Synthetic peptides as tools in chemical immunology

Doelman, W.

Synthetic Peptides as tools in Chemical Immunology

proefschrift

ter verkrijging van
de graad van doctor aan de Universiteit Leiden,
op gezag van rector magnificus prof.dr.ir. H. Bijl,
volgens besluit van het college voor promoties
te verdedigen op donderdag 9 februari 2023
klokke 10:00 uur

door

Ward Doelman

geboren te Utrecht
in 1994

Promotores:	Prof. Dr. S.I. van Kasteren
	Prof. Dr. H.S. Overkleeft
Promotiecommissie:	Prof. Dr. M. Ubbink
	Prof. Dr. N.I. Martin
	Prof. Dr. A.J. Fairbanks (Canterbury, New Zealand)
	Prof. Dr. J.D.C. Codée
	Dr. M.T.C. Walvoort (RUG)

Cover design by Stijn Doelman

Printed by Ridderprint

Table of contents

1

Synthesis of glycopeptide conjugates for immunological studies

This work was published as: W. Doelman and S.I. van Kasteren *Org. Biomol. Chem.* **2022**, 20, 6487-6507

Glycosylation is one of the key post-translational modifications (PTMs) of proteins.[1] Like all PTMs, glycans are not directly encoded by the genome. Genetic techniques can therefore not be readily used to study the effects of glycosylation. Furthermore, the glycans introduced onto proteins using the cellular glycosylation machinery are heterogenous in nature. This means that isolated glycoproteins exist as mixtures modified with different glycans; so-called glycoforms.[2] Determining the relationship between glycoprotein functions and specific oligosaccharide structures is therefore challenging.

This is particularly poignant in immunology, where protein glycosylation plays a major role in many key processes, like regulation of immunotolerance,[3,4] uptake of antigens[5,6], the creation of neo-epitopes[7,8], and even the protection of the foetus.[9] The precise study of these processes has been hampered by a dearth of well-defined reagents. In some cases, well-defined glycans, in the absence of any protein scaffold, can be used to study these functions. For instance, the carbohydrate binding specificity of many lectins have been determined using synthetic oligosaccharides in absence of a protein scaffold.[10,11] However, for many processes, the combination of carbohydrate and protein is key. For example, antigen (cross-)presentation is thought to be enhanced by uptake of the antigen via lectins[12,13] and therefore requires a covalent attachment of the protein and the (specific) oligosaccharide.

Entire glycoproteins, bearing a well-defied glycan, are formidable synthetic targets. Their use is therefore often not feasible. Synthetic, glycosylated peptides can offer a useful alternative; a compromise between reality and synthetic accessibility for biochemical studies. Additionally, synthetic glycosylated peptides in themselves are being actively developed as vaccine candidates.[14] These have been shown to induce glycosylation-specific immune responses.[15,16] Examples of antigens that have been tried as targets for glycopeptide vaccines are the envelope glycoprotein of human immunodeficiency virus (HIV),[17] as well as certain tumor associated antigens.[18]

From a synthetic perspective, the synthesis of glycosylated peptides is still a challenge in itself, as it involves the combination of two types of bio-organic chemistry: peptide synthesis and carbohydrate chemistry. While these two fields are not inherently incompatible, there are challenges to overcome for successful glycopeptide synthesis. This review will focus on the synthesis of glycopeptides and glycopeptide conjugates useful for immunological studies. To give a good overview of the field both early and recent developments will be highlighted.

Overview of protein glycosylation

Before discussing the synthetic challenges involved, it is important to understand the structure of naturally glycosylated peptides. Native glycosylation of peptides and proteins generally happens in two forms: O-glycosylation, were the reducing end of an oligosaccharide is attached to the hydroxy-function of a serine or threonine (or sometimes tyrosine) residue[1,19], and N-glycosylation, where the oligosaccharide is attached to the carboxamide function of an asparagine residue.[1,20] Not only the nature of the glycosidic bond to the peptide is inherently different between these two types of glycosylation; the general structure of the N- and O-linked glycans is also fundamentally different and each presents their own unique synthetic (and biological) challenges.

The simplest form of O-glycosylation is the introduction of β-GlcNAc onto serine or threonine (**Figure 1**, **1**). This is a regulatory modification that is, unlike the more complex forms of O-glycosylation, reversable.[21] Despite this, it seems to be an immunologically relevant peptide modification, as O-GlcNAcylated peptides have been shown to be presented by major histocompatibility complexes (MHC) *in vivo*.[22] The non-dynamic types of O-glycosylation start

with the introduction of an α-linked N-acetyl galactosamine (GalNAc) residue (**2**), also called the Tn-antigen, onto serine or threonine. This single carbohydrate can then be enzymatically elaborated towards more complicated structures. For instance, the introduction of galactose onto the 3-OH creates the T-antigen (**3**), while 2,6-sialylation creates the STn-antigen (**4**). More elaborate structures are produced by enzymatic extension of different core structures. The four O-glycan cores most important in humans are also shown in **Figure 1** (**3**,**5-7**). The biosynthesis and biochemical functions of these more complex O-glycosylation patterns are, as of yet, poorly understood.[23] It cannot, for example, be predicted from the structure where on the protein this modification will be introduced, nor is the glycosylation machinery well defined. Besides these common modifications, glycosylation of serine and threonine with mannose, fucose, galactose and xylose have also been shown to exist within the human glycoproteome.[1]

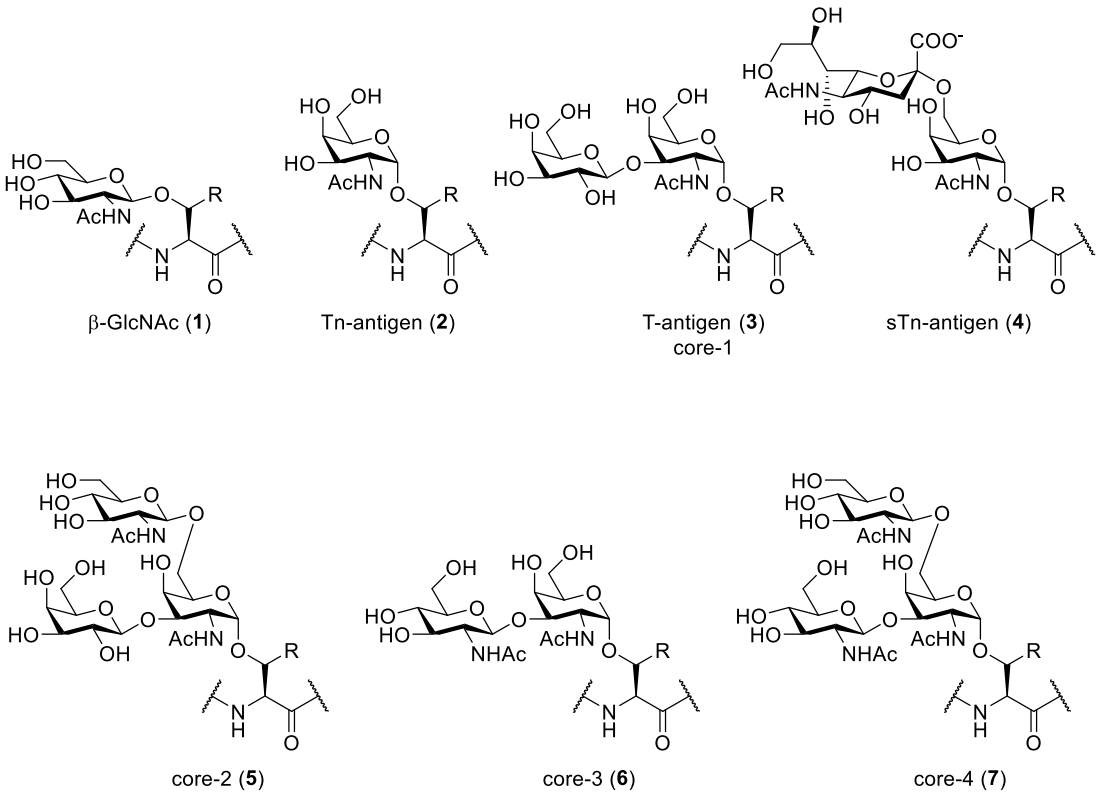

Figure 1. Some examples of O-glycosylation. β-GlcNAcylation of Serine or Threonine (**1**) is a commons regulatory PTM that competes with phosphorylation. Minimal O-glycosylation (**2-4**) patterns known to be relevant in cancer. More complex O-glycosylation is branched of different O-glycan cores represented by compounds **2,5,6,7**. All of these modifications occur both on serine (R = H) or threonine (R = CH_3).

One of the most well-studied examples of protein O-glycosylation is the mucin family of glycoproteins. The members of this family are produced primarily by epithelial cells and are either cell-membrane bound or secreted into the extracellular matrix. While elaborate O-glycosylation is suspected to exist on many proteins, the total amount and structural diversity found within this protein family is striking. Aberrant glycosylation of mucins, resulting in the proteins being decorated with the more simplistic forms of O-glycosylation (**2-4**), is found in

several types of cancer.[24] Targeting of these hypoglycosylated proteins by the immune system is a very active area of research for the development of onco-immunology based cancer treatments.[25]

N-glycosylation is biochemically distinct from O-glycosylation. Unlike O-glycosylation, the location of N-glycosylation can be easily predicted: Introduction of N-glycans occurs at asparagine residues that are part of the consensus sequence Asn-Xxx-Ser/Thr, with Xxx representing any amino acid except proline.[1] Furthermore, the structure of the glycan is very different from those seen for O-glycans. Every N-glycan has the same core structure, that is Manα1-6(Manα1-3)Manβ1-4GlcNAcβ1-4GlcNac (**8**), containing a rare β-mannoside linkage (**Figure 2**).[26] Generally, this core structure is further elaborated with additional glycosylation. One commonly seen N-glycan structure is the so-called "high mannose", or Man_9, N-glycan (**9**), a modification that is introduced early in the biosynthesis of N-glycosylated proteins.[26] Remodeling and elaboration of these immature N-glycans by the cellular glycosylation machinery leads to more elaborate N-glycans, the so-called "complex" type, such as a so-called biantennary and sialylated structure **10.**

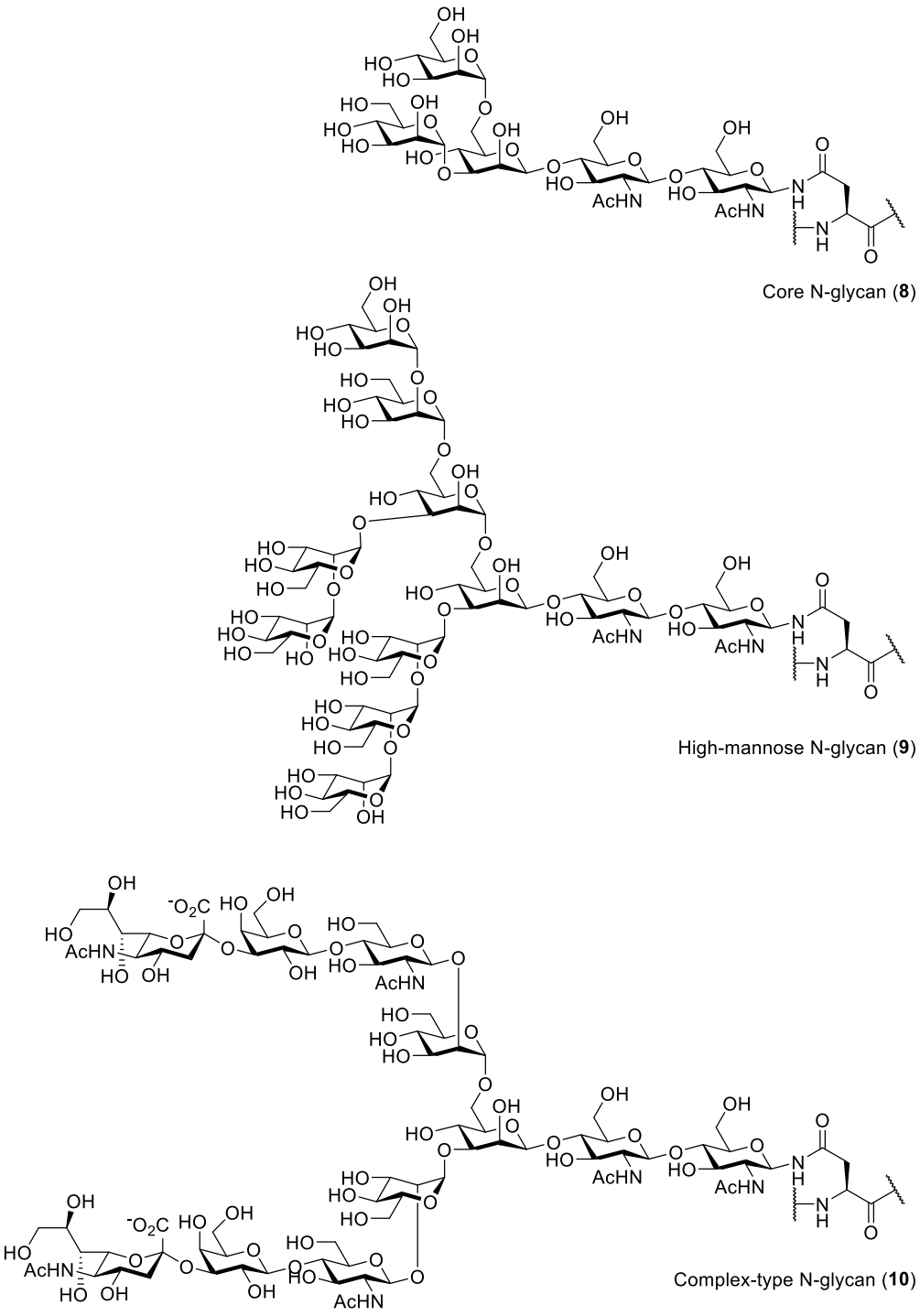

Figure 2. Examples of asparagine residues decorated with N-glycans. Structure **8** represents the core pentasaccharide seen in all natural N-glycans. Structure **9** is an example of the high-mannose or immature N-glycan, while **10** is an example of a sialylated complex N-glycan.

Chemical approaches towards synthetic glycopeptides

Synthetic strategies towards the production of well-defined glycopeptides can take one of three approaches:

1) *Total chemical synthesis*, where the entire molecule is produced using organic transformations;
2) *Chemoenzymatic synthesis*, where parts of the synthesis are accomplished using enzymatic transformations;
3) *Conjugation based approaches*, where the covalent linkage of peptide and oligosaccharide is achieved using one of various chemical approaches. These approaches usually yield a glycoconjugate containing one or more unnatural linkages.

While the first two approaches produce glycopeptides identical to naturally glycosylated peptides, this last approach will produce neoglycopeptides that, while not identical to native molecules, can be used to study the biochemical functions of glycosylation in some instances.[14,27–32]

For some applications, like the development of vaccines against glycosylated epitopes, having the entire, natively glycosylated amino acid in the peptide sequence is of crucial importance. This is necessary to produce antibodies and T-cell responses against a specific antigen *in vivo* without producing antibodies against unnatural linker-structures.[33] However, the majority of lectin interactions only require certain oligosaccharide substructures derived from larger O- or N-glycans.[10,29,30,34] For these areas of research, where the interactions under study only depend on a substructure of the glycan, simplified glycopeptides or glycoconjugates can be used. These can mimic some of the effects of natural glycosylation and can be used in place of natively glycosylated peptides. Specific areas of (immunological) interest these conjugates have seen use are the study of lectin mediated peptide uptake,[13,28] modulation of cytokine production[29,35] or targeting of specific cell-types.[27,36] The increased synthetic accessibility of these glycoconjugates enables the synthesis and evaluation of more variants, in turn enabling more in-depth studies of glycan function. Therefore, conjugation methods to synthesize non-natively glycosylated peptides in a facile (compared to synthesis of native structures) manner will be described in more detail.

1. Total chemical synthesis of glycopeptides

Total synthesis of O-glycosylated peptides

The total chemical synthesis of O-glycosylated peptides is usually carried out using a building block-based approach, where the entire glycosylated serine or threonine residue is first synthesized as an Fmoc-protected building block. These amino acids are then incorporated into the desired peptide sequence using standard Fmoc-SPPS conditions. However, unlike the synthesis of peptides containing only standard, non-glycosylated amino acids, some considerations need to be made. The typical TFA mediated global deprotection of the synthesized peptides can lead to hydrolysis of certain glycosidic bonds, with α-fucosides and sialic acids being the most sensitive.[37–39] This was famously demonstrated by Unverzagt and Kunz during the synthesis of a peptide containing an asparagine residue glycosylated with fucosylated chitobiose.[37] During deprotection, they found that the acid lability of the α-fucoside linkage was protecting-group dependent. Compound **11**, bearing benzyl protection groups on the fucose hydroxy-groups, was not resistant to acidic treatment, while acetylated compound **13** was (**Figure 3A**). Additionally, alkaline conditions, like the Fmoc-deprotection step or the coupling step itself, can cause β-elimination of glycosylated threonine (**Figure 3B**) or epimerization of glycosylated serine.[40,41]

The use of particular protecting groups on the sugar part of the glycopeptide can help alleviate these problems, but require careful consideration during synthesis of the glycosylated amino acid building blocks. O-Acetyls are most often employed, as they improve the acid stability of the molecule, while enabling removal under mild enough conditions to avoid the aforementioned base-mediated side reactions. Treatment with dilute solutions of NaOMe,[42] NaOH[43] or hydrazine[44] can often be used to selectively liberate the protected glycoside without affecting the peptide or glycosidic bonds.

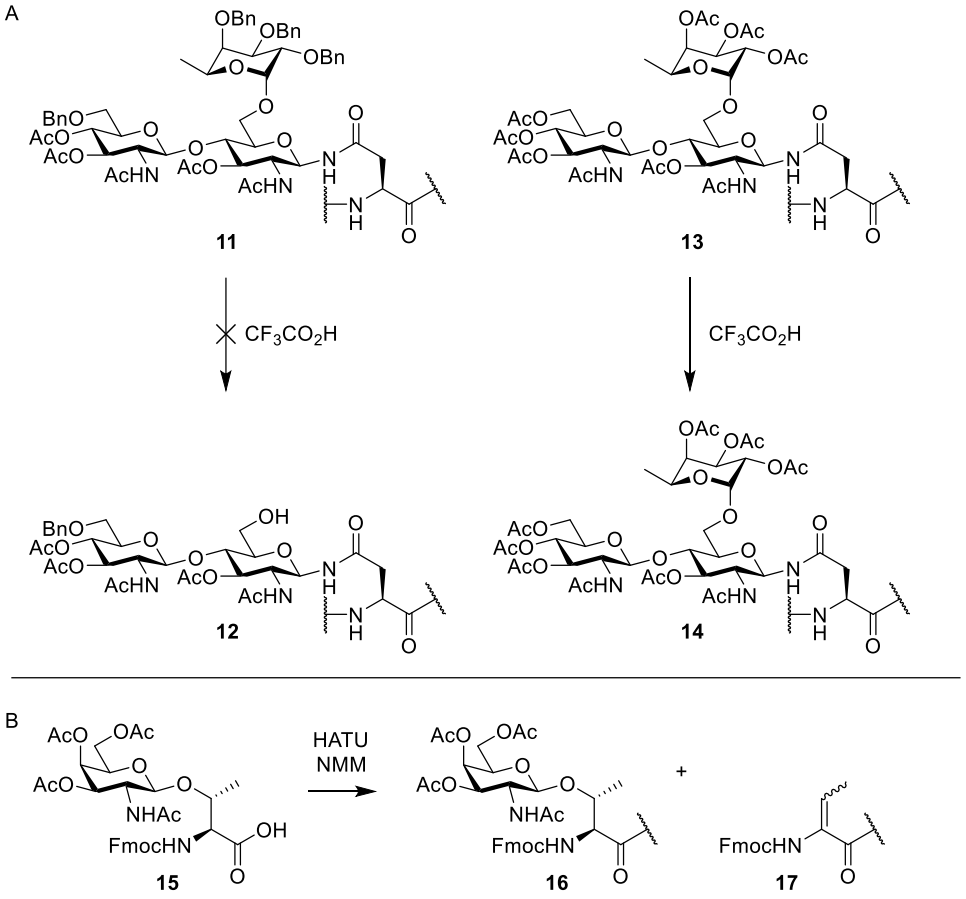

Figure 3. A) TFA mediated deglycosylation observed by Unverzagt and Kunz.[37] During TFA mediated deprotection of a peptide containing a trisaccahride (**11**) cleavage of the α-fucoside bond was observed yielding partially deprotected glycopeptide **12**. A peptide containing an acetyl protected trisaccharide (**13**), when treated under similar conditions, did fully retain the fucose residue. B) Base mediated β-elimination of an O-glycosylated threonine residue as observed by Zhang et al.[40]

These days, peptides containing (simple) O-glycosylation patterns are synthesized as a matter of course, with many useful building blocks readily available from commercial sources. This, of course, is made possible by decades of development, that are briefly highlighted here. The initial development of synthetic methods to produce O-glycosylated peptides started in the 1980s.[45–47] Kunz introduced the building block approach described above, synthesizing the first of Fmoc-protected O-glycosylated amino acids, using esters to protect the sugar hydroxyl groups (**Figure 4A**). The common approach to introduce the α-glycosidic bond between the amino acid and the galactosamine, that is glycosylation with a 2-azido donor followed by reduction and acetylation, was used. These amino acids were used to produce several tripeptides decorated with both Tn- and T-antigen structures.[47] Paulsen then applied a similar building block to Fmoc-SPPS, producing an octapeptide bearing five threonine residues modified with α-GalNAc,[42] opening up the way towards more complicated glycopeptides.

The synthesis of glycopeptides bearing sialic acid containing O-glycans, a key modification highly abundant on certain tumors,[48] would take another decade.[43,49] As an example, the synthesis of a sialyl Tn-antigen building block (**26**) and incorporation into a peptide fragment

from the HIV glycopeptide gp120[50] (**27**) by Kihlberg is given in **Figure 4B**.[49] This synthesis, like the one outlined above, used an azide function on the galactose C-2 to mediate formation of the α-glycosidic bond, followed by transformation to the desired acetamide function. This synthesis also exemplifies an early use of an acid labile protecting group, in the form of the isopropylidene, on a glycosylated amino acid building block. Since the sialic acid containing amino acid is introduced as the methyl ester, final deprotection has to be carried out using a hydroxide solution, in order to obtain the free acid.

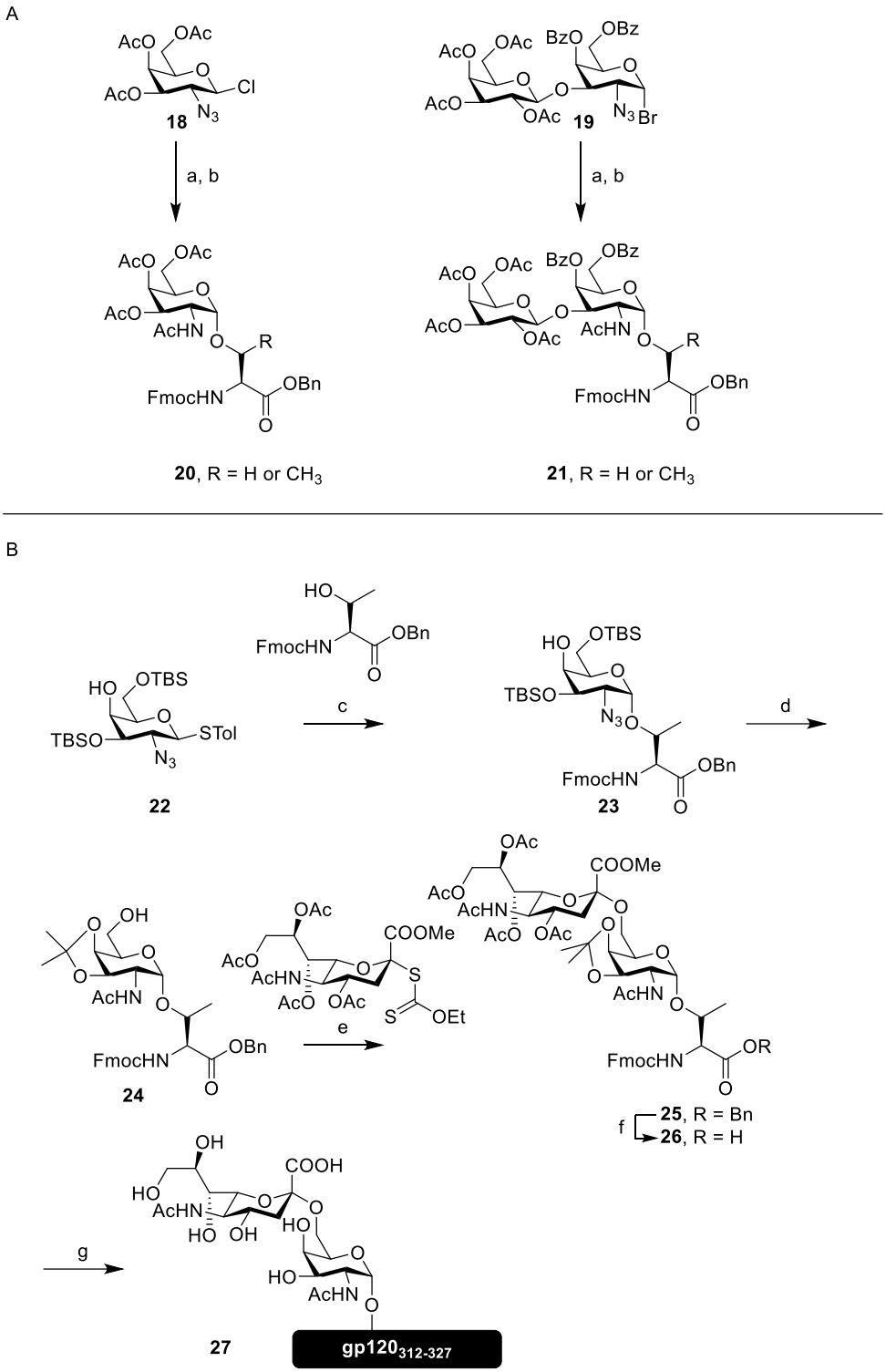

Figure 4. A) First synthesis of the Tn- (**20**) and T-antigen (**21**) as Fmoc-protected amino acids, as described by Kunz.[47] B) Synthesis of a Sialo-Tn antigen building block (**26**) and use of this building block in Fmoc-SPPS, as described by Kihlberg and coworkers.[49] Reagents and conditions: a) Fmoc-Ser-OBn or Fmoc-Thr-OBn, Ag^{+}, 30-65% b) i) $NaBH_4$, $NiCl_2$ ii) Ac_2O, pyridine, 60-86% c) NBS, Bu_4NOTf, DCM, -28°C, 71% (α/β mixture) d) i) AcSH, pyridine, 67% ii) AcOH, MeOH, THF, 60°C, 86% iii) DMP, TsOH, 85% e) MeSBr, AgOTf, DCM, MeCN, -78°C, 49% f) H_2, Pd/C, EtOAc, 88% g) i) Fmoc-SPPS ii) TFA, PhSMe, $HSCH_2CH_2SH$ iii) NaOMe, MeOH iv) NaOH, H_2O, v) RP-HPLC, 12%

With the synthesis of the glycopeptides via Fmoc-SPPS reaching greater maturity, the complexity, as well as the diversity, of the oligosaccharide structures has increased.[51–55] For instance, the group of Westerlind developed a microarray containing a wide variety of mucin-protein derived glycopeptides, enabling the profiling of the antibody response of mice vaccinated with different MUC-glycopeptide based vaccine candidates.[56]

Besides mucin-derived peptides, other O-glycosylated peptides have been the object of study. As an example, glycopeptide ligands for the P- and E-selectin receptors on white blood cells are an important class of O-glycosylated peptides.[57] P-selectin binds to the sialyl-Lewis^X (sLe^X) tetrasaccharide (Neu5Acα2-3Galβ1-4(Fucα1-3)GlcNAcβ), a synthetically challenging target on its own. Total synthesis of a 12-mer peptide, derived from the protein P-selectin glycoprotein ligand-1 (PSGL-1), containing a threonine residue glycosylated with a hexasaccharide containing the sLe^X structure was achieved by Baumann et al.[58]

Recently, renewed interest in the development of O-glycosylated amino acid building blocks has been seen. Several novel acid-labile protecting group strategies have been developed, enabling a one-step deprotection of the resin-bound glycopeptide. These approaches use electron-rich benzyl ethers[59,60] or silyl ethers.[49,61,62] While these are promising developments simplifying the synthesis of O-glycosylated peptides, they have only been applied to peptides bearing mono- or disaccharides, and have yet to be proven in the synthesis of glycopeptides bearing larger protected glycans.

Total synthesis of N-glycosylated peptides

While generally more challenging than the synthesis of O-glycosylated peptides, due to the high complexity of even “simple” N-glycans, some total syntheses of N-glycosylated peptides have also been carried out. In contrast to the synthesis of O-glycosylated peptides, where the glycosidic linkage between amino acid and oligosaccharide is often introduced in an early stage, most syntheses of N-glycosylated amino-acids or peptides produce the crucial glycoside-asparagine linkages at a late stage in the synthesis. Most commonly, the entire glycan, either with or without protecting groups, is produced as a glycosyl amine, that is then used in an amide-bond forming reaction with an aspartic acid sidechain.

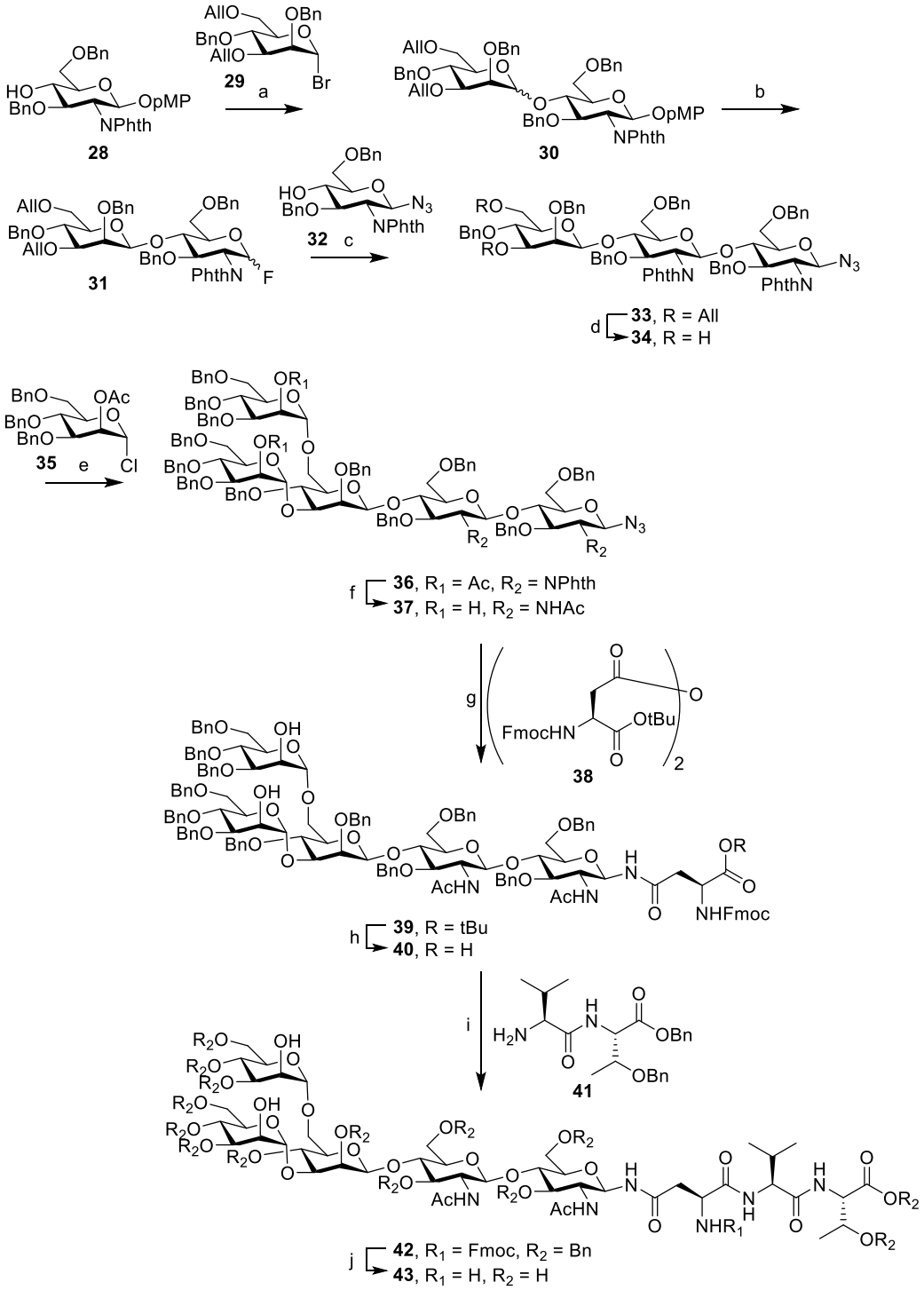

Figure 5. Ogawa's synthesis of an Fmoc-asparagine building block carrying the core N-glycan structure (**40**), and solution phase synthesis of a simple tripeptide bearing this glycan (**43**). In contrast to the synthesis of O-glycosylated building blocks for peptide synthesis, the introduction of the amino acid happens after production of the full glycan. Reagents and conditions: a) silver silica-alumina, DCM, 72% (α/β = 7/8) b) i) CAN, H_2O, MeCN, MePh, 70% ii) DAST, DCM, quant. c) $AgClO_4$, hafnocene dichloride, DCM, 79% d) $\{Ir(COD)[PCH_3(C_6H_5)_2]_2\}PF_6$, THF, 79% e) AgOTf, DCM, -40°C, 80% f) i) $NH_2CH_2CH_2NH_2$, nBuOH ii) Ac_2O, MeOH, 0°C, 80% g) Lindlar, H_2, MeOH, 79% h) TFA, DCM, 89% i) EDC, HOBt, DCM, 90% j) i) morpholine ii) Pd/C, H_2, AcOH, H_2O, 58%

Early work on N-glycosylated peptides used a similar building block approach as was used for the synthesis of O-glycosylated peptides. The group of Ogawa managed the first synthesis of a tripeptide carrying the core-pentasaccharide.[63] This synthesis, outlined in **Figure 5**, starts with the complete synthesis of the pentasaccharide azide **37**. In this synthesis, no particular care was taken to selectively produce the β-mannoside linkage in compound **30**, preferring instead to separate the two diastereomers. After allyl ether deprotection (**34**) and introduction of the final two mannose moieties (**36**), the phthalimide functions were converted to the acetamides (**37**). To introduce the (orthogonally protected) asparagine residue, the anomeric azide was selectively reduced by hydrogenation over Lindlar catalyst to obtain the glycosyl amine. This intermediate was then condensed with anhydride **38** in the same pot, to limit hydrolysis of the sensitive anomeric amine. TFA mediated deprotection of the *tert*-butyl ester produced Fmoc-amino acid **40**, usable for Fmoc-SPPS of glycopeptides. In this case, however, solution phase peptide synthesis was employed, with EDC mediated coupling to dipeptide **41** yielding the protected tripeptide **42**. Fmoc-deprotection followed by hydrogenolysis yielded the desired deprotected glycopeptide **43**.

Further development of this building block approach by Unverzagt produced a pentapeptide decorated with a heptasaccharide N-glycan, again by in solution peptide synthesis.[64,65] This glycosylated amino acid, bearing no protective groups on the sugar hydroxy functions, was later also used in Fmoc-SPPS, where the choice of solid support turned out to be critical to mediate effective introduction of this extremely polar amino acid.[66] When using glycosylated amino acids without hydroxyl-group protection, side reactions, in the form of unwanted acylation, limit the maximum length of the peptide that can be synthesized.[67] However, when the glycoside was protected with acetyl groups, via on-resin acetylation, another set of unspecified side-reactions still prevented the synthesis of N-glycosylated peptides longer than 20 amino acids.[68]

To avoid these problems, the total synthesis of N-glycosylated peptides is usually carried out via an convergent approach. This is most often accomplished using the so-called Lansbury aspartylation (**Figure 6**).[69,70] In this reaction, a glycosylamine derivative of the oligosaccharide is condensed with a partially protected peptide, containing an activated aspartic acid residue. This approach is not free of side reactions, with aspartimide formation and the associated formation of iso-aspartate and loss of stereochemistry of the aspartic acid residue being key problems.[71]

Still, in this manner the total synthesis of highly complex N-glycosylated peptides was achieved, with the chemical synthesis of homogeneously glycosylated Erythropoietin by Danishefsky and coworkers the most famous example.[72] Also, a glycopeptide derived from the HIV envelope protein, a potential vaccine candidate, was produced by total synthesis. This peptide was used to isolate a so-called broadly neutralizing antibody (BnAb) from the plasma of a HIV patient, as well as induce production of antibodies in a Rhesus Macaque model. [73]

However, to further avoid the side reactions associated with chemical introduction of N-glycans or N-glycosylated amino acids, as well as the laborious work of producing said glycan by synthesis, many examples of N-glycopeptide synthesis have instead been carried out using chemoenzymatic and semisynthetic means.

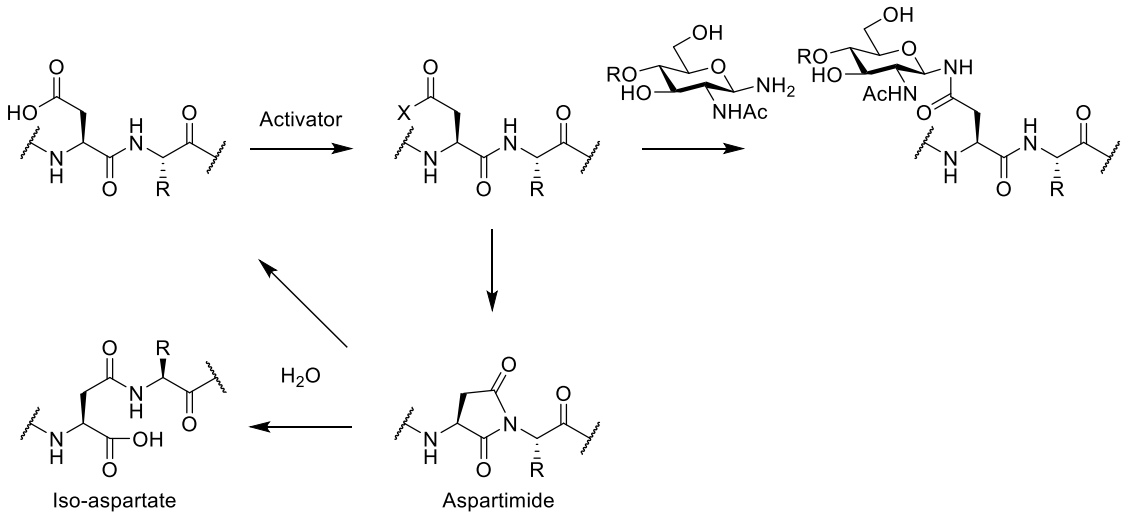

Figure 6. Lansbury aspartylation and the associated aspartimide formation side reactions. The acid function of an unprotected aspartic acid sidechain is activated using a coupling reagent, and the active ester is reacted with a free glycosyl amine. As a sidereaction, the activated ester of aspartic acid can react with the C-terminal amide, forming an aspartimide. Hydrolysis at the C^{α}-side leads to the formation of an iso-aspartate residue. X = active ester.

2. Chemoenzymatic (semi)synthesis of glycopeptides

Since N-glycans all have the same pentasaccharide core, the enzymes that deal with this part of the glycan are often somewhat promiscuous. This is especially true for the family of *endo*-β-N-acetylglucosaminidases (ENGases), which catalyze the cleavage of the majority of an N-glycan from a peptide, by hydrolyzing the glycosidic bond between the first and second GlcNAc at the reducing and of the oligosaccharide.[74] It was soon realized that these enzymes could, under the right conditions, be made to perform transglycosylation reactions between an asparagine residue containing a full N-glycan and another bearing only an N-acetyl glucosamyl.[75] The discovery that these enzymes were capable of using oxazoline donors[76] instead of glycosylated asparagine derivatives helped to further develop this effective enzymatic glycosylation method. Directed mutagenesis of several ENGase enzymes lead to the development of specific mutants that had limited hydrolytic capacity, removing the most pronounced side reaction and increasing the yield of these enzymatic glycosylations.[77,78] In **Figure 7A**, the general method of ENGase mediated peptide glycosylation, using an oxazoline donor glycoside, is shown.

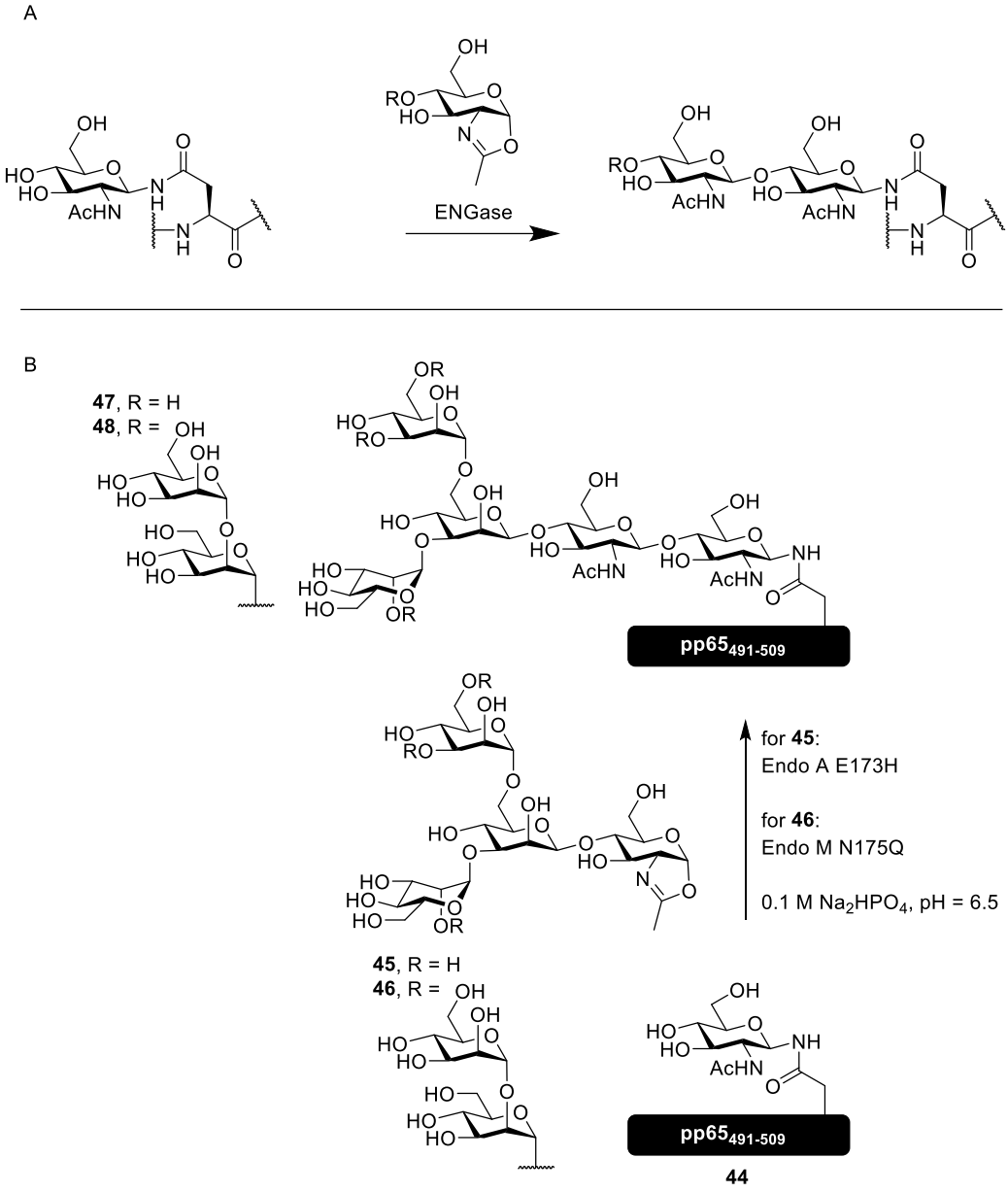

Figure 7. A) general overview of ENGase mediated glycosylation of a peptide containing an N-GlcNAc asparagine residue with an oxazoline donor. B) ENGase mediated synthesis of several N-glycosylated derivatives of the cytomegalovirus derived peptide pp65$_{491\text{-}509}$ by McIntosh et al.[79] Both synthetic oxazoline donor **44** as well as semisynthetic oxazoline donor **45**, produced from an N-glycopeptide obtained from soy flour, were enzymatically introduced onto glycopeptide **43**, producing vaccine candidates **46** and **47**.

ENGase mediated synthesis has been used to synthesize a peptide derived from the HIV glycoprotein gp120, containing two core pentasaccharides,[80] and a vaccine candidate glycopeptide against cytomegalovirus (CMV), decorated with either a core-pentasaccharide (**47**, **Figure 7B**) or a full high mannose-type glycan (**48**). As the peptide sequence under investigation contains two distinct N-glycosylation sites, the effect of glycosylating one or both sites was evaluated. The found that while glycosylation of Asn$_{507}$ had negligible inhibitory effect on T-cell activation, introduction of the N-glycans onto both Asn$_{495}$ and Asn$_{507}$ completely inhibited T-cell activation.[79]

ENGase mediated glycopeptide synthesis has also used to synthesize lectin binding peptides; Yamaguchi *et al.* produced, by total chemical synthesis, an oxazoline donor of a bis-phosphorylated high-mannose type N-glycan (**49**), and used this to produce a cyclic peptide containing two phosphorylated N-glycans (**50**, **Figure 8**). This molecule had a nanomolar affinity for the cation-independent mannose-6-phophate receptor (CI-MPR). The cyclic nature of the peptide was found to be critical, as linear glycopeptide **51** had a 20-fold lower affinity for the CI-MPR.[81] Besides the synthesis of N-glycosylated peptides, ENGase catalyzed glycosylation has also been extensively applied to the production of single glycoform N-glycosylated proteins, including remodeling of the N-glycans on the Fc-domain of antibodies.[82–85]

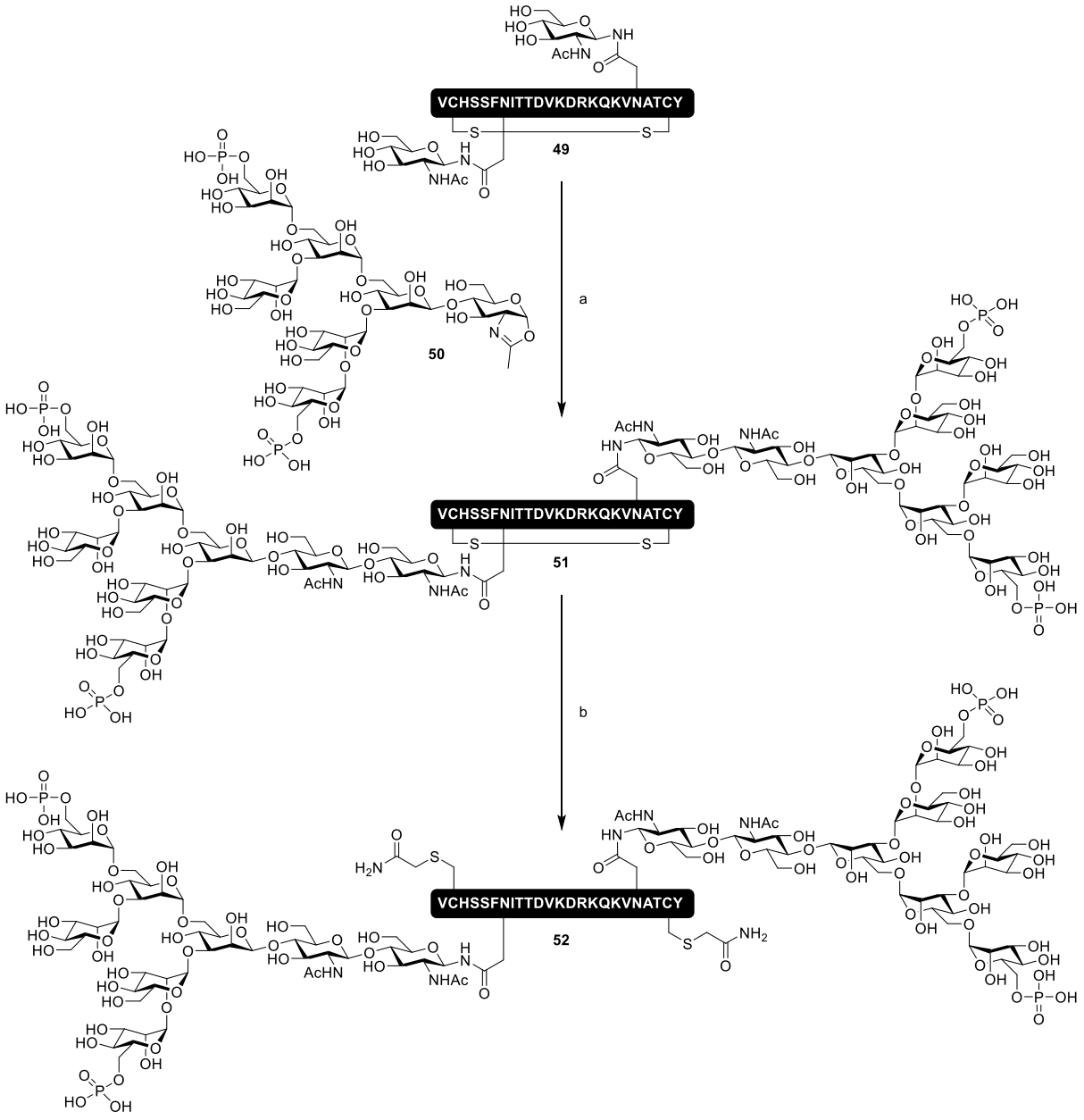

Figure 8. ENGase mediated synthesis of a CI-MPR binding cyclic phosphorylated glycopeptide **51** by Yamaguchi et al.[81] Reagents and conditions: a) Endo A N171A, Tris buffer (pH 7.1) b) i) DTT ii) Iodoacetamide

Another area where biochemical methods have improved the study of N-glycosylated peptides is in the production of the N-glycosylated asparagine building blocks and oxazoline donors required for the above syntheses. Methods have been developed to isolate N-glycopeptide carrying specific N-glycans from biological sources. This was first demonstrated by the isolation of sialoglycopeptide (SGP) from egg yolk, a hexapeptide bearing a biantennary sialoglycan.[86] This peptide was used directly with Endo M (one of the ENGases) to produce a glycosylated form of the CD52 peptide,[87] as well as being chemically transformed into an oxazoline donor for other ENGase mediated reactions.[88,89] Furthermore, after peptidase mediated liberation of the glycosylated asparagine followed by selective introduction of an Fmoc-group and protection of the sialic acid residues as benzyl esters[67] or phenacyl (Pac) esters,[90] this semisynthetic glycosylated amino acid has been used in SPPS for the facile production of N-glycosylated peptides.[91,92] These protecting groups inhibited the acid mediated hydrolysis of the sensitive glycosidic bond of sialic acid, enabling both Fmoc- and Boc-SPPS approaches. A high mannose type N-glycan ($Man_9GlcNAc_2$-Asn) can, in a similar manner, be isolated from soybean flour[93,94] or egg yolks,[95] and has also been used in ENGase mediated glycotransfer reactions[79,96] as well as SPPS.[97]

Another enzymatic approach that has furthered the synthesis of N-glycopeptides is enzyme-based glycan remodeling. This is the enzymatically removal and/or addition of specific glycosides to an N-glycan. Enzymes have most commonly been employed to install sialic acids onto peptides bearing synthetic complex-type N-glycans[65], or for introduction of the so-called core-fucose moiety (α-fucosylation of the 6-OH of the reducing-end GlcNAc in the core pentasaccharide).[98] More extensive remodeling of N-glycosylated asparagine has also been reported. The group of Kajihara used partial acidic hydrolysis of glycosylated asparagine obtained from egg-yolk SGP, followed by further enzymatic hydrolysis to produce various N-glycosylated asparagine residues. These were subsequently used in peptide synthesis.[99] More recently, the group of Boons showed the production of various N-glycosylated asparagine structures by enzymatic remodeling of the biantennary N-glycan isolated from egg yolk.[100,101] This method has, however, not yet been employed for the synthesis of N-glycosylated peptides.

Chemo-enzymatic approaches have also been applied to the synthesis of O-glycans, by enzymatically elaborating synthetic O-glycosylated peptides. These approaches start by the chemical synthesis of a peptide containing an α-GalNAc-Ser/Thr as a starting point for enzymatic introduction of additional saccharides. Sialic acids have been introduced in a stereoselective manner using this approach[102], a feat that can be challenging using organic synthesis techniques.[103] More complex oligosaccharides have also been made chemoenzymatically; for instance, a glycosulfopeptide derived from PGSL-1 has been produced by enzymatic elaboration of an α-GalNac containing synthetic peptide.[104] Producing O-glycosylated peptides from non-glycosylated starting material has also been accomplished, as shown by the group of Clausen, who synthesized various glycoforms of a 60-mer MUC1 repeat peptide.[105] Two of the peptides produced in this manner were then used to immunize

mice, where production of specific antibodies was observed. Using the various differently glycosylated MUC1 peptides produced by the authors, they were able to precisely determine the specificity of these antibodies.[105,106]

3. Unnatural glycoconjugate peptides

The glycans of many glycoproteins are very complex (as described above). However, the core of the glycan often does not partake in shaping its biological role.[10] In order to study the role glycosylation plays in immunological processes without having the perform highly complex glycopeptide total synthesis, conjugation strategies to produce non-natural glycosylated peptides have been developed. These non-natural structures enable the rapid production of glycopeptide conjugates. This in turn facilitates the study of the role of glycosylation in certain (immune)cellular processes. It also enables more rapid synthesis of libraries of glycopeptides bearing various oligosaccharides, enabling powerful studies in carbohydrate structure/activity relationships.[28–31]

Simplified and stabilized glycosylated amino acid building blocks

Peptides decorated with simplified glycans – either attached via a native or non-native linkage – can provide useful tools for studying the effect of glycosylation on immune reactions. Various approaches have been developed based on this premise. These primarily differ from each other by how close they mimic the chemical structure of natively glycosylated peptides. They can be viewed to be on a spectrum from nearly-native down to glycopeptide conjugates using completely non-native linkages. On the nearly-native side of the spectrum, there are the simplified N-glycans. Here asparagine is, via a natural N-glycosidic linkage, decorated with a truncated glycan. Next are the stabilized linkages, described below, where labile parts of the glycosylated amino acid are replaced with more stable bioisosteres. For example, replacing the oxygen in a glycosidic bond for a sulfur atom renders the glycoside resistant to enzymatic hydrolysis.[107] While these are not equivalent to the linkages found in nature, these still have a high degree of similarity to the native structures. On the fully non-native end of the spectrum, completely non-amino acid based building blocks are used to attach a glycoside to a peptide, usually by amide bond formation with the N-terminal or lysine-sidechain amine group(s).

The simplified N-glycan mimics, as the most natural-like of the simplified glycans, still retain some key properties of the glycans they are mimicking, *i.e.* the presence of a glycosidic bond with asparagine. Peptides produced via the simplified N-glycan approach are capable of mimicking certain functional aspects of N-glycans, while circumventing production of the entire, synthetically complex natural N-glycan. The group of Kunz has, for example, developed glycopeptide ligands for the lectin E-selectin, containing asparagine linked Sialyl-Le^X determinants (**53**, **Figure 9A**).[108,109] Simplified N-glycans, bearing other, non-sialylated and immunologically important Lewis-type sugars, like Le^X [29,110] and Le^A [111] have also been described.

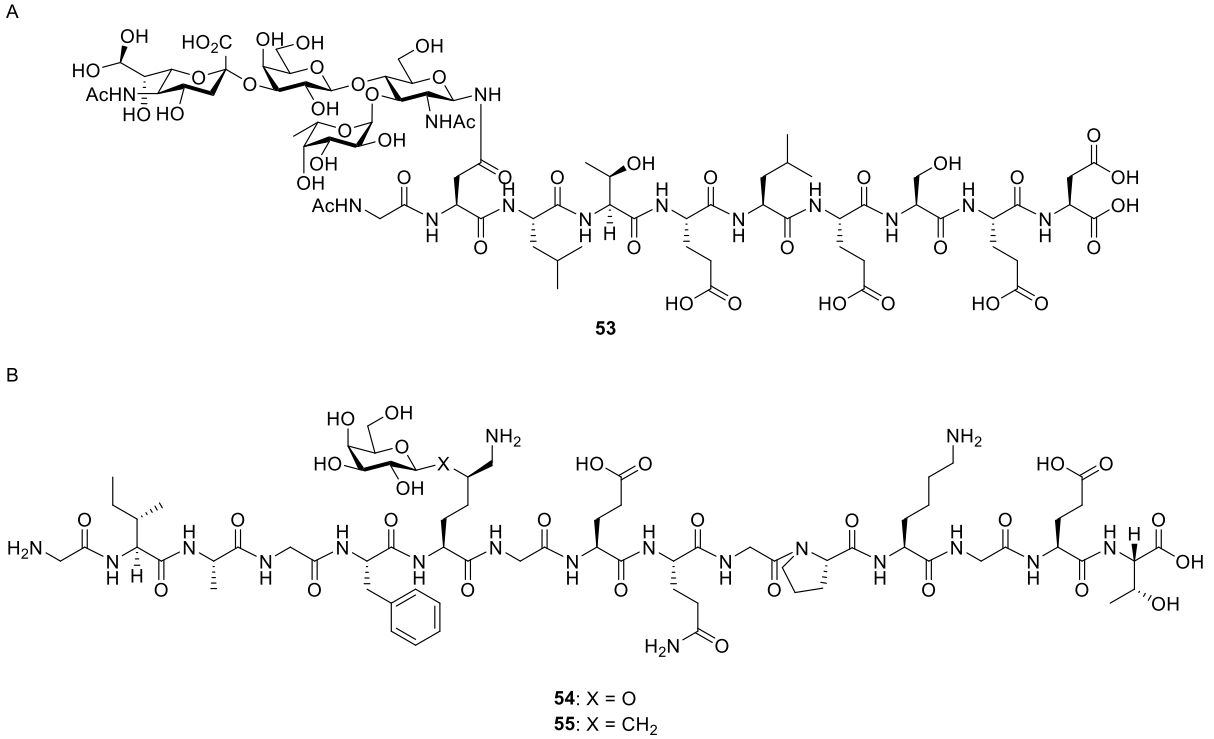

Figure 9. Examples of simplified and stabilized glycopeptides. A) A synthetic N-glycopeptide bearing a simplified N-glycan produced by Filser et al.[108] By including only the part of the N-glycan required for lectin binding, here the sialyl-Lewis^X determinant, the synthetic complexity of glycopeptides can be limited without compromising on functional activity. B) Structure of the native (**54**) and stabilized (**55**) variants of a neoglycoepitope derived from collagen type II synthesized by Gustafsson *et al*.[112] Peptide **55** was still able to induce a T-cell response, despite the non-native glycosidic linkage.

Stabilized building blocks, on the other hand, were developed not to simplify chemical synthesis, but to increase (bio)chemical stability of the glycopeptide. These approaches are occasionally used to suppress the chemical side reactions described earlier. More commonly, stabilized building blocks are applied in glycopeptide synthesis to prevent the enzymatic hydrolysis of natural linkages in biological systems.[21,113] These actions of cellular enzymes can be a complication when studying the effect of peptide glycosylation in biological systems. To suppress enzymatic degradation, stabilized glycosylated amino acid building blocks have been developed, based on S- or C- glycosidic linkages. Cys(β-GlcNAc), as mentioned before, is a good functional mimic of Ser(β-GlcNAc), that is resistant to hydrolysis by the glycosidase O-GlcNAcase.[107] An S-glycoside analogue of a Tn-antigen containing MUC1-peptide has also been developed and tested as a vaccine candidate. The antibodies obtained from mice immunized with this peptide were able to recognize a human tumor cell line, indicating that the unnatural linkage does not necessarily impede the ability of a synthetic glycopeptide to induce an immune response to the native antigen.[114] This result further exemplifies the ability of S-glycopeptides to mimic the functions of O-glycopeptides. C-glycosides have been similarly used in immunological studies. For instance, the group of Kihlberg produced a glycopeptide epitope, derived from type II collagen containing a galactosylated δ-hydroxylysine (**54**, **Figure 9B**), as well as a C-glycoside mimic of this moiety (**55**).[112] This peptide may play a key role in

the pathogenesis of rheumatoid arthritis (RA).[115,116] The C-glycoside analogue **55** was able to activated T-cell hybridomas, although at a lower level compared to the natural peptide. Stabilized glycopeptides can also bind lectins; for instance, C-mannoside decorated peptides have been successfully used as DC-SIGN ligands.[117]

Finally, sometimes glycosylated building blocks bearing very little resemblance to the natively glycosylated amino acids are used. Here, a glycoside is coupled, usually via the anomeric lactol function, to a linker bearing a carboxylic acid. These can be coupled on-resin or in solution to the N-terminus of the peptide or to the sidechain amine of lysine residues. These linkers can take the form of a simple hydroxylated carboxylic acid, as used by Kantchev *et al.*[118] These molecules were used to decorate vaccine peptides with glycans and study the effect of lectin mediated uptake on antigen (cross-)presentation. An alternative glycoside derivatization strategy was developed by the group of Roche (**Figure 10**). Here, the free reducing-end lactol of a glycoside (**56**) is reacted with the amine group of glutamic acid (**57**), forming the hemiaminal. Cyclization with the sidechain carboxylic acid formed the pyroglutamate derivative, stabilizing the N-glycosidic bond (**59**).[119] After hydrogenolysis of the benzyl ester protecting the carboxylic ester (**60**) the glycans were coupled in solution phase to various oligolysine peptides (producing, for example, **61**). Various glycoclusters were build using this method. These were then used to study the binding specificity of the mannose receptor.[28] The same group later further expanded on this approach, using it to target antigenic peptides to DC-SIGN in order to improve antigen cross-presentation. Here, they showed a glycan-dependent effect on T-cell activation.[120]

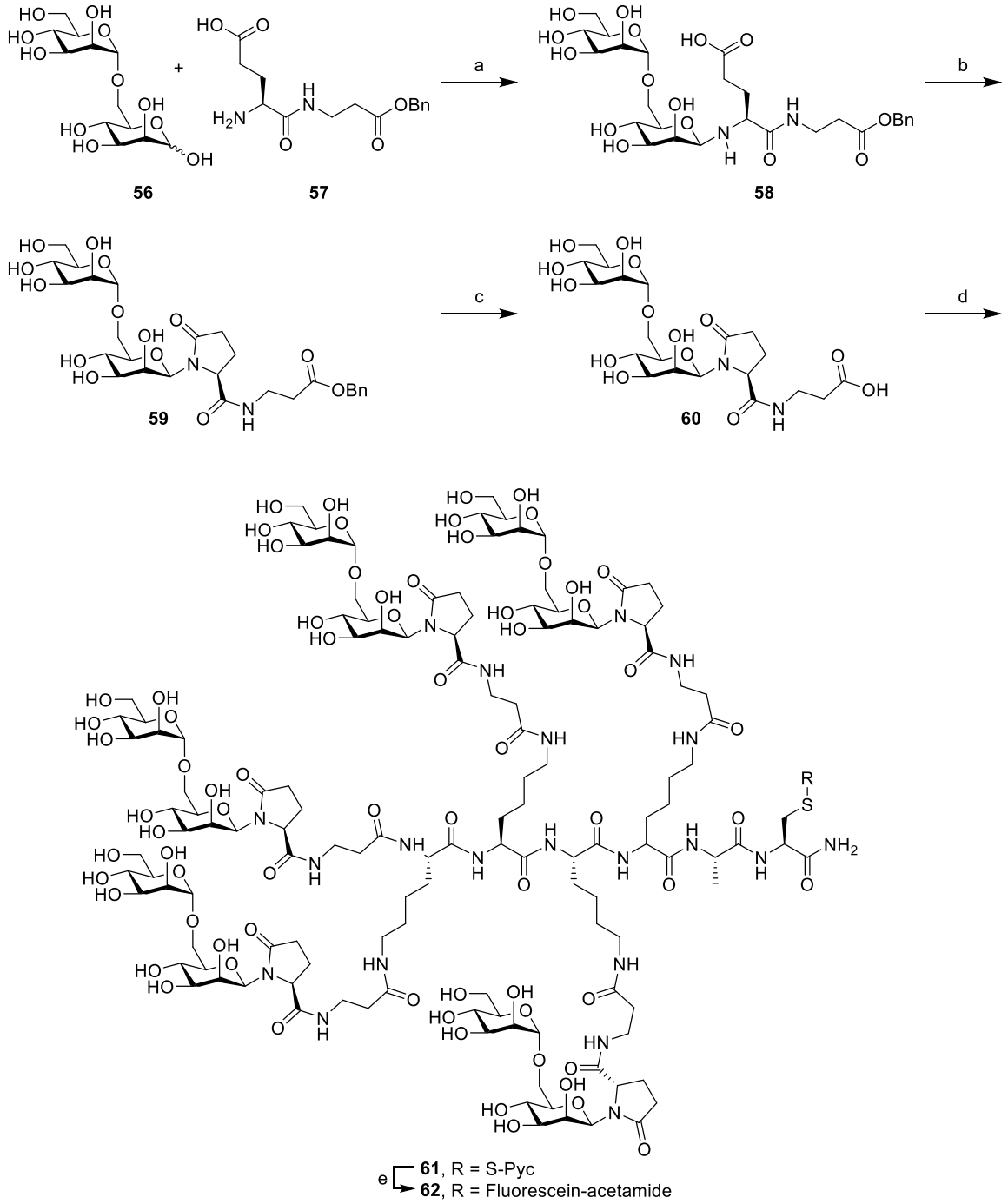

Figure 10. Example synthesis of the fluorophore labeled oligomannose clusters synthesized by Frison et al.[28] Reagents and conditions: a) imidazole, NMP, 50°C b) BOP, imidazole c) H_2, Pd/C d) Lys-Lys-Lys-Lys-Ala-Cys(S-Pyc)-NH_2, HBTU, HOBt, DiPEA, NMP e) i) TCEP, NMP, NaPi pH = 7.2 ii) Fluorescien-iodoacetamide

All of these strategies still rely on introduction of glycosyl building blocks into the peptide on the solid support or in solution. This often requires large amounts of the glyco-building block under investigation and are often limited by low peptide yields. In order to limit the need for large amounts of precious oligosaccharide, conjugation methods were developed, where the carbohydrate part of the molecule can be conjugated to the peptide after SPPS and HPLC

purification. This requires far less of the precious oligosaccharide, enabling the use of more complex sugars.

Late-stage glycoconjugation using organic transformations

Many glycopeptide conjugation strategies are based around the unique reactivity of the amino acid cysteine.[121] The thiol function of this amino acid represents unique reactivity compared to the 19 other amino acids, enabling some form of chemoselectivity. Various groups have exploited the fact that thiolates are soft nucleophiles to introduce oligosaccharide modifications to peptides (**Figure 11**). The group of Stenvall used a bromoethyl linker on the reducing end of several oligosaccharides (for instance **64**) to produce O-glycan mimicking neoglycopeptides.[122] In a similar manner, maleimidosugars (**67**) have been used as well.[123] Alternatively, the ability of thiols to form disulfides under mild conditions was exploited to produce disulfide linked oligosaccharides (**72**) by the groups of Davis[124], and Boons[125], using thioglycoside **70** and **71** respectively.

Another class of thiol selective chemistry that can be applied to cysteine is the photoinduced thiole-ene reaction,[126] which has been used to produce glycoconjugate **75** using allyl glycoside **74**.[127,128] Alternatively, the reactivity of thiols can also be used in the opposite direction. The thiol-ene reaction can also be performed by reacting a thiol glycoside (**77**) to an alkene containing peptide (**76**), producing neoglycopeptide **78**.[129] The nucleophilicity of thioglycosides was also exploited to synthesize peptides containing S-glycosylated cysteine residues in an unconventional manner. The nucleophilic opening of an aziridine amino acid (**79**) on solid support was used to produce an S-glycoside mimic of the Tn-antigen (**81**).[130]

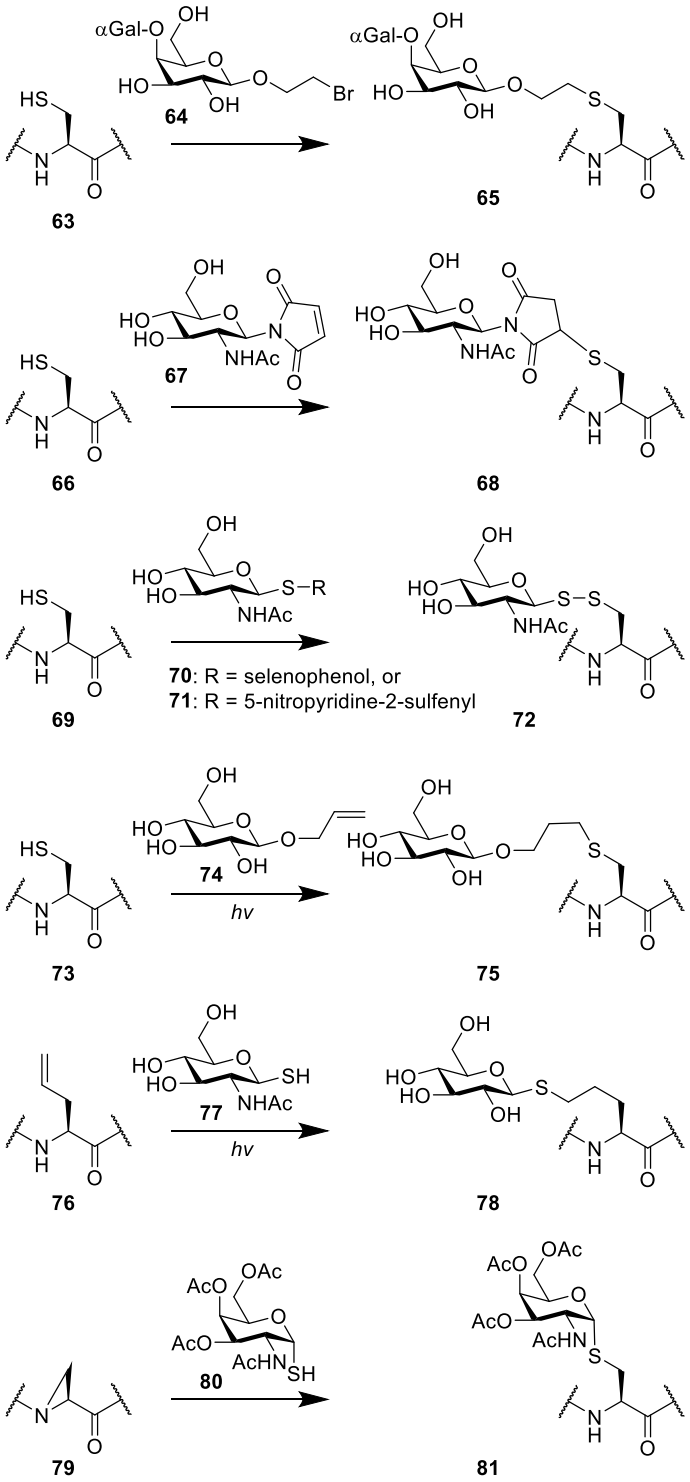

Figure 11. Examples of thiol-based glycoconjugate synthesis.

However, the above-described approaches all rely on thiolate functions to mediate chemoselective ligation, making these approaches incompatible with peptides containing natural cysteine residues. Earlier attempts at making glycoconjugation reactions orthogonal to common peptide functionalities hinged on the reactivity between the aldehyde function present in carbohydrates and oxy-amine functionalities (**Figure 12**). As a simple example, the oxy-amine derivative of serine (**82**) can be used to chemoselectively ligate a free lactol.[131] The

downside of this ligation approach is that it primarily forms the ring-opened configuration of the reducing end glycoside (**84**).[132] When the nitrogen in this oxy-amine is alkylated (**85**), the cyclic form of the glycoside is conserved after ligation (**86**).[133,134] Another approach, that more closely mimics the structure of N-glycans, uses the hydrazide derivative of aspartic acid (**87**). Conjugation with the free lactol of GlcNAc (**83**) leads to the formation of an anomeric β-hydrazide (**88**), a close mimic of a native N-glycan, with an additional nitrogen in between the glycoside and the asparagine residue.[131] The condensation of oxy-amines with carbonyl functionalities has also been used in the form of a chemoselective ligation between a peptide containing a ketone containing amino acid (**89**) and a hydroxylamine-glycoside (**90**).[135]

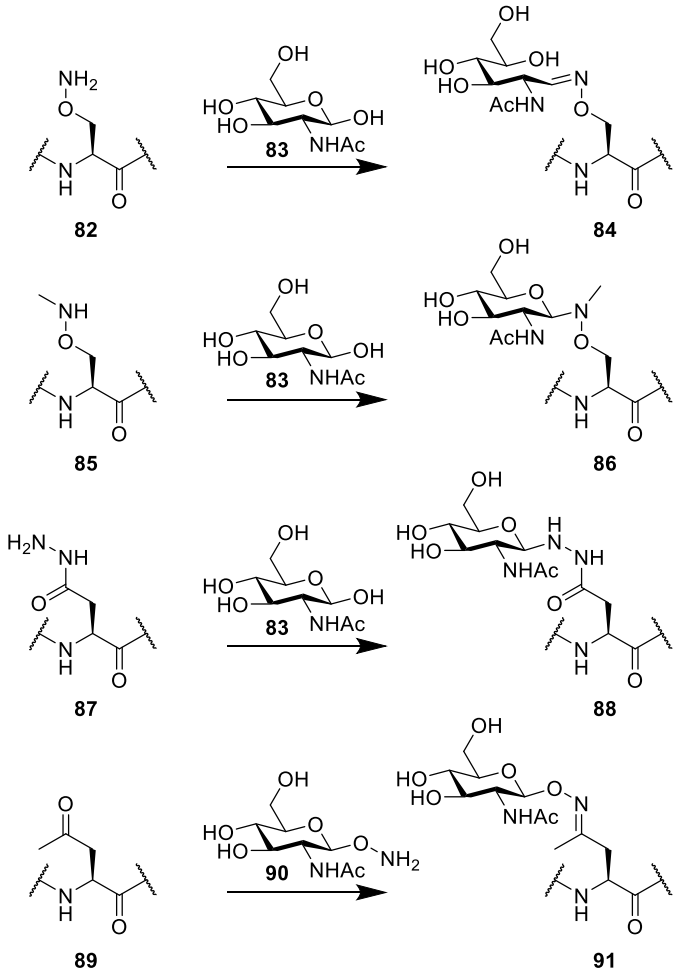

Figure 12. Various glycoconjugation approaches used for the synthesis of neoglycopeptides, based on the unique reactivity of oxy-amine and hydrazide derivatives.

Metal-catalyzed late stage conjugations

One downside to the aforementioned conjugation methods is that they are quite limited in scope, often not producing the desired results when dealing with complex oligosaccharides or peptides. Recently, metal-catalyzed ligation reactions have shown their ability to produce glycoconjugate peptides by true bio-orthogonal means, while simultaneously producing high yields using complex substrates. The earliest work on metal catalyzed synthesis of glycoconjugates made use of the olefin-crossmetathesis reaction. McGarvey et al. used

protected peptides containing an allylglycine residue, together with a C-glycoside bearing an anomeric allyl modification.[136] Later, the utility of cross-metathesis to produce larger glycoconjugate peptides in aqueous medium was demonstrated by the group of Davis, as they showed effective cross-metathesis between an S-allyl cysteine containing protein and β-allyl glucose or α-allyl mannose.[137]

However, the most popular metal-catalyzed cross-coupling reaction used for the production of glycopeptide conjugates is the copper-catalyzed azide-alkyne cycloaddition (CuAAC). In this reaction, an alkylic azide reacts with an alkyne group to form a triazole structure. The reaction is mediated by Cu(I) catalysis and compatible with a wide variety of solvents including water and other polar media usable for the dissolution of unprotected peptides. Soon after the reactions' discovery,[138,139] the group of Rutjes produced the first triazole-linked glycopeptide by reacting protected dipeptides, containing the unnatural amino acid propargylglycine, with acetyl-protected 1-azido-glucose and -cellobiose.[140] The utility of the reaction for the modification of unprotected peptides was discovered soon after. Walsh produced several variants of the peptide antibiotic tyrocidine containing one or more propargylglycine residues. These were, in unprotected form, conjugated with several unprotected sugars, modified with an anomeric azidoethanol function, displaying for the first time the utility of the CuAAC reaction in the late-stage introduction of glycosylation onto a peptide scaffold.[141] This was further exemplified by the work of Davis[34] and Brimble,[142,143] producing various unnatural glycopeptides.

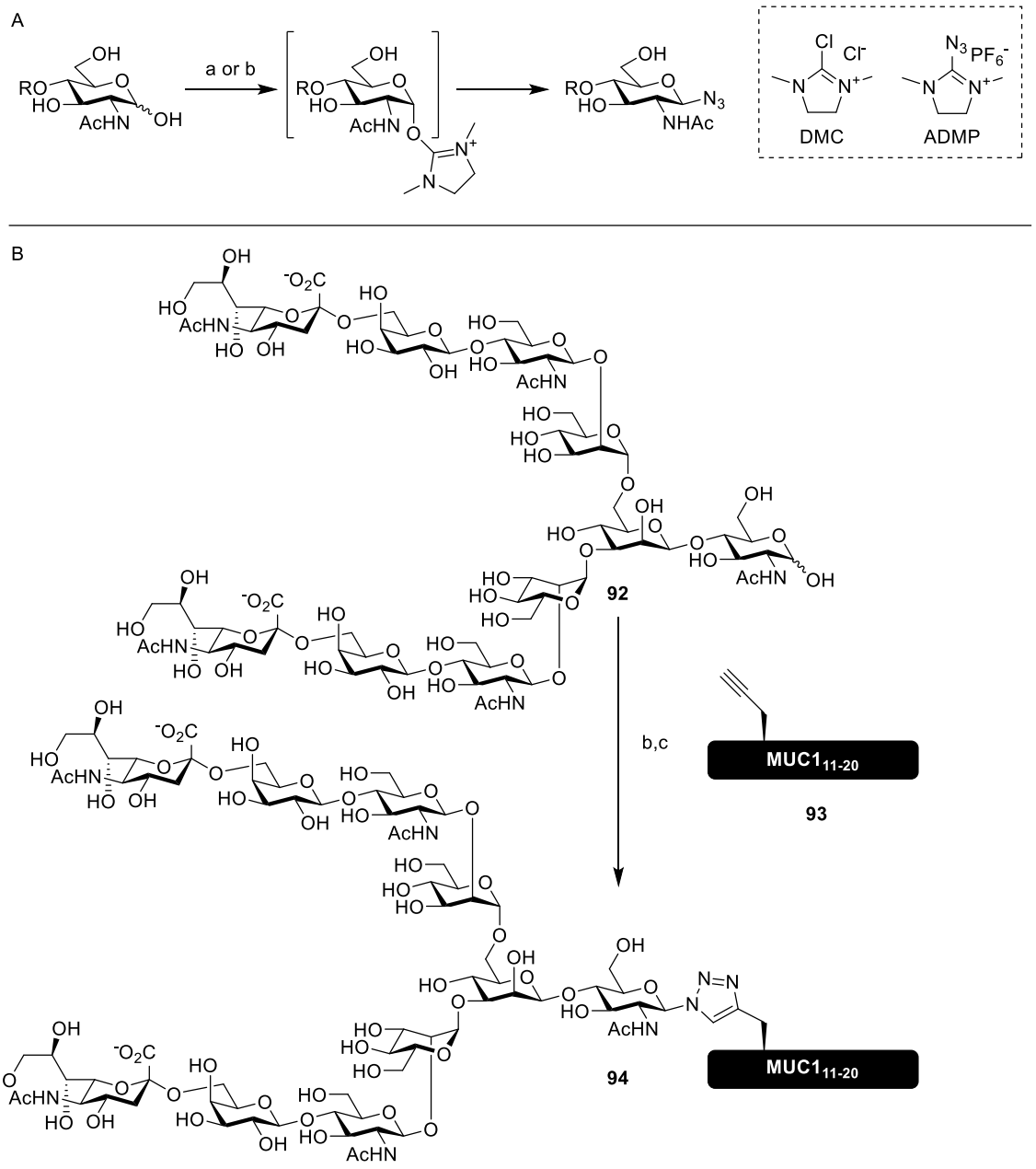

Figure 13. A) DMC[144] or ADMP[145] mediated synthesis of azidoglycosides from unprotected sugars in water. B) One pot synthesis of a glycoconjugate MUC1-peptide (**94**) using ADMP mediated conversion of lactol **92** into the glycosyl azide. CuAAC conjugation in the same pot with alkyne-containing peptide **93**, where Thr_{16} was replaced with propargylglycine, yielded the desired glycoconjugate.[145] Reagents and conditions: a) DMC, 2,6-lutidine, NaN_3, H_2O b) ADMP, Et_3N, D_2O, MeCN c) **93**, $CuSO_4$, ascorbic acid

To further streamline the synthesis of glycoconjugate peptides via CuAAC, novel methods to produce glycosyl azides from reducing sugars were developed. Shoda introduced the reagent 2-chloro-1,3-dimethylimidazolinium chloride (DMC) for the activation of anomeric lactol towards nucleophiles like sodium azide, producing exclusively the β-azide on glucose-configured reducing sugars (**Figure 13A**).[144] This method enables the use of oligosaccharides isolated from natural sources, like the biantennary N-glycan isolated from egg yolk described in section 2, to be conveniently conjugated to peptides containing one or more alkyne handles.

Fairbanks further improved on this approach by utilizing a more efficient reagent for the introduction of the azide, 2-azido-1,3-dimethylimidazolinium hexafluorophosphate (ADMP), and using this approach to synthesize several non-natively glycosylated MUC1 derivatives, among them compound **94**, bearing a biantennary sialoglycan (**Figure 13B**).[145]

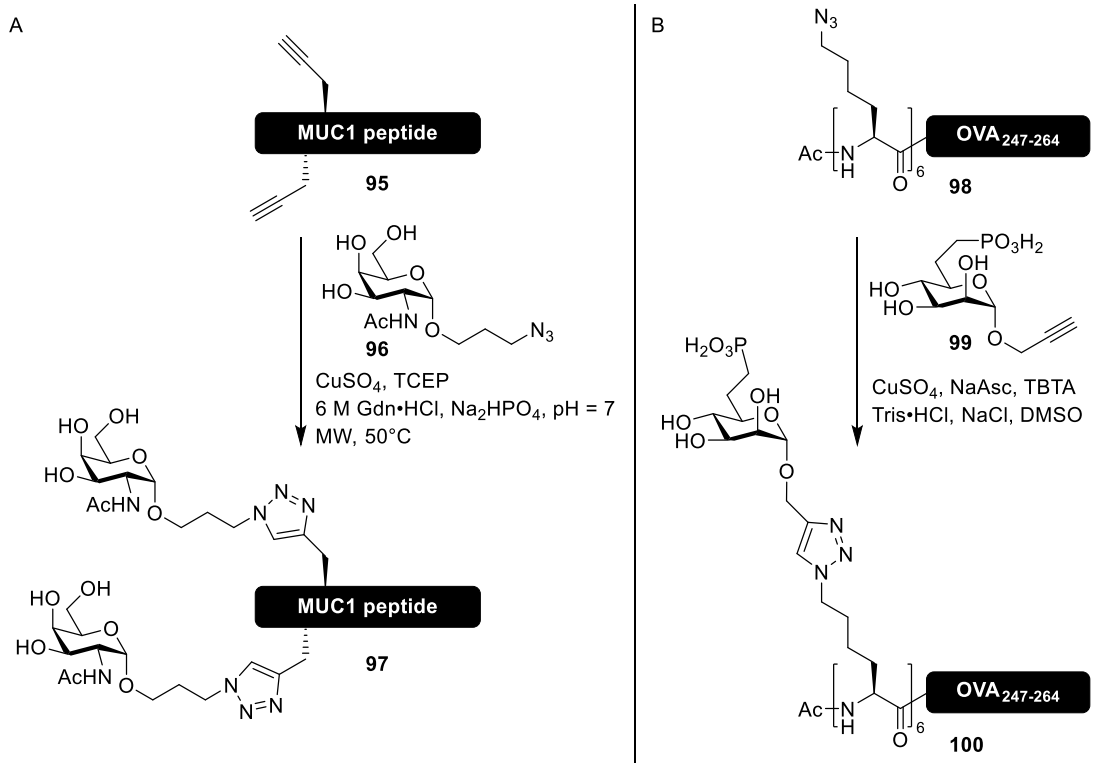

Figure 14. A) Synthesis of MUC1 derived neo-glycopeptides bearing click-based Tn-antigen mimics by Lee *et al*.[146] Selected threonine and/or serine residues were replaced with propargyl-glycine in the peptide sequence, and a CuAAC reaction with the Tn-antigen mimic **96** facilitated the synthesis of neoglycopeptides. B) Synthesis of an antigenic peptide derived from chicken ovalbumin bearing a glycocluster of mannose-6-phosphate receptor binding glycans by Reintjes et al.[32] By synthesizing a peptide bearing multiple azidonorleucine residues on the N-terminus, followed by CuAAC conjugation using propargyl glycoside **99**, the effect of multivalent glycan presentation on antigen uptake could be studied.

The CuAAC mediated synthesis of glycoconjugates was soon utilized in the synthesis of more glycosylated antigenic peptides. The group of Brimble used CuAAC to synthesize six different MUC1 derived peptides containing 1-5 Tn-antigen mimics, introduced using a late-stage click reaction between unprotected peptides and glycosides (**Figure 14A**).[146] More recently, CuAAC-based approaches have been used to rapidly produce large libraries of antigenic peptides containing various oligosaccharides, in order to study the role peptide glycosylation has in antigen (cross)-presentation. The group of Codee investigated the binding of mannosylated gp100 antigen, an often studied cancer epitope,[147] to the lectins DC-SIGN[31] and Langerin.[148] To study the effects of both multivalency and carbohydrate configuration, large libraries of glycopeptides bearing 1,2,3 or 6 azide handles, usable for the introduction of alkyne-modified oligomannosides, were produced. While the higher valency conjugates

showed an increase in affinity for the targeted receptors, this did not translate into improved presentation of the antigens to T-cells.[31,148]

In a similar manner, stabilized ligands for the mannose-6-phosphate receptor, in the form of mannose-6-phophonate, conjugated to epitopes derived from chicken ovalbumin, were produced (**Figure 14B**).[32] All of these works were based on the synthesis of peptides bearing several azidonorleucine residues, conjugated to different carbohydrates all bearing an anomeric propargyl group.

CuAAC-based neoglycopeptide synthesis strategies have now shown to be able to quickly deliver various unnatural but functional glycoconjugate peptides. It is expected that these methods will be further exploited in the future to elucidate the complex roles of lectins in the immune system.

Conclusion

Over the last few decades, the development of glycopeptides and glycopeptides conjugates has aided our understanding of glycobiology and glyco-immunology. Various glycosylated peptides are being actively studied as potential peptide vaccines, the hypoglycosylated mucin peptides and mannosylated HIV-gp120 derivatives as the most important examples. Glycosylation is also used to enhance peptide uptake and to shape the response of immune cells, by targeting immunolectins with various oligosaccharides. The contemporary development of efficient and rapid glyco-conjugation methods, key among which are the methods utilizing the copper catalyzed click reaction, creates the opportunity to generate many unnatural but functionally interesting glycoconjugates. These in turn enable an ever increasing amount of studies in carbohydrate structure/activity relationships. In the future, these developments could lead to better vaccines and other immune-response shaping synthetic molecules.

Outline of this thesis

The research described in this thesis explores the use of peptide chemistry to produce novel molecules to study immunological processes. **Chapter 2** describes the synthesis of a series of N-linked neoglycopeptides, including a Le^X containing peptide that is able to bind to DC-SIGN and modulate monocyte derived dendritic cell (moDC) cytokine production. **Chapter 3** explores the biophysical and immunological differences between citrullinated derivatives of human and murine MOG_{35-55}, a peptide thought to be critical to the development of multiple sclerosis. **Chapter 4** describes the synthesis of several antigenic peptides decorated with both oligosaccharides and a fluorophore, usable for the visualization of lectin binding, (glycan-mediated) uptake and intracellular routing of the antigenic peptide. In **Chapter 5** development of a cyclic, glycosylated ligand for cholera toxin subunit B (CTB) is described. **Chapter 6** describes a novel synthetic method to introduce the *trans*-cyclooctene (TCO) carbamate protecting group onto lysine residues in peptides, enabling the synthesis of peptides bearing both free and TCO-protected lysines. **Chapter 7** summarizes the research described in the thesis, and outlines novel directions that the presented works could be taken in the future.

References

(1) Schjoldager, K. T.; Narimatsu, Y.; Joshi, H. J.; Clausen, H. Global View of Human Protein Glycosylation Pathways and Functions. *Nat. Rev. Mol. Cell Biol. 2020 2112* **2020**, *21* (12), 729–749. https://doi.org/10.1038/S41580-020-00294-X.

(2) Rudd, P. M.; Dwek, R. A. Glycosylation: Heterogeneity and the 3D Structure of Proteins. *Crit. Rev. Biochem. Mol. Biol.* **1997**, *32* (1), 1–100. https://doi.org/10.3109/10409239709085144.

(3) Gringhuis, S. I.; den Dunnen, J.; Litjens, M.; van der Vlist, M.; Geijtenbeek, T. B. H. Carbohydrate-Specific Signaling through the DC-SIGN Signalosome Tailors Immunity to Mycobacterium Tuberculosis, HIV-1 and Helicobacter Pylori. *Nat. Immunol.* **2009**, *10* (10), 1081–1088. https://doi.org/10.1038/ni.1778.

(4) Lübbers, J.; Rodríguez, E.; van Kooyk, Y. Modulation of Immune Tolerance via Siglec-Sialic Acid Interactions. *Front. Immunol.* **2018**, *9*, 2807. https://doi.org/10.3389/FIMMU.2018.02807/BIBTEX.

(5) Burgdorf, S.; Lukacs-Kornek, V.; Kurts, C. The Mannose Receptor Mediates Uptake of Soluble but Not of Cell-Associated Antigen for Cross-Presentation. *J. Immunol.* **2006**, *176* (11), 6770–6776. https://doi.org/10.4049/JIMMUNOL.176.11.6770.

(6) Royer, P.-J.; Emara, M.; Yang, C.; Al-Ghouleh, A.; Tighe, P.; Jones, N.; Sewell, H. F.; Shakib, F.; Martinez-Pomares, L.; Ghaemmaghami, A. M. The Mannose Receptor Mediates the Uptake of Diverse Native Allergens by Dendritic Cells and Determines Allergen-Induced T Cell Polarization through Modulation of IDO Activity. *J. Immunol.* **2010**, *185* (3), 1522–1531. https://doi.org/10.4049/JIMMUNOL.1000774.

(7) Hafstrand, I.; Badia-Martinez, D.; Josey, B. J.; Norström, M.; Buratto, J.; Pellegrino, S.; Duru, A. D.; Sandalova, T.; Achour, A. Crystal Structures of H-2Db in Complex with the LCMV-Derived Peptides GP92 and GP392 Explain Pleiotropic Effects of Glycosylation on Antigen Presentation and Immunogenicity. *PLoS One* **2017**, *12* (12), e0189584. https://doi.org/10.1371/journal.pone.0189584.

(8) Apostolopoulos, V.; Yuriev, E.; Ramsland, P. A.; Halton, J.; Osinski, C.; Li, W.; Plebanski, M.; Paulsen, H.; McKenzie, I. F. C. A Glycopeptide in Complex with MHC Class I Uses the GalNAc Residue as an Anchor. *Proc. Natl. Acad. Sci. U. S. A.* **2003**, *100* (25), 15029–15034. https://doi.org/10.1073/pnas.2432220100.

(9) Rizzuto, G.; Brooks, J. F.; Tuomivaara, S. T.; McIntyre, T. I.; Ma, S.; Rideaux, D.; Zikherman, J.; Fisher, S. J.; Erlebacher, A. Establishment of Fetomaternal Tolerance through Glycan-Mediated B Cell Suppression. *Nature* **2022**, *603* (7901), 497–502. https://doi.org/10.1038/s41586-022-04471-0.

(10) Blixt, O.; Head, S.; Mondala, T.; Scanlan, C.; Huflejt, M. E.; Alvarez, R.; Bryan, M. C.; Fazio, F.; Calarese, D.; Stevens, J.; Razi, N.; Stevens, D. J.; Skehel, J. J.; Van Die, I.; Burton, D. R.; Wilson, I. A.; Cummings, R.; Bovin, N.; Wong, C. H.; Paulson, J. C. Printed Covalent Glycan Array for Ligand Profiling of Diverse Glycan Binding Proteins. *Proc. Natl. Acad. Sci. U. S. A.* **2004**, *101* (49), 17033–17038. https://doi.org/10.1073/PNAS.0407902101.

(11) van Liempt, E.; Bank, C. M. C.; Mehta, P.; García-Vallejo, J. J.; Kawar, Z. S.; Geyer, R.; Alvarez, R. A.; Cummings, R. D.; Kooyk, Y. van; van Die, I. Specificity of DC-SIGN for Mannose- and Fucose-Containing Glycans. *FEBS Lett.* **2006**, *580* (26), 6123–6131. https://doi.org/10.1016/j.febslet.2006.10.009.

(12) Burgdorf, S.; Kautz, A.; Böhnert, V.; Knolle, P. A.; Kurts, C. Distinct Pathways of Antigen Uptake and Intracellular Routing in CD4 and CD8 T Cell Activation. *Science* **2007**, *316* (5824), 612–616. https://doi.org/10.1126/science.1137971.

(13) Rauen, J.; Kreer, C.; Paillard, A.; Van Duikeren, S.; Benckhuijsen, W. E.; Camps, M. G.; Valentijn, A. R. P. M.; Ossendorp, F.; Drijfhout, J. W.; Arens, R.; Burgdorf, S. Enhanced Cross-Presentation and Improved CD8+ T Cell Responses after Mannosylation of Synthetic Long Peptides in Mice. *PLoS One* **2014**, *9* (8), e103755. https://doi.org/10.1371/journal.pone.0103755.

(14) Anderluh, M.; Berti, F.; Bzducha-Wróbel, A.; Chiodo, F.; Colombo, C.; Compostella, F.; Durlik, K.; Ferhati, X.; Holmdahl, R.; Jovanovic, D.; Kaca, W.; Lay, L.; Marinovic-Cincovic, M.; Marradi, M.; Ozil, M.; Polito, L.; Reina, J. J.; Reis, C. A.; Sackstein, R.; Silipo, A.; Švajger, U.; Vaněk, O.; Yamamoto, F.; Richichi, B.; van Vliet, S. J. Recent Advances on Smart Glycoconjugate Vaccines in Infections and Cancer. *FEBS J.* **2021**. https://doi.org/10.1111/febs.15909.

(15) Galli-Stampino, L.; Meinjohanns, E.; Frische, K.; Meldal, M.; Jensen, T.; Werdelin, O.; Mouritsen, S. T-Cell Recognition of Tumor-Associated Carbohydrates: The Nature of the Glycan Moiety Plays a Decisive Role in Determining Glycopeptide Immunogenicity. *Cancer Res.* **1997**, *57* (15), 3214–3222.

(16) Soliman, C.; Yuriev, E.; Ramsland, P. A. Antibody Recognition of Aberrant Glycosylation on the Surface of Cancer Cells. *Curr. Opin. Struct. Biol.* **2017**, *44*, 1–8. https://doi.org/10.1016/j.sbi.2016.10.009.

(17) Fernández-Tejada, A.; Haynes, B. F.; Danishefsky, S. J. Designing Synthetic Vaccines for HIV. *Expert Rev. Vaccines* **2015**, *14* (6), 815–831. https://doi.org/10.1586/14760584.2015.1027690.

(18) Brockhausen, I.; Melamed, J. Mucins as Anti-Cancer Targets: Perspectives of the Glycobiologist. *Glycoconj. J.* **2021**, *38* (4), 459–474. https://doi.org/10.1007/s10719-021-09986-8.

(19) Dutta, D.; Mandal, C.; Mandal, C. Unusual Glycosylation of Proteins: Beyond the Universal Sequon and Other Amino Acids. *Biochim. Biophys. Acta - Gen. Subj.* **2017**, *1861* (12), 3096–3108. https://doi.org/10.1016/j.bbagen.2017.08.025.

(20) Spiro, R. G. Protein Glycosylation: Nature, Distribution, Enzymatic Formation, and Disease Implications of Glycopeptide Bonds. *Glycobiology* **2002**, *12* (4), 43R-56R. https://doi.org/10.1093/glycob/12.4.43R.

(21) Yang, X.; Qian, K. Protein O-GlcNAcylation: Emerging Mechanisms and Functions. *Nat. Rev. Mol. Cell Biol.* **2017**, *18* (7), 452–465. https://doi.org/10.1038/nrm.2017.22.

(22) Haurum, J. S.; Høier, I. B.; Arsequell, G.; Neisig, A.; Valencia, G.; Zeuthen, J.; Neefjes, J.; Elliott, T. Presentation of Cytosolic Glycosylated Peptides by Human Class I Major Histocompatibility Complex Molecules in Vivo. *J. Exp. Med.* **1999**, *190* (1), 145–150. https://doi.org/10.1084/JEM.190.1.145.

(23) Wandall, H. H.; Nielsen, M. A. I.; King-Smith, S.; de Haan, N.; Bagdonaite, I. Global Functions of O-Glycosylation: Promises and Challenges in O-Glycobiology. *FEBS J.* **2021**, *288* (24), 7183–7212. https://doi.org/10.1111/FEBS.16148.

(24) Chugh, S.; Gnanapragassam, V. S.; Jain, M.; Rachagani, S.; Ponnusamy, M. P.; Batra, S. K. Pathobiological Implications of Mucin Glycans in Cancer: Sweet Poison and Novel Targets. *Biochim. Biophys. Acta - Rev. Cancer* **2015**, *1856* (2), 211–225. https://doi.org/10.1016/J.BBCAN.2015.08.003.

(25) Kumar, A. R.; Devan, A. R.; Nair, B.; Vinod, B. S.; Nath, L. R. Harnessing the Immune System against Cancer: Current Immunotherapy Approaches and Therapeutic Targets. *Molecular Biology Reports*. Springer Science and Business Media B.V. December 1, 2021, pp 8075–8095. https://doi.org/10.1007/s11033-021-06752-9.

(26) Aebi, M.; Bernasconi, R.; Clerc, S.; Molinari, M. N-Glycan Structures: Recognition and Processing in the ER. *Trends Biochem. Sci.* **2010**, *35* (2), 74–82. https://doi.org/10.1016/j.tibs.2009.10.001.

(27) Fehres, C. M.; Kalay, H.; Bruijns, S. C. M.; Musaafir, S. A. M.; Ambrosini, M.; Van Bloois, L.; Van Vliet, S. J.; Storm, G.; Garcia-Vallejo, J. J.; Van Kooyk, Y. Cross-Presentation through Langerin and DC-SIGN Targeting Requires Different Formulations of Glycan-Modified Antigens. *J. Control. Release* **2015**, *203*, 67–76.

(28) Frison, N.; Taylor, M. E.; Soilleux, E.; Bousser, M.-T.; Mayer, R.; Monsigny, M.; Drickamer, K.; Roche, A.-C. Oligolysine-Based Oligosaccharide Clusters. *J. Biol. Chem.* **2003**, *278* (26), 23922–23929. https://doi.org/10.1074/jbc.M302483200.

(29) Doelman, W.; Marqvorsen, M. H. S.; Chiodo, F.; Bruijns, S. C. M.; van der Marel, G. A.; van Kooyk, Y.; van Kasteren, S. I.; Araman, C. Synthesis of Asparagine Derivatives Harboring a Lewis X Type DC-SIGN Ligand and Evaluation of Their Impact on Immunomodulation in Multiple Sclerosis. *Chem. Eur. J.* **2021**, *27* (8), 2742–2752. https://doi.org/10.1002/chem.202004076.

(30) Riera, R.; Hogervorst, T. P.; Doelman, W.; Ni, Y.; Pujals, S.; Bolli, E.; Codée, J. D. C.; van Kasteren, S. I.; Albertazzi, L. Single-Molecule Imaging of Glycan–Lectin Interactions on Cells with Glyco-PAINT. *Nat. Chem. Biol.* **2021**, *17* (12), 1281–1288. https://doi.org/10.1038/s41589-021-00896-2.

(31) Li, R. J. E.; Hogervorst, T. P.; Achilli, S.; Bruijns, S. C.; Arnoldus, T.; Vivès, C.; Wong, C. C.; Thépaut, M.; Meeuwenoord, N. J.; van den Elst, H.; Overkleeft, H. S.; van der Marel, G. A.; Filippov, D. V.; van Vliet, S. J.; Fieschi, F.; Codée, J. D. C.; van Kooyk, Y. Systematic Dual Targeting of Dendritic Cell C-Type Lectin Receptor DC-SIGN and TLR7 Using a Trifunctional Mannosylated Antigen. *Front. Chem.* **2019**, *7*, 650. https://doi.org/10.3389/fchem.2019.00650.

(32) Reintjens, N. R. M. M.; Tondini, E.; Vis, C.; McGlinn, T.; Meeuwenoord, N. J.; Hogervorst, T. P.; Overkleeft, H. S.; Filippov, D. V.; Marel, G. A. van der; Ossendorp, F.; Codée, J. D. C. C.; van der Marel, G. A.; Ossendorp, F.; Codée, J. D. C. C. Multivalent, Stabilized Mannose-6-Phosphates for the Targeted Delivery of Toll-Like Receptor Ligands and Peptide Antigens. *ChemBioChem* **2021**, *22* (2), 434–440. https://doi.org/10.1002/CBIC.202000538.

(33) Beckwith, D. M.; Cudic, M. Tumor-Associated O-Glycans of MUC1: Carriers of the Glyco-Code and Targets for Cancer Vaccine Design. *Semin. Immunol.* **2020**, *47*. https://doi.org/10.1016/J.SMIM.2020.101389.

(34) van Kasteren, S. I.; Kramer, H. B.; Jensen, H. H.; Campbell, S. J.; Kirkpatrick, J.; Oldham, N. J.; Anthony, D. C.; Davis, B. G. Expanding the Diversity of Chemical Protein Modification Allows Post-Translational Mimicry. **2007**, *446* (7139), 1105–1109. https://doi.org/10.1038/nature05757.

(35) García-Vallejo, J. J.; Ambrosini, M.; Overbeek, A.; van Riel, W. E.; Bloem, K.; Unger, W. W. J.; Chiodo, F.; Bolscher, J. G.; Nazmi, K.; Kalay, H.; van Kooyk, Y. Multivalent Glycopeptide Dendrimers for the Targeted Delivery of Antigens to Dendritic Cells. *Mol. Immunol.* **2013**, *53* (4), 387–397. https://doi.org/10.1016/j.molimm.2012.09.012.

(36) Rentzsch, M.; Wawrzinek, R.; Zelle-Rieser, C.; Strandt, H.; Bellmann, L.; Fuchsberger, F. F.; Schulze, J.; Busmann, J.; Rademacher, J.; Sigl, S.; Del Frari, B.; Stoitzner, P.; Rademacher, C. Specific Protein Antigen Delivery to Human Langerhans Cells in Intact Skin. *Front. Immunol.* **2021**, *12*, 4338. https://doi.org/10.3389/fimmu.2021.732298.

(37) Kunz, H.; Unverzagt, C. Protecting-Group-Dependent Stability of Intersaccharide Bonds—Synthesis of a Fucosyl-Chitobiose Glycopeptide. *Angew. Chemie Int. Ed. English* **1988**, *27* (12), 1697–1699. https://doi.org/10.1002/ANIE.198816971.

(38) Urge, L.; Otvos, L.; Lang, E.; Wroblewski, K.; Laczko, I.; Hollosi, M. Fmoc-Protected, Glycosylated Asparagines Potentially Useful as Reagents in the Solid-Phase Synthesis of N-Glycopeptides. *Carbohydr. Res.* **1992**, *235* (C), 83–93. https://doi.org/10.1016/0008-6215(92)80080-K.

(39) Ito, S.; Asahina, Y.; Hojo, H. Investigation of Protecting Group for Sialic Acid Carboxy Moiety toward Sialylglycopeptide Synthesis by the TFA-Labile Protection Strategy. *Tetrahedron* **2021**, *97*, 132423. https://doi.org/10.1016/J.TET.2021.132423.

(40) Zhang, Y.; Muthana, S. M.; Barchi, J. J.; Gildersleeve, J. C. Divergent Behavior of Glycosylated Threonine and Serine Derivatives in Solid Phase Peptide Synthesis. *Org. Lett.* **2012**, *14* (15), 3958–3961. https://doi.org/10.1021/ol301723e.

(41) Zhang, Y.; Muthana, S. M.; Farnsworth, D.; Ludek, O.; Adams, K.; Barchi, J. J.; Gildersleeve, J. C. Enhanced Epimerization of Glycosylated Amino Acids during Solid-Phase Peptide Synthesis. *J. Am. Chem. Soc.* **2012**, *134* (14), 6316–6325. https://doi.org/10.1021/ja212188r.

(42) Paulsen, H.; Merz, G.; Weichert, U. Solid-Phase Synthesis of O-Glycopeptide Sequences. *Angew. Chemie Int. Ed. English* **1988**, *27* (10), 1365–1367. https://doi.org/10.1002/ANIE.198813651.

(43) Liebe, B.; Kunz, H. Solid-Phase Synthesis of a Tumor-Associated Sialyl-TN Antigen Glycopeptide with a Partial Sequence of the "Tandem Repeat" of the MUC-1 Mucin. *Angew. Chemie Int. Ed. English* **1997**, *36* (6), 618–621. https://doi.org/10.1002/ANIE.199706181.

(44) Bielfeldt, T.; Peters, S.; Meldal, M.; Bock, K.; Paulsen, H. A New Strategy for Solid-Phase Synthesis of O-Glycopeptides. *Angew. Chemie Int. Ed. English* **1992**, *31* (7), 857–859. https://doi.org/10.1002/ANIE.199208571.

(45) Kauth, H.; Kunz, H. Synthese von Geschützten Serin-Glycopeptiden Durch N-Terminale Peptidketten-Verlängerung. *Liebigs Ann. der Chemie* **1983**, *1983* (3), 360–366. https://doi.org/10.1002/JLAC.198319830303.

(46) Paulsen, H.; Paal, M.; Schultz, M. Syntheseblock β-D-Gal (1→3)-D-GalNAc Zur Selektiv-Simultanen Anknüpfung an Peptide Zu O-Glycopeptiden. *Tetrahedron Lett.* **1983**, *24* (17), 1759–1762. https://doi.org/10.1016/S0040-4039(00)81763-3.

(47) Kunz, H.; Birnbach, S. Synthesis of O-Glycopeptides of the Tumor-Associated TN- and T-Antigen Type and Their Binding to Bovine Serum Albumin. *Angew. Chemie Int. Ed. English* **1986**, *25* (4), 360–362. https://doi.org/10.1002/ANIE.198603601.

(48) Bhatia, R.; Gautam, S. K.; Cannon, A.; Thompson, C.; Hall, B. R.; Aithal, A.; Banerjee, K.; Jain, M.; Solheim, J. C.; Kumar, S.; Batra, S. K. Cancer-Associated Mucins: Role in Immune Modulation and Metastasis. *Cancer Metastasis Rev. 2019 381* **2019**, *38* (1), 223–236. https://doi.org/10.1007/S10555-018-09775-0.

(49) Elofsson, M.; A. Salvador, L.; Kihlberg, J. Preparation of Tn and Sialyl Tn Building Blocks Used in Fmoc Solid-Phase Synthesis of Glycopeptide Fragments from HIV Gp120. *Tetrahedron* **1997**, *53* (1), 369–390. https://doi.org/10.1016/S0040-4020(96)00992-1.

(50) Yoon, V.; Fridkis-Hareli, M.; Munisamy, S.; Lee, J.; Anastasiades, D.; Stevceva, L. The GP120 Molecule of HIV-1 and Its Interaction with T Cells. *Curr. Med. Chem.* **2010**, *17* (8), 741–749. https://doi.org/10.2174/092986710790514499.

(51) Schwarz, J. B.; Kuduk, S. D.; Chen, X. T.; Sames, D.; Glunz, P. W.; Danishefsky, S. J. A Broadly Applicable Method for the Efficient Synthesis of α-O-Linked Glycopeptides and Clustered Sialic Acid Residues. *J. Am. Chem. Soc.* **1999**, *121* (12), 2662–2673. https://doi.org/10.1021/ja9833265.

(52) Glunz, P. W.; Hintermann, S.; Williams, L. J.; Schwarz, J. B.; Kuduk, S. D.; Kudryashov, V.; Lloyd, K. O.; Danishefsky, S. J. Design and Synthesis of Le(y)-Bearing Glycopeptides That Mimic Cell Surface Le(y) Mucin Glycoprotein Architecture. *J. Am. Chem. Soc.* **2000**, *122* (30), 7273–7279. https://doi.org/10.1021/ja0011820.

(53) Brocke, C.; Kunz, H. Synthetic Glycopeptides of the Tandem Repeat Sequence of the Epithelial Mucin MUC4 with Tumour-Associated Carbohydrate Antigens. *Synlett* **2003**, *2003* (13), 2052–2056. https://doi.org/10.1055/S-2003-42029/ID/32.

(54) Pett, C.; Schorlemer, M.; Westerlind, U. A Unified Strategy for the Synthesis of Mucin Cores 1–4 Saccharides and the Assembled Multivalent Glycopeptides. *Chem. – A Eur. J.* **2013**, *19* (50), 17001–17010. https://doi.org/10.1002/CHEM.201302921.

(55) Pett, C.; Westerlind, U. A Convergent Strategy for the Synthesis of Type-1 Elongated Mucin Cores 1–3 and the Corresponding Glycopeptides. *Chem. – A Eur. J.* **2014**, *20* (24), 7287–7299. https://doi.org/10.1002/CHEM.201400162.

(56) Pett, C.; Cai, H.; Liu, J.; Palitzsch, B.; Schorlemer, M.; Hartmann, S.; Stergiou, N.; Lu, M.; Kunz, H.; Schmitt, E.; Westerlind, U. Microarray Analysis of Antibodies Induced with Synthetic Antitumor Vaccines: Specificity against Diverse Mucin Core Structures. *Chem. – A Eur. J.* **2017**, *23* (16), 3875–3884. https://doi.org/10.1002/CHEM.201603921.

(57) Somers, W. S.; Tang, J.; Shaw, G. D.; Camphausen, R. T. Insights into the Molecular Basis of Leukocyte Tethering and Rolling Revealed by Structures of P- and E-Selectin Bound to SLeX and PSGL-1. *Cell* **2000**, *103* (3), 467–479. https://doi.org/10.1016/S0092-8674(00)00138-0.

(58) Baumann, K.; Kowalczyk, D.; Kunz, H. Total Synthesis of the Glycopeptide Recognition Domain of the P-Selectin Glycoprotein Ligand 1. *Angew. Chem. Int. Ed.* **2008**, *47* (18), 3445–3449. https://doi.org/10.1002/ANIE.200705762.

(59) Takeda, N.; Takei, T.; Asahina, Y.; Hojo, H. Sialyl Tn Unit with TFA-Labile Protection Realizes Efficient Synthesis of Sialyl Glycoprotein. *Chem. – A Eur. J.* **2018**, *24* (11), 2593–2597. https://doi.org/10.1002/CHEM.201706127.

(60) Asahina, Y.; Kawakami, T.; Hojo, H. Glycopeptide Synthesis Based on a TFA-Labile Protection Strategy and One-Pot Four-Segment Ligation for the Synthesis of O-Glycosylated Histone H2A. *European J. Org. Chem.* **2019**, *2019* (9), 1915–1920. https://doi.org/10.1002/EJOC.201801885.

(61) Toonstra, C.; Amin, M. N.; Wang, L. X. Site-Selective Chemoenzymatic Glycosylation of an HIV-1 Polypeptide Antigen with Two Distinct N-Glycans via an Orthogonal Protecting Group Strategy. *J. Org. Chem.* **2016**, *81* (15), 6176–6185.

(62) Yan, B.; Li, W.; Hackenberger, C. P. R. A Silyl Ether-Protected Building Block for O-GlcNAcylated Peptide Synthesis to Enable One-Pot Acidic Deprotection. *Org. Biomol. Chem.* **2021**, *19* (37), 8014–8017. https://doi.org/10.1039/D1OB00510C.

(63) Matsuo, I.; Nakahara, Y.; Ito, Y.; Nukada, T.; Nakahara, Y.; Ogawa, T. Synthesis of a Glycopeptide Carrying a N-Linked Core Pentasaccharide. *Bioorg. Med. Chem.* **1995**, *3* (11), 1455–1463. https://doi.org/10.1016/0968-0896(95)00139-8.

(64) Unverzagt, C. Chemoenzymatic Synthesis of a Sialylated Diantennary N-Glycan Linked to Asparagine. *Carbohydr. Res.* **1997**, *305* (3–4), 423–431. https://doi.org/10.1016/S0008-6215(97)10056-8.

(65) Unverzagt, C. Building Blocks for Glycoproteins: Synthesis of the Ribonuclease B Fragment 21-25 Containing an Undecasaccharide N-Glycan. *Tetrahedron Lett.* **1997**, *38* (32), 5627–5630. https://doi.org/10.1016/S0040-4039(97)01278-1.

(66) Mezzato, S.; Schaffrath, M.; Unverzagt, C. An Orthogonal Double-Linker Resin Facilitates the Efficient Solid-Phase Synthesis of Complex-Type N-Glycopeptide Thioesters Suitable for Native Chemical Ligation. *Angew. Chem. Int. Ed.* **2005**, *44* (11), 1650–1654. https://doi.org/10.1002/anie.200461125.

(67) Yamamoto, N.; Ohmori, Y.; Sakakibara, T.; Sasaki, K.; Juneja, L. R.; Kajihara, Y. Solid-Phase Synthesis of Sialylglycopeptides through Selective Esterification of the Sialic Acid Residues of an Asn-Linked Complex-Type Sialyloligosaccharide. *Angew. Chem. Int. Ed.* **2003**, *42* (22), 2537–2540. https://doi.org/10.1002/anie.200250572.

(68) Piontek, C.; Varón Silva, D.; Heinlein, C.; Pöhner, C.; Mezzato, S.; Ring, P.; Martin, A.; Schmid, F. X.; Unverzagt, C. Semisynthesis of a Homogeneous Glycoprotein Enzyme: Ribonuclease C: Part 2. *Angew. Chem. Int. Ed.* **2009**, *48* (11), 1941–1945. https://doi.org/10.1002/ANIE.200804735.

(69) Anisfeld, S. T.; Lansbury, P. T. A Convergent Approach to the Chemical Synthesis of Asparagine-Linked Glycopeptides. *J. Org. Chem.* **2002**, *55* (21), 5560–5562. https://doi.org/10.1021/JO00308A009.

(70) Cohen-Anisfeld, S. T.; Lansbury, P. T. A Practical, Convergent Method for Glycopeptide Synthesis. *J. Am. Chem. Soc.* **2002**, *115* (23), 10531–10537. https://doi.org/10.1021/JA00076A010.

(71) Wang, P.; Aussedat, B.; Vohra, Y.; Danishefsky, S. J. An Advance in the Chemical Synthesis of Homogeneous N-Linked Glycopolypeptides by Convergent Aspartylation. *Angew. Chem. Int. Ed.* **2012**, *51* (46), 11571–11575. https://doi.org/10.1002/ANIE.201205038.

(72) Wang, P.; Dong, S.; Shieh, J. H.; Peguero, E.; Hendrickson, R.; Moore, M. A. S.; Danishefsky, S. J. Erythropoietin Derived by Chemical Synthesis. *Science* **2013**, *342* (6164), 1357–1360. https://doi.org/10.1126/science.1245095.

(73) Alam, S. M.; Aussedat, B.; Vohra, Y.; Meyerhoff, R. R.; Cale, E. M.; Walkowicz, W. E.; Radakovich, N. A.; Anasti, K.; Armand, L.; Parks, R.; Sutherland, L.; Scearce, R.; Joyce, M. G.; Pancera, M.; Druz, A.; Georgiev, I. S.; Von Holle, T.; Eaton, A.; Fox, C.; Reed, S. G.; Louder, M.; Bailer, R. T.; Morris, L.; Abdool-Karim, S. S.; Cohen, M.; Liao, H. X.; Montefiori, D. C.; Park, P. K.; Fernández-Tejada, A.; Wiehe, K.; Santra, S.; Kepler, T. B.; Saunders, K. O.; Sodroski, J.; Kwong, P. D.; Mascola, J. R.; Bonsignori, M.; Moody, M. A.; Danishefsky, S.; Haynes, B. F. Mimicry of an HIV Broadly Neutralizing Antibody Epitope with a Synthetic Glycopeptide. *Sci. Transl. Med.* **2017**, *9* (381). https://doi.org/10.1126/SCITRANSLMED.AAI7521/SUPPL_FILE/AAI7521_SM.PDF.

(74) Fairbanks, A. J. The ENGases: Versatile Biocatalysts for the Production of Homogeneous N-Linked Glycopeptides and Glycoproteins. *Chem. Soc. Rev.* **2017**, *46* (16), 5128–5146. https://doi.org/10.1039/C6CS00897F.

(75) Yamamoto, K.; Kadowaki, S.; Watanabe, J.; Kumagai, H. Transglycosylation Activity of Mucor Hiemalis Endo-β-N-Acetylglucosaminidase Which Transfers Complex Oligosaccharides to the N-Acetylglucosamine Moieties of Peptides. *Biochem. Biophys. Res. Commun.* **1994**, *203* (1), 244–252. https://doi.org/10.1006/BBRC.1994.2174.

(76) Fujita, M.; Shoda, S. ichiro; Haneda, K.; Inazu, T.; Takegawa, K.; Yamamoto, K. A Novel Disaccharide Substrate Having 1,2-Oxazoline Moiety for Detection of Transglycosylating Activity of Endoglycosidases. *Biochim. Biophys. Acta - Gen. Subj.* **2001**, *1528* (1), 9–14. https://doi.org/10.1016/S0304-4165(01)00164-7.

(77) Umekawa, M.; Huang, W.; Li, B.; Fujita, K.; Ashida, H.; Wang, L. X.; Yamamoto, K. Mutants of Mucor Hiemalis Endo-β-N-Acetylglucosaminidase Show Enhanced Transglycosylation and Glycosynthase-like Activities. *J. Biol. Chem.* **2008**, *283* (8), 4469–4479. https://doi.org/10.1074/JBC.M707137200.

(78) Umekawa, M.; Li, C.; Higashiyama, T.; Huang, W.; Ashida, H.; Yamamoto, K.; Wang, L. X. Efficient Glycosynthase Mutant Derived from Mucor Hiemalis Endo-β-N-Acetylglucosaminidase Capable of Transferring Oligosaccharide from Both Sugar Oxazoline and Natural N-Glycan. *J. Biol. Chem.* **2010**, *285* (1), 511–521. https://doi.org/10.1074/JBC.M109.059832.

(79) McIntosh, J. D.; Brimble, M. A.; Brooks, A. E. S.; Dunbar, P. R.; Kowalczyk, R.; Tomabechi, Y.; Fairbanks, A. J. Convergent Chemo-Enzymatic Synthesis of Mannosylated Glycopeptides; Targeting of Putative Vaccine Candidates to Antigen Presenting Cells. *Chem. Sci.* **2015**, *6* (8), 4636–4642. https://doi.org/10.1039/c5sc00952a.

(80) Li, H.; Li, B.; Song, H.; Breydo, L.; Baskakov, I. V.; Wang, L. X. Chemoenzymatic Synthesis of HIV-1 V3 Glycopeptides Carrying Two N-Glycans and Effects of Glycosylation on the Peptide Domain. *J. Org. Chem.* **2005**, *70* (24), 9990–9996. https://doi.org/10.1021/jo051729z.

(81) Yamaguchi, T.; Amin, M. N.; Toonstra, C.; Wang, L. X. Chemoenzymatic Synthesis and Receptor Binding of Mannose-6-Phosphate (M6P)-Containing Glycoprotein Ligands Reveal Unusual Structural Requirements for M6P Receptor Recognition. *J. Am. Chem. Soc.* **2016**, *138* (38), 12472–12485. https://doi.org/10.1021/jacs.6b05762.

(82) Priyanka, P.; Parsons, T. B.; Miller, A.; Platt, F. M.; Fairbanks, A. J. Chemoenzymatic Synthesis of a Phosphorylated Glycoprotein. *Angew. Chemie* **2016**, *128* (16), 5142–5145. https://doi.org/10.1002/ANGE.201600817.

(83) Ochiai, H.; Huang, W.; Wang, L. X. Expeditious Chemoenzymatic Synthesis of Homogeneous N-Glycoproteins Carrying Defined Oligosaccharide Ligands. *J. Am. Chem. Soc.* **2008**, *130* (41), 13790–13803. https://doi.org/10.1021/JA805044X/SUPPL_FILE/JA805044X_SI_001.PDF.

(84) Kurogochi, M.; Mori, M.; Osumi, K.; Tojino, M.; Sugawara, S. I.; Takashima, S.; Hirose, Y.; Tsukimura, W.; Mizuno, M.; Amano, J.; Matsuda, A.; Tomita, M.; Takayanagi, A.; Shoda, S. I.; Shirai, T. Glycoengineered Monoclonal Antibodies with Homogeneous Glycan (M3, G0, G2, and A2) Using a Chemoenzymatic Approach Have Different Affinities for FcγRIIIa and Variable Antibody-Dependent Cellular Cytotoxicity Activities. *PLoS One* **2015**, *10* (7), e0132848. https://doi.org/10.1371/JOURNAL.PONE.0132848.

(85) Lin, C. W.; Tsai, M. H.; Li, S. T.; Tsai, T. I.; Chu, K. C.; Liu, Y. C.; Lai, M. Y.; Wu, C. Y.; Tseng, Y. C.; Shivatare, S. S.; Wang, C. H.; Chao, P.; Wang, S. Y.; Shih, H. W.; Zeng, Y. F.; You, T. H.; Liao, J. Y.; Tu, Y. C.; Lin, Y. S.; Chuang, H. Y.; Chen, C. L.; Tsai, C. S.; Huang, C. C.; Lin, N. H.; Ma, C.; Wu, C. Y.; Wong, C. H. A Common Glycan Structure on Immunoglobulin G for Enhancement of Effector Functions. *Proc. Natl. Acad. Sci. U. S. A.* **2015**, *112* (34), 10611–10616. https://doi.org/10.1073/pnas.1513456112.

(86) Seko, A.; Koketsu, M.; Nishizono, M.; Enoki, Y.; Ibrahim, H. R.; Juneja, L. R.; Kim, M.; Yamamoto, T. Occurrence of a Sialylglycopeptide and Free Sialylglycans in Hen's Egg Yolk. *Biochim. Biophys. Acta - Gen. Subj.* **1997**, *1335* (1–2), 23–32. https://doi.org/10.1016/S0304-4165(96)00118-3.

(87) Li, H.; Singh, S.; Zeng, Y.; Song, H.; Wang, L. X. Chemoenzymatic Synthesis of CD52 Glycoproteins Carrying Native N-Glycans. *Bioorg. Med. Chem. Lett.* **2005**, *15* (4), 895–898. https://doi.org/10.1016/J.BMCL.2004.12.066.

(88) Huang, W.; Li, C.; Li, B.; Umekawa, M.; Yamamoto, K.; Zhang, X.; Wang, L. X. Glycosynthases Enable a Highly Efficient Chemoenzymatic Synthesis of N-Glycoproteins Carrying Intact Natural N-Glycans. *J. Am. Chem. Soc.* **2009**, *131* (6), 2214–2223. https://doi.org/10.1021/ja8074677.

(89) Huang, W.; Yang, Q.; Umekawa, M.; Yamamoto, K.; Wang, L. X. Arthrobacter Endo-β-N-Acetylglucosaminidase Shows Transglycosylation Activity on Complex-Type N-Glycan Oxazolines: One-Pot Conversion of Ribonuclease B to Sialylated Ribonuclease C. *ChemBioChem* **2010**, *11* (10), 1350–1355. https://doi.org/10.1002/cbic.201000242.

(90) Murakami, M.; Okamoto, R.; Izumi, M.; Kajihara, Y.; Murakami, M.; Okamoto, R.; Izumi, M.; Kajihara, Y. Chemical Synthesis of an Erythropoietin Glycoform Containing a Complex-Type Disialyloligosaccharide. *Angew. Chem. Int. Ed.* **2012**, *51* (15), 3567–3572. https://doi.org/10.1002/ANIE.201109034.

(91) Yamamoto, N.; Takayanagi, A.; Sakakibara, T.; Dawson, P. E.; Kajihara, Y. Highly Efficient Synthesis of Sialylglycopeptides Overcoming Unexpected Aspartimide Formation during Activation of Fmoc-Asn(Undecadisialyloligosaccharide)-OH. *Tetrahedron Lett.* **2006**, *47* (8), 1341–1346. https://doi.org/10.1016/j.tetlet.2005.12.064.

(92) Kajihara, Y.; Yoshihara, A.; Hirano, K.; Yamamoto, N. Convenient Synthesis of a Sialylglycopeptide-Thioester Having an Intact and Homogeneous Complex-Type Disialyl-Oligosaccharide. *Carbohydr. Res.* **2006**, *341* (10), 1333–1340. https://doi.org/10.1016/j.carres.2006.04.037.

(93) Evers, D. L.; Hung, R. L.; Thomas, V. H.; Rice, K. G. Preparative Purification of a High-Mannose TypeN-Glycan from Soy Bean Agglutinin by Hydrazinolysis and Tyrosinamide Derivatization. *Anal. Biochem.* **1998**, *265* (2), 313–316. https://doi.org/10.1006/ABIO.1998.2895.

(94) Wang, L.-X.; Ni, J.; Singh, S.; Li, H. Binding of High-Mannose-Type Oligosaccharides and Synthetic Oligomannose Clusters to Human Antibody 2G12: Implications for HIV-1 Vaccine Design. *Chem. Biol.* **2004**, *11* (1), 127–134. https://doi.org/10.1016/J.CHEMBIOL.2003.12.020.

(95) Makimura, Y.; Kiuchi, T.; Izumi, M.; Dedola, S.; Ito, Y.; Kajihara, Y. Efficient Synthesis of Glycopeptide-α-Thioesters with a High-Mannose Type Oligosaccharide by Means of Tert-Boc-Solid Phase Peptide Synthesis. *Carbohydr. Res.* **2012**, *364*, 41–48. https://doi.org/10.1016/J.CARRES.2012.10.011.

(96) Wang, L. X.; Song, H.; Liu, S.; Lu, H.; Jiang, S.; Ni, J.; Li, H. Chemoenzymatic Synthesis of HIV-1 Gp41 Glycopeptides: Effects of Glycosylation on the Anti-HIV Activity and α-Helix Bundle-Forming Ability of Peptide C34. *ChemBioChem* **2005**, *6* (6), 1068–1074. https://doi.org/10.1002/CBIC.200400440.

(97) Kiuchi, T.; Izumi, M.; Mukogawa, Y.; Shimada, A.; Okamoto, R.; Seko, A.; Sakono, M.; Takeda, Y.; Ito, Y.; Kajihara, Y. Monitoring of Glycoprotein Quality Control System with a Series of Chemically Synthesized Homogeneous Native and Misfolded Glycoproteins. *J. Am. Chem. Soc.* **2018**, *140* (50), 17499–17507. https://doi.org/10.1021/jacs.8b08653.

(98) Li, C.; Zhu, S.; Ma, C.; Wang, L. X. Designer A1,6-Fucosidase Mutants Enable Direct Core Fucosylation of Intact N-Glycopeptides and N-Glycoproteins. *J. Am. Chem. Soc.* **2017**, *139* (42), 15074–15087. https://doi.org/10.1021/jacs.7b07906.

(99) Kajihara, Y.; Suzuki, Y.; Yamamoto, N.; Sasaki, K.; Sakakibara, T.; Juneja, L. R. Prompt Chemoenzymatic Synthesis of Diverse Complex-Type Oligosaccharides and Its Application to the Solid-Phase Synthesis of a Glycopeptide with Asn-Linked Sialyl-Undeca- and Asialo-Nonasaccharides. *Chem. Eur. J.* **2004**, *10* (4), 971–985. https://doi.org/10.1002/chem.200305115.

(100) Wang, Z.; Chinoy, Z. S.; Ambre, S. G.; Peng, W.; McBride, R.; De Vries, R. P.; Glushka, J.; Paulson, J. C.; Boons, G. J. A General Strategy for the Chemoenzymatic Synthesis of Asymmetrically Branched N-Glycans. *Science* **2013**, *341* (6144), 379–383. https://doi.org/10.1126/science.1236231.

(101) Liu, L.; Prudden, A. R.; Capicciotti, C. J.; Bosman, G. P.; Yang, J. Y.; Chapla, D. G.; Moremen, K. W.; Boons, G. J. Streamlining the Chemoenzymatic Synthesis of Complex N-Glycans by a Stop and Go Strategy. *Nat. Chem.* **2019**, *11* (2), 161–169. https://doi.org/10.1038/s41557-018-0188-3.

(102) Malekan, H.; Fung, G.; Thon, V.; Khedri, Z.; Yu, H.; Qu, J.; Li, Y.; Ding, L.; Lam, K. S.; Chen, X. One-Pot Multi-Enzyme (OPME) Chemoenzymatic Synthesis of Sialyl-Tn-MUC1 and Sialyl-T-MUC1 Glycopeptides Containing Natural or Non-Natural Sialic Acid. *Bioorg. Med. Chem.* **2013**, *21* (16), 4778–4785. https://doi.org/10.1016/J.BMC.2013.02.040.

(103) Vibhute, A. M.; Komura, N.; Tanaka, H. N.; Imamura, A.; Ando, H. Advanced Chemical Methods for Stereoselective Sialylation and Their Applications in Sialoglycan Syntheses. *Chem. Rec.* **2021**, *21* (11), 3194–3223. https://doi.org/10.1002/tcr.202100080.

(104) Leppänen, A.; Mehta, P.; Ouyang, Y. Bin; Ju, T.; Helin, J.; Moore, K. L.; Van Die, I.; Canfield, W. M.; McEver, R. P.; Cummings, R. D. A Novel Glycosulfopeptide Binds to P-Selectin and Inhibits Leukocyte Adhesion to P-Selectin. *J. Biol. Chem.* **1999**, *274* (35), 24838–24848. https://doi.org/10.1074/jbc.274.35.24838.

(105) Sørensen, A. L.; Reis, C. A.; Tarp, M. A.; Mandel, U.; Ramachandran, K.; Sankaranarayanan, V.; Schwientek, T.; Graham, R.; Taylor-Papadimitriou, J.; Hollingsworth, M. A.; Burchell, J.; Clausen, H. Chemoenzymatically Synthesized Multimeric Tn/STn MUC1 Glycopeptides Elicit Cancer-Specific Anti-MUC1 Antibody Responses and Override Tolerance. *Glycobiology* **2006**, *16* (2), 96–107. https://doi.org/10.1093/GLYCOB/CWJ044.

(106) Tarp, M. A.; Sørensen, A. L.; Mandel, U.; Paulsen, H.; Burchell, J.; Taylor-Papadimitriou, J.; Clausen, H. Identification of a Novel Cancer-Specific Immunodominant Glycopeptide Epitope in the MUC1 Tandem Repeat. *Glycobiology* **2007**, *17* (2), 197–209. https://doi.org/10.1093/GLYCOB/CWL061.

(107) De Leon, C. A.; Levine, P. M.; Craven, T. W.; Pratt, M. R. The Sulfur-Linked Analogue of O-GlcNAc (S-GlcNAc) Is an Enzymatically Stable and Reasonable Structural Surrogate for O-GlcNAc at the Peptide and Protein Levels. *Biochemistry* **2017**, *56* (27), 3507–3517. https://doi.org/10.1021/acs.biochem.7b00268.

(108) Filser, C.; Kowalczyk, D.; Jones, C.; Wild, M. K.; Ipe, U.; Vestweber, D.; Kunz, H. Synthetic Glycopeptides from the E-Selectin Ligand 1 with Varied Sialyl Lewisx Structure as Cell-Adhesion Inhibitors of E-Selectin. *Angew. Chem. Int. Ed.* **2007**, *46* (12), 2108–2111. https://doi.org/10.1002/ANIE.200604442.

(109) Sprengard, U.; Schudok, M.; Schmidt, W.; Kretzschmar, G.; Kunz, H. Multiple Sialyl Lewisx N-Glycopeptides: Effective Ligands for E-Selectin. *Angew. Chemie Int. Ed. English* **1996**, *35* (3), 321–324. https://doi.org/10.1002/ANIE.199603211.

(110) von dem Bruch, K.; Kunz, H. Synthesis of N-Glycopeptide Clusters with Lewisx Antigen Side Chains and Their Coupling to Carrier Proteins. *Angew. Chemie Int. Ed. English* **1994**, *33* (1), 101–103. https://doi.org/10.1002/anie.199401011.

(111) März, J.; Kunz, H. Synthesis of Selectively Deprotectable Asparagine Glycoconjugates with a Lewis a Antigen Side Chain. *Synlett* **1992**, *1992* (7), 589–590. https://doi.org/10.1055/s-1992-21426.

(112) Gustafsson, T.; Hedenström, M.; Kihlberg, J. Synthesis of a C-Glycoside Analogue of β-D-Galactosyl Hydroxylysine and Incorporation in a Glycopeptide from Type II Collagen. *J. Org. Chem.* **2006**, *71* (5), 1911–1919. https://doi.org/10.1021/jo052256z.

(113) Gramer, M. J.; Goochee, C. F.; Chock, V. Y.; Brousseau, D. T.; Sliwkowski, M. B. Removal of Sialic Acid from a Glycoprotein in CHO Cell Culture Supernatant by Action of an Extracellular CHO Cell Sialidase. *Bio/Technology 1995 137* **1995**, *13* (7), 692–698. https://doi.org/10.1038/nbt0795-692.

(114) Companión, I.; Guerreiro, A.; Mangini, V.; Castro-López, J.; Escudero-Casao, M.; Avenoza, A.; Busto, J. H.; Castillón, S.; Jiménez-Barbero, J.; Asensio, J. L.; Jiménez-Osés, G.; Boutureira, O.; Peregrina, J. M.; Hurtado-Guerrero, R.; Fiammengo, R.; Bernardes, G. J. L.; Corzana, F. Structure-Based Design of Potent Tumor-Associated Antigens: Modulation of Peptide Presentation by Single-Atom O/S or O/Se Substitutions at the Glycosidic Linkage. *J. Am. Chem. Soc.* **2019**, *141* (9), 4063–4072. https://doi.org/10.1021/jacs.8b13503.

(115) Michaëlsson, E.; Andersson, M.; Holmdahl, R.; Engström, Å. Identification of an Immunodominant Type-II Collagen Peptide Recognized by T Cells in H-2q Mice: Self Tolerance at the Level of Determinant Selection. *Eur. J. Immunol.* **1992**, *22* (7), 1819–1825. https://doi.org/10.1002/EJI.1830220722.

(116) Broddefalk, J.; Bäcklund, J.; Almqvist, F.; Johansson, M.; Hoimdahl, R.; Kihlberg, J. T Cells Recognize a Glycopeptide Derived from Type II Collagen in a Model for Rheumatoid Arthritis. *J. Am. Chem. Soc.* **1998**, *120* (31), 7676–7683. https://doi.org/10.1021/ja980489k.

(117) Hogervorst, T. P.; Li, R. J. E.; Marino, L.; Bruijns, S. C. M.; Meeuwenoord, N. J.; Filippov, D. V.; Overkleeft, H. S.; Van Der Marel, G. A.; Van Vliet, S. J.; Van Kooyk, Y.; Codeé, J. D. C. C-Mannosyl Lysine for Solid Phase Assembly of Mannosylated Peptide Conjugate Cancer Vaccines. *ACS Chem. Biol.* **2020**, *15* (3), 728–739. https://doi.org/10.1021/acschembio.9b00987.

(118) Kantchev, E. A. B.; Chang, C. C.; Chang, D. K. Direct Fmoc/Tert-Bu Solid Phase Synthesis of Octamannosyl Polylysine Dendrimer-Peptide Conjugates. *Biopolym. - Pept. Sci. Sect.* **2006**, *84* (2), 232–240. https://doi.org/10.1002/bip.20403.

(119) Frison, N.; Marceau, P.; Roche, A. C.; Monsigny, M.; Mayer, R. Oligolysine-Based Saccharide Clusters: Synthesis and Specificity. *Biochem. J.* **2002**, *368* (Pt 1), 111. https://doi.org/10.1042/BJ20020673.

(120) Srinivas, O.; Larrieu, P.; Duverger, E.; Boccaccio, C.; Bousser, M. T.; Monsigny, M.; Fonteneau, J. F.; Jotereau, F.; Roche, A. C. Synthesis of Glycocluster−Tumor Antigenic Peptide Conjugates for Dendritic Cell Targeting. *Bioconjug. Chem.* **2007**, *18* (5), 1547–1554. https://doi.org/10.1021/BC070026G.

(121) Gunnoo, S. B.; Madder, A. Chemical Protein Modification through Cysteine. *ChemBioChem* **2016**, *17* (7), 529–553. https://doi.org/10.1002/CBIC.201500667.

(122) Bengtsson, M.; Broddefalk, J.; Dahmén, J.; Henriksson, K.; Kihlberg, J.; Lönn, H.; Srinivasa, B. R.; Stenvall, K. Convergent Synthesis of Neoglycopeptides by Coupling of 2-Bromoethyl Glycosides to Cysteine and Homocysteine Residues in T Cell Stimulating Peptides. *Glycoconjugate J. 1998 153* **1998**, *15* (3), 223–231. https://doi.org/10.1023/A:1006988810800.

(123) Shin, I.; Jung, H. J.; Lee, M. R. Chemoselective Ligation of Maleimidosugars to Peptides/Protein for the Preparation of Neoglycopeptides/Neoglycoprotein. *Tetrahedron Lett.* **2001**, *42* (7), 1325–1328. https://doi.org/10.1016/S0040-4039(00)02286-3.

(124) Gamblin, D. P.; Garnier, P.; Kasteren, S. van; Oldham, N. J.; Fairbanks, A. J.; Davis, B. G. Glyco-SeS: Selenenylsulfide-Mediated Protein Glycoconjugation—A New Strategy in Post-Translational Modification. *Angew. Chemie* **2004**, *116* (7), 846–851. https://doi.org/10.1002/ANGE.200352975.

(125) Macindoe, W. M.; Van Oijen, A. H.; Boons, G. J. A Unique and Highly Facile Method for Synthesising Disulfide Linked Neoglycoconjugates: A New Approach for Remodelling of Peptides and Proteins. *Chem. Commun.* **1998**, No. 7, 847–848. https://doi.org/10.1039/A708701B.

(126) Nolan, M. D.; Scanlan, E. M. Applications of Thiol-Ene Chemistry for Peptide Science. *Frontiers in Chemistry*. Frontiers Media S.A. November 12, 2020, p 1060. https://doi.org/10.3389/fchem.2020.583272.

(127) Dondoni, A.; Massi, A.; Nanni, P.; Roda, A. A New Ligation Strategy for Peptide and Protein Glycosylation: Photoinduced Thiol–Ene Coupling. *Chem. – A Eur. J.* **2009**, *15* (43), 11444–11449. https://doi.org/10.1002/CHEM.200901746.

(128) Piccirillo, G.; Pepe, A.; Bedini, E.; Bochicchio, B. Photoinduced Thiol-Ene Chemistry Applied to the Synthesis of Self-Assembling Elastin-Inspired Glycopeptides. *Chem. – A Eur. J.* **2017**, *23* (11), 2648–2659. https://doi.org/10.1002/CHEM.201604831.

(129) Alexander, S. R.; Lim, D.; Amso, Z.; Brimble, M. A.; Fairbanks, A. J. Protecting Group Free Synthesis of Glycosyl Thiols from Reducing Sugars in Water; Application to the Production of N -Glycan Glycoconjugates. *Org. Biomol. Chem.* **2017**, *15* (10), 2152–2156. https://doi.org/10.1039/C7OB00112F.

(130) Galonić, D. P.; Van Der Donk, W. A.; Gin, D. Y. Site-Selective Conjugation of Thiols with Aziridine-2-Carboxylic Acid-Containing Peptides. *J. Am. Chem. Soc.* **2004**, *126* (40), 12712–12713. https://doi.org/10.1021/JA046793X/SUPPL_FILE/JA046793XSI20040831_023609.PDF.

(131) Peluso, S.; Imperiali, B. Asparagine Surrogates for the Assembly of N-Linked Glycopeptide Mimetics by Chemoselective Ligation. *Tetrahedron Lett.* **2001**, *42* (11), 2085–2087. https://doi.org/10.1016/S0040-4039(01)00104-6.

(132) Finch, P.; Merchant, Z. The Structures of D-Arabinose and D-Glucose Oximes. *J. Chem. Soc. Perkin Trans. 1* **1975**, *0* (17), 1682–1686. https://doi.org/10.1039/p19750001682.

(133) Carrasco, M. R.; Nguyen, M. J.; Burnell, D. R.; MacLaren, M. D.; Hengel, S. M. Synthesis of Neoglycopeptides by Chemoselective Reaction of Carbohydrates with Peptides Containing a Novel N'-Methyl-Aminooxy Amino Acid. *Tetrahedron Lett.* **2002**, *43* (33), 5727–5729. https://doi.org/10.1016/S0040-4039(02)01212-1.

(134) Peri, F.; Dumy, P.; Mutter, M. Chemo- and Stereoselective Glycosylation of Hydroxylamino Derivatives: A Versatile Approach to Glycoconjugates. *Tetrahedron* **1998**, *54* (40), 12269–12278. https://doi.org/10.1016/S0040-4020(98)00763-7.

(135) Rodriguez, E. C.; Marcaurelle, L. A.; Bertozzi, C. R. Aminooxy-, Hydrazide-, and Thiosemicarbazide-Functionalized Saccharides: Versatile Reagents for Glycoconjugate Synthesis. *J. Org. Chem.* **1998**, *63* (21), 7134–7135. https://doi.org/10.1021/jo981351n.

(136) McGarvey, G. J.; Benedum, T. E.; Schmidtmann, F. W. Development of Co- and Post-Translational Synthetic Strategies to C-Neoglycopeptides. *Org. Lett.* **2002**, *4* (21), 3591–3594. https://doi.org/10.1021/ol0264861.

(137) Lin, Y. A.; Chalker, J. M.; Floyd, N.; Bernardes, G. J. L.; Davis, B. G. Allyl Sulfides Are Privileged Substrates in Aqueous Cross-Metathesis: Application to Site-Selective Protein Modification. *J. Am. Chem. Soc.* **2008**, *130* (30), 9642–9643. https://doi.org/10.1021/ja8026168.

(138) Tornøe, C. W.; Christensen, C.; Meldal, M. Peptidotriazoles on Solid Phase: [1,2,3]-Triazoles by Regiospecific Copper(I)-Catalyzed 1,3-Dipolar Cycloadditions of Terminal Alkynes to Azides. *J. Org. Chem.* **2002**, *67* (9), 3057–3064. https://doi.org/10.1021/jo011148j.

(139) Rostovtsev, V. V.; Green, L. G.; Fokin, V. V.; Sharpless, K. B. A Stepwise Huisgen Cycloaddition Process: Copper(I)-Catalyzed Regioselective "Ligation" of Azides and Terminal Alkynes. *Angew. Chem. Int. Ed.* **2002**, *41* (14), 2596–2599. https://doi.org/10.1002/1521-3773(20020715)41:14<2596::AID-ANIE2596>3.0.CO;2-4.

(140) Kuijpers, B. H. M.; Groothuys, S.; Keereweer, A. R.; Quaedflieg, P. J. L. M.; Blaauw, R. H.; Van Delft, F. L.; Rutjes, F. P. J. T. Expedient Synthesis of Triazole-Linked Glycosyl Amino Acids and Peptides. *Org. Lett.* **2004**, *6* (18), 3123–3126. https://doi.org/10.1021/ol048841o.

(141) Lin, H.; Walsh, C. T. A Chemoenzymatic Approach to Glycopeptide Antibiotics. *J. Am. Chem. Soc.* **2004**, *126* (43), 13998–14003. https://doi.org/10.1021/ja045147v.

(142) Lee, D. J.; Mandai, K.; Harris, P. W. R.; Brimble, M. A.; Kent, S. B. H. A One-Pot Approach to Neoglycopeptides Using Orthogonal Native Chemical Ligation and Click Chemistry. *Org. Lett.* **2009**, *11* (22), 5270–5273. https://doi.org/10.1021/ol902131n.

(143) Miller, N.; Williams, G. M.; Brimble, M. A. Synthesis of Fish Antifreeze Neoglycopeptides Using Microwave-Assisted "Click Chemistry." *Org. Lett.* **2009**, *11* (11), 2409–2412. https://doi.org/10.1021/ol9005536.

(144) Tanaka, T.; Nagai, H.; Noguchi, M.; Kobayashi, A.; Shoda, S. I. One-Step Conversion of Unprotected Sugars to β-Glycosyl Azides Using 2-Chloroimidazolinium Salt in Aqueous Solution. *Chem. Commun.* **2009**, No. 23, 3378–3379. https://doi.org/10.1039/B905761G.

(145) Lim, D.; Brimble, M. A.; Kowalczyk, R.; Watson, A. J. A.; Fairbanks, A. J. Protecting-Group-Free One-Pot Synthesis of Glycoconjugates Directly from Reducing Sugars. *Angew. Chemie* **2014**, *126* (44), 12101–12105. https://doi.org/10.1002/ANGE.201406694.

(146) Lee, D. J.; Harris, P. W. R.; Brimble, M. A. Synthesis of MUC1 Neoglycopeptides Using Efficient Microwave-Enhanced Chaotrope-Assisted Click Chemistry. *Org. Biomol. Chem.* **2011**, *9* (5), 1621–1626. https://doi.org/10.1039/C0OB01043J.

(147) Kawakami, Y.; Rosenberg, S. A. Immunobiology of Human Melanoma Antigens MART-1 and Gp100 and Their Use for Immuno-Gene Therapy. *Int. Rev. Immunol.* **1997**, *14* (2–3), 173–192. https://doi.org/10.3109/08830189709116851.

(148) Li, R. J. E.; Hogervorst, T. P.; Achilli, S.; Bruijns, S. C. M.; Spiekstra, S.; Vivès, C.; Thépaut, M.; Filippov, D. V.; van der Marel, G. A.; van Vliet, S. J.; Fieschi, F.; Codée, J. D. C.; van Kooyk, Y. Targeting of the C-Type Lectin Receptor Langerin Using Bifunctional Mannosylated Antigens. *Front. Cell Dev. Biol.* **2020**, *8*, 556. https://doi.org/10.3389/fcell.2020.00556.

2

Synthesis of asparagine derivatives harboring a Lewis^X-type DC-SIGN ligand and evaluation of their immunomodulation

This work was published as: W. Doelman, M.H.S. Marqvorsen, F. Chiodo, S.C.M. Bruijns, G.A. van der Marel, Y. van Kooyk, S.I. van Kasteren, C. Araman, *Chem. Eur. J.* **2021**, 27, 2742-2752

Introduction

Multiple Sclerosis (MS) is a group of auto-immune neurodegenerative diseases characterized by the formation of lesions in the patient's brain that lead to loss of function.[1] The pathology of MS is not fully understood, but degradation of myelin sheath seems to be a critical step in the disease pathogenesis.[2] Myelin sheaths are comprised of myelin, an insulating substance consisting of lipids, proteins and other molecules, and are responsible for fast information transfer through axons.[3] Several proteinogenic components of myelin sheath have been shown to become antigenic upon their degradation.[4] For example, myelin oligodendrocyte glycoprotein (MOG), an exclusively CNS-resident protein found on the surface of

oligodendrocytes and myelin sheaths, acts as an autoantigen in an MS-like animal model, the so-called experimental autoimmune encephalomyelitis (EAE).[5]

MOG is a membrane bound glycoprotein, decorated with an *N*-glycan[6] on Asn_{31}, with an approximate molecular mass of 26 kDa.[7,8] It comprises 245 amino acids (AA) and belongs to the immunoglobulin superfamily (Ig). Over the last few decades, it has been shown that antibodies against MOG are circulating in the bloodstream of patients suffering from various demyelinating diseases such as MS and *N*-methyl-D-aspartate receptor-encephalitis.[9] It has also been shown that a peptide fragment comprising AAs 35-55, MOG_{35-55}, is an immunodominant peptide in EAE.[10,11]

Recently, a potential mechanism behind the pathogenicity of this MOG_{35-55}-peptide in EAE was discovered: after post-translational citrullination (deimination of the guanidine moiety of arginine), the peptide was shown to form amyloid-like aggregates intracellularly, where they appear to be cytotoxic.[12,13] Citrullination of myelin proteins is considered to be critical in MS. For example, another antigenic myelin protein, myelin basic protein (MBP), has been shown to have increased citrullination in myelin samples from MS patients.[14] Together, these advances led to the hypothesis that post-translational citrullination of MOG, via cytotoxic peptide aggregates, could be in part responsible for the neurodegeneration observed in MS and EAE.

In light of the above findings, the effect of the native *N*-glycan at position 31 on the aggregation behavior of the citrullinated peptide was questioned. Inhibition of aggregation by glycosylation could be expected based on the work on *O*-glycosylation of serine or threonine residues, which has previously been shown to inhibit the aggregation of a tau derived peptide, a highly aggregation-prone protein family involved in Alzheimer's disease.[15] The introduction of *N*-glycans (and their mimics) on peptides derived from prion protein[16] and the full-length prion protein[17] has also been shown to decrease or even abrogate aggregation. Therefore, a study on the effects of glycosylation on the previously described aggregation of citrullinated MOG peptides was called for.

Furthermore, the N-glycan present on MOG may play a second role in its pathological mechanisms: previous studies on the glycosylation of MOG suggest that specific *N*-glycan structures can modulate the immunological tolerance through the dendritic cell-specific intercellular adhesion molecule-3–grabbing nonintegrin (DC-SIGN) receptor.[18] This receptor has been shown to recognize the fucose-containing Lewis-type glycans,[19] especially the trisaccharide Galβ1-4(Fucα1-3)GlcNAc, better known as $Lewis^X$ (Le^X), which has been shown to be highly abundant on natively glycosylated MOG.[20]

Studies using synthetic neoglycopeptides bearing DC-SIGN binding *N*-glycan mimics may shed light on the role of a putative interaction between DC-SIGN and MOG in MS. MOG_{31-55}-peptides decorated with Le^X and Le^X derived oligosaccharides (LacNAc and Fucα1-3GlcNAc) on the N-terminal asparagine (Asn_{31}) were therefore synthesized and the effect of these

modifications on the aggregation-proneness of the peptides was assessed, and the results of these studies are described in this Chapter. To minimize artefacts stemming from various non-native linkers[21–23], the oligosaccharides are attached via the native anomeric amide linkage that normally occurs in N-glycans. To achieve this, the recently published method for the synthesis of glycosylated asparagine derivatives was extended to larger oligosaccharides.[24] By using the asparagine building blocks obtained in this manner with the previously established model peptide, MOG_{31-55}[12], the effect of glycosylation on citrullination-dependent aggregation of MOG could be evaluated. Subsequently, the binding of Le^X-decorated neoglycopeptides to DC-SIGN was confirmed by solid-phase immunoassays using recombinant DC-SIGN-Fc fusion protein.[25] Finally, a cytokine secretion assay in monocyte derived dendritic cells (moDCs) from human donors was utilized to analyze the degree of modulation for IL-10 (anti-inflammatory) and IL-12p70 (pro-inflammatory) production by Le^X-decorated peptides.

Results and Discussion

N-glycosylation of asparagine is of prime importance for a variety of protein functions such as signaling and folding.[26] Studying these functions however, is challenging, as the typical size and complexity of an *N*-glycan poses a considerable synthetic challenge. *N*-glycosylated peptides have been generated using semisynthetic methods involving synthesis and/or isolation of carbohydrate segments which can be linked covalently using endohexosaminidases[27,28], or extended via specific glycosyltransferases as recently demonstrated by Boons and colleagues.[29,30] Synthetic preparation of an entire peptide bearing a natural *N*-glycan has also been reported.[31–33]

Previous work has shown that fucosylated glycans interact with DC-SIGN without the need for an *N*-glycan core structure.[34–38] This formed the inspiration to synthesize a Le^X *N*-glycan derivative similar to the one developed by von dem Bruch and Kunz.[39] This glycosylated asparagine could then be incorporated as residue 31 on the MOG_{31-55} peptide, enabling the facile synthesis of MOG_{31-55} derived neoglycopeptides. These would enable the study of the DC-SIGN binding properties of glycosylated MOG_{31-55}, without needing to produce a full Lewis^X containing N-glycan (Figure 1). To study the effect glycosylation has on the citrulline driven aggregation of MOG_{31-55}, citrullinated forms of MOG_{31-55}, also bearing different N-glycan derivatives, could be synthesized. Since MOG_{31-55} has three arginine residues, seven different permutation of citrullinated derivatives could be considered. Replacing Arg_{41} and Arg_{46} with citrulline seemed to most interesting, as it had previously been shown that this citrullination pattern has some of the most pronounced aggregation behaviour.[12] These arginine residue are also within the reported MHC-I restricted epitope (for non-human primates) MOG_{40-48}.[40] Furthermore, the citrullination of either of these positions has previously been extensively studied in a rodent EAE model.[41]

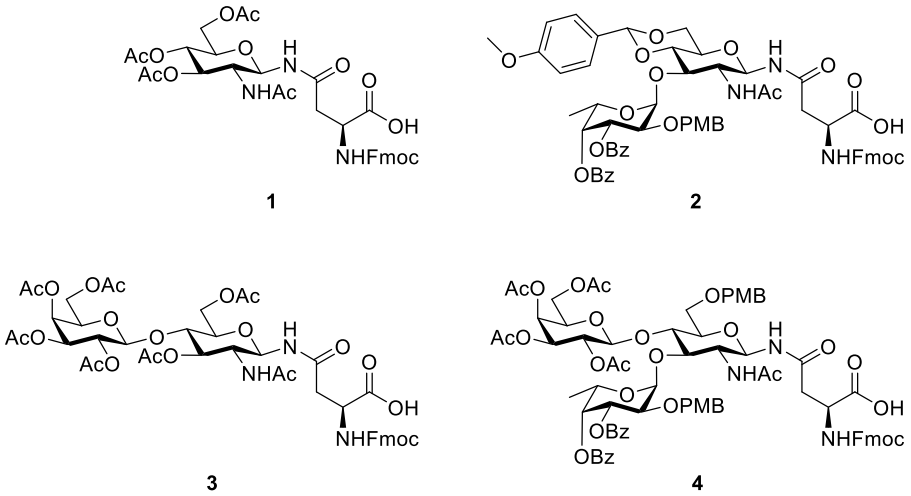

Figure 1. Desired glycosylated Fmoc-asparagine building blocks **1**-**4**.

Three Fmoc-SPPS (solid phase peptide synthesis) compatible glycosyl amide derivatives of asparagine were designed and synthesized (Figure **1**, **1-4**), one (compound **4**) containing a Le^X structure and two (compounds **2** and **3**) featuring a Fucα1-3GlcNAc and LacNAc, respectively, attached to the asparagine side chain via the reducing ends of respective sugars. The LacNAc construct (**3**) was included as a negative control for DC-SIGN binding, as the interaction of Le^X with the receptor has been shown to be fucose dependent.[35]

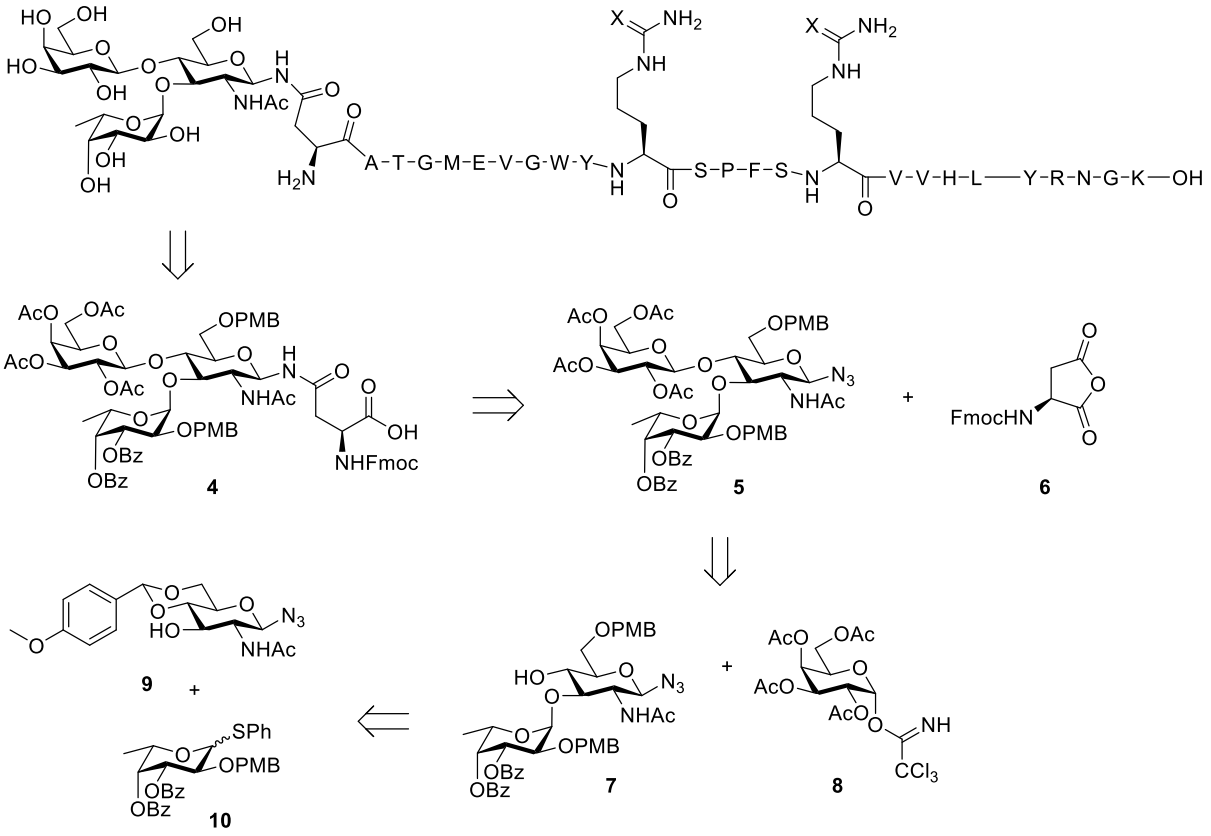

Figure 2. Retrosynthetic analysis of the synthesis of Le^X decorated MOG$_{31-55}$ peptides using building block **4**. A similar approach can be used to produce building blocks **1-3** and incorporate these into peptides. X = NH (Arg) or X = O (Cit).

As exemplified by the structure of Le^X containing protected building block **4** (Figure 1), the synthetic strategy was based on the utilization of acid labile *para*-methoxybenzyl (PMB) and *para*-methoxybenzylidene groups, which would be removed during the TFA mediated global peptide deprotection in standard Fmoc-based solid phase peptide synthesis, and on ester protective groups, which can be removed using hydrazine in methanol after the acidic global deprotection of the peptide. A synthetic strategy was designed so that these protecting groups would be introduced on the monosaccharide building blocks and used throughout the synthesis, avoiding late-stage protecting group manipulation.

The condensation between the glycosyl amine and the sidechain of asparagine for the synthesis of the Fmoc-asparagine building blocks was accomplished using the recently developed two-step one-pot approach for the synthesis of glycosylated asparagine derivatives.[24] This method uses Fmoc-aspartic anhydride (**6**) as an activated Fmoc-aspartic acid derivative, while avoiding protecting group manipulation on the C$^\alpha$-carbonyl. In this method, a Staudinger reduction is used to transform a glycosyl azide into a glycosyl amine.[42–44] The crude glycosyl amine is then redissolved in DMSO, and reacted with Fmoc-aspartic anhydride. The glycosyl amine regioselectively opens the anhydride ring on the C$^\gamma$ side, generating a protected glycosyl asparagine amino acid (Figure 2).[45] The polarity of the solvent is crucial for this regioselectivity, with DMSO generally giving the best results.[46] The synthesis

of the Le^X azide derivative **5** itself will be carried out by first introducing the fucose moiety on the 3-OH of GlcNAc, using donor **10** and acceptor **9**, followed by reductive opening of the *para*-methoxybenzylidine function to generate **7**. This disaccharide acceptor can then be glycosylated with galactoside donor **8**, producing Le^X azide **5**.

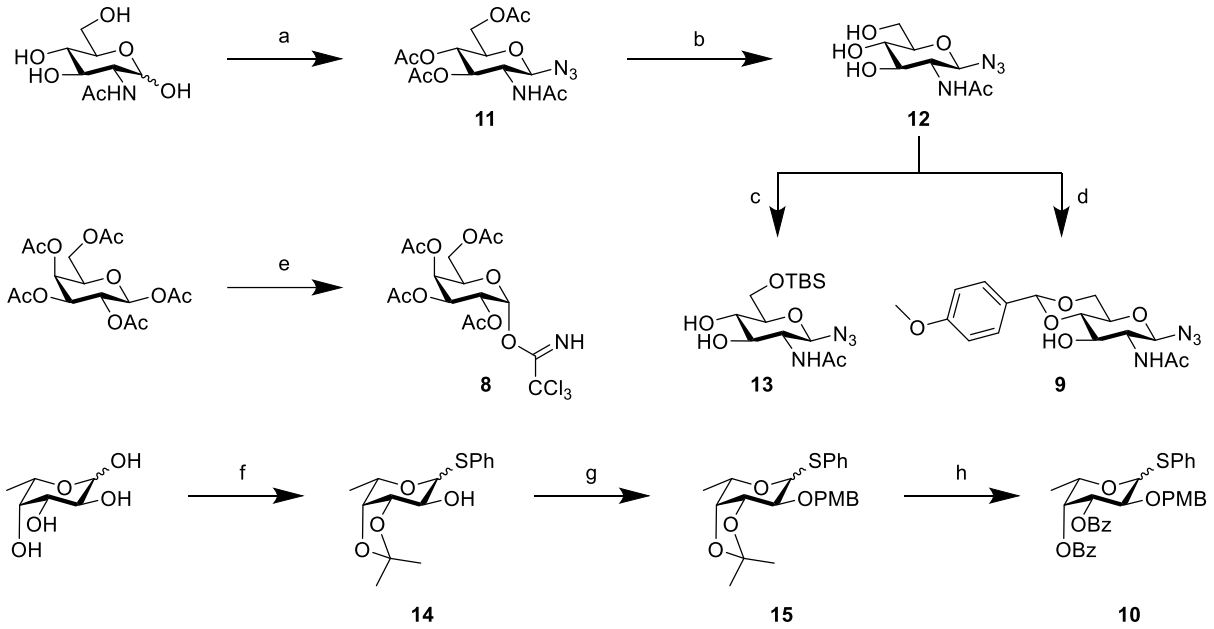

Figure 3. Synthesis of acceptor glycosides **9** and **13**, donor galactoside **8** and donor fucoside **10**. Reagents and conditions: a) i) AcCl, RT ii) NaN_3, DMF, RT, 2h, 42% b) Na, MeOH, RT, 1h c) TBSCl, pyridine, RT, 2h, 84% d) anisaldehyde dimethyl acetal, CSA, ACN, 50 °C, 300 mbar, 3h, 65% e) i) N,N-dimethylaminopropylamine, THF, RT 1h ii) CCl_3CN, DBU, DCM, 1 h RT, 60% over two steps f) i) Ac_2O, pyridine ii) $BF_3{\cdot}Et_2O$, PhSH, toluene iii) Na, MeOH iv) 2,2-dimethoxypropane, CSA, acetone, 80% over four steps g) NaH, PMB-Cl, DMF, 0°C → RT, 2h, 84% h) i) AcOH, H_2O, 80°C, 1h ii) BzCl, pyridine, RT, 2h, 64% over two steps

In the first step towards the glycosyl azides, the monosaccharide building blocks were constructed (Figure 3). N-acetyl glucosaminyl azide **11** was synthesized from N-acetyl glucosamine by acetylation and simultaneous introduction of the anomeric chloride,[47] followed by substitution of the chloride with sodium azide in DMF. This gave **11** in 42% yield over two steps. The acetyl groups were removed under Zemplén conditions and the resulting compound **12** was reacted either with anisaldehyde dimethyl acetal in the presence of CSA to fashion *para*-methoxybenzylidene protected acceptor **9** in 65% yield, or with TBS-Cl in pyridine to produce acceptor **13** in 84% yield. The synthesis of galactosyl imidate donor **8** was accomplished by selective hydrolysis of the anomeric acetate in galactose pentaacetate using N,N-dimethylaminopropylamine[48], followed by formation of the anomeric imidate using trichloroacetonitrile in the presence of catalytic DBU. Lastly, fucosyl donor **10** was constructed starting from L-fucose. Sequential acetylation, introduction of the thiophenol, deacetylation and formation of an isopropylidene gave **14** in 80% yield over four steps. The free 2-OH was then alkylated with *para*-methoxybenzyl chloride, mediated by NaH, to produce compound **15**. Hydrolysis of the isopropylidene group in **15** using 50% aqueous acetic acid at 80°C resulted in liberation of the diol without removing the acid labile PMB group. This was

followed by benzoylation with benzoyl chloride in pyridine, producing donor **10** in 64% over two steps.

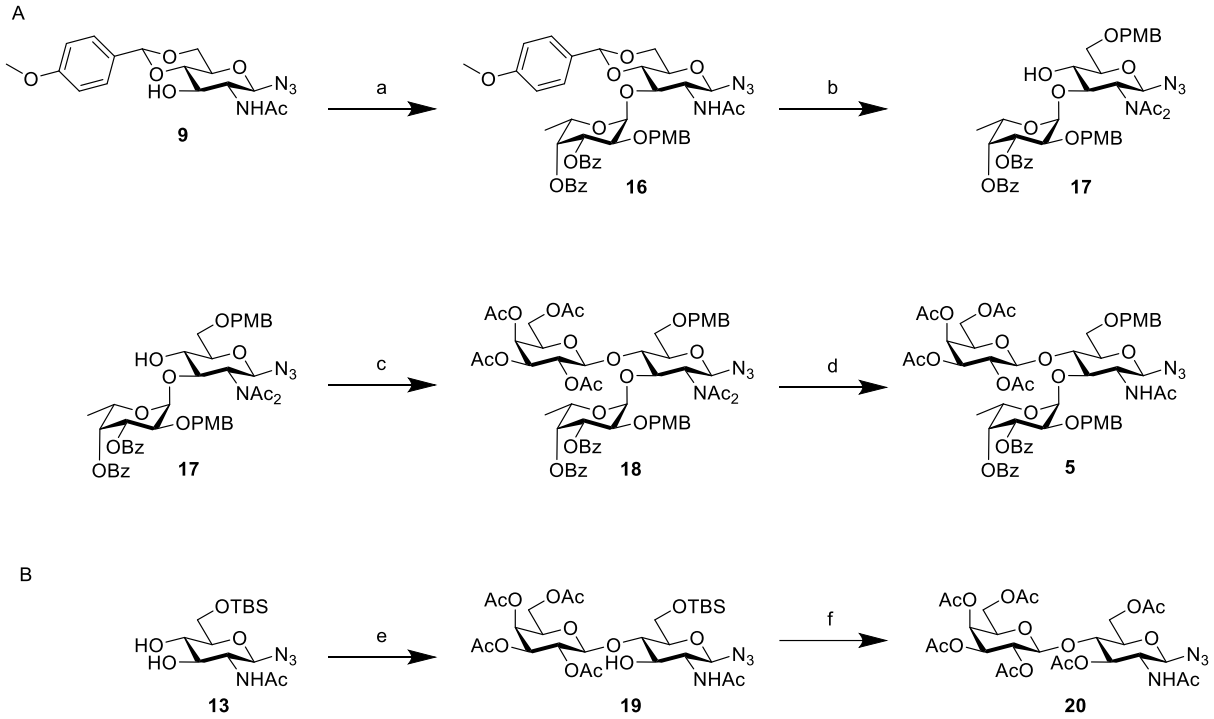

Figure 4. Synthesis of Lewis X azide (A) **15** and LacNAc azide **17** (B). Reagents and conditions: a) **11**, NIS, TMSOTf, 4 Å molecular sieves, DCM, DMF, 0°C, 71% b) i) AcCl, DiPEA, DCM, 89% ii) BH_3, Bu_2BOTf, THF, -50 °C, 81% c) **8**, TMSOTf, DCM, 4 Å molecular sieves, DCM, -15°C, 77% d) N,N-dimethylaminopropylamine, THF, 87% e) **8**, $BF_3{\cdot}Et_2O$, DCM, -40°C, 56% f) i) HF·pyridine ii) Ac_2O, DMAP, DCM, 85% over two steps

The synthesis of protected Le^X glycosyl azide **5** (Figure 4A) started from *para*-methoxybenzylidene-protected glycosyl azide **9** by NIS/TMSOTf-promoted fucosylation with thioglycoside **10** to afford disaccharide **16** in 71% yield. Next, reductive opening of the *para*-methoxybenzylidene group in **16** was carried out to produce **7** (Figure 2). However, the presence of the acetamido group in this glycosyl acceptor hindered the glycosylation, an often encountered problem with *N*-acetyl-glucosamine derived acceptors.[49] Accordingly, disaccharide **16** was first treated with an excess of acetyl chloride and diisopropylethylamine (DiPEA) to convert the amide into the less interfering imide in 89% yield.[50] Reductive opening of the *para*-methoxybenzylidene with BH_3/Bu_2BOTf was performed as described,[51] affording compound **17** in 81% yield. Then, galactosylation with trichloroacetimidate donor **8** yielded the desired protected trisaccharide **18** in 77% yield. Chemoselective deacetylation of **18** using N,N-dimethylaminopropylamine[48] afforded **5** in 87% yield.

The protected lactosaminyl azide **17** was prepared using a literature protocol for regioselective glycosylation of 1,6-protected GlcNAc derivatives.[52,53] Silyl-protected glycosyl azide **13** was subjected to $BF_3{\cdot}Et_2O$ promoted galactosylation with trichloroacetimidate donor **8**, affording the partially protected disaccharide **19** in a 56% yield (Figure 4B). This compound

was treated with HF·pyridine for removal of the *tert*-butyldimethylsilyl (TBS) group, followed by acetylation to afford the desired peracetylated glycosyl azide **20** in 85% yield over 2 steps.

Asparagine derivatives **1-4** were prepared following a general synthetic strategy involving the Staudinger reduction of a glycosyl azide followed by direct reaction of the resulting glycosyl amine with Fmoc aspartic anhydride to perform a nucleophilic ring opening (Figure 5A).[24] Accordingly, Fmoc-Asn(Ac_4GlcNAc)-OH (**1**) was synthesized from glycosyl azide **11**[54] in three steps by PMe_3-mediated azide reduction, followed by addition of H_2O to the crude iminophosphorane to obtain the intermediate glycosyl amine. The desired asparagine derivative was formed by redissolving the crude glycosyl amine in DMSO followed by addition of Fmoc aspartic anhydride. Precipitation directly afforded the desired SPPS building block **1** in 69% yield.

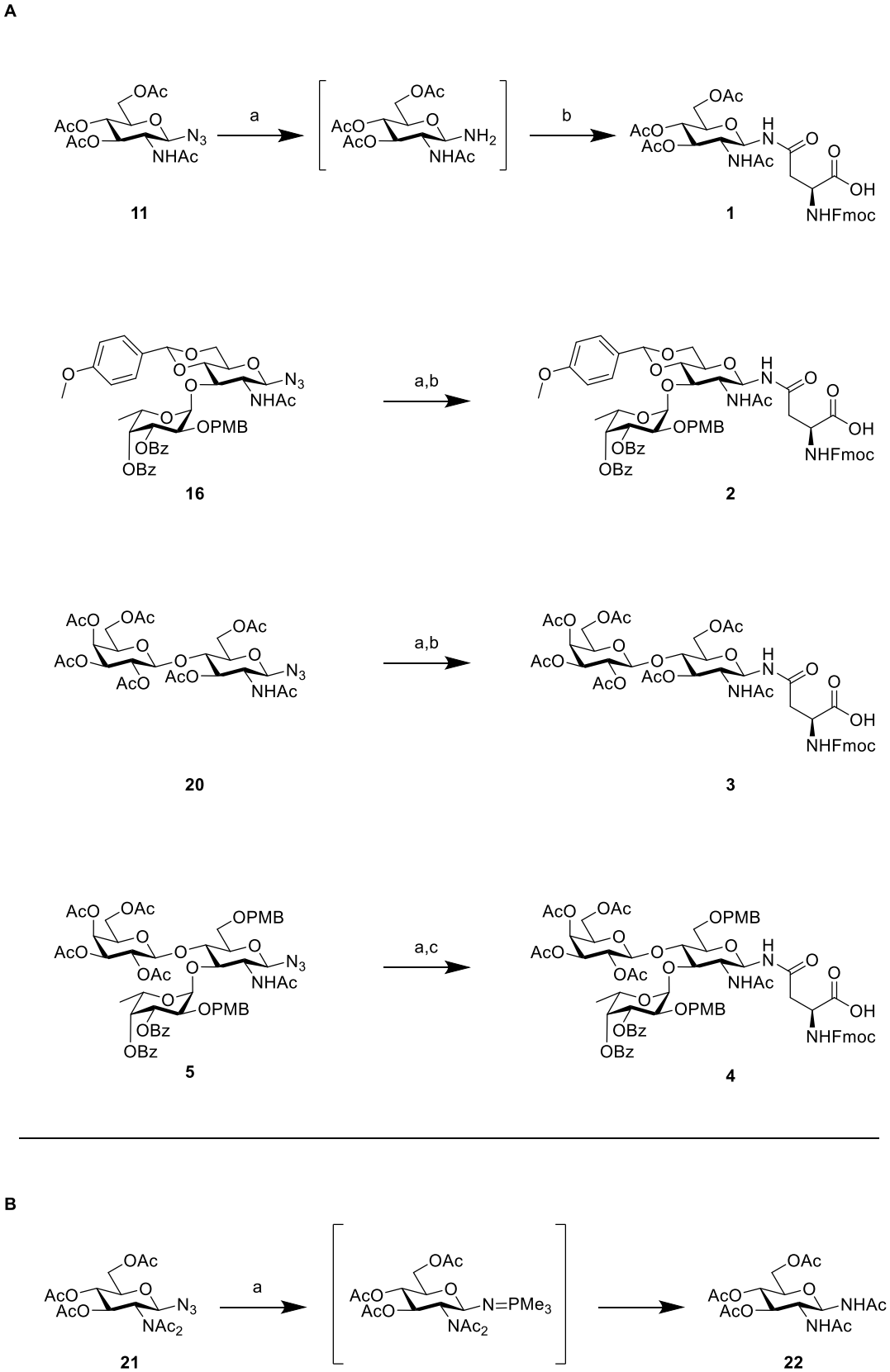

Figure 5. A) Synthesis of glycosylated Fmoc-asparagine derivatives **1**-**4** via the two step Staudinger reduction/aspartic anhydride coupling approach. B) observed reaction when performing Staudinger reduction of diacetylimide **21**. Reagents and conditions: a) i) PMe_3, THF ii) H_2O b) Fmoc-aspartic anhydride, DMSO, 69% (**1**), 65% (**2**), 63% (**3**) c) Fmoc-aspartic anhydride, DMA, 74%

The above sequence proved similarly useful for the preparation of the other desired glycosylated asparagine building blocks (**2**-**4**, Figure 5A). However, precipitation or extraction were found to be less efficient for small scale purification of the more complex carbohydrates, and therefore these compounds were subjected to silica gel chromatography for purification. Using this approach, the fucosylated glycosyl azide **16** was converted to its corresponding SPPS building block **2** in 65% yield, while lactosyl compound **20** was similarly converted to compound **3** in 63% yield. (Figure 5). For the trisaccharide glycosyl azide, conversion of the NAc_2 functionality back to the acetamide was required, as Staudinger reduction of **18** afforded conversion to an unknown side product. Acetyl migration is a likely explanation, as Staudinger reduction of the model NAc_2 protected glycosyl azide **21** afforded clean conversion to the more readily assignable glycosyl acetamide **22** (Figure 5B). Glycosyl azide **5** was coupled to Fmoc aspartic anhydride yielding the desired Le^X SPPS building block **4** as an inseparable 10:1 mixture with its corresponding iso-asparagine isomeric product. It has been shown that dimethylacetamide (DMA) gives similar regioselectivity as DMSO when used as solvent for aspartic anhydride ring opening reactions.[46] However, the lower melting point of this solvent allows for aspartic anhydride ring-opening at 0°C, potentially increasing regioselectivity. Indeed, this solvent and temperature change resulted in the desired Le^X asparagine **4** being formed in 74% yield with complete regioselectivity.

The syntheses of the desired glycopeptides started with the automated SPPS of the immobilized MOG_{32-55} peptide **23** on Tentagel®S-RAM resin, using HCTU as the coupling reagent. This peptide was then manually elongated at the N-terminus with either of the glycosylated asparagine derivatives **1**-**4** using DEPBT as the coupling reagent to prevent aspartimide formation, as described by Yamamoto *et al*.[55] The general synthetic strategy used for the synthesis of the glycopeptides is outlined in Figure 6.

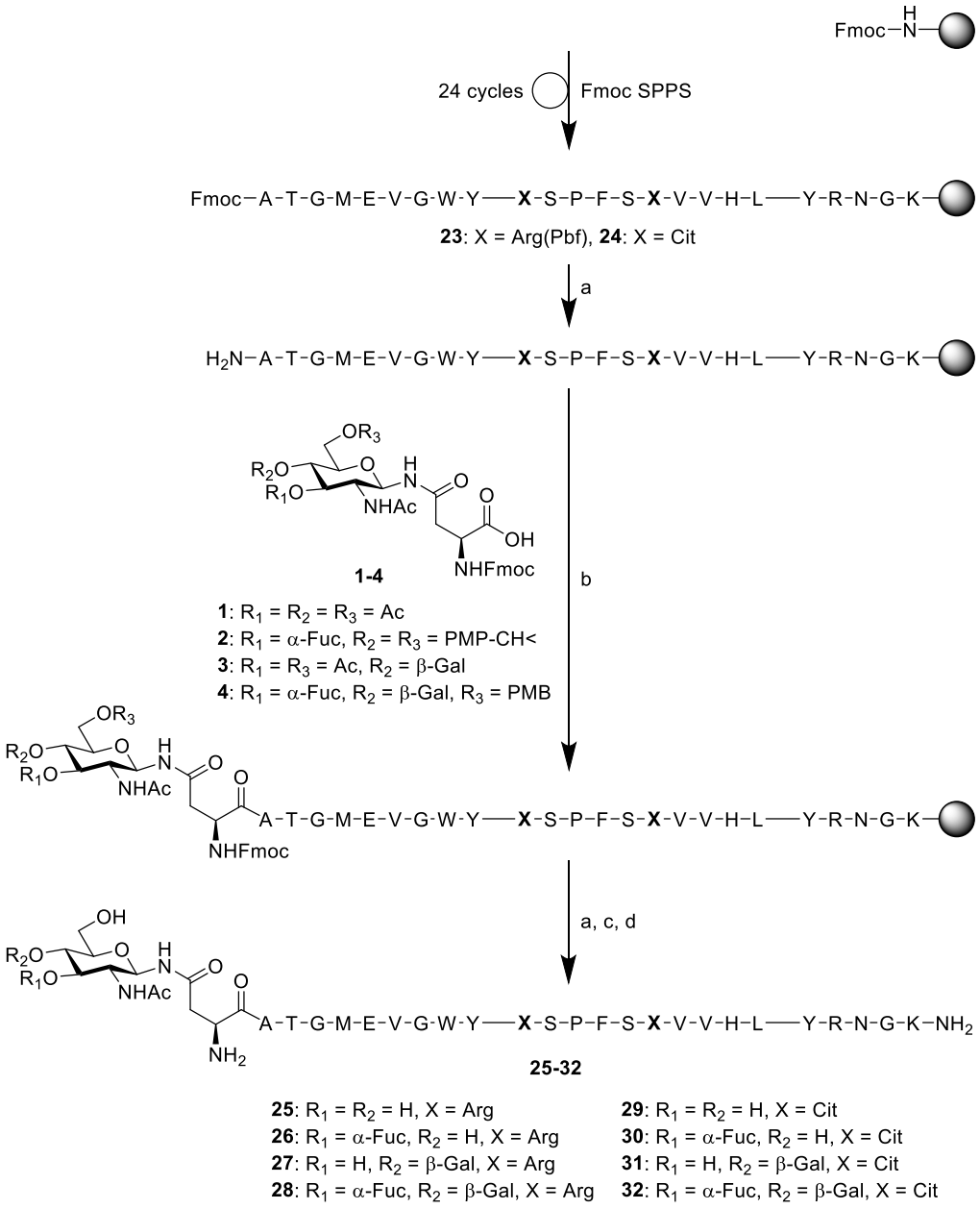

Figure 6. Synthetic strategy employed for the synthesis of MOG_{31-55} glycopeptides **25-32** starting from fully protected immobilized peptides **23** and **24**. X = Arg (**25-28**) or Cit (**29-32**). Reagents and conditions: a) 20% piperidine in DMF b) **1-4**, DEPBT. DiPEA, DMF c) TFA, TIS, H_2O, DCM d) $H_2H_4 \cdot H_2O$, MeOH.

Immobilized peptides **25** and **27** were cleaved from the solid support under standard cleavage conditions (95:2.5:2.5 TFA/TIS/H_2O (v/v) mixture for 2 hours). To prevent potential hydrolysis of the acid labile α-fucosyl bonds[56] in peptides **26** and **28**, more dilute acidic conditions (50:2.5:2.5:45 TFA/TIS/H_2O/DCM (v/v) mixture for 4 hours) were applied. The reaction time under these less acidic conditions had to be extended to ensure complete removal of the 2,2,4,6,7-pentamethyldihydrobenzofuran-5-sulfonyl (Pbf) protecting groups, which are more acid stable than the other side chain protecting groups (Boc/tBu/Trt) used in the synthesis.[57]

To remove the remaining ester protecting groups on the carbohydrate moieties, the crude peptides were treated with 10% hydrazine monohydrate in methanol. The resulting fully

deprotected glycopeptides were then purified by preparative reverse-phase (RP) HPLC and the target neoglycopeptides **25-28** were isolated in moderate to good yields after RP-HPLC (Table 1).

Table 1. Yields of glycopeptides **25-32** obtained using the synthetic strategy outlined in Figure 6 after preparative HPLC. The number for each compound is given together with the HPLC yield based on crude mass.

Amino acid	X = Arg	X = Cit
GlcNAc (**1**)	**25** (4.0 %)	**29** (8.6 %)
Fucα1-3GlcNAc (**2**)	**26** (5.6 %)	**30** (2.1 %, 5.7 %[a])
LacNAc (**3**)	**27** (5.8 %)	**31** (5.6 %)
Lewis X (**4**)	**28** (4.1 %)	**32** (6.1 %, 4.8 %[a])

[a] The product containing methionine oxidation was isolated separately.

Next, peptides carrying both post-translational modifications under investigation, glycosylation and citrullination, were synthesized. These peptide were designated peptides **29-32** and prepared using the same procedures as the non-citrullinated glycopeptides, starting from peptide **24**, synthesized using Fmoc-citrulline as the 41st and 46th amino acid. Similar levels of glycosyl amino acid incorporation and similar RP-HPLC yields were achieved during the synthesis of these glycopeptides (Table 1).

The influence of glycosylation on the structure and behavior of MOG_{31-55} was assessed using a variety of biophysical and biochemical experiments. First, solution circular dichroism (CD) spectra of peptides **26-28** and **30-32** were taken to see if these would indicate any difference in biophysical behavior. All peptides showed a pre-dominantly random-coiled structure. The effect of addition of the α-helix stabilizer TFE (50% v/v in PBS) or SDS at non-micellar concentrations (4 mM) was also evaluated (Figure 7). These results indicate the peptides are not prone to β-sheet formation.

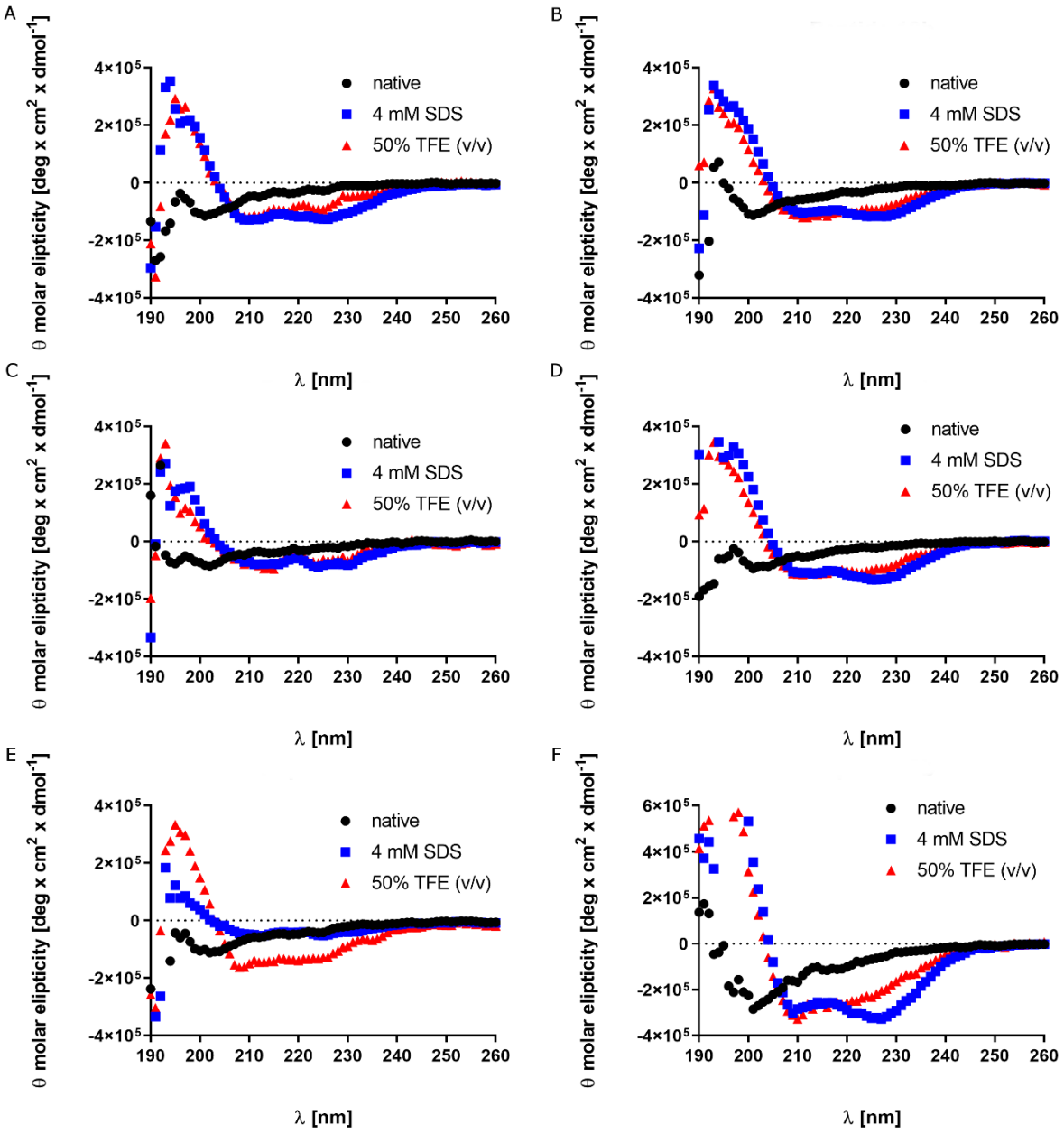

Figure 7. Circular Dichroism spectra of the glycopeptides. A) peptide **26** B) peptide **27** C) peptide **28** D) peptide **30** E) peptide **31** F) peptide **32**

Next, the susceptibility of all glycopeptides to form amyloid-like aggregates was evaluated using the previously described Thioflavin T (ThT) fluorescence assay.[12] In this assay, a fluorogenic substrate, Thioflavin T, was used to detect whether such aggregation occurs. This dye, upon binding to the typical cross β-sheet structures found in amyloid-like aggregates, undergoes an increase in fluorescence quantum yield and a shift of absorption/emission maxima, resulting in an increase in observed fluorescence.[58] The non-citrullinated peptides did not show aggregation at 10 µM (Figure 8A). For the citrullinated peptides, the differently glycosylated peptides displayed distinct aggregation behavior.

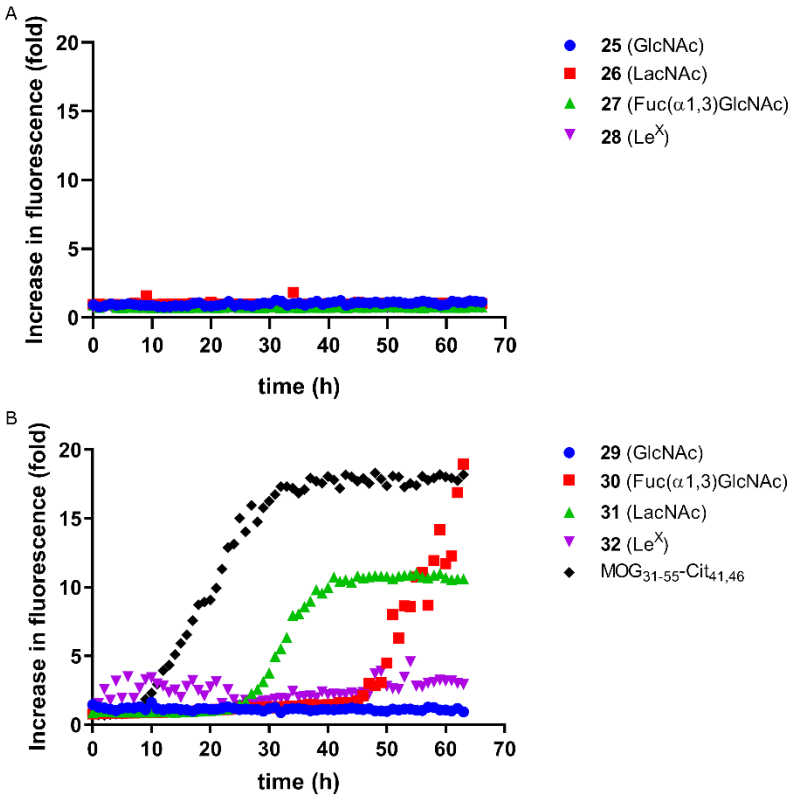

Figure 8. ThT aggregation assay of non-citrullinated (A) and citrullinated (B) glycosylated MOG31-55 peptides 17a-20b. Peptides were tested at a concentration of 10 µM. Positive control (black diamonds) is nonglycosylated MOG31-55 citrullinated at positions 41 and 46. All data were recorded at an excitation wavelength of 444 ± 9 nm and an emission wavelength of 485 ± 9 nm. All samples were used at a pH of 5.0 and aggregation assays were performed at least three times and with experimental triplicates.

While all glycosylated peptides showed reduced aggregation propensity compared to the non-glycosylated control, large differences between the differently glycosylated structures were found (Figure 8B). The peptide containing a single GlcNAc (**29**) did not show any aggregation over the entire duration of the assay. This exemplifies the powerful effect glycosylation can have on peptide aggregation. The peptide containing the DC-SIGN ligand Le^X (**32**) showed a similar inhibition of aggregation to that of GlcNAc, suggesting the potential in controlling immune household and not the neurodegenerative mechanism in MS. However, the other glycosylated peptides tested, that is Fucα1-3GlcNAc containing peptide **30** and LacNAc containing peptide **31**, did still aggregate after longer incubation times, indicating that glycan structure plays a role in this process (Figure 8B).

In previous studies[12] it was shown that citrullinated MOG_{35-55} peptides are cytotoxic to murine bone marrow derived dendritic cells (BMDCs). Citrullinated MOG_{31-55} however was not yet tested. To analyze whether native, glycosylated or citrullinated MOG_{31-55} variants show similar cytotoxicity to those of citrullinated MOG_{35-55}, cell viability assays were conducted using 3-(4,5-dimethylthiazol-2-yl)-2,5-diphenyltetrazolium bromide (MTT) as described previously (Figure 9).[12] In this assay, the mitochondrial activity of the cells under investigation is determined by their ability to enzymatically convert MTT into formazan. Formation of this

compound is determined by detection of absorption at 540 nm. By comparing the amount of signal at 540 nm to that produced to the same amount of non-treated cells, the percentage of living cells can be determined.

BMDCs were treated with citrullinated peptides **29-32** as well as their non-glycosylated counterpart (MOG_{31-55}-$Cit_{41,46}$) at four different concentrations (40, 20, 10 and 5 µM). None of the tested peptides showed significant decrease in viability of BMDCs at any concentration tested. As expected, the remaining glycosylated MOG_{31-55} derivatives **25-28** as well as the native variant did also not exhibit any significant drop in cell viability in BMDCs.

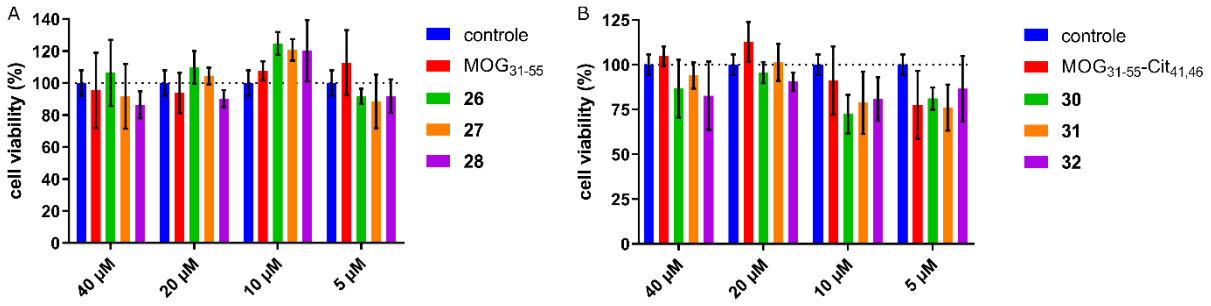

Figure 9. Cell viability as determined by MTT of BMDCs incubated for 3-4 hours with varying concentrations of A) non-citrullinated MOG peptides **21a**-**23a** (N=3) or B) citrullinated MOG peptides **21b**-**23b** (N=6)

From this data, it may be concluded that the glycosylated MOG_{31-55} peptides do not display altered biophysical properties as measured by CD. Furthermore, glycosylated peptide **29** and **32** showed a complete absence of aggregation propensity. No major cytotoxic effects were observed for citrullinated and glycosylated MOG_{31-55} derivatives **29-32** in BMDCs, which renders them useful for subsequent studies to explore the impact of DC-SIGN binding on moDCs.

Next, the ability of the *N*-glycosylated peptides to bind DC-SIGN was assessed by ELISA.[59] For this, the peptides were adsorbed on high-binding 96-well plates and incubated with a recombinant DC-SIGN-Fc construct consisting of the N-terminally truncated extracellular domain (K_{62}-A_{404}) of human DC-SIGN fused to the Fc region of human IgG1 at the N-terminus.[25] This was followed by incubation with a HRP-conjugated anti-IgG1 and 3,3',5,5'-tetramethylbenzidine (TMB) as a substrate for the conjugated HRP. The amount of DC-SIGN-Fc bound to the glycopeptides was determined readout of absorbence at 450 nm (Figure 10). Le^X peptides **28** and **32** were recognized by DC-SIGN-Fc, while the other fucosylated glycopeptides were recognized to a lesser extent (**26, 30**). LacNAc decorated peptides **27** and **31** showed no binding, as expected. A detectable binding of the GlcNAcylated peptide **25** was also observed, in line with previous reports that GlcNAc itself is a ligand for DC-SIGN; albeit a weak one with an IC_{50} of 5 mM *in vitro*.[60] This DC-SIGN binding was not seen for the other GlcNAc containing peptide, **29**.

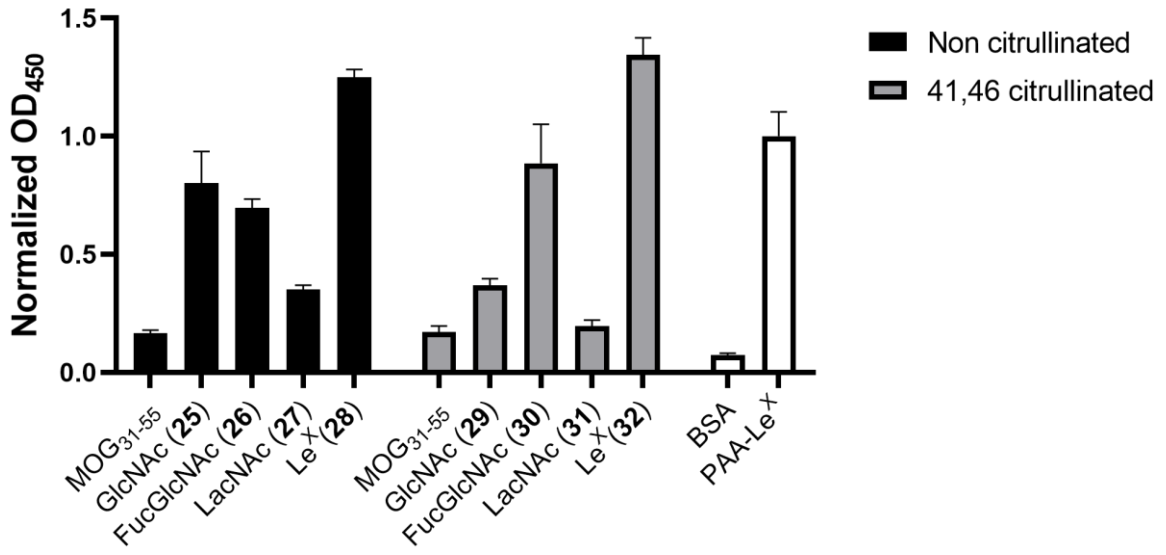

Figure 10. DC-SIGN-Fc ELISA. Lewis X decorated polymer (PAA-LeX) was used as the positive control, while for the negative control no peptide was added, meaning they are fully blocked with BSA. The DC-SIGN ELISA has been performed three times showing similar results. The graph shows data of one representative experiment out of three independent experiments performed in duplicate. Error bars represent standard deviation.

Finally, the downstream effects of stimulation of human monocytes-derived dendritic cells (moDCs) with Le^X decorated peptide **28** was investigated, as this peptide showed good binding to DC-SIGN in the ELISA. Since DC-SIGN is absent on murine DCs,[61] human dendritic cells, derived from donor blood, were used for this experiment. A well-established assay[62] was utilized, where the release of anti- and pro-inflammatory cytokines, IL-10 and IL-12p70 respectively, is measured. When stimulated with TLR4 ligands, DCs become pro-inflammatory, inducing the secretion of IL12p70. Simultaneous stimulation of DC-SIGN with fucosylated glycans induces an upregulation of IL-10 secretion and a down-regulation of IL-12p70 secretion, switching the immune response towards tolerance instead of inflammation. MoDCs from three donors were stimulated with peptide **28** or non-glycosylated MOG_{31-55} at multiple concentrations (14, 7 and 3.5 µM). This was done in presence or absence of the TLR4 ligand LPS (from *E. coli* at 10 ng/mL). After 16 hours, the concentrations of secreted cytokines were measured.[63] No cytokine production was observed upon stimulation of moDCs with peptide in the absence of LPS (Supporting Figure S1). However, upon co-stimulation with LPS, a glycan-dependent effect on IL-12p70 secretion at all concentration tested was observed. In Figure 11A the ratio of IL-10/IL-12p70 secretion is plotted for a single donor (representative for three independent experiments, N=3). An increase of the IL10/IL12P70 ratio was found for the Le^X decorated neoglycopeptide **28** over the non-glycosylated control at all concentrations tested. This increase in IL10/IL12p70 ratio shows that stimulation with peptide **28** leads to a more tolerogenic response compared to non-glycosylated MOG_{31-55}.

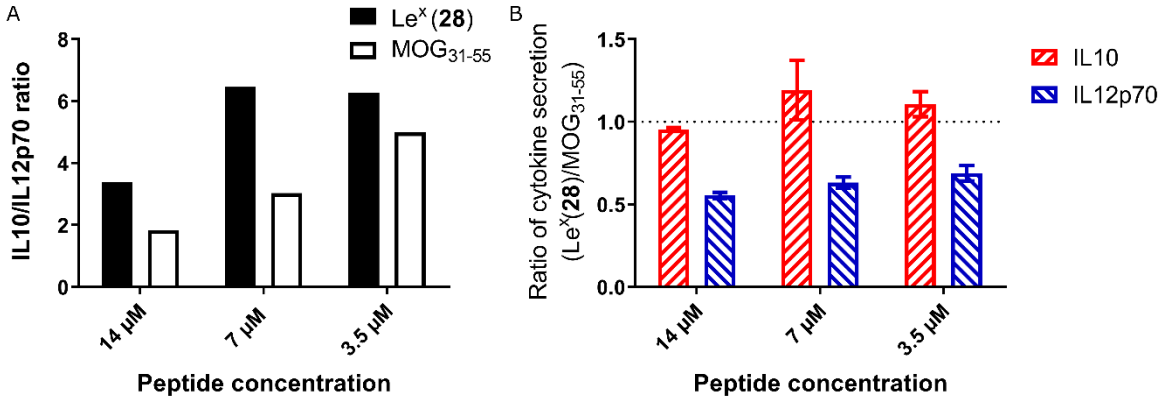

Figure 11. In vitro moDC cytokine profiling upon exposure to **28** A) Ratio of IL10/IL12p70 secretion measured upon moDC stimulation with either **28** or non-glycosylated control in the presence of 10 ng/mL of LPS. This graph is a representative plot from one donor (N=3). B) Normalized ratios for IL-10 and IL-12p70 secretion between non-glycosylated peptide MOG$_{31-55}$ and peptide **28** harboring Le^X incubated with moDCs at different concentrations in the presence 10 ng/mL LPS. Here a ratio of 1 means cytokine production is the same for both peptides, while a ratio of 0.5 means cytokine production is halved for **28** compared to non-glycosylated peptide. The results are the average of three experiments performed using cells from three separate donors, each measured in duplicate.

Figure 11B shows the ratio of cytokine secretion between stimulation of moDCs with **28** and non-glycosylated MOG$_{31-55}$ for all donors (N=3). A reduction in secretion of pro-inflammatory cytokine IL-12p70 is observed, while secretion of anti-inflammatory IL-10 remains unchanged. This indicates the increase in IL10/IL12p70 ratio is mostly driven by a decrease in IL12p70 secretion. Since the DC-SIGN-Fc binding ELISA shows a binding interaction between the Le^X decorated peptide and not the non-glycosylated peptide, a DC-SIGN driven process is strongly suggested.

Conclusion

In this chapter, the development of a synthetic route for three novel SPPS compatible glycosylated Fmoc-asparagine building blocks, including an asparagine derivative of the important DC-SIGN ligand Le^X is described. These building blocks have been synthesized from the corresponding glycosyl-azides using a Staudinger-reduction/aspartic anhydride ring-opening approach. By careful choice of protecting groups during the oligosaccharide assembly, the amount of protecting group manipulations could be kept to a minimum, and final glycopeptide deprotection was accomplished in a straightforward manner. This was demonstrated by the synthesis of glycosylated derivatives of the peptide MOG$_{31-55}$ in good yields and purity, as well as derivatives that are both glycosylated and citrullinated.

Using these synthetic neoglycopeptides, it was demonstrated that glycosylation has a powerful effect on the citrullination driven aggregation of this model peptide. All evaluated peptides carrying both glycosylation and citrullination had slowed induction of aggregation compared to the non-glycosylated control, with the GlcNAc (**29**) and Le^X (**32**) decorated peptides showing no glycosylation at all. Furthermore, it was shown that Le^X, while linked to

asparagine directly via an amide bond, is capable of binding to DC-SIGN, *via* ELISA. In a final experiment it was shown that peptide **28**, decorated with Le^X on asparagine, is able to elicit a tolerogenic response (reduced IL12p70 secretion compared to non-glycosylated counterpart), when used to stimulate moDCs. This indicates that peptides bearing the simplified Le^X N-glycan described in this chapter could be useful tools to study the role of DC-SIGN stimulation on immunotolerance. Given the straightforward synthesis of building block **4** and efficient incorporation of this structure into peptides using SPPS, this offers a new tool to perform experiments on lectin driven immunomodulation.

Experimental Section

General methods for synthesis and characterization of compounds

Solvents were purchased from Honeywell, VWR or Alfa Aesar. Anhydrous solvents were prepared by drying over 4Å molecular sieves. Reagents purchased from chemical suppliers were used without further purification, unless stated otherwise. All reactions were performed under nitrogen atmosphere and/or under exclusion of H_2O, unless stated otherwise. Reactions were followed by thin layer chromatography which was performed using TLC silica gel 60 F254 on aluminium sheets, supplied by Merck. Compounds were visualized using UV absorption (254 nm) and/or a spray reagent, either permanganate (5 g/L $KMnO_4$, 25 g/L K_2CO_3) or sulfuric acid (10% v/v in EtOH). ^1H and ^{13}C NMR spectra were recorded using a Brüker AV400 (400 /101 MHz) and COSY and HSQC 2D experiments were used to assign peaks. Recorded data was interpreted and analyzed using MestReNova 12 software. Chemical shifts are reported in ppm (δ) in reference to an internal standard (TMS) or the residual solvent peak. High resolution mass spectra were recorded by direct injection (2 µL of a 2 µM solution in H_2O/MeCN 1:1 and 0.1% formic acid) on a mass spectrometer (Thermo Fisher Exactive HF Orbitrap) equipped with an electrospray ion source in positive mode. The high resolution mass spectrometer was calibrated prior to measurements with a calibration mixture (Thermo Finnigan). The optical rotation of chirally pure compounds was measured on an Anton Paar MCP110 polarimeter at 25°C. IR spectra were recorded using a Shimadzu IRSpirit fourier transform infrared spectrometer.

General methods for SPPS

An automated synthesizer (PTI Tribute UV-IR synthesizer, Gyros Protein Technologies) was utilized. If not stated otherwise, peptides were synthesized on Tentagel S RAM resin (Rapp Polymere GmbH, Germany) on a 100 µmol scale using 5.0 equiv of each amino acid (AA) with respect to the resin loading. Fmoc protected amino acids were purchased from either Novabiochem or Sigma-Aldrich. For the amino acids that require sidechain protection, the following protecting groups were used: tBu for Ser, Thr and Tyr; OtBu for Asp and Glu; Trt for Asn, Gln and His; Boc for Lys and Trp; Pbf for Arg. An equimolar quantity of 2-(6-chloro-1-H-benzotriazole-1-yl)-1,1,3,3-tetramethylaminium hexafluorophosphate (HCTU) was used as activator. Coupling cycles of 1 h were utilized, and unreacted amines were capped after each cycle using a solution of 500 µL of acetic anhydride, 250 µL of DIPEA, and 4.25 mL of DMF for 5 min at room temperature twice. Fmoc deprotection was accomplished with 20% piperidine in DMF (3 x 5 min). Cleavage of non-glycosylated peptides was accomplished using a 95:2.5:2.5 mixture of TFA/TES/H_2O for 3 hours, followed by precipitation from cold diethyl ether and recovery of the precipitate by centrifugation. Peptides were characterized using electrospray ionization mass spectrometry (ESI-MS) on a Thermo Finnigan LCQ Advantage Max LC-MS instrument with a Surveyor PDA plus UV detector on an analytical C18 column (Phenomenex, 3 µm, 110 Å, 50 mm × 4.6 mm) in combination with buffers A (H_2O), B (MeCN), and C (1% aq TFA). Quality of crude peptides was evaluated with a linear gradient of 10-50% B with a constant 10% C over 10 minutes, while final peptide quality was evaluated using a linear gradient of 5-65% B with a constant 10% C over 30 minutes.

Incorporation of glycosylated amino acids

Synthesis of glycopeptides was carried out at 25 µmol scale. Fmoc group was removed from the resin bound peptide using 2 x 2 mL of 20% (v/v) piperidine in DMF (3 + 7 min). After Fmoc deprotection, the resin was washed five times with DMF (5 x 5 mL). Fully protected glycosylated asparagine (2 eq, 50 µmol) was dissolved in 500 µL of a 0.3 M solution of 3-(diethoxyphosphoryloxy)-1,2,3-benzotriazin-4(3H)-one (DEPBT) in DMF by the addition of DIPEA (8.7 µL, 2 eq, 50 µmol). The mixture was agitated for at least 5 minutes or until all amino acid had been dissolved. The solution containing the activated amino acid was added to the resin and the resin was incubated overnight under mild agitation. After overnight coupling, the resin was washed with DMF (5 x 5 mL) and a small portion was deprotected to confirm incorporation of the glycosylated amino acid. Fmoc deprotection was carried out as normal using a freshly prepared piperidine solution. Full cleavage of the peptide was achieved using 2 mL of 95:2.5:2.5 (v/v) mixture of TFA/TES/H_2O for 2 hours or 50:2.5:2.5:45 (v/v) mixture of TFA/TES/H_2O/DCM for 4 hours for fucose containing peptides. The deprotected peptide was precipitated in cold diethyl ether (10 mL) and the resin was washed with DCM (1 mL) which was added to the ether phase. After centrifugation, the pellet was washed with a small amount of diethyl ether (3-5 mL) and centrifugated again. To facilitate the removal of the ester protection groups, the peptide was suspended in methanol (2.25 mL) in a roundbottom flask and placed under N_2 atmosphere, followed by the addition of hydrazine monohydrate (0.25 mL). After stirring overnight, the reaction progress was checked by LC-MS. When complete deprotection was confirmed the volatiles were removed *in vacuo* to yield the crude glycopeptide. Preparative reverse phase HPLC on a Waters AutoPurification system (eluent A: H_2O + 0.2% TFA; eluent B: ACN) with a preparative Gemini C18 column (5 µm, 150 x 21.2 mm) yielded the final products.

N^{γ}-[3,4,6-tri-O-acetyl-2-deoxy-2-acetamido-β-D-glucopyranosyl]-N^{α}-fluorenylmethoxycarbonyl-L-asparagine (1)

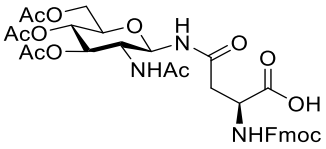

Glycosyl azide **11** (200 mg, 0.54 mmol) was dissolved in THF (0.76 mL) and the solution was cooled in an icebath. 0.54 mL of a 1 M solution of trimethylphosphine (1.0 eq, 0.54 mmol) in THF was added dropwise over 2 minutes, during which gas evolution was observed. The icebath was removed, and the reaction was stirred for 5 minutes before H2O (10 eq, 97 µL, 5.4 mmol) was added. The reaction was stirred at room temperature for 1.5 hours, after which it was concentrated. The residue containing the crude glycosyl amine was redissolved in DMSO (1.8 mL) and Fmoc-aspartic anhydride[45] (1.0 eq, 181 mg, 0.54 mmol) was added. The reaction was stirred for 2 hours at room temperature. The DMSO solution was added dropwise to a centrifuge tube containing 30 mL of a 2:1 mixture of diethyl ether and ethyl acetate and a precipitate started to form. The compound was left to fully precipitate for 16 hours at room temperature, after which it was collected by centrifugation. The supernatant was discarded and the pellet was washed with a small amount of the diethyl ether/ethyl acetate mixture. After removing the volatiles under reduced pressure, the title compound was obtained as a white amorphous solid (255 mg, 0.37 mmol, 69%). **^{1}H NMR** (500 MHz, DMSO-d6) δ 8.60 (d, J = 9.8 Hz, 1H, $N^{\gamma}H$), 7.99 – 7.78 (m, 3H, N<u>H</u>C(O)CH_3, Fmoc-Ar), 7.71 (d, J = 7.5 Hz, 2H, Fmoc-Ar), 7.51 (d, J = 8.5 Hz, 1H, $N^{\alpha}H$), 7.41 (t, J = 7.5 Hz, 2H, Fmoc-Ar), 7.32 (t, J = 7.4 Hz, 2H, Fmoc-Ar), 5.18 (t, J = 9.8 Hz, 1H, H1), 5.10 (t, J = 9.8 Hz, 1H, H3), 4.82 (t, J = 9.8 Hz, 1H, H4), 4.38 (q, J = 7.5 Hz, 1H, Asn-CH), 4.33 – 4.13 (m, 4H, Fmoc-CH_2, Fmoc-CH, H6a), 3.94 (d, J = 11.3 Hz, 1H, H6b), 3.88 (q, J = 9.8 Hz, 1H, H2), 3.84

– 3.78 (m, 1H, H5), 2.66 (dd, J = 16.3, 5.4 Hz, 1H, Asn-CHH), 1.99 (s, 3H, OC(O)CH_3), 1.96 (s, 3H, OC(O)CH_3), 1.90 (s, 3H, OC(O)CH_3), 1.72 (s, 3H, NHC(O)CH_3). **^{13}C NMR** (126 MHz, DMSO-d6) δ = 173.0 (C=O), 170.1 (C=O), 169.9 (C=O), 169.6 (C=O), 169.6 (C=O), 169.4 (C=O), 155.9 (C=O), 143.8 (Fmoc-Ar), 143.8 (Fmoc-Ar), 140.7 (Fmoc-Ar), 127.7 (Fmoc-Ar), 127.1 (Fmoc-Ar), 125.3 (Fmoc-Ar), 120.2 (Fmoc-Ar), 78.1 (C1), 73.4 (C3), 72.3 (C5), 68.4 (C4), 65.8 (Fmoc-CH_2), 61.9 (C6), 52.2 (C2), 50.0 (Asn-CH), 46.6 (Fmoc-CH), 36.9 (Asn-CH_2), 22.6 (NHC(O)CH_3), 20.6 (OC(O)CH_3), 20.4 (OC(O)CH_3), 20.4 (OC(O)CH_3). **HRMS** (ESI) m/z: [M + H^+] calcd for $C_{33}H_{37}N_3O_{13}H$ 684.23991, found 684.23920.

N$^\gamma$-[3,4-di-O-benzoyl-2-O-(4-methoxybenzyl)-α-L-fucopyranoside-(1→3)-4,6-O-(4-methoxybenzylidene)-2-deoxy-2-acetamido-β-D-glucopyranosyl]-N$^\alpha$-fluorenylmethoxycarbonyl-L-asparagine (2)

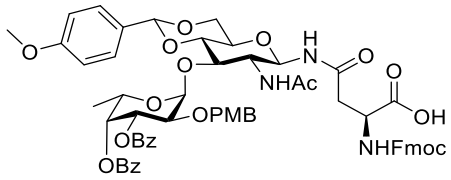

Glycosyl azide **16** (168 mg, 0.2 mmol) was dissolved in dry THF (2 mL) and trimethylphosphine was added as a 1 M solution in THF (1.1 eq, 220 µL, 0.22 mmol). The reaction was stirred for 10 minutes at room temperature and H_2O (50 eq, 180 µL, 10 mmol) was added. After stirring for 1 hour at room temperature, the reaction was concentrated and the residue was dissolved in DMSO (2 mL). Fmoc-aspartic anhydride[45] (1.0 eq, 67 mg, 0.2 mmol) was added and the reaction mixture was stirred for 1 hour at room temperature. The solvent was removed *in vacuo* and the crude was subjected to silica gel column chromatography (0 → 8% MeOH in DCM, Δ = 1%). This yielded the title compound (150 mg, 0.13 mmol, 65%). **$[\alpha]_D^{25}$** = -73.3 (c 1.00 in $CHCl_3$). **^{1}H NMR** (400 MHz, DMSO-d6) δ 8.46 (d, J = 9.4 Hz, 1H, N$^\gamma$H), 8.16 (d, J = 9.0 Hz, 1H, NHC(O)CH_3), 7.87 (t, J = 8.0 Hz, 3H, CH_{arom}), 7.81 – 7.64 (m, 5H, CH_{arom}), 7.64 – 7.47 (m, 5H, CH_{arom}), 7.47 – 7.26 (m, 8H, N$^\alpha$H, CH_{arom}), 7.18 – 7.04 (m, 2H, CH_{arom}), 6.97 – 6.89 (m, 2H, CH_{arom}), 6.73 – 6.62 (m, 2H, CH_{arom}), 5.71 (s, 1H, PMP-CH_{acetal}), 5.42 – 5.33 (m, 2H, H1', H3'), 5.23 (d, J = 3.5 Hz, 1H, H4'), 5.15 (t, J = 9.5 Hz, 1H, H1), 4.55 – 4.43 (m, 2H, H5', PMB-CHH), 4.39 – 4.30 (m, 2H, PMB-CHH, Asn-CH), 4.30 – 4.17 (m, 4H, Fmoc-CH_2, H5, Fmoc-CH), 4.13 (t, J = 9.5 Hz, 1H, H3), 3.99 (dd, J = 10.7, 3.5 Hz, 1H, H2'), 3.95 – 3.84 (m, 1H, H2), 3.76 – 3.60 (m, 9H, H6, H4, OCH_3, OCH_3), 2.66 (dd, J = 16.1, 5.6 Hz, 1H, Asn-CHH), 1.82 (s, 3H, NHC(O)CH_3), 0.46 (d, J = 6.4 Hz, 3H, H6'). **^{13}C NMR** (101 MHz, DMSO-d6) δ = 170.2 (C=O), 169.7 (C=O), 165.6 (C=O), 164.8 (C=O), 159.7 (C_q), 158.8 (C_q), 155.9 (C=O), 143.9 (Fmoc-Ar), 143.8 (Fmoc-Ar), 140.7 (Fmoc-Ar), 133.7 (CH_{arom}), 133.5 (CH_{arom}), 130.0 (C_q), 129.2 (CH_{arom}), 129.1 (C_q), 129.0 (CH_{arom}), 128.8 (CH_{arom}), 128.5 (CH_{arom}), 127.8 (CH_{arom}), 127.8 (CH_{arom}), 127.7 (CH_{arom}), 127.1 (CH_{arom}), 125.3 (CH_{arom}), 120.1 (CH_{arom}), 113.4 (CH_{arom}), 100.9 (PMP-CH), 96.2 (C1'), 79.4 (C1, C4), 75.3 (C3), 72.3 (C4'), 71.5 (C2'), 70.0 (PMB-CH_2), 69.6 (C3'), 68.0 (C5), 67.8 (C6), 65.8 (Fmoc-CH_2), 63.9 (C5'), 55.1 (OCH_3, C2), 55.0 (OCH_3), 50.4 (Asn-CH), 46.6 (Fmoc-CH), 37.3 (Asn-CH_2), 23.1 (NHC(O)CH_3), 15.2, (C6'). **HRMS** (ESI) m/z: [M + H^+] calcd for $C_{63}H_{63}N_3O_{18}H$ 1150.41794, found 1150.41741.

N$^\gamma$-[2,3,4,6-tetra-O-acetyl-β-D-galactopyranoside-(1→4)-6,3-di-O-acetyl-2-deoxy-2-acetamido-β-D-glucopyranosyl]-N$^\alpha$-fluorenylmethoxycarbonyl-L-asparagine (3)

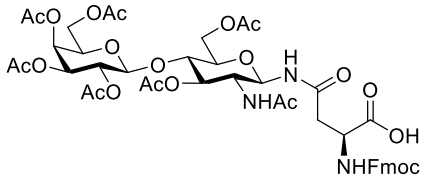

Glycosyl azide **20** (0.74 mmol, 488 mg) was dissolved in THF (7.4 mL) and a 1 M solution of trimethylphosphine in THF (1.5 eq, 1.1 mL, 1.1 mmol) was added and the reaction was stirred at room temperature. H_2O (50 eq, 0.67 mL, 37 mmol) was added and the

reaction was further stirred for 60 minutes. The volatiles were removed *in vacuo* and the crude glycosyl amine was redissolved in DMSO (7.4 mL). Fmoc-aspartic anhydride (1 eq, 0.74 mmol, 249 mg) was added and the reaction was stirred for 75 minutes. The solvent was removed *in vacuo* and the crude was subjected to silica gel column chromatography (0 → 8% MeOH in DCM, Δ = 1%) to yield the title product (455 mg, 0.47 mmol, 63%). $[\alpha]_D^{20}$ = +0,2 (c 1.00 in MeOH) **^{1}H NMR** (400 MHz, DMSO-d6) δ 8.58 (d, J = 9.1 Hz, 1H, N$^{\gamma}$H), 7.89 (d, *J* = 7.7 Hz, 2H, Fmoc-Ar), 7.86 (d, J = 9.5 Hz, 1H, NHC(O)CH$_3$), 7.71 (d, J = 7.5 Hz, 2H, Fmoc-Ar), 7.42 (t, J = 7.3 Hz, 3H, Fmoc-Ar, N$^{\alpha}$H), 7.33 (t, J = 7.4 Hz, 2H, Fmoc-Ar), 5.23 (d, J = 3.7 Hz, 1H, H4'), 5.16 (dd, J = 10.3, 3.6 Hz, 1H, H3'), 5.10 (t, J = 9.5 Hz, 1H, H1), 4.97 (t, J = 9.5 Hz, 1H, H3), 4.84 (dd, J = 10.3, 8.0 Hz, 1H, H2'), 4.70 (d, J = 8.0 Hz, 1H, H1'), 4.36 – 4.15 (m, 6H, Asn-CH, Fmoc-CH$_2$, H6a, H5', Fmoc-CH), 4.09 – 3.95 (m, 3H, H6b, H6'), 3.81 (q, J = 9.5 Hz, 1H, H2), 3.73 – 3.55 (m, 2H, H4, H5), 2.63 (dd, J = 16.3, 5.3 Hz, 1H, Asn-CH$_2$), 2.11 (s, 3H, C(O)CH$_3$), 2.07 (s, 3H, C(O)CH$_3$), 2.01 (s, 3H, C(O)CH$_3$), 2.01 (s, 3H, C(O)CH$_3$), 1.94 (s, 3H, C(O)CH$_3$), 1.90 (s, 3H, C(O)CH$_3$), 1.71 (s, 3H, NH(CO)CH$_3$). **^{13}C NMR** (101 MHz, DMSO-d6) δ = 173.1 (C=O), 170.4 (C=O), 170.0 (C=O), 169.9 (C=O), 169.6 (C=O), 169.5 (C=O), 169.3 (C=O), 169.2 (C=O), 155.8 (C=O), 143.8 (Fmoc-Ar), 140.7 (Fmoc-Ar), 127.7 (Fmoc-Ar), 127.1 (Fmoc-Ar), 125.3 (Fmoc-Ar), 120.2 (Fmoc-Ar), 99.9 (C1'), 77.9 (C1), 76.2 (C4), 73.8 (C3), 73.5 (C5), 70.4 (C3'), 69.7 (C5'), 68.9 (C2'), 67.1 (C4'), 65.7 (Fmoc-CH$_2$), 62.5 (C6), 60.9 (C6'), 52.3 (C2), 50.3 (Asn-CH), 46.6 (Fmoc-CH), 37.1 (Asn-CH$_2$), 22.7 (NHC(O)CH$_3$), 20.7 (C(O)CH$_3$), 20.6 (C(O)CH$_3$), 20.5 (C(O)CH$_3$), 20.4 (C(O)CH$_3$), 20.4 (C(O)CH$_3$) **HRMS** (ESI) m/z: [M + H$^+$] calcd for $C_{45}H_{53}N_3O_{21}H$ 972.32443, found 972.32357

N$^{\gamma}$-{2,3,4,6-tetra-O-acetyl-β-D-galactopyranoside-(1→4)-[3,4-di-O-benzoyl-2-O-(4-methoxybenzyl)-α-L-fucopyranoside-(1→3)]-6-O-(4-methoxybenzyl)-2-deoxy-2-acetamido-β-D-glucopyranosyl}-N$^{\alpha}$-fluorenylmethoxycarbonyl-L-asparagine (4)

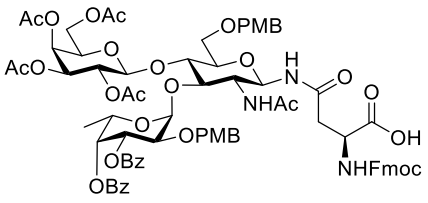

Glycosyl azide **5** (53 mg, 45 µmol) was dissolved in dry THF (0.45 mL) and cooled to 0°C in an icebath. 75 µL of a 1 M trimethylphosphine solution in THF was added dropwise. The reaction was stirred for 5 minutes at 0°C and for 5 minutes at room temperature. H_2O (50 eq, 40 µL, 2.25 mmol) was added and the reaction was stirred for 2 hours at room temperature. The volatiles were removed *in vacuo* and the crude glycosyl amine was redissolved in DMA (450 µL). The reaction mixture was again cooled in an icebath and aspartic anhydride[45] (1 eq, 15 mg, 45µmol) was added. The reaction was stirred and allowed to warm to room temperature overnight. The solvent was removed by evaporation and the crude glycoaminoacid was subjected to silica gel column chromatography (0 → 25% acetone in DCM + 0.5% acetic acid, $\Delta_{acetone}$ = 5%) to yield the title compound (49 mg, 33 µmol, 73%). Traces of acetic acid were removed by sequential co-evaporation with dioxane (3 x 2 mL), toluene (3 x 2 mL) and $CHCl_3$ (3 x 2 mL). $[\alpha]_D^{25}$ = -94.2 (c 1.00 in $CHCl_3$). **^{1}H NMR** (400 MHz, $CDCl_3$) δ 7.98 – 7.89 (m, 2H, CH_{arom}), 7.78 – 7.64 (m, 5H, N$^{\gamma}$H, CH_{arom}), 7.64 – 7.51 (m, 3H, CH_{arom}), 7.51 – 7.40 (m, 3H, CH_{arom}), 7.40 – 7.19 (m, 9H, NHC(O)CH$_3$, CH_{arom}), 7.07 (d, J = 8.6 Hz, 2H, CH_{arom}), 6.91 (d, J = 8.6 Hz, 2H, CH_{arom}), 6.66 (d, J = 8.3 Hz, 2H, CH_{arom}), 6.41 (d, J = 8.4 Hz, 1H, N$^{\alpha}$H), 5.63 – 5.54 (m, 2H, H4', H3'), 5.47 (d, J = 3.4 Hz, 1H, H1'), 5.33 (d, J = 3.7 Hz, 1H, H4'), 5.09 (dd, J = 10.4, 8.0 Hz, 1H, H2''), 4.99 (t, J = 7.8 Hz, 1H, H1), 4.85 (dd, J = 10.4, 3.6 Hz, 1H, H3''), 4.81 – 4.70 (m, 1H, H5'), 4.69 – 4.43 (m, 5H, PMB-CH$_2$, Asn-CH, Fmoc-CH, H1''), 4.39 – 4.22 (m, 5H, Fmoc-CH$_2$, PMB-CHH, H6''), 4.22 – 4.03 (m, 4H, PMB-CHH, H2, H2', H4), 3.95 (t, J = 8.4 Hz, 1H, H3), 3.82 – 3.63 (m, 8H, OCH$_3$, H6, OCH$_3$), 3.57 – 3.44 (m, 2H, H5, H5''), 2.90 – 2.72 (m, 2H, Asn-

CH_2), 2.17 (s, 3H, C(O)CH_3), 2.07 – 1.91 (m, 12H, 4 x C(O)CH_3), 1.24 (d, J = 6.5 Hz, 3H, H6'). **^{13}C NMR** (101 MHz, $CDCl_3$) δ = 173.5 (C=O), 173.2 (C=O), 171.8 (C=O), 170.5 (C=O), 170.4 (C=O), 170.0 (C=O), 169.8 (C=O), 165.9 (C=O), 165.3 (C=O), 159.6 (C_q), 159.5 (C_q), 156.4 (C=O), 143.9 (Fmoc-Ar), 143.7 (Fmoc-Ar), 141.2 (Fmoc-Ar), 141.2 (Fmoc-Ar), 133.3 (CH_{arom}), 133.1 (CH_{arom}), 130.3 (CH_{arom}), 129.8 (CH_{arom}), 129.7 (CH_{arom}), 129.6 (CH_{arom}), 129.6 (C_q), 129.5 (C_q), 128.9 (C_q), 128.5 (CH_{arom}), 128.3 (CH_{arom}), 127.7 (CH_{arom}), 127.1 (CH_{arom}), 125.3 (CH_{arom}), 125.2 (CH_{arom}), 119.9 (CH_{arom}), 114.1 (CH_{arom}), 114.0 (CH_{arom}), 99.4 (C1''), 97.4 (C1'), 79.7 (C1), 76.0 (C5, C3), 73.3 (C4), 73.3 (C2'), 73.3 (PMB-CH_2), 72.7 (PMB-CH_2), 72.5 (C4'), 71.0 (C5''), 70.8 (C3''), 70.1 (C3'), 69.3 (C2''), 67.8 (C6), 67.2 (Fmoc-CH_2), 66.9 (C4''), 65.8 (C5'), 61.0 (C6''), 55.3 (OCH_3), 55.2 (OCH_3), 53.6 (C2), 50.5 (Asn-CH), 47.1 (Fmoc-CH), 37.9 (Asn-CH_2), 22.8 (NHC(O)$\underline{C}H_3$), 20.8 (C(O)$\underline{C}H_3$), 20.8 (C(O)$\underline{C}H_3$), 20.7 (C(O)$\underline{C}H_3$), 20.6 (C(O)$\underline{C}H_3$), 16.1 (C6'). **HRMS** (ESI) m/z: [M + Na^+] calcd for $C_{77}H_{83}N_3O_{27}Na$ 1504.51061, found 1504.51004

Azido 3,4,6-tri-O-acetyl-2-deoxy-2-acetamido-β-D-glucopyranoside (11)

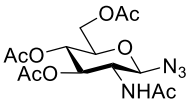

N-acetyl glucosamine was converted into the 2-acetamido-3,4,6-tri-*O*-acetyl-2-deoxy-α-D-glucopyranosyl chloride as described by Horton[47]. Briefly, N-acetyl glucosamine (11.0 g, 50 mmol) was carefully added to acetyl chloride (25.0 ml, 350 mmol). The resulting suspension was heated to 30°C for 30 minutes, followed by overnight stirring at room temperature. The reaction mixture was diluted with chloroform (100 mL) and washed with ice water (100 g ice and 25 mL water). The organic layer was washed with ice cold saturated $NaHCO_{3\ (aq)}$ (100 mL) and dried over $MgSO_4$. The solution was concentrated to 20% of the original volume and Et_2O (100 mL) was added. The product was allowed to crystalized overnight to yield 2-acetamido-3,4,6-tri-*O*-acetyl-2-deoxy-α-D-glucopyranosyl chloride in a 3.6:1 mixture with 2-acetamido-3,4,6-tri-*O*-acetyl-2-deoxy-α-D-glucopyranosyl acetate, which was collected by filtration and dried *in vacuo*. This mixture was used without further purification in the next step. The crude glycosyl chloride was dissolved in DMF (125 mL) and NaN_3 (3.25 g, 50 mmol) was added. The reaction was stirred for 2 hours at room temperature until TLC (100% EtOAc) confirmed complete consumption of the glycosyl chloride. The reaction mixture was diluted with saturated aqueous $NaHCO_3$ and the product was extracted with DCM. The organic layer was washed with a second portion of saturated aqueous $NaHCO_3$ and dried over $MgSO_4$, filtered and concentrated. The mixture containing the β-glycosyl azide and α-glycosyl acetate was dissolved in THF (125 mL) and N,N-dimethylaminopropylamine (70 mmol, 8.8 mL) was added. The reaction mixture was stired at room temperature two hours, resulting in the selective hydrolysis of the anomeric acetate as described by Andersen et al.[48] The reaction mixture was diluted with DCM and washed with 1 M aqueous HCl. The organic layer was dried over $MgSO_4$, filtered and concentrated. Silica gel column chromatography (80% EtOAc in DCM) gave the title compound (7.82 g, 21 mmol, 42%). $\mathbf{[\alpha]_D^{25}}$ = -41.6° (c 1.00 in $CHCl_3$) $\mathbf{\nu_{max}/cm^{-1}}$ 2117.80 (N_3), 1747.18 (CO), 1664.19 (CO) **^{1}H NMR** (400 MHz, $CDCl_3$) δ 5.66 (d, J = 8.9 Hz, 1H, NH), 5.25 (dd, J = 10.6, 9.3 Hz, 1H, H3), 5.11 (t, J = 9.7 Hz, 1H, H4), 4.76 (d, J = 9.3 Hz, 1H, H1), 4.28 (dd, *J* = 12.5, 4.8 Hz, 1H, H6a), 4.17 (dd, J = 12.4, 2.3 Hz, 1H, H6b), 3.92 (dt, J = 10.7, 9.1 Hz, 1H, H2), 3.79 (ddd, J = 10.0, 4.8, 2.3 Hz, 1H, H5), 2.11 (s, 3H, C(O)CH_3), 2.05 (s, 3H, C(O)CH_3), 2.04 (s, 3H, C(O)CH_3), 1.99 (s, 3H, C(O)CH_3) **^{13}C NMR** (101 MHz, $CDCl_3$) δ = 171.0 (C=O), 170.8 (C=O), 170.7 (C=O), 169.4 (C=O), 88.5 (C1), 74.0 (C5), 72.2 (C3), 68.3 (C4), 62.0 (C6), 54.1 (C2), 23.3 (NHC(O)$\underline{C}H_3$), 20.8 (C(O)$\underline{C}H_3$), 20.7 (C(O)$\underline{C}H_3$), 20.7 (C(O)$\underline{C}H_3$) **HRMS** (ESI) m/z: [M + H^+] calcd for $C_{14}H_{20}N_4O_8H$ 373.13539, found 373.13521.

Azido 2-deoxy-2-acetamido-β-D-glycopyranoside (12)

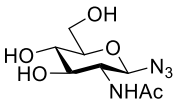

Acetylated glycosyl azide **11** (4.3g, 11.6 mmol) was dissolved in methanol (115 mL) and put under inert atmosphere. Elemental sodium was added until the pH reached 11 (as indicated by wet pH paper) and the reaction was stirred at room temperature for 2 hours, after which TLC (100% EtOAc) indicated full consumption of starting material. The reaction was neutralized with amberlite H^+ resin and the resin was filtered off. The volatiles were removed *in vacuo* to yield the title compound in quantitative yield. This compound was used without further purification. **ν_{max}/cm^{-1}** 2117.80 (N_3) 1644.16 (CO) **^{1}H NMR** (400 MHz, MeOD) δ 4.51 (d, J = 9.2 Hz, 1H, H1), 3.90 (dd, J = 12.1, 1.8 Hz, 1H, H6a), 3.74 – 3.63 (m, 2H, H6b, H2), 3.47 (dd, J = 9.6, 8.5 Hz, 1H, H3), 3.41 – 3.36 (m, 2H, H4, H5), 2.00 (s, 3H, NHC(O)C$\underline{H}_3$) **^{13}C NMR** (101 MHz, MeOD) δ 173.8 (C=O), 90.1 (C1), 80.3 (C4), 75.7 (C3), 71.6 (C5), 62.6 (C6), 56.7 (C2), 22.9 (NHC(O)$\underline{C}H_3$) **HRMS** (ESI) m/z: [M + H+] calcd for C8H14N4O5H 247.10370, found 247.10360

Azido 4,6-O-(4-methoxybenzylidene)-2-deoxy-2-acetamido-β-D-glucopyranoside (9)

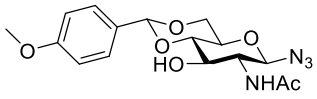

Deacetylated glycosyl azide **12** (492 mg, 2.0 mmol) was suspended in dry acetonitrile (8 mL) and anisaldehyde dimethyl acetal (2 eq., 660 µL, 4.0 mmol) and CSA (0,1 eq., 46 mg, 0,2 mmol) were added. The reaction was kept at 50 °C and 300 mbar on a rotary evaporator for 3h. The reaction was quenched by the addition of trimethylamine (100 µL) and the volatiles were removed under reduced pressure. The crude was recrystallized from methanol to yield the title compound (475 mg, 1,3 mmol, 65%) **$[\alpha]_D^{25}$** = -70.0° (c 0.10 in $CHCl_3$) **ν_{max}/cm^{-1}** 2114.94 (N_3), 1651.31 (CO) **^{1}H NMR** (400 MHz, DMSO-d_6) δ 7.99 (d, J = 8.4 Hz, 1H, NH), 7.37 (d, J = 8.8 Hz, 2H, CH_{arom}), 6.93 (d, J = 8.8 Hz, 2H, CH_{arom}), 5.57 (s, 1H, PMP-CH_{acetal}), 5.45 (d, J = 5.2 Hz, 1H, 3-OH), 4.60 (d, J = 8.8 Hz, 1H, H1), 4.21 (dd, J = 10.1, 4.3 Hz, 1H, H6), 3.75 (s, 3H, OCH_3), 3.74 – 3.44 (m, 5H, H6, H2, H3, H4, H5), 1.86 (s, 3H, NHC(O)C$\underline{H}_3$) **^{13}C NMR** (101 MHz, DMSO-d_6) δ 169.62 (NH$\underline{C}$(O)CH_3), 159.63, 129.98 (C_q), 127.74, 113.38 (CH_{arom}), 100.73 (PMP-$\underline{C}$H), 88.83 (C1), 80.79 (C4), 70.26 (C3), 68.19 (C5), 67.49 (C6), 55.42 (C2), 55.16 (OCH_3), 22.97 (NHC(O)$\underline{C}H_3$) **HRMS** (ESI) m/z: [M + H^+] calcd for $C_{16}H_{20}N_4O_6H$ 365.14556, found 365.14532

Azido 6-(*tert*-butyldimethylsilyl)-2-deoxy-2-acetamido-β-D-glucopyranoside (13)

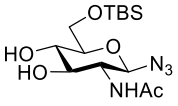

Deacetylated glycosyl azide **12** (1.23 g, 5 mmol) was co-evaporated three times with toluene and dissolved in 50 mL of dry pyridine. TBS-Cl (1.5 eq, 2.7 mL, 7.5 mmol) was added and the reaction was stirred at room temperature. After 2 hours, TLC (10% MeOH in EtOAc) indicated complete consumption of the starting material. The reaction mixture was poured into H_2O (100 mL) and transferred to a separatory funnel. DCM (200 mL) and 1 M HCl (aq) (100 mL) were added and the organic layer was collected. The organic layer was dried over $MgSO_4$, filtered and concentrated. Traces of pyridine were removed with toluene co-evaporation. Silica gel column chromatography (0% → 1% → 2% → 5% → 10% MeOH in EtOAc) yielded the title compound (1.51 g, 4.19 mmol, 84%). **$[\alpha]_D^{20}$** = -57,4 (c 1.00 in $CHCl_3$) **ν_{max}/cm^{-1}** 2114.94 (N_3), 1648.45 (CO) **^{1}H NMR** (400 MHz, $CDCl_3$) δ 6.90 (d, J = 7.9 Hz, 1H, NH), 5.08 (d, J = 4.2 Hz, 1H, 3-OH), 4.63 (d, J = 8.7 Hz, 1H, H1), 4.30 (d, J = 3.2 Hz, 1H, 4-OH), 3.91 (ddd, J = 19.5, 11.2, 4.1 Hz, 2H, H6), 3.73 – 3.56 (m, 2H, H2, H3), 3.52 (td, J = 8.8, 8.4, 3.2 Hz, 1H, H4), 3.42 (dt, J = 8.8, 4.5 Hz, 1H, H5), 2.04 (s, 3H, NHC(O)C$\underline{H}_3$), 0.91 (s, 9H, tBu), 0.11 (d, J = 1.3 Hz, 6H, Si-CH_3) **^{13}C NMR** (101 MHz, $CDCl_3$) δ = 172.7 (C=O), 88.5 (C1), 77.7 (C5), 74.5 (C3),

71.6 (C4), 63.6 (C6), 55.4 (C2), 25.9 (tBu), 23.3 (NHC(O)$\underline{C}H_3$), 18.4 (Si-C), -5.2 (Si-CH_3) **HRMS** (ESI) m/z: [M + Na^+] calcd for $C_{14}H_{28}N_4O_5SiNa$ 383.1721, found 383.1729

2,3,4,6-tetra-O-acetyl-α-D-galactopyranosyl trichloroacetimidate (8)

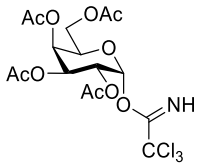

1,2,3,4,6-tetra-O-acetyl-β-D-galactopyranose (7.8 g, 20 mmol) was dissolved in dry THF (100 mL) and N,N-dimethylaminopropylamine (5 eq, 12,8 mL) was added according to the procedure of Andersen *et al.*[48] The reaction was stirred at room temperature for 1.5 hours, after which TLC (1/1 EtOAc/pentane) showed full conversion. The reaction was diluted with DCM and washed with 1 M aqueous HCl. The organic layer was collected, dried over $MgSO_4$, filtered and concentrated. The crude was co-evaporated once with toluene and dissolved in dry DCM (100 mL). Trichloroacetonitrile (5 eq, 10 mL, 100 mmol) and DBU (0.1 eq, 0.3 mL, 2 mmol) were added. The reaction was stirred at room temperature for 1 h, after which TLC (1/1 EtOAc/pentane) showed full conversion. Celite was added to the reaction and the volatiles were removed *in vacuo*. Silica gel column chromatography on neutralized silica (30% → 40% → 50% Et_2O in pentane) yielded the title compound (5.87 g, 11.6 mmol, 58%, corrected for residual diethyl ether), which was immediately stored at -20°C under an N_2 atmosphere. **^{1}H NMR** (400 MHz, $CDCl_3$) δ 8.69 (s, 1H, NH), 6.60 (d, J = 3.5 Hz, 1H, H1), 5.57 (dd, J = 3.2, 1.3 Hz, 1H, H4), 5.43 (dd, J = 10.8, 3.2 Hz, 1H, H3), 5.36 (dd, J = 10.8, 3.5 Hz, 1H, H2), 4.49 – 4.41 (m, 1H, H5), 4.17 (dd, J = 11.3, 6.6 Hz, 1H, H6a), 4.09 (dd, J = 11.3, 6.7 Hz, 1H, H6b), 2.18 (s, 3H, C(O)CH_3), 2.04 (s, 3H, C(O)CH_3), 2.03 (s, 3H, C(O)CH_3), 2.02 (s, 3H, C(O)CH_3) **^{13}C NMR** (101 MHz, $CDCl_3$) δ 170.4 (C=O), 170.2 (C=O), 170.0 (C=O), 161.0 (C=NH), 93.6 (C1), 69.0 (C5), 67.6 (C3), 67.4 (C4), 66.9 (C2), 61.3 (C6), 20.7 (C(O)$\underline{C}H_3$), 20.7 (C(O)$\underline{C}H_3$), 20.7 (C(O)$\underline{C}H_3$), 20.6 (C(O)$\underline{C}H_3$)

Phenyl 3,4-O-isopropylidene-1-thio-L-fucopyranoside (14)

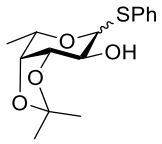

L-fucose (16,4 g, 100 mmol) was suspended in ethyl acetate (250 mL) and pyridine (7.5 eq., 60 mL, 750 mmol) was added. The mixture was cooled in an icebath and acetic anhydride (7.5, eq., 70 mL, 750 mmol) and DMAP (0.1 eq., 1,2 g, 10 mmol) were added. The reaction was stirred and allowed to warm to room temperature. After 4 hours, TLC indicated starting material consumption and all compound was dissolved. The reaction was again cooled with an icebath and methanol was added to quench the reaction. The organic phase was washed with 1 M HCl, saturated $NaHCO_3$ and brine, dried over $MgSO_4$, filtered, and concentrated. This compound was used in the next reaction without purification. **^{1}H NMR** (400 MHz, $CDCl_3$) δ 6.34 (d, J = 3.0 Hz, 1H, H1), 5.39 – 5.28 (m, 3H, H2, H3, H4), 4.28 (q, J = 6.6 Hz, 1H, H5), 2.19 (s, 3H, C(O)CH_3), 2.16 (s, 3H, C(O)CH_3), 2.02 (s, 3H, C(O)CH_3), 2.01 (s, 3H, C(O)CH_3), 1.16 (d, J = 6.6 Hz, 3H, H6) **^{13}C NMR** (101 MHz, $CDCl_3$) δ 170.5 (C=O), 170.2 (C=O), 170.0 (C=O), 169.2 (C=O), 90.0 (C1), 70.6, 67.8, 67.3, 66.5 (C2, C3, C4, C5), 21.0 (C(O)$\underline{C}H_3$), 20.7 (C(O)$\underline{C}H_3$), 20.6 (C(O)$\underline{C}H_3$), 20.6 (C(O)$\underline{C}H_3$), 16.0 (C6). The intermediate was coevaporated once with toluene and then dissolved in toluene (100 mL). Thiophenol (1.1 eq., 11,3 mL, 110 mmol) was then added and the mixture was cooled in an icebath. $BF_3{\cdot}Et_2O$ (3.0 eq., 37 mL, 300 mmol) was added and after 15 minutes the icebath was removed. After one hour TLC indicated complete consumption of the starting material. The reaction was diluted with toluene and washed five

times with saturated aqueous $NaHCO_3$. The organic phase was dried over $MgSO_4$, filtered, and concentrated to yield the thioglycoside in a 1:4 α:β ratio. This compound was used in the next reaction without purification. **^{1}H NMR** (300 MHz, $CDCl_3$) δ 7.55 – 7.24 (m, 6H, CH_{arom}), 5.94 (d, J = 4.9 Hz, 1H, H1α), 5.40 – 5.29 (m, 3H, H2α, H3α, H4α), 5.27 (dd, J = 3.3, 1.2 Hz, 1H, H4β), 5.21 (t, J = 9.9 Hz, 1H, H2β), 5.05 (dd, J = 9.9, 3.3 Hz, 1H, H3β), 4.71 (d, J = 9.9 Hz, 1H, H1β), 4.61 (q, J = 6.5 Hz, 1H, H5α), 3.84 (q, J = 6.4 Hz, 1H, H5β), 2.17 (s, 3H, C(O)CH_3 (α)), 2.15 (s, 3H, C(O)CH_3 (β)), 2.10 (s, 3H, C(O)CH_3 (α)), 2.09 (s, 3H, C(O)CH_3 (β)), 2.02 (s, 3H, C(O)CH_3 (α)), 1.98 (s, 3H, C(O)CH_3 (β)), 1.24 (d, J = 6.4 Hz, 3H, C6β), 1.13 (d, J = 6.5 Hz, 3H, C6α) **^{13}C NMR** (75 MHz, $CDCl_3$) δ 170.7 (C=O), 170.2 (C=O), 169.6 (C=O), 132.4 $C(C_q)$, 131.8 (CH_{arom}), 129.2 (CH_{arom}), 129.0 (CH_{arom}), 128.0 (CH_{arom}), 127.6 (CH_{arom}), 86.6 (C1β), 85.6 (C1α), 73.2 (C5β), 72.5 (C3β), 71.0 (C4α), 70.4 (C4β), 68.7, 68.2 (C2α, C3α), 67.4 (C2β), 65.6 (C5α), 21.0 (C(O)$\underline{C}H_3$), 20.7 (C(O)$\underline{C}H_3$), 16.6 (C6β), 16.0 (C6α). The acetylated thioglycoside was suspended in methanol (500 mL). Metallic sodium was added until the pH was 12 and the reaction was left to stir overnight. The reaction was neutralized with amberlite H^+ resin, filtered and concentrated to give the deacetylated intermediate. This compound was used in the next reaction without purification. **^{1}H NMR** (400 MHz, MeOD) δ 7.56 – 7.45 (m, 2H, CH_{arom}), 7.32 – 7.18 (m, 4H, CH_{arom}), 5.60 (d, J = 5.6 Hz, 1H, H1α), 4.58 (d, J = 9.6 Hz, 1H, H1β), 4.40 (q, J = 6.6 Hz, 1H, H5α), 4.17 (dd, J = 10.1, 5.6 Hz, 1H, H2α), 3.75 – 3.70 (m, 2H, H3α, H4α), 3.70 – 3.57 (m, 3H, H4β, H2β, H5β), 3.53 (dd, J = 9.2, 3.3 Hz, 1H, H3β), 1.25 (d, J = 6.5 Hz, 3H, H6β), 1.19 (d, J = 6.6 Hz, 3H, H6α). **^{13}C NMR** (101 MHz, MeOD) δ 132.8 (C_q), 131.9 (CH_{arom}), 129.8 (CH_{arom}), 129.7 (CH_{arom}), 127.9 (CH_{arom}), 91.0 (C1α), 89.7 (C1β), 76.2 (C3β), 75.7 (C5β), 73.2 (C3α), 72.9 (C4β), 72.3 (C4α), 70.6 (C2β), 69.5 (C2α), 68.5 (C5α), 17.0 (C6β), 16.5 (C6α). The crude triol was dissolved in acetone (500 mL). 2,2-Dimethoxypropane (4.0 eq., 49 mL, 400 mmol) and CSA (0,1 eq., 2,3 g, 10 mmol) were added. The reaction was stirred at room temperature for 1 hour, after which TLC analysis indicated consumption of stating material. The reaction was quenched with Et_3N (2 mL) and concentrated. Silica gel column chromatography (50% Et_2O/pentane) yielded the title compound as an inseparable mixture of anomers (1:4, α:β) (23,7 g, 80 mmol, 80%). **^{1}H NMR** (400 MHz, $CDCl_3$) δ 7.62 – 7.46 (m, 2H, CH_{arom}), 7.36 – 7.25 (m, 4H, CH_{arom}), 5.56 (d, *J* = 4.9 Hz, 1H, H1α), 4.57 (qd, *J* = 6.6, 2.3 Hz, 1H, H5α), 4.43 (d, *J* = 10.2 Hz, 1H, H1β), 4.20 – 4.08 (m, 3H, H2α, H3α, H4α), 4.08 – 4.02 (m, 2H, H3β, H4β), 3.88 (qd, *J* = 6.6, 2.0 Hz, 1H, H5β), 3.55 (ddd, *J* = 10.2, 6.4, 2.5 Hz, 1H, H2β), 2.72 (d, *J* = 6.0 Hz, 1H, 2-OHα), 2.65 (d, *J* = 2.5 Hz, 1H, 2-OHβ), 1.52 (s, 3H, C(CH_3)$C\underline{H}_3$ α), 1.46 – 1.41 (m, 6H, H6β, C(CH_3)$C\underline{H}_3$ β), 1.38 – 1.35 (m, 6H, H6α, C($C\underline{H}_3$)CH_3 α), 1.35 (s, 3H, C($C\underline{H}_3$)CH_3 β). **^{13}C NMR** (101 MHz, $CDCl_3$) δ 132.7 (CH_{arom}), 132.3 (C_q), 131.4 (CH_{arom}), 129.2 (CH_{arom}), 129.0 (CH_{arom}), 128.1 (CH_{arom}), 127.4 (CH_{arom}), 110.0 ($C_{q,acetal}$β), 109.5 ($C_{q,acetal}$α), 88.4 (C1α), 87.9 (C1β), 79.2 (C3β), 76.4 (C4β), 75.9 (C3α, C4α), 72.9 (C5β), 71.4 (C2β), 70.1 (C2α), 65.5 (C5α), 28.2 (C(CH_3)$\underline{C}H_3$ β), 28.0 (C(CH_3)$\underline{C}H_3$ α), 26.5 (C($\underline{C}H_3$)CH_3 β), 26.1 (C($\underline{C}H_3$)CH_3 α), 17.1 (C6β), 16.4 (C6α) **HRMS** (ESI) m/z: [M + Na^+] calcd for $C_{15}H_{20}O_4SNa$ 319.09745, found 319.09718

Phenyl 3,4-O-isopropylidene-2-O-(4-methoxybenzyl)-1-thio-L-fucopyranoside (15)

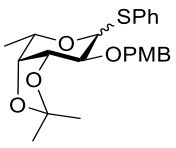

Thioglycoside **14** (1.48 g, 5.0 mmol) was dissolved in dry DMF (25 mL). The reaction was cooled in an icebath and a 60% w/w NaH dispersion in mineral oil (1,2 eq., 240 mg, 6.0 mmol) was added. The reaction was stirred for 15 minutes before PMB-Cl (2 eq., 1,56 g, 10 mmol) was added. The reaction was cooled for an additional 15 minutes before the icebath was removed. The reaction was then stirred for an additional 2 hours at room temperature. The reaction mixture was diluted with chloroform, and washed twice with water

and once with brine. The organics were dried over $MgSO_4$, filtered and concentrated. Silicagel column chromatography (10% → 15% → 20% Et_2O in pentane) gave the title compound (1.75 g, 4.2 mmol, 84%) as a mixture of anomers (1:9, α:β). **^{1}H NMR** (400 MHz, $CDCl_3$) δ 7.52 (d, J = 7.4 Hz, 2H, CH_{arom}β), 7.47 (d, J = 7.7 Hz, 2H, CH_{arom}α), 7.33 (d, J = 8.2 Hz, 2H, CH_{arom}), 7.30 – 7.12 (m, 4H, CH_{arom}), 6.85 (d, J = 8.2 Hz, 2H, CH_{arom}), 5.58 (d, J = 5.2 Hz, 1H, H1α), 4.74 (d, J = 10.9 Hz, 1H, PMB-CH_2β), 4.71 – 4.61 (m, 2H, PMB-CH_2α), 4.61 – 4.45 (m, 3H, PMB-CH_2β, H1β, H5α), 4.27 (t, J = 6.3 Hz, 1H, H3α), 4.18 (t, J = 5.9 Hz, 1H, H3β), 4.05 (d, J = 5.3 Hz, 1H, H4α), 3.97 (d, *J* = 5.9 Hz, 1H, H4β), 3.86 (t, J = 6.0 Hz, 1H, H2α), 3.81 – 3.65 (m, 4H, OCH_3, H5β), 3.47 (dd, J = 9.7, 5.9 Hz, 1H, H2β), 1.40 (s, 3H, C(CH_3)C$\underline{H}_3$), 1.36 (d, J = 6.7 Hz, 3H, H6β), 1.34 (s, 3H, C(C$\underline{H}_3$)CH_3), 1.27 (d, J = 6.7 Hz, 3H, H6α) **^{13}C NMR** (101 MHz, $CDCl_3$) δ 159.2 (C_q), 133.7 (C_q), 131.8 (CH_{arom}), 130.6 (CH_{arom}), 130.0 (CH_{arom}), 129.8 (CH_{arom}), 129.5 (CH_{arom}), 128.8 (CH_{arom}), 128.7 (CH_{arom}), 127.2 (CH_{arom}), 126.6 (CH_{arom}), 113.7 (CH_{arom}), 113.6 (CH_{arom}), 109.5 ($C_{q,acetal}$β), 109.1 ($C_{q,acetal}$α), 85.9 (C1β), 85.7 (C1α), 79.7 (C3β), 77.6 (C2β), 76.3 (C4β), 75.7 (C4α), 75.4 (C2α), 74.5 (C3α), 72.9 (PMB-CH_2), 72.2 (C5β), 64.9 (C5α), 55.1 (OCH_3), 27.8 (C(CH_3)C$\underline{H}_3$β), 27.6 (C(CH_3)C$\underline{H}_3$α), 26.3 (C(C$\underline{H}_3$)CH_3β), 25.9 (C(C$\underline{H}_3$)CH_3α), 16.8 (C6β), 16.2 (C6α) **HRMS** (ESI) m/z: [M + H^+] calcd for $C_{23}H_{28}O_5SH$ 417.17302, found 417.17284

Phenyl 3,4-di-O-benzoyl-2-O-(4-methoxybenzyl)-1-thio-L-fucopyranoside (10)

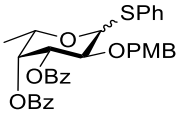

Thioglycoside **15** (7.98g, 19.2 mmol) was suspended in water (50 mL) and acetic acid (50 mL) and heated to 80°C for one hour. The volatiles were removed under reduced pressure and were further removed with toluene co-evaporation. The crude intermediate was then dissolved in pyridine (125 mL) and cooled in an icebath. Benzoyl chloride (3.0 eq., 6.8 mL, 57.6 mmol) was added and the reaction was stirred at room temperature for 2 hours. The reaction was quenched with water, diluted with ethyl acetate and washed successively with 1 M HCl and saturated $NaHCO_3$. The organic layer was dried over $MgSO_4$, filtered and concentrated. Silica gel column chromatography (10% → 20% → 30% Et_2O in pentane) gave the title compound (7.19 g, 12.3 mmol, 64%) as a mixture of anomers (1:4, α:β). **^{1}H NMR** (400 MHz, $CDCl_3$) δ 8.00 – 7.90 (m, 3H, CH_{arom}), 7.85 – 7.67 (m, 5H, CH_{arom}), 7.67 – 7.56 (m, 2H, CH_{arom}), 7.56 – 7.42 (m, 5H, CH_{arom}), 7.42 – 7.34 (m, 3H, CH_{arom}), 7.34 – 7.16 (m, 4H, CH_{arom}), 7.11 – 7.04 (m, 2H, CH_{arom}), 6.74 (d, J = 8.7 Hz, 2H, CH_{arom}), 6.70 – 6.61 (m, 2H CH_{arom}), 5.80 (d, J = 5.4 Hz, 1H, C1α), 5.69 (dd, J = 3.3, 1.1 Hz, 1H, H4α), 5.63 (dd, J = 3.3, 0.9 Hz, 1H, H4β), 5.42 (dd, J = 9.6, 3.3 Hz, 1H, H3β), 4.80 (d, J = 9.6 Hz, 1H, H1β), 4.73 (d, J = 10.3 Hz, 1H, PMB-C$\underline{H}$Hβ), 4.67 (d, J = 12.0 Hz, 1H, PMB-C$\underline{H}$Hα), 4.57 (d, J = 12.0 Hz, 1H, PMB-CH$\underline{H}$α), 4.52 (d, J = 10.3 Hz, 1H, PMB-CH$\underline{H}$β), 4.39 (dd, J = 10.5, 5.4 Hz, 1H, H2α), 4.02 (qd, *J* = 6.6, 0.9 Hz, 1H, H5β), 3.95 (t, J = 9.6 Hz, 1H, H2β), 3.74 (s, 3H, OCH_3α), 3.68 (s, 3H, OCH_3β), 1.32 (d, J = 6.6 Hz, 3H, H6β), 1.19 (d, J = 6.5 Hz, 3H, H6α) **^{13}C NMR** (101 MHz, $CDCl_3$) δ 165.9 (C=O), 165.5 (C=O), 159.3 (C_q), 133.5 (CH_{arom}), 133.4 (CH_{arom}), 133.2 (CH_{arom}), 133.1 (C_q), 132.8 (CH_{arom}), 131.7 (CH_{arom}), 130.0 (CH_{arom}), 129.9 (CH_{arom}), 129.8 (CH_{arom}), 129.8 (CH_{arom}), 129.7 (CH_{arom}), 129.6 (C_q), 129.6 (C_q), 129.1 (CH_{arom}), 128.9 (CH_{arom}), 128.6 (CH_{arom}) , 128.6 (CH_{arom}), 128.4 (CH_{arom}), 128.3 (CH_{arom}), 127.9 (CH_{arom}), 127.3 (CH_{arom}), 113.8 (CH_{arom}), 113.7 (CH_{arom}), 87.2 (C1α), 87.1 (C1β), 75.3 (C3β), 75.0 (PMB-CH_2β), 74.5 (C2β), 73.5 (C5α), 72.5 (C2α), 72.2 (C3α), 72.0 (PMB-CH_2α), 71.8 (C4β), 71.1 (C3α), 66.0 (C5α), 55.2 (OCH_3), 16.9 (C6β), 16.2 (C6α) **HRMS** (ESI) m/z: [M + NH_4^+] calcd for $C_{34}H_{32}O_7SNH_4$ 602.22070, found 602.22042

Azido 3,4-di-O-benzoyl-2-O-(4-methoxybenzyl)-α-L-fucopyranoside-(1→3)-4,6-O-(4-methoxybenzylidene)-2-deoxy-2-acetamido-β-D-glucopyranoside (16)

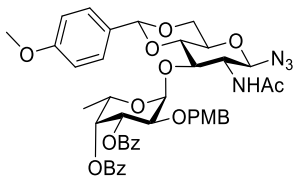

Donor **10** (1.5 eq., 1.76 mg, 3.0 mmol) and acceptor **9** (728 mg, 2.0 mmol) were co-evaporated 3 times with toluene, backfilling the flask with N_2 after every co-evaporation round, and placed under a N_2 atmosphere. The sugars were dissolved in dry DCM (36 mL) with dry DMF (4 mL). Activated 4Å molecular sieves (1 g) were added and the solution was stirred for 90 minutes. The reaction mixture was then cooled in an icebath and NIS (2.0 eq., 900 mg, 4.0 mmol) and TMSOTf (0.1 eq., 37 µL) were added. The reaction was stirred and allowed to warm to room temperature overnight. The reaction was filtered, diluted with DCM and washed with a 1:1 mixture of 10% $Na_2S_2O_3$ (aq) and saturated $NaHCO_3$ (aq). The organic layer was dried over $MgSO_4$, filtered and concentrated. Silica gel column chromatography (30% → 40% → 50% → 60% EtOAc in pentane) yielded the title compound (1.19 g, 1.42 mmol, 71%). $[\alpha]_D^{25}$ = -144.0 (c 1.00 in $CHCl_3$) **νmax/cm^{-1}** 2117.80 (N_3), 1724.29 (CO) **^{1}H NMR** (400 MHz, $CDCl_3$) δ 8.00 – 7.89 (m, 2H, CH_{arom}), 7.82 – 7.75 (m, 2H, CH_{arom}), 7.64 – 7.56 (m, 1H, CH_{arom}), 7.54 – 7.40 (m, 5H, CH_{arom}), 7.33 – 7.27 (m, 2H, CH_{arom}), 7.15 – 7.08 (m, 2H, CH_{arom}), 6.88 (d, J = 8.8 Hz, 2H, CH_{arom}), 6.74 (d, J = 8.6 Hz, 2H, CH_{arom}), 6.05 (d, J = 6.9 Hz, 1H, NH), 5.73 (dd, J = 10.5, 3.3 Hz, 1H, H3'), 5.53 (s, 1H, PMP-CH_{acetal}), 5.50 (dd, J = 3.4, 1.4 Hz, 1H, H4'), 5.28 (d, J = 9.3 Hz, 1H, H1), 5.15 (d, J = 3.5 Hz, 1H, H1'), 4.61 (d, J = 11.4 Hz, 1H, PMB-C<u>H</u>H), 4.54 (d, J = 11.4 Hz, 1H, PMB-CH<u>H</u>), 4.51 – 4.42 (m, 2H, H3, H5'), 4.38 (dd, J = 10.5, 4.2 Hz, 1H, H5), 4.13 (dd, J = 10.5, 3.4 Hz, 1H, H2'), 3.84 – 3.70 (m, 7H, 2 x OCH_3, H6a), 3.70 – 3.57 (m, 2H, H6b, H4), 3.25 (td, J = 9.3, 6.9 Hz, 1H, H2), 1.81 (s, 3H, NHC(O)C<u>H</u>$_3$), 0.73 (d, J = 6.5 Hz, 3H, H6'). 13C NMR (101 MHz, $CDCl_3$) δ 171.4 (C=O), 166.0 (C=O), 165.7 (C=O), 160.4 (C_q), 159.6 (C_q), 133.4 (CH_{arom}), 133.2 (CH_{arom}), 129.8 (CH_{arom}), 129.7 (CH_{arom}), 129.7 (CH_{arom}), 129.6 (C_q), 129.6 (C_q), 128.6 (CH_{arom}), 128.4 (CH_{arom}), 127.8 (CH_{arom}), 114.1 (CH_{arom}), 113.7 (CH_{arom}), 102.1 (PMP-CH), 98.6 (C1'), 87.9 (C1), 80.7 (C4), 75.5 (C3), 74.2 (C2'), 73.4 (PMB-CH_2), 72.6 (C4'), 70.9 (C3'), 68.6 (C6), 68.5 (C5), 65.6 (C5'), 58.4 (C2), 55.4 (OCH_3), 55.3 (OCH_3), 23.4 (NHC(O)<u>C</u>H$_3$), 15.6 (C6') **HRMS** (ESI) m/z: [M + H$^+$] calcd for $C_{44}H_{46}N_4O_{13}H$ 839.31341, found 839.31311

Azido 3,4-di-O-benzoyl-2-O-(4-methoxybenzyl)-α-L-fucopyranoside-(1→3)-6-O-(4-methoxybenzyl)-2-deoxy-2-(N-acetylacetamido)-β-D-glucopyranoside (17)

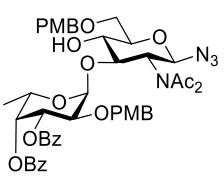

Dissacharide **16** (436 mg, 0.52 mmol) was dissolved in anhydrous DCM and DiPEA (10 eq., 870 µL, 5 mmol) and acetyl chloride (50 eq., 1.8 mL, 25 mmol) were added. The reaction was stirred for 2 hours at room temperature, after which TLC (10% EtOAc in DCM) indicated full conversion. The reaction mixture was diluted with DCM and the organic layer was washed with saturated aqueous $NaHCO_3$. The organic layer was dried over $MgSO_4$, filtered and concentrated. Silica gel column chromatography (30% → 40% → 50% Et_2O in pentane) yielded the diacetylated intermediate (406 mg, 0.46 mmol, 89%). $[\alpha]_D^{25}$ = -105.2 (c 0.50 in $CHCl_3$). **ν_{max}/cm^{-1}** 2119.23 (N_3), 1727.15 (CO) **^{1}H NMR** (400 MHz, $CDCl_3$) δ 7.94 – 7.87 (m, 2H, CH_{arom}), 7.78 – 7.71 (m, 2H, CH_{arom}), 7.63 – 7.55 (m, 1H, CH_{arom}), 7.52 – 7.39 (m, 5H, CH_{arom}), 7.32 – 7.26 (m, 2H, CH_{arom}), 7.12 – 7.04 (m, 2H, CH_{arom}), 6.91 – 6.83 (m, 2H, CH_{arom}), 6.68 (d, J = 8.7 Hz, 2H, CH_{arom}), 5.75 – 5.66 (m, 2H, H1, H3'), 5.51 (s, 1H, PMP-CH_{acetal}), 5.42 (dd, J = 3.3, 1.4 Hz, 1H, H4'), 4.79 (dd, J = 9.6, 8.6 Hz, 1H, H3), 4.74 (d, J = 3.5 Hz, 1H, H1'), 4.52 – 4.37 (m, 4H, PMB-CH_2, H5', H5), 4.06 (dd, J = 10.6, 3.5 Hz, 1H, H2'), 3.85 – 3.70 (m, 8H, 2 x OCH_3, H6), 3.70 – 3.61 (m, 2H, H4, H2), 2.50 (s,

3H, N(C(O)CH_3)C(O)C$\underline{H}_3$), 2.30 (s, 3H, N(C(O)C$\underline{H}_3$)C(O)CH_3), 0.52 (d, J = 6.4 Hz, 3H, H6'). **^{13}C NMR** (101 MHz, $CDCl_3$) δ 175.2 (C=O), 174.6 (C=O), 165.9 (C=O), 165.8 (C=O), 160.5 (C_q), 159.5 (C_q), 133.3 (CH_{arom}), 133.2 (CH_{arom}), 130.5 (CH_{arom}), 129.8 (CH_{arom}), 129.7 (CH_{arom}), 129.4 (C_q), 129.2 (C_q), 128.5 (CH_{arom}), 128.4 (CH_{arom}), 128.0 (CH_{arom}), 113.8 (CH_{arom}), 113.7 (CH_{arom}), 102.5 (PMP-C$\underline{H}$), 98.8 (C1'), 87.5 (C1), 80.9 (C4), 73.6 (C3), 73.4 (PMB-CH_2), 72.6 (C4'), 71.8 (C2'), 71.3 (C3'), 68.6 (C6), 68.0 (C5), 65.4 (C5'), 64.1 (C2), 55.4 (OCH_3), 55.2 (OCH_3), 28.6 (N(C(O)CH_3)C(O)$\underline{C}H_3$), 25.6 (N(C(O)$\underline{C}H_3$)C(O)CH_3), 15.2 (C6'). **HRMS** (ESI) m/z: [M + Na^+] calcd for $C_{46}H_{48}N4O_{14}Na$ 903.30592, found 903.30478. The 4-methoxybenzylidene protected disaccharide (461 mg, 0.52 mmol) was dissolved in dry THF and cooled to -70°C. BH_3·THF was added as a 1.0 M solution in THF (5 eq, 2.6 mmol, 2.6 mL) and the reaction was stirred for 15 minutes at this temperature. Then Bn_2BOTf was added as a 1.0 M solution in DCM (2 eq, 1 mmol, 1 mL) and the reaction was stirred for an additional 15 minutes at -70°C. The reaction was then heated to -50°C and stirred overnight. The reaction was quenched by careful addition of 0.5 mL of Et_3N followed by 15 mL MeOH and was stirred at room temperature for 30 minutes. The reaction mixture was concentrated *in vacuo* and subjected to silica gel column chromatography (40% → 50% →60 % Et_2O in pentane). This yielded the title compound (370 mg, 0.42 mmol, 81%). **$[\alpha]_D^{25}$** = -93.2 (c 1.00 in $CHCl_3$) **ν_{max}/cm^{-1}** 2117.80 (N_3), 1724.29 (CO) **^{1}H NMR** (400 MHz, $CDCl_3$) δ 7.95 – 7.88 (m, 2H, CH_{arom}), 7.80 – 7.73 (m, 2H, CH_{arom}), 7.67 – 7.59 (m, 1H, CH_{arom}), 7.54 – 7.42 (m, 3H, CH_{arom}), 7.35 – 7.26 (m, 4H, CH_{arom}), 7.11 – 7.04 (m, 2H, CH_{arom}), 6.90 (d, *J* = 8.6 Hz, 2H, CH_{arom}), 6.74 (d, *J* = 8.6 Hz, 2H, CH_{arom}), 5.67 – 5.59 (m, 3H, H1, H3', H4'), 4.93 (d, *J* = 3.6 Hz, 1H, H1'), 4.66 – 4.39 (m, 6H, PMB-CH_2, PMB-CH_2, H3, H5'), 4.10 (dd, *J* = 10.3, 3.6 Hz, 1H, H2'), 4.01 (s, 1H, 4-OH), 3.85 – 3.79 (m, 4H, H6a, OCH_3), 3.78 – 3.72 (m, 4H, H6b, OCH_3), 3.71 – 3.62 (m, 3H, H2, H4, H5), 2.41 (s, 3H, N(C(O)CH_3)C(O)C$\underline{H}_3$), 2.37 (s, 3H, N(C(O)C$\underline{H}_3$)C(O)CH_3)), 1.21 (d, *J* = 6.5 Hz, 3H, H6') **^{13}C NMR** (101 MHz, $CDCl_3$) δ 175.4 (C=O), 174.3 (C=O), 165.8 (C=O), 165.4 (C=O), 159.5 (C_q), 159.4 (C_q), 133.5 (CH_{arom}), 133.3 (CH_{arom}), 130.0 (CH_{arom}), 129.9 (CH_{arom}), 129.7 (CH_{arom}), 129.5 (CH_{arom}), 129.2 (C_q), 128.6 (CH_{arom}), 128.4 (CH_{arom}), 113.9 (CH_{arom}), 99.7 (C1'), 86.8 (C1), 82.6 (C3), 76.7 (C4), 73.4 (PMB-CH_2), 72.7 (PMB-CH_2), 72.1 (C4'), 71.4 (C5), 71.3 (C2'), 70.3 (C3'), 68.7 (C6), 66.7 (C5'), 62.3 (C2), 55.4 (OCH_3), 55.3 (OCH3), 28.4 (N(C(O)$\underline{C}H_3$)C(O)CH_3), 25.6 (N(C(O)CH_3)C(O)$\underline{C}H_3$), 16.2 (C6') **HRMS** (ESI) m/z: [M + NH_4^+] calcd for $C_{46}H_{50}N_4O_{14}NH_4$ 900.36618, found 900.36581

Azido 2,3,4,6-tetra-O-acetyl-β-D-galactopyranoside(1→4)-[3,4-di-O-benzoyl-2-O-(4-methoxybenzyl)-α-L-fucopyranoside-(1→3)]-6-O-(4-methoxybenzyl)-2-deoxy-2-(N-acetylacetamido)-β-D-glucopyranoside (18)

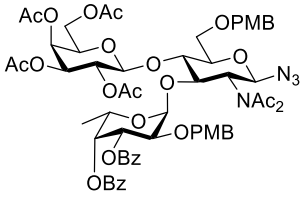

Donor **8** (5 eq., 737 mg, 1.5 mmol) and acceptor **17** (266 mg, 0,3 mmol) were co-evaporated 3 times with toluene, backfilling the flask with N_2 after every co-evaporation round, and placed under a N_2 atmosphere. The sugars were dissolved in dry DCM (3 mL) and activated 4Å molecular sieves (300 mg) were added. The mixture was stirred 30 minutes at room temperature and subsequently cooled to -10°C. TMS triflate (0.1 eq, 5.6 µl, 0.03 mmol) was added and the reaction was stirred over night at -10°C. The reaction was quenched by addition of Et_3N (0.1 mL) and allowed to warm to room temperature. The reaction mixture was diluted with DCM, filtered, further diluted with toluene and concentrated *in vacuo*. Silica gel column chromatography (40 → 70% Et_2O in pentane, Δ=5%) yielded the title compound (283 mg, 0.23 mmol, 77%). **$[\alpha]_D^{25}$** = -104.4 (c 1.00 in $CHCl_3$) **^{1}H NMR** (400 MHz, $CDCl_3$) δ 7.99 – 7.92 (m, 2H, CH_{arom}), 7.78 –

7.71 (m, 2H, CH_{arom}), 7.65 – 7.58 (m, 1H, CH_{arom}), 7.50 – 7.42 (m, 3H, CH_{arom}), 7.36 – 7.30 (m, 2H, CH_{arom}), 7.26 (dd, J = 8.3, 7.4 Hz, 3H, CH_{arom}), 7.13 (d, J = 8.6 Hz, 2H, CH_{arom}), 6.97 (d, J = 8.7 Hz, 2H, CH_{arom}), 6.70 (d, J = 8.6 Hz, 2H, CH_{arom}), 5.66 (dd, J = 3.3, 1.4 Hz, 1H, H4'), 5.64 – 5.54 (m, 2H, H3', H1), 5.38 (dd, J = 3.6, 1.0 Hz, 1H, H4''), 5.14 (q, J = 6.5 Hz, 1H, H5'), 5.04 (dd, J = 10.3, 8.3 Hz, 1H, H2''), 4.86 – 4.67 (m, 5H, H3'', PMB-C<u>H</u>H, H1', H1'', H3), 4.60 (dd, J = 11.5, 6.1 Hz, 1H, H6''a), 4.50 (s, 2H, PMB-CH_2), 4.46 – 4.38 (m, 2H, PMB-CH<u>H</u>, H6''b), 4.11 (dd, J = 10.6, 3.7 Hz, 1H, H2'), 4.05 (dd, J = 10.0, 8.9 Hz, 1H, H4), 3.88 – 3.68 (m, 8H, OCH_3, H6, OCH_3), 3.59 (t, J = 9.4 Hz, 1H, H2), 3.56 – 3.49 (m, 2H, H5, H5''), 2.51 (s, 3H, N(C(O)CH_3)C(O)C<u>H</u>$_3$), 2.25 (s, 3H, N(C(O)C<u>H</u>$_3$)C(O)CH_3), 2.24 (s, 3H, C(O)CH_3), 2.10 (s, 3H, C(O)CH_3), 2.00 (s, 3H, C(O)CH_3), 1.98 (s, 3H, C(O)CH_3), 1.24 (d, J = 6.6 Hz, 3H, H6') **^{13}C NMR** (101 MHz, $CDCl_3$) δ = 175.5 (C=O), 174.8 (C=O), 170.9 (C=O), 170.5 (C=O), 170.2 (C=O), 168.9 (C=O), 166.1 (C=O), 165.4 (C=O), 159.8 (C_q), 159.5 (C_q), 133.3 (CH_{arom}), 133.0 (CH_{arom}), 130.8 (CH_{arom}), 130.0 (C_q), 130.0 (CH_{arom}), 129.9 (CH_{arom}), 129.8 (C_q), 129.6 (CH_{arom}), 129.4 (C_q), 128.5 (CH_{arom}), 128.3 (CH_{arom}), 114.3 (CH_{arom}), 113.7 (CH_{arom}), 99.7 (C1''), 97.8 (C1'), 86.9 (C1), 76.6 (C5''), 74.3 (C4), 73.7 (PMB-CH_2), 73.5 (PMB-CH_2), 72.9 (C4'), 71.8 (C3', C3, C2'), 71.3 (C3''), 71.1 (C5), 69.2 (C2''), 67.0 (C4''), 66.9 (C6), 64.9 (C5'), 64.3 (C2), 61.1 (C6''), 55.4 (OCH_3), 55.3 (OCH_3), 28.8 (N(C(O)CH_3)C(O)C<u>H</u>$_3$), 25.8 (N(C(O)C<u>H</u>$_3$)C(O)CH_3), 21.0 (C(O)C<u>H</u>$_3$), 20.9 (C(O)C<u>H</u>$_3$), 20.8 (C(O)C<u>H</u>$_3$), 20.7 (C(O)C<u>H</u>$_3$), 16.0 (C6'). **HRMS** (ESI) m/z: [M + Na^+] calcd for $C_{60}H_{68}N_4O_{23}Na$ 1235.41666, found 1235.41654

Azido 2,3,4,6-tetra-O-acetyl-β-D-galactopyranoside-(1→4)-[3,4-di-O-benzoyl-2-O-(4-methoxybenzyl)-α-L-fucopyranoside-(1→3)]-6-O-(4-methoxybenzyl)-2-deoxy-2-acetamido-β-D-glucopyranoside (5)

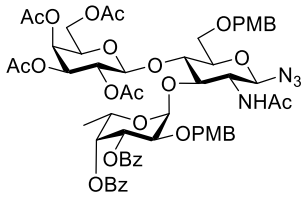

Protected trisaccharide **18** (61 mg, 50 µmol) was dissolved in dry THF (1 mL) and N,N-dimethylaminopropylamine (10 eq, 63 µL, 0.5 mmol) was added. The reaction was stirred for 30 minutes at room temperature and another portion of N,N-dimethylaminopropylamine (10 eq, 63 µL, 0.5 mmol) was added. After further stirring for 1 hour, TLC (15% EtOAc in DCM) indicated full conversion. The reaction mixture was diluted with DCM and washed with 1 M HCl (aq). The organic layer was dried over $MgSO_4$, filtered and concentrated *in vacuo*. Silica gel column chromatography (0% → 10% → 15% → 20% EtOAc in DCM) yielded the title compound (51 mg, 42 µmol, 87%). **$[\alpha]_D^{25}$** = -76.0 (c 1.00 in $CHCl_3$) **^{1}H NMR** (400 MHz, $CDCl_3$) δ 8.02 – 7.94 (m, 2H, CH_{arom}), 7.79 – 7.73 (m, 2H, CH_{arom}), 7.65 – 7.58 (m, 1H, CH_{arom}), 7.51 – 7.44 (m, 3H, CH_{arom}), 7.33 – 7.28 (m, 3H, CH_{arom}), 7.17 (d, J = 8.6 Hz, 2H, , CH_{arom}), 6.95 (d, J = 8.6 Hz, 2H, CH_{arom}), 6.76 (d, J = 8.7 Hz, 2H, CH_{arom}), 6.03 (d, J = 7.5 Hz, 1H, NH), 5.68 – 5.61 (m, 2H, H4', H3'), 5.38 (dd, J = 3.6, 1.1 Hz, 1H, H4''), 5.26 (d, J = 8.2 Hz, 1H, H1), 5.21 (d, J = 3.6 Hz, 1H, H1'), 5.08 (dd, J = 10.4, 8.1 Hz, 1H, H2''), 4.99 – 4.86 (m, 2H, H5', H3''), 4.73 – 4.67 (m, 2H, PMB-C<u>H</u>H, H1''), 4.64 (d, J = 11.6 Hz, 1H, PMB-C<u>H</u>H), 4.57 (d, J = 11.7 Hz, 1H, PMB-CH<u>H</u>), 4.46 – 4.31 (m, 4H, PMB-CH<u>H</u>, H6'', H3), 4.18 (dd, J = 9.7, 3.5 Hz, 1H, H1'), 4.06 (t, J = 8.3 Hz, 1H, H4), 3.85 – 3.78 (m, 5H, OCH_3, H6), 3.75 (s, 3H, OCH_3), 3.64 – 3.55 (m, 2H, H5'', H5), 3.33 (q, J = 8.1 Hz, 1H, H2), 2.21 (s, 3H, C(O)CH_3), 2.07 (s, 3H, C(O)CH_3), 2.02 (s, 3H, C(O)CH_3), 1.98 (s, 3H, C(O)CH_3), 1.89 (s, 3H, NHC(O)C<u>H</u>$_3$), 1.25 (d, J = 6.6 Hz, 3H, H6') **^{13}C NMR** (101 MHz, $CDCl_3$) δ = 171.0 (C=O), 170.6 (C=O), 170.5 (C=O), 170.2 (C=O), 169.4 (C=O), 166.1 (C=O), 165.3 (C=O), 159.6 (C_q), 159.6 (C_q), 133.3 (CH_{arom}), 133.0 (CH_{arom}), 129.9 (CH_{arom}), 129.8 (C_q), 129.8 (CH_{arom}), 129.7 (CH_{arom}), 129.7 (CH_{arom}), 128.6 (CH_{arom}), 128.3 (CH_{arom}), 114.1 (CH_{arom}), 114.0 (CH_{arom}), 99.6 (C1''), 97.3 (C1'), 87.2 (C1), 76.7 (C5), 73.6 (C2', C4), 73.5 (C3), 73.4 (PMB-CH_2), 73.1 (PMB-CH_2), 72.8 (C4'), 71.1 (C5''), 71.0 (C3''), 71.0 (C3'), 69.2

(C2''), 67.4 (C6), 67.0 (C4''), 65.2 (C5'), 61.1 (C6''), 57.0 (C2), 55.4 (OCH_3), 55.3 (OCH_3), 23.5 ($NHC(O)\underline{C}H_3$), 20.9 ($C(O)\underline{C}H_3$), 20.9 ($C(O)\underline{C}H_3$), 20.7 ($C(O)\underline{C}H_3$), 16.1 (C6'). **HRMS** (ESI) m/z: [M + Na^+] calcd for $C_{58}H_{66}N_4O_{22}Na$ 1193.40609, found 1193.40573

Azido 2,3,4,6-tetra-O-acetyl-β-D-galactopyranoside-(1→4)-6-(*tert*-butyldimethylsilyl)-2-deoxy-2-acetamido-β-D-glucopyranoside (19)

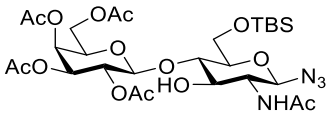

Donor **8** (1.5 eq, 368 mg, 0.75 mmol) and acceptor **13** (180 mg, 0.5 mmol) were co-evaporated 3 times with toluene and put under N_2. The sugars were dissolved in dry DCM (5 mL) and stirred with activated 4 Å molecular sieves (0.5 g) for 2 hours at room temperature. The reaction was cooled to -40°C and $BF_3{\cdot}Et_2O$ (1.6 eq, 100 µL, 0.8 mmol) was added. The reaction was stirred at -40°C overnight and formation of disaccharide product was confirmed by TLC (70% EtOAc in pentane). The reaction was quenched with Et_3N (0.5 mL), diluted with DCM, filtered, diluted with toluene and concentrated. Silica gel column chromatography (60% → 70% → 80% EtOAc in pentane) yielded the title compound (193 mg, 0.28 mmol, 56%). $\mathbf{[\alpha]_D^{20}}$ = +5,8 (c 1.00 in $CHCl_3$) $\mathbf{\nu_{max}/cm^{-1}}$ 2115.65 (N_3), 1752.19 (CO) **^{1}H NMR** (400 MHz, $CDCl_3$) δ 6.17 (d, J = 8.5 Hz, 1H, NH), 5.40 (dd, J = 3.4, 1.0 Hz, 1H, H4'), 5.22 (dd, J = 10.5, 8.0 Hz, 1H, H2'), 4.99 (dd, J = 10.5, 3.4 Hz, 1H, H3'), 4.69 – 4.61 (m, 2H, H1, H1'), 4.15 (d, J = 6.5 Hz, 2H, H6'), 4.06 (bs, 1H, 3-OH), 4.01 (t, J = 6.5 Hz, 1H, H5'), 3.90 – 3.72 (m, 3H, H6, H3), 3.69 – 3.57 (m, 2H, H4, H2), 3.43 (ddd, J = 9.6, 3.4, 1.5 Hz, 1H, H5), 2.17 (s, 3H, $C(O)CH_3$), 2.08 (s, 3H, $C(O)CH_3$), 2.07 (s, 3H, $C(O)CH_3$), 2.03 (s, 3H, $NHC(O)C\underline{H}_3$), 1.99 (s, 3H, $C(O)CH_3$), 0.92 (s, 9H, tBu), 0.11 (s, 3H, Si-CH_3), 0.10 (s, 3H, Si-CH_3) **^{13}C NMR** (101 MHz, $CDCl_3$) δ = 171.0 (C=O), 170.6 (C=O), 170.2 (C=O), 170.1 (C=O), 169.4 (C=O), 101.6 (C1'), 87.9 (C1), 80.5 (C4), 76.7 (C5), 71.9 (C3), 71.4 (C5'), 70.9 (C3'), 68.7 (C2'), 66.8 (C4'), 61.4 (C6'), 61.2 (C6), 55.6 (C2), 25.9 (tBu), 23.4 ($NHC(O)\underline{C}H_3$), 20.7 ($C(O)\underline{C}H_3$), 20.6 ($C(O)\underline{C}H_3$), 20.6 ($C(O)\underline{C}H_3$), 20.6 ($C(O)\underline{C}H_3$), 18.3 (Si-C_q), -5.0 (Si-CH_3), -5.2 (Si-CH_3) **HRMS** (ESI) m/z: [M + Na^+] calcd for $C_{28}H_{46}N_4O_{14}SiNa$ 713.2672, found 713.2695

Azido 2,3,4,6-tetra-O-acetyl-β-D-galactopyranoside-(1→4)-6,3-di-O-acetyl-2-deoxy-2-acetamido-β-D-glucopyranoside (20)

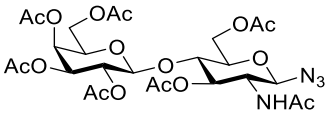

Silyl protected disaccharide **19** (517 mg, 0.75 mmol) was dissolved in dry THF (7.5 mL) in a plastic tube. HF·pyridine complex (16 eq, 310 µL, 12 mmol) was added and the reaction was stirred overnight. Completion of the reaction was assessed by TLC (100% EtOAc) and the reaction mixture was diluted with DCM. The organic layer was washed with aqueous saturated $NaHCO_3$ (3:1 ratio of DCM:H_2O) and the aqueous layer was back extracted with DCM. The combined organic layers were dried over $MgSO_4$, filtered and concentrated, yielding 380 mg (0.66 mmol) of crude intermediate. The crude desilylated disaccharide was dissolved in dry pyridine (6.6 mL) and cooled to 0°C in an ice bath. Acetic anhydride (10 eq, 620 µL, 6.6 mmol) and DMAP (0.1 eq, 9 mg, 0.07 mmol) were added. The reaction was stirred overnight at room temperature and reaction completion was confirmed by TLC (100% EtOAc). The reaction was quenched with methanol and concentrated. Pyridine traces were removed with toluene co-evaporation. Silica gel column chromatography (70% → 80% → 90% EtOAc in pentane) yielded the title compound (421 mg, 0.64 mmol, 85%). $\mathbf{[\alpha]_D^{20}}$ = -26,4 (c 1.00 in $CHCl_3$) $\mathbf{\nu_{max}/cm^{-1}}$ 2116.37 (N_3), 1744.32 (CO) **^{1}H NMR** (400 MHz, $CDCl_3$) δ 6.53 (d, J = 9.6 Hz, 1H, NH), 5.37 (dd, J = 3.4, 1.2 Hz, 1H, H4'), 5.19 – 5.03 (m, 2H, H3, H2'), 4.99 (dd, J = 10.5, 3.4 Hz, 1H, H3'), 4.64 – 4.50 (m, 3H, H1, H1', H6a), 4.21

– 4.01 (m, 4H, H6', H6b, H2), 3.93 (t, J = 7.1 Hz, 1H, H5'), 3.84 (t, J = 9.1 Hz, 1H, H4), 3.73 (ddd, J = 9.1, 5.0, 2.2 Hz, 1H, H5), 2.17 (s, 3H, C(O)CH_3), 2.14 (s, 3H, C(O)CH_3), 2.11 (s, 3H, C(O)CH_3), 2.07 (s, 3H, C(O)CH_3), 2.07 (s, 3H, C(O)CH_3), 1.99 (s, 3H, NHC(O)C$\underline{H}_3$), 1.97 (s, 3H, C(O)CH_3) **^{13}C NMR** (101 MHz, $CDCl_3$) δ = 171.0 (C=O), 170.5 (C=O), 170.4 (C=O), 170.3 (C=O), 170.1 (C=O), 170.0 (C=O), 169.3 (C=O), 101.3 (C1'), 88.3 (C1), 76.1 (C4), 74.5 (C5), 73.1 (C3), 70.8 (C3'), 70.7 (C5'), 69.0 (C2'), 66.6 (C4'), 61.9 (C6), 60.6 (C6'), 53.0 (C2), 23.0 (NHC(O)$\underline{C}H_3$), 20.9 (C(O)$\underline{C}H_3$), 20.8 (C(O)$\underline{C}H_3$), 20.6 (C(O)$\underline{C}H_3$), 20.6 (C(O)$\underline{C}H_3$), 20.5 (C(O)$\underline{C}H_3$), 20.5 (C(O)$\underline{C}H_3$) **HRMS** (ESI) m/z: [M + Na^+] calcd for $C_{26}H_{36}N_4O_{16}Na$ 683.2019, found 683.2029

3,4,6-tri-O-acetyl-2-deoxy-2-(acetylacetamido)-β-D-glucopyranosyl azide (21)

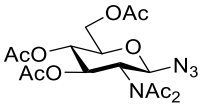

Glycosyl azide **11** (186 mg, 0.5 mmol) was dissolved in anhydrous DCM (5 mL). DiPEA (2 eq, 175 µL, 1.0 mmol) and acetyl chloride (10 eq, 350 µL, 5.0 mmol) were added and the reaction was stirred at room temperature. After 2 hours TLC (20% pentane in EtOAc) inducated complete consumption of the starting material. The reaction mixture was diluted with DCM and washed with saturated aqueous $NaHCO_3$. The organic layer was dried over $MgSO_4$ and concentrated. Silica gel column chromatography (1/1 Et_2O/pentane) yielded the title compound (112 mg, 0.27 mmol, 54%). **^{1}H NMR** (400 MHz, $CDCl_3$) δ 5.86 (d, J = 8.7 Hz, 1H, H1), 5.82 (dd, J = 10.3, 8.9 Hz, 1H, H3), 5.10 (dd, J = 10.3, 8.9 Hz, 1H, H4), 4.37 (dd, J = 12.5, 4.6 Hz, 1H, H6a), 4.14 (dd, J = 12.5, 2.2 Hz, 1H, H6b), 3.92 (ddd, J = 10.3, 4.6, 2.2 Hz, 1H, H5), 3.62 (dd, J = 10.3, 8.7 Hz, 1H, H2), 2.38 (s, 3H, NHC(O)CH_3), 2.37 (s, 3H, NHC(O)C$\underline{H}_3$), 2.11 (s, 3H, C(O)CH_3), 2.04 (s, 3H, C(O)CH_3), 2.00 (s, 3H, C(O)CH_3) **^{13}C NMR** (101 MHz, $CDCl_3$) δ = 174.7 (C=O), 173.4 (C=O), 170.6 (C=O), 169.6 (C=O), 87.1 (C1), 73.6 (C5), 70.2 (C3), 68.8 (C4), 61.7 (C2), 61.7 (C6), 27.8 (NHC(O)C$\underline{H}_3$), 25.1 (NHC(O)$\underline{C}H_3$), 20.7 (C(O)$\underline{C}H_3$), 20.6 (C(O)$\underline{C}H_3$), 20.4 (C(O)$\underline{C}H_3$)

3,4,6-tri-O-acetyl-2-deoxy-2-(acetamido)-β-D-glucopyranosyl acetamide (22)

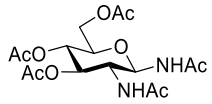

Acetylimide protected sugar **21** (40 mg, 0.1 mmol) was dissolved in THF (2 mL) and a 1 M solution of trimethylphosphine (1.5 eq, 150 µL, 0.15 mmol) was added. The reaction was stirred for 5 minutes before H_2O (50 eq, 90 µL 5 mmol) was added. The reaction was stirred for 1 hour and the volatiles were removed *in vacuo*. NMR analysis (DMSO-d6) indicated full conversion to the anomeric acetamide. **^{1}H NMR** (400 MHz, DMSO-d_6) δ 8.56 (d, J = 9.3 Hz, 1H, C1-N$\underline{H}$), 7.99 (d, J = 9.2 Hz, 1H, C2-N$\underline{H}$), 5.15 (t, J = 9.6 Hz, 1H, H1), 5.09 (dd, J = 10.3, 9.5 Hz, 1H, H3), 4.80 (t, J = 9.8 Hz, 1H, H4), 4.16 (dd, J = 12.4, 4.3 Hz, 1H, H6a), 3.94 (dd, J = 12.4, 2.2 Hz, 1H, H6b), 3.90 – 3.76 (m, 2H, H2, H5), 1.99 (s, 3H, C(O)CH_3), 1.96 (s, 3H, C(O)CH_3), 1.90 (s, 3H, C(O)CH_3), 1.82 (s, 3H, C(O)CH_3), 1.74 (s, 3H, C(O)CH_3)

Asn(GlcNAc)-Ala-Thr-Gly-Met-Asp-Val-Gly-Trp-Tyr-Arg-Ser-Pro-Phe-Ser-Arg-Val-Val-His-Leu-Tyr-Arg-Asn-Gly-Lys-NH_2 (25)

Using the general method of glycopeptide synthesis, asparagine derivative **1** was coupled to immobilized peptide **23**, producing compound **25** in 4.0% (3.1 mg) yield after RP-HPLC. **LC-MS** RT = 14.0 min (C18, 5-65% B over 30 minutes) **LRMS** calcd $[M+3H]^{3+}$ = 1043.18; observed M/z = 1043.42

Asn(FucGlcNAc)-Ala-Thr-Gly-Met-Asp-Val-Gly-Trp-Tyr-Arg-Ser-Pro-Phe-Ser-Arg-Val-Val-His-Leu-Tyr-Arg-Asn-Gly-Lys-NH_2 (26)

Using the general method of glycopeptide synthesis, asparagine derivative **2** was coupled to immobilized peptide **23**, producing compound **26** in 5.6% (2.4 mg) yield after RP-HPLC. **LC-MS** RT = 14.0 min (C18, 5-65% B over 30 minutes) **LRMS** calcd $[M+3H]^{3+}$ = 1091.87, $[M+2H]^{2+}$ = 1637.30; observed M/z = 1092.50, 1637.83

Asn(LacNAc)-Ala-Thr-Gly-Met-Asp-Val-Gly-Trp-Tyr-Arg-Ser-Pro-Phe-Ser-Arg-Val-Val-His-Leu-Tyr-Arg-Asn-Gly-Lys-NH_2 (27)

Using the general method of glycopeptide synthesis, asparagine derivative **3** was coupled to immobilized peptide **23**, producing compound **27** in 5.8% (2.3 mg) yield after RP-HPLC. **LC-MS** RT = 13.9 min (C18, 5-65% B over 30 minutes) **LRMS** calcd $[M+3H]^{3+}$ = 1097.20, $[M+2H]^{2+}$ = 1645.30; observed M/z = 1097.92, 1645.92

Asn(Le^X)-Ala-Thr-Gly-Met-Asp-Val-Gly-Trp-Tyr-Arg-Ser-Pro-Phe-Ser-Arg-Val-Val-His-Leu-Tyr-Arg-Asn-Gly-Lys-NH_2 (28)

Using the general method of glycopeptide synthesis, asparagine derivative **4** was coupled to immobilized peptide **23**, producing compound **28** in 4.1% (1.7 mg) yield after RP-HPLC. **LC-MS** RT = 13.9 min (C18, 5-65% B over 30 minutes) **LRMS** calcd $[M+3H]^{3+}$ = 1145.89, $[M+2H]^{2+}$ = 1718.34; observed M/z = 1146.50, 1718.83

Asn(GlcNAc)-Ala-Thr-Gly-Met-Asp-Val-Gly-Trp-Tyr-Cit-Ser-Pro-Phe-Ser-Cit-Val-Val-His-Leu-Tyr-Arg-Asn-Gly-Lys-NH_2 (29)

Using the general method of glycopeptide synthesis, asparagine derivative **1** was coupled to immobilized peptide **24**, producing compound **29** in 8.6% (6.7 mg) yield after RP-HPLC. **LC-MS** RT = 15.1 min (C18, 5-65% B over 30 minutes) **LRMS** $[M+3H]^{3+}$ = 1043.84, $[M+2H]^{2+}$ = 1565.26; observed M/z = 1044.08, 1565.50

Asn(FucGlcNAc)-Ala-Thr-Gly-Met-Asp-Val-Gly-Trp-Tyr-Cit-Ser-Pro-Phe-Ser-Cit-Val-Val-His-Leu-Tyr-Arg-Asn-Gly-Lys-NH_2 (30)

Using the general method of glycopeptide synthesis, asparagine derivative **2** was coupled to immobilized peptide **24**, producing compound **30** in 2.1% (2.2 mg) yield as well as the product containing a single methionine oxidation (5.7 %, 6.1 mg) after RP-HPLC. **LC-MS** RT = 15.1 min (C18, 5-65% B over 30 minutes) **LRMS** calcd $[M+3H]^{3+}$ = 1092.50, $[M+2H]^{2+}$ = 1638.29; observed M/z = 1092.58, 1638.17

Asn(LacNAc)-Ala-Thr-Gly-Met-Asp-Val-Gly-Trp-Tyr-Cit-Ser-Pro-Phe-Ser-Cit-Val-Val-His-Leu-Tyr-Arg-Asn-Gly-Lys-NH_2 (31)

Using the general method of glycopeptide synthesis, asparagine derivative **3** was coupled to immobilized peptide **24**, producing compound **31** in 5.6% (3.9 mg) yield after RP-HPLC. **LC-MS** RT = 14.9 min (C18, 5-65% B over 30 minutes) **LRMS** calcd $[M+3H]^{3+}$ = 1097.86, $[M+2H]^{2+}$ = 1646.29; observed M/z = 1098.17, 1646.33

Asn(Le^X)-Ala-Thr-Gly-Met-Asp-Val-Gly-Trp-Tyr-Cit-Ser-Pro-Phe-Ser-Cit-Val-Val-His-Leu-Tyr-Arg-Asn-Gly-Lys-NH_2 (32)

Using the general method of glycopeptide synthesis, asparagine derivative **4** was coupled to immobilized peptide **24**, producing compound **32** in 5.3% (1.9 mg) yield as well as the product containing a single methionine oxidation (3.9 %, 1.4 mg) after RP-HPLC. **LC-MS** RT = 15.0 min (C18, 5-65% B over 30 minutes) **LRMS** calcd $[M+3H]^{3+}$ = 1146,54, $[M+2H]^{2+}$ = 1719.31; observed M/z =1146.75, 1719.42

Biophysical and biochemical methods

ThT Fluorescence Aggregation Assays

Aggregation assays were modified according to Araman et al.[12] Briefly, a mixture of 199 µL of peptide (10 µM) and 1 µL of ThT pipetted to 96-well plates and the fluorescence in each well was measured with a kinetic interval of 10 min peptides at 37 °C using the CLARIOstar® *Plus* plate reader. The measurements were performed with an excitation wavelength of 444 nm and an emission wavelength of 485 nm with a bandwidth of 10 nm.

Circular Dichroism (CD) Spectroscopy

Circular dichroism spectroscopy was performed at room temperature using a Jasco J-815 CD spectrometer with a 1 mm path-length cell and a bandwidth of 2.0 nm. The peptides were prepared in 20 mM NaOAc buffer (pH 5.0) with a final peptide concentration of 0.1−0.2 mg/mL.. Spectra were recorded from 260 to 190 nm at an interval of 1 nm. Each spectrum was the average of five scans and blank subtraction. Further analysis was performed via addition of 4 mM sodium dodecyl sulfate (SDS) (β-sheet enhancer) or 50% trifluoroethanol (TFE) (α-helix enhancer).

Cell Viability Assay with 3-(4,5-Dimethylthiazol-2-yl)-2,5-diphenyltetrazolium Bromide (MTT)

The cell viability of BMDCs was tested via the MTT assay. In a typical experiments, BMDCs were seeded in a 96-well plate at a density of 2.5×10^4 cells/well and treated with varying amounts of peptides **26-28** as well as **29-32** in IMDM (40, 20, 10, and 5 µM) incubated overnight at 37 °C and 5% CO_2. Medium with (control) and medium without 2.5×10^4 cells (blank) served used as controls. Upon overnight incubation, cells were centrifuged (300*g* for 5 min at 4 °C), the supernatant was discarded, and 100 µL of 0.5 mg/mL MTT in PBS was added to each well. Upon incubation for 3–4 h at 37 °C and formation of intracellular formazan crystals, the supernatant was removed and the crystals were dissolved in DMSO (75-100 µL). The plate was incubated for a further 30 min at 37 °C, and the absorbance was measured at 540 nm (A_{540}) as well as 570 nm (CLARIOstar® *Plus*). The following equation was used to assess cell viability:

$$\%\ \text{cell viability} = \frac{A_{540}(\text{sample}) - A_{540}(\text{blank})}{A_{540}(\text{control}) - A_{540}(\text{blank})}$$

DC-SIGN ELISA

DC-SIGN ELISA was performed according to the method published elsewhere.[59] Briefly, 2 mM peptide stock solutions in DMSO were diluted to 14 µM with PBS before incubating 50 µL/well in high-binding 96-well plates (Nunc Maxisorp) at room temperature for 2 hours for coating. The wells were then washed twice with 150 µL of a calcium and magnesium-containing buffer [TSM: 20 mM tris(hydroxymethyl)aminomethane (Tris)-HCl, pH 8.0; 150 mM NaCl; 1 mM $CaCl_2$; 2 mM $MgCl_2$] and blocked using 100 uL TSM buffer containing 1% BSA for 45 min. at room temperature. The blocking solution was removed and wells were then incubated 45 min. at room temperature with 1µg/mL of DC-SIGN-Fc (extracellular portion of DC-SIGN, residues 64 to 404, fused at the C-terminus to a human IgG1/Fc fragment into the Sig-pIgG1-Fc vector) in TSM buffer containing 0.5% BSA. After two washes with TSM buffer, HRP-linked goat anti-human IgG-Fc, 400 µg/mL diluted 1:250 in TSM containing 0.5% BSA was added and incubated for 1 hour at room temperature. After 2 washes with TSM buffer, TMB substrate in citric acid buffer containing a catalytic amount of H_2O_2 was added, and the plate was read on a spectrophotometer at 450 nm. Polyacrylamide polymers (PAA), functionalized with LeX was purchased from Lectinity, MW approx. 20 KDa, carbohydrate content around 20% mol., and used as positive control (20 µg/mL to coat the ELISA wells).

Generation and stimulation of moDC

Peripheral blood mononuclear cells (PBMCs) were isolated from buffy coats of healthy volunteers (Sanquin, Amsterdam, The Netherlands) by centrifugation on a Ficoll gradient as previously described.[64] Briefly, blood was mixed with PBS 1% citrate and layered on the Ficoll. After 30 min centrifugation, the interphase containing monocytes and lymphocytes was collected, washed with PBS/Citrate and the pellet was resuspended in complete RPMI medium. PBMCs were then loaded on a Percoll layer (GE Healthcare, Chicago, U.S.) and after centrifugation, the interphase was collected, washed and resuspended in complete RPMI. moDC were generated by culturing monocytes for 5-7 days at a concentration of 1.25×10^6/mL in complete RPMI (Lonza, Basel, Switzerland) containing 500 U/mL IL-4 (ImmunoTools, Friesoythe, Germany) and 800 U/mL Granulocyte Macrophage Colony stimulating Factor (GM-CSF) (ImmunoTools). On day four moDC ($0.5\text{-}1 \times 10^5$) were stimulated with different concentration of the reported glycosylated peptides (14, 7 and 3.5 µM) in RPMI-1640, supplemented with 10% FCS, L-Glutamine (2 mM), and penicillin/streptomycin (100 U/ml) at 37°C, 5% CO_2 for 16 hours. Lipopolysaccharide (LPS, *E. coli* 0111:B4, Sigma-Aldrich, cat#L4391, 10 ng/mL) was used as control.

Cytokine ELISA

Human IL-10 and IL-12p70 ELISA Kit Duo Set R&D systems were used following the manufacturer instructions. Briefly, anti-human IL-10 or IL-12p70 was coated overnight in 50 mM Na2CO3, pH 9.7, in Nunc Maxisorp plates. After washing with PBS 0.05% Tween, and blocked for 30 min with 1% BSA in PBS, moDC supernatants were added together with the corresponding detection antibody for 2 h at RT. Cytokines were detected with Streptavidin-PO (Biosource Finnigan, Waltham, U.S.) adding substrate buffer [(110 mM citric acid (Merck), 110 mM sodium acetate (Fisher scientific, Waltham, U.S.), pH 4] and 100 µg/mL TMB solution (Sigma) with a catalytic amount of H2O2, and stopping the enzymatic reaction with 0.8M H2SO4. UV absorbance was measured at 450 nm on an ELISA reader (Bio-Rad Benchmark, Hercules, U.S.).

Supporting Figures

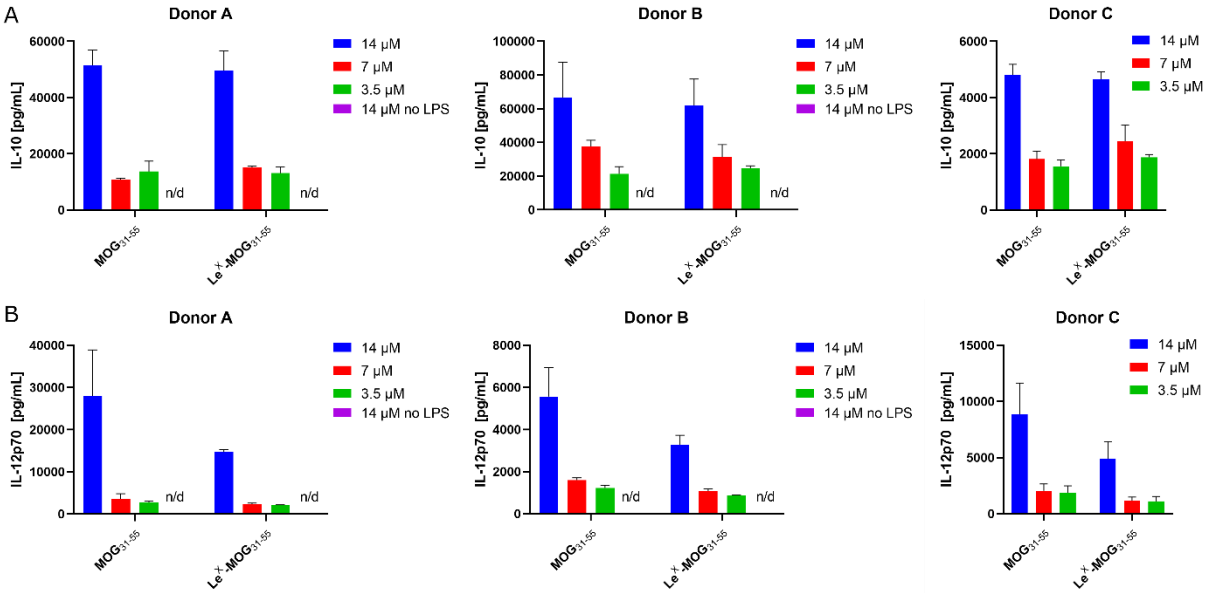

Figure S1. Concentrations of secreted of IL10 (A) and IL12p70 (B) measured for Donors A, B and C upon stimulation with MOG_{31-55} or the glycosylated peptide Le^X-MOG_{31-55} (**28**). Cells were stimulated with 10 ng/mL of LPS unless stated otherwise ("no LPS"). n/d = not detected

References

(1) Dobson, R.; Giovannoni, G. Multiple Sclerosis – a Review. *European Journal of Neurology*. John Wiley & Sons, Ltd (10.1111) January 1, 2019, pp 27–40. https://doi.org/10.1111/ene.13819.

(2) Steinman, L. Multiple Sclerosis: Two-Stage Disease. *Nat. Immunol.* **2001**, *2* (9), 762–764. https://doi.org/10.1038/ni0901-762.

(3) Snaidero, N.; Simons, M. Myelination at a Glance. *J. Cell Sci.* **2014**, *127* (14), 2999–3004. https://doi.org/10.1242/jcs.151043.

(4) Whitaker, J. N. The Appearance of a New Antigenic Determinant during the Degradation of Myelin Basic Protein. *J. Neuroimmunol.* **1982**, *2* (3–4), 201–207. https://doi.org/10.1016/0165-5728(82)90054-6.

(5) Adelmann, M.; Wood, J.; Benzel, I.; Fiori, P.; Lassmann, H.; Matthieu, J. M.; Gardinier, M. V.; Dornmair, K.; Linington, C. The N-Terminal Domain of the Myelin Oligodendrocyte Glycoprotein (MOG) Induces Acute Demyelinating Experimental Autoimmune Encephalomyelitis in the Lewis Rat. *J. Neuroimmunol.* **1995**, *63* (1), 17–27. https://doi.org/10.1016/0165-5728(95)00124-7.

(6) Jung, J.; Dudek, E.; Michalak, M. The Role of N-Glycan in Folding, Trafficking and Pathogenicity of Myelin Oligodendrocyte Glycoprotein (MOG). *Biochim. Biophys. Acta - Mol. Cell Res.* **2014**, *1853* (9), 2115–2121. https://doi.org/10.1016/j.bbamcr.2014.12.023.

(7) Pham-Dinh, D.; Mattei, M. G.; Nussbaum, J. L.; Roussel, G.; Pontarotti, P.; Roeckel, N.; Mather, I. H.; Artzt, K.; Lindahl, K. F.; Dautigny, A. Myelin/Oligodendrocyte Glycoprotein Is a Member of a Subset of the Immunoglobulin Superfamily Encoded within the Major Histocompatibility Complex. *Proc. Natl. Acad. Sci. U. S. A.* **1993**, *90* (17), 7990–7994. https://doi.org/10.1073/pnas.90.17.7990.

(8) Linnington, C.; Webb, M.; Woodhams, P. L. A Novel Myelin-Associated Glycoprotein Defined by a Mouse Monoclonal Antibody. *J. Neuroimmunol.* **1984**, *6* (6), 387–396. https://doi.org/10.1016/0165-5728(84)90064-X.

(9) Peschl, P.; Bradl, M.; Höftberger, R.; Berger, T.; Reindl, M. Myelin Oligodendrocyte Glycoprotein: Deciphering a Target in Inflammatory Demyelinating Diseases. *Front. Immunol.* **2017**, *8*, 529. https://doi.org/10.3389/fimmu.2017.00529.

(10) Mendel, I.; de Rosbo, N. K.; Ben-Nun, A. A Myelin Oligodendrocyte Glycoprotein Peptide Induces Typical Chronic Experimental Autoimmune Encephalomyelitis in H-2b Mice: Fine Specificity and T Cell Receptor Vβ Expression of Encephalitogenic T Cells. *Eur. J. Immunol.* **1995**, *25* (7), 1951–1959. https://doi.org/10.1002/eji.1830250723.

(11) Jagessar, S. A.; Holtman, I. R.; Hofman, S.; Morandi, E.; Heijmans, N.; Laman, J. D.; Gran, B.; Faber, B. W.; van Kasteren, S. I.; Eggen, B. J. L.; 't Hart, B. A. Lymphocryptovirus Infection of Nonhuman Primate B Cells Converts Destructive into Productive Processing of the Pathogenic CD8 T Cell Epitope in Myelin Oligodendrocyte Glycoprotein. *J. Immunol.* **2016**, *197* (4), 1074–1088. https://doi.org/10.4049/jimmunol.1600124.

(12) Araman, C.; van Gent, M. E.; Meeuwenoord, N. J.; Heijmans, N.; Marqvorsen, M. H. S.; Doelman, W.; Faber, B. W.; 't Hart, B. A.; Van Kasteren, S. I. Amyloid-like Behavior of Site-Specifically Citrullinated Myelin Oligodendrocyte Protein (MOG) Peptide Fragments inside EBV-Infected B-Cells Influences Their Cytotoxicity and Autoimmunogenicity. *Biochemistry* **2019**, *58* (6), 763–775. https://doi.org/10.1021/acs.biochem.8b00852.

(13) Eisenberg, D.; Jucker, M. The Amyloid State of Proteins in Human Diseases. *Cell*. Cell Press March 16, 2012, pp 1188–1203. https://doi.org/10.1016/j.cell.2012.02.022.

(14) Wood, D. D.; Bilbao, J. M.; O'Connors, P.; Moscarello, M. A. Acute Multiple Sclerosis (Marburg Type) Is Associated with Developmentally Immature Myelin Basic Protein. *Ann. Neurol.* **1996**, *40* (1), 18–24. https://doi.org/10.1002/ana.410400106.

(15) Frenkel-Pinter, M.; Richman, M.; Belostozky, A.; Abu-Mokh, A.; Gazit, E.; Rahimipour, S.; Segal, D. Selective Inhibition of Aggregation and Toxicity of a Tau-Derived Peptide Using Its Glycosylated Analogues. *Chem. Eur. J.* **2016**, *22* (17), 5945–5952. https://doi.org/10.1002/chem.201504950.

(16) Bosques, C. J.; Imperiali, B. The Interplay of Glycosylation and Disulfide Formation Influences Fibrillization in a Prion Protein Fragment. *Proc. Natl. Acad. Sci.* **2003**, *100* (13), 7593–7598. https://doi.org/10.1073/pnas.1232504100.

(17) Araman, C.; Thompson, R. E.; Wang, S.; Hackl, S.; Payne, R. J.; Becker, C. F. W. Semisynthetic Prion Protein (PrP) Variants Carrying Glycan Mimics at Position 181 and 197 Do Not Form Fibrils. *Chem. Sci.* **2017**, *8* (9), 6626–6632. https://doi.org/10.1039/c7sc02719b.

(18) Geijtenbeek, T. B. H.; van Vliet, S. J.; Koppel, E. A.; Sanchez-Hernandez, M.; Vandenbroucke-Grauls, C. M. J. E.; Appelmelk, B.; van Kooyk, Y. Mycobacteria Target DC-SIGN to Suppress Dendritic Cell Function. *J. Exp. Med.* **2003**, *197* (1), 7–17. https://doi.org/10.1084/jem.20021229.

(19) van Liempt, E.; Bank, C. M. C.; Mehta, P.; García-Vallejo, J. J.; Kawar, Z. S.; Geyer, R.; Alvarez, R. A.; Cummings, R. D.; Kooyk, Y. van; van Die, I. Specificity of DC-SIGN for Mannose- and Fucose-Containing Glycans. *FEBS Lett.* **2006**, *580* (26), 6123–6131. https://doi.org/10.1016/j.febslet.2006.10.009.

(20) García-Vallejo, J. J.; Ilarregui, J. M.; Kalay, H.; Chamorro, S.; Koning, N.; Unger, W. W.; Ambrosini, M.; Montserrat, V.; Fernandes, R. J.; Bruijns, S. C. M.; van Weering, J. R. T.; Paauw, N. J.; O'Toole, T.; van Horssen, J.; van der Valk, P.; Nazmi, K.; Bolscher, J. G. M.; Bajramovic, J.; Dijkstra, C. D.; 't Hart, B. A.; van Kooyk, Y. CNS Myelin Induces Regulatory Functions of DC-SIGN–Expressing, Antigen-Presenting Cells via Cognate Interaction with MOG. *J. Exp. Med.* **2014**, *211* (7), 1465–1483. https://doi.org/10.1084/jem.20122192.

(21) Buskas, T.; Li, Y.; Boons, G.-J. The Immunogenicity of the Tumor-Associated Antigen Lewisy May Be Suppressed by a Bifunctional Cross-Linker Required for Coupling to a Carrier Protein. *Chem. Eur. J.* **2004**, *10* (14), 3517–3524. https://doi.org/10.1002/chem.200400074.

(22) Cai, H.; Zhang, R.; Orwenyo, J.; Giddens, J.; Yang, Q.; LaBranche, C. C.; Montefiori, D. C.; Wang, L.-X. Multivalent Antigen Presentation Enhances the Immunogenicity of a Synthetic Three-Component HIV-1 V3 Glycopeptide Vaccine. *ACS Cent. Sci.* **2018**, *4* (5), 582–589. https://doi.org/10.1021/acscentsci.8b00060.

(23) Marqvorsen, M. H. S.; Araman, C.; Van Kasteren, S. I. Going Native: Synthesis of Glycoproteins and Glycopeptides via Native Linkages to Study Glycan-Specific Roles in the Immune System. *Bioconjugate Chemistry*. American Chemical Society October 3, 2019, pp 2715–2726. https://doi.org/10.1021/acs.bioconjchem.9b00588.

(24) Marqvorsen, M. H. S.; Paramasivam, S.; Doelman, W.; Fairbanks, A. J.; van Kasteren, S. I. Efficient Synthesis and Enzymatic Extension of an N -GlcNAz Asparagine Building Block. *Chem. Commun.* **2019**, *55* (36), 5287–5290. https://doi.org/10.1039/C9CC02051A.

(25) Geijtenbeek, T. B. H.; Van Duijnhoven, G. C. F.; Van Vliet, S. J.; Krieger, E.; Vriend, G.; Figdor, C. G.; Van Kooyk, Y. Identification of Different Binding Sites in the Dendritic Cell-Specific Receptor DC-SIGN for Intercellular Adhesion Molecule 3 and HIV-1. *J. Biol. Chem.* **2002**, *277* (13), 11314–11320. https://doi.org/10.1074/jbc.M111532200.

(26) Aebi, M. N-Linked Protein Glycosylation in the ER. *Biochim. Biophys. Acta - Mol. Cell Res.* **2013**, *1833* (11), 2430–2437. https://doi.org/10.1016/J.BBAMCR.2013.04.001.

(27) McIntosh, J. D.; Brimble, M. A.; Brooks, A. E. S.; Dunbar, P. R.; Kowalczyk, R.; Tomabechi, Y.; Fairbanks, A. J. Convergent Chemo-Enzymatic Synthesis of Mannosylated Glycopeptides; Targeting of Putative Vaccine Candidates to Antigen Presenting Cells. *Chem. Sci.* **2015**, *6* (8), 4636–4642. https://doi.org/10.1039/c5sc00952a.

(28) Tomabechi, Y.; Krippner, G.; Rendle, P. M.; Squire, M. A.; Fairbanks, A. J. Glycosylation of Pramlintide: Synthetic Glycopeptides That Display in Vitro and in Vivo Activities as Amylin Receptor Agonists. *Chem. Eur. J.* **2013**, *19* (45), 15084–15088. https://doi.org/10.1002/chem.201303303.

(29) Liu, L.; Prudden, A. R.; Capicciotti, C. J.; Bosman, G. P.; Yang, J. Y.; Chapla, D. G.; Moremen, K. W.; Boons, G. J. Streamlining the Chemoenzymatic Synthesis of Complex N-Glycans by a Stop and Go Strategy. *Nat. Chem.* **2019**, *11* (2), 161–169. https://doi.org/10.1038/s41557-018-0188-3.

(30) Wang, Z.; Chinoy, Z. S.; Ambre, S. G.; Peng, W.; McBride, R.; De Vries, R. P.; Glushka, J.; Paulson, J. C.; Boons, G. J. A General Strategy for the Chemoenzymatic Synthesis of Asymmetrically Branched N-Glycans. *Science* **2013**, *341* (6144), 379–383. https://doi.org/10.1126/science.1236231.

(31) Geng, X.; Dudkin, V. Y.; Mandal, M.; Danishefsky, S. J. In Pursuit of Carbohydrate-Based HIV Vaccines, Part 2: The Total Synthesis of High-Mannose-Type Gp120 Fragments—Evaluation of Strategies Directed to Maximal Convergence. *Angew. Chem. Int. Ed.* **2004**, *43* (19), 2562–2565. https://doi.org/10.1002/anie.200353626.

(32) Walczak, M. A.; Hayashida, J.; Danishefsky, S. J. Building Biologics by Chemical Synthesis: Practical Preparation of Di- and Triantennary N-Linked Glycoconjugates. *J. Am. Chem. Soc.* **2013**, *135* (12), 4700–4703. https://doi.org/10.1021/ja401385v.

(33) Luber, T.; Niemietz, M.; Karagiannis, T.; Mönnich, M.; Ott, D.; Perkams, L.; Walcher, J.; Berger, L.; Pischl, M.; Weishaupt, M.; Eller, S.; Hoffman, J.; Unverzagt, C. A Single Route to Mammalian N-Glycans Substituted with Core Fucose and Bisecting GlcNAc. *Angew. Chemie* **2018**, *130* (44), 14751–14757. https://doi.org/10.1002/ANGE.201807742.

(34) Appelmelk, B. J.; van Die, I.; van Vliet, S. J.; Vandenbroucke-Grauls, C. M. J. E.; Geijtenbeek, T. B. H.; van Kooyk, Y. Cutting Edge: Carbohydrate Profiling Identifies New Pathogens That Interact with Dendritic Cell-Specific ICAM-3-Grabbing Nonintegrin on Dendritic Cells. *J. Immunol.* **2003**, *170* (4), 1635–1639. https://doi.org/10.4049/jimmunol.170.4.1635.

(35) Guo, Y.; Feinberg, H.; Conroy, E.; Mitchell, D. A.; Alvarez, R.; Blixt, O.; Taylor, M. E.; Weis, W. I.; Drickamer, K. Structural Basis for Distinct Ligand-Binding and Targeting Properties of the Receptors DC-SIGN and DC-SIGNR. *Nat. Struct. Mol. Biol.* **2004**, *11* (7), 591–598. https://doi.org/10.1038/nsmb784.

(36) Fehres, C. M.; Kalay, H.; Bruijns, S. C. M.; Musaafir, S. A. M.; Ambrosini, M.; Van Bloois, L.; Van Vliet, S. J.; Storm, G.; Garcia-Vallejo, J. J.; Van Kooyk, Y. Cross-Presentation through Langerin and DC-SIGN Targeting Requires Different Formulations of Glycan-Modified Antigens. *J. Control. Release* **2015**, *203*, 67–76.

(37) Frison, N.; Taylor, M. E.; Soilleux, E.; Bousser, M.-T.; Mayer, R.; Monsigny, M.; Drickamer, K.; Roche, A.-C. Oligolysine-Based Oligosaccharide Clusters. *J. Biol. Chem.* **2003**, *278* (26), 23922–23929. https://doi.org/10.1074/jbc.M302483200.

(38) Timpano, G.; Tabarani, G.; Anderluh, M.; Invernizzi, D.; Vasile, F.; Potenza, D.; Nieto, P. M.; Rojo, J.; Fieschi, F.; Bernardi, A. Synthesis of Novel DC-SIGN Ligands with an α-Fucosylamide Anchor. *ChemBioChem* **2008**, *9* (12), 1921–1930. https://doi.org/10.1002/cbic.200800139.

(39) von dem Bruch, K.; Kunz, H. Synthesis of N-Glycopeptide Clusters with Lewisx Antigen Side Chains and Their Coupling to Carrier Proteins. *Angew. Chemie Int. Ed. English* **1994**, *33* (1), 101–103. https://doi.org/10.1002/anie.199401011.

(40) Jagessar, S. A.; Heijmans, N.; Blezer, E. L. A.; Bauer, J.; Blokhuis, J. H.; Wubben, J. A. M.; Drijfhout, J. W.; van den Elsen, P. J.; Laman, J. D.; Hart, B. A. '. Unravelling the T-Cell-Mediated Autoimmune Attack on CNS Myelin in a New Primate EAE Model Induced with MOG 34-56 Peptide in Incomplete Adjuvant. *Eur. J. Immunol.* **2012**, *42* (1), 217–227. https://doi.org/10.1002/eji.201141863.

(41) Carrillo-Vico, A.; Leech, M. D.; Anderton, S. M. Contribution of Myelin Autoantigen Citrullination to T Cell Autoaggression in the Central Nervous System. *J. Immunol.* **2010**, *184* (6), 2839–2846. https://doi.org/10.4049/jimmunol.0903639.

(42) Inazu, T.; Kobayashi, K. A New Simple Method for the Synthesis of N^{α}-Fmoc-N^{β}-Glycosylated-L-Asparagine Derivatives. *Synlett* **1993**, *1993* (11), 869–870. https://doi.org/10.1055/s-1993-22637.

(43) Bianchi, A.; Bernardi, A. Traceless Staudinger Ligation of Glycosyl Azides with Triaryl Phosphines: Stereoselective Synthesis of Glycosyl Amides. *J. Org. Chem.* **2006**, *71* (12), 4565–4577. https://doi.org/10.1021/jo060409s.

(44) Toonstra, C.; Amin, M. N.; Wang, L. X. Site-Selective Chemoenzymatic Glycosylation of an HIV-1 Polypeptide Antigen with Two Distinct N-Glycans via an Orthogonal Protecting Group Strategy. *J. Org. Chem.* **2016**, *81* (15), 6176–6185.

(45) Ibatullin, F. M.; Selivanov, S. I. Reaction of N-Fmoc Aspartic Anhydride with Glycosylamines: A Simple Entry to N-Glycosyl Asparagines. *Tetrahedron Lett.* **2009**, *50* (46), 6351–6354. https://doi.org/10.1016/j.tetlet.2009.08.106.

(46) Yang, C. P.; Su, C. S. Effects of Solvents and Additives on the Reaction of N-Benzyloxycarbonyl-L-Aspartic Anhydride with L-Phenylalanine Methyl Ester (Synthesis of Aspartame). *J. Org. Chem.* **1986**, *51* (26), 5186–5191. https://doi.org/10.1021/jo00376a025.

(47) Horton, D. 2-Acetamido-3,4,6-Tri-O-Acetyl-2-Deoxy-α-d-Glucopyranosyl Chloride. In *General Carbohydrate Method*; 1972; Vol. 46, pp 282–285. https://doi.org/10.1016/b978-0-12-746206-6.50056-4.

(48) Andersen, S. M.; Heuckendorff, M.; Jensen, H. H. 3-(Dimethylamino)-1-Propylamine: A Cheap and Versatile Reagent for Removal of Byproducts in Carbohydrate Chemistry. *Org. Lett.* **2015**, *17* (4), 944–947. https://doi.org/10.1021/acs.orglett.5b00041.

(49) Liao, L.; Auzanneau, F.-I. The Amide Group in N-Acetylglucosamine Glycosyl Acceptors Affects Glycosylation Outcome. *J. Org. Chem.* **2005**, *70* (16), 6265–6273. https://doi.org/10.1021/jo050707+.

(50) Liao, L.; Auzanneau, F.-I. Glycosylation of N -Acetylglucosamine: Imidate Formation and Unexpected Conformation. *Org. Lett.* **2003**, *5* (15), 2607–2610. https://doi.org/10.1021/ol034669x.

(51) Hernández-Torres, J. M.; Achkar, J.; Wei, A. Temperature-Controlled Regioselectivity in the Reductive Cleavage of p-Methoxybenzylidene Acetals. *J. Org. Chem.* **2004**, *69* (21), 7206–7211. https://doi.org/10.1021/jo048999m.

(52) Sato, S.; Ito, Y.; Nukada, T.; Nakahara, Y.; Ogawa, T. Total Synthesis of X Hapten, III3 Fucα-NLc4 Cer. *Carbohydr. Res.* **1987**, *167* (C), 197–210. https://doi.org/10.1016/0008-6215(87)80279-3.

(53) van Kasteren, S. I.; Kramer, H. B.; Jensen, H. H.; Campbell, S. J.; Kirkpatrick, J.; Oldham, N. J.; Anthony, D. C.; Davis, B. G. Expanding the Diversity of Chemical Protein Modification Allows Post-Translational Mimicry. **2007**, *446* (7139), 1105–1109. https://doi.org/10.1038/nature05757.

(54) Tomabechi, Y.; Squire, M. A.; Fairbanks, A. J. Endo-β-N-Acetylglucosaminidase Catalysed Glycosylation: Tolerance of Enzymes to Structural Variation of the Glycosyl Amino Acid Acceptor. *Org. Biomol. Chem.* **2014**, *12* (6), 942–955. https://doi.org/10.1039/C3OB42104J.

(55) Yamamoto, N.; Takayanagi, A.; Sakakibara, T.; Dawson, P. E.; Kajihara, Y. Highly Efficient Synthesis of Sialylglycopeptides Overcoming Unexpected Aspartimide Formation during Activation of Fmoc-Asn(Undecadisialyloligosaccharide)-OH. *Tetrahedron Lett.* **2006**, *47* (8), 1341–1346. https://doi.org/10.1016/j.tetlet.2005.12.064.

(56) Urge, L.; Otvos, L.; Lang, E.; Wroblewski, K.; Laczko, I.; Hollosi, M. Fmoc-Protected, Glycosylated Asparagines Potentially Useful as Reagents in the Solid-Phase Synthesis of N-Glycopeptides. *Carbohydr. Res.* **1992**, *235* (C), 83–93. https://doi.org/10.1016/0008-6215(92)80080-K.

(57) Isidro-Llobet, A.; Álvarez, M.; Albericio, F. Amino Acid-Protecting Groups. *Chem. Rev.* **2009**, *109* (6), 2455–2504. https://doi.org/10.1021/cr800323s.

(58) Biancalana, M.; Koide, S. Molecular Mechanism of Thioflavin-T Binding to Amyloid Fibrils. *Biochimica et Biophysica Acta - Proteins and Proteomics*. Elsevier July 1, 2010, pp 1405–1412. https://doi.org/10.1016/j.bbapap.2010.04.001.

(59) Chiodo, F.; Marradi, M.; Tefsen, B.; Snippe, H.; van Die, I.; Penadés, S. High Sensitive Detection of Carbohydrate Binding Proteins in an ELISA-Solid Phase Assay Based on Multivalent Glyconanoparticles. *PLoS One* **2013**, *8* (8), e73027. https://doi.org/10.1371/journal.pone.0073027.

(60) Porkolab, V.; Chabrol, E.; Varga, N.; Ordanini, S.; Sutkevičiute, I.; Thépaut, M.; García-Jiménez, M. J.; Girard, E.; Nieto, P. M.; Bernardi, A.; Fieschi, F. Rational-Differential Design of Highly Specific Glycomimetic Ligands: Targeting DC-SIGN and Excluding Langerin Recognition. *ACS Chem. Biol.* **2018**, *13* (3), 600–608. https://doi.org/10.1021/acschembio.7b00958.

(61) Garcia-Vallejo, J. J.; van Kooyk, Y. The Physiological Role of DC-SIGN: A Tale of Mice and Men. *Trends in Immunology*. Elsevier Current Trends October 1, 2013, pp 482–486. https://doi.org/10.1016/j.it.2013.03.001.

(62) García-Vallejo, J. J.; Ambrosini, M.; Overbeek, A.; van Riel, W. E.; Bloem, K.; Unger, W. W. J.; Chiodo, F.; Bolscher, J. G.; Nazmi, K.; Kalay, H.; van Kooyk, Y. Multivalent Glycopeptide Dendrimers for the Targeted Delivery of Antigens to Dendritic Cells. *Mol. Immunol.* **2013**, *53* (4), 387–397. https://doi.org/10.1016/j.molimm.2012.09.012.

(63) Gringhuis, S. I.; den Dunnen, J.; Litjens, M.; van der Vlist, M.; Geijtenbeek, T. B. H. Carbohydrate-Specific Signaling through the DC-SIGN Signalosome Tailors Immunity to Mycobacterium Tuberculosis, HIV-1 and Helicobacter Pylori. *Nat. Immunol.* **2009**, *10* (10), 1081–1088. https://doi.org/10.1038/ni.1778.

(64) Stolk, D. A.; de Haas, A.; Vree, J.; Duinkerken, S.; Lübbers, J.; van de Ven, R.; Ambrosini, M.; Kalay, H.; Bruijns, S.; van der Vliet, H. J.; de Gruijl, T. D.; van Kooyk, Y. Lipo-Based Vaccines as an Approach to Target Dendritic Cells for Induction of T- and INKT Cell Responses. *Front. Immunol.* **2020**, *11*, 990. https://doi.org/10.3389/fimmu.2020.00990.

3

Citrullinated human and murine MOG_{35-55} display distinct biophysical and biochemical behavior

W. Doelman, R.C. Reijnen, N. van Driel, I. Philippens, S.I. van Kasteren and M.C. Araman contributed to the work presented in this chapter

Introduction

Multiple Sclerosis (MS) is a family of neurodegenerative autoimmune diseases that presents itself pathologically in the form of neuroinflammation, demyelination and axonal damage.[1] Most patients (±85%) start with the remitting-relapsing form of the disease (RRMS), where episodes of neurological impairment (relapse) are followed by periods of symptom free survival (remission). A large cohort (±60%) of these patients later progresses into secondary progressive MS (SPMS), where neurological damage is chronic. A small portion of the patients

(10-15%) starts off with a progressive form of the disease. This is called primary progressive MS (PPMS).[2] While treatments exist to manage the remitting form of the disease, the progressive forms are untreatable at present.[3]

While involvement of the immune system is well established, the critical autoantigen that induces the autoimmune response has not been identified yet. Some candidate autoantigens are myelin basic protein (MBP), proteolipidprotein (PLP) and myelin oligodendrocyte glycoprotein (MOG).[4] Of these proteins, MOG was found in animal models to be critical for the induction of demyelinating disease.[5,6] In these studies, some regions of this protein have been found to induce strong immune responses, especially the peptide spanning residues 35-55 (MOG_{35-55}).[7,8]

One key area of active research in MS is that of post-translational modification of myelin proteins, in particular citrullination. Citrullination is the enzymatic deimidation of arginine, converting the guanidine function into a urea function. This reaction is carried out by a group of enzymes called the peptidyl arginine deimidases (PADs).[9] Hypercitrullination of MBP,[10,11] as well as a general increase in citrullinated proteins in brain samples[12] have been shown to be hallmarks of MS. Therefore, the biophysical and biochemical effects of citrullination on MPB and other myelin proteins, like MOG, is an area of active research.

Recently, the observation was made that the previously mentioned immunodominant peptide of murine MOG, $mMOG_{35-55}$, showed amyloid-like aggregation behavior after posttranslational citrullination.[13] Amyloid-like aggregation starts with a peptide (or protein) folding into a stable, β-sheet rich conformation. These structures can then associate with each other, forming oligomers and finally polymeric fibrils. This process is thermodynamically favorable, and formed fibrils have been shown to nucleate further amyloid formation, creating a positive feedback loop that drives the process towards further aggregation.[14]

This observation may place MS into the constantly growing class of amyloid diseases. This category contains many other incurable neurodegenerative diseases including Alzheimer's and Parkinson's disease. In these diseases, the formation of amyloids, from the Aβ peptide in Alzheimer's disease[15] and the protein α-synuclein in Parkinson's disease[16], produce fibrils that appear to be involved in disease progression. While amyloid-like aggregates have not been shown inside MS patient brain autopsies, the potential involvement of amyloids in MS pathology and disease progression is an exciting line of inquiry. Specifically, the speculative involvement of an amyloidogenic process might explain some of the features of progressive MS, as well as the switch from RRMS to SPMS, both of which are yet poorly understood.[17]

However, the above-described research on MOG_{35-55} aggregation was conducted using a peptide derived from the murine sequence of MOG. MOG, and specifically the immunodominant regions involved, are highly conserved between species. While this is a helpful feature for animal experiments, some single amino acid polymorphisms are present and their effects need to be considered. Specifically, the murine and human sequence of the MOG_{35-55} peptide differs by one residue, with the murine Ser_{42} residue substituted for Pro in

humans (Figure 1). MOGs of other commonly used laboratory animals (*i.e.*, rats and common marmosets) also feature a Ser$_{42}$ residue. It is not unlikely that the switch from Ser to Pro drives human MOG$_{35-55}$ to behave different from that of these animal models.

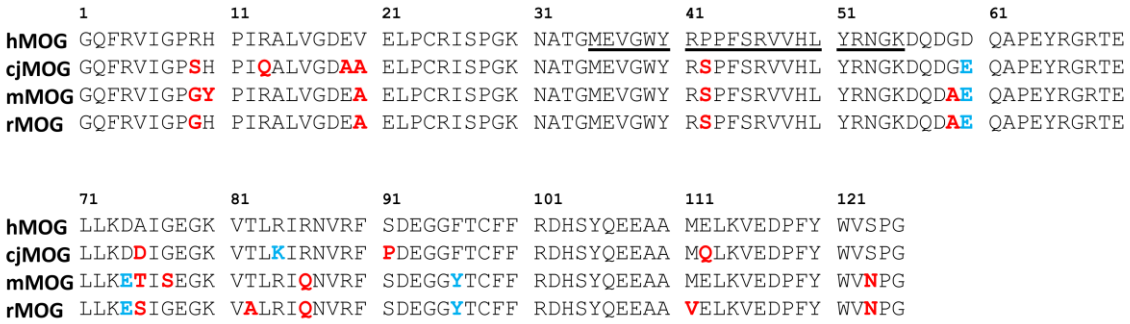

Figure 1. Amino acid sequence of the extracellular part (AAs 1-125) of Myelin Oligodendrocyte Glycoprotein (MOG) for human (hMOG), *Callithrix jacchus* or common marmoset (cjMOG), mice (mMOG) and rat (rMOG). Residues that are mutated compared to the human protein are marked red, while minor, highly similar, mutations are marked in blue. The immunodominant portion, MOG$_{35-55}$, is underlined.

In this chapter, the amyloidogenic properties of citrullinated human and murine MOG$_{35-55}$ peptides are compared to each other. To investigate the sensitivity of the aggregation of citrullinated MOG$_{35-55}$ peptides to variation on position 42, some further modifications on this position were also screened, that covered the intermediate chemical space between the mouse and human MOG-peptides. Finally, the immunological consequences of these Ser-to-Pro modifications were evaluated using an earlier described B-cell cross-presentation assay in the marmoset.[18]

Results and discussion

To investigate whether amyloid-like aggregation is unique to the mouse peptide, hMOG$_{35-55}$ peptides bearing the same citrullination patterns as the strongest aggregating mouse peptides, hMOG$_{35-55}$-Cit$_{41,46}$ and hMOG$_{35-55}$-Cit$_{46,52}$, were synthesized. The hMOG$_{35-55}$ peptide, bearing no Arg-to-Cit substitutions, was also synthesized as a control. All peptides were synthesized on Tentagel S RAM resin for its ease of synthesis, yielding the desired C-terminally amidated peptides, as previously reported in Chapter 2 and by Araman *et al.*[13]

Next, MOG$_{35-55}$ peptides where Ser$_{42}$ was replaced with alanine, threonine, or the unnatural amino acid L-aminobutyric acid (Abu), structurally close analogues of serine, were synthesized. These isosteres of serine were hypothesized to show comparable amyloid-like aggregation and were postulated to reveal something about the importance of position 42 for aggregation. Furthermore, proline hydroxylation,[19] an oxidative modification of proline that introduces a hydroxyl group onto the proline pyrrolidine ring, was considered as a potential modifier of the aggregation of the human peptide, since the hydroxy function of serine could be critical to the aggregation. In order to test this hypothesis, peptides replacing Pro$_{42}$ or Pro$_{43}$ with 4-

hydroxyproline were also synthesized. A complete overview of all the synthesized peptides, together with a qualitative indication of their aggregation propensity and the chemical yield after Fmoc-SPPS synthesis and RP-HPLC purification, is given in Table 1.

Table 1. Overview of all synthesized peptides. In every peptide sequence the amino acids changed from the human sequence hMOG$_{35-55}$ are highlighted in boldface. [a] explanation of aggregation symbols: -, no aggregation at all concentrations; +, slow aggregation at some concentrations; ++, rapid aggregation at some concentrations, +++, rapid concentration at all concentrations; [b] synthesis was previously described in Araman *et al.*[13]

Name	Sequence	Aggregation[a]	Yield (%)
hMOG$_{35-55}$	MEVGWYRPPFSRVVHLYRNGK-NH_2	-	26
hMOG$_{35-55}$-Cit$_{41,46}$	MEVGWY***Cit***PPFS***Cit***VVHLYRNGK-NH_2	-	12
hMOG$_{35-55}$-Cit$_{46,52}$	MEVGWYRPPFS***Cit***VVHLY***Cit***NGK-NH_2	-	22
mMOG$_{35-55}$	MEVGWYR**S**PFSRVVHLYRNGK-NH_2	-	-[b]
mMOG$_{35-55}$-Cit$_{41,46}$	MEVGWY***Cit*****S**PFS***Cit***VVHLYRNGK-NH_2	+++	-[b]
mMOG$_{35-55}$-Cit$_{46,52}$	MEVGWYR**S**PFS***Cit***VVHLY***Cit***NGK-NH_2	+++	-[b]
MOG$_{35-55}$-Ala$_{42}$-Cit$_{41,46}$	MEVGWY***Cit*****A**PFS***Cit***VVHLYRNGK-NH_2	-	24
MOG$_{35-55}$-Ala$_{42}$-Cit$_{46,52}$	MEVGWYR**A**PFS***Cit***VVHLY***Cit***NGK-NH_2	++	21
MOG$_{35-55}$-Thr$_{42}$-Cit$_{41,46}$	MEVGWY***Cit*****T**PFS***Cit***VVHLYRNGK-NH_2	-	35
MOG$_{35-55}$-Thr$_{42}$-Cit$_{46,52}$	MEVGWYR**T**PFS***Cit***VVHLY***Cit***NGK-NH_2	-	16
MOG$_{35-55}$-Abu$_{42}$-Cit$_{41,46}$	MEVGWY***CitAbu***PFS***Cit***VVHLYRNGK-NH_2	++	30
MOG$_{35-55}$-Abu$_{42}$-Cit$_{46,52}$	MEVGWYR***Abu***PFS***Cit***VVHLY***Cit***NGK-NH_2	-	38
MOG$_{35-55}$-Hyp$_{42}$-Cit$_{41,46}$	MEVGWY***CitHyp***PFS***Cit***VVHLYRNGK-NH_2	-	13
MOG$_{35-55}$-Hyp$_{42}$-Cit$_{46,52}$	MEVGWYR***Hyp***PFS***Cit***VVHLY***Cit***NGK-NH_2	-	30
hMOG$_{35-55}$-Hyp$_{43}$-Cit$_{41,46}$	MEVGWY***Cit***P***Hyp***FS***Cit***VVHLYRNGK-NH_2	-	27
hMOG$_{35-55}$-Hyp$_{43}$-Cit$_{46,52}$	MEVGWYRP***Hyp***FS***Cit***VVHLY***Cit***NGK-NH_2	-	23

The formation of amyloid like aggregates was quantified using the fluorogenic dye Thioflavin T,[20] as described in Chapter 2. This dye strongly increases its fluorescence upon binding to the typical cross-beta sheet-like structures that are present in amyloid-like aggregates. This allowed for the study of the kinetics of aggregate formation. The peptides were incubated at 37°C in a sodium acetate buffer at pH 5, conditions previously determined to be optimal for mMOG$_{35-55}$-Cit$_{41,46}$ and mMOG$_{35-55}$-Cit$_{46,52}$, (as these peptides are produced after uptake in the lysosome, where the environment is acidic) for up to 16 hours while the amyloid aggregation was followed by measuring the increase of the ThT fluorescent signal, as compared to a sample containing no peptide. As expected, neither hMOG$_{35-55}$ (Figure 2A) nor mMOG$_{35-55}$ (Figure 2B) showed amyloid-like aggregation under these conditions. Surprisingly, while mMOG$_{35-55}$-Cit$_{41,46}$ (Figure 2D) and mMOG$_{35-55}$-Cit$_{46,52}$ (Figure 2F) peptides showed clear increase in ThT signal over time as expected, this effect was absent for the hMOG$_{35-55}$-Cit$_{41,46}$ (Figure 2C) and for hMOG$_{35-55}$-Cit$_{46,52}$ (Figure 2E) peptides. This indicates that these peptides, unlike their murine counterparts, are *not* amyloidogenic.

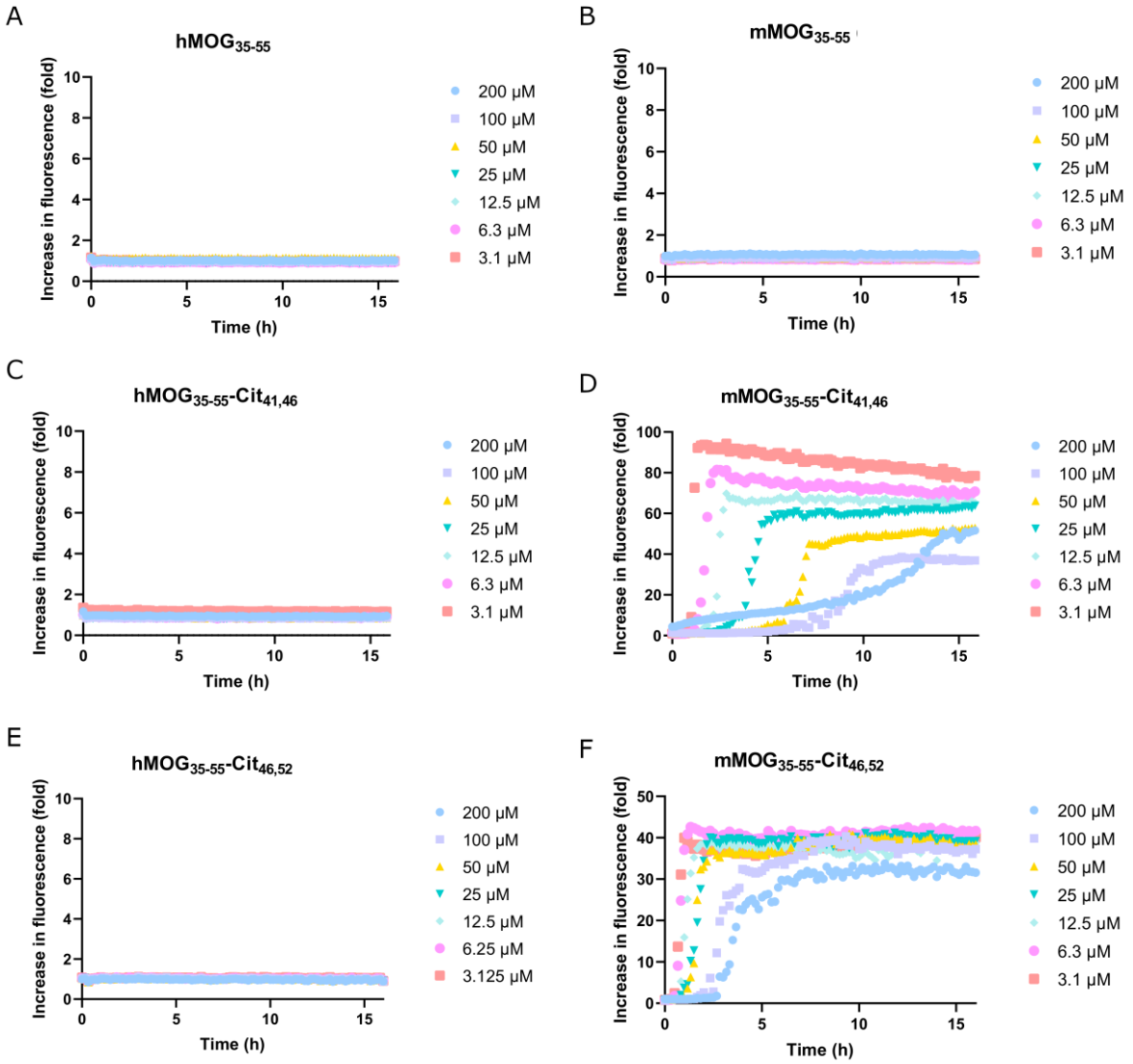

Figure 2. A-F) ThT aggregation assays showing the aggregation properties of hMOG$_{35-55}$ and mMOG$_{35-55}$ and their citrullinated variants at pH=5 (20 mM NaOAc buffer) and 37°C.

To assess whether the hMOG peptides had any propensity to aggregate at all, a seeding experiment was performed by which solutions of the human peptide were seeded with aggregates of mMOG$_{35-55}$-Cit$_{46,52}$. To this end, 200 µL of a 40 µM mMOG$_{35-55}$-Cit$_{46,52}$ solution in pH 5 NaOAc buffer was incubated at 37°C for 24 hours, followed by centrifugation at 20,000 g for 30 minutes. After discarding the supernatant, the seeds were homogenized in 200 µL buffer and co-incubated with either hMOG$_{35-55}$-Cit$_{41,46}$ or hMOG$_{35-55}$-Cit$_{46,52}$. No aggregation was observed in these experiments, indicating that nucleation is not the missing factor that can induce aggregation of citrullinated hMOG$_{35-55}$ peptides.

Next, the series of peptides containing the close analogues of serine, that is alanine, threonine and aminobutyric acid, were similarly evaluated using the ThT assay (Figure 3).

Firstly, alanine modification was assessed, where Ser$_{42}$ was substituted by an alanine residue. In this series, MOG$_{35-55}$-Ala$_{42}$-Cit$_{41,46}$ showed little increase in ThT fluorescence over 16h

(Figure 3A), whereas MOG_{35-55}-Ala_{42}-$Cit_{46,52}$ did show a clear increase in ThT signal (Figure 3B). However, when compared to the original serine containing peptide, $mMOG_{35-55}$-$Cit_{46,52}$, the aggregation was slower. This difference in time of onset was obtained by fitting a sigmoidal aggregation curve to the data obtained at a concentration of 3.1, 6.3 and 12.5 µM.[21] However, the quality of the fit was poor, indicating that the alanine substituted peptide does not fit the sigmoidal aggregation model well, making calculations of the differences of the rate of aggregation complicated. However, with these limitations kept in mind, an t_{50} (time to reaching 50% of maximum fluorescence) of 6.1 ± 0.2 hours was obtained for this peptide at 6.3 µM concentration. This gives a Δt_{50} of 5.3 hours compared to $mMOG_{35-55}$-$Cit_{46,52}$, for which a t_{50} of 0.79 ± 0.012 hours was found at the same concentration.

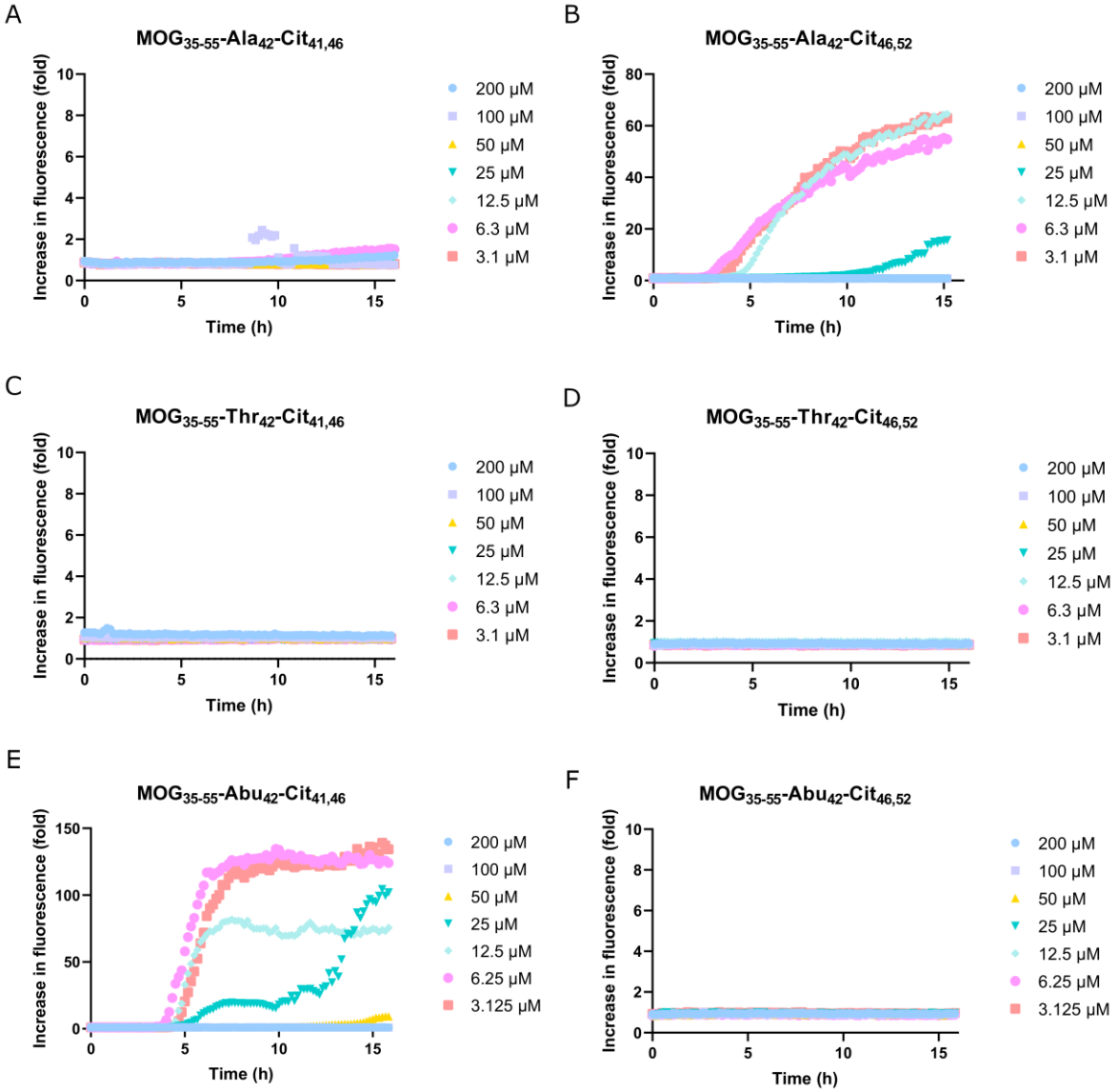

Figure 3. ThT aggregation assays showing the aggregation properties of MOG_{35-55}-$Cit_{41,46}$ and MOG_{35-55}-$Cit_{46,52}$ when Ser_{42} is replaced with either alanine (A, B), threonine (C, D), L-2-aminobutyric acid (Abu) (E, F)

The peptides with the Ser-to-Thr substitution at position 42, MOG_{35-55}-Thr_{42}-$Cit_{41,46}$ and MOG_{35-55}-Thr_{42}-$Cit_{46,52}$, were considered next. These peptides, again showed no increase in ThT fluorescence for the entire duration of the measurement (Figures 3C&3D).

The peptides in which Ser was substituted for the unnatural amino acid L-aminobutyric acid showed the opposite effect on aggregation from the alanine containing peptide was observed, as MOG_{35-55}-Abu_{42}-$Cit_{41,46}$ (Figure 3E) showed amyloid-like aggregation behavior in the ThT assay while its counterpart MOG_{35-55}-Abu_{42}-$Cit_{46,52}$ (Figure 3F) did not. The citrullinated $hMOG_{35-55}$ peptides containing 4-hydroxyproline (Hyp) in place of Pro_{42} and/or Pro_{43} were evaluated as these peptides represent a biologically accessible hybrid between the human and the mouse peptides (i.e. containing both a hydroxyl-functionality and a proline). None of these showed an increase in ThT fluorescence after 16 hours (Figure 4). This indicates that simple oxidation of proline to hydroxyproline is insufficient to turn a nonaggregating peptide into an aggregating one.

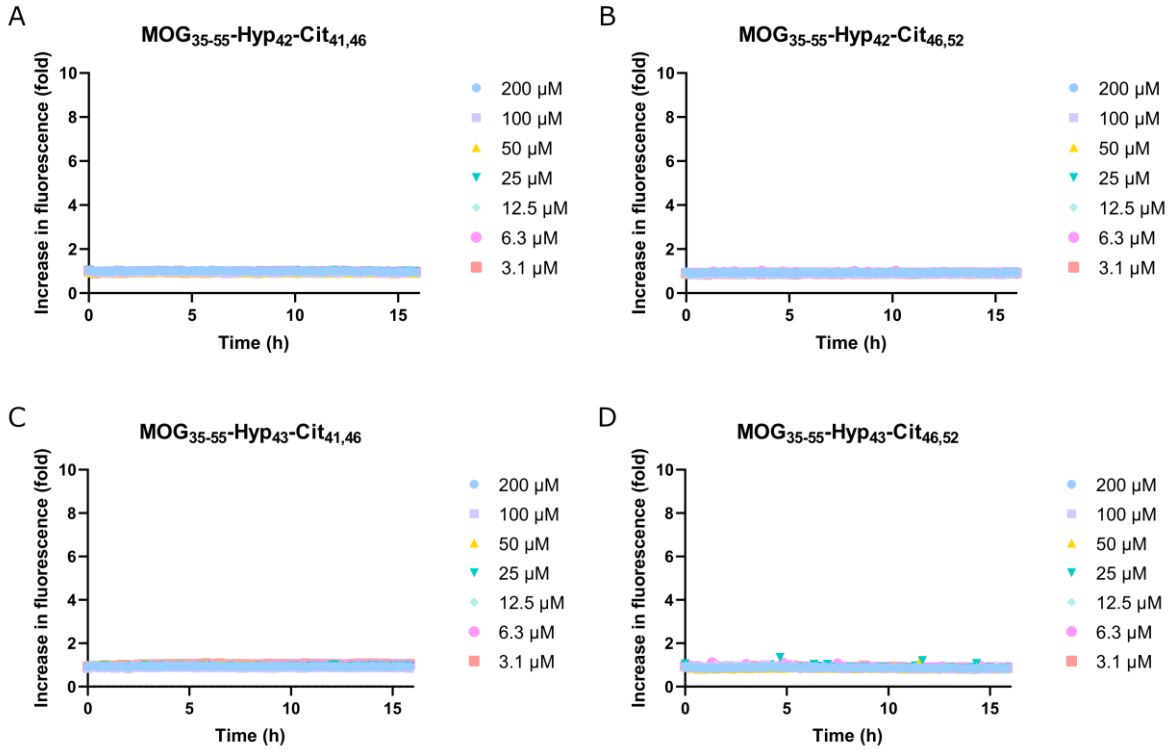

Figure 4. ThT aggregation assays showing the aggregation properties of citrullinated $hMOG_{35-55}$ peptides hydroxylated on either Pro_{42} (A, B) or Pro_{43} (C, D)

In conclusion, it seems that the primary hydroxyl functionality of serine is of key importance to this aggregation process as none of the peptides containing an aliphatic amino acid instead of serine displayed the same level of aggregation. The lack of aggregation seen with amino acids bearing a secondary alcohol, as well as the erratic aggregation of the alkylic amino acids could imply that both the size of the sidechain and the serine hydroxyl group have key roles in the aggregation process.

These findings could have great impact on the interpretation of immunological experiments carried out with these peptides in animal-model studies. One of these models, and one of the more refined animal models of multiple sclerosis-like neuroinflammation and neurodegeneration, is the experimental autoimmune encephalomyelitis (EAE) model in the common marmoset (*Callitrix jacchus*) developed by the 't Hart group. In this model, in contrast to many of the earlier murine models, immunization with the $hMOG_{35-55}$ peptide, in the absence of any immune adjuvant, induces severe neurological inflammation and impairment.[18,22] This finding underlines the great immune stimulating potential of this short MOG peptide.

Further characterization of this model found a critical role for B-cells as antigen presenting cells for the activation of $CD8^+$ T-cells. Surprisingly, it was found that the immunodominant epitope $hMOG_{40-48}$ was presented via the non-classical MHC I molecule Caja-E, a close marmoset analogue to the human HLA-E complex.[18] In an *in vitro* assay using cells derived from these monkeys, it had previously been shown that the aggregating citrullinated peptides $mMOG_{35-55}$-$Cit_{41,46}$ and $mMOG_{35-55}$-$Cit_{41,46}$, in contrast to non-citrullinated $mMOG_{35-55}$, did *not* induce T-cell proliferation, instead displaying cytotoxicity.[13]

An important unanswered biological question stemming from this was whether the changes in aggregation of citrullinated $mMOG_{35-55}$ between mouse and human sequences affected T-cell responses against the dominant MHC-I-restricted epitopes contained within these sequences. With the remarkable difference in amyloidogenic potential between the human and murine peptides now known, it was next investigated what, if any, effect this has on the cross-presentation potential of these peptides.

To this end, T-cell activation by the different human and murine MOG_{35-55} peptides was evaluated. For this assay, cells isolated from the axillary lymph node (ALN) of marmosets immunized with $hMOG_{34-56}$ were utilized, as reported previously.[13,23] Briefly, EBV-infected marmoset B-lymphoblastoid cells (BLCs) were lethally irradiated and incubated with different concentration (10, 3 and 1 µM) of the peptides for 1 hour. After this incubation period, freshly thawed marmoset ALN cells were added to the BLC culture and co-cultured for 48 hours and the proliferation of the lymphocyte cells was determined via an [^{3}H]thymidine incorporation assay. From this assay a stimulation index (SI, ratio of proliferation of treated cells versus untreated control) was calculated, and a SI > 2 was considered T-cell activation. The experiment was carried out with cells isolated from three different marmosets and the individual responses as well as the mean response were plotted in Figure 5.

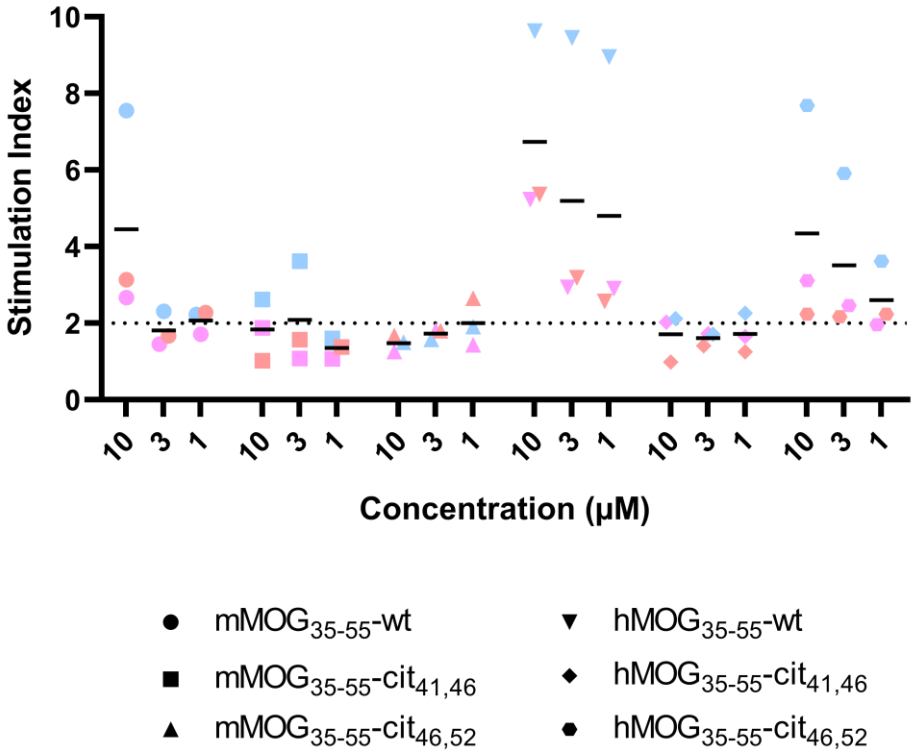

Figure 5. B-cells isolated from rhMOG immunized marmosets where stimulated with different peptides at the indicated concentrations for 1 hours. T-cells were added and proliferation was measured using a [^{3}H]thymidine incorporation assays. A stimulation index (ratio of proliferation for stimulated T-cells versus unstimulated control, SI) was plotted for each condition and SI > 2 was taken as the cut-off for T-cell activation. The experiment was carried out using material from three different animals (N=3), with the individual responses shown as three distinct colors.

A strong response against $hMOG_{35-55}$ was observed at all concentrations tested, which was expected as this was the immunogen used to immunize the marmosets. The peptide derived from the murine (and also marmoset) sequence, $mMOG_{35-55}$ also induced a strong proliferation at the highest tested concentration (10 µM). The citrullinated human peptide $hMOG_{35-55}$-$Cit_{46,52}$ produced a strong increase in T-cell proliferation, while the murine counterpart $mMOG_{35-55}$-$Cit_{46,52}$ shows no proliferation. Finally, neither $mMOG_{35-55}$-$Cit_{41,46}$ nor $hMOG_{35-55}$-$Cit_{41,46}$ produced a T-cell response in this assay. While previous work had already indicated immunological differences between human and murine MOG_{35-55} using a murine system,[24] this striking difference of T-cell activation between $mMOG_{35-55}$-$Cit_{46,52}$ and $hMOG_{35-55}$-$Cit_{46,52}$ was unknown.

Conclusion

The role of citrullination in both MS and EAE is currently poorly understood. While evidence exists for an increase of citrullination of the key myelin protein Myelin Basic Protein (MBP)[25] as well as a general increase in protein citrullination in white matter[26] in MS patients, citrullination of MOG itself has never been directly detected. However, in the animal model of MS, EAE, MOG is the most commonly studied autoantigen, and the effect of citrullination on the key antigenic peptide MOG_{35-55} has been studied extensively.[27–30]

The recently described aggregation behavior of citrullinated $mMOG_{35-55}$[13] opened up a new avenue for MOG mediated disease progression in MS, where the aggregation of citrullinated peptide could potentially directly induce neurodegeneration once sufficient levels of citrullination are achieved. However, the findings in this chapter show that the aggregation of citrullinated MOG_{35-55} is inherent only to the peptides containing serine on position 42, a polymorphism that is present in many of the commonly studied laboratory animals (mice, rats, common marmosets), but is replaced by proline in the human sequence of MOG. This one amino acid change renders the peptide completely resistant to amyloid like aggregation under the conditions that were optimal for the murine peptides.

In order to better understand the large effect this single amino acid substitution has on the peptide properties, a series of single amino acid substitutions were synthesized and screened for their aggregation behavior. The results obtained here indicate that serine is critical for the observed effect, with all amino acid substitutions tested producing either a far weaker aggregating peptide or, in most cases, a non-aggregating peptide.

The aforementioned previous study on the aggregating citrullinated murine peptides had also shown non-immunogenic properties of these peptides in an EBV infected B-cell cross-presentation assay. Unexpectedly, one of the human citrullinated peptides tested here, $hMOG_{35-55}$-$Cit_{46,52}$, showed strong T-cell activation in the same assay, raising questions about the validity of the animal models for the study of the autoantigenic responses in MS. A potential explanation for the discrepancy in T-cell activation is the aggregation behavior of the murine peptide. The murine citrullinated peptide might form an insoluble aggregate either inside or outside of the cell, inhibiting both (productive) peptide processing and epitope presentation. It is currently unknown whether the aggregated forms of the murine peptides are resistant to degradation and how this influences antigen processing. However, one could speculate that the formed aggregates might prohibit production of the key epitope peptide, limiting T-cell activation in this way. Additionally, while not studied here, cytotoxicity of aggregated peptide towards T-cells has been put forward as a potential reason for lack of T-cell activation observed with the citrullinated $mMOG_{35-55}$ peptides.[13]

Taken together, more work is needed in validating multiple sclerosis animal models using myelin oligodendrocyte glycoprotein as a model autoantigen, especially when studying the effects of citrullination.

Experimental

General peptide synthesis

SPPS of peptides was carried out using manual synthesis on a 50 µmol on Tentagel S RAM resin (Rapp Polymere GmbH, Germany) when a C-terminal carboxamide was desired, or on chloro-(2'-chloro)-trityl (CTC) polystyrene resin when a C-terminal carboxylic acid was intended. Fmoc protected amino acids were purchased from either Novabiochem or Sigma-Aldrich. For the amino acids that require sidechain protection, the following protecting groups were used: tBu for Ser, Thr, Tyr and Hyp; OtBu for Asp and Glu; Trt for Asn, Gln and His; Boc for Lys and Trp; Pbf for Arg. To load the first amino acid onto CTC resin, 2 eq of the desired amino acid together with 5 eq of DiPEA dissolved in anhydrous DCM (1.25 mL) are added to the resin which was gently agitated overnight. The loaded resin was then washed with DCM and capped using a mixture of MeOH/DiPEA/DCM (2:1:17) for one hour. To extend the growing peptide chain, 5 eq of Fmoc-amino acid was mixed together with an equimolar quantity of 2-(6-Chloro-1-H-benzotriazole-1-yl)-1,1,3,3-tetramethylaminium hexafluorophosphate (HCTU) in DMF at an concentration of 0.5 M, followed by the addition of 10 eq of diisopropylethylamine (DiPEA) and preactivation for 2 minutes. Coupling reaction were carried out for 30-45 minutes. Fmoc deprotection was accomplished by repeated treatment with 20% piperidine in DMF (3 + 7 min). Global deprotection and resin cleavage of peptides was accomplished using a 95:2.5:2.5 mixture of TFA/TIS/H_2O for 3 hours, followed by precipitation from cold diethyl ether (1:9 ratio TFA to ether) and recovery of the precipitate by centrifugation. Crude, tryptophan containing peptides were dissolved in MilliQ water an lyophilized overnight in order to remove the residual carboxylate. Preparative reverse phase HPLC on a Waters AutoPurification system (eluent A: H_2O + 0.2% TFA; eluent B: ACN) with a preparative Gemini C18 column (5 µm, 150 x 21.2 mm) yielded the final products. Peptides were characterized using electrospray ionization mass spectrometry (ESI-MS) on a Thermo Finnigan LCQ Advantage Max LC-MS instrument with a Surveyor PDA plus UV detector on an analytical C18 column (Phenomenex, 3 µm, 110 Å, 50 mm × 4.6 mm) in combination with buffers A (H_2O), B (MeCN), and C (1% aq TFA). Quality of crude and purified peptides was evaluated with a linear gradient of 10-50% B with a constant 10% C over 10 minutes. Preparative reverse phase HPLC on a Waters AutoPurification system (eluent A: H_2O + 0.2% TFA; eluent B: ACN) with a preparative Gemini C18 column (5 µm, 150 x 21.2 mm) yielded the final products.

Table of synthesized peptides

Table 2. Overview of all synthesized peptides. [a] synthesis was previously described in Araman *et al.*[13]

Name	Sequence	Expected mass [M+2H]	Found mass [M+2H]	Yield (%)
$mMOG_{35-55}$	MEVGWYRSPFSRVVHLYRNGK-NH_2	-	-	-[a]
$hMOG_{35-55}$	MEVGWYRPPFSRVVHLYRNGK-NH_2	1295.7	1296.3	25.6
$hMOG_{35-55}$-$Cit_{41,46}$	MEVGWY*Cit*PPFS*Cit*VVHLYRNGK-NH_2	1296.5	1297.3	12.4
$hMOG_{35-55}$-$Cit_{46,52}$	MEVGWYRPPFS*Cit*VVHLY*Cit*NGK-NH_2	1296.5	1297.4	22.4
$mMOG_{35-55}$-$Cit_{41,46}$	MEVGWY*Cit*SPFS*Cit*VVHLYRNGK-NH_2	-	-	-[a]
$mMOG_{35-55}$-$Cit_{46,52}$	MEVGWYRSPFS*Cit*VVHLY*Cit*NGK-NH_2	-	-	-[a]

MOG$_{35-55}$-Ala$_{42}$-Cit$_{41,46}$	MEVGWY*Cit*APFS*Cit*VVHLYRNGK-NH_2	1283.7	1284.2	24.2
MOG$_{35-55}$-Ala$_{42}$-Cit$_{46,52}$	MEVGWYRAPFS*Cit*VVHLY*Cit*NGK-NH_2	1283.7	1284.2	21.1
MOG$_{35-55}$-Thr$_{42}$-Cit$_{41,46}$	MEVGWY*Cit*TPFS*Cit*VVHLYRNGK-NH_2	1298.7	1299.1	34.9
MOG$_{35-55}$-Thr$_{42}$-Cit$_{46,52}$	MEVGWYRTPFS*Cit*VVHLY*Cit*NGK-NH_2	1298.7	1299.1	15.8
MOG$_{35-55}$-Abu$_{42}$-Cit$_{41,46}$	MEVGWY*CitAbu*PFS*Cit*VVHLYRNGK-NH_2	1290.7	1291.2	30.2
MOG$_{35-55}$-Abu$_{42}$-Cit$_{46,52}$	MEVGWYR*Abu*PFS*Cit*VVHLY*Cit*NGK-NH_2	1290.7	1291.3	38.3
MOG$_{35-55}$-Hyp$_{42}$-Cit$_{41,46}$	MEVGWY*CitHyp*PFS*Cit*VVHLYRNGK-NH_2	1304.7	1305.3	13.0
MOG$_{35-55}$-Hyp$_{42}$-Cit$_{46,52}$	MEVGWYR*Hyp*PFS*Cit*VVHLY*Cit*NGK-NH_2	1304.7	1305.1	30.0
hMOG$_{35-55}$-Hyp$_{43}$-Cit$_{41,46}$	MEVGWY*Cit*P*Hyp*FS*Cit*VVHLYRNGK-NH_2	1304.7	1305.1	27.1
hMOG$_{35-55}$-Hyp$_{43}$-Cit$_{46,52}$	MEVGWYRP*Hyp*FS*Cit*VVHLY*Cit*NGK-NH_2	1304.7	1305.3	23.4

ThT Fluorescence Aggregation Assays

Aggregation assays were carried out in 96-well plate format using a Infinite M1000 Pro Tecan plate reader. The excitation and emission wavelengths were set to 444 nm and 485 nm respectively, with a bandwidth of 10 nm. For each peptide under investigation, a 200 µM stock in sodium ascorbate buffer (20 mM, pH=5) was prepared and from this stock a serial diluted was made using the same buffer. Of these solutions, 199 µL of peptide stock was added into a well and mixed with 1 µL of 1 mM Thioflavin T stock solution, prepared in the same NaOAc buffer, for a final dye concentration of 5 µM. Every concentration of peptide was measured in triplicate. The plate was kept at 37°C and the fluorescence was measured every ten minutes for 16 hours. The fluorescence was normalized against a well containing 5 µM Thioflavin T in buffer that was measured alongside the assay.

T-cell Culture Assay

Mononuclear cells (MNC) were isolated from the axillary lymph node (ALN) from three adult common marmosets (*Callithrix jacchus*). These animals were used in EAE studies, to induce EAE the animals were immunised with MOG_{34-56} (Cambridge research biochemicals Ltd.) emulsified in IFA. EBV infected marmoset B-cells (BCLs) were used as antigen presenting cells.

For the proliferation assay the marmoset BCLs were collected and washed with PBS and irradiated with 70Gy in RPMI (Gibco) without FCS. BCLs were plated in 96-well round bottom plates (Greiner) at the concentration of $1{\cdot}10^3$ cells/well and incubated for 1H in an incubator with 5% CO_2 and 37°C with different concentration of the peptides (1 µM, 3 µM and 10 µM), the medium was used as a negative control. After 1 hour, thawed MNC were added to the BCLs at a concentration of $1{\cdot}10^5$ cells/well. After 48 hour 25µL of [methyl-3H] thymidine (0.1 mCi/mL stock; PerkinElmer) was added. 18 hour later the cells were harvested using a Filtermate Harvester (PerkinElmer) on a microfilter plate. When the plate had dried, 25µL of Ultima Gold™ (PerkinElmer) was added and measured on a MicroBeta2 counter (PerkinElmer).

References

(1) Thompson, A. J.; Baranzini, S. E.; Geurts, J.; Hemmer, B.; Ciccarelli, O. Multiple Sclerosis. *The Lancet*. Lancet Publishing Group April 21, 2018, pp 1622–1636. https://doi.org/10.1016/S0140-6736(18)30481-1.

(2) Dendrou, C. A.; Fugger, L.; Friese, M. A. Immunopathology of Multiple Sclerosis. *Nat. Rev. Immunol.* **2015**, *15* (9), 545–558. https://doi.org/10.1038/nri3871.

(3) Milo, R.; Kahana, E. Multiple Sclerosis: Geoepidemiology, Genetics and the Environment. *Autoimmunity Reviews*. Elsevier March 1, 2010, pp A387–A394. https://doi.org/10.1016/j.autrev.2009.11.010.

(4) Fraussen, J.; Claes, N.; de Bock, L.; Somers, V. Targets of the Humoral Autoimmune Response in Multiple Sclerosis. *Autoimmun. Rev.* **2014**, *13* (11), 1126–1137. https://doi.org/10.1016/j.autrev.2014.07.002.

(5) McFarland, H. I.; Lobito, A. A.; Johnson, M. M.; Nyswaner, J. T.; Frank, J. A.; Palardy, G. R.; Tresser, N.; Genain, C. P.; Mueller, J. P.; Matis, L. A.; Lenardo, M. J. Determinant Spreading Associated with Demyelination in a Nonhuman Primate Model of Multiple Sclerosis. *J. Immunol.* **1999**, *162* (4), 2384–2390.

(6) Smith, P. A.; Heijmans, N.; Ouwerling, B.; Breij, E. C.; Evans, N.; van Noort, J. M.; Plomp, A. C.; Delarasse, C.; Hart, B.; Pham-Dinh, D.; Amor, S. Native Myelin Oligodendrocyte Glycoprotein Promotes Severe Chronic Neurological Disease and Demyelination in Biozzi ABH Mice. *Eur. J. Immunol.* **2005**, *35* (4), 1311–1319. https://doi.org/10.1002/eji.200425842.

(7) Bernard, C. C. A.; Johns, T. G.; de Rosbo, N. K.; Ichikawa, M. A Peptide from Myelin Oligodendrocyte Glycoprotein That Induces Demyelinating Encephalomyelitis Resembling Multiple Sclerosis. *J. Neuroimmunol.* **1994**, *54* (1–2), 153. https://doi.org/10.1016/0165-5728(94)90266-6.

(8) Mendel, I.; Rosbo, N. K. de; Ben-Nun, A. Delineation of the Minimal Encephalitogenic Epitope within the Immunodominant Region of Myelin Oligodendrocyte Glycoprotein: Diverse Vβ Gene Usage by T Cells Recognizing the Core Epitope Encephalitogenic for T Cell Receptor Vβb and T Cell Receptor Vβa H-2b Mice. *Eur. J. Immunol.* **1996**, *26* (10), 2470–2479. https://doi.org/10.1002/EJI.1830261030.

(9) Vossenaar, E. R.; Zendman, A. J. W.; Van Venrooij, W. J.; Pruijn, G. J. M. PAD, a Growing Family of Citrullinating Enzymes: Genes, Features and Involvement in Disease. *BioEssays*. John Wiley & Sons, Ltd November 1, 2003, pp 1106–1118. https://doi.org/10.1002/bies.10357.

(10) Wood, D. D.; Moscarello, M. A. The Isolation, Characterization, and Lipid-Aggregating Properties of a Citrulline Containing Myelin Basic Protein. *J. Biol. Chem.* **1989**, *264* (9), 5121–5127. https://doi.org/10.1016/s0021-9258(18)83707-3.

(11) Kim, J. K.; Mastronardi, F. G.; Wood, D. D.; Lubman, D. M.; Zand, R.; Moscarello, M. A. Multiple Sclerosis: An Important Role for Post-Translational Modifications of Myelin Basic Protein in Pathogenesis *. *Mol. Cell. Proteomics* **2003**, *2* (7), 453–462. https://doi.org/10.1074/MCP.M200050-MCP200.

(12) Luchicchi, A.; Hart, B.; Frigerio, I.; van Dam, A. M.; Perna, L.; Offerhaus, H. L.; Stys, P. K.; Schenk, G. J.; Geurts, J. J. G. Axon-Myelin Unit Blistering as Early Event in MS Normal Appearing White Matter. *Ann. Neurol.* **2021**, *89* (4), 711–725. https://doi.org/10.1002/ana.26014.

(13) Araman, C.; Van Gent, M. E.; Meeuwenoord, N. J.; Heijmans, N.; Marqvorsen, M. H. S.; Doelman, W.; Faber, B. W.; 't Hart, B. A.; Van Kasteren, S. I. Amyloid-like Behavior of Site-Specifically Citrullinated Myelin Oligodendrocyte Protein (MOG) Peptide Fragments inside EBV-Infected B-Cells Influences Their Cytotoxicity and Autoimmunogenicity. *Biochemistry* **2019**, *58* (6), 763–775. https://doi.org/10.1021/acs.biochem.8b00852.

(14) Harrison, R. S.; Sharpe, P. C.; Singh, Y.; Fairlie, D. P. Amyloid Peptides and Proteins in Review. In *Reviews of Physiology, Biochemistry and Pharmacology*; Amara, S. G., Bamberg, E., Fleischmann, B., Gudermann, T., Hebert, S. C., Jahn, R., Lederer, W. J., Lill, R., Miyajima, A., Offermanns, S., Zechner, R., Eds.; Springer Berlin Heidelberg: Berlin, Heidelberg, 2007; pp 1–77. https://doi.org/10.1007/112_2007_0701.

(15) Chen, G. F.; Xu, T. H.; Yan, Y.; Zhou, Y. R.; Jiang, Y.; Melcher, K.; Xu, H. E. Amyloid Beta: Structure, Biology and Structure-Based Therapeutic Development. *Acta Pharmacologica Sinica*. Nature Publishing Group July 17, 2017, pp 1205–1235. https://doi.org/10.1038/aps.2017.28.

(16) Zhang, G.; Xia, Y.; Wan, F.; Ma, K.; Guo, X.; Kou, L.; Yin, S.; Han, C.; Liu, L.; Huang, J.; Xiong, N.; Wang, T. New Perspectives on Roles of Alpha-Synuclein in Parkinson's Disease. *Front. Aging Neurosci.* **2018**, *10*, 370. https://doi.org/10.3389/FNAGI.2018.00370/BIBTEX.

(17) Correale, J.; Gaitán, M. I.; Ysrraelit, M. C.; Fiol, M. P. Progressive Multiple Sclerosis: From Pathogenic Mechanisms to Treatment. *Brain* **2017**, *140* (3), 527–546. https://doi.org/10.1093/brain/aww258.

(18) Jagessar, S. A.; Heijmans, N.; Blezer, E. L. A.; Bauer, J.; Blokhuis, J. H.; Wubben, J. A. M.; Drijfhout, J. W.; van den Elsen, P. J.; Laman, J. D.; Hart, B. A. '. Unravelling the T-Cell-Mediated Autoimmune Attack on CNS Myelin in a New Primate EAE Model Induced with MOG 34-56 Peptide in Incomplete Adjuvant. *Eur. J. Immunol.* **2012**, *42* (1), 217–227. https://doi.org/10.1002/eji.201141863.

(19) Zurlo, G.; Guo, J.; Takada, M.; Wei, W.; Zhang, Q. New Insights into Protein Hydroxylation and Its Important Role in Human Diseases. *Biochim. Biophys. Acta - Rev. Cancer* **2016**, *1866* (2), 208–220. https://doi.org/10.1016/j.bbcan.2016.09.004.

(20) Biancalana, M.; Koide, S. Molecular Mechanism of Thioflavin-T Binding to Amyloid Fibrils. *Biochimica et Biophysica Acta - Proteins and Proteomics*. Elsevier July 1, 2010, pp 1405–1412. https://doi.org/10.1016/j.bbapap.2010.04.001.

(21) Sabareesan, A. T.; Udgaonkar, J. B. Amyloid Fibril Formation by the Chain B Subunit of Monellin Occurs by a Nucleation-Dependent Polymerization Mechanism. *Biochemistry* **2014**, *53* (7), 1206–1217. https://doi.org/10.1021/bi401467p.

(22) Jagessar, S. A.; Kap, Y. S.; Heijmans, N.; Van Driel, N.; Van Straalen, L.; Bajramovic, J. J.; Brok, H. P. M.; Blezer, E. L. A.; Bauer, J.; Laman, J. D.; 'T Hart, B. A. Induction of Progressive Demyelinating Autoimmune Encephalomyelitis in Common Marmoset Monkeys Using MOG34-56 Peptide in Incomplete Freund Adjuvant. *J. Neuropathol. Exp. Neurol.* **2010**, *69* (4), 372–385. https://doi.org/10.1097/NEN.0b013e3181d5d053.

(23) Jagessar, S. A.; Heijmans, N.; Blezer, E. L. A.; Bauer, J.; Weissert, R.; 't Hart, B. A. Immune Profile of an Atypical EAE Model in Marmoset Monkeys Immunized with Recombinant Human Myelin Oligodendrocyte Glycoprotein in Incomplete Freund's Adjuvant. *J. Neuroinflammation* **2015**, *12* (1), 169. https://doi.org/10.1186/s12974-015-0378-5.

(24) Oliver, A. R.; Lyon, G. M.; Ruddle, N. H. Rat and Human Myelin Oligodendrocyte Glycoproteins Induce Experimental Autoimmune Encephalomyelitis by Different Mechanisms in C57BL/6 Mice. *J. Immunol.* **2003**, *171* (1), 462–468. https://doi.org/10.4049/JIMMUNOL.171.1.462.

(25) Moscarello, M. A.; Wood, D. D.; Ackerley, C.; Boulias, C. Myelin in Multiple Sclerosis Is Developmentally Immature. *J. Clin. Invest.* **1994**, *94* (1), 146–154. https://doi.org/10.1172/JCI117300.

(26) Faigle, W.; Cruciani, C.; Wolski, W.; Roschitzki, B.; Puthenparampil, M.; Tomas-Ojer, P.; Sellés-Moreno, C.; Zeis, T.; Jelcic, I.; Schaeren-Wiemers, N.; Sospedra, M.; Martin, R. Brain Citrullination Patterns and T Cell Reactivity of Cerebrospinal Fluid-Derived CD4+ T Cells in Multiple Sclerosis. *Front. Immunol.* **2019**, *0* (APR), 540. https://doi.org/10.3389/FIMMU.2019.00540.

(27) Carrillo-Vico, A.; Leech, M. D.; Anderton, S. M. Contribution of Myelin Autoantigen Citrullination to T Cell Autoaggression in the Central Nervous System. *J. Immunol.* **2010**, *184* (6), 2839–2846. https://doi.org/10.4049/jimmunol.0903639.

(28) Haanstra, K. G.; Wubben, J. A. M.; Jonker, M.; Hart, B. A. t. Induction of Encephalitis in Rhesus Monkeys Infused with Lymphocryptovirus-Infected B-Cells Presenting MOG34–56 Peptide. *PLoS One* **2013**, *8* (8), e71549. https://doi.org/10.1371/JOURNAL.PONE.0071549.

(29) Jagessar, S. A.; Holtman, I. R.; Hofman, S.; Morandi, E.; Heijmans, N.; Laman, J. D.; Gran, B.; Faber, B. W.; van Kasteren, S. I.; Eggen, B. J. L.; 't Hart, B. A. Lymphocryptovirus Infection of Nonhuman Primate B Cells Converts Destructive into Productive Processing of the Pathogenic CD8 T Cell Epitope in Myelin Oligodendrocyte Glycoprotein. *J. Immunol.* **2016**, *197* (4), 1074–1088. https://doi.org/10.4049/jimmunol.1600124.

(30) Morandi, E.; Jagessar, S. A.; 't Hart, B. A.; Gran, B. EBV Infection Empowers Human B Cells for Autoimmunity: Role of Autophagy and Relevance to Multiple Sclerosis. *J. Immunol.* **2017**, *199* (2), 435–448.

4

Synthesis of glycosylated and fluorescently labeled antigenic peptides for immune-receptor interaction studies

Part of this work was published as: Riera, R.; Hogervorst, T.P.; Doelman, W.; Ni, Y.; Pujals, S.; Bolli, E.; Codée, J.D.C.; van Kasteren, S.I.; Albertazzi, L. Single-Molecule Imaging of Glycan–Lectin Interactions on Cells with Glyco-PAINT. *Nat. Chem. Biol.* **2021**, *17* (12), 1281–1288

L. Verschoor and R.W.R van den Kieboom also contributed to the work presented in this chapter

Introduction

Glycans have a critical role in immune response modulation through their interaction with immune lectins.[1–3] Immune cells express a variety of such lectins – protein receptors for glycans – and use these to distinguish self from non-self, leading to subsequent secretion of specific cytokines[4,5] and receptor-mediated endocytosis of the glycosylated material.[6]

One well-studied example of an immune lectin is the mannose receptor (MR, CD206), also known as the macrophage mannose receptor.[7] This protein contains multiple domains with different binding specificities.[8] It has eight C-type lectin domains (CTLs) for which evidence suggests only one, CTL4, is active.[9] The other domains do seem to play a role in recognition of larger glycan structures, like yeast mannan.[10] The CTLs of the mannose receptor not only bind mannosides and oligomannosides, but also fucosides and N-acetyl-glucosamine-containing carbohydrates.[11]

In addition to the CTL-domain, the MR has two additional binding domains: a fibronectin type II domain, capable of binding collagen fragments,[12] and a cysteine-rich lectin domain (CRD) capable of binding to sulfated sugars, particularly 4-sulfo-N-acetyl-galactosamine and 3-sulfo-galactose containing oligosaccharides.[13]

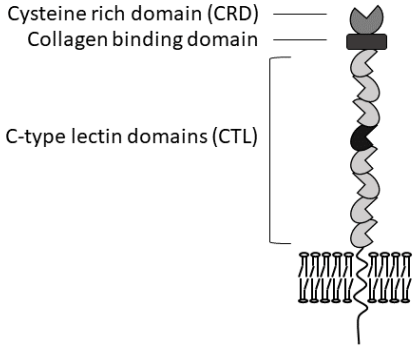

Figure 1. Cartoon representation of the mannose receptor (CD206). The CTL domain that is responsible for most of the calcium dependent oligosaccharide binding affinity (CTL4) is highlighted.

The biology of the MR is intriguing: it appears to enhance uptake of attached ligands in a receptor-dependent fashion, yet it possesses no internal signaling domains. In 2006, Kurts and co-workers[14] observed that MR-ligands showed enhanced antigen cross-presentation, while leaving MHC-II restricted antigen presentation unaffected. This effect seemed to be caused by differential routing of mannose receptor associated antigen compared to non-MR binding soluble antigen. As shown globally in Figure 2, regular pinocytosis of antigen targets an antigen to lysosomes, resulting in MHC class II presentation and activation of $CD4^+$ T-cells. MR-mediated uptake, however, results in sequestering of antigen in early endosomes, resulting in epitope presentation via MHC class I and activation of $CD8^+$ T-cells. This striking observation was deemed of importance to the field of vaccinology, as strong activation of a $CD8^+$ T-cell response is critical for anti-viral and anti-tumor vaccine regimes.[15] Achieving this using conventional vaccination strategies has proven difficult to date.[16]

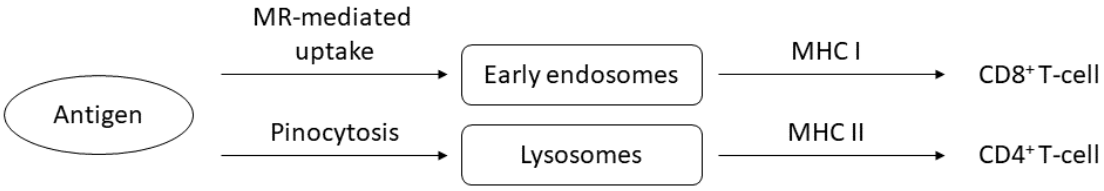

Figure 2. Simplified overview of the different routing of antigens and the different T-cell activations this results in, depending on MR-mediated uptake of antigen or uptake by pinocytosis.

Decoration of synthetic vaccines with MR-ligands is an area of active research.[17,18] Yet, to date, no direct correlation between mannoside-lectin binding characteristics and improved T-cell activation of a vaccine candidate has been made. This is largely due to the generally weak (mM to µM affinity) binding of carbohydrates to lectins.[11] This weak binding makes studying carbohydrate-lectin interactions using established techniques like surface plasmon resonance (SPR) or isothermal titration calorimetry (ITC) difficult. However, recently a microscopy-based method was developed that allowed for the evaluation of glycan-lectin interactions on the surface of a cell, using a points accumulation for imaging in nanoscale topography (PAINT) microscopy technique.

In PAINT microscopy, single molecule interactions are detected only when the fluorescent molecule under study is bound to some larger structure; the diffusional motion of unbound probe blurs the fluorescent signal to below detection limits. Interactions that slow the probe's diffusion for a certain length of time (hundreds of milliseconds), like glycan-lectin interactions, can be made visible as distinct events. The frequency these events are observed is correlated to the on-rate of the interaction, while the time (number of frames) they are visible is directly related to the off-rate. Glycoclusters were synthesized, containing various valences and configurations of carbohydrates, all containing a single fluorophore. By treating cells expressing the MR on the cell surface with low concentration (1-5 nM) of these probes, direct measurements of the lectin binding kinetics could be made for the first time. This method, dubbed "glyco-PAINT"[19] enables the direct, single molecule, observation of fluorescently labeled glycoclusters binding to the mannose receptor and the extraction of binding information from the approach.

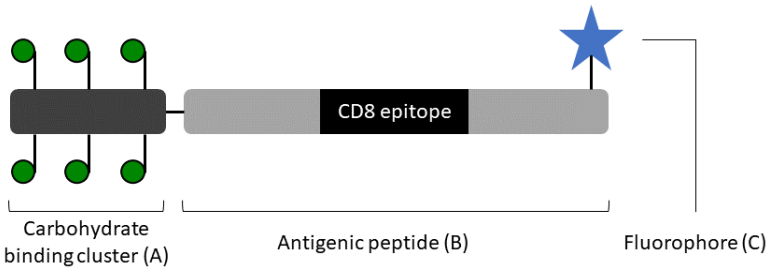

Figure 3. General design of the model antigenic peptides containing a mannose receptor binding carbohydrate cluster (A), an antigenic peptide containing a $CD8^+$ T-cell epitope (B) and a fluorophore (C) for tracking via glyco-PAINT.

It was envisaged that this technique could also be used to directly determine MR-binding kinetics of synthetic glycosylated vaccines. If this could then be combined with a $CD8^+$ T-cell activation study, a correlation between on-cell lectin binding kinetics and antigen cross-presentation could finally be established. This chapter describes the synthesis of a series of such glycosylated model peptides (Figure 3), containing a carbohydrate binding cluster (A, Figure 3), a CD8 T-cell epitope within flanking regions (B, Figure 3) and a fluorophore to allow glyco-PAINT of the constructs (C, Figure 3).

Results and Discussion

In order to study antigen uptake and cross-presentation using glyco-PAINT, a synthetic antigenic peptide bearing both one or more glycans as well as a fluorophore had to be designed and synthesized (Figure 4). As a first step in the design, the antigenic peptide was selected. The commonly employed model antigen $OVA_{247\text{-}264}$ was chosen as a first model antigen.[20,21] This peptide contains the MHC class I restricted epitope $OVA_{257\text{-}264}$ (SIINFEKL), commonly used in the study of antigen cross-presentation in mice and reagents for its immunological analysis are widely available. The $OVA_{247\text{-}264}$ peptide is often C-terminally extended with a A_5K spacer and previous work has indicated that the C-terminal lysine residue of this spacer can be modified with various functionalities without impairing antigen uptake and presentation.[21,22] This residue was therefore considered the preferred site for fluorophore introduction.

Similar previous work has also indicated that attachment of one or more azido-lysine residues N-terminal of the peptide is well tolerated in cross-presentation.[17,23] Propargylated glycans can then be installed by copper(I)-catalyzed azide alkyne cycloaddition (CuAAC). Variation of the number of azidolysines, as well as the spacing between the azidolysine residues enables the study of the effects multivalency has on the binding and internalization of glycosylated peptides. By introducing spacers of varying length between the azidolysine cluster and the N-terminus of the antigenic peptide, further optimization of the glycan-mediated uptake might be achieved. In the initial study, two spacers are compared: a single glycine residue and a triethylene-glycol based spacer, as described in Chapter 5. This last option could improve both aqueous solubility of the peptide as well as increasing the peptide's flexibility, and form an interesting contrast to the less flexible glycine spacer. Both of these spacer options are compatible with in-line Fmoc-SPPS, simplifying synthetic accessibility.

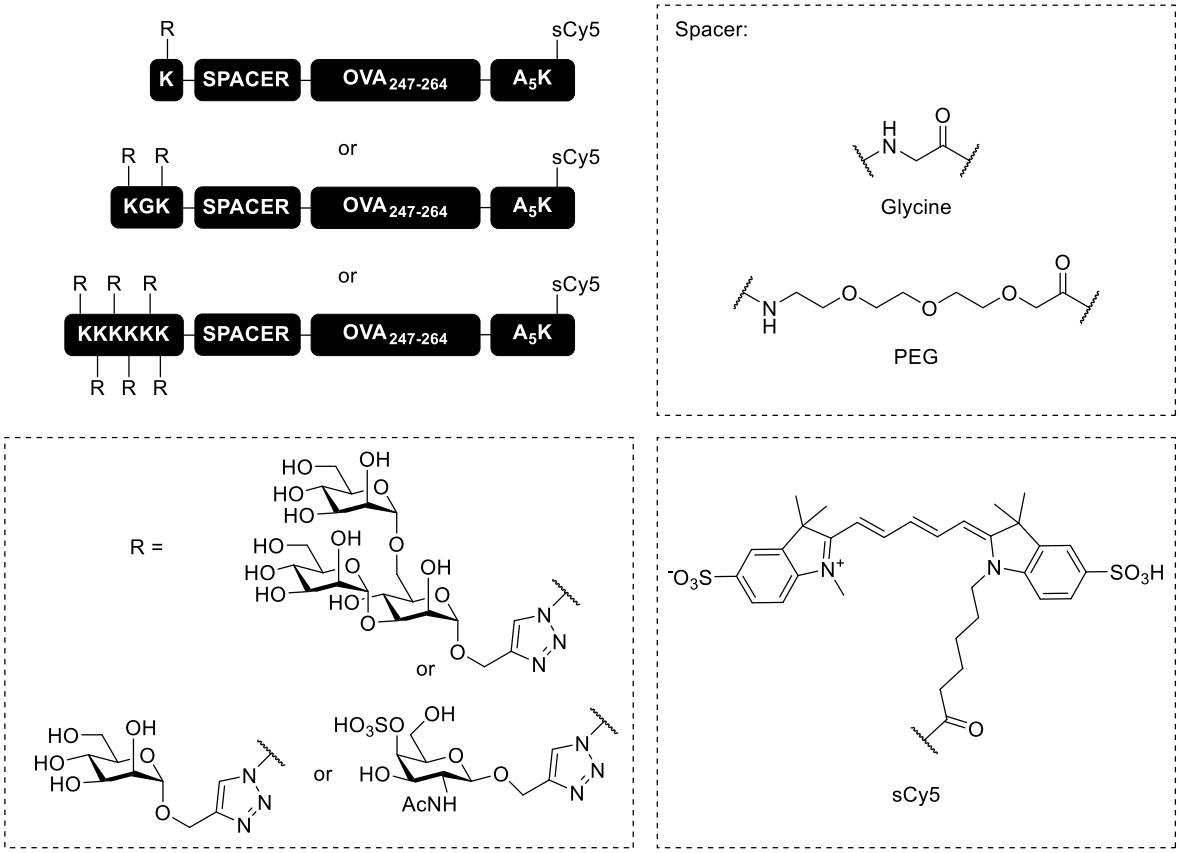

Figure 4. Overview of the proposed target peptides for the glyco-PAINT based studies on the correlation of mannose-receptor binding and CD8 T-cell cross-presentation. The $OVA_{247-264}$ peptide sequence contains the well-studied $OVA_{257-264}$ epitope, which is C-terminally extended with the amino acid sequence AAAAAK. This C-terminal lysine is then used for the introduction of the sulfoCy5 fluorophore. N-terminally an optional spacer can be introduced, followed by a cluster of one, two or six azidolysine residues conjugated with propargylated glycans via CuAAC chemistry.

Introduction of the propargylated glycans using CuAAC conjugation will be carried out as the last step, on the fluorescently labeled peptide scaffold (Figure 5A). The introduction of this fluorophore on the C-terminal lysine will be accomplished using on-resin coupling methods. To selectively modify this residue over the lysine residue that is present in the $OVA_{247-264}$ sequence, the C-terminal residue will be protected with the acid-labile monomethoxytrityl (Mmt) protective group, which can be liberated in a highly selective fashion. The synthesis of the fully protected, resin-bound antigenic peptide, containing the azidolysine residue required for carbohydrate conjugation, can be achieved using standard Fmoc-SPPS.

As the glycans of choice, mono- and trimannosides **1** and **2** (Figure 5B) were considered as good model mannosides to target the CTL domain of the mannose receptor, based on the data obtained in the original Glyco-PAINT experiments. These structures were previously shown to be on the lower and higher end of mannose receptor affinity respectively.[19] Furthermore, to target the CRD of the mannose receptor, a sulfated GalNAc derivative (**3**) was added to the library.[24,25] For the fluorophore, required to enable peptide tracking by Glyco-PAINT, the sulfo-

Cy5 dye (**4**) was selected. This dye is water soluble, super-resolution microscopy compatible,[26] and synthetically accessible.[27]

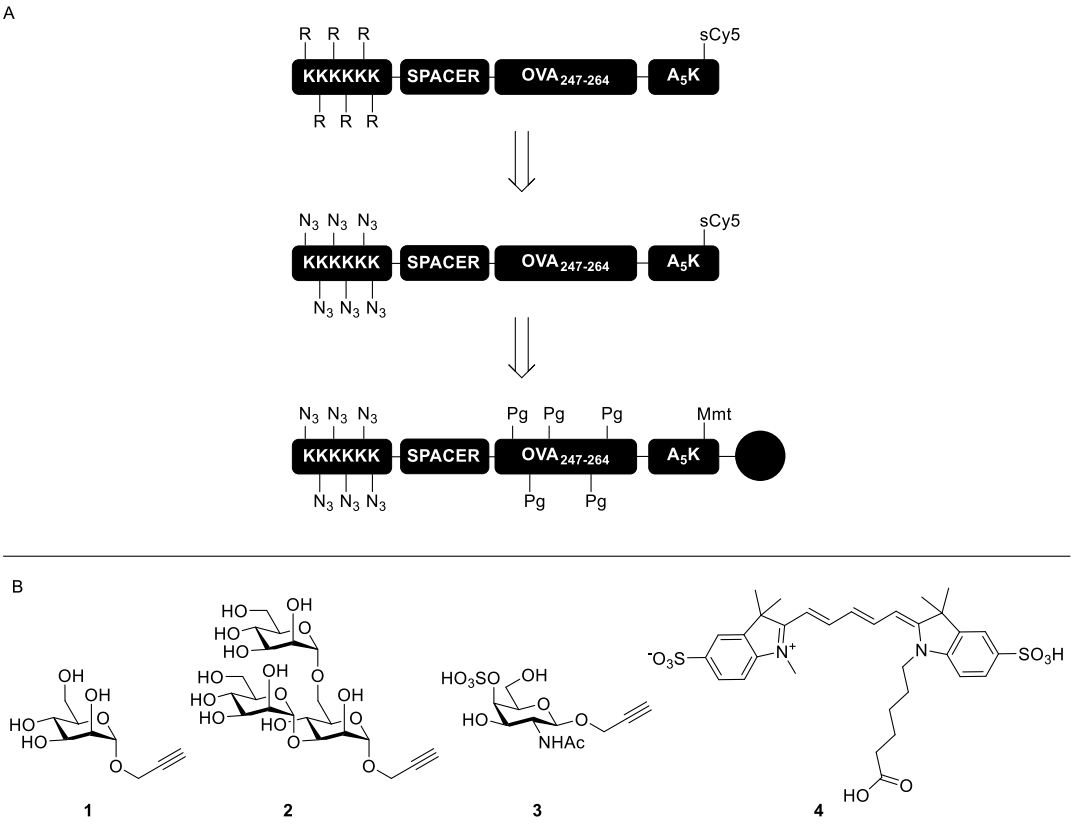

Figure 5. A) Retrosynthetic analysis of one of the target peptides. The R-groups represent different glycans linked via triazole-linkage, as in Figure 4. B) synthetic building blocks, required to furnish the differently glycosylated mannose receptor targeting fluorescent peptides.

To synthesize trimannoside **2**, a modified synthesis based on the work of Fairbanks and co-workers was explored.[28] In this work, this trimannoside was synthesized bearing a benzyl protecting group on the reducing end anomeric center. Replacing this with a propargyl group had no negative effect on the synthesis, as shown in Figure 6.

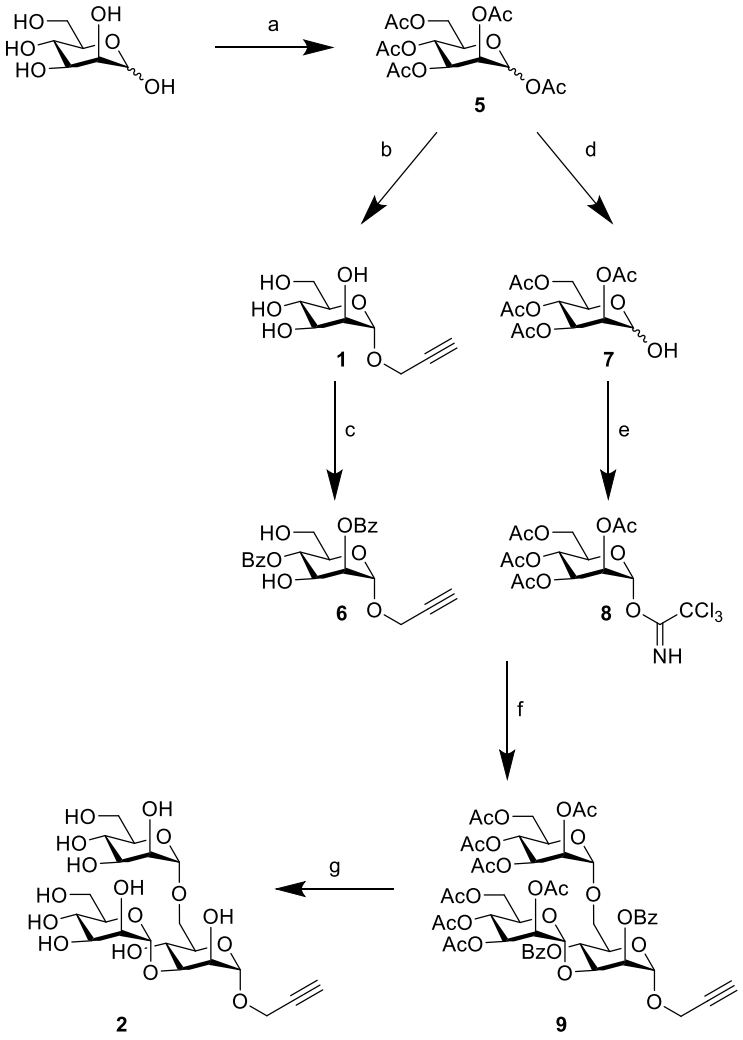

Figure 6. Synthesis of trimannoside **6**. Reagents and conditions: a) Ac_2O, pyridine, 93% b) i) Propargyl-OH, $BF_3{\cdot}Et_2O$, DCM, 63% ii) NaOMe, MeOH, 93% c) $Ph(OMe)_3$, TsOH, MECN ii) TFA, H_2O, 61% d) N,N-dimethylaminopropylamine, THF, 72% e) CCl_3CN, DBU, DCM, 70% f) $BF_3{\cdot}Et_2O$, 4Å molecular sieves, DCM, 62% g) Na(s), MeOH, 68%.

The first step of the synthesis was the acetylation of D-mannose to yield peracetylated sugar **5**. Propargyl alcohol was introduced at the anomeric position using $BF_3{\cdot}Et_2O$ as a catalyst, followed by Zemplén deacetylation with sodium methoxide in methanol to produce **1**. A portion of this sugar was reserved for later peptide conjugation. The bulk was regioselectively benzoylated on the 2- and 4-positions:[28,29] treatment of **1** with trimethylorthobenzoate and *para*-toluenesulfonic acid gave the 2,3:4,6-bis-orthoester intermediate, which can be hydrolyzed in the presence of TFA to give predominately the 2,4-benzoylated glycosyl acceptor **6**.

Intermediate **5** was also used to create lactol **7** using the selective anomeric deacetylation procedure reported by Andersen *et al.*[30] This intermediate was converted into trichloroacetimidate donor **8** using trichloroacetonitrile and catalytic DBU. The protected trisaccharide **9** was formed in 62% yield by reacting 4 equivalents of **8** with glycosyl acceptor

6, using $BF_3{\cdot}Et_2O$ as the activator. Deprotection of the ester groups under Zemplén conditions produced the propargyl-modified trimannoside **2**.

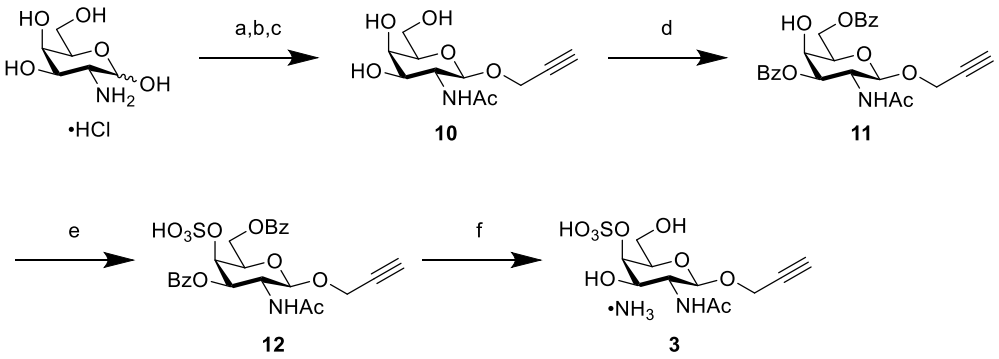

Figure 7. Synthesis of sulfated N-acetylgalactosamine derivative **3**. Reagents and conditions: a) Ac_2O, pyridine 84% b) propargyl-OH, $Yb(OTf)_3$ DCM, 94% c) NaOMe, MeOH, quant. d) BzCl, pyridine, DMF, -40°C, 55% e) $SO_3{\cdot}$pyridine, pyridine, 91% f) NH_3, H_2O, 75%.

The synthesis of the sulfated galactosamine derivative **3** began with the acetylation of D-galactosamine hydrochloride to yield peracetylated galactosamine in exclusively the β-configuration. The anomeric position was modified with propargyl alcohol using $Yb(OTf)_3$ as catalyst.[31] This was followed by deacetylation to produce propargylated *N*-acetylgalactosamine **10**. This intermediate was then benzoylated on the 3,6-positions. Initially, the conditions described by Imperiali and coworkers[32] were attempted, but the solubility of compound **10** in pyridine at -40°C was too low for the reaction to work efficiently. By dissolving the starting material in DMF, followed by cooling to -40°C and careful addition of benzoyl chloride in pyridine, the desired product **11** was obtained in 55% yield. This intermediate was sulfated using $SO_3{\cdot}$pyridine complex in 91% yield (**12**). Deacetylation using ammonium hydroxide produced the desired sulfated *N*-acetylgalactosamine **3**.

With the carbohydrate building blocks in hand, the focus was shifted to the synthesis of the fluorophore. The synthesis of such sulfated derivatives of cyanine dyes were originally described by Waggoner and coworkers.[27] To bring the structure in line with the commercially available cyanine dyes, a methyl substituent was placed on the indole nitrogen, instead of the ethyl used in the original publication (Figure 8).

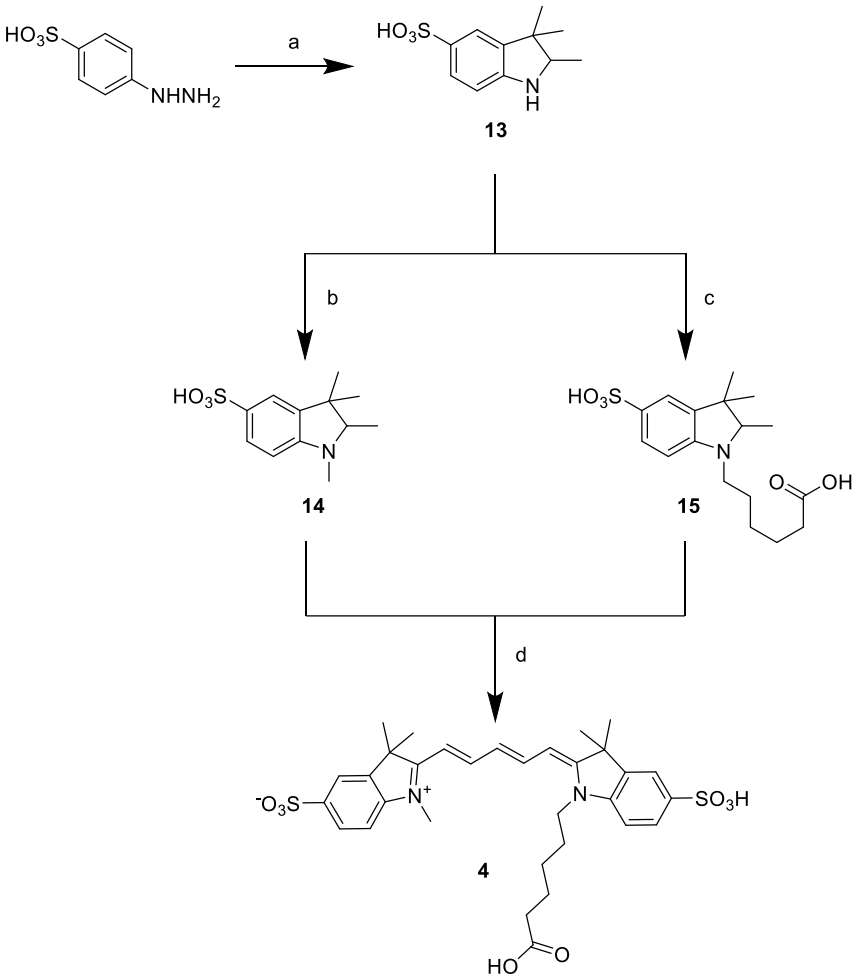

Figure 8. Synthesis of sulfoCy5 fluorophore **16**. Reagents and conditions: a) 3-methylbutanone, AcOH, 65% b) i) NaOAc, MeOH ii) MeI, MeCN, 80% c) i) KOAc, MeOH ii) 6-bromohexanoic acid, 1,2-dichlorobenzene, quant d) i) malonaldehyde bis(phenylimine) HCl, AcOH, Ac_2O, quant ii) Ac_2O, pyridine, 7%.

The synthesis of **4** started with a Fischer indole synthesis, yielding indoline **13** from *p*-hydrazinobenzenesulfonic acid and 3-methylketone. This indoline was alkylated with either iodomethane, producing **14**, or with 6-bromohexanoic acid, to produce **15.** To produce **4**, **14** was first reacted with an excess malonaldehyde bis(phenylimine), followed by a quick workup and further reaction with **15** to yield the asymmetric dye. Using RP-HPLC, the final product was obtained as the free carboxylic acid (**4**).

For the first attempt at a glycosylated and fluorophore labeled antigenic peptide, a simple monovalent design was endeavored (Figure 9). As a spacer moiety between the azidolysine residue and the antigenic peptide, a single glycine residue was introduced.

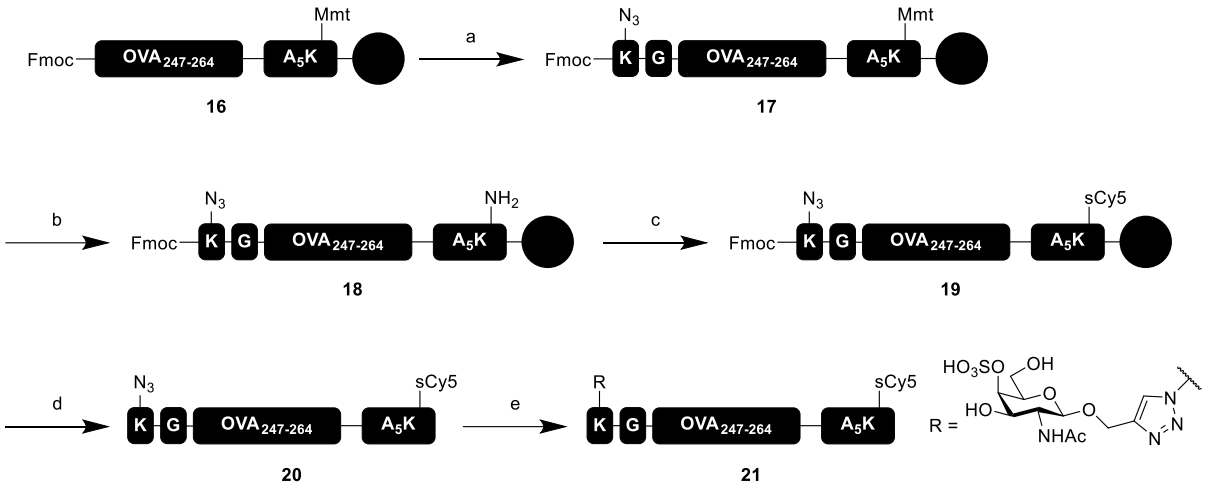

Figure 9. Synthesis of fluorescently labeled and glycosylated peptide **21**. Reagents and conditions: a) SPPS (2 cycles, HCTU, Fmoc-Gly-OH, Fmoc-Lys(N_3)-OH) b) i) AcOH, TFE, DCM ii) Et_3N, DMF c) **4**, HCTU, DiPEA, DMF d) i) 20% (v/v) piperidine/DMF ii) TFA, TIS, H_2O iii) RP-HPLC, 5.0 % e) **3**, $CuSO_4$, NaAsc, THPTA, 40°C, 74%.

The synthesis of resin bound peptide **16** was started by coupling of the Mmt-protected lysine onto Tentagel S RAM resin. Automated SPPS was then used to couple five alanine residues, followed by the native sequence of $OVA_{247-264}$. This peptide was then elongated with a glycine residue, followed by azidolysine, to yield resin bound peptide **17**. From this peptide, the Mmt-group was removed selectively using a mildly acetic mixture (1:2:7, AcOH/TFE/DCM)[33] followed by extensive washing with Et_3N in DMF to remove excess acetic acid. Fluorophore **4** was then coupled to the deprotected lysine sidechain using HCTU as a coupling agent. After coupling overnight, resin bound peptide **19** was obtained. Removal of the N-terminal Fmoc in **19** was followed by cleavage using a standard TFA deprotection mixture (95:2.5:2.5, TFA/TIS/H_2O) to yield a product mixture that, according to LC-MS analysis, contained product **20**, tainted with large quantities of a peptide with a mass spectrum indicating over-labeling with **4** (Δm = +624 Da), suggesting a second unprotected amine was present in (part of) resin bound peptide **18**. This could be caused by either unintentional cleavage of the Boc protecting group of the other lysine residue in the sequence, or by accidental partial cleavage of the Fmoc protecting group during the washing steps, with the latter being the most likely. The mixture was subjected to RP-HPLC and peptide **20** was isolated successfully in a yield of 5.0%. Next, conjugation of peptide **20** to the propargylated sulfosugar **3** under copper catalysis was attempted. Many different conditions for bioconjugation using copper catalysis have been described.[34,35] Initially, copper iodide was used as the source of Cu(I), with DiPEA and THPTA added to stabilize this reactive species, as was described previously for the synthesis of mannose glycoclusters.[19,36] However, this combination of reagents performed erratically, showing efficient conversion in some cases and no conversion in others. A different approach was taken instead: $CuSO_4$ was used as the copper source and was reduced *in situ* to Cu(I) using sodium ascorbate. The ligand THPTA[34] was added to stabilize the catalytically active species. The solvents were sparged with nitrogen before use, in order to remove dissolved oxygen that could potentially oxidize the Cu(I) species back to Cu(II). The purification of the product was

carried out using size exclusion chromatography with HW-40 resin[36], to remove the unreacted sugar, copper salts and small molecule ligands used in the reaction. The fluorophore present in the product allows for facile detection of product containing fractions via UV monitoring. This way, peptide **21** was obtained in a 74% yield.

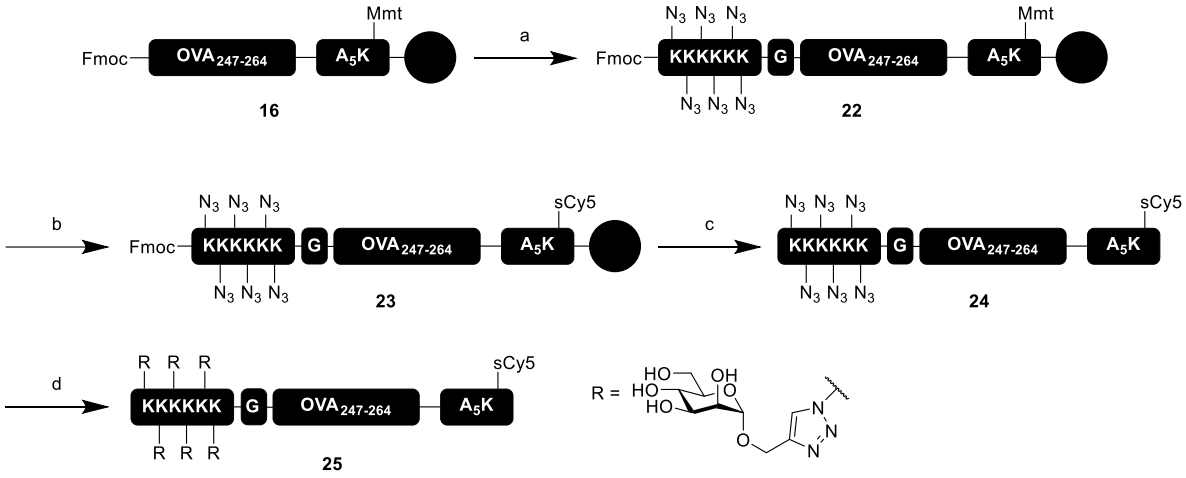

Figure 10. Synthesis hexaazide peptide scaffold **25**. Reagents and condition: a) SPPS (7 cycles, HCTU, Fmoc-Gly-OH, 6 x Fmoc-Lys(N_3)-OH) b) i) AcOH, TFE, DCM ii) Et_3N, DMF iii) **4**, HCTU, DiPEA, DMF c) i) 20% (v/v) piperidine/DMF ii) TFA, TIS, H_2O iii) RP-HPLC, 2.4% d) a) **1**, $CuSO_4$, NaAsc, THTPA, DMSO.

A peptide bearing 6 azidolysine residues was chosen as the next target as this would allow the comparison of MR-ligand valency on antigen cross-presentation. The synthesis of this peptide was started from resin bound peptide **16**, which was elongated with a single glycine residue, followed by six azidolysine residues to yield resin-bound intermediate **22**. The Mmt protecting group on **22** was cleaved under mild acidic conditions (AcOH/TFE/DCM, 1:2:7) followed by basic washes. Coupling of fluorophore **4** to the unmasked amine, mediated by HCTU, produced resin bound peptide **23**. Fmoc cleavage and global deprotection of the peptide using a TFA cocktail (95:2.5:2.5, TFA/TIS/H_2O) yielded crude **24**. This intermediate was again highly contaminated by large quantities of doubly labeled peptide. After RP-HPLC, pure **24** was obtained in 2.4% yield.

As, due to the low yields of SPPS, only limited quantities of **24** were available, the conjugation with propargyl mannoside **1** was attempted on a test-scale. Gratifyingly, the click reaction proceeded without incident, generating compound **25** cleanly based on LC-MS analysis (Figure 10). However, after purification over HW-40 size exclusion resin, some problems were encountered. The ammonium acetate used as buffer salt during the purification was not fully removable by lyophilization, even after repeated rounds of lyophilization. This, combined with the small scale of the reaction, meant the final yield of **25** could not be determined accurately. As the isolated yield of peptide **24** was rather poor, resynthesis using larger quantities of the peptide was not an immediate option. Therefore, improvements to the synthesis of the scaffold were considered a first priority.

To increase the yield of the fluorophore labeled scaffold peptide, the over-labeling problem in the fluorophore labeling step had to be eliminated. Since this problem is most likely caused by unintentional deprotection of the N-terminal Fmoc, acetylation of the N-terminus before fluorophore coupling was considered a viable strategy to explore.

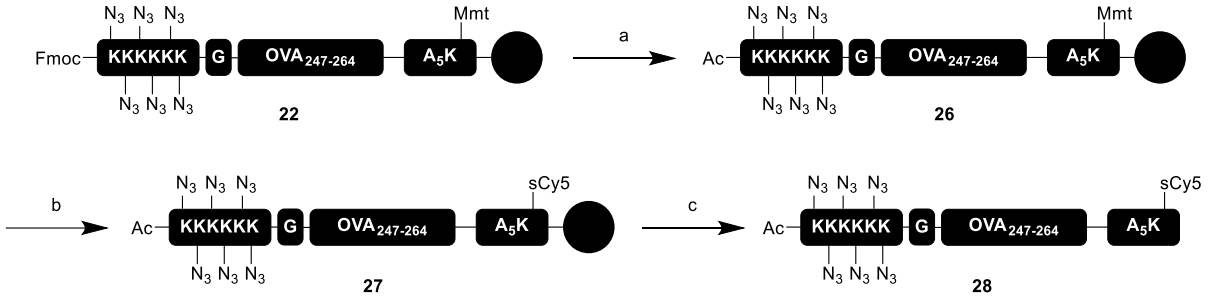

Figure 11. Synthesis of acetylated scaffold **29** from resin bound intermediate **23**. Reagents and conditions: a) i) 20 % (v/v) piperidine/DMF ii) Ac_2O, DiPEA, DMF b) i) AcOH, TFE, DCM ii) Et_3N, DMF iii) **4**, HCTU, DiPEA, DMF c) i) TFA, TIS, H_2O ii) RP-HPLC, 6.2%.

Previously synthesized intermediate **22** was N-terminally deprotected and acetylated by treating the resin bound peptide with a mixture of Ac_2O and DiPEA in DMF, producing resin bound peptide **26** (Figure 11). This peptide was then selectively deprotected and the fluorophore was introduced as before, producing **27**. After global deprotection of the peptide followed by RP-HPLC purification, **28** was obtained in 6.2% yield, a marked increase over the previous synthesis.

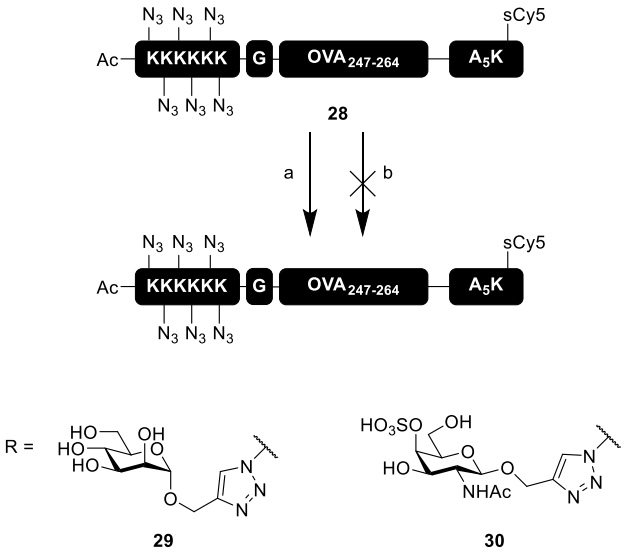

Figure 12. Conjugation of peptide scaffold **29** with mannoside **1** and attempted conjugation with sulfated glycoside **3**. Reagents and conditions: a) **1**, $CuSO_4$, NaAsc, THTPA, DMSO, 20% b) **3**, $CuSO_4$, NaAsc, THTPA, DMSO.

This peptide was again conjugated to monomannoside **1**. The solubility of the scaffold **28** was quite low even when using DMSO as main solvent, but conjugation with the mannoside did proceed to completion. During size exclusion chromatography over HW-40 resin, ammonium

bicarbonate was used as the buffer salt, which is easier to remove by lyophilization. This enabled the isolation of compound **29** in 20% yield. Next, an attempt was made to modify peptide **28** with sulfated glycan **3**. Unlike the modification with the neutrally charged mannoside, the Cu-catalyzed conjugation proceeded sluggishly for this sugar. LC-MS analysis after 72 hours of reaction time indicated the presence of a mixture of peptides, bearing various amounts of sugar **3**. The main component of the mixture had a mass-spectrum indicative of conjugation of only three sugars to the peptide. At the same time, the reaction mixture had started to turn gel-like, further indicating the low solubility of the scaffold as a problematic factor. After an additional 48 hours of reaction time, the complexity of the mixture had further increased and no products or intermediates could be identified by mass spectrometry analysis. Further dilution with DMSO or DMF could not redissolve the peptide, hindering thorough analysis and further conversion. At this point, the reaction was abandoned.

As these solubility issues were seriously hindering the synthesis of more complex peptides, the earlier described polyethyleneglycol spacer was considered as a replacement for the glycine spacer used up to now. This spacer should increase solubility in both organic and aqueous solvents, hopefully keeping the molecule in solution during the copper-catalyzed glycoconjugation. However, the length and flexibility of this moiety can also have considerable effect on the binding kinetics of the glycocluster, so direct comparison between peptides containing different spacers need to be considered carefully. The synthesis of a short PEG spacer compatible with Fmoc-SPPS will be described in Chapter 5, and this same spacer will be used here.

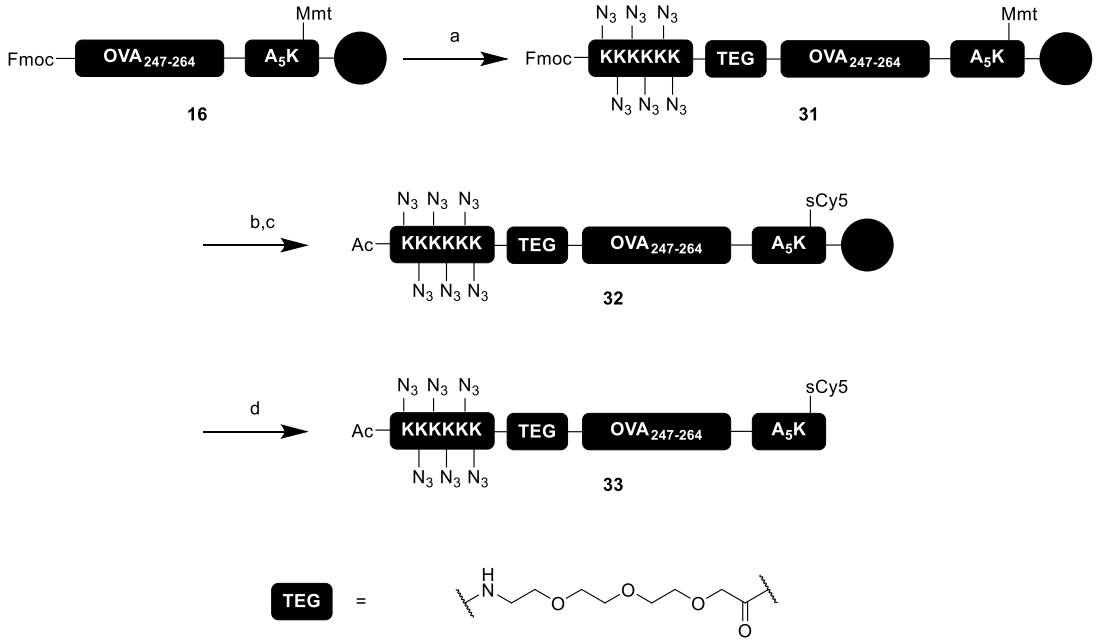

Figure 13. Synthesis of scaffold peptide **34** containing a polyethylene glycol spacer. Reagents and conditions: a) SPPS (7 cycles, HCTU, Fmoc-PEG-OH, 6 x Fmoc-Lys(N_3)-OH) b) i) 20 % (v/v) piperidine/DMF ii) Ac_2O, DiPEA, DMF c) i) AcOH, TFE, DCM ii) Et_3N, DMF iii) **4**, HCTU, DiPEA, DMF d) i) TFA, TIS, H_2O ii) RP-HPLC, 7.4%.

By extending resin bound peptide **16** with this PEG spacer, followed by elongation with six azidolysine residues, resin bound peptide **31** was obtained successfully. N-terminal acetylation followed by selective Mmt deprotection and HCTU mediated coupling of fluorophore **4** yielded resin bound peptide **32**. Global deprotection of this molecule followed by RP-HPLC purification yielded compound **33** in 7.4% yield. As expected, the solubility of this molecule was improved compared to the previously described compound **28**. Next, copper catalyzed click reactions with all three propargylated glycans were carried out on this scaffold.

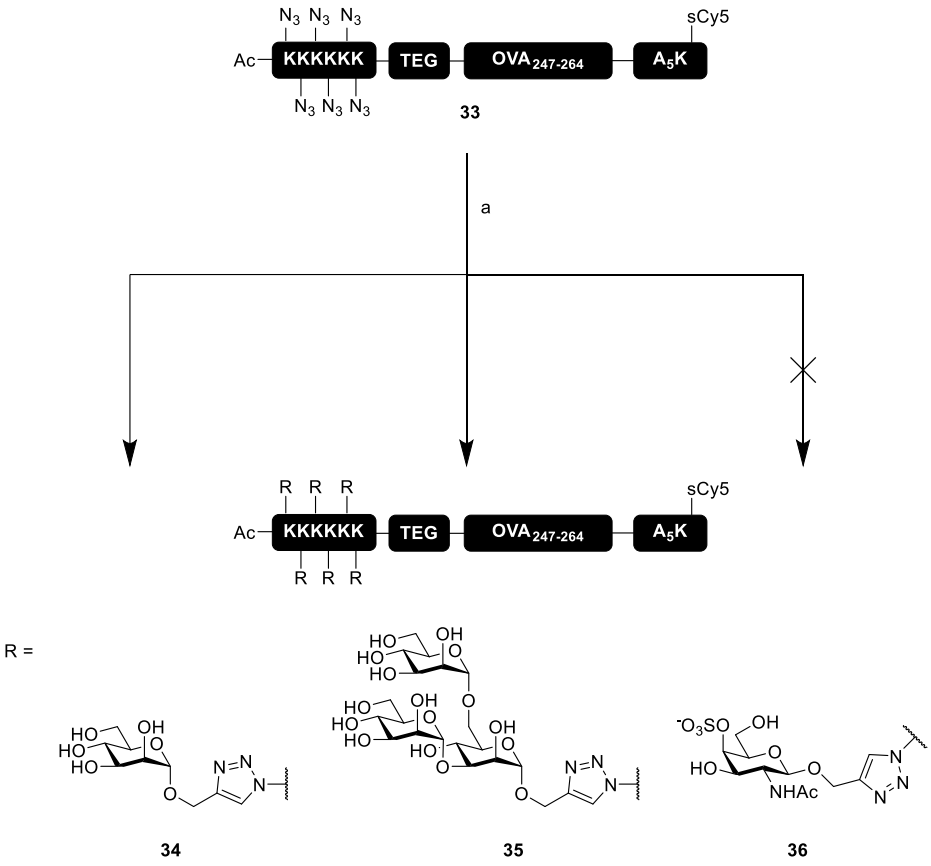

Figure 14. Synthesis of three different glycoconjugates based on scaffold **34**. Reagents and conditions: a) **1**, **2** or **3**, $CuSO_4$, NaAsc, THPTA, DMSO, 40°C, (**35:** 85%, **36:** 54%, **37:** -).

Conjugation of scaffold **33** with both the monomannoside **1** and trimannoside **2** worked without major issue in 85% and 54% yield respectively. The increase in yield observed for the hexa-monomannoside (compared to compound **29**) could indicate that the increase in solubility helps the reaction or the following purification. Sulfated glycan **3** was also subjected to copper catalyzed click with scaffold **33** in an attempt to produce conjugate **36**, and initially LC-MS analysis indicated formation of the desired glycopeptide from this reaction. An attempt was made to isolate this product using size exclusion chromatography, but after lyophilization of the main peak no product was observed by LC-MS analysis.

Since earlier work has found a correlation between multivalency and both lectin binding and cross-presentation, peptides with a different valency were explored next. Using the methods described above, synthesis of a peptide bearing two N-terminal azidolysine residues, with a glycine spacer between them, was carried out (Figure 15).

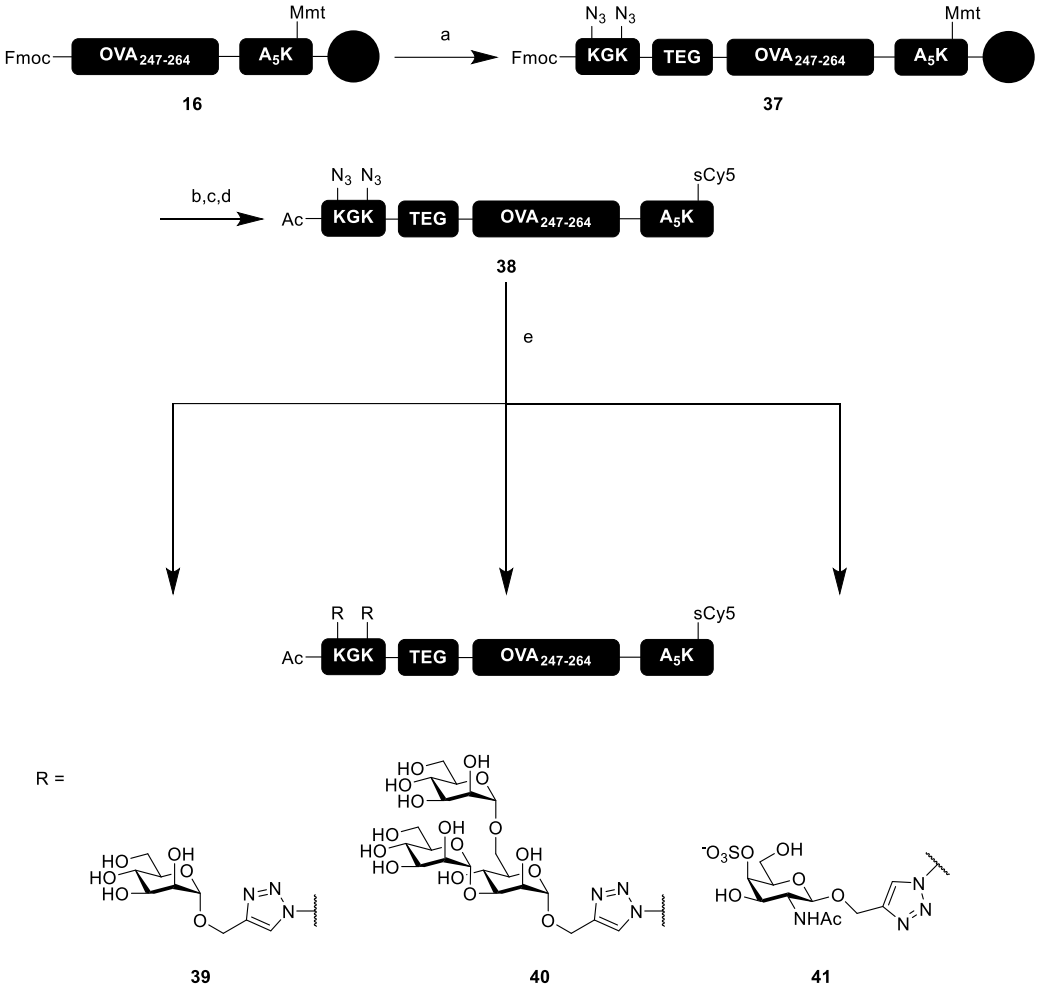

Figure 15. Synthesis of bivalent peptide scaffold **39** and glycoconjugates **40**, **41** and **42**. Reagents and conditions: a) SPPS (4 cycles, HCTU, Fmoc-PEG-OH, Fmoc-Lys(N_3)-OH, Fmoc-Gly-OH, Fmoc-Lys(N_3)-OH) b) i) 20 % (v/v) piperidine/DMF ii) Ac_2O, DiPEA, DMF c) i) AcOH, TFE, DCM ii) Et_3N, DMF iii) **4**, HCTU, DiPEA, DMF d) i) TFA, TIS, H_2O ii) RP-HPLC, 6.6% e) **1**, **2** or **3**, $CuSO_4$, NaAsc, THPTA, DMSO, 40°C, (**40:** 60%, **41:** 60%, **42:** 52%)**.**

Manual elongation of the resin bound peptide **16** with the TEG-spacer followed by Lys(N_3)-Gly-Lys(N_3) proceeded smoothly. This was followed by acetylation of the N-terminus, selective lysine deprotection and fluorophore incorporation. After global deprotection with TFA (95:2.5:2.5, TFA/TIS/H_2O) and RP-HPLC scaffold **38** was obtained in 6.6% yield. This scaffold was derivatized with all three propargylated glycans, producing all three bivalently glycosylated peptides in decent yields. Of particular note here is the fact that compound **41**, bearing two of the sulfo-GalNAc moieties was obtained without incident in fair yield. This indicates that the problems encountered while attempting to synthesize compounds **30** and **36** are most likely arriving from the amount of sulfated glycans introduced and are not an inherent problem of the sulfated glycan.

To evaluate whether the binding of these novel antigenic peptides could indeed be studied by glyco-PAINT, a binding density measurement was performed. In this experiment, the same mannose-receptor expressing Chinese hamster ovary (CHO) cells used for the original glyco-PAINT experiments were used.[19] Since CHO cells do not express any mannose-binding lectins by themselves, non-modified CHOs were used as negative controls. During the measurement, 1 nM of molecule **34** was added to the cells and a total of 5000 frames, with a 50 ms frame integration time, were recorded. Using the tracking software TrackMate[37] individual single-molecule binding events were detected as fluorescent puncta in the images. Next, using the tracking capability of the software, these individual binding events were linked together into tracks, effectively grouping together peptide-MR interactions that persisted over several frames. These tracks were converted to density maps by plotting the total amount of tracks per μm^2. These maps, together with the brightfield images of the cells, are shown in Figure 16.

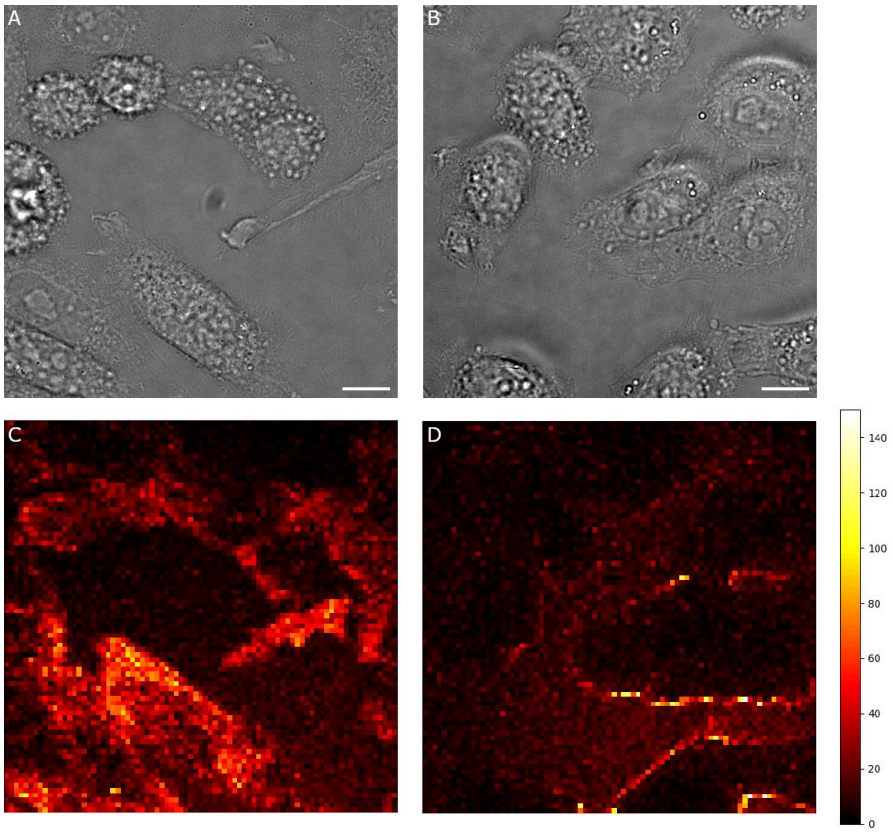

Figure 16. An example of glyco-PAINT used to determine binding affinity of glycosylated antigenic peptide **34**. Top half of figure: Brightfield images showing A) MR-transformed CHO and B) non-transfected wildtype CHO cells. Bottom half of figure: Density maps showing binding in events/μm^2 for C) MR-transformed CHO cells and D) non-transfected CHO cells. A single pixel in the density maps represents 1 μm^2 of cell area. The scale bar in brightfield images represents 10 µm.

In these maps, the difference in binding density between MR-expressing cells and the wild-type is apparent. This suggests that 1) the glycosylated antigenic peptides do indeed have binding interaction with the mannose receptor and 2) Glyco-PAINT can be used to measure the kinetics of this binding. In the near future, all glycosylated peptides described in this

chapter will be evaluated in this manner, and k_{off} and relative k_{on} values will be determined for all. Once these data are obtained, T-cell assays will be carried out using the different constructs to determine whether a correlation between one or more parameters of MR-binding and level of T-cell activation exist, using a dendritic cell mediated cross-presentation assay.

Conclusion

The effects glycosylation has on antigen (cross-)presentation are as of now not yet fully understood. Novel methods and tools to study lectin interaction, uptake and routing of, and T-cell activation by, glycosylated antigens are a key region of investigation. The glyco-PAINT method was developed to better measure the binding of glycans to lectins on a cell membrane, allowing for more accurate determination of some of the parameters involved in uptake of glycosylated antigen. Here, a series of glycosylated peptides were synthesized in an attempt to apply the glyco-PAINT methodology to glycosylated versions of the well-studied antigenic peptide $OVA_{247-264}$.

Incorporation of the required fluorophore was carried out by modification of the C-terminal A_5K modification. On-resin introduction of the fluorophore enabled facile conjugation of the fluorophore to the desired lysine residue, and the modified peptides were isolated in reasonable yields after RP-HPLC. For the introduction of the multivalent glycans, a strategy based on the introduction of a multivalent clickable scaffold, in the form of one or more azidolysine residues on the N-terminal side of the peptide, was utilized. These azide containing peptides can be modified with different propargylated glycans, creating diversity in both multivalency and glycan structure. Besides the already known propargyl mono- and trimannoside structures, a new novel sulfated GalNAc derivative, as a ligand for the cysteine rich domain of the mannose receptor, was developed.

During the synthesis of the larger scaffolds, some solubility problems were encountered. The solubility of the peptide was improved by the introduction of a PEG based spacer between the antigenic peptide and the poly-azidolysine scaffold. Using this improved scaffold, hexavalent peptides **34** and **35** could be synthesized successfully, as well as bivalent peptides **39**, **40** and **41**. Interestingly, both attempts to couple six sulfo-GalNAc molecules onto a hexavalent scaffold failed. Whether this is a problem caused by the high degree of sulfation, by negatively influencing either the click reaction or the following purification, remains to be investigated.

An initial glyco-PAINT experiment was carried out using peptide **34**, showing that this construct does indeed show MR-dependent binding interactions with cells. The technique will be further utilized to fully characterize the MR binding of molecules **34**,**35** and **39-41**.

Experimental

General methods for synthesis and characterization of compounds

Solvents were purchased from Honeywell, VWR or Alfa Aesar. Anhydrous solvents were prepared by drying over 4Å molecular sieves. Reagents purchased from chemical suppliers were used without further purification, unless stated otherwise. All reactions were performed under nitrogen atmosphere and/or under exclusion of H_2O, unless stated otherwise. Reactions were followed by thin layer chromatography which was performed using TLC silica gel 60 F254 on aluminium sheets, supplied by Merck. Compounds were visualized using UV absorption (254 nm) and/or a spray reagent, either permanganate (5 g/L $KMnO_4$, 25 g/L K_2CO_3) or sulfuric acid (10% v/v in EtOH). ^1H and ^{13}C NMR spectra were recorded using a Brüker AV400 (400 / 101 MHz) or a Brüker AV300 (300 / 75 MHz) and COSY and HSQC 2D experiments were used to assign peaks. Recorded data was interpreted and analyzed using MestReNova 12 software. Chemical shifts are reported in ppm (δ) in reference to an internal standard (TMS) or the residual solvent peak. High resolution mass spectra were recorded by direct injection (2 µL of a 2 µM solution in H_2O/MeCN 1:1 and 0.1% formic acid) on a mass spectrometer (Thermo Fisher Exactive HF Orbitrap) equipped with an electrospray ion source in positive mode. The high resolution mass spectrometer was calibrated prior to measurements with a calibration mixture (Thermo Finnigan). LC-MS characterization of compound was carried out using an electrospray ionization mass spectrometry (ESI-MS) on a Thermo Finnigan LCQ Advantage Max LC-MS instrument with a Surveyor PDA plus UV detector on an analytical C18 column (Phenomenex, 3 µm, 110 Å, 50 mm × 4.6 mm) in combination with buffers A (H_2O) and B (MeCN) containing a constant 10% C (1% aq TFA).

1,2,3,4,6-penta-O-acetate-D-mannopyranose (5)

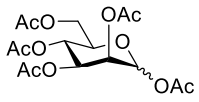

D-mannose (9.20 g, 50 mmol) was suspended in EtOAc (250 mL). Pyridine (10 eq., 40 mL, 500 mmol) and acetic anhydride (10 eq., 47 mL, 500 mmol) were added and the reaction was stirred overnight at room temperature. The reaction mixture was diluted with 250 ml EtOAc and washed once with 1M HCl (1 L) and twice with saturated $NaHCO_3$ (2 x 1 L) solution. The resulting organic layer was dried over $MgSO_4$, filtered and concentrated. Penta-acetyl mannose **5** was obtained as a viscous yellow oil (18.43 g, 47.2 mmol, 93%). The product was used in the next reaction steps without further purification. Spectral data was in accordance with earlier published results.[38]

Propargyl 2,3,4,6-tetra-O-acetyl-α-D-mannopyranoside (S1)

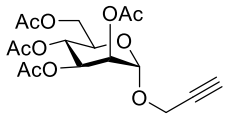

A solution of **5** (3.90 g, 10 mmol) in anhydrous DCM (50 mL) was cooled to 0°C in an ice bath. Propargyl alcohol (5 eq., 2.9 ml, 50 mmol) and $BF_3{\cdot}Et_2O$ (10 eq, 12.3 mL, 100 mmol) were added and the solution was warmed to room temperature. After 96 hours, the reaction was quenched by the addition of saturated aqueous $NaHCO_3$ (200 mL). The reaction mixture was further diluted by the addition of DCM (200 mL) and the organic layer was separated. The organic layer was washed once with saturated aqueous $NaHCO_3$ (200 mL) and twice with water. The organic layer was dried over $MgSO_4$, filtered and concentrated. Silica gel column chromatography (10→50% EtOAc in pentane) yielded **S1** as a colourless oil (2.43 g, 6.3 mmol, 63%). **^{1}H NMR** (300 MHz, $CDCl_3$) δ 5.36 – 5.26 (m, 3H, H2, H3, H4), 5.04 (d, *J* = 1.7 Hz, 1H, H1), 4.34 – 4.25 (m,

3H, H5, CH_2-propargyl), 4.12 (dd, *J* = 12.2, 2.5 Hz, 1H, H6a), 4.07 – 3.99 (m, 1H, H6b), 2.49 (t, *J* = 2.4 Hz, 1H, CH-propargyl), 2.17 (s, 3H, C(O)CH_3), 2.11 (s, 3H, C(O)CH_3), 2.05 (s, 3H, C(O)CH_3), 2.00 (s, 3H, C(O)CH_3). **^{13}C NMR** (75 MHz, $CDCl_3$) δ 170.8 (C=O), 170.1 (C=O), 170.0 (C=O), 169.8 (C=O), 96.3 (C1), 75.7 (CH-propargyl), 69.4 (C2), 69.1 (C5), 69.0 (C4), 66.1 (C3), 62.4 (C6), 55.1 (CH_2-propargyl), 21.0 (C(O)$\underline{C}H_3$), 20.9 (C(O)$\underline{C}H_3$), 20.8 (C(O)$\underline{C}H_3$).

Propargyl α-D-mannopyranoside (1)

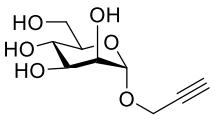

Acetylated glycoside **S1** (1.07 g, 2.76 mmol) was dissolved in MeOH (25 mL). a 30% (w/w) NaOMe in methanol solution (80 µL) was added and the reaction mixture was stirred for four hours. After TLC analysis indicated completion of the reaction, the reaction mixture was neutralized with Amberlyst H^+ resin. The resin was filtered off and the solution was concentrated *in vacuo*. Propargyl mannoside **1** was obtained as a crystalline white solid (0.56 g, 2.56 mmol, 93%). **^{1}H NMR** (300 MHz, MeOD) δ 4.96 (d, *J* = 1.7 Hz, 1H, H1), 4.27 (d, *J* = 2.4 Hz, 2H, CH_2-propargyl), 3.89 – 3.57 (m, 5H, H2, H3, H4, H6), 3.51 (ddd, *J* = 8.7, 5.8, 2.3 Hz, 1H, H5), 2.86 (t, *J* = 2.4 Hz, 1H, CH-propargyl). **^{13}C NMR** (75 MHz, MeOD) δ 99.8 (C1), 76.0 (CH propargyl), 75.0 (C5), 72.5 (C4), 72.0 (C2), 68.4 (C3), 62.8 (C6), 54.8 (CH_2-propargyl). **HRMS** (ESI) m/z: [M + Na^+] calcd for $C_9H_{14}O_6$ 241.0683, found 241.0681.

Propargyl 2,4-di-O-benzoyl-α-D-mannopyranoside (6)

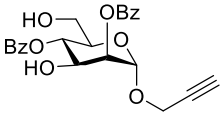

Glycoside **1** (0.53 g, 2.5 mmol) was dissolved in MECN (12.5 ml). Trimethyl orthobenzoate (2,5 eq., 1.1 ml, 6.2 mmol) and TsOH (0.1 eq., 48 mg, 0.25 mmol) were added and the solution was swirled until all solids were dissolved. The solution was stirred for another 5 minutes and the MECN was removed *in vacuo*. The obtained solid was redissolved in fresh MECN (5 ml) and 10% aqueous TFA (5 ml) was added. The solution was stirred for another 15 minutes and subsequently concentrated to dryness. The crude solid was purified by column chromatography (1:1 EtOAc:pentane) to obtain pure **6** as a white solid (0.65 g, 1.52 mmol, 61%). **^{1}H NMR** (300 MHz, $CDCl_3$) δ 8.13 – 8.03 (m, 4H, CH_{arom}), 7.65 – 7.56 (m, 2H, CH_{arom}), 7.51 – 7.41 (m, 4H CH_{arom}), 5.52 (t, *J* = 10.0 Hz, 1H, H4), 5.45 (dd, *J* = 3.5, 1.7 Hz, 1H, H2), 5.25 (d, *J* = 1.7 Hz, 1H, H1), 4.44 (dd, *J* = 10.0, 3.5 Hz, 1H, H3), 4.33 (d, *J* = 2.4 Hz, 2H, CH_2-propargyl), 4.00 (ddd, *J* = 10.0, 4.1, 2.4 Hz, 1H, H5), 3.86 – 3.70 (m, 2H, H6), 2.51 (t, *J* = 2.4 Hz, 1H, CH-propargyl). **^{13}C NMR** (75 MHz, $CDCl_3$) δ 167.4 (C=O), 166.1 (C=O), 133.9 (CH_{arom}), 133.8 (CH_{arom}), 130.1 (CH_{arom}), 129.3 (C_q), 129.1 (C_q), 128.8 (CH_{arom}), 128.7 (CH_{arom}), 96.7 (C1), 78.4 (C_q-propargyl) 75.6 (CH-propargyl), 72.8 (C2), 71.2 (C5), 70.3 (C4), 68.7 (C3), 61.5 (C6), 55.4 (CH_2-propargyl). **HRMS** (ESI) m/z: [M + Na^+] calcd for $C_{23}H_{22}O_8$ 449.1207, found: 449.1202.

2,3,4,6-tetra-O-acetyl-D-mannopyranose (7)

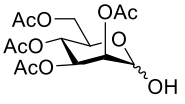

Anomeric deacetylation was carried out according to the procedure of Andersen et al.[30] Acetylated sugar **5** (9.93 g, 25 mmol) was dissolved in THF (125 mL). DMAPA (5 eq., 15.7 ml, 125 mmol) was added to the solution and the reaction mixture was stirred for 2 hours, after which TLC analysis indicated full consumption of starting material. The solution was transferred to a separation funnel and diluted with DCM (500 mL). The organic layer was washed successively with 1M HCl (500 mL) and brine (500 mL). The organic layer was dried over $MgSO_4$, filtered and concentrated producing the partially deacetylated sugar **7** (6.39 g, 18.3 mmol, 72%). This product was used in the next step without further purification. **^{1}H NMR** (300 MHz, $CDCl_3$) δ 5.42 (dd, J

= 10.0, 3.3 Hz, 1H, H3), 5.37 – 5.20 (m, 3H, H1, H2, H4), 4.62 (d, J = 4.2 Hz, 1H, 1-OH), 4.32 – 4.21 (m, 2H, H5, H6a), 4.19 – 4.09 (m, 1H, H6b), 2.17 (s, 3H, C(O)CH_3), 2.11 (s, 3H, C(O)CH_3), 2.06 (s, 3H, C(O)CH_3), 2.01 (s, 3H, C(O)CH_3). **^{13}C NMR** (75 MHz, $CDCl_3$) δ 171.0 (C=O), 170.4 (C=O), 170.2 (C=O), 170.0 (C=O), 92.1 (C1), 70.3 (C2), 68.9 (C3), 68.3 (C5), 66.3 (C4), 62.7 (C6), 20.9 (C(O)$\underline{C}H_3$), 20.8 (C(O)$\underline{C}H_3$), 20.8 (C(O)$\underline{C}H_3$).

Trichloroacetimidate 2,3,4,6-tetra-O-acetyl-D-mannopyranoside (8)

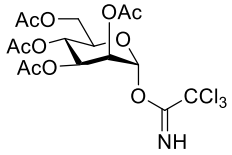

Partially protected compound **7** (1.74 g, 5.0 mmol) was co-evaporated three times with toluene. The flask was backfilled with N_2 and the sugar was dissolved in anhydrous DCM (25 mL). Trichloroacetonitrile (5 eq., 2.5 ml, 25 mmol) and DBU (0.1 eq., 77 mg, 0.5 mmol) were added and the reaction was allowed to stir at room temperature for 2.5 hours. Celite was added to the reaction and the volatiles were removed *in vacuo*. Silica gel column chromatography on neutralized silical (1:1 Et_2O:pentane) yielded trichloroacetimidate **8** a colorless solid (1.64 g, 3.34 mmol, 70%). **^{1}H NMR** (300 MHz, $CDCl_3$) δ 8.80 (s, 1H, C(NH)CCl_3), 6.29 (d, *J* = 1.9 Hz, 1H, H1), 5.50 – 5.39 (m, 3H, H2, H3, H4), 4.32 – 4.24 (m, 1H, H6a), 4.24 – 4.13 (m, 2H, H5, H6b), 2.21 (s, 3H, C(O)CH_3), 2.09 (s, 3H, C(O)CH_3), 2.07 (s, 3H, C(O)CH_3), 2.01 (s, 3H, C(O)CH_3). **^{13}C NMR** (75 MHz, $CDCl_3$) δ 170.0 (C=O), 169.9 (C=O), 169.9 (C=O), 169.7 (C=O), 159.9 ($\underline{C}$(NH)CCl_3), 94.6 (C1), 71.3 (C5), 68.9 (C2) , 68.0 (C3), 65.5 (C4), 62.2 (C6), 20.9 (C(O)$\underline{C}H_3$), 20.8 (C(O)$\underline{C}H_3$), 20.8 (C(O)$\underline{C}H_3$), 20.7 (C(O)$\underline{C}H_3$).

Propargyl 2,3,4,6-tetra-O-acetyl-α-D-mannopyranosyl-(1→6)-[2,3,4,6-tetra-O-acetyl-α-D-mannopyranosyl-(1→3)]-2,4-di-O-benzoyl-α-D-mannopyranoside (9)

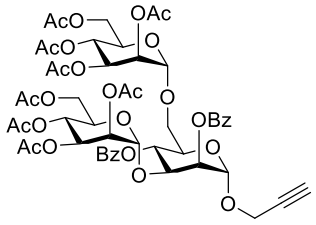

Glycosyl acceptor **6** (0.21 g, 0.5 mmol) was co-evaporated 3 times with toluene and dissolved in anhydrous DCM (25 mL) under an N_2 atmosphere. In a separate dry flask imidate donor **8** (4 eq., 0.99 g, 2.0 mmol) was dissolved in anhydrous DCM (5 mL). The solution containing the imidate was transferred to the reaction flask with a syringe and activated 4Å molecular sieves (1.26 g) were added. After stirring for one hour $BF_3{\cdot}Et_2O$ (2 eq, 0.12 ml, 1.0 mmol) was added and the solution was stirred overnight. The reaction was quenched by adding Et_3N (20 eq., 2.8 mL). The reaction mixture was filtered over celite and water (150 mL) was added. The layers were separated and the aqueous layer extracted twice with DCM (2 x 50 mL). The organic fractions were combined, dried and concentrated. The crude compound was purified by silica gel column chromatography (30% EtOAc in DCM) to produce pure **9** as a colorless solid (0.34 g, 0.31 mmol, 62%). **^{1}H NMR** (400 MHz, $CDCl_3$) δ 8.18 – 8.13 (m, 2H, CH_{arom}), 8.06 – 8.01 (m, 2H, CH_{arom}), 7.67 – 7.52 (m, 4H, CH_{arom}), 7.49 – 7.43 (m, 2H, CH_{arom}), 5.65 (t, *J* = 10.0 Hz, 1H), 5.55 (dd, *J* = 3.4, 1.8 Hz, 1H), 5.34 (dd, *J* = 10.1, 3.4 Hz, 1H), 5.29 – 5.20 (m, 3H), 5.11 – 5.06 (m, 2H), 4.98 (d, *J* = 1.9 Hz, 1H), 4.88 (dd, *J* = 2.9, 1.8 Hz, 1H), 4.81 (d, *J* = 1.7 Hz, 1H), 4.49 (dd, *J* = 9.8, 3.4 Hz, 1H), 4.37 (d, *J* = 2.4 Hz, 2H, CH_2-propargyl), 4.25 – 3.97 (m, 8H), 3.91 (dd, *J* = 10.8, 6.7 Hz, 1H), 3.62 (dd, *J* = 10.8, 2.2 Hz, 1H), 2.56 (t, *J* = 2.4 Hz, 1H, CH-propargyl), 2.14 (s, 3H, C(O)CH_3), 2.12 (s, 3H, C(O)CH_3), 2.05 (s, 3H, C(O)CH_3), 1.99 (s, 3H, C(O)CH_3), 1.95 (s, 3H, C(O)CH_3), 1.94 (s, 3H, C(O)CH_3), 1.85 (s, 3H, C(O)CH_3), 1.83 (s, 3H, C(O)CH_3). **^{13}C NMR** (101 MHz, $CDCl_3$) δ 170.8 (C=O), 170.7 (C=O), 170.1 (C=O), 169.9 (C=O), 169.8 (C=O), 169.2 (C=O), 166.0 (C=O), 165.4 (C=O), 133.8 (CH_{arom}), 133.7 (CH_{arom}), 130.1 (CH_{arom}), 130.0 (CH_{arom}), 129.2 (C_q), 128.9 (CH_{arom}), 128.8 (C_q), 128.7 (CH_{arom}), 99.5, 97.3, 96.2, 78.1 (C_q-propargyl), 75.8 (CH-propargyl), 75.0, 71.6, 70.1, 69.4, 69.3, 69.1, 68.8, 68.7, 68.4, 66.8, 66.1, 65.9, 62.5, 62.4, 55.1 (CH_2-propargyl),

21.0 (C(O)$\underline{C}H_3$), 20.9 (C(O)$\underline{C}H_3$), 20.8 (C(O)$\underline{C}H_3$), 20.7 (C(O)$\underline{C}H_3$), 20.5 (C(O)$\underline{C}H_3$). **HRMS** (ESI) m/z: [M + NH_4^+] calcd for $C_{51}H_{58}O_{26}$ 1104.3555, found 1104.3553

Propargyl α-D-mannopyranosyl-(1→6)-[α-D-mannopyranosyl-(1→3)]-α-D-mannopyranoside (2)

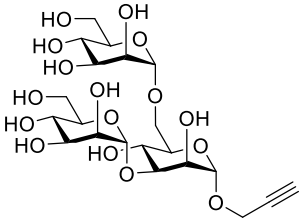

A small amount of sodium metal was dissolved in 5 ml MeOH (pH > 12). The methoxide solution was added to a flask containing **9** (0.32 g, 0.29 mmol) and the solution was stirred for 6 days. The reaction mixture was acidified with Amberlyst H+ and filtered. The solution was concentrated to dryness and the product was redissolved in 2 ml MeOH. The product was precipitated from 30 ml ice-cold diethyl ether. The ether was removed via centrifugation and the solids were washed with fresh Et_2O. The product was dried under vacuum yielding pure **2** as a white powder (0.12 g, 0.22 mmol, 68%). The obtained spectral data was consistent to earlier published results.[39] **^{1}H NMR** (400 MHz, MeOD) δ 5.06 (d, *J* = 1.4 Hz, 1H), 4.84 (d, *J* = 1.5 Hz, 1H), 4.26 (t, *J* = 2.1 Hz, 2H, CH_2-propargyl), 4.04 (dd, *J* = 3.0, 1.8 Hz, 1H), 4.00 – 3.90 (m, 2H), 3.89 – 3.58 (m, 18H), 2.89 (t, *J* = 2.4 Hz, 1H, CH-propargyl). **^{13}C NMR** (101 MHz, MeOD) δ 104.0, 101.5, 100.2, 80.7, 76.1 (CH-propargyl), 74.9, 74.4, 73.8, 72.6, 72.4, 72.1, 72.1, 71.2, 68.7, 68.5, 67.3, 67.1, 62.8, 55.0 (CH_2-propargyl). **HRMS** (ESI) m/z: [M + NH_4^+] calcd for $C_{21}H_{34}O_{16}$ 560.2185, found 560.2189

1,3,4,5-tetra-O-acetyl-2-deoxy-2-acetamido-β-D-galactopyranoside (S2)

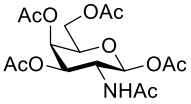

This reaction was carried out as described by Wipf et al.[40] Galactosamine hydrochloride (2.16 g, 10 mmol) was suspended in anhydrous pyridine (20 mL) and acetic anhydride (12 eq, 11.3 mL, 120 mmol) was added. The reaction was stirred overnight and decanted into ice cold water (200 mL). The precipitate was collected by filtration and dried in vacuo, yielding the title compound **S2** (3.25 g, 8.4 mmol, 84%) as a white solid. Traces of water were removed by co-evaporation with toluene. **^{1}H NMR** (400 MHz, $CDCl_3$) δ 5.70 (d, J = 8.8 Hz, 1H, H1), 5.45 (d, J = 9.6 Hz, 1H, NH), 5.38 (dd, J = 3.4, 1.2 Hz, 1H, H4), 5.09 (dd, J = 11.3, 3.3 Hz, 1H, H3), 4.45 (dt, J = 11.4, 9.2 Hz, 1H, H2), 4.21 – 4.07 (m, 2H, H6), 4.03 (td, J = 6.5, 1.2 Hz, 1H, H5), 2.18 (s, 3H, C(O)CH_3), 2.14 (s, 3H, C(O)CH_3), 2.05 (s, 3H, C(O)CH_3), 2.03 (s, 3H, C(O)CH_3), 1.95 (s, 3H, C(O)CH_3). **^{13}C NMR** (101 MHz, $CDCl_3$) δ 170.9 (C=O), 170.6 (C=O), 170.4 (C=O), 170.3 (C=O), 169.7 (C=O), 93.2 (C1), 72.0 (C5), 70.4 (C3), 66.5 (C4), 61.4 (C6), 50.0 (C2), 23.5 (C(O)$\underline{C}H_3$), 21.0 (C(O)$\underline{C}H_3$), 20.8 (C(O)$\underline{C}H_3$), 20.8 (C(O)$\underline{C}H_3$).

Propargyl 3,4,5-tri-O-acetyl-2-deoxy-2-acetamido-β-D-galactopyranoside (S3)

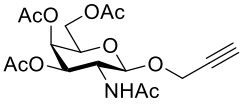

Compound **S2** (778 mg, 2 mmol) was suspended in anhydrous DCM (10 mL). Propargyl alcohol (10 eq, 1.15 mL, 20 mmol) and $Yb(OTf)_3$ (5 mol%, 62 mg) were added. The mixture was refluxed overnight. TLC analysis (100% EtOAc) indicated complete consumption of starting material and the reaction was allowed to cool to room temperature. The reaction mixture was further diluted with DCM and washed once with H_2O. The organic layer was dried over $MgSO_4$ and concentrated under reduced pressure. Silica gel column chromatography (4/1 EtOAc/pentane → 100% EtOAc) yielded compound **S3** as a white solid (569 mg, 1.88 mmol, 94%). **^{1}H NMR** (400 MHz, $CDCl_3$) δ 6.12 (d, J = 8.8 Hz, 1H, NH), 5.38 (d, J = 2.9 Hz, 1H, H4), 5.32 (dd, J = 11.2, 3.4 Hz, 1H, H3), 4.90 (d, J = 8.4 Hz, 1H, H1), 4.40 (d, J = 2.3 Hz, 2H, CH2-propargyl), 4.21 – 3.96 (m, 4H, H6, H2, H5), 2.51 (t, J = 2.3 Hz, 1H, CH-propargyl), 2.16 (s, 3H, C(O)CH_3), 2.06 (s, 3H, C(O)CH_3), 2.01 (s, 3H,

C(O)CH_3), 1.98 (s, 3H, C(O)CH_3). **^{13}C NMR** (101 MHz, $CDCl_3$) δ 170.8 (C=O), 170.5 (C=O), 170.4 (C=O), 98.7 (C1), 78.7 (Cq-propargyl), 75.4 (CH-propargyl), 70.8 (C5), 70.0 (C3), 66.8 (C4), 61.5 (C6), 55.9 (CH_2-propargyl), 51.0 (C2), 23.5 (C(O)$\underline{C}H_3$), 20.7 (C(O)$\underline{C}H_3$).

Propargyl 2-deoxy-2-acetamido-β-D-galactopyranoside (10)

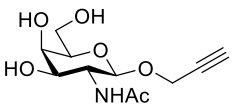

Compound **S3** (555 mg, 1.83 mmol) was dissolved in MeOH (18 mL) and a catalytic amount of metallic sodium was added. After 2 h, TLC (10% MeOH in EtOAc) indicated full consumption of starting material. The reaction was quenched by the addition of Amberlite® H+ resin and filtered. The volatiles were removed under reduced pressure and **10** was obtained in quantitative yield as a white solid. **^{1}H NMR** (400 MHz, MeOD) δ 4.57 (d, J = 8.4 Hz, 1H, H1), 4.37 (dd, J = 2.4, 1.0 Hz, 2H, CH2-propargyl), 3.93 (dd, J = 10.7, 8.4 Hz, 1H, H2), 3.84 (dd, J = 3.4, 1.0 Hz, 1H, H4), 3.78 (dd, J = 11.4, 7.0 Hz, 1H, H6a), 3.73 (dd, J = 11.4, 5.2 Hz, 1H, H6b), 3.63 (dd, J = 10.7, 3.3 Hz, 1H, H3), 3.51 (ddd, J = 6.8, 5.2, 1.1 Hz, 1H, H5), 2.85 (t, J = 2.4 Hz, 1H, CH-propargyl), 1.99 (s, 3H, NHC(O)C$\underline{H}_3$). **^{13}C NMR** (101 MHz, MeOD) δ 100.8 (C1), 80.1 (Cq-propargyl), 76.9 (C5), 76.0 (CH-propargyl), 73.1 (C3), 69.6 (C4), 62.5 (C6), 56.3 (CH_2-propargyl), 54.0 (C2), 23.0 (NHC(O)$\underline{C}H_3$).

Propargyl 3,6-di-O-benzoyl-2-deoxy-2-acetamido-β-D-galactopyranoside (11)

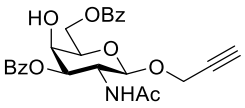

Deprotected sugar **10** (470 mg, 1.8 mmol) was co-evaporated with toluene (3x) and dissolved in anhydrous DMF (3.6 mL). The reaction mixture was cooled to -40°C before a solution of benzoyl chloride (2.2 eq, 465 µL, 3.96 mmol) in anhydrous pyridine (1.8 mL) was added dropwise. The reaction mixture was kept at -40°C for 1 h before allowing it to warm to room temperature. The reaction was stirred an additional 20 h, when TLC (70% EtOAc in pentane) indicated complete consumption of starting material. The reaction mixture was concentrated under reduced pressure and subjected to silica gel column chromatography (1/1 EtOAc/pentane → 9/1 EtOAc/pentane). This yielded the title compound **11** as a white solid (469 mg, 1.0 mmol, 55%). **^{1}H NMR** (400 MHz, MeOD) δ 8.10 – 8.01 (m, 4H, CH_{arom}), 7.66 – 7.56 (m, 2H, CH_{arom}), 7.53 – 7.42 (m, 4H, CH_{arom}), 5.19 (dd, J = 11.1, 3.2 Hz, 1H, H3), 4.60 (dd, J = 11.3, 7.4 Hz, 1H, H6a), 4.55 – 4.44 (m, 2H, H6b, H2), 4.43 – 4.34 (m, 2H, CH_2-propargyl), 4.28 (dd, J = 3.3, 1.1 Hz, 1H, H4), 4.08 (ddd, J = 7.4, 5.2, 1.1 Hz, 1H, H5), 2.87 (t, J = 2.4 Hz, 1H, CH-propargyl), 1.87 (s, 3H, NHC(O)C$\underline{H}_3$). **^{13}C NMR** (101 MHz, MeOD) δ 173.6 (C=O), 167.7 (C=O), 167.5 (C=O), 134.5 (CH_{arom}), 134.4 (CH_{arom}), 131.2 (C_q), 131.1 (C_q), 130.9 (CH_{arom}), 130.6 (CH_{arom}), 129.6 (CH_{arom}), 129.6 (CH_{arom}), 100.4 (C1), 79.7 (C_q-propargyl), 76.5 (CH-propargyl), 75.7 (C3), 74.0 (C5), 67.2 (C4), 64.8 (C6), 56.4 (CH_2-propargyl), 51.2 (C2), 22.8 (NHC(O)$\underline{C}H_3$).

Propargyl 3,6-di-O-benzoyl-4-O-sulfo-2-deoxy-2-acetamido-β-D-galactopyranoside (12)

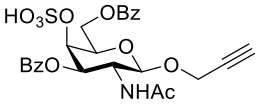

Compound **11** (65 mg, 0.14 mmol) was dissolved in anhydrous pyridine (2.8 mL) and SO_3·pyridine complex (5 eq, 111 mg, 0.7 mmol) was added and the reaction was heated to 50°C. After 1.5 h, TLC (100% EtOAc) indicated full consumption of starting material. The reaction was allowed to cool to room temperature, after which the mixture was concentrated under reduced pressure. Silica gel column chromatography (EtOAc → 1/4 MeOH/EtOAc) yielded the title compound **12** (70 mg, 128 µmol, 91%) as a white solid. **^{1}H NMR** (400 MHz, MeOD) δ 8.17 – 8.00 (m, 4H, Bz), 7.63 – 7.52 (m, 2H, Bz), 7.51 – 7.40 (m, 4H, Bz), 5.31 (dd, J = 11.2, 3.3 Hz, 1H, H3), 5.04 (d, J = 3.2 Hz, 1H, H4), 4.67 (d, J = 6.5 Hz, 2H, H6), 4.43 – 4.31 (m, 3H, H2,

CH2-propargyl), 4.17 (td, J = 6.1, 5.7, 0.9 Hz, 1H, H5), 2.85 (t, J = 2.4 Hz, 1H, CH-propargyl), 1.87 (s, 3H, C(O)CH_3). **^{13}C NMR** (101 MHz, MeOD) δ 167.8 (C=O), 134.3 (CH_{arom}), 134.0 (CH_{arom}), 131.4 (C_q), 131.4 (C_q), 131.1 (CH_{arom}), 130.7 (CH_{arom}), 129.5 (CH_{arom}), 129.3 (CH_{arom}), 100.2 (C1), 79.5 (Cq-propargyl), 76.6 (CH-propargyl), 73.7 (C5), 73.3 (C3), 73.2 (C4), 65.4 (C6), 56.4 (CH2-propargyl), 51.6 (C2), 22.8 (C(O)$\underline{C}H_3$). **HRMS** (ESI) m/z: [M + Na^+] calcd $C_{25}H_{25}NO_{11}S$ 570.1041, found 570.1042

Propargyl 4-O-sulfo-2-deoxy-2-acetamido-β-D-galactopyranoside ammonium salt (3)

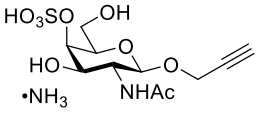

Compound **12** (90 mg, 0.16 mmol) was suspended in 28% aqueous ammonia (1.6 mL) and stirred at RT for 24h, at which time TLC (20% MeOH in EtOAc) indicated complete consumption of starting material. The reaction mixture was then diluted with water and washed with diethyl ether (3x). The organic layer was discarded and the aqueous layer concentrated under reduced pressure. The obtained residue was subjected to silica gel column chromatography (EtOAc → 1/1 MeOH/EtOAc) and the purified product was lyophilized to yield the title compound **3** as a with powder (42 mg, 0.12 mmol, 75%). **^{1}H NMR** (400 MHz, D_2O) δ 4.72 – 4.68 (m, 1H, H1), 4.66 (d, J = 2.1 Hz, 1H, H4), 4.39 (t, J = 2.4 Hz, 2H, CH_2-propargyl), 3.91 – 3.84 (m, 2H, H3, H2), 3.82 – 3.76 (m, 3H, H6, H5), 2.87 (t, J = 2.4 Hz, 1H, CH-propargyl), 2.01 (s, 3H, C(O)CH_3). **^{13}C NMR** (101 MHz, D_2O) δ 175.0 (C=O), 99.6 (C1), 78.7 (C_q-propargyl), 76.1 (CH-propargyl), 75.6 (C4), 74.5 (C5), 69.9 (C3), 60.9 (C6), 56.7 (CH_2-propargyl), 52.5 (C2), 22.2 (C(O)$\underline{C}H_3$). **HRMS** (ESI) m/z: [M + Na^+] calcd $C_{11}H_{16}NO_9SNa$ 384.0336, found 384.0338

2,3,3-trimethyl-3H-indole-5-sulfonic acid (13)

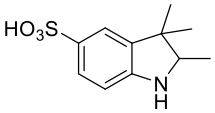

4-Hydrazinobenzenesulfonic acid (1.97 g, 10 mmol) was suspended in AcOH. 3-methyl-2-butanone (3 eqv., 2.58 g, 30 mmol) was added and the reaction mixture was refluxed for 3h. After cooling back to room temperature, the reaction mixture was triturated with EtOAc, the precipitate was collected by centrifugation and washed with cold EtOAc to give compound **13** as a pink powder (1.56 g, 6.5 mmol, 65%). **^{1}H NMR** (300 MHz, DMSO) δ 7.92 (d, *J* = 1.7 Hz, 1H), 7.87 (dd, *J* = 8.1, 1.7 Hz, 1H), 7.54 (d, *J* = 8.1 Hz, 1H), 1.43 (s, *J* = 7.2 Hz, 6H, C(CH_3)$_2$).

1,2,3,3-tetramethyl-3H-indol-1-ium-5-sulfonate (14)

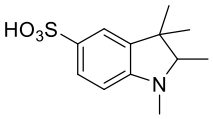

2,3,3-trimethyl-3H-indole-5-sulfonic acid (**13**) (0.550 g, 2.3 mmol) was dissolved in MeOH (11.5 mL). NaOAc (1.1 eqv., 0.205 g, 2.5 mmol) was added and the reaction mixture was stirred at RT for 15 min. The reaction mixture was concentrated under reduced pressure, co-evaporated with toluene (3x) and suspended in acetonitrile (11.5 mL). Iodomethane (2 eqv., 0.29 mL, 4.6 mmol) was added and the reaction mixture was stirred at 80°C for 22h. The reaction mixture was siluted by the addition of additional acetonitrile and the residue was obtained by decantation. This residue was washed three times with acetone to give compound **14** as a red solid (0.474 g, 1.9 mmol, 80%). **^{1}H NMR** (400 MHz, MeOD) δ 8.05 (d, *J* = 1.2 Hz, 1H, CH_{arom}), 7.96 (dd, *J* = 8.4, 1.2 Hz, 1H, CH_{arom}), 7.85 (d, *J* = 8.4 Hz, 1H, CH_{arom}), 4.08 (s, 3H, NCH_3), 1.61 (s, 6H, C(CH_3)$_2$).

1-(5-carboxypentyl)-2,3,3-trimethyl-3H-indol-1-ium-5-sulfonate (15)

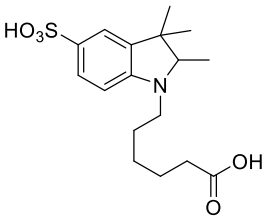

2,3,3-trimethyl-3H-indole-5-sulfonic acid (**13**) (0.718 g, 3 mmol) was dissolved in MeOH (12 mL). KOAc (1.1 eqv., 0.324 g, 3.3 mmol) was added and the reaction mixture was stirred at RT for 15 min. The reaction mixture was concentrated under reduced pressure, co-evaporated with toluene (3x) and suspended in 1,2-dichlorobenzene (12 mL). 6-bromohexanoic acid (1.25 eqv., 0.732 g, 3.75 mmol) was added and the reaction mixture was stirred at 110°C for 23h. The solvent was removed by decantation and the residue was washed 3 times with isopropanol to give compound **15** as a red powder (1.08 g, 3 mmol, quantitative). **^{1}H NMR** (400 MHz, MeOD) δ 8.13 (t, *J* = 4.5 Hz, 1H, CH_{arom}), 8.05 (dd, *J* = 8.4, 1.5 Hz, 1H, CH_{arom}), 7.96 – 7.89 (m, 1H, CH_{arom}), 4.53 (t, *J* = 4.5 Hz, 2H, $NC\underline{H}_2CH_2CH_2CH_2CH_2C(O)OH$), 2.37 – 2.27 (m, 2H, $NCH_2CH_2CH_2CH_2C\underline{H}_2C(O)OH$), 2.03 – 1.92 (m, 2H, $NCH_2C\underline{H}_2CH_2CH_2CH_2C(O)OH$), 1.77 – 1.65 (m, 4H, $NCH_2CH_2C\underline{H}_2C\underline{H}_2CH_2C(O)OH$), 1.62 (s, 6H, $C(CH_3)_2$).

Sulpho Cy5-OH (4)

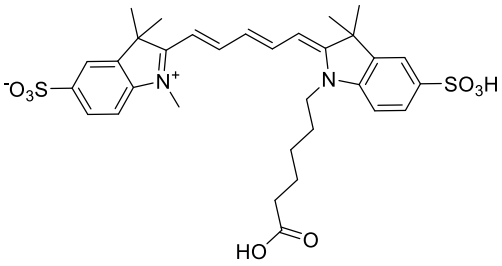

2,3,3-trimethyl-3H-indole-5-sulfonic acid (**14**) (0.999 g, 3.9 mmol) was dissolved in AcOH (20 mL) and Ac_2O (54 eqv., 20 mL, 210 mmol). Malonaldehyde bis(phenylimine) monohydrochloride (1.1 eqv., 1.11 g, 4.3 mmol) was added and the reaction mixture was refluxed for 4h. The reaction mixture was concentrated under reduced pressure, precipitated in EtOAc and washed 3 times with EtOAc to give the intermediate as a dark yellow solid (1.8 g, 3.9 mmol, quantitative). **LC-MS** RT = 4.7 min (C18, 10-90% B over 9 minutes) **LRMS** calcd $[M]^+$ = 425.15 observed M/z = 425.13

This intermediate (0,424 g, 1 mmol) and compound **15** (0.353 g, 1 mmol) were dissolved in pyridine (10 mL). Ac_2O (105 eqv., 10 mL, 105 mmol) was added and the reaction mixture was stirred at 110°C for 4h. The reaction mixture was triturated with EtOAc, the precipitate was collected by centrifugation and washed 3 times with isopropanol. Reverse phase HPLC yielded the title compound as dark blue solid (42 mg, 65 µmol, 7%). **^{1}H NMR** (400 MHz, D_2O) δ 7.85 (d, *J* = 12.4 Hz, 2H, C-CH=C$\underline{H}$-CH=C$\underline{H}$-CH=C), 7.74 (d, *J* = 5.1 Hz, 2H, aromatic), 7.73 – 7.68 (m, 2H, aromatic), 7.23 (dd, *J* = 8.3, 3.6 Hz, 2H, aromatic), 6.33 (t, *J* = 12.2 Hz, 1H, C-CH=CH-C$\underline{H}$=CH-CH=C), 3.98 – 3.88 (m, 2H, $NC\underline{H}_2CH_2CH_2CH_2CH_2C(O)OH$), 3.48 (s, 3H, NCH_3), 2.29 (t, *J* = 7.3 Hz, 2H, $NCH_2CH_2CH_2CH_2C\underline{H}_2C(O)OH$), 1.75 – 1.64 (m, 2H, $NCH_2C\underline{H}_2CH_2CH_2CH_2C(O)OH$), 1.60 – 1.48 (m, 14H, $NCH_2CH_2CH_2C\underline{H}_2CH_2C(O)OH$, 2x $C(CH_3)_2$), 1.41 – 1.28 (m, 2H, $NCH_2CH_2C\underline{H}_2CH_2CH_2C(O)OH$). **LC-MS** RT = 4.3 min (C18, 10-90% B over 9 minutes) **LRMS** calcd $[M]^+$ = 643.21 observed M/z = 643.33

SPPS procedures

General procedure for automated SPPS

Peptides were synthesized using automated Fmoc-SPPS on a Liberty Blue^{tm} automated microwave peptide synthesizer (CEM corporation). Synthesis was performed 100 µmol scale on Tentagel S RAM resin (loading 0.20-0.25 mmol/g, Rapp Polymere GmbH, Germany). Resin was first swollen for 5 minutes in DMF prior to amino acid coupling. Activation was achieved using DIC/Oxyma coupling as is

recommended by the manufacturer. The following amino acids were used: Fmoc-Ala-OH, Fmoc-Arg(Pbf)-OH, Fmoc-Asn(Trt)-OH, Fmoc-Asp(OtBu)-OH, Fmoc-Gln(tBu)-OH, Fmoc-Glu(OtBu), Fmoc-Gly-OH, Fmoc-Ile-OH, Fmoc-Leu-OH, Fmoc-Lys(Boc)-OH, Fmoc-Lys(Mmt)-OH, Fmoc-Phe-OH, Fmoc-Ser(tBu)-OH, Fmoc-Val-OH. All amino acids were obtained from Novabiochem except Fmoc-Lys(Mmt)-OH which was obtained from CEM corporation. Standard coupling was achieved using 5 equivalents amino acid as a 0.2 M amino acid/DMF solution, 5 equivalents DIC as a 0.5 M of DIC/DMF solution and 5 equivalents Oxyma as a 1 M Oxyma/DMF solution (also containing 0.2 M DiPEA), at 90°C for 2 minutes. Standard Fmoc deprotection was achieved by 20% (v/v) piperidine in DMF at 90°C for 90 seconds, repeated once. To analyze the quality of the peptide, a small amount of resin (~1mg) was treated with 200 µL of a TFA cocktail (95:2.5:2.5, TFA/H_2O/TIS) for 2 hours, after which the TFA was filtered into 800 µL of ice cold Et_2O. After five minutes the formed precipitate was collected by centrifugation and the supernatant discarded. The pellet was dissolved in 200 µL 1:1:1 H_2O/MeCN/tBuOH and subjected to LC-MS analysis. Peptides were characterized using electrospray ionization mass spectrometry (ESI-MS) on a Thermo Finnigan LCQ Advantage Max LC-MS instrument with a Surveyor PDA plus UV detector on an analytical C18 column (Phenomenex, 3 µm, 110 Å, 50 mm × 4.6 mm) in combination with buffers A (H_2O), B (MeCN), and C (1% aq TFA). Quality of crude was evaluated with a linear gradient of 10-90% B with a constant 10% C over 10 minutes.

General procedures for manual SPPS

Manual elongation of peptides was carried out in a fritted syringe at either 25 or 5 µmol scale. Fmoc deprotection was achieved using 20 % (v/v) piperidine in DMF in two steps, reacting 3 and 7 minutes respectively. Fmoc-Gly-OH was coupled using 5 equivalents of amino acid together with 5 equivalents of HCTU (as a 0.5 M solution) and 10 equivalents DiPEA for 45 minutes. Fmoc-Lys(N_3)-OH was coupled using 2 equivalents together with 2 equivalents HCTU (as a 0.2 M in DMF solution) and 4 equivalents of DiPEA for 90 minutes. Fmoc-TEG-OH (Chapter 5) was coupled using 4 equivalents, together with 4 equivalents HCTU and 8 equivalents DiPEA in 1 mL of DMF for 45 minutes. Analysis of the quality of the resin-bound peptide was carried out as above.

General procedure for N-terminal acetylation

The N-terminal Fmoc was cleaved by treating the resin twice with a 20% (v/v) solution of piperidine in DMF, for 3 and 7 minutes. This was followed by the addition of a solution containing 10 % (v/v) Ac_2O and 5 % (v/v) DiPEA in DMF (1 mL for 25 µmol resin bound peptide). This resin was acetylated for 15 minutes under gentle agitation, followed by draining the acetylation solution and thorough washing of the resin with DMF.

General procedure for fluorophore labeling

Fluorophore labeling of peptides was generally carried out on a 5 µmol scale. The resin was first swelled in DCM, followed by selective Mmt deprotection. The Mmt group protecting the C-terminal lysine residue, the resin was treated with a mildly acidic mixture consisting of 10 % (v/v) AcOH and 20 % (v/v) TFE in DCM (1 mL) for one hour.[33] After this time has elapsed, the resin was washed three times with DCM and three times with DMF. To remove residual acetic acid, the resin was then treated with a 10 % TEA in DMF mixture (2 x 10 min) followed by an additional three washes with DMF. One equivalent of fluorophore **16** was dissolved in a 50 mM solution of HCTU together with 2 equivalents of DiPEA. This mixture was added to the drained resin and allowed to react under gentle agitation overnight

protected from light. After overnight coupling the solution was drained and the resin was thoroughly washed with DMF.

General procedure for peptide global deprotection and purification

Peptide cleavage was carried out using a standard TFA cleavage cocktail (TFA:H_2O:TIS 95:2.5:2.5) using 1 mL per 25 µmol of resin bound peptide. Before initiating cleavage, the resin was thoroughly washed with DCM and drained. The TFA cocktail was added and mixed with the resin under gentle agitation for one hour, after which it was drained into a centrifuge tube containing ice cold diethyl ether (10:1 ratio Et_2O:TFA). When deprotecting fluorophore modified peptides, the cleavage reaction was protected from light as much as possible and a 20:1 ratio of Et_2O to TFA was used. The diethylether/TFA mixture was chilled for a minimum of 10 minutes to increase peptide recovery and the precipitated peptide was recovered by centrifugation. The supernatant was discarded and the pellet washed with a small amount of Et_2O, followed again by centrifugation. This pellet was dissolved in a mixture of H_2O/MeCN/tBuOH and subjected to RP-HPLC purification on a Gilson GX281 semipreparative HPLC. This machine was equipped with a Gemini-NX C18 column (5 µm, 110 A, 250 x 10.0 mm) using a flow of 5 mL/min and buffers A = 0.1% TFA in H_2O and B = MeCN. Peak detection was done using a UV-Vis detector set to 225 nm or 610 nm for fluorescently labeled peptides. Quality of purified peptides was determined using an electrospray ionization mass spectrometry (ESI-MS) on a Thermo Finnigan LCQ Advantage Max LC-MS instrument with a Surveyor PDA plus UV detector on an analytical C18 column (Phenomenex, 3 µm, 110 Å, 50 mm × 4.6 mm) in combination with buffers A (H_2O), B (MeCN), and C (1% aq TFA). Quality of the peptides was evaluated with a linear gradient of 10-50% B with a constant 10% C over 9 minutes or a linear gradient of 10-90% B with a constant 10% C over 9 minutes.

Fmoc-Asp(OtBu)-Glu(OtBu)-Val-Ser(tBu)-Gly-Leu-Glu(OtBu)-Gln(Trt)-Leu-Glu(OtBu)-Ser(tBu)-Ile-Ile-Asn(Trt)-Phe-Glu(OtBu)-Lys(Boc)-Leu-Ala-Ala-Ala-Ala-Ala-Lys(Mmt)-RAM-Tentagel S (16)

Peptide was synthesized on a 100 µmole scale using the general automated synthesis procedures. **LC-MS** RT = 5.3 min (C18, 10-90% B over 9 minutes) **LRMS** calcd $[M+2H]^{2+}$ = 1384.21, $[M+3H]^{3+}$ = 923.14 observed M/z = 1384.75, 923.50

Fmoc-Lys(N_3)-Gly-Asp(OtBu)-Glu(OtBu)-Val-Ser(tBu)-Gly-Leu-Glu(OtBu)-Gln(Trt)-Leu-Glu(OtBu)-Ser(tBu)-Ile-Ile-Asn(Trt)-Phe-Glu(OtBu)-Lys(Boc)-Leu-Ala-Ala-Ala-Ala-Ala-Lys(Mmt)-RAM-Tentagel S (17)

Resin bound peptide **16** (10 µmol) was elongated manually with Fmoc-Gly-OH and Fmoc-Lys(N_3)-OH. **LC-MS** RT = 5.6 min (C18, 10-90% B over 9 minutes) **LRMS** calcd $[M+2H]^{2+}$ = 1490.00, $[M+3H]^{3+}$ = 993.67 observed M/z = 1490.33, 994.08

Lys(N_3)-Gly-Asp-Glu-Val-Ser-Gly-Leu-Glu-Gln-Leu-Glu-Ser-Ile-Ile-Asn-Phe-Glu-Lys-Leu-Ala-Ala-Ala-Ala-Ala-Lys(sCy5)-NH_2 (20)

The C-terminal Lys(Mmt) of resin bound peptide **17** (10 µmol) was chemoselectively deprotected followed by coupling of **4** (1.0 eq, 6.4 mg, 10 µmol) as described in the general methods. Global deprotection followed by RP-HPLC purification yielded compound **20** as a blue solid (1.69 mg, 0.50 µmol, 5.0%). **LC-MS** RT = 7.2 min (C18, 10-50% B over 9 minutes) **LRMS** calcd $[M+2H]^{2+}$ = 1691.33, $[M+3H]^{3+}$ = 1127.88 observed M/z = 1691.25, 1128.17

Fmoc-Lys(N_3)-Lys(N_3)-Lys(N_3)-Lys(N_3)-Lys(N_3)-Lys(N_3)-Gly-Asp(OtBu)-Glu(OtBu)-Val-Ser(tBu)-Gly-Leu-Glu(OtBu)-Gln(Trt)-Leu-Glu(OtBu)-Ser(tBu)-Ile-Ile-Asn(Trt)-Phe-Glu(OtBu)-Lys(Boc)-Leu-Ala-Ala-Ala-Ala-Ala-Lys(Mmt)-RAM-Tentagel S (22)

Resin bound peptide **16** (25 µmol) was elongated manually with Fmoc-Gly-OH and Fmoc-Lys(N_3)-OH. **LC-MS** RT = 8.0 min (C18, 10-90% B over 9 minutes) **LRMS** calcd $[M+2H]^{2+}$ = 1875.48, $[M+3H]^{3+}$ = 1250.65 observed M/z = 1875.80, 1250.93

Lys(N_3)-Lys(N_3)-Lys(N_3)-Lys(N_3)-Lys(N_3)-Lys(N_3)-Gly-Asp-Glu-Val-Ser-Gly-Leu-Glu-Gln-Leu-Glu-Ser-Ile-Ile-Asn-Phe-Glu-Lys-Leu-Ala-Ala-Ala-Ala-Ala-Lys(sCy5)-NH_2 (24)

The C-terminal Lys(Mmt) of resin bound peptide **22** (5 µmol) was chemoselectively deprotected followed by coupling of **4** (1.0 eq, 3.2 mg, 5 µmol) as described in the general methods. Global deprotection followed by RP-HPLC purification yielded compound **24** as a blue solid (0.49 mg, 0.12 µmol, 2.4%). **LC-MS** RT = 5.4 min (C18, 10-90% B over 9 minutes) **LRMS** calcd $[M+3H]^{3+}$ = 1384.69 observed M/z = 1385.00

Ac-Lys(N_3)-Lys(N_3)-Lys(N_3)-Lys(N_3)-Lys(N_3)-Lys(N_3)-Gly-Asp-Glu-Val-Ser-Gly-Leu-Glu-Gln-Leu-Glu-Ser-Ile-Ile-Asn-Phe-Glu-Lys-Leu-Ala-Ala-Ala-Ala-Ala-Lys(sCy5)-NH_2 (28)

Resin bound peptide **22** (5 µmol) was N-terminally acetylated according to the standard conditions. This was followed by chemoselective deprotection of the Mmt group and coupling of **4** (1.0 eq, 3.2 mg, 5 µmol) as described in the general methods. Global deprotection followed by RP-HPLC purification yielded compound **28** as a blue solid (1.30 mg, 0.31 µmol, 6.2%). **LC-MS** RT = 6.4 min (C18, 10-90% B over 9 minutes) **LRMS** calcd $[M+3H]^{3+}$ = 1398.70 observed M/z = 1399.00

Fmoc-Lys(N_3)-Lys(N_3)-Lys(N_3)-Lys(N_3)-Lys(N_3)-Lys(N_3)-TEG-Asp(OtBu)-Glu(OtBu)-Val-Ser(tBu)-Gly-Leu-Glu(OtBu)-Gln(Trt)-Leu-Glu(OtBu)-Ser(tBu)-Ile-Ile-Asn(Trt)-Phe-Glu(OtBu)-Lys(Boc)-Leu-Ala-Ala-Ala-Ala-Ala-Lys(Mmt)-RAM-Tentagel S (31)

Resin bound peptide **16** (25 µmol) was elongated manually with Fmoc-TEG-OH and Fmoc-Lys(N_3)-OH. **LC-MS** RT = 7.6 min (C18, 10-90% B over 9 minutes) **LRMS** calcd $[M+2H]^{2+}$ = 1941.52, $[M+3H]^{3+}$ = 1294.68 observed M/z = 1941.53, 1294.80

Ac-Lys(N_3)-Lys(N_3)-Lys(N_3)-Lys(N_3)-Lys(N_3)-Lys(N_3)-TEG-Asp-Glu-Val-Ser-Gly-Leu-Glu-Gln-Leu-Glu-Ser-Ile-Ile-Asn-Phe-Glu-Lys-Leu-Ala-Ala-Ala-Ala-Ala-Lys(sCy5)-NH_2 (33)

Resin bound peptide **31** (5 µmol) was N-terminally acetylated according to the standard conditions. This was followed by chemoselective deprotection of the Mmt group and coupling of **4** (1.0 eq, 3.2 mg, 5 µmol) as described in the general methods. Global deprotection followed by RP-HPLC purification yielded compound **33** as a blue solid (1.60 mg, 0.37 µmol, 7.4%). **LC-MS** RT = 6.0 min (C18, 10-90% B over 9 minutes) **LRMS** calcd $[M+3H]^{3+}$ = 1443.06 observed M/z = 1443.00

Fmoc-Lys(N_3)-Gly-Lys(N_3)-TEG-Asp(OtBu)-Glu(OtBu)-Val-Ser(tBu)-Gly-Leu-Glu(OtBu)-Gln(Trt)-Leu-Glu(OtBu)-Ser(tBu)-Ile-Ile-Asn(Trt)-Phe-Glu(OtBu)-Lys(Boc)-Leu-Ala-Ala-Ala-Ala-Ala-Lys(Mmt)-RAM-Tentagel S (37)

Resin bound peptide **16** (25 µmol) was elongated manually with Fmoc-TEG-OH, Fmoc-Lys(N_3)-OH and Fmoc-Gly-OH. **LC-MS** RT = 6.5 min (C18, 10-90% B over 9 minutes) **LRMS** calcd $[M+2H]^{2+}$ = 1661.86, $[M+3H]^{3+}$ = 1108.24 observed M/z = 1662.00, 1108.67

Ac-Lys(N_3)-Gly-Lys(N_3)-TEG-Asp-Glu-Val-Ser-Gly-Leu-Glu-Gln-Leu-Glu-Ser-Ile-Ile-Asn-Phe-Glu-Lys-Leu-Ala-Ala-Ala-Ala-Ala-Lys(sCy5)-NH_2 (38)

Resin bound peptide **37** (5 µmol) was N-terminally acetylated according to the standard conditions. This was followed by chemoselective deprotection of the Mmt group and coupling of **4** (1.0 eq, 3.2 mg, 5 µmol) as described in the general methods. Global deprotection followed by RP-HPLC purification yielded compound **38** as a blue solid (1.24 mg, 0.33 µmol, 6.6%). **LC-MS** RT = 5.0 min (C18, 10-90% B over 9 minutes) **LRMS** calcd $[M+2H]^{2+}$ = 1883.93, $[M+3H]^{3+}$ = 1256.28 observed M/z = 1884.42, 1256.67

CuAAC glycopeptide conjugation

General procedures for CuAAC modification of peptides

Peptides were dissolved in degassed DMSO and glycans in either degassed DMSO or degassed MilliQ water. These were mixed together in a 1.5 mL Eppendorf tube, followed by addition of a copper click mix. This click mix typically consistent of 1 part 0.1 M $CuSO_4$ (in MQ), 2 parts 0.1 M sodium ascorbate (in MQ) and 3 parts 0.1 M THPTA (in DMSO), giving a solution with a total Cu(I) concentration of around 15 mM. Of this solution, enough was added to be 0.15 equivalents compared to the peptide. The reaction was heated in a 40°C shaker block, and every 24 hours 1 equivalent of 0.1 M sodium ascorbate was added. Periodically, a 0.5 µL sample was diluted into 39.5 µL of 1:1:1 H_2O/MeCN/tBuOH and analyzed by LC-MS to evaluate reaction progression. After full conversion of the peptide towards the desired conjugate was observed, the reaction mixture was subjected to size exclusion chromatography over Toyopearl HW-40 size exclusion resin using 150 mM NH_4OAc or 150 mM NH_4HCO_3 (containing 20% MeCN) as the buffer. Fractions showing absorbance at 610 nm were combined and lyophilized.

Lys(4-SO_4-GalNAc)-Gly-Asp-Glu-Val-Ser-Gly-Leu-Glu-Gln-Leu-Glu-Ser-Ile-Ile-Asn-Phe-Glu-Lys-Leu-Ala-Ala-Ala-Ala-Ala-Lys(sCy5)-NH_2 (21)

Compound **20** (0.5 µmol) was dissolved in 15 µl degassed DMSO and sugar **3** was added (2 eq., 10 µL of 0.1 M solution in H_2O). A click mix was prepared by mixing CuI (1 eq, 0.1 M), THPTA (3 eq, 0.3 M) and DiPEA (2 eq, 0.2 M) and 1 µL of this mixture was added to the reaction mix. After SEC purification and lyophilization compound **21** was obtained as a blue powder (1.37 mg, 0.37 µmol, 74%). **LC-MS** RT = 7.0 min (C18, 10-50% B over 9 minutes) **LRMS** calcd $[M+2H]^{2+}$ = 1860.86, $[M+3H]^{3+}$ = 1240.93 observed M/z = 1860.83, 1240.92

Lys(Man)-Lys(Man)-Lys(Man)-Lys(Man)-Lys(Man)-Lys(Man)-Gly-Asp-Glu-Val-Ser-Gly-Leu-Glu-Gln-Leu-Glu-Ser-Ile-Ile-Asn-Phe-Glu-Lys-Leu-Ala-Ala-Ala-Ala-Ala-Lys(sCy5)-NH_2 (25)

Compound **24** (50 nmol, 5 mM in DMSO) was mixed with propargyl mannoside **1** (7.5 eq., 7.5 µL of 50 mM solution in 1:1 H_2O/DMSO). 0.5 µL of the standard click mix was added and the reaction carried out at 40°C. After SEC purification and lyophilization compound **25** was obtained as a blue powder (0.67 mg). **LC-MS** RT = 6.7 min (C18, 10-50% B over 9 minutes) **LRMS** calcd $[M+3H]^{3+}$ = 1821.19, $[M+4H]^{4+}$ = 1366.14 observed M/z = 1821.00, 1366.08

Ac-Lys(Man)-Lys(Man)-Lys(Man)-Lys(Man)-Lys(Man)-Lys(Man)-Gly-Asp-Glu-Val-Ser-Gly-Leu-Glu-Gln-Leu-Glu-Ser-Ile-Ile-Asn-Phe-Glu-Lys-Leu-Ala-Ala-Ala-Ala-Ala-Lys(sCy5)-NH_2 (29)

Compound **28** (100 nmol, 50 mM in DMSO) was mixed with propargyl mannoside **1** (12 eq., 6 µL of 200 mM solution in 1:1 H_2O/DMSO). 1 µL of the standard click mix was added and the reaction carried out

at 40°C. After SEC purification and lyophilization compound **29** was obtained as a blue powder (0.11 mg, 20 nmol, 20%). **LC-MS** RT = 6.7 min (C18, 10-50% B over 9 minutes) **LRMS** calcd $[M+3H]^{3+}$ = 1835.22, $[M+4H]^{4+}$ = 1376.67 observed M/z = 1835.25, 1376.92

Ac-Lys(Man)-Lys(Man)-Lys(Man)-Lys(Man)-Lys(Man)-Lys(Man)-TEG-Asp-Glu-Val-Ser-Gly-Leu-Glu-Gln-Leu-Glu-Ser-Ile-Ile-Asn-Phe-Glu-Lys-Leu-Ala-Ala-Ala-Ala-Ala-Lys(sCy5)-NH_2 (34)

Compound **33** (100 nmol, 50 mM in DMSO) was mixed with propargyl mannoside **1** (12 eq., 6 µL of 200 mM solution in DMSO). 1 µL of the standard click mix was added and the reaction carried out at 40°C. After SEC purification and lyophilization compound **34** was obtained as a blue powder (0.48 mg, 85 nmol, 85%). **LC-MS** RT = 4.3 min (C18, 10-50% B over 9 minutes) **LRMS** calcd $[M+3H]^{3+}$ = 1879.21, $[M+4H]^{4+}$ = 1409.66 observed M/z = 1879.33, 1409.83

Ac-Lys(triMan)-Lys(triMan)-Lys(triMan)-Lys(triMan)-Lys(triMan)-Lys(triMan)-TEG-Asp-Glu-Val-Ser-Gly-Leu-Glu-Gln-Leu-Glu-Ser-Ile-Ile-Asn-Phe-Glu-Lys-Leu-Ala-Ala-Ala-Ala-Ala-Lys(sCy5)-NH_2 (35)

Compound **34** (100 nmol, 50 mM in DMSO) was mixed with propargyl mannoside **2** (12 eq., 6 µL of 200 mM solution in DMSO). 1 µL of the standard click mix was added and the reaction carried out at 40°C. After SEC purification and lyophilization compound **35** was obtained as a blue powder (0.41 mg, 54 nmol, 54%). **LC-MS** RT = 4.2 min (C18, 10-50% B over 9 minutes) **LRMS** calcd $[M+4H]^{4+}$ = 1896.07, $[M+5H]^{5+}$ = 1517.06 observed M/z = 1896.08, 1517.17

Ac-Lys(Man)-Gly-Lys(Man)-TEG-Asp-Glu-Val-Ser-Gly-Leu-Glu-Gln-Leu-Glu-Ser-Ile-Ile-Asn-Phe-Glu-Lys-Leu-Ala-Ala-Ala-Ala-Ala-Lys(sCy5)-NH_2 (39)

Compound **38** (100 nmol, 25 mM in DMSO) was mixed with propargyl mannoside **1** (4 eq., 2 µL of 200 mM solution in DMSO). 1 µL of the standard click mix was added and the reaction carried out at 40°C. After SEC purification and lyophilization compound **39** was obtained as a blue powder (0.25 mg, 60 nmol, 60%). **LC-MS** RT = 6.8 min (C18, 10-50% B over 9 minutes) **LRMS** calcd $[M+3H]^{3+}$ = 1402.00 observed M/z = 1402.08

Ac-Lys(triMan)-Gly-Lys(triMan)-TEG-Asp-Glu-Val-Ser-Gly-Leu-Glu-Gln-Leu-Glu-Ser-Ile-Ile-Asn-Phe-Glu-Lys-Leu-Ala-Ala-Ala-Ala-Ala-Lys(sCy5)-NH_2 (40)

Compound **38** (100 nmol, 25 mM in DMSO) was mixed with propargyl mannoside **2** (4 eq., 2 µL of 200 mM solution in DMSO). 1 µL of the standard click mix was added and the reaction carried out at 40°C. After SEC purification and lyophilization compound **40** was obtained as a blue powder (0.29 mg, 60 nmol, 60%). **LC-MS** RT = 6.6 min (C18, 10-50% B over 9 minutes) **LRMS** calcd $[M+3H]^{3+}$ = 1618.07 observed M/z = 1618.08

Ac-Lys(4-SO_4-GalNAc)-Gly-Lys(4-SO_4-GalNAc)-TEG-Asp-Glu-Val-Ser-Gly-Leu-Glu-Gln-Leu-Glu-Ser-Ile-Ile-Asn-Phe-Glu-Lys-Leu-Ala-Ala-Ala-Ala-Ala-Lys(sCy5)-NH_2 (41)

Compound **38** (100 nmol, 25 mM in DMSO) was mixed with propargyl N-acetylgalactosamine **3** (4 eq., 2 µL of 200 mM solution in DMSO). 1 µL of the standard click mix was added and the reaction carried out at 40°C. After SEC purification and lyophilization compound **41** was obtained as a blue powder (0.23 mg, 52 nmol, 52%). **LC-MS** RT = 6.8 min (C18, 10-50% B over 9 minutes) **LRMS** calcd $[M+3H]^{3+}$ = 1482.66 observed M/z = 1482.67

Glyco-PAINT data acquisition and analysis

CHO-MR and wt CHO cells were cultured as described previously.[19] Image acquisition was carried out on a NIKON Ti-2 microscope in a 512 x 512 pixel region (pixel dimensions: 0.160 µm x 0.160 µm). At least 5000 frames were collected using a 50 ms acquisition time. A 640 nm laser at 40 mW was used to illuminate the fluorescent molecules.

Data analysis was carried out using the open source Fiji package. First, individual fluorescent puncta were detected using the LoG (Laplacian of Gaussian) detector of the TrackMate plug-in, with the estimated object diameter set to 0.480 µm and median filter preprocessing turned on. Next, these detected puncta were tracked over time using the 'simple LAP tracker' option, with 'linking max distance' and 'gap-closing max distance' set to 0.6 µm and 'gap-closing max frame gap' set to 3. From the resulting tracks, only tracks containing > 3 individual spots were included for further analysis. Heatmaps were generated from 5000 frames analyzed over the whole image. The average position of every track was rounded down on both the x and y axis, effectively binning events per μm^2. The resulting track density was plotted as a 2D histogram using matplotlib.

References

(1) Rudd, P. M.; Elliott, T.; Cresswell, P.; Wilson, I. A.; Dwek, R. A. Glycosylation and the Immune System. *Science* **2001**, *291* (5512), 2370–2376. https://doi.org/10.1126/science.291.5512.2370.

(2) Torigoe, S.; Schutt, C. R.; Yamasaki, S. Immune Discrimination of the Environmental Spectrum through C-Type Lectin Receptors. *Int. Immunol.* **2021**, *33* (12), 847–851. https://doi.org/10.1093/intimm/dxab074.

(3) Rabinovich, G. A.; van Kooyk, Y.; Cobb, B. A. Glycobiology of Immune Responses. *Ann. N. Y. Acad. Sci.* **2012**, *1253* (1), 1–15. https://doi.org/10.1111/J.1749-6632.2012.06492.X.

(4) Nigou, J.; Zelle-Rieser, C.; Gilleron, M.; Thurnher, M.; Puzo, G. Mannosylated Lipoarabinomannans Inhibit IL-12 Production by Human Dendritic Cells: Evidence for a Negative Signal Delivered Through the Mannose Receptor. *J. Immunol.* **2001**, *166* (12), 7477–7485. https://doi.org/10.4049/JIMMUNOL.166.12.7477.

(5) Gringhuis, S. I.; den Dunnen, J.; Litjens, M.; van der Vlist, M.; Geijtenbeek, T. B. H. Carbohydrate-Specific Signaling through the DC-SIGN Signalosome Tailors Immunity to Mycobacterium Tuberculosis, HIV-1 and Helicobacter Pylori. *Nat. Immunol.* **2009**, *10* (10), 1081–1088. https://doi.org/10.1038/ni.1778.

(6) Denda-Nagai, K.; Aida, S.; Saba, K.; Suzuki, K.; Moriyama, S.; Oo-puthinan, S.; Tsuiji, M.; Morikawa, A.; Kumamoto, Y.; Sugiura, D.; Kudo, A.; Akimoto, Y.; Kawakami, H.; Bovin, N. V.; Irimura, T. Distribution and Function of Macrophage Galactose-Type C-Type Lectin 2 (MGL2/CD301b): Efficient Uptake and Presentation of Glycosylated Antigens by Dendritic Cells. *J. Biol. Chem.* **2010**, *285* (25), 19193–19204. https://doi.org/10.1074/jbc.M110.113613.

(7) Martinez-Pomares, L. The Mannose Receptor. *J. Leukoc. Biol.* **2012**, *92* (6), 1177–1186. https://doi.org/10.1189/JLB.0512231.

(8) East, L.; Isacke, C. M. The Mannose Receptor Family. *Biochim. Biophys. Acta - Gen. Subj.* **2002**, *1572* (2–3), 364–386. https://doi.org/10.1016/S0304-4165(02)00319-7.

(9) Mullin, N. P.; Hall, K. T.; Taylor, M. E. Characterization of Ligand Binding to a Carbohydrate-Recognition Domain of the Macrophage Mannose Receptor. *J. Biol. Chem.* **1994**, *269* (45), 28405–28413. https://doi.org/10.1016/s0021-9258(18)46942-6.

(10) Taylor, M. E.; Drickamer, K. Structural Requirements for High Affinity Binding of Complex Ligands by the Macrophage Mannose Receptor. *J. Biol. Chem.* **1993**, *268* (1), 399–404. https://doi.org/10.1016/S0021-9258(18)54164-8.

(11) Feinberg, H.; Jégouzo, S. A. F.; Lasanajak, Y.; Smith, D. F.; Drickamer, K.; Weis, W. I.; Taylor, M. E. Structural Analysis of Carbohydrate Binding by the Macrophage Mannose Receptor CD206. *J. Biol. Chem.* **2021**, *296*, 100368–100369. https://doi.org/10.1016/j.jbc.2021.100368.

(12) Napper, C. E.; Drickamer, K.; Taylor, M. E. Collagen Binding by the Mannose Receptor Mediated through the Fibronectin Type II Domain. *Biochem. J.* **2006**, *395* (3), 579–586. https://doi.org/10.1042/BJ20052027.

(13) Leteux, C.; Chai, W.; Loveless, R. W.; Yuen, C. T.; Uhlin-Hansen, L.; Combarnous, Y.; Jankovic, M.; Maric, S. C.; Misulovin, Z.; Nussenzweig, M. C.; Feizi, T. The Cysteine-Rich Domain of the Macrophage Mannose Receptor Is a Multispecific Lectin That Recognizes Chondroitin Sulfates a and B and Sulfated Oligosaccharides of Blood Group Lewisa and Lewisx Types in Addition to the Sulfated N-Glycans of Lutropin. *J. Exp. Med.* **2000**, *191* (7), 1117–1126. https://doi.org/10.1084/JEM.191.7.1117.

(14) Burgdorf, S.; Kautz, A.; Böhnert, V.; Knolle, P. A.; Kurts, C. Distinct Pathways of Antigen Uptake and Intracellular Routing in CD4 and CD8 T Cell Activation. *Science* **2007**, *316* (5824), 612–616. https://doi.org/10.1126/science.1137971.

(15) Butler, N. S.; Nolz, J. C.; Harty, J. T. Immunologic Considerations for Generating Memory CD8 T Cells through Vaccination. *Cell. Microbiol.* **2011**, *13* (7), 925–933. https://doi.org/10.1111/J.1462-5822.2011.01594.X.

(16) Ott, P. A.; Hu, Z.; Keskin, D. B.; Shukla, S. A.; Sun, J.; Bozym, D. J.; Zhang, W.; Luoma, A.; Giobbie-Hurder, A.; Peter, L.; Chen, C.; Olive, O.; Carter, T. A.; Li, S.; Lieb, D. J.; Eisenhaure, T.; Gjini, E.; Stevens, J.; Lane, W. J.; Javeri, I.; Nellaiappan, K.; Salazar, A. M.; Daley, H.; Seaman, M.; Buchbinder, E. I.; Yoon, C. H.; Harden, M.; Lennon, N.; Gabriel, S.; Rodig, S. J.; Barouch, D. H.; Aster, J. C.; Getz, G.; Wucherpfennig, K.; Neuberg, D.; Ritz, J.; Lander, E. S.; Fritsch, E. F.; Hacohen, N.; Wu, C. J. An Immunogenic Personal Neoantigen Vaccine for Patients with Melanoma. *Nature* **2017**, *547* (7662), 217–221. https://doi.org/10.1038/nature22991.

(17) Rauen, J.; Kreer, C.; Paillard, A.; Van Duikeren, S.; Benckhuijsen, W. E.; Camps, M. G.; Valentijn, A. R. P. M.; Ossendorp, F.; Drijfhout, J. W.; Arens, R.; Burgdorf, S. Enhanced Cross-Presentation and Improved CD8+ T Cell Responses after Mannosylation of Synthetic Long Peptides in Mice. *PLoS One* **2014**, *9* (8), e103755. https://doi.org/10.1371/journal.pone.0103755.

(18) McIntosh, J. D.; Brimble, M. A.; Brooks, A. E. S.; Dunbar, P. R.; Kowalczyk, R.; Tomabechi, Y.; Fairbanks, A. J. Convergent Chemo-Enzymatic Synthesis of Mannosylated Glycopeptides; Targeting of Putative Vaccine Candidates to Antigen Presenting Cells. *Chem. Sci.* **2015**, *6* (8), 4636–4642. https://doi.org/10.1039/c5sc00952a.

(19) Riera, R.; Hogervorst, T. P.; Doelman, W.; Ni, Y.; Pujals, S.; Bolli, E.; Codée, J. D. C.; van Kasteren, S. I.; Albertazzi, L. Single-Molecule Imaging of Glycan–Lectin Interactions on Cells with Glyco-PAINT. *Nat. Chem. Biol.* **2021**, *17* (12), 1281–1288. https://doi.org/10.1038/s41589-021-00896-2.

(20) Rosalia, R. A.; Quakkelaar, E. D.; Redeker, A.; Khan, S.; Camps, M.; Drijfhout, J. W.; Silva, A. L.; Jiskoot, W.; Hall, T. van; Veelen, P. A. van; Janssen, G.; Franken, K.; Cruz, L. J.; Tromp, A.; Oostendorp, J.; Burg, S. H. van der; Ossendorp, F.; Melief, C. J. M. Dendritic Cells Process Synthetic Long Peptides Better than Whole Protein, Improving Antigen Presentation and T-Cell Activation. *Eur. J. Immunol.* **2013**, *43* (10), 2554–2565. https://doi.org/10.1002/EJI.201343324.

(21) Gential, G. P. P.; Hogervorst, T. P.; Tondini, E.; van de Graaff, M. J.; Overkleeft, H. S.; Codée, J. D. C.; van der Marel, G. A.; Ossendorp, F.; Filippov, D. V. Peptides Conjugated to 2-Alkoxy-8-Oxo-Adenine as Potential Synthetic Vaccines Triggering TLR7. *Bioorg. Med. Chem. Lett.* **2019**, *29* (11), 1340–1344. https://doi.org/10.1016/J.BMCL.2019.03.048.

(22) Reintjens, N. R. M.; Tondini, E.; De Jong, A. R.; Meeuwenoord, N. J.; Chiodo, F.; Peterse, E.; Overkleeft, H. S.; Filippov, D. V.; Van Der Marel, G. A.; Ossendorp, F.; Codée, J. D. C. Self-Adjuvanting Cancer Vaccines from Conjugation-Ready Lipid A Analogues and Synthetic Long Peptides. *J. Med. Chem.* **2020**, *63* (20), 11691–11706. https://doi.org/10.1021/acs.jmedchem.0c00851.

(23) Reintjens, N. R. M. M.; Tondini, E.; Vis, C.; McGlinn, T.; Meeuwenoord, N. J.; Hogervorst, T. P.; Overkleeft, H. S.; Filippov, D. V.; Marel, G. A. van der; Ossendorp, F.; Codée, J. D. C. C.; van der Marel, G. A.; Ossendorp, F.; Codée, J. D. C. C. Multivalent, Stabilized Mannose-6-Phosphates for the Targeted Delivery of Toll-Like Receptor Ligands and Peptide Antigens. *ChemBioChem* **2021**, *22* (2), 434–440. https://doi.org/10.1002/CBIC.202000538.

(24) Liu, Y.; Chirino, A. J.; Misulovin, Z.; Leteux, C.; Feizi, T.; Nussenzweig, M. C.; Bjorkman, P. J. Crystal Structure of the Cysteine-Rich Domain of Mannose Receptor Complexed with a Sulfated Carbohydrate Ligand. *J. Exp. Med.* **2000**, *191* (7), 1105–1116.

https://doi.org/10.1084/JEM.191.7.1105.

(25) Liu, Y.; Misulovin, Z.; Bjorkman, P. J. The Molecular Mechanism of Sulfated Carbohydrate Recognition by the Cysteine-Rich Domain of Mannose Receptor. *J. Mol. Biol.* **2001**, *305* (3), 481–490. https://doi.org/10.1006/JMBI.2000.4326.

(26) Li, H.; Vaughan, J. C. Switchable Fluorophores for Single-Molecule Localization Microscopy. *Chemical Reviews*. American Chemical Society September 26, 2018, pp 9412–9454. https://doi.org/10.1021/acs.chemrev.7b00767.

(27) Mujumdar, R. B.; Ernst, L. A.; Mujumdar, S. R.; Lewis, C. J.; Waggoner, A. S. Cyanine Dye Labeling Reagents: Sulfoindocyanine Succinimidyl Esters. *Bioconjug. Chem.* **2002**, *4* (2), 105–111. https://doi.org/10.1021/BC00020A001.

(28) Rising, T. W. D. F.; Claridge, T. D. W.; Davies, N.; Gamblin, D. P.; Moir, J. W. B.; Fairbanks, A. J. Synthesis of N-Glycan Oxazolines: Donors for Endohexosaminidase Catalysed Glycosylation. *Carbohydr. Res.* **2006**, *341* (10), 1574–1596. https://doi.org/10.1016/j.carres.2006.03.007.

(29) Oscarson, S.; Tidén, A. K. Syntheses of the Octyl and Tetradecyl Glycosides of 3,6-Di-O-α-d-Mannopyranosyl-α-d-Mannopyranose and of 3,4-Di-O-α-d-Mannopyranosyl-α-d-Mannopyranose. A New Way for 2,4-Di-O-Protection of Mannopyranosides. *Carbohydr. Res.* **1993**, *247* (C), 323–328. https://doi.org/10.1016/0008-6215(93)84266-9.

(30) Andersen, S. M.; Heuckendorff, M.; Jensen, H. H. 3-(Dimethylamino)-1-Propylamine: A Cheap and Versatile Reagent for Removal of Byproducts in Carbohydrate Chemistry. *Org. Lett.* **2015**, *17* (4), 944–947. https://doi.org/10.1021/acs.orglett.5b00041.

(31) Christensen, H.; Christiansen, M. S.; Petersen, J.; Jensen, H. H. Direct Formation of β-Glycosides of N-Acetyl Glycosamines Mediated by Rare Earth Metal Triflates. *Org. Biomol. Chem.* **2008**, *6* (18), 3276–3283. https://doi.org/10.1039/b807064d.

(32) Weerapana, E.; Glover, K. J.; Chen, M. M.; Imperiali, B. Investigating Bacterial N-Linked Glycosylation: Synthesis and Glycosyl Acceptor Activity of the Undecaprenyl Pyrophosphate-Linked Bacillosamine. *J. Am. Chem. Soc.* **2005**, *127* (40), 13766–13767. https://doi.org/10.1021/ja054265v.

(33) Aletras, A.; Barlos, K.; Gatos, D.; Koutsogianni, S.; MAMOS, P. Preparation of the Very Acid-sensitive Fmoc-Lys(Mtt)-OH Application in the Synthesis of Side-chain to Side-chain Cyclic Peptides and Oligolysine Cores Suitable for the Solid-phase Assembly of MAPs and TASPs. *Int. J. Pept. Protein Res.* **1995**, *45* (5), 488–496. https://doi.org/10.1111/j.1399-3011.1995.tb01065.x.

(34) Hong, V.; Presolski, S. I.; Ma, C.; Finn, M. G. Analysis and Optimization of Copper-Catalyzed Azide-Alkyne Cycloaddition for Bioconjugation. *Angew. Chem. Int. Ed.* **2009**, *48* (52), 9879–9883. https://doi.org/10.1002/anie.200905087.

(35) Moorman, R. M.; Collier, M. B.; Frohock, B. H.; Womble, M. D.; Chalker, J. M. Halide Inhibition of the Copper-Catalysed Azide–Alkyne Cycloaddition. *Org. Biomol. Chem.* **2015**, *13* (7), 1974–1978. https://doi.org/10.1039/C4OB02479F.

(36) Li, R. J. E.; Hogervorst, T. P.; Achilli, S.; Bruijns, S. C.; Arnoldus, T.; Vivès, C.; Wong, C. C.; Thépaut, M.; Meeuwenoord, N. J.; van den Elst, H.; Overkleeft, H. S.; van der Marel, G. A.; Filippov, D. V.; van Vliet, S. J.; Fieschi, F.; Codée, J. D. C.; van Kooyk, Y. Systematic Dual Targeting of Dendritic Cell C-Type Lectin Receptor DC-SIGN and TLR7 Using a Trifunctional Mannosylated Antigen. *Front. Chem.* **2019**, *7*, 650. https://doi.org/10.3389/fchem.2019.00650.

(37) Tinevez, J. Y.; Perry, N.; Schindelin, J.; Hoopes, G. M.; Reynolds, G. D.; Laplantine, E.; Bednarek, S. Y.; Shorte, S. L.; Eliceiri, K. W. TrackMate: An Open and Extensible Platform for Single-Particle

Tracking. *Methods* **2017**, *115*, 80–90. https://doi.org/10.1016/J.YMETH.2016.09.016.

(38) Patel, M. K.; Vijayakrishnan, B.; Koeppe, J. R.; Chalker, J. M.; Doores, K. J.; Davis, B. G. Analysis of the Dispersity in Carbohydrate Loading of Synthetic Glycoproteins Using MALDI-TOF Mass Spectrometry. *Chem. Commun.* **2010**, *46* (48), 9119–9121. https://doi.org/10.1039/c0cc03420g.

(39) Wong, C. S.; Hoogendoorn, S.; Van Der Marel, G. A.; Overkleeft, H. S.; Codée, J. D. C. Targeted Delivery of Fluorescent High-Mannose-Type Oligosaccharide Cathepsin Inhibitor Conjugates. *Chempluschem* **2015**, *80* (6), 928–937. https://doi.org/10.1002/CPLU.201500004.

(40) Wipf, P.; Eyer, B. R.; Yamaguchi, Y.; Zhang, F.; Neal, M. D.; Sodhi, C. P.; Good, M.; Branca, M.; Prindle, T.; Lu, P.; Brodsky, J. L.; Hackam, D. J. Synthesis of Anti-Inflammatory α-and β-Linked Acetamidopyranosides as Inhibitors of Toll-like Receptor 4 (TLR4). *Tetrahedron Lett.* **2015**, *56* (23), 3097–3100. https://doi.org/10.1016/J.TETLET.2014.11.048.

5

Synthesis of pre-organized cyclic ligands for the Cholera toxin B-subunit

Introduction

Cholera is the disease caused by the bacterium *Vibrio Cholerae*. It is probably most famous for being the subject of the first-ever epidemiology study, when John Snow showed the role of the local water supply in the deadly spread of Cholera in London in 1854.[1] However, despite this historical nature and intimate knowledge of the disease, it remains a major health problem today. Cholera is responsible for an estimated 100,000 deaths annually, primarily in developing countries. It often rears its head in crisis situations, where a clean water supply is absent. The disease is characterized by a watery diarrhea that induces death by dehydration unless adequately treated with anitbiotics.[2]

The causative agent of Cholera is a secreted protein toxin named cholera toxin (CT). CT consists of an A subunit, which is non-covalently attached to a ring of five copies of a second subunit, aptly named "subunit B" (CTB). The overall stoichiometry of the toxin is therefore AB_5 (Figure 1B).[3] The A subunit (CTA) contains the catalytic domain of the toxin. Once the complex has entered the gut endothelial cells, CTA disassociates from the pentameric ring of B subunits as two fragments; CTA1 and CTA2. CTA1 acts as an ADP-ribosyltransferase in the cytosol, leading to ADP-ribosylation of the alpha subunit of the heterotrimeric G-protein (Gsα). This modification leads to the overproduction of cAMP by activation of adenylate cyclase, which in turn leads to the phosphorylation of the chloride transporter cystic fibrosis transmembrane conductance regulator (CFTR). This activates the transport of chloride ions out of the cell, leading to the efflux of water due to the resulting change in osmotic pressure.[4]

CTB is responsible for cell entry of CT. It does so by binding carbohydrates on the epithelial cell surface, leading to internalization via an as of yet unknown mechanism. In the 70s, three different research groups found the ganglioside GM1 (Figure 1A) to be the main ligand for CTB.[5–7] This interaction has been shown to have a K_d of about 60 nM, as measured by surface plasmon resonance (SPR), which is unusually strong for a lectin-carbohydrate interaction.[8] The role of GM1 as the receptor for CT is not unambiguous: fucosylated oligosaccharides, such as Lewis X and Lewis Y[8] or the A, B and H blood group antigens[9], were recently found to also be ligands for CTB, binding to a separate, secondary binding site on the protein. Further evidence questioning the importance of GM1 came from a study by Wands *et al.*[10] who were unable to detect GM1 gangliosides on the human colonic epithelial cell line T84, despite this cell line being commonly used to study CTB internalization.[11,12] This was compounded by Yrlid and co-workers who showed that the CT mediated diarrheal response in GM1 deficient mice is no different from that of wildtype mice.[13] All these data support the hypothesis that non GM1-carbohydrates (such as the Lewis-type glycans) are the main ligands for CTB in the human intestine.

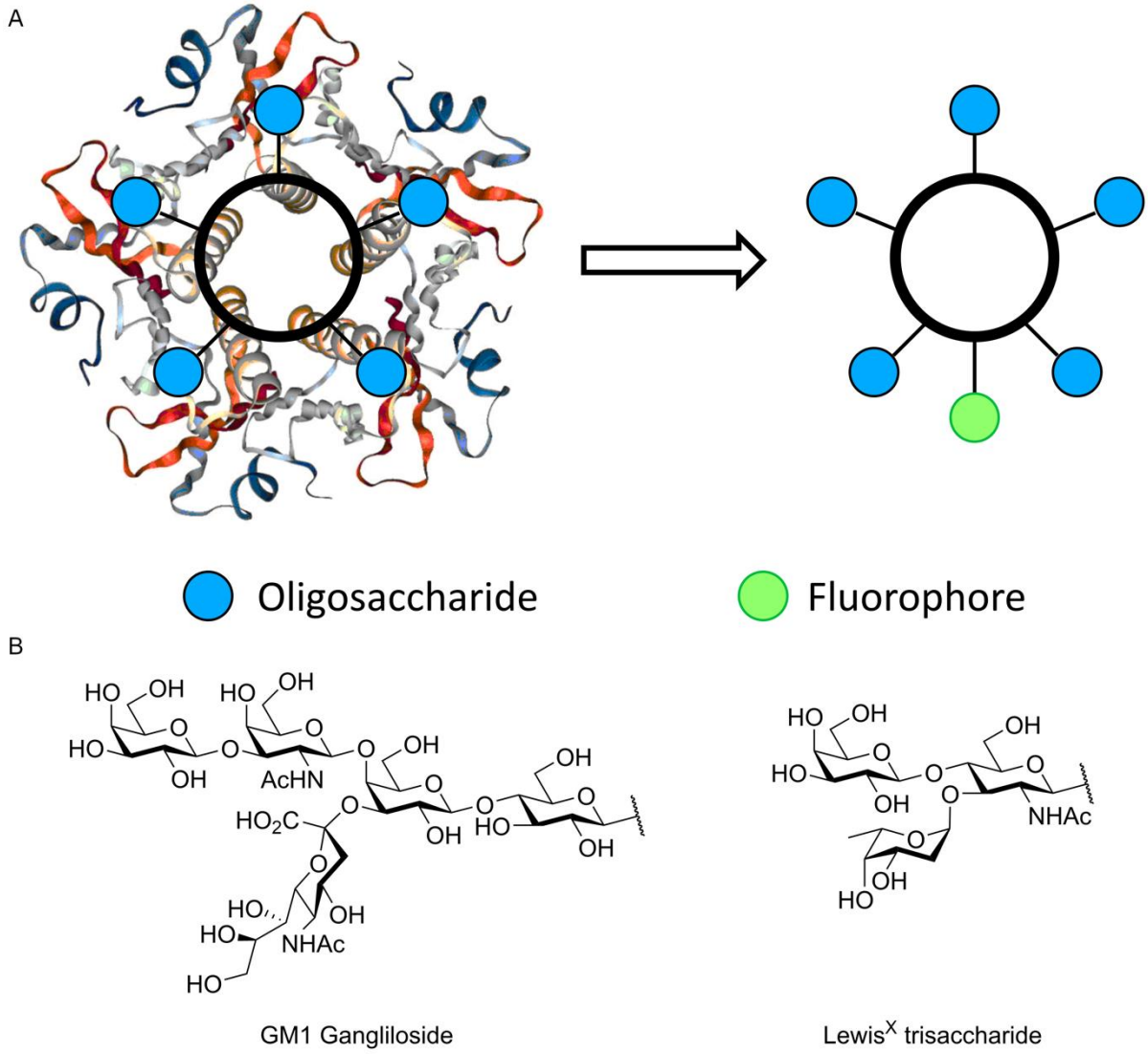

Figure 1. A) Cartoon displaying the general structure and biding mode of pentavalent CTB ligands and the proposed incorporation of a fluorophore for fluorescent detection (protein structure was adapted from PDB: 1CHQ). B) Structure of the GM1 ganglioside and the Lewis X trisaccharide.

Since carbohydrate-mediated uptake of CT is a key process in the disease progress of cholera, several competitive inhibitors for the carbohydrate binding sites have been developed. While monovalent ligands are also known,[14] most approaches focus on exploiting the pentavalent nature of the protein to increase affinity. Multiple pentavalent scaffolds have been modified with carbohydrates and used as CTB ligands. One of the oldest designs is the pentacyclen based design pioneered by Fan *et al*.[15] Other designs based on calixarene structures[16] or scaffolds based on cyclic peptides have also been studied.[17] In all of these designs, long, polyethylene glycol based linkers are placed between the scaffold core and the carbohydrate ligands, to span the distance between the different binding sites. This is necessary since the diameter of the CTB ring is about 50 Å, with the distance between neighboring binding sites about 35 Å.[18] This makes the protein substantially larger than the diameter of most cyclic cores.

To date, no ligand has been synthesized that allows for the detection of CTB via fluorescent techniques. A ligand like that could be useful for the detection of cholera toxin in waste water[19] or the study of pathogen-host interactions by fluorescent microscopy. To this end, one of the known scaffold designs could be modified to allow for the incorporation of a fluorophore. Figure 1B shows a cartoon displaying this general idea. Of the earlier described designs, the cyclic peptide-based ligands appear the most promising for this application, given the vast amounts of known chemistry for the synthesis and derivatization of peptidic molecules. For the carbohydrate ligand, the Lewis^X trisaccharide was chosen over the more commonly used GM1 pentasaccharide, since recent studies have indicated this as the more relevant ligand for CT.

To allow efficient binding to the multivalent CTB lectin, a pre-organized multivalent carbohydrate ligand was envisaged. By synthesizing a cyclic peptide scaffold containing 5 carbohydrate attachment points, as well as an attachment point for a fluorophore, this pentavalency was deemed achievable (Figure 1B). Linkers of defined length between the trisaccharides and the cyclic peptide were also included in the design, as Fan and coworkers have shown spacer length to be critical for a strong binding interaction.[17] The cyclic peptide would consist of six lysine residues, five of which would be attached to the linker modified carbohydrates and one would serve as the fluorophore attachment point. In between the lysine residues spacer moieties will be added to give the cyclic peptide the correct circumference. By using a combination of amide bond forming reactions and copper catalyzed click chemistry, the core scaffold can be elaborated with different oligosaccharides or fluorophores in a modular fashion. This chapter describes the synthesis of such a peptidic scaffold as well as the synthesis of the full, pentavalent Lewis^X-based fluorescent CTB ligand (Scheme 1).

Results and discussion

The ideal fluorescent, peptide based, CTB ligand would have a cyclic core consisting of lysine residues used for functionalization, spaced out into an optimal ring size by spacer amino acids. The work of Fan and coworkers[17] on cyclic peptide based CTB ligands already showed aminohexanoic acid to be an effective spacer for these structures. From this same work it was deduced that a linker length of 8 ethylene glycol units between the peptide core and the Lewis^X trisaccharides should be optimal. The fluorophore itself can be attached directly to the scaffold, since it should not interact with the protein. All of this taken together gives target structure I, which is retrosynthetically analyzed in Scheme 1.

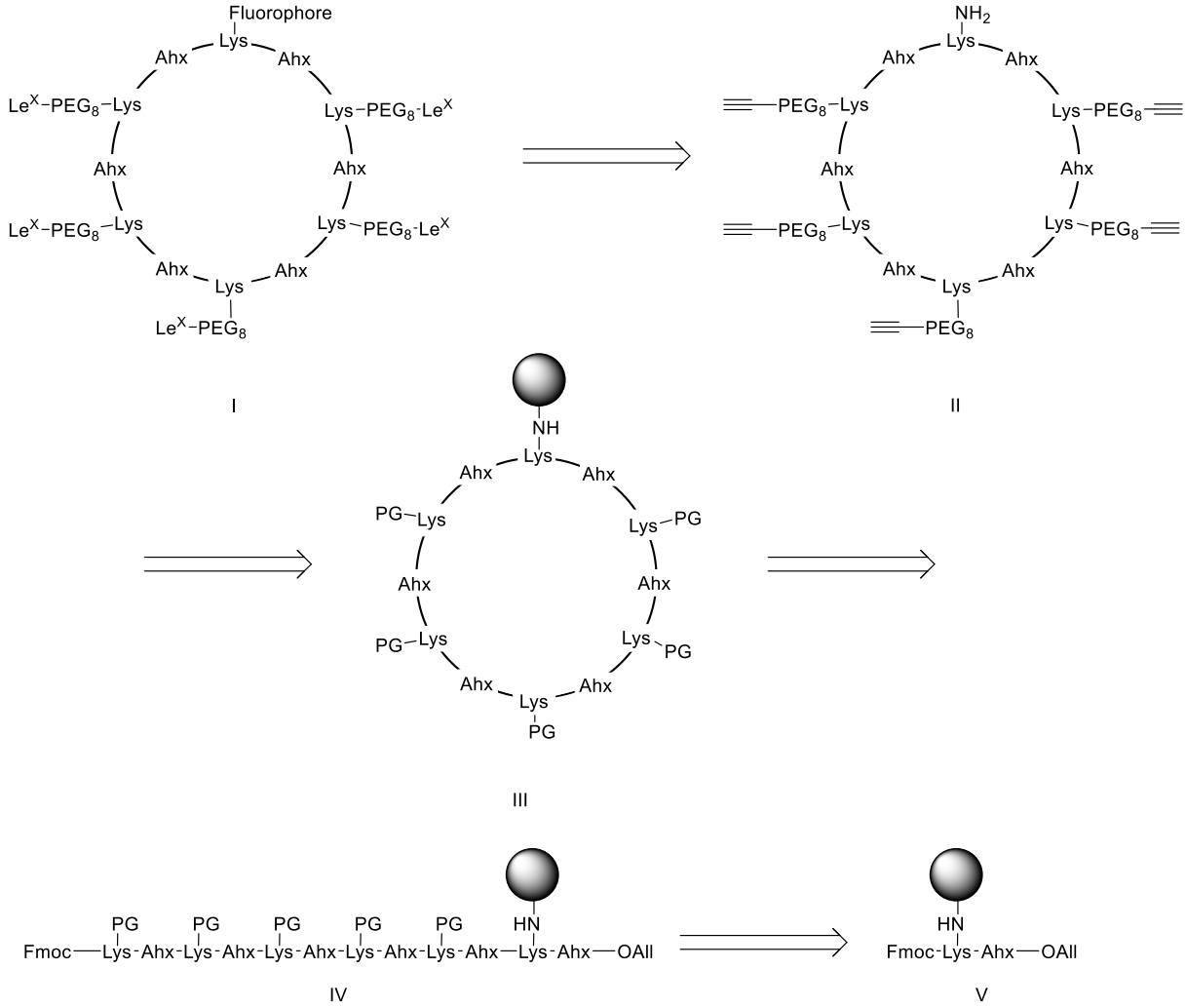

Scheme 1. Retrosynthetic analysis of the cyclic scaffold presenting pentavalent carbohydrate ligands and a fluorophore.

In order to synthesize the desired ligand, a cyclic scaffold containing five carbohydrate attachment points and a single fluorophore attachment site, three things need to be kept in mind: i) introduction of the carbohydrate should happen late-stage using high yielding chemistry, as the sugars are precious, ii) introduction of the fluorophore can most easily be accomplished in the form of an amide forming reaction using a fluorophore NHS-ester, as these reagents are generally commercially available and allow for efficient labeling, and iii) the attachment points used for both oligosaccharides and fluorophore should not interfere with cyclisation of the scaffold.

The first point, efficient late-stage attachment of carbohydrates, can be accomplished using copper(I) catalyzed click chemistry, as previously demonstrated in Chapter 4. A synthesis producing a protected azido-Lewis^X was previously described in Chapter 2, and deprotection of this advanced intermediate should yield a clickable Le^X for the conjugation reaction. To conjugate this oligosaccharide to the scaffold, an alkyne terminated polyethylene glycol molecule could be considered as the linker of choice, as these are often used as biocompatible linkers.[20] Incorporation onto the peptidic scaffold would be accomplished in a facile manner

by amide coupling a carboxylic acid terminated linker to a lysine sidechain. A sixth, unmodified lysine residue would then enable late-stage fluorophore labeling. (Scheme 1, intermediate II) This scaffold itself would be constructed from a properly protected cyclic intermediate (Scheme 1, intermediate III). This leaves the formation of the cyclic peptidic core as the last consideration. On-resin head-to-tail cyclization of a properly orthogonally protected peptide would enable the rapid synthesis of this scaffold using well established chemistry.

To allow for on-resin backbone cyclization, as well as selective coupling of linkers to five of the six lysine sidechains, a strategy of triple orthogonal protected amines is required. (Scheme 1, intermediate IV) To enable a head-to-tail cyclisation approach for the synthesis of the scaffold core, the peptide will be anchored to the solid support via the sidechain of one of the lysine residues, in the form of a carbamate linkage with a resin-bound *para*-hydroxybenzyl functionality, enabling release of the peptide under acidic treatment.[21] The C-terminus of the peptide will remain masked in the form of an allyl ester until the cyclisation reaction is carried out. Using the standard Fmoc protecting group on the N-terminus of the linear peptide immediately creates orthogonality with the acid labile resin anchoring, as well as the allyl ester, while also being synthetically the most straightforward, given the commercial availability of building blocks bearing this protecting group. The remaining lysine sidechains could be protected using highly acid labile trityl based protecting groups. While these types of acid sensitive protected lysine building blocks are commonly used for on-resin sidechain modifications,[22,23] the compatibility with the resin anchoring carbamate linkage needs to be investigated. The synthesis of the linear peptide will start from an immobilized dipeptide bearing a C-terminal allyl ester and an N-terminal Fmoc (Scheme 1, intermediate V).

The synthesis of the cyclic peptide was initiated with the synthesis of fully protected dipeptide **2**, bearing a N-terminal Fmoc, a C-terminal allyl ester and a Boc-group protecting the lysine sidechain. This synthesis commenced with the allylation of 6-aminohexanoic acid using $SOCl_2$ as an activator to obtain amine **1** in 94% yield, followed by HCTU mediated coupling to Fmoc-Lys(Boc)-OH, giving the desired dipeptide **2** in 92% yield. To create the carbamate linkage between the resin and the lysine sidechain, the Boc protecting group was removed by treatment with a 1/1 mixture of TFA/DCM (v/v) for 15 minutes, followed by removal of the volatiles *in vacuo*. This afforded crude peptide **3**, which was dissolved in 1 M DiPEA in DCM, in order to neutralize the acid, and *para*-nitrophenolcarbonate-actived Tentagel S NPC resin was added. After stirring for 16 hours, the peptide was immobilized on the resin, affording intermediate **4**.

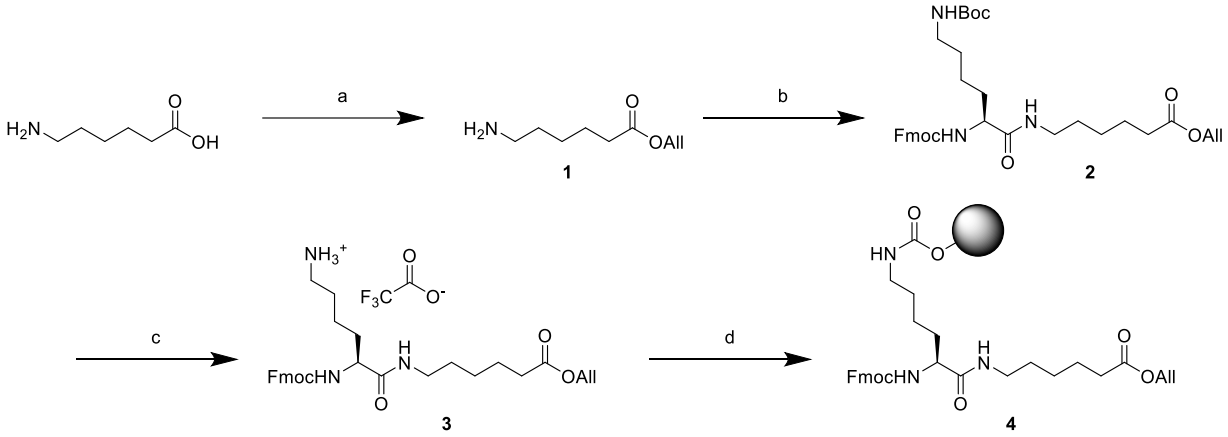

Scheme 2. Synthesis of fully protected dipeptide **3** followed by resin-anchoring via the lysine sidechain. Reagents and conditions: a) allyl alcohol, $SOCl_2$, 0°C, 94% b) Fmoc-Lys(Boc)-OH, HCTU, DiPEA, DMF, 92% c) TFA, DCM d) Tentagel S NPC, DiPEA, DCM.

To answer the question of protecting group orthogonality between the resin linker and the protecting groups used for the lysine sidechain, model immobilized peptide **5a** was first synthesized by extending **4** with Fmoc-Ahx-OH and Fmoc-Lys(Mtt)-OH. A series of deprotection conditions (Table 1, #1-4) were tested on this immobilized peptide. After deprotection, the resin was treated with Ac_2O and DiPEA followed by resin cleavage with a standard 95% TFA cocktail. By performing LC-MS analysis of the crude peptide, the amount of protecting group liberation could be determined by peak integration, by comparing peak intensity of the acetylated versus non-acetylated peptide. In order to determine whether resin cleavage took place during the trityl deprotection, the flowthrough of the reaction was concentrated *in vacuo,* redissolved in 1:1:1 H_2O/MeCN/tBuOH and subjected to LC-MS analysis as well.

Table 1. Optimization of lysine sidechain deprotection in presence of the acid-labile carbamate resin linkage.

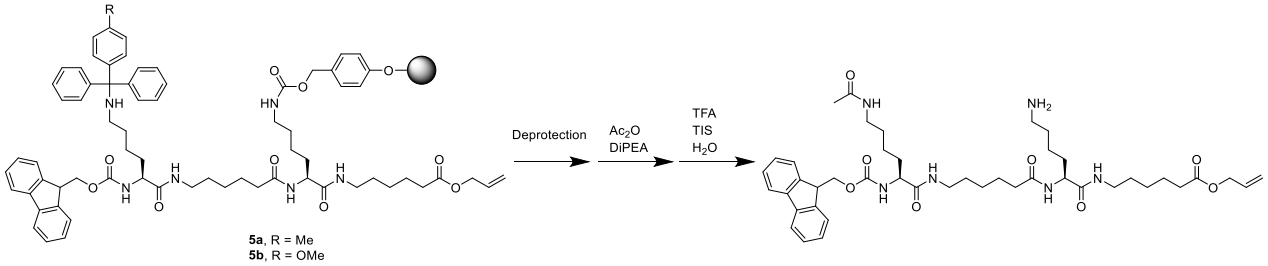

#	Reagent	R =	Time	Remark
1	1% TFA/DCM (v/v)	CH_3	30 min	10% Mtt deprotection
2	1% TFA/DCM (v/v)	CH_3	7 x 2 min	Peptide cleaved from resin
3	1% TFA/DCM + 1% TES (v/v)	CH_3	1 h	50% Mtt deprotection
4	1:2:7 AcOH/TFE/DCM (v/v)	CH_3	1 h	50% Mtt deprotection
5	1% TFA/DCM (v/v)	OCH_3	30 min	Peptide (partially) cleaved from resin
6	**1:2:7 AcOH/TFE/DCM (v/v)**	**OCH_3**	**1 h**	**Full Mmt deprotection**

The typical method for the selective liberation of Lys(Mtt) is treatment with 1% TFA in DCM (v/v) for 30 minutes (entry 1) or multiple very short incubations, repeated until the yellow color, indicative of liberated trityl carbocations, stops appearing (entry 2). While the single acidic treatment was mostly unsuccessful in liberating Mtt, the repeated incubations was able fully deprotect the protecting group, however simultaneously also fully cleaving the solid support linker. Since retritylation of the sidechain could play a role in the poor conversion found for entry 1, this reaction was reattempted with the addition of TES as a cation scavenger (entry 3). While this increased the level of conversion from 10% to 50%, these numbers are nevertheless insufficient for the efficient synthesis of the desired modified peptide. As a final alternative, the resin bound peptide was treated with a mixture of acetic acid and trifluoroethanol in DCM, as described by Aletras *et al.*[24], for one hour. However, this again yielded an unacceptable low conversion to the desired partially deprotected peptide.

Disappointingly, no condition for the full deprotection could be found that was able to fully liberate methyltrityl on lysine while simultaneously being fully orthogonal to the resin linker. Since most conditions led to partial liberation of the trityl without touching the resin linker, a more acid labile protecting group, in the form of 4-methoxytrityl, was incorporated instead, yielding resin bound peptide **5b**. This immobilized peptide was subjected to the same screening approach. When treating this immobilized peptide with 1% TFA in DCM (v/v) for half an hour (entry 5), some peptide liberation was observed, in contrast to what was observed earlier with resin bound peptide **5a** under the same conditions. Gratifyingly, when using the acetic acid/trifluoroethanol mixture (entry 6) complete amine liberation with full retention of support linkage was observed. With an effective orthogonal deprotection strategy in hand, the synthesis of the cyclic peptide itself was investigated next.

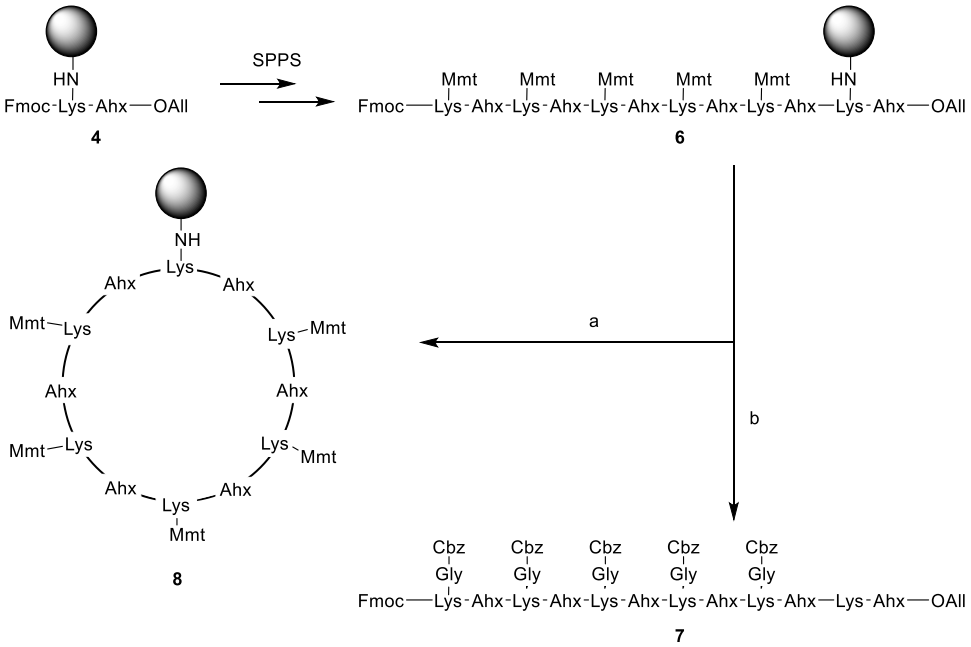

Scheme 3. Synthesis of fully protected cyclic scaffold **8** and exploration of deprotection and coupling of five Lys(Mmt) lysine residues. Reagents and conditions: a) i) $Pd(PPh_3)_4$, $PhSiH_3$, DCM ii) 2% DBU/DMF (v/v) iii) PyAOP, DiPEA, DMF b) i) AcOH, TFE, DCM ii) Cbz-Gly-OH, HCTU, DiPEA, DMF iii) TFA, TIS, DCM.

The immobilized linear peptide **6** was first synthesized using standard Fmoc based SPPS, using only two equivalents to couple the precious Fmoc-Lys(Mmt)-OH building block. Before cyclization could commence, first the C- and N-terminus of the peptide had to be liberated. The C-terminal allyl ester was cleaved using repeated treatment with $Pd(PPh_3)_4$ and phenylsilane. Complete removal of the protecting group was confirmed by a test cleavage of a small portion of resin (~1mg) followed by LC-MS analysis. Initially, the N-terminus was deprotected using 20% piperidine in DMF, as is typical in Fmoc based SPPS. However, this led to the formation of a C-terminal piperidine amide during the cyclization reaction, even when extensive washes were carried out between deprotection and cyclization. Presumably piperidine forms a salt bridge with the deprotected C-terminus, retaining the base on the resin. By deprotecting the N-terminus using 2% DBU in DMF (v/v) instead, this side reaction could be suppressed. Cyclization was attempted by treating the resin with a solution containing PyBOP as the condensation agent and DiPEA as general base for 16 hours, as was described by Fan and co-workers.[17] However, even after repeated 16 hour treatment, some non-cyclized material was still present. By using a more reactive condensation agent, PyAOP,[25] full consumption of linear peptide could be attained after a single 16 hour reaction.

With the fully cyclized peptide in hand, the deprotection and subsequent amide formation of the five lysine residues was explored. It was decided to optimize this reaction on the linear peptide **6**, since cyclisation side-products could conceivably make analysis of incompletely acylated mixtures more cumbersome. To this end, resin bound peptide **6** was first treated with acetic acid and trifluoroethanol in DCM for one hour, followed by DCM and DMF washes. Here, a cheap model carboxylic acid was needed to test the coupling reaction. Cbz-Gly-OH was used, as its lack of steric bulk on the C-α position combined and good UV absorption for LC-MS analysis makes this an ideal test reagent. Therefore, the partially deprotected immobilized peptide was reacted with a mixture of Cbz-Gly-OH, HCTU and DiPEA, which were first preactivated together for 5 minutes before addition to the resin. After 1 hour the resin was thoroughly washed with DMF and DCM and the bound peptide was liberated by treatment with a 95% TFA cocktail (95:2.5:2.5 TFA/H_2O/TIS), followed by LC-MS analysis. Here, besides the desired product **7**, peaks belonging to species where one, two or three lysine residues were acetylated, instead of the desired acylation with Cbz-glycine, were observed. This side reaction presumably happens because of residual acetic acid in the resin matrix, which is activated by HCTU. Some different post-deprotection wash protocols were evaluated, with a thorough washing with 10% TEA in DMF (v/v) for 2 x 15 minutes giving a sufficiently clean result.

Next, the synthesis of the required long PEG linkers was evaluated. At first, the method of Zhang *et al.*[26], where long, functionalized and monodisperse PEG spacers are synthesized starting from a common building block, was attempted. However, this method turned out to be cumbersome and low yielding, so it was decided to make the required long linkers using on-resin amide bond formation from two shorter linkers **11** and **15**, the synthesis of which is shown in Scheme 4.

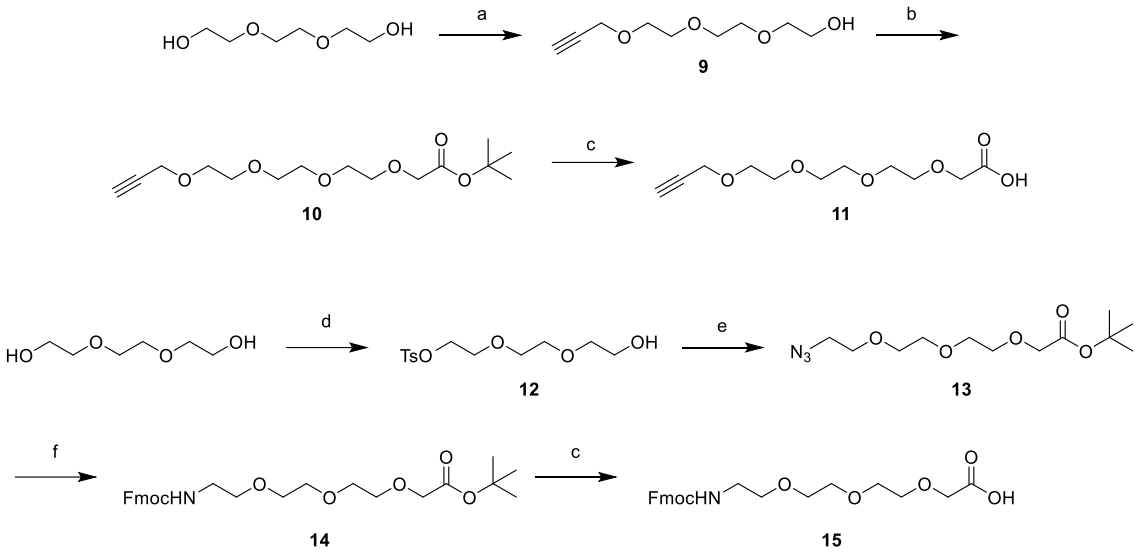

Scheme 4. Synthesis of PEG linkers **11** and **15** from triethylene glycol. Reagents and conditions: a) propargyl bromide, NaH, THF, 89% b) *tert*-butyl bromoacetate, NaH, THF, 64% c) TFA, DCM, **11** quant, **15** quant d) TsCl, Et_3N, DCM, 86% e) i) NaN_3, DMF, 70°C ii) *tert*-butyl bromoacetate, NaH, THF, 50% over two steps f) i) PPh_3, H_2O, THF ii) Fmoc-OSu, N-methylmorpholine, DCM, 90%.

Briefly, the propargyl terminated TEG linker **11** was synthesized by selective monoalkylation of triethylene glycol with propargyl bromide, mediated by NaH, obtaining the alkyne **9** in 89% yield, followed by alkylation of the second alcohol with *tert*-butyl bromoacetate, again mediated by NaH, in 64% yield, producing **10**. This protected acid was then treated with TFA to give **11** in quantitative yield. Similarly, the synthesis of Fmoc protected TEG-linker **15** was commenced by monotosylation of triethylene glycol, performed with *para*-toluenesulfonyl chloride in presence of triethylamine, to produce **12** in 86% yield. Next, substitution with sodium azide in DMF at elevated temperature, followed by alkylation with *tert*-butylbromoacetate and NaH in THF, produced intermediate **13** in 50% yield. The azide was converted to an amine by Staudinger reduction with triphenylphosphine and water and immediately protected with an Fmoc group using Fmoc-OSu and *N*-methylmorpholine, yielding fully protected linker **14** in 90% yield. After deprotection of the *tert*-butyl ester with TFA, **15** was obtained in quantitative yield.

In order to obtain scaffold **19**, fully protected cyclic peptide **8** was first treated with the Mmt cleavage cocktail, giving resin bound peptide **16**. After extensive washing, TEG linker **15** was coupled using HCTU as the condensation reagent in presence of DiPEA, producing resin-bound peptide **17**. This was followed by Fmoc deprotection and coupling of linker **11** under the same conditions. This resin bound molecule (**18**) was then treated with a 95% TFA cocktail for one hour, liberating the resin bound scaffold. The obtained crude mixture was purified over RP-HPLC, but the desired molecule was obtained in extremely poor yield (< 1%).

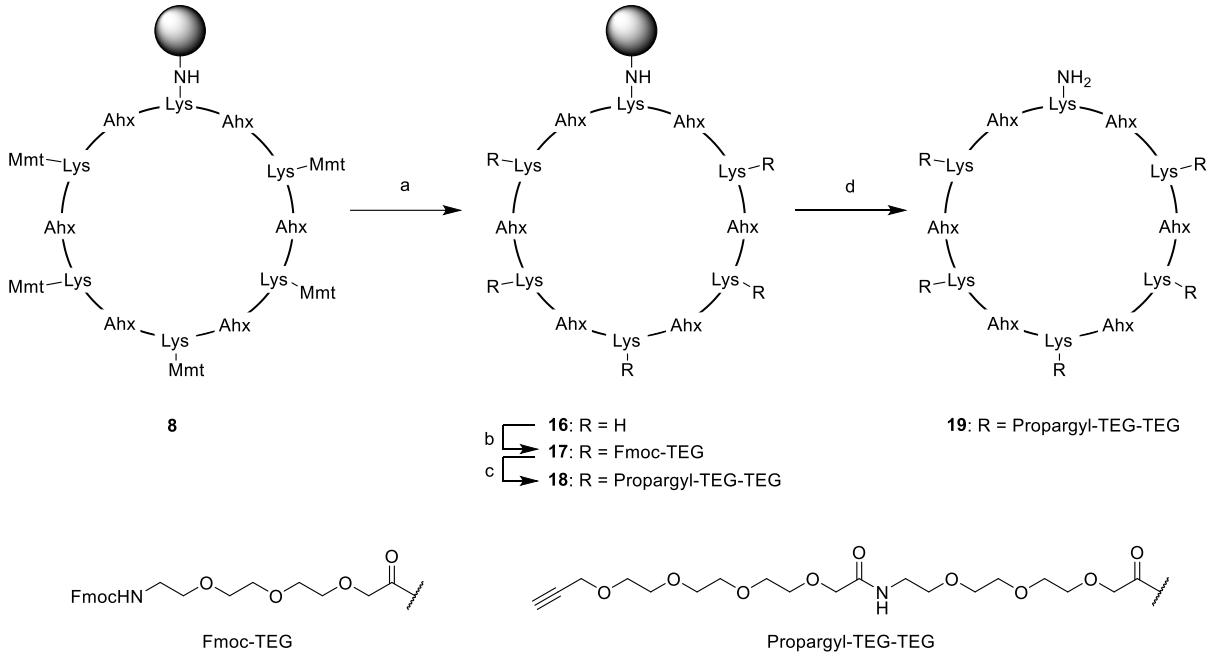

Scheme 5. Synthesis of cyclic scaffold **19**. Reagents and conditions: a) AcOH, TFE, DCM b) **15**, HCTU, DiPEA c) **11**, HCTU, DiPEA d) TFA, TIS, H_2O.

Careful investigation of LC-MS spectra obtained when test-cleaving immobilized peptides **17** and **18** revealed incomplete linker incorporation, especially in the second acylation step (**17** → **18**). By changing the coupling reagent used in these reactions from HCTU to PyAOP, an increased conversion to the desired molecule could be achieved. When the molecule was resynthesized using this altered method, a new complication was observed. When analyzing the mass spectrum (Figure 2A) of the crude molecule, the two main ions observed were found to have m/z = 1768.25 and m/z = 1415.00. While the first mass is readily assigned as the z=2 ion of the expected product **19** (exact mass = 3533.07 Da), the second ion would belong to an unlikely z=2.5 ionization. A more likely explanation would be the formation of the cyclic dimer, where first two linear peptides couple to form a linear dimer, followed by cyclization. This would imply the observed masses are actually the z = 4 and z = 5 ions of the dimer molecule (exact mass = 7066.15 Da). This kind of side reaction has been observed more often when performing on-resin cyclisation reactions.[27] In order to better understand the amount of cyclic monomer versus cyclic dimer that is being formed, an improved way of analyzing cyclic intermediate **8** was envisioned. Since a cyclic polylysine derivative as has been synthesized here has very little retention on reverse phase silica, a method to increase the retention time and separation between monomer and dimer peaks on LC-MS was used, as outlined in Figure 2B. Capitalizing on the ability to selectively liberate the Mmt groups on the lysine sidechains, a hydrophobic moiety could be introduced, increasing retention on reverse phase silica. Benzoyl groups where chosen as the moiety of choice both for their ease of introduction using benzoic anhydride in DCM as well as their added benefit of having good UV absorption properties, aiding the analysis of the mixture by LC-UV.

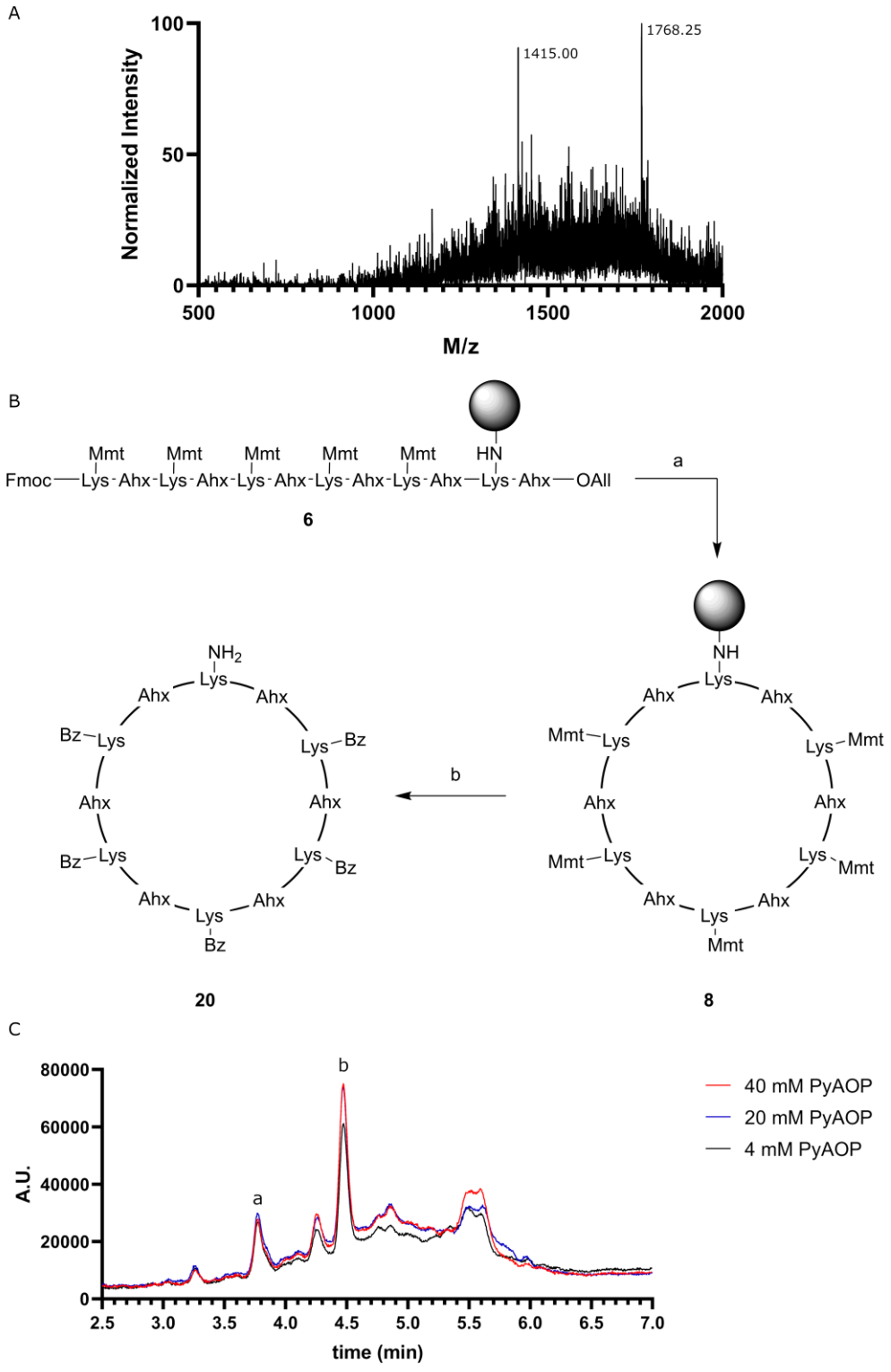

Figure 2. A) Partial mass spectrum obtained when analyzing crude **19**, the two largest peaks are annotated. B) Outline of the methodology used to analyze cyclization products. C) Partial LC-UV chromotagram of the benzoylated derivatives Reagents and conditions: a) i) $Pd(PPh_3)_4$, $PhSiH_3$, DCM ii) DBU, DMF iii) PyAOP, DiPEA, DMF b) i) AcOH, TFE, DCM ii) Bz_2O, DiPEA, DCM iii) TFA, H_2O, TIS C) partial LC-UV analysis (gradient: 30-70% B over 10 minutes) of cyclization reactions carried out using different concentrations of PyAOP. Peak (a) was assigned as the desired monocyclized product and (b) as the undesired dimeric cyclic product.

To evaluate the effect the concentration of the condensation agent PyAOP has on the cyclization, three test cyclization reactions were carried out. The Mmt groups of the immobilized peptides were then removed, followed by benzoylation and resin cleavage. The crude cleavage products were then analyzed by LC-MS, and the traces are shown in Figure 2C. As can be seen in this chromatogram, the majority of observed product was in the form of the cyclic dimer, regardless of concentration of PyAOP. A similar result was obtained when the cyclization was carried out in DMSO instead of DMF. These results suggest that the prevalence to form dimers is inherent to the structure of linear peptide **6**.

One variable that might be key to the formation of the undesired peptide cyclic peptide is the length of the linear peptide used in the cyclization reaction. Replacing aminohexanoic acid with a shorter spacer, for instance the four carbon long aminobutyric acid, might decrease the peptide's propensity to form cyclic dimers over the desired cyclic monomer. In order to test this, a new immobilized dipeptide **23** was synthesized (Scheme 6). The synthesis started with the formation of an allylester on Boc-aminobutynoic acid, mediated by EDC, in presence of DiPEA and DMAP as nucleophilic catalyst, producing **21** in 75% yield. This was followed by Boc deprotection in 1/1 (v/v) TFA/DCM. After removing the volatiles *in vacuo* the crude amine was immediately coupled to Fmoc-Lys(Boc)-OH, affording dipeptide **22** in 90% yield. This dipeptide was then, after facile removal of the Boc group protecting the lysine side chain, loaded onto Tentagel S NPC resin to afford immobilized intermediate **23**.

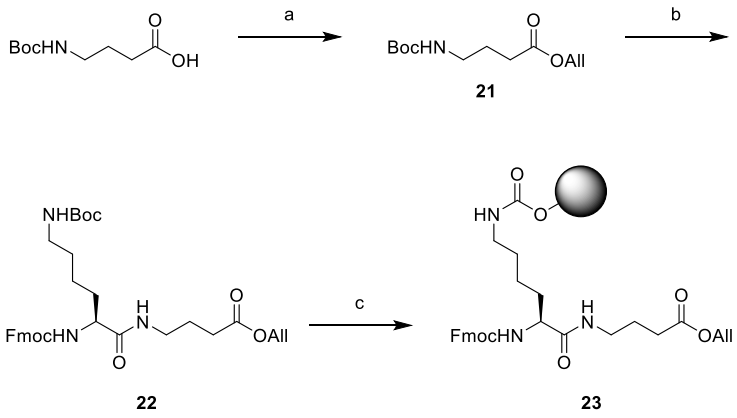

Scheme 6. Synthesis of immobilized dipeptide **23**. Reagents and conditions: a) Allyl alcohol, EDC, DMAP, DiPEA, DCM, 16h, 75% b) i) TFA, DCM, 15 min ii) Fmoc-Lys(Boc)-OH, HCTU, DiPEA, DMF, 2h, 90% over two steps c) i) TFA, DCM, 15 min ii) Tentagel S NPC, DiPEA, DCM, 16 h.

With immobilized dipeptide **23** in hand, synthesis of the full scaffold proceeded smoothly, as presented in Scheme 7. The full linear peptide **24** was synthesized as before, and deallylation using $Pd(PPh_3)_4$ and $PhSiH_3$ proceeded smoothly. After removal of the Fmoc using 2% DBU in DMF cyclisation was attempted using PyAOP. After overnight treatment, a small portion of the resin was again subjected to selective Mmt removal followed by benzoylation with benzoic anhydride. After resin liberation with the 95% TFA cocktail, LC-MS analysis showed the desired monocyclic molecule as the main product. The rest of immobilized peptide **25** was then

subjected to the same deprotection condition to liberate the Mmt groups. After vigorous washing to remove remaining acetic acid, Fmoc protected TEG linker **15** was coupled using PyAOP as the condensation agent in presence of DiPEA. The Fmoc group was removed using the conventional method (20% piperidine in DMF (v/v)) and the propargyl terminated TEG **11** was coupled to the linkers, again mediated by PyAOP/DiPEA. The peptide was released from the resin using the standard 95% TFA cocktail and purified by preparative RP-HPLC, yielding **29** in 4.6% yield.

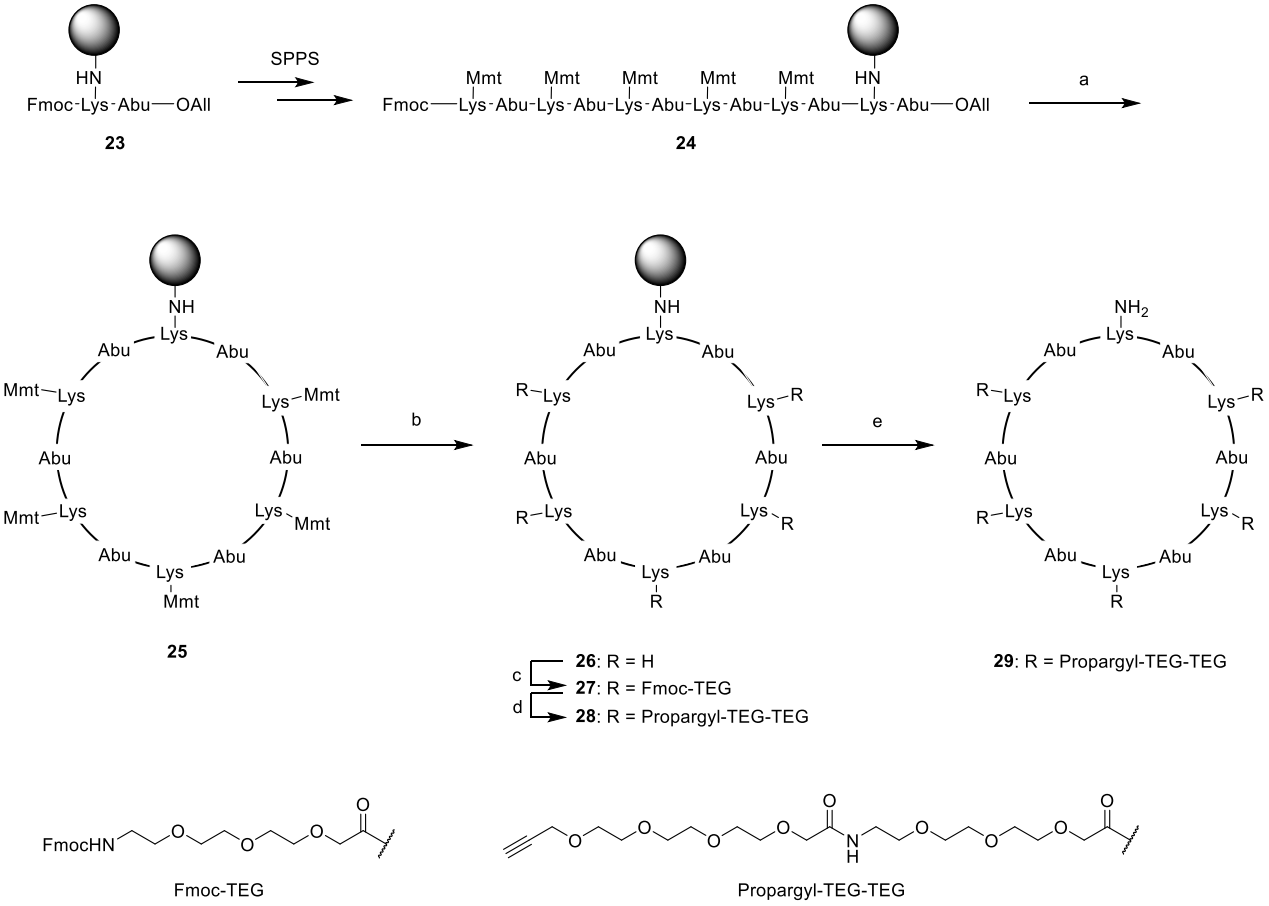

Scheme 7. Synthesis of cyclic Abu containing peptide **29**. Reagents and conditions: a) i) $Pd(PPh_3)_4$, $PhSiH_3$, DCM ii) DBU, DMF iii) PyAOP, DiPEA, DMF b) AcOH, TFE, DCM c) **15**, PyAOP, DiPEA, DMF d) i) piperidine, DMF ii) **11**, PyAOP, DiPEA, DMF e) TFA, TIS, H_2O.

With the peptidic scaffold now in hand, the next step was the synthesis of the clickable sugars. Besides Lewis^X azide, an 1-azido derivative of galactose was also synthesized to explore binding differences caused by interaction with the distinct pockets, since galactose has been shown to interact with the GM1 binding pocket of CTB.[28]

The synthesis of clickable galactoside **32** started from commercially available 1,2,3,4,6-penta-O-acetyl-β-galactopyranoside by introduction of an anomeric chloride using $TiCl_4$ in refluxing DCM, producing α-chloride **30** in 93% yield. A simple S_N2-like substitution with NaN_3 produced the protected azidosugar **31** in 83% yield, which was then deacetylated under Zemplén conditions to produce compound **32** in 92% yield. The synthesis of the azido Lewis X trisaccharide started off with fully protected sugar **34**, the synthesis of which was described

in Chapter 2. The *para*-methoxybenzyl protecting groups were removed oxidatively using DDQ, yielding the partially deprotected compound **35** in 71% yield. To remove the remaining ester protecting groups, Zemplén conditions were again employed, producing compound **36** in quantitative yield.

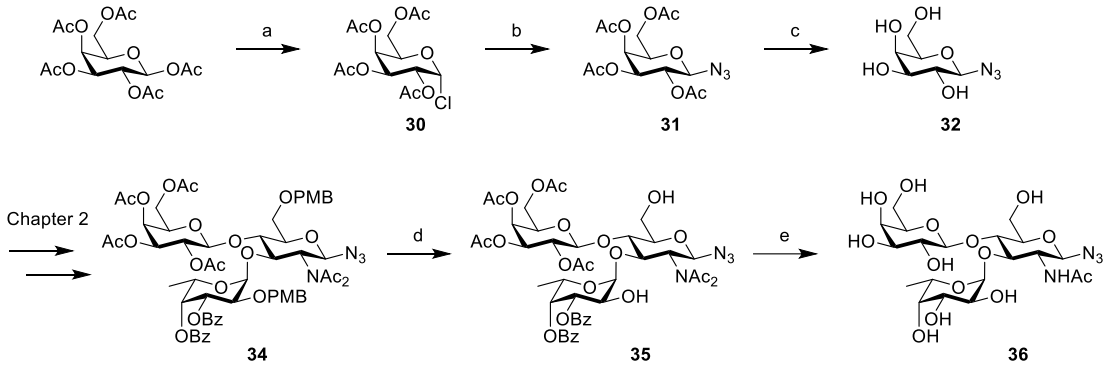

Scheme 8. Synthesis of galactoside **32** and trisaccharide **36**. Reagents and conditions: a) $TiCl_4$, DCM, 40°C, 1h, 93% b) NaN_3, DMF, 50°C, 3h, 82% c) NaOMe, MeOH, 1.5h, 92% d) DDQ, H_2O, DCM, 71% e) NaOMe, MeOH, 24h, quant.

An attempt was then made to couple these glycosides to the pentameric scaffolds. Scaffold **29** was dissolved in DMSO (50 mM), and glycosyl azides were added as 0.2 M stocks (2 eq per alkyne for **32** and 1.2 eq per alkyne for **36**). A copper click mix was prepared (1:3:2 $CuSO_4$/THPTA/sodium ascorbate) and 15 mol% Cu(I) was added to the reaction mixture. The reactions were gently agitated at 40°C for 48h, after which a small sample was taken out for LC-MS analysis, confirming full conversion to the pentaglycosylated products. Size exclusion purification of **37** and **39**, on HW40 resin using an ammonium acetate buffer, was attempted. While the products were obtained in reasonable purity according to LC-MS analysis, removal of remaining salts proved troublesome. Repeated cycles of dissolution in aqueous acetonitrile, followed by lyophilization were carried out, to no avail. An attempt was made to exchange the acetate ions for hydroxy ions using an anion exchange resin, but this resulted into partial degradation of the material. Instead, an alternative synthetic route was employed, where purification after the click reaction was omitted. To this end, 100 nmol of scaffold **29** was again reacted with sugar **32** in the presence of Cu(I) to give **37**. When LC-MS indicated product formation, DiPEA was added, followed by Atto655-NHS, to label the free lysine. Initial attempts to carry out the reaction at room temperature yielded no conversion, so the reaction was heated to 40°C for 16 hours, creating the desired labeled glycoconjugates. These were again isolated using HW40 size exclusion chromatography. This time, an ammonium bicarbonate buffer was used, since this salt is easier removed by lyophilization and the increase pH (compared to ammonium acetate) is of little concern. Using this method, pentavalent glycoconjugate **38** was isolated in 87% yield and the more complex conjugate **40** was isolated in 42%.

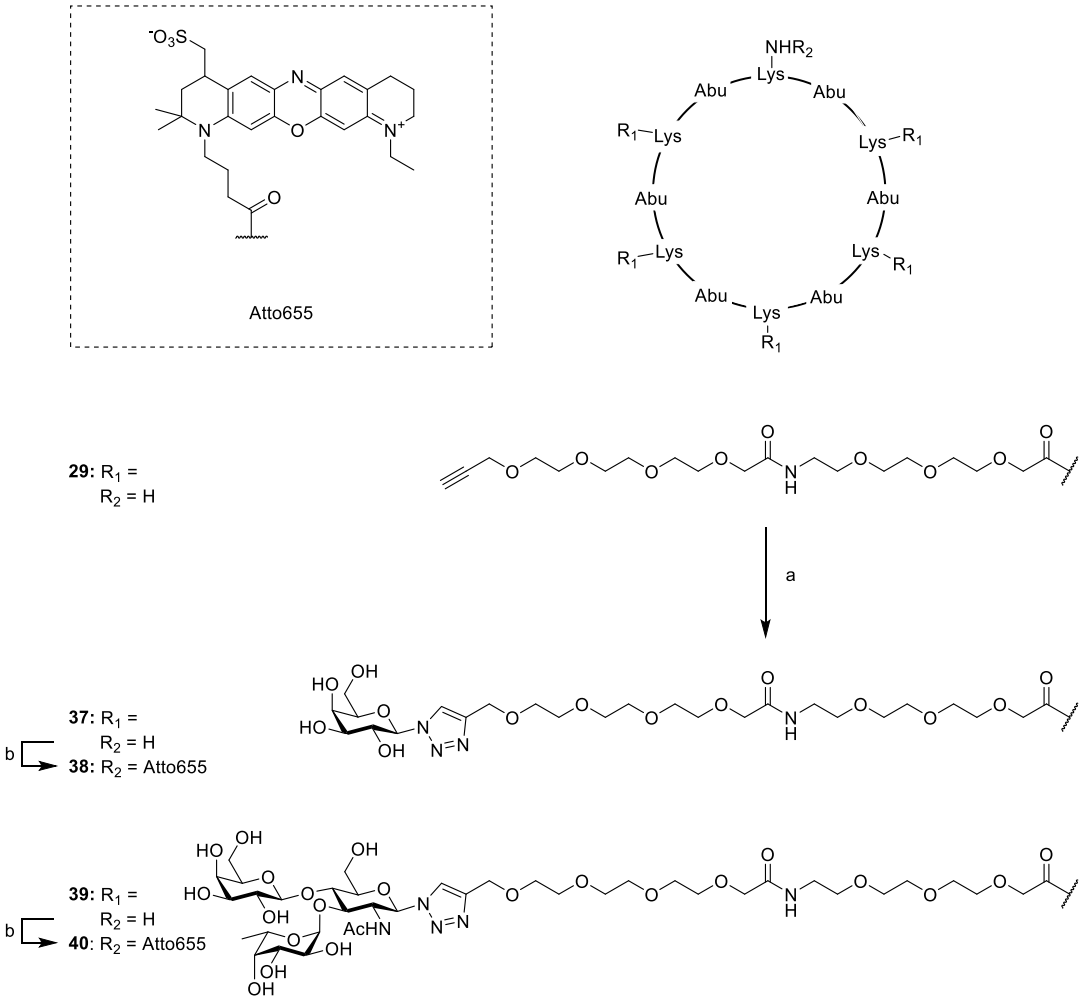

Scheme 9. Synthesis of the final glycoconjugates **38** and **40**. Reagents and conditions: a) **32** or **36**, $CuSO_4$, THPTA, sodium ascorbate, 40°C, 48h b) Atto655-NHS, DiPEA, 40°C, 16h, **38** (87% over 2 steps), **40** (42% over 2 steps).

Conclusion

Since the interactions between carbohydrate binding proteins and their ligands tend to be weak, multivalency is often exploited to increase affinity.[29] As technologies are developed that are able to effectively visualize these kinds of interactions, multivalent scaffolds containing fluorophores for microscopy analysis become more relevant.[30] The combination of the key role the multivalent lectin CTB plays in cholera infection and the unmet medical needs concerning this disease makes CTB an interesting target for further development of multivalent carbohydrate probes. While many different multivalent CTB binding scaffolds have been developed over the years as inhibitors for the cholera toxin itself, modifying one of these to allow for introduction of a fluorescent detector group is non-trivial. Cyclic peptide-based inhibitors seemed like a logical target, as robustness and flexibility of modern solid support peptide synthesis helps the rapid production of these target molecules.

However, the synthesis and late stage functionalization of cyclic peptides is still not without its challenges. As seen in this chapter, cyclization reactions can give unexpected side products, like the aforementioned cyclic dimer. Here, it seems that ring size is still a concern, even while

working under the pseudo-dilution conditions of on-resin cyclization. Fortunately, decreasing the length of the linear peptide, and therefore the circumference of the cyclic molecule, enabled smooth cyclization. Based on previous literature the change from a 6 carbon spacer to a 4 carbon spacer is unlikely to negatively impact the multivalent binding of the molecule to CTB.[17]

Another point of attention is protecting group orthogonality, which in many cases is not fully explored. In this case, conditions where the trityl-based protective groups on the lysine sidechains could be fully removed without touching the resin linker had to be discovered. Here, the extremely acid-sensitive monomethoxytrityl group afforded the desired selectivity and deprotection efficiency. This allowed for the direct incorporation of the polyethylene glycol-based linkers using standard SPPS chemistry, avoiding handling the polyamine intermediate or performing complicated in-solution chemistry after resin liberation. Instead, the completed scaffold molecule was purified by RP-HPLC and derivatized using CuAAC chemistry, following by amine labeling with a commercially available fluorophore NHS ester. This way, cumbersome HPLC purification was avoided for the precious final compound, which could instead be purified over size exclusion chromatography.

In conclusion, this chapter describes the synthesis of a fluorescently labeled pentavalent ligand for CTB bearing either five galactose or five Lewis^X ligands. In the future, this ligand will be applied for the visualization of cholera toxin in cholera infected zebrafish. Furthermore, variants of this scaffold presenting different numbers of specific carbohydrates will be evaluated as ligands for different lectins, for instance DC-SIGN[31] or the mannose-6-phophate[32] receptor.

Experimental

General methods for synthesis and characterization of compounds

Solvents were purchased from Honeywell, VWR or Alfa Aesar. Anhydrous solvents were prepared by drying over 4Å molecular sieves. Reagents purchased from chemical suppliers were used without further purification, unless stated otherwise. All reactions were performed under nitrogen atmosphere and/or under exclusion of H_2O, unless stated otherwise. Reactions were followed by thin layer chromatography which was performed using TLC silica gel 60 F254 on aluminium sheets, supplied by Merck. Compounds were visualized using UV absorption (254 nm) and/or a spray reagent, either permanganate (5 g/L $KMnO_4$, 25 g/L K_2CO_3) or sulfuric acid (10% v/v in EtOH). ^1H and ^{13}C NMR spectra were recorded using a Brüker AV400 (400 /101 MHz) and COSY and HSQC 2D experiments were used to assign peaks. Recorded data was interpreted and analyzed using MestReNova 12 software. Chemical shifts are reported in ppm (δ) in reference to an internal standard (TMS) or the residual solvent peak. High resolution mass spectra were recorded by direct injection (2 µL of a 2 µM solution in H_2O/MeCN 1:1 and 0.1% formic acid) on a mass spectrometer (Thermo Fisher Exactive HF Orbitrap) equipped with an electrospray ion source in positive mode. The high resolution mass spectrometer was calibrated prior to measurements with a calibration mixture (Thermo Finnigan). IR spectra were recorded using a Shimadzu IRSpirit fourier transform infrared spectrometer.

SPPS methods

Loading of Tentalgel NPC resin

Protected dipeptide **2** or **22** (500 µmol) were weighed out into a 50 mL round bottom flask. DCM (2 mL) and TFA (2 mL) were added and the resulting suspension was stirred for 15 minutes, during which the solid fully dissolved. Next, the volatiles were removed *in vacuo* and residual TFA was removed by toluene co-evaporation (3x2 mL). The residue was taken up in 1 M DiPEA in anhydrous DCM (2 mL) and Tentagel S NPC (400 mg, 0.26 mmol/g loading) was added. Another 3 mL of anhydrous DCM were added and the resulting suspension was stirred under an N_2 atmosphere overnight. The next day, the suspension was transferred to a fritted syringe and washed extensively with DCM (3x10 mL) and DMF (3x10 mL).

Manuel synthesis of linear peptides

For the synthesis of linear precursor of the cyclic peptides, manual SPPS protocols were employed on a 100 µmol scale. Liberation of the Fmoc protecting group was accomplished using 20% (v/v) piperidine in DMF (2x 10 mL, 3+7 min), followed by extensive washing with DMF (5x10 mL). The sequence was extended alternatively with either a spacer amino acid (Fmoc-Ahx-OH or Fmoc-Abu-OH) or Fmoc-Lys(Mmt)-OH. For the spacer amino acids, 4 eq to resin loading were used, together with 4 eq HCTU (as 0.4 M solution in DMF) and 8 eq DiPEA and the coupling reaction was carried out for 45 minutes. Fmoc-Lys(Mmt)-OH was coupled using 2 eq of amino acid to resin loading, together with 2 eq HCTU (as a 0.2 M in DMF solution) together with 4 eq of DiPEA, and the reaction was run for 1.5 h. After each coupling, the resin was washed thoroughly with DMF (4x10 mL) before the next round of Fmoc deprotection was started. After synthesis of the full-length linear peptide, the quality of the immobilized peptide was checked by treating a small (~1mg) portion of resin using 200 µL 95% TFA cocktail (95:2.5:2.5 TFA/TIS/H_2O) for 1 hour. After this time the TFA was drained into ~800 µL of ice

cold Et_2O and the formed precipitate was collected by centrifugation. The supernatant was discarded and the pellet redissolved in 200 µL 1:1:1 H_2O/ACN/tBuOH and subjected to LC-MS analysis.

General method for on resin cyclization

This general protocol was used on a scale of 50 µmol of resin bound linear peptide. The C-terminal allyl ester protecting group was removed using $Pd(PPh_3)_4$ and $PhSiH_3$ as scavenger. The resin was first extensively washed with DCM (5x 10 mL). DCM was degassed by bubbling N_2 through ~10mL of DCM for ~1.5 minutes. $Pd(PPh_3)_4$ (11.6 mg, 10 µmol) was weighed in an Eppendorf reaction vessel and dissolved in 1 mL of degassed DCM. $PhSiH_3$ (61 µL, 500 µmol) was added and the resulting solution was added to the drained resin. The resin was then reacted at room temperature under light agitation for 15 minutes. The solution was drained from the resin and the resin was washed once with DCM (5 mL). This procedure was repeated 3 more times to fully liberate the C-terminus of the peptide. Following allyl ester cleavage, the resin was thoroughly washed with DCM (5x 5 mL). Before continuing, the complete removal of the allyl ester was confirmed by the cleavage of a small portion of resin (1 mg) in 95% TFA cocktail followed by LC-MS analysis. The resin was then washed with DMF (3x 5 mL), followed by Fmoc cleavage by 2% DBU (v/v) in DMF (3x5 mL, 5 min each) and extensive DMF washes (3x 5 mL). The resin was then washed 2 times with anhydrous DMF (2x 5 mL) and transferred to a flask, were it was suspended in 20 mL of anhydrous DMF and placed under an N_2 atmosphere. PyAOP (250 µmol, 52 mg, 5 eq) and DiPEA (500 µmol, 35 µL, 10 eq) were added, and the suspension was stirred overnight. The next day, the resin was transferred back to the fritted syringe, drained and washed extensively with DMF (3x5 mL) and DCM (3x5 mL). The drained resin was stored at -20°C.

General method for cyclization analysis

A small portion of resin bearing immobilized cyclic peptide (~1 mg) was treated with 500 µL of a mixture of 1:2:7 AcOH/TFE/DCM for 1 hour followed by extensive washing with DCM (3x2 mL). The deprotected immobilized peptide was then treated with a solution of benzoic anhydride (50 mg) and DiPEA (25 µL) in DCM (450 mL) for 15 minutes. After extensive washing (5x2 mL DCM) 200 µL of a 95% TFA cocktail was added and the resulting suspension was stirred by light agitation for 1 h. The TFA was drained into 800 µL of icecold Et_2O and the formed suspension was collected by centrifugation. The supernatant was discarded and the pellet dissolved in DMSO (200µL) and subjected to LC-MS analysis.

Modification of cyclic peptides with TEG linkers

This general protocol was used on a scale of 50 µmol of resin bound cyclic peptide. The resin was suspended in DCM for 20 minutes to swell the resin before synthesis In order to remove the Mmt protection groups, the resin was suspended in 2 mL of 1:2:7 AcOH/TFE/DCM for 1 hour. This was followed by extensive washing with DCM (3x5 mL) and DMF (3x 5 mL). The resin was then treated with a 10% (v/v) solution of Et_3N in DMF (2x 5 mL, 15 min each) followed by though washing with DMF (5x 5 mL). To a solution of TEG linker **15** (500µmol, 10 eq) in DMF (0.5 M) was added PyAOP (260 mg, 500 µmol, 10 eq) and DiPEA (174 µL, 1 mmol, 20 eq) and the solution was allowed to preactivate for 5 minutes before being added to the drained resin. The suspension was reacted at room temperature under gentle agitation overnight, and the resin was drained and extensively washed with DMF (4x 5 mL). The Fmoc groups were removed as stated before (20% piperidine (v/v) in DMF, 2x 5 mL, 3+7 min) followed by extensive washing with DMF (5x 5 mL). Propargylated TEG **11** (123 mg, 500µmol, 10 eq) and PyAOP (260 mg, 500 µmol, 10 eq) were dissolved in DMF (1 mL) and DiPEA (174 µL, 1 mmol, 20

eq) was added. The suspension was reacted at room temperature under gentle agitation overnight, and the resin was drained and extensively washed with DMF (3x 5 mL) and DCM (3x 5 mL). The resin was then treated with 2 mL of a 95% TFA cocktail (95:2.5:2.5 TFA:TIS:H_2O) for one hour. The TFA solution was filtered through the syringe frit into ice cold Et_2O (10 mL) and the resulting precipitate was collected by centrifugation. The crude scaffold was then subjected to RP-HPLC to obtain the pure compound.

Solution phase synthesis

6-Aminohexanoic acid allyl ester hydrochloride (1)

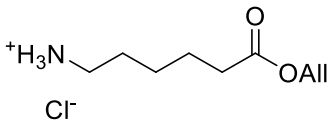

To an icebath cooled flask containing allyl alcohol (10 mL) thionyl chloride (3 mL, 40 mmol, 10 eq) was added dropwise. 6-aminohexanoic acid (524 mg, 4 mmol) was carefully added to the mixture and the reaction was allowed to warm up to room temperature overnight. The volatiles were removed *in vacuo* and the remaining solid was washed with Et_2O to obtain allyl ester **1** in 94% yield (775 mg, 3.74 mmol). This compound was used in the next step without further purification. **^{1}H NMR** (400 MHz, DMSO) δ 8.06 (s, 3H), 5.91 (ddt, J = 17.2, 10.7, 5.5 Hz, 1H), 5.28 (dq, J = 17.2, 1.6 Hz, 1H), 5.20 (dq, J = 10.5, 1.4 Hz, 1H), 4.53 (dt, J = 5.4, 1.4 Hz, 2H), 2.72 (t, J = 7.5 Hz, 2H), 2.33 (t, J = 7.4 Hz, 2H), 1.60 – 1.48 (m, 4H), 1.36 – 1.25 (m, 2H) **^{13}C NMR** (101 MHz, DMSO) δ 172.5, 132.8, 117.8, 64.3, 38.5, 33.2, 26.6, 25.3, 23.9

Fmoc-Lys(Boc)-Ahx-OAll (2)

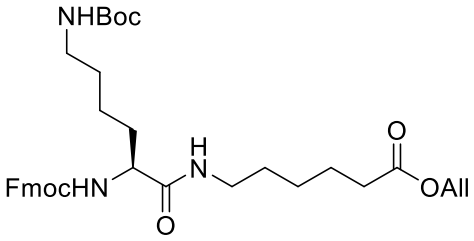

Fmoc-Lys(Boc)-OH (281 mg, 0.6 mmol, 1.2 eq) was dissolved in dry DMF (2 mL) and HCTU (248 mg, 0.6 mmol, 1.2 eq) and DiPEA (260 µL, 1.5 mmol, 3 eq) were added. The mixture was stirred for 5 minutes before hydrochloride salt **1** (103 mg, 0.5 mmol) was added. The reaction was stirred for 2 hours, diluted with EtOAc (50 mL) and washed successively with 1 M $HCl_{(aq)}$, saturated aqueous $NaHCO_3$ and brine. The organic layer was dried over $MgSO_4$, filtered and concentrated. Silica gel column chromatography (1/1 EtOAc/pentane) yielded dipeptide **2** in 92% yield (287 mg, 0.46 mmol) **^{1}H NMR** (400 MHz, $CDCl_3$) δ 7.73 (d, J = 7.5 Hz, 2H, Fmoc-Ar), 7.55 (d, J = 7.1 Hz, 2H, Fmoc-Ar), 7.36 (t, J = 7.2 Hz, 2H, Fmoc-Ar), 7.30 – 7.23 (m, 2H, Fmoc-Ar), 6.71 (s, 1H, NH), 6.01 – 5.79 (m, 2H, NH, -C<u>H</u>=CH_2), 5.28 (d, J = 17.2 Hz, 1H, -CH=C<u>H</u>H), 5.21 (d, J = 10.4 Hz, 1H, -CH=CH<u>H</u>), 4.86 (s, 1H, NH), 4.54 (d, J = 5.6 Hz, 2H, Allyl-CH_2), 4.41 – 4.24 (m, 2H, Fmoc-CH_2), 4.24 – 4.12 (m, 2H, α-Lys), 3.31 – 2.95 (m, 4H, ε-Ahx, ε-Lys), 2.27 (t, J = 7.4 Hz, 2H, α-Ahx), 1.91 – 1.16 (m, 21H, β-Lys, β-Ahx, γ-Lys, γ-Ahx, δ-Lys, δ-Ahx, tBu). **^{13}C NMR** (101 MHz, $CDCl_3$) δ 173.2 (C=O), 171.8 (C=O), 156.4 (C=O), 156.2 (C=O), 143.7 (Fmoc-C_q), 141.2 (Fmoc-C_q), 132.2 (-<u>C</u>H=CH_2), 127.7 (Fmoc-Ar), 127.0 (Fmoc-Ar), 125.0 (Fmoc-Ar), 119.9 (Fmoc-Ar), 118.2 (-CH=<u>C</u>H_2), 79.0 (tBu-C_q), 67.0 (Fmoc-CH_2), 65.0 (Allyl-CH_2), 54.8 (α-Lys), 47.0 (Fmoc-CH), 40.0, 39.2 (ε-Lys, ε-Ahx), 33.9 (α-Ahx), 32.3 (β-Lys), 29.6, 29.0, 28.4 (tBu-CH_3), 26.2, 24.3, 22.5 (β-Lys, β-Ahx, γ-Lys, γ-Ahx, δ-Lys, δ-Ahx). **HRMS** (ESI) m/z $[M + H]^+$ calcd for $C_{35}H_{47}N_3O_7H$ 622.3487 found 622.3487

4-(*tert*-Butoxycarbonylamino)butyric acid allyl ester (21)

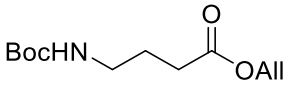

4-(*tert*-Butoxycarbonylamino)butyric acid (1.22g, 6.0 mmol) was dissolved in DCM and the solution was cooled in an ice bath. Allyl alcohol (2 mL, 30

mmol, 5 eq), EDC·HCl (1.38 g, 7.2 mmol, 1.2 eq), DiPEA (5.2 mL, 30 mmol, 5 eq) and DMAP (67 mg, 0.6 mmol, 0.1 eq) were added successively. The reaction was allowed to warm to room temperature overnight after which TLC analysis (40% EtOAc/pentane + 0.1% AcOH) indicated starting material consumption. The reaction mixture was diluted with DCM and washed with 1 M $HCl_{(aq)}$ and sat. aq. $NaHCO_3$, dried over $MgSO_4$ and filtered. The dried organics were concentrated to give allyl ester **21** in 75% yield (1.09 g, 4.5 mmol). This compound was used without further purification. **^{1}H NMR** (300 MHz, $CDCl_3$) δ 5.91 (ddt, *J* = 17.1, 10.4, 5.7 Hz, 1H, -C<u>H</u>=CH_2), 5.31 (dq, J = 17.2, 1.6 Hz, 1H, -CH=C<u>H</u>H), 5.26 – 5.15 (m, 2H, -CH=CH<u>H</u>, NH), 4.58 (dt, J = 5.7, 1.3 Hz, 2H, Allyl-CH_2), 3.16 (q, J = 6.5 Hz, 2H, α-Abu), 2.39 (t, J = 7.4 Hz, 2H, γ-Abu), 1.83 (p, J = 7.1 Hz, 2H, β-Abu), 1.43 (s, 9H, tBu) **^{13}C NMR** (75 MHz, $CDCl_3$) δ 172.6 (C(O)OAll), 155.8 (C(O)OtBu), 131.9 (-<u>C</u>H=CH_2), 117.9 (-CH=<u>C</u>H_2), 78.6, (tBu-C_q), 64.8 (Allyl-CH_2), 39.6 (γ-Abu), 31.2 (α-Abu), 28.1 (tBu-CH_3), 25.0 (β-Abu)

Fmoc-Lys(Boc)-Abu-OAll (22)

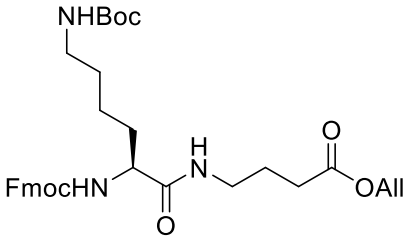

Protected amino acid **21** (1.09 g, 4.5 mmol) was dissolved in DCM (5 mL) and TFA (5 mL) was added. The resulting mixture was stirred for 15 minutes before the volatiles were removed *in vacuo*. The crude amine was co-evaporated thrice with toluene (3 x 5 mL) to remove traces of TFA and kept under N_2. In a separate flask, Fmoc-Lys(Boc)-OH (2.53 g, 5.4 mmol, 1.2) and HCTU (2.24 g, 5.4 mmol, 1.2 eq) were dissolved in DMF (18 mL), followed by the addition of DiPEA (3.9 mL, 22.5 mmol, 5 eq). The resulting solution was stirred for 5 minutes before being added to the flask containing the crude amine. The reaction was stirred overnight at room temperature and TLC analysis (1/1 EtOAc/pentane) indicated the formation of a product. The reaction mixture was diluted with EtOAc and washed successively with 1 M $HCl_{(aq)}$, saturated aqueous $NaHCO_3$ and brine. The organic layer was dried over $MgSO_4$, filtered and concentrated. Silica gel column chromatography (1/1 EtOAc/pentane) produced dipeptide **22** in 90% yield (2.56 g, 4.3 mmol). **^{1}H NMR** (400 MHz, DMSO) δ 7.96 – 7.88 (m, 3H, Abu-N$^{\gamma}$H, Fmoc-Ar), 7.74 (dd, J = 7.4, 3.6 Hz, 2H, Fmoc-Ar), 7.49 – 7.39 (m, 3H, Lys-N$^{\alpha}$H), 7.34 (t, J = 7.4 Hz, 2H, Fmoc-Ar), 6.79 (t, J = 5.6 Hz, 1H, Lys-N$^{\varepsilon}$H), 5.90 (ddt, J = 17.2, 10.7, 5.4 Hz, 1H, -C<u>H</u>=CH_2), 5.28 (dq, J = 17.2, 1.6 Hz, 1H, -CH=C<u>H</u>H), 5.19 (dq, J = 10.5, 1.4 Hz, 1H, CH=CH<u>H</u>), 4.53 (dt, J = 5.4, 1.4 Hz, 2H, Allyl-CH_2), 4.30 – 4.18 (m, 3H, Fmoc-CH_2, Fmoc-CH), 3.90 (td, *J* = 8.5, 5.4 Hz, 1H, α-Lys), 3.15 – 3.02 (m, 2H, γ-Abu), 2.97 – 2.83 (m, 2H, ε-Lys), 2.35 (t, J = 7.5 Hz, 2H, α-Abu), 1.66 (p, J = 7.1 Hz, 2H, β-Abu), 1.61 – 1.46 (m, 2H, β-Lys), 1.43 – 1.18 (m, 13H, tBu, γ-Lys, δ-Lys) **^{13}C NMR** (101 MHz, DMSO) δ 172.8 (C=O), 172.4 (C=O), 156.4 (C=O), 156.0 (C=O), 144.4 (Fmoc-C_q), 144.3 (Fmoc-C_q), 141.2 (Fmoc-C_q), 133.2 (-<u>C</u>H=CH_2), 128.1 (Fmoc-Ar), 127.5 (Fmoc-Ar), 125.8 (Fmoc-Ar), 120.6 (Fmoc-Ar), 118.1 (-CH=<u>C</u>H_2), 77.8 (tBu-C_q), 66.0 (Fmoc-CH_2), 64.8 (Allyl-CH_2), 55.2 (α-Lys), 47.1 (Fmoc-CH), 38.2 (γ-Abu), 32.1 (β-Lys), 31.2 (α-Abu), 29.7 (δ-Lys), 28.7 (tBu-CH_3), 24.9 (β-Abu), 23.4 (γ-Lys) **HRMS** (ESI) m/z [M + H]$^+$ calcd for $C_{33}H_{43}N_3O_7H$ 594.3174 found 594.3174

2-(2-(2-(prop-2-yn-1-yloxy)ethoxy)ethoxy)ethan-1-ol (9)

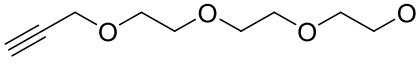

Triethylene glycol (3.0 g, 20 mmol, 2 eq) was dissolved in anhydrous THF (50 mL) and cooled to 0°C in and ice bath. A dispersion of NaH (60% w/w) in mineral oil (0.52 g, 13 mmol, 1.3 eq) was added and the reaction was stirred at 0°C for 30 minutes, followed by the addition of propargyl bromide (1.1 mL, 10 mmol). The reaction was stirred for another 2 hours at 0°C followed by 15 hours at room temperature, at which

point TLC analysis (1/4 acetone/DCM) indicated complete consumption of starting material. The reaction was quenched by the addition of H_2O (2 mL), dried over $MgSO_4$, filtered and concentrated *in vacuo*. Silica gel column chromatography (5% → 20% acetone/DCM) yielded the desired alcohol **9** as a yellow oil in 89% yield (1.66 g, 8.9 mmol). **^{1}H NMR** (400 MHz, $CDCl_3$) δ 4.20 (d, J = 2.4 Hz, 2H, CH2 propargyl), 3.76 – 3.64 (m, 10H), 3.62 – 3.57 (m, 2H), 3.25 (s, 1H, OH), 2.51 (t, J = 2.4 Hz, 1H, CH propargyl) **^{13}C NMR** (101 MHz, $CDCl_3$) δ 79.4 (C propargyl), 74.7 (CH propargyl), 72.4, 70.4, 70.1, 70.1, 68.8, 61.34 58.2 (CH2 propargyl)

tert-butyl 3,6,9,12-tetraoxapentadec-14-ynoate (10)

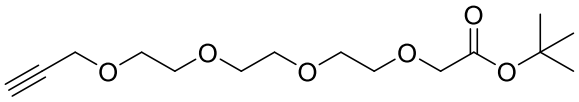

Alcohol **9** (5.37 g, 28.5 mmol) was dissolved in anhydrous THF (140 mL) and cooled to 0°C. A dispersion of NaH (60% w/w) in mineral oil (1.6 g, 40 mmol, 1.4 eq) was added and the suspension was stirred for 30 minutes at 0°C. *tert*-butylbromoacetate (6.4 mL, 43 mmol 1.5 eq) was added to the reaction mixture and the reaction was stirred for an additional 90 minutes at 0°C, followed by the removal of the icebath. The reaction was stirred at room temperature for 20 hours, after which TLC analysis (10% acetone/DCM) indicated consumption of starting material. The reaction mixture was poured in water (700 mL) and the aqueous layer extracted with DCM. The organic layer was dried over $MgSO_4$, filtered and concentrated. Silica gel column chromatography (1% → 10% acetone/DCM) yielded the desired ester **10** as a yellow oil in 64% yield (5.48g, 18.1 mmol). **^{1}H NMR** (400 MHz, $CDCl_3$) δ 4.21 (d, J = 2.4 Hz, 2H, CH2 propargyl), 4.03 (s, 2H, $OCH_2C(O)O$), 3.75 – 3.64 (m, 12H), 2.45 (t, J = 2.4 Hz, 1H, CH propargyl), 1.48 (s, 9H, $C(CH_3)_3$) **^{13}C NMR** (101 MHz, $CDCl_3$) δ 169.6 (C=O), 81.5 ($\underline{C}(CH_3)_3$), 79.6 (C propargyl), 74.6 (CH propargyl), 70.9, 70.7, 70.6, 70.4, 69.1, 69.0 ($O\underline{C}H_2C(O)O$), 58.4 (CH_2 propargyl), 28.1 ($C(\underline{C}H_3)_3$)

3,6,9,12-tetraoxapentadec-14-ynoic acid (11)

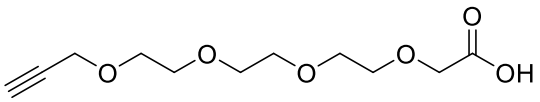

tert-butyl ester **10** (1.16g, 3.8 mmol) was dissolved in DCM (7.6 mL) and TFA (2.9 mL, 38 mmol, 10 eq) was added. The reaction mixture was stirred at room temperature for 1 hour, after which TLC analysis (10% acetone/DCM) indicated full consumption of the starting material. The volatiles were removed *in vacuo* and the resulting residue was dissolved in ddH_2O and lyophilized to obtain **11** as a yellow oil in quantitative yield (918 mg, 3.72 mmol). **^{1}H NMR** (400 MHz, $CDCl_3$) δ 9.31 (s, 1H, COOH), 4.21 (d, J = 2.4 Hz, 2H, CH_2 propargyl), 4.19 (s, 2H, $OCH_2C(O)O$), 3.79 – 3.74 (m, J = 5.8, 2.7 Hz, 2H), 3.74 – 3.66 (m, 10H), 2.47 (t, J = 2.3 Hz, 1H, CH propargyl). **^{13}C NMR** (101 MHz, $CDCl_3$) δ 173.4 (C=O), 79.5 (C propargyl), 74.8 (CH propargyl), 71.2, 70.9, 70.6, 70.4, 70.3, 70.3, 69.1, 68.6 ($O\underline{C}H_2C(O)O$), 58.4 (CH_2 propargyl) **ν_{max}/cm^{-1}** 3255 (Alkyne), 1742 (C=O) **HRMS** (ESI) m/z: $[M + Na]^+$ calcd for $C_{11}H_{18}O_6Na$ 269.0996, found 269.0993

2-(2-(2-hydroxyethoxy)ethoxy)ethyl 4-methylbenzenesulfonate (12)

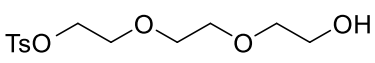

Triethylene glycol (14 mL, 100 mmol, 10 eq) and Et_3N (2.1 mL, 15 mmol, 1.5 eq) were dissolved together in anhydrous DCM (14 mL). The mixture was cooled to 0°C in an icebath and tosyl chloride (1.9 g, 10 mmol) was added portionwise. The reaction was stirred for 72 hours and TLC analysis (10% acetone/DCM) indicated full consumption of tosyl chloride. The reaction mixture was then diluted with DCM (100 mL), washed with water (2x 50

mL) and the combined aqueous layers were back-extracted with DCM (50 mL). The combined organic layers were then washed with 1 M $HCl_{(aq)}$, dried over $MgSO_4$, filtered and concentrated under reduced pressure, giving the desired monosubstituted ethylene glycol **12** in 86% yield (2.60 g, 8.55 mmol). **^{1}H NMR** (400 MHz, $CDCl_3$) δ 7.79 (d, J = 8.2 Hz, 2H, Ts-Ar), 7.35 (d, J = 8.2 Hz, 2H, Ts-Ar), 4.20 – 4.14 (m, 2H, CH_2OTs), 3.75 – 3.67 (m, 4H, PEG-CH_2), 3.60 (s, 4H, PEG-CH_2), 3.58 – 3.54 (m, 2H, PEG-CH_2), 2.77 (s, 1H, OH), 2.44 (s, 3H, Ts-CH_3). **^{13}C NMR** (101 MHz, $CDCl_3$) δ 144.9, 132.7, 129.8, 127.9 (Ts-Ar), 72.4, 70.6, 70.5, 70.2, 69.2, 68.5, 61.5 (PEG-CH_2), 21.6 (Ts-CH_3)

tert-butyl 2-(2-(2-(2-azidoethoxy)ethoxy)ethoxy)acetate (13)

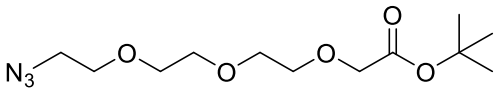

Tosylate **12** (2.60 g, 8.5 mmol) was dissolved in anhydrous DMF (8.5 mL) and NaN_3 (1.1 g, 17 mmol, 2 eq) was added. The reaction was heated to 70°C and stirred at this temperature for 36 hours, after which TLC analysis indicated full consumption of starting material. The reaction was allowed to cool to room temperature, diluted with H_2O (100 mL) and extracted four times with DCM (4x 50 mL). The combined organic layers were dried over $MgSO_4$, filtered and concentrated *in vacuo*. The crude azide was then dissolved in anhydrous THF (8 mL), together with tert-butyl bromoacetate (3.2 mL, 21 mmol, 2.5 eq). The reaction mixture was then cooled to 0°C in an icebath and a 60% (w/w) dispersion of NaH in mineral oil was added (840 mg, 21 mmol, 2.5 eq) portionwise. After addition was complete, the reaction was allowed to warm to room temperature over night and was quenched by the addition of saturated aqueous $NaHCO_3$ (50 mL). The aqueous layer was extracted twice with DCM (2x 50 mL) and the combined aqueous layers were dried over $MgSO_4$, filtered and concentrated under reduced pressure. Silica gel column chromatography (20% → 40% EtOAc/pentane) gave the desired ethylene glycol derivative **13** in 50% yield (1.23 g, 4.27 mmol). **^{1}H NMR** (400 MHz, $CDCl_3$) δ 4.03 (s, 2H, $OCH_2C(O)O$), 3.76 – 3.65 (m, 10H), 3.39 (t, J = 5.0 Hz, 2H, CH_2N_3), 1.48 (s, 9H, $C(CH_3)_3$). **^{13}C NMR** (101 MHz, $CDCl_3$) δ 169.6 (C=O), 81.5 ($\underline{C}(CH_3)_3$), 70.7, 70.7, 70.6, 70.6, 70.0, 69.0 (PEG-CH_2), 50.7 (CH_2N_3), 28.1 ($C(\underline{C}H_3)_3$). **ν_{max}/cm^{-1}** 2111 (N_3), 1747 (C=O)

tert-butyl 1-(9H-fluoren-9-yl)-3-oxo-2,7,10,13-tetraoxa-4-azapentadecan-15-oate (14)

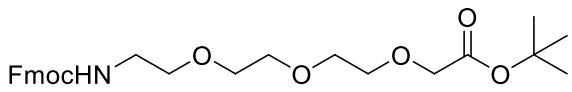

Azide **13** (3.76 g, 13 mmol) was dissolved in anhydrous THF (85 mL) and cooled to 0°C in an ice bath. PPh_3 (4.46 g, 17 mmol, 1.3 eq) was added and the reaction was stirred at room temperature for 24 h. When TLC analysis (10% acetone/DCM) indicated full consumption of starting material, H_2O (610 µL 34 mmol, 2.6 eq) was added and the reaction was stirred for an additional 24 h. When TLC analysis (10% MeOH/DCM + 0.1% Et_3N) indicated full consumption of the iminophosphorane intermediate, the reaction mixture was diluted with H_2O (150 mL). The aqueous layer was washed three times with toluene each toluene layers was separately extracted with water. The combined aqueous layers were concentrated to give the crude amine as a yellow oil. This oil was dissolved in DCM (100 mL) and Fmoc-OSu (5.26 g, 15.6 mmol, 1.2 eq) and N-methylmorpholine (1.4 mL, 13 mmol, 1 eq) were added. The reaction mixture was stirred at room temperature for 1 h, when TLC analysis (10% MeOH/DCM indicate full consumption of the amine. The reaction mixture was then washed once with H_2O and twice with 1 M $HCl_{(aq)}$. Each aqueous layer was back-extracted with DCM and the combined organic layers were dried over $MgSO_4$, filtered and concentrated under reduced pressure. Silica gel column chromatography (40% → 80% EtOAc/pentane) gave the desired protected ethylene glycol **14** in 90% yield (5.7 g, 11.7 mmol). **^{1}H NMR** (400 MHz,

$CDCl_3$) δ 7.75 (d, J = 7.5 Hz, 2H, Fmoc-Ar), 7.60 (d, J = 7.4 Hz, 2H, Fmoc-Ar), 7.38 (t, J = 7.4 Hz, 2H, Fmoc-Ar), 7.30 (td, J = 7.4, 1.0 Hz, 2H, Fmoc-Ar), 5.52 (s, 1H, NH), 4.39 (d, J = 7.0 Hz, 2H, Fmoc-CH_2), 4.21 (t, J = 6.9 Hz, 1H, Fmoc-CH), 3.99 (s, 2H, $OCH_2C(O)O$), 3.73 – 3.59 (m, 8H, PEG-CH_2), 3.56 (t, J = 4.9 Hz, 2H), 3.39 (dd, J = 10.4, 5.2 Hz, 2H, CH_2NH), 1.45 (s, 9H, $C(CH_3)_3$) **^{13}C NMR** (101 MHz, CDCl3) δ 169.6 (C=O), 156.5 (C=O), 144.00, 141.27, 127.63, 127.03, 125.10, 119.93 (Fmoc-Ar), 81.6 ($\underline{C}(CH_3)_3$), 77.5, 70.7, 70.5, 70.3, 70.0 (PEG-CH_2), 68.9 ($O\underline{C}H_2C(O)O$), 66.5 (Fmoc-CH_2), 47.2 (Fmoc-CH), 40.9 (CH_2NH), 28.1 ($C(\underline{C}H_3)_3$)

1-(9H-fluoren-9-yl)-3-oxo-2,7,10,13-tetraoxa-4-azapentadecan-15-oic acid (15)

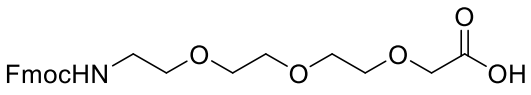

tert-butyl ester **14** (1.46 g, 3 mmol) was dissolved in TFA (15 mL) and the reaction was stirred at room temperature for 2 h, after which TLC analysis (60% EtOAc/pentane) indicated full consumption of starting material. The volatiles were removed *in vacuo* to give building block **15** in quantitative yield (1.47g, 3 mmol). **^{1}H NMR** (400 MHz, $CDCl_3$) δ 9.05 (s, 1H, C(O)OH), 7.76 (d, J = 7.5 Hz, 2H, Fmoc-Ar), 7.60 (d, J = 7.4 Hz, 2H, Fmoc-Ar), 7.39 (t, J = 7.4 Hz, 2H, Fmoc-Ar), 7.31 (t, J = 7.4 Hz, 2H, Fmoc-Ar), 5.57 (s, 1H, NH), 4.53 – 4.34 (m, J = 21.1, 10.1 Hz, 2H, Fmoc-CH_2), 4.22 (t, J = 7.0 Hz, 1H, Fmoc-CH), 4.18 – 4.10 (m, 2H, $OC\underline{H}_2C(O)OH$), 3.78 – 3.51 (m, 10H), 3.40 (s, 2H, $C\underline{H}_2NH$). **^{13}C NMR** (101 MHz, CDCl3) δ 173.1 (C=O), 156.9 (C=O), 144.0, 141.3, 127.7, 127.1, 125.2, 120.0 (Fmoc-Ar), 71.1, 70.5, 70.2, 70.1, 70.0 (PEG-CH_2), 68.5 ($O\underline{C}H_2C(O)OH$), 66.8 (Fmoc-CH_2), 47.2 (Fmoc-CH), 40.9 (CH_2NH). **HRMS** (ESI) m/z $[M + Na]^+$ calcd for $C_{23}H_{27}NO_7Na$ 452.1680 found 452.1678

2,3,4,6-tetra-O-acetyl-α-D-galactopyranosyl chloride (30)

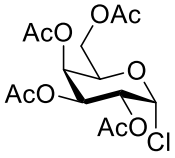

1,2,3,4,6-penta-O-acetyl-β-D-galactopyranoside (3.9 g, 10 mmol) was dissolved in anhydrous DCM (38 mL) and a 1M $TiCl_4$ solution in DCM (12 mL, 12 mmol, 1.2 eq) was added. The reaction was heated to reflux for 1 hour, after which TLC analysis (1/1 EtOAc/pentane) indicated full conversion of the starting material to a higher running spot. The reaction was allowed to cool to room temperature, diluted with DCM and washed with saturated aqueous $NaHCO_3$ and brine. The organic layer was dried over $MgSO_4$, filtered and concentrated. The crude was loaded onto a silica in DCM and eluted in 1/1 EtOAc/pentane to remove residual titanium salts. After removal of the solvent galatosyl chloride **30** was obtained in 93% yield (3.29g, 9.25 mmol, 93%) and used in the next step without further purification. **^{1}H NMR** (400 MHz, $CDCl_3$) δ 6.40 (d, J = 3.8 Hz, 1H, H1), 5.52 (d, J = 2.0 Hz, 1H, H4), 5.40 (dd, J = 10.7, 3.1 Hz, 1H, H3), 5.25 (dd, J = 10.7, 3.9 Hz, 1H, H2), 4.55 (t, J = 6.4 Hz, 1H, H5), 4.19 (dd, J = 11.4, 6.1 Hz, 1H, H6a), 4.11 (dd, J = 11.4, 6.9 Hz, 1H, H6b), 2.16 (s, 3H, Ac), 2.11 (s, 3H, Ac), 2.06 (s, 3H, Ac), 2.01 (s, 3H, Ac) **^{13}C NMR** (101 MHz, $CDCl_3$) δ 169.9 (C=O), 169.7 (C=O), 169.6 (C=O), 169.3 (C=O), 91.1 (C1), 69.2 (C5), 67.5 (C2), 66.9 (C4), 66.7 (C3), 60.8 (C6), 20.3 (Ac), 20.2 (Ac), 20.2 (Ac)

2,3,4,6-tetra-O-acetyl-β-D-galactopyranosyl azide (31)

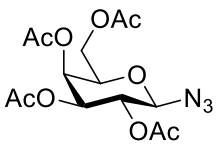

Glycosyl chloride **30** (3.29 g, 9.3 mmol) was dissolved in anhydrous DMF (19 mL) and NaN_3 (1.21 g, 18.6 mmol, 2 eq) was added. The reaction mixture was heated to 50°C for three hours, after which TLC analysis (1/9 EtOAc/DCM) indicated full consumption of starting material. The reaction was allowed to cool to room temperature. The reaction mixture was then diluted with saturated aqueous $NaHCO_3$ (200 mL) and extracted with Et_2O (200 mL). The organic layer was washed with brine (200 mL), dried over $MgSO_4$ and concentrated. Silica gel column chromatography (40% → 50% Et_2O/pentane) yielded azido sugar

31 in 82% yield (2.82 g, 7.58 mmol). **^{1}H NMR** (400 MHz, $CDCl_3$) δ 5.43 (d, J = 3.2 Hz, 1H, H4), 5.20 – 5.03 (m, 2H, H2, H3), 4.68 (d, J = 8.5 Hz, 1H, H1), 4.18 (d, J = 6.7 Hz, 2H, H6), 4.14 – 4.07 (m, 1H, H5), 2.18 (s, 3H, Ac), 2.10 (s, 3H, Ac), 2.06 (s, 3H, Ac), 1.99 (s, 3H, Ac) **^{13}C NMR** (101 MHz, $CDCl_3$) δ 170.0 (C=O), 169.9 (C=O), 169.6 (C=O), 169.1 (C=O), 87.9 (C1), 72.5 (C5), 70.4 (C3), 67.8 (C2), 66.7 (C4), 61.1 (C6), 20.3 (Ac), 20.3 (Ac), 20.2 (Ac)

β-D-galactopyranosyl azide (32)

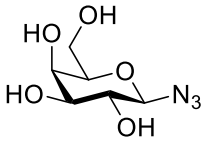

A fresh solution of sodium methoxide was prepared by dissolving a small chuck of sodium metal in methanol (10 mL). The pH of the solution was checked to be 11 and protected glycoside **31** was added. The reaction was stirred at room temperature for 1.5 hours, after which TLC analysis (4/1 EtOAc/pentane) indicated full consumption of starting material. The reaction mixture was neutralized with Amberlite H^+ resin, filtered and concentrated. The obtained material was lyophilized to obtain monosaccharide **32** in 92% yield (189 mg, 0.92 mmol). **^{1}H NMR** (400 MHz, D_2O) δ 4.63 (d, J = 8.7 Hz, 1H, H1), 3.92 (d, J = 3.4 Hz, 1H, H4), 3.80 – 3.67 (m, 3H, H6, H5), 3.64 (dd, J = 9.9, 3.4 Hz, 1H, H3), 3.47 (dd, J = 9.8, 8.8 Hz, 1H, H2) **^{13}C NMR** (101 MHz, D_2O) δ 90.5 (C1), 77.2 (C5), 72.6 (C3), 70.3 (C2), 68.5 (C4), 60.9 (C6)

Azido 2,3,4,6-tetra-O-acetyl-β-D-galactopyranoside(1→4)-[3,4-di-O-benzoyl-α-L-fucopyranoside-(1→3)]-2-deoxy-2-(N-acetylacetamido)-β-D-glucopyranoside (35)

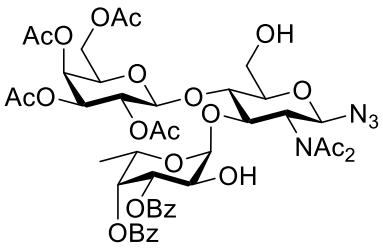

Protected trisaccharide **34** (243 mg, 0.2 mmol, see Chapter 2 for the preparation of this molecule) was dissolved in DCM (1.9 mL) and H_2O (0.1 mL). 2,3-Dichloro-5,6-dicyano-1,4-benzoquinone (182 mg, 0.8 mmol, 4 eq) was added and the resulting suspension was stirred overnight. The next day, TLC analysis (1/1 EtOAc/pentane) indicated full consumption of starting material. The reaction mixture was diluted with DCM and quenched by the addition of saturated aqueous $NaHCO_3$. The layers were separated and the aqueous layer was re-extracted with DCM. The combined organic layers were dried over $MgSO_4$, filtered and concentrated. Silicagel column chromatography (1/1 EtOAc/pentane) yielded partially deprotected trisaccharide **35** in 71% yield (138 mg, 142 µmol). **^{1}H NMR** (400 MHz, $CDCl_3$) δ 8.04 (dd, J = 8.4, 1.3 Hz, 2H, Bz), 7.82 (dd, J = 8.3, 1.2 Hz, 2H, Bz), 7.60 (tt, J = 7.0, 1.3 Hz, 1H, Bz), 7.51 – 7.42 (m, 3H, Bz), 7.32 – 7.24 (m, 2H, Bz), 5.69 (d, J = 2.7 Hz, 1H, H4''), 5.64 (d, J = 8.8 Hz, 1H, H1), 5.57 (dd, J = 10.5, 3.4 Hz, 1H, H3''), 5.48 (dd, J = 3.3, 0.7 Hz, 1H, H4'), 5.20 – 5.07 (m, 3H, H2', H5'', H3'), 4.91 – 4.83 (m, 3H, H1'', H1', H6'a), 4.79 (t, J = 9.5 Hz, 1H, H3), 4.24 (dd, J = 10.5, 4.0 Hz, 1H, H2''), 4.17 (dd, J = 11.7, 6.1 Hz, 1H, H6'b), 4.03 (d, J = 11.3 Hz, 1H, H6a), 4.00 – 3.91 (m, 2H, H5', H4), 3.87 (d, J = 9.9 Hz, 1H, H6b), 3.68 (t, J = 9.3 Hz, 1H, H2), 3.56 (d, J = 9.9 Hz, 1H, H5), 2.51 (s, 3H, Ac), 2.45 (s, 3H, Ac), 2.28 (s, 3H, Ac), 2.08 (s, 3H, Ac), 2.06 (s, 3H, Ac), 2.00 (s, 3H, Ac), 1.31 (d, J = 6.6 Hz, 3H, H6'') **^{13}C NMR** (101 MHz, $CDCl_3$) δ 175.4 (C=O), 174.5 (C=O), 170.9 (C=O), 170.6 (C=O), 170.2 (C=O), 169.0 (C=O), 166.3 (C=O), 166.2 (C=O), 133.4 (Bz-CH), 133.1 (Bz-CH), 129.9 (Bz-CH), 129.7 (Bz-CH), 129.7 (Bz-C_q), 129.6 (Bz-C_q), 128.6 (Bz-CH), 128.3 (Bz-CH), 100.1 (C1'), 98.3 (C1''), 86.8 (C1), 77.1 (C5), 74.1 (C4), 72.3 (C4''), 72.0 (C5'), 71.8 (C3''), 71.6 (C3), 71.0 (C3'), 69.1 (C2'), 67.5 (C2''), 67.3 (C4'), 65.2 (C5''), 64.1 (C2), 61.7 (C6'), 59.9 (C6), 28.4 (Ac), 25.8 (Ac), 21.0 (Ac), 20.8 (Ac), 20.7 (Ac), 16.1 (C6'')

β-D-galactopyranoside(1→4)-[α-L-fucopyranoside-(1→3)]-2-deoxy-2-acetamido-β-D-glucopyranosyl azide (36)

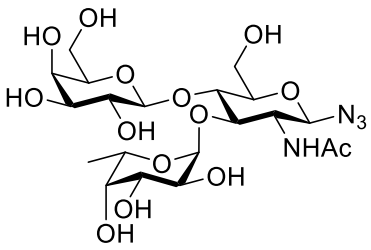

A fresh solution of sodium methoxide was prepared by dissolving a small chuck of sodium metal in methanol (2 mL). The pH of the solution was checked to be 12 before it was added to a separate flask containing partially protected glycoside **35** (155 mg, 160 µmol). After 24 hours, LC-MS analysis indicated full conversion to the desired product. The reaction mixture was neutralized by addition of amberlite H^+ ion exchange resin and the solution was carefully transferred into a centrifuge tube containing ice-cold Et_2O (20 mL). The resin was washed twice with methanol (2x1 mL) and these washes were also added to the ether. A precipitate was formed that was isolated by centrifugation. The supernatant was discarded and the pellet was washed once with Et_2O (5 mL). The pellet was then transferred to a flask and dried under vacuum, yielding desired oligosaccharide **36** in quantitative (94 mg) yield. **^{1}H NMR** (400 MHz, D_2O) δ 4.99 (d, J = 4.0 Hz, 1H, H1''), 4.76 – 4.73 (m, 1H, H5''), 4.68 (d, J = 8.8 Hz, 1H, H1), 4.34 (d, J = 7.8 Hz, 1H, H1'), 3.93 – 3.51 (m, 13H), 3.48 (dd, J = 7.6, 4.4 Hz, 1H, H5), 3.38 (dd, J = 9.7, 7.9 Hz, 1H, H2), 1.93 (s, 3H, Ac), 1.06 (d, J = 6.6 Hz, 3H, H6'') **^{13}C NMR** (101 MHz, D_2O) δ 174.5 (C=O), 101.8 (C1'), 98.8 (C1''), 88.6 (C1), 77.4, 74.9, 74.9 (C5), 72.9, 72.4, 71.9, 71.0, 69.2, 68.3, 67.7, 66.7 (C5''), 61.5 (C6), 59.6 (C6'), 55.3 (C2), 22.2 (Ac), 15.3 (C6'') **HRMS** (ESI) m/z $[M + Na]^+$ calcd for $C_{20}H_{34}N_4O_{14}Na$ 577.1964 found 577.1966

***Cyclo*(-Lys-Abu-Lys(TEG-TEG-propargyl)-Abu-Lys(TEG-TEG-propargyl)-Abu-Lys(TEG-TEG-propargyl)-Abu-Lys(TEG-TEG-propargyl)-Abu-Lys(TEG-TEG-propargyl)-Abu-) (29)**

Following the general procedures for cyclization and sidechain modification, compound **29** was isolated using RP-HPLC in 4.6% (7.7 mg, 2.3 µmol) yield. **LC-MS** RT = 4.4 min (C18, 10-90% B over 9 minutes) **LRMS** calcd $[M+3H]^{3+}$ = 1122.96, $[M+2H]^{2+}$ = 1683.95; observed M/z = 1123.25, 1684.08 **HRMS** (ESI) m/z $[M + 4H]^{4+}$ calcd for $C_{155}H_{269}N_{23}O_{57}H_4$ 842.2287 found 842.2289

***Cyclo*(-Lys(Atto655)-Abu-Lys(TEG-TEG-triazole-β-Gal)-Abu-Lys(TEG-TEG-triazole-β-Gal)-Abu-Lys(TEG-TEG-triazole-β-Gal)-Abu-Lys(TEG-TEG-triazole-β-Gal)-Abu-Lys(TEG-TEG-triazole-β-Gal)-Abu-) (38)**

To a solution of scaffold **29** (100 nmol, 50 mM in DMSO) was added a solution of glycosyl azide **32** in water (10 eq, 5 µL of 200 mM). A click mix was prepared by mixing 1 µL of 0.1 M $CuSO_4$, 2 µL 0.1 M sodium ascorbate and 3 µL of 0.1 M THPTA, and 1 µL of this mixture was added to the scaffold solution. The solution was gently agitated and heated to 40°C for 48h, after which a 0.5 µL portion was taken out and diluted into 35 µL 1:1:1 H_2O/MeCN/tBuOH and subjected to LC-MS analysis, indicating full conversion to the desired glycoconjugate. The reaction mixture was diluted with 200 µL MilliQ water and lyophilized. The crude glycoconjugate was redissolved in 50 µL DMSO and a solution of DiPEA in DMSO (10 eq, 10 µL of 100 mM) was added, followed by a solution of Atto655-NHS in DMSO (2 eq, 40 µL of 5 mM). The solution was gently agitated and heated to 40°C for 16h, after which a 1 µL portion was taken out and diluted into 39 µL 1:1:1 H_2O/MeCN/tBuOH and subjected to LC-MS analysis, indicating formation of the labeled molecule. The crude was diluted with water and subjected to HW40 size exclusion chromatography in a NH_4OAc buffer containing 10% MeCN. The fractions containing fluorophore labeled product were pooled and lyophilized, producing compound **38** in 87% yield (0.43

mg, 87 nmol) as a blue powder. **LC-MS** RT = 5.7 min (C18, 00-50% B over 9 minutes). **LRMS** calcd $[M+4H]^{4+}$ = 1226.36, $[M+3H]^{3+}$ = 1634.81; observed M/z = 1126.42, 1634.83

Cyclo(-Lys(Atto655)-Abu-Lys(TEG-TEG-triazole-Le^X)-Abu-Lys(TEG-TEG-triazole-Le^X)-Abu-Lys(TEG-TEG-triazole-Le^X)-Abu-Lys(TEG-TEG-triazole-Le^X)-Abu-Lys(TEG-TEG-triazole-Le^X)-Abu-) (40)

To a solution of scaffold **29** (100 nmol, 50 mM in DMSO) was added a solution of glycosyl azide **36** in DMSO (6 eq, 6 µL of 100 mM). A click mix was prepared by mixing 1 µL of 0.1 M $CuSO_4$, 2 µL 0.1 M sodium ascorbate and 3 µL of 0.1 M THPTA, and 1 µL of this mixture was added to the scaffold solution. The solution was gently agitated and heated to 40°C for 48h, after which a 0.5 µL portion was taken out and diluted into 35 µL 1:1:1 H_2O/MeCN/tBuOH and subjected to LC-MS analysis, indicating full conversion to the desired glycoconjugate. Next, a solution of DiPEA in DMSO (10 eq, 10 µL of 100 mM) was added, followed by a solution of Atto655-NHS in DMSO (2 eq, 40 µL of 5 mM). The solution was gently agitated and heated to 40°C for 16h, after which a 1 µL portion was taken out and diluted into 39 µL 1:1:1 H_2O/MeCN/tBuOH and subjected to LC-MS analysis, indicating formation of the labeled molecule. The crude was diluted with water and subjected to HW40 size exclusion chromatography in a NH_4OAc buffer containing 10% MeCN. The fractions containing fluorophore labeled product were pooled and lyophilized, producing compound **40** in 42% yield (0.29 mg, 42 nmol) as a blue powder. **LC-MS** RT = 4.3 min (C18, 10-50% B over 9 minutes). **LRMS** calcd $[M+5H]^{5+}$ = 1330.43, $[M+4H]^{4+}$ = 1662.78; observed M/z = 1330.50, 1662.83

References

(1) CAMERON, D.; JONES, I. G. John Snow, the Broad Street Pump and Modern Epidemiology. *Int. J. Epidemiol.* **1983**, *12* (4), 393–396. https://doi.org/10.1093/IJE/12.4.393.

(2) Clemens, J. D.; Nair, G. B.; Ahmed, T.; Qadri, F.; Holmgren, J. Cholera. *Lancet* **2017**, *390* (10101), 1539–1549. https://doi.org/10.1016/S0140-6736(17)30559-7.

(3) Fan, E.; Merritt, E. A.; Verlinde, C. L. M. J.; Hol, W. G. J. AB5 Toxins: Structures and Inhibitor Design. *Current Opinion in Structural Biology*. Elsevier Current Trends December 1, 2000, pp 680–686. https://doi.org/10.1016/S0959-440X(00)00152-4.

(4) Wernick, N. L. B. B.; Chinnapen, D. J.-F.; Cho, J. A.; Lencer, W. I. Cholera Toxin: An Intracellular Journey into the Cytosol by Way of the Endoplasmic Reticulum. *Toxins (Basel).* **2010**, *2* (3), 310–325. https://doi.org/10.3390/toxins2030310.

(5) Cuatrecasas, P. Interaction of Vibrio Cholerae Enterotoxin with Cell Membranes. *Biochemistry* **1973**, *12* (18), 3547–3558. https://doi.org/10.1021/bi00742a031.

(6) King, C. A.; Heyningen, W. E. V. Deactivation of Cholera Toxin by a Sialidase-Resistant Monosialosylganglioside. *J. Infect. Dis.* **1973**, *127* (6), 639–647. https://doi.org/10.1093/infdis/127.6.639.

(7) Holmgren, J.; Lönnroth, I.; Svennerholm, L. Tissue Receptor for Cholera Exotoxin: Postulated Structure from Studies with GM1 Ganglioside and Related Glycolipids. *Infect. Immun.* **1973**, *8* (2), 208.

(8) Heim, J. B.; Hodnik, V.; Heggelund, J. E.; Anderluh, G.; Krengel, U. Crystal Structures of Cholera Toxin in Complex with Fucosylated Receptors Point to Importance of Secondary Binding Site. *Sci. Rep.* **2019**, *9* (1), 1–14. https://doi.org/10.1038/s41598-019-48579-2.

(9) Heggelund, J. E.; Burschowsky, D.; Bjørnestad, V. A.; Hodnik, V.; Anderluh, G.; Krengel, U. High-Resolution Crystal Structures Elucidate the Molecular Basis of Cholera Blood Group Dependence. *PLoS Pathog.* **2016**, *12* (4), e1005567. https://doi.org/10.1371/journal.ppat.1005567.

(10) Wands, A. M.; Fujita, A.; McCombs, J. E.; Cervin, J.; Dedic, B.; Rodriguez, A. C.; Nischan, N.; Bond, M. R.; Mettlen, M.; Trudgian, D. C.; Lemoff, A.; Quiding-Järbrink, M.; Gustavsson, B.; Steentoft, C.; Clausen, H.; Mirzaei, H.; Teneberg, S.; Yrlid, U.; Kohler, J. J. Fucosylation and Protein Glycosylation Create Functional Receptors for Cholera Toxin. *Elife* **2015**, *4* (OCTOBER2015). https://doi.org/10.7554/eLife.09545.

(11) Lencer, W.; Delp, C.; Neutra, M.; Madara, J. Mechanism of Cholera Toxin Action on a Polarized Human Intestinal Epithelial Cell Line: Role of Vesicular Traffic. *J. Cell Biol.* **1992**, *117* (6), 1197–1209. https://doi.org/10.1083/JCB.117.6.1197.

(12) Lencer, W. I.; Constable, C.; Moe, S.; Rufo, P. A.; Wolf, A.; Jobling, M. G.; Ruston, S. P.; Madara, J. L.; Holmes, R. K.; Hirst, T. R. Proteolytic Activation of Cholera Toxin and Escherichia Coli Labile Toxin by Entry into Host Epithelial Cells: SIGNAL TRANSDUCTION BY A PROTEASE-RESISTANT TOXIN VARIANT *. *J. Biol. Chem.* **1997**, *272* (24), 15562–15568. https://doi.org/10.1074/JBC.272.24.15562.

(13) Cervin, J.; Wands, A. M.; Casselbrant, A.; Wu, H.; Krishnamurthy, S.; Cvjetkovic, A.; Estelius, J.; Dedic, B.; Sethi, A.; Wallom, K.-L. L.; Riise, R.; Bäckström, M.; Wallenius, V.; Platt, F. M.; Lebens, M.; Teneberg, S.; Fändriks, L.; Kohler, J. J.; Yrlid, U. GM1 Ganglioside-Independent Intoxication by Cholera Toxin. *PLoS Pathog.* **2018**, *14* (2), e1006862. https://doi.org/10.1371/journal.ppat.1006862.

(14) Minke, W. E.; Roach, C.; Hol, W. G. J.; Verlinde, C. L. M. J. Structure-Based Exploration of the Ganglioside GM1 Binding Sites of Escherichia Coli Heat-Labile Enterotoxin and Cholera Toxin for the Discovery of Receptor Antagonists. *Biochemistry* **1999**, *38* (18), 5684–5692. https://doi.org/10.1021/bi982649a.

(15) Fan, E.; Zhang, Z.; Minke, W. E.; Hou, Z.; Verlinde, C. L. M. J.; Hol, W. G. J. High-Affinity Pentavalent Ligands of Escherichia Coli Heat-Labile Enterotoxin by Modular Structure-Based Design [10]. *J. Am. Chem. Soc.* **2000**, *122* (11), 2663–2664. https://doi.org/10.1021/ja993388a.

(16) Garcia-Hartjes, J.; Bernardi, S.; Weijers, C. A. G. M.; Wennekes, T.; Gilbert, M.; Sansone, F.; Casnati, A.; Zuilhof, H. Picomolar Inhibition of Cholera Toxin by a Pentavalent Ganglioside GM1os-Calix[5]Arene. *Org. Biomol. Chem.* **2013**, *11* (26), 4340–4349. https://doi.org/10.1039/c3ob40515j.

(17) Zhang, Z.; Liu, J.; Verlinde, C. L. M. J.; Hol, W. G. J.; Fan, E. Large Cyclic Peptides as Cores of Multivalent Ligands: Application to Inhibitors of Receptor Binding by Cholera Toxin. *J. Org. Chem.* **2004**, *69* (22), 7737–7740. https://doi.org/10.1021/jo0489770.

(18) Pickens, J. C.; Mitchell, D. D.; Liu, J.; Tan, X.; Zhang, Z.; Verlinde, C. L. M. J.; Hol, W. G. J.; Fan, E. Nonspanning Bivalent Ligands as Improved Surface Receptor Binding Inhibitors of the Cholera Toxin B Pentamer. *Chem. Biol.* **2004**, *11* (9), 1205–1215. https://doi.org/10.1016/J.CHEMBIOL.2004.06.008.

(19) Achtsnicht, S.; Neuendorf, C.; Faßbender, T.; Nölke, G.; Offenhäusser, A.; Krause, H.-J.; Schröper, F. Sensitive and Rapid Detection of Cholera Toxin Subunit B Using Magnetic Frequency Mixing Detection. *PLoS One* **2019**, *14* (7), e0219356. https://doi.org/10.1371/JOURNAL.PONE.0219356.

(20) Erak, M.; Bellmann-Sickert, K.; Els-Heindl, S.; Beck-Sickinger, A. G. Peptide Chemistry Toolbox – Transforming Natural Peptides into Peptide Therapeutics. *Bioorg. Med. Chem.* **2018**, *26* (10), 2759–2765. https://doi.org/10.1016/J.BMC.2018.01.012.

(21) Alsina, J.; Rabanal, F.; Chiva, C.; Giralt, E.; Albericio, F. Active Carbonate Resins: Application to the Solid-Phase Synthesis of Alcohol, Carbamate and Cyclic Peptides. *Tetrahedron* **1998**, *54* (34), 10125–10152. https://doi.org/10.1016/S0040-4020(98)00606-1.

(22) Reintjens, N. R. M. M.; Tondini, E.; Vis, C.; McGlinn, T.; Meeuwenoord, N. J.; Hogervorst, T. P.; Overkleeft, H. S.; Filippov, D. V.; Marel, G. A. van der; Ossendorp, F.; Codée, J. D. C. C.; van der Marel, G. A.; Ossendorp, F.; Codée, J. D. C. C. Multivalent, Stabilized Mannose-6-Phosphates for the Targeted Delivery of Toll-Like Receptor Ligands and Peptide Antigens. *ChemBioChem* **2021**, *22* (2), 434–440. https://doi.org/10.1002/CBIC.202000538.

(23) Ning, X.; Liu, D.; Liu, S.; Zhang, M.; Shen, H. Modification of Oligopeptides on Aspartic Acid or Lysine Residues by Solid-Phase Synthesis through On-Resin Side-Chain Conjugation. *Synlett* **2018**, *29* (19), 2588–2594. https://doi.org/10.1055/S-0037-1611060.

(24) Aletras, A.; Barlos, K.; Gatos, D.; Koutsogianni, S.; MAMOS, P. Preparation of the Very Acid-sensitive Fmoc-Lys(Mtt)-OH Application in the Synthesis of Side-chain to Side-chain Cyclic Peptides and Oligolysine Cores Suitable for the Solid-phase Assembly of MAPs and TASPs. *Int. J. Pept. Protein Res.* **1995**, *45* (5), 488–496. https://doi.org/10.1111/j.1399-3011.1995.tb01065.x.

(25) Albericio, F.; Cases, M.; Alsina, J.; Triolo, S. A.; Carpino, L. A.; Kates, S. A. On the Use of PyAOP, a Phosphonium Salt Derived from HOAt, in Solid-Phase Peptide Synthesis. *Tetrahedron Lett.* **1997**, *38* (27), 4853–4856. https://doi.org/10.1016/S0040-4039(97)01011-3.

(26) Zhang, H.; Li, X.; Shi, Q.; Li, Y.; Xia, G.; Chen, L.; Yang, Z.; Jiang, Z.-X. Highly Efficient Synthesis of Monodisperse Poly(Ethylene Glycols) and Derivatives through Macrocyclization of Oligo(Ethylene Glycols). *Angew. Chem. Int. Ed.* **2015**, *54* (12), 3763–3767. https://doi.org/10.1002/ANIE.201410309.

(27) Thakkar, A.; Trinh, T. B.; Pei, D. Global Analysis of Peptide Cyclization Efficiency. *ACS Comb. Sci.* **2013**, *15* (2), 120–129. https://doi.org/10.1021/CO300136J.

(28) O'Neal, C. J.; Amaya, E. I.; Jobling, M. G.; Holmes, R. K.; Hol, W. G. J. Crystal Structures of an Intrinsically Active Cholera Toxin Mutant Yield Insight into the Toxin Activation Mechanism. *Biochemistry* **2004**, *43* (13), 3772–3782. https://doi.org/10.1021/bi0360152.

(29) Fehres, C. M.; Kalay, H.; Bruijns, S. C. M.; Musaafir, S. A. M.; Ambrosini, M.; Van Bloois, L.; Van Vliet, S. J.; Storm, G.; Garcia-Vallejo, J. J.; Van Kooyk, Y. Cross-Presentation through Langerin and DC-SIGN Targeting Requires Different Formulations of Glycan-Modified Antigens. *J. Control. Release* **2015**, *203*, 67–76.

(30) Riera, R.; Hogervorst, T. P.; Doelman, W.; Ni, Y.; Pujals, S.; Bolli, E.; Codée, J. D. C.; van Kasteren, S. I.; Albertazzi, L. Single-Molecule Imaging of Glycan–Lectin Interactions on Cells with Glyco-PAINT. *Nat. Chem. Biol.* **2021**, *17* (12), 1281–1288. https://doi.org/10.1038/s41589-021-00896-2.

(31) van Kooyk, Y.; Geijtenbeek, T. B. H. DC-SIGN: Escape Mechanism for Pathogens. *Nat. Rev. Immunol. 2003 39* **2003**, *3* (9), 697–709. https://doi.org/10.1038/nri1182.

(32) Ghosh, P.; Dahms, N. M.; Kornfeld, S. Mannose 6-Phosphate Receptors: New Twists in the Tale. *Nat. Rev. Mol. Cell Biol. 2003 43* **2003**, *4* (3), 202–213. https://doi.org/10.1038/nrm1050.

6

Synthesis of peptides containing a combination of free and 2-*trans*-cyclooctene carbamate protected lysine residues

W. Doelman, N.A.M. Ligthart, M.M.E. Isendoorn, D.V. Filippov, S.I. van Kasteren and M.A.T. van de Plassche contributed to the work presented in this chapter

Introduction

Dissociative bio-orthogonal reactions are a quickly developing field of chemical biology.[1] In these reactions, a protected bioactive molecule – where the protecting group blocks the biological function of the molecule in some manner – are removed using a bio-compatible chemical reaction. This restores the molecule's biological activity, giving chemical control over the activity of a molecule inside a living system. The very first example of such a reaction was

shown in 2006, when Streu and Meggers showed intracellular cleavage of an Alloc protecting group using a ruthenium complex.[2] Since then, a large amount similar, bio-compatible bond cleavage reactions have been developed, both using transition metal catalysis and organic reactions.[3] Using these reactions, spatial and/or temporal control over biological functions, such as receptor-ligand interactions[4] or cytotoxic activity[5,6] has been achieved.

Among the currently known dissociative bio-orthogonal reactions, the "click-to-release"-reaction, first demonstrated by Robillard,[6] has become one of the main reactions of choice. The "click" part of the name is the inverse electron demand Diels-Alder (IEDDA) reaction between a 2-*trans*-cyclooctene (2-TCO) (Figure 1, I) and a 1,2,4,5-tetrazine. In this reaction an unstable dihydropyridazine intermediate (II) is formed, which can adopt a different tautomeric form (III). This tautomer can eliminate the leaving group on the allylic position of the TCO, "releasing" a molecule (IV), and forming a pyridazine (V) as a byproduct. Different functional groups have been successfully uncaged in this manner, among them amines,[6–9] carboxylic acids[10] and alcohols.[11,12]

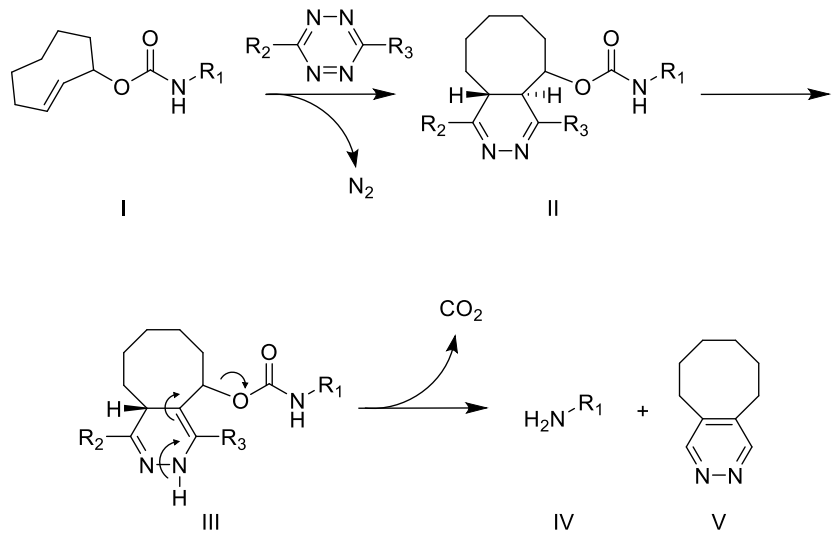

Figure 1. Mechanism of the click-to-release reaction between an amine protected with an allylic TCO-carbamate and a 1,2,4,5-tetrazine. In this reaction, the TCO (I) reacts with a tetrazine to form the click-product (II) with gaseous nitrogen as the byproduct. This intermediate tautomerizes to a different dihydropyridazine (III) which eliminates the allylic carbamate. After CO_2 release, the deprotected amine (IV) is formed, as well as a byproduct (V).

The reaction has properties that make it favorable for use as a biocompatible deprotection reaction. Firstly, the uncaging reaction has fast kinetics.[13] Secondly, the tetrazine reagents have low toxicity and good bioavailability.[5,14] As a result, the system has been successfully used for the *in vivo* deprotection of a kinase enzyme,[14] for the dissociation of antibody-drug conjugates[15], and is even pursued in a Phase I clinical trial for localized drug activation, using a TCO caged form of the anticancer drug doxorubicin.[16]

Allylic trans-cyclooctenes have also been used for the protection of peptides. For example, to shield a T-cell epitope from recognition by its cognate T-cell clone. Addition of tetrazine (*in*

vitro or *in vivo*) allowed for the controlled activation of the T-cell in space and time.[17] Further expansion of this approach to more complicated peptides has been hindered by the extreme acid-lability of the trans-cyclooctene moiety.[18,19] As any concentration of trifluoroacetic acid (TFA; commonly employed as a deprotection reagent in the solid support synthesis of peptides) led to the partial deprotection and/or isomerization to the unreactive *cis*-isomer,[4,19] on-resin modification of lysine residues during Fmoc-SPPS (solid phase peptide synthesis) with TCO was not viable. Therefore, the only known approaches were post-synthetic modification of lysine sidechains with TCO reagents. Using either a compatible protection group to temporarily block the N-terminus, like the Msc-group used by van de Gracht *et al.*[17] (Figure 2A) or a permanent modification of the N-terminus, for instance acetylation,[20] peptides bearing a single lysine function could be modified. However, none of these strategies provided the necessary selectivity to modify peptides containing multiple lysine functions. The lack of a good protecting group strategy has limited the effective use of TCO-modified peptides to those containing only a single lysine residue.

A synthetic approach, whereby (longer) peptides can be synthesized that contain both a 2-TCO-protected lysine, as well as unreacted lysines, is therefore an unmet chemical need. Particularly, as this would allow the extension of the above T-cell activation study, to also study the processing of long peptide antigens by antigen presenting cells, as was previously done using a Staudinger-reduction approach.[21] La-Venia *et al.*[19] (Figure 2B) have developed an approach, where short peptides containing multiple lysines carrying a non-allylic TCO group (4-TCO), were synthesized. This method was based on an acid-mediated global deprotection of the synthesized peptide on resin, followed by introduction of the 4-TCO onto the lysine sidechain and NaOH mediated release of the peptide from resin. Additional lysine residues could be protected using either the Alloc group or as a trifluoroacetate amide, which remain stable during acidic deprotection but could be removed orthogonally to the 4-TCO later using either $Pd(PPh_3)_4$ with morpholine (for Alloc) or NaOH (for the trifluoroacetamide). The palladium treatment would likely result in the removal of an allylic TCO, rendering the approach less promising for use with 2-TCO protecting groups. The use of trifluoroacetamide protection could be a promising approach for the synthesis of 2-TCO protected peptides. Since it is known 2-TCO groups are stable to nucleophilic base,[17] deprotection of amines, as well as cleavage of the resin linker, with NaOH should be possible. However, it is known that nucleophilic base mediated cleavage from SPPS resin is often problematic on longer peptides or peptides containing a sterically hindered C-terminal amino acid.[22,23] This method has not been tested on longer peptides and is incompatible with peptides carrying groups labile to nucleophilic base. Therefore, an alternative strategy that could utilize the regular, highly efficient acidic resin cleavage used in standard Fmoc-SPPS would greatly benefit the development of more complex *trans*-cyclooctene protected peptides.

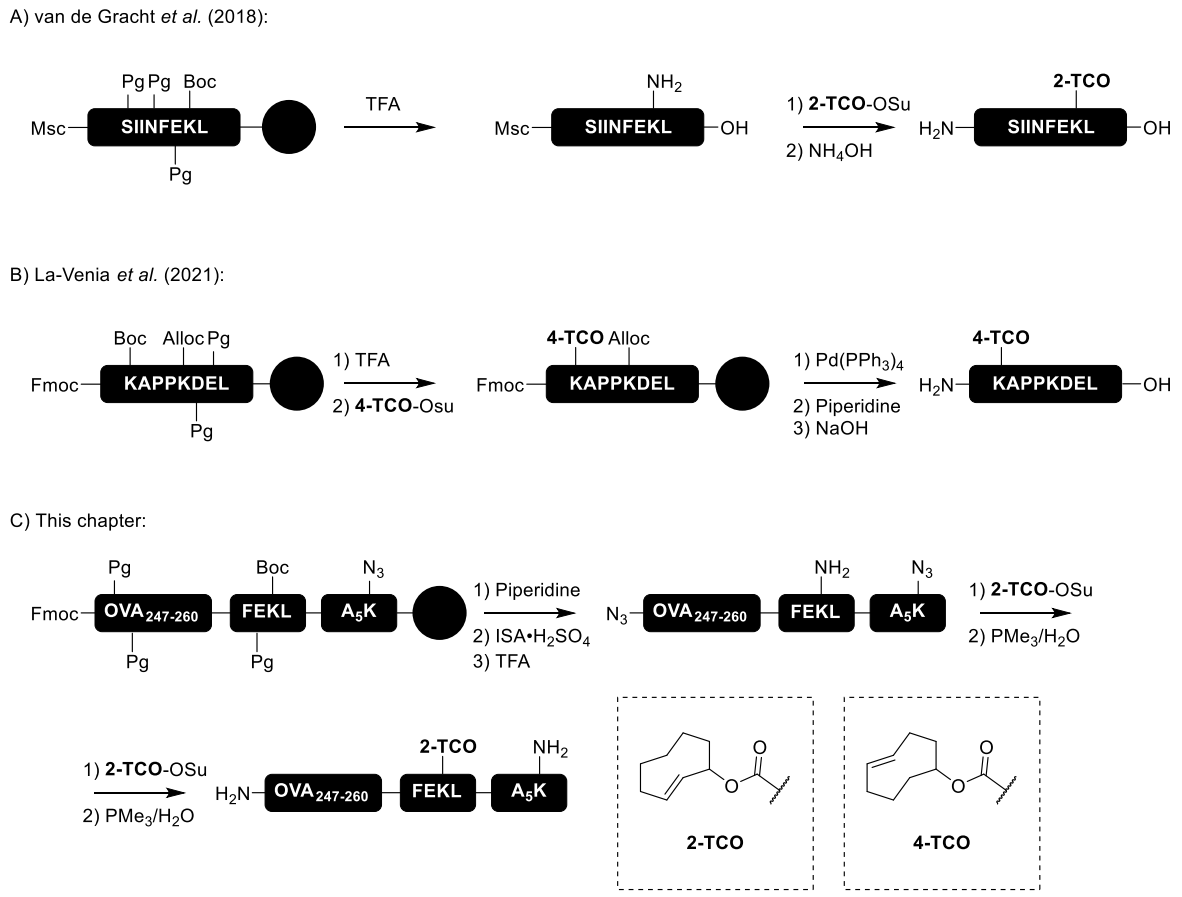

Figure 2. Overview of published methods to synthesize TCO functionalized peptides. A) Hybrid synthesis using the base-labile Msc group as temporary N-terminal protecting group[17] b) Full on-resin method published by Vrabel to introduce 4-TCO groups onto peptides.[19] C) Novel hybrid approach described in this chapter. Here, azide groups are used to temporary mask amine functions.

It was here postulated that an azide protection strategy could be used (Figure 2C). Lysine residues not intended for 2-TCO protection could be introduced as the commercially available azidolysine building block. For the N-terminus, multiple on-resin diazotransfer reactions have been reported, using either triflic azide[24] or the more easily handled imidazole-1-sulfonyl azide (ISA).[25,26] This second reagent was first described by Goddar-Borger and Stick as the HCl salt,[27] however the later reported bisulfate salt[28] is preferred since the hydrochloride salt has been reported to decompose to HN_3 over time. Hansen and co-workers have reported a protocol for on-resin diazotransfer where ISA·H_2SO_4 is used in DMF with DiPEA as base.[25] Alternatively, the α-azido forms of some amino acids are also commercially available. The azide is stable during basic Fmoc-deprotection and acidic resin cleavage,[29] and can be reduced to the corresponding amine using a mild phosphine reduction, often called the Staudinger reduction,[30] a transformation successfully used before on synthetic peptides.[31,32]

In this chapter, a novel approach is described that allows the facile incorporation of a 2-TCO (from this point on simply referred to as TCO) protected lysine in a peptide containing multiple lysine residues. This is achieved by masking all amines as azides during SPPS, except the lysine to which the TCO carbamate is introduced, which is Boc protected as h during normal SPPS

(Figure 2C). Introduction of the TCO happens after full peptide assembly and cleavage from the resin, completely avoiding acid when the TCO group is present, while still utilizing the standard, optimized, Fmoc-SPPS protocols. Here, it is shown that TCO is compatible with this azide reduction, enabling facile synthesis of peptides containing a combination of TCO-protected and free lysine residues.

Results and Discussion

To validate the utility of azide as a protective group of amines in peptides during the synthesis of TCO protected peptides, a model peptide was designed that contained both an azidolysine, free lysine and azido-N-terminus (**3**, Figure 3). The peptide was synthesized using manual SPPS on Tentagel S RAM resin. For the introduction of the precious azidolysine building block on the resin two equivalents (in relation to the manufacturer specified resin loading), instead of the typical five, were utilized. The rest of the peptide was synthesized using standard Fmoc-SPPS conditions. After synthesis of the full resin bound hexapeptide **1**, the N-terminal amine was masked as an azide using the protocol of Hansen *et al.*[25], using ISA·H_2SO_4 in DMF with DiPEA as base. This method was preferred over aqueous diazotransfer reactions,[26,33] since the solubility of fully protected peptides in aqueous mixtures was expected to be poor.

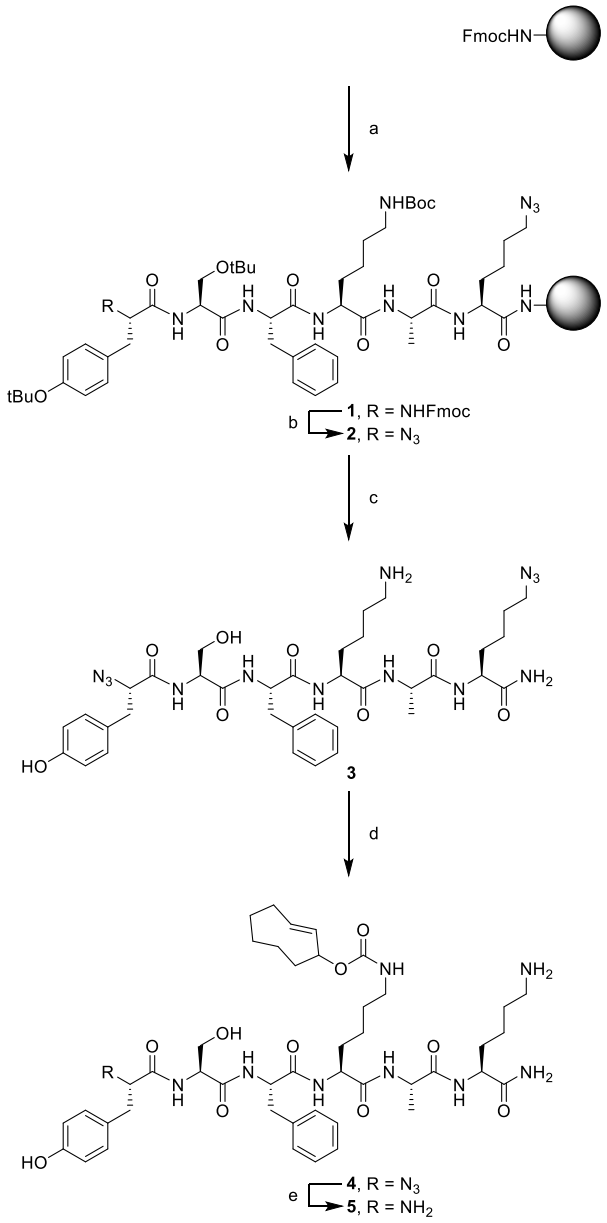

Figure 3. Synthesis of example TCO caged peptide **5**. Reagents and conditions: a) Fmoc-SPPS b) i) 20 % v/v piperidine, DMF ii) ISA·H_2SO_4, DiPEA c) TFA, TIS, H_2O d) TCO-OSu, DiPEA, DMF e) i) PMe_3, H_2O, DMF ii) RP-HPLC, 2.1%

This diazotransfer reaction with 3 equivalents of ISA·H_2SO_4 and 5 equivalents of DiPEA, gave full conversion to resin-bound peptide **2**, as determined by LC-MS analysis of the crude peptide after acidic cleavage of a small amount of resin. After full resin liberation and global deprotection with a standard TFA cocktail (95:2.5:2.5, TFA/TIS/H_2O) the crude peptides **3** was precipitated from cold diethyl ether and residual TFA removed by co-evaporation with toluene. To introduce the 2-TCO carbamate, a small excess of TCO-OSu together with 5 equivalents of DiPEA were dissolved in DMF and added to the crude peptide. After two hours, LC-MS analysis indicated complete conversion to the TCO protected peptide **4**. The final step was the reduction of the azides. For this, a solution of PMe_3 in THF was added, to form the iminophosphorane intermediate, followed by water, to hydrolyze this intermediate to the

corresponding amine. After one hour, full consumption of peptide **4** was confirmed by LC-MS and the crude peptide was precipitated. RP-HPLC was carried out, using acetic acid instead of TFA as the pH modulator in the aqueous buffer, and peptide **5** was obtained in 2.1% yield.

The integrity of the TCO cage was validated by deprotection of a small aliquot of the purified peptide with 3,6-dimethyl-1,2,4,5-tetrazine followed by LC-MS analysis, which confirmed complete removal of the TCO-group, indicating that none had isomerized to the non-reactive *cis*-cyclooctene by-product.

With the successful application of both the diazotransfer reaction and Staudinger reduction established, the method was next used to synthesize an immuno-relevant peptide. The model antigen $OVA_{247\text{-}264}A_5K$, a peptide derived from chicken ovalbumin, C-terminally extended with the amino acid sequence AAAAAK, is used to study the antigen processing and presentation of MHC class I restricted antigens.[34,35] This peptide contains the MHC class I restricted epitope $OVA_{257\text{-}264}$ (SIINFEKL),[36] an often used model antigen to study T-cell activation with murine immune cells. Previously, antigen processing studies have been carried out by masking the lysine in this epitope with TCO. The second lysine on the C-terminus of the $OVA_{247\text{-}264}A_5K$ peptide precluded a similar approach to study processing of the extended peptide. Using the azide based protecting group strategy enables the synthesis of this complex, TCO protected peptide.

The synthesis was again initiated with the coupling of Fmoc-Lys(N_3)-OH onto Tentagel S RAM resin using two equivalents of amino acid and HCTU as the coupling agent. The rest of the peptide was assembled using an automated peptide synthesizer to yield resin bound peptide **6** (Figure 4). After Fmoc removal, the resin was treated again with ISA·H_2SO_4 and DiPEA in DMF. After a TFA mediated test cleavage, the main peak in the chromatogram could be assigned to peptide **8**, confirming that formation of the N-terminal azide had proceeded to near completion. Since some peptide with an unreacted N-terminal amine was still present, the resin-bound peptide was treated with a solution of Ac_2O and DiPEA in DMF to acetylate any remaining free amines.

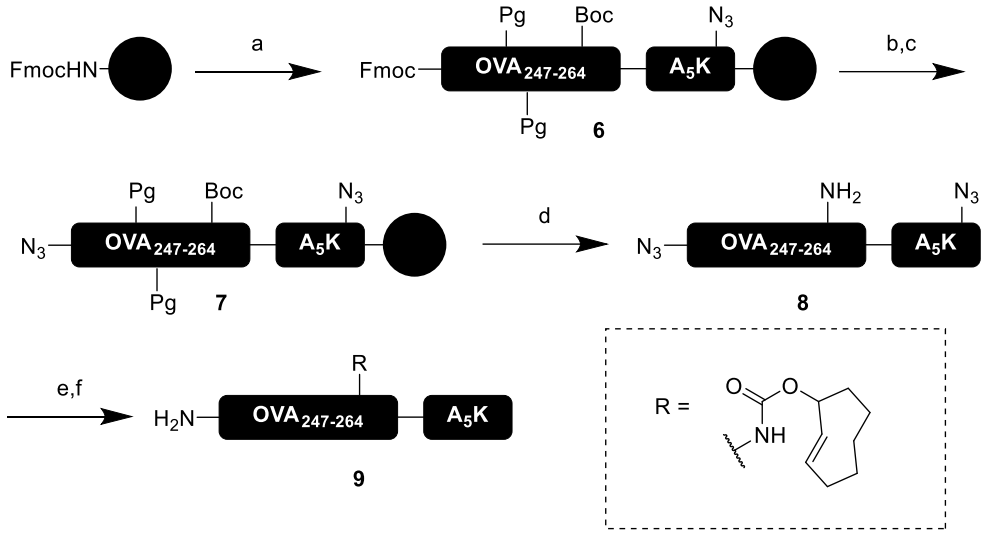

Figure 4. Synthesis $OVA_{247-264}A_5K$, bearing an allylic TCO on Lys_{263} (**11**). Reagents and conditions: a) Fmoc-SPPS b) 20% piperidine (v/v), DMF c) $ISA{\cdot}H_2SO_4$, DiPEA, DMF d) TFA, TIS, H_2O e) TCO-OSu, DiPEA, DMF f) i) PMe_3, H_2O, DMF ii) RP-HPLC, 5.4%

The protected peptide **7** was then cleaved from resin and deprotected (with the exception of the azides) and precipitated from cold diethyl ether, producing crude **8**. Residual TFA was removed by toluene co-evaporation. Then, a mixture of TCO-OSu and 20 equivalents of DiPEA in DMF were added to the peptide, in order to introduce the TCO onto the free lysine residue. After 2 hours, LC-MS analysis indicated the formation of the TCO conjugated intermediate. Finally, the azides were reduced using PMe_3 and water. After one hour, LC-MS analysis indicated complete reduction of both azides. Crude peptide **9** was recovered from solution by ether precipitation and the desired TCO protected peptide was isolated using RP-HPLC in 5.4% yield.

In a similar manner, a TCO protected peptide was also made from the C-terminally non-extended peptide $OVA_{247-264}$ (Figure 5). The critical lysine within the $OVA_{257-264}$ peptide, Lys_{263}, was again caged with an allylic TCO carbamate. This peptide was synthesized on Tentagel S Ac resin, to produce the C-terminal carboxylic acid needed for epitope binding to the MHC complex.[37] Standard Fmoc-SPPS produced resin-bound peptide **10**. Initial attempts to introduce the N-terminal azide via the described diazotransfer reaction with $ISA{\cdot}H_2SO_4$ in DMF yielded poor conversion. An alternative approach was taken, where a solution of $ISA{\cdot}H_2SO_4$ in water, using Na_2CO_3 as base, was used. This resulted in complete conversion of the N-terminal amine into an azide. TCO conjugation and Staudinger reduction were carried out as before, resulting in the isolation of peptide **12** in a rather poor 1.4% yield.

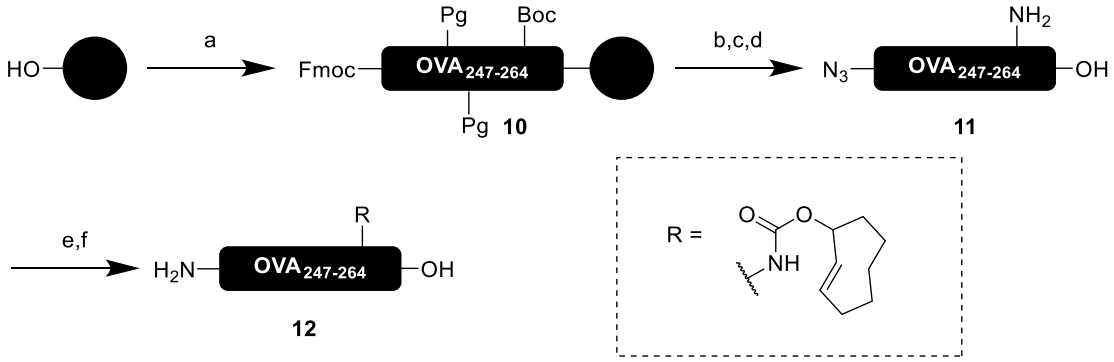

Figure 5. Synthesis of TCO protected $OVA_{247-264}$, peptide **14**. Reagents and conditions: a) Fmoc-SPPS b) 20% (v/v) piperidine, DMF c) ISA·H_2SO_4, DiPEA, DMF d) TFA, TIS, H_2O e) TCO-OSu, DiPEA, DMF f) i) PMe_3, H_2O, DMF ii) RP-HPLC, 1.4%.

The TCO-caged $OVA_{247-264}A_5K$ peptide **9** was tested in a T-cell activation assay. In this assay, the dendritic cell-line D1 is preincubated with varying concentration of either peptide **9** or the non-protected control. After two hours, the caged peptides were uncaged by the addition of 10 µM tetrazine **13**[38] (Figure 6A) for one hour. Then, the D1 cells were co-cultured with B3Z T-cell hybridoma cells.[39] In these cells, the expression of the enzyme LacZ is under the control of the nuclear factor of activated T cells (NF-AT) promotor, meaning LacZ production is induced when the cells become activated by T-cell receptor (TCR) stimulation. LacZ mediated hydrolysis of the chromogenic substrate chlorophenol red-β-D-galactopyranoside (CPRG) was then used as a reporter of T-cell activation, by measuring absorption at 570 nm.[40] The response to 100 nM $OVA_{247-264}$ was used as a positive control (Figure 6B).

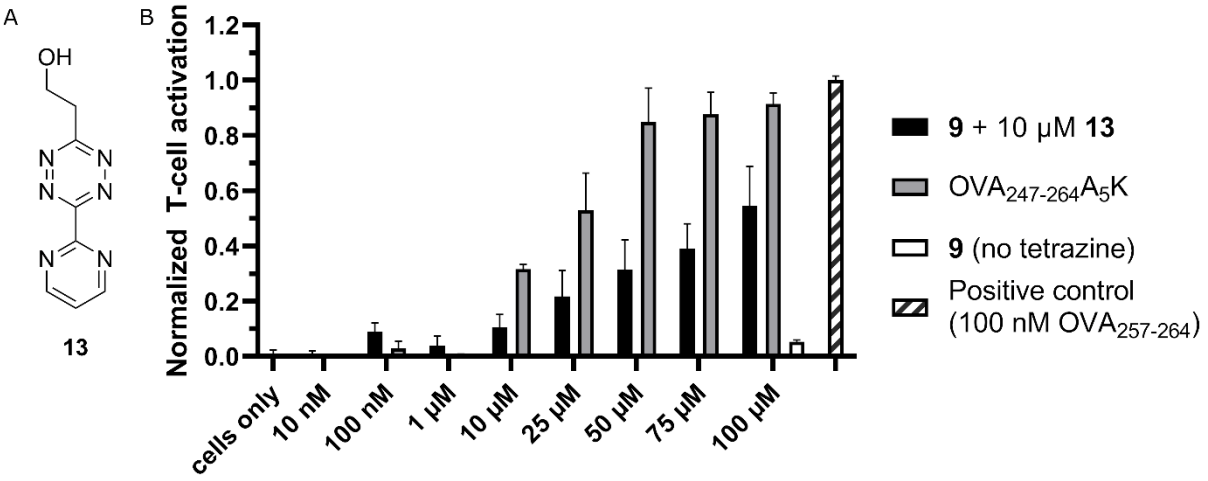

Figure 6. A) Structure of tetrazine **13**, used in the on-cell uncaging experiment. B) Graph of the normalized T-cell response measured for either peptide **9** (with or without uncaging with tetrazine **13**) or the non-caged control $OVA_{247-264}A_5K$. T-cell assays were carried out by N.A.M. Ligthart (Leiden University).

In the absence of tetrazine, very low levels of T-cell activation were observed when cells were treated with 100 µM of peptide **9**. When tetrazine **13** was added, T-cell activation following a clear dose-response relation was found, with the highest concentration of 100 µM showing nearly 60% of the level of T-cell activation of non-caged $OVA_{247-264}A_5K$.

Over the last two decades, it has become apparent that the direct conjugation of an innate immune activating molecule to a peptide vaccine can greatly enhance its immunogenicity.[41] To this end, Toll-like receptor (TLR) ligands are often conjugated to synthetic peptides.[42,43] This results in activation and maturation of dendritic cells and improved cross-presentation of the T-cell epitope.[34]

Studying the processing and presentation of these peptide conjugate vaccines is crucial to their further development. The development of model constructs that give chemical control over the antigen presentation kinetics would be very useful. Here, as a proof of concept, such a peptide was synthesized, based on the $OVA_{247\text{-}264}A_5K$ model antigen. This antigenic peptide can be conjugated to the hTLR2 ligand mini-uPam to enhance its immunogenicity. This ligand is a derivative of the TLR2 ligand Pam_3SK_4, a small lipopeptide, optimized for lower lipophilicity.[44] Since this mini-uPam moiety contains multiple ester functionalities, the synthetic strategies previously reported based on NaOH labile protecting groups, were not feasible for the synthesis of such a conjugate. The Staudinger-reduction based approach shown here, however, has no such limitations, enabling the synthesis of **18**.

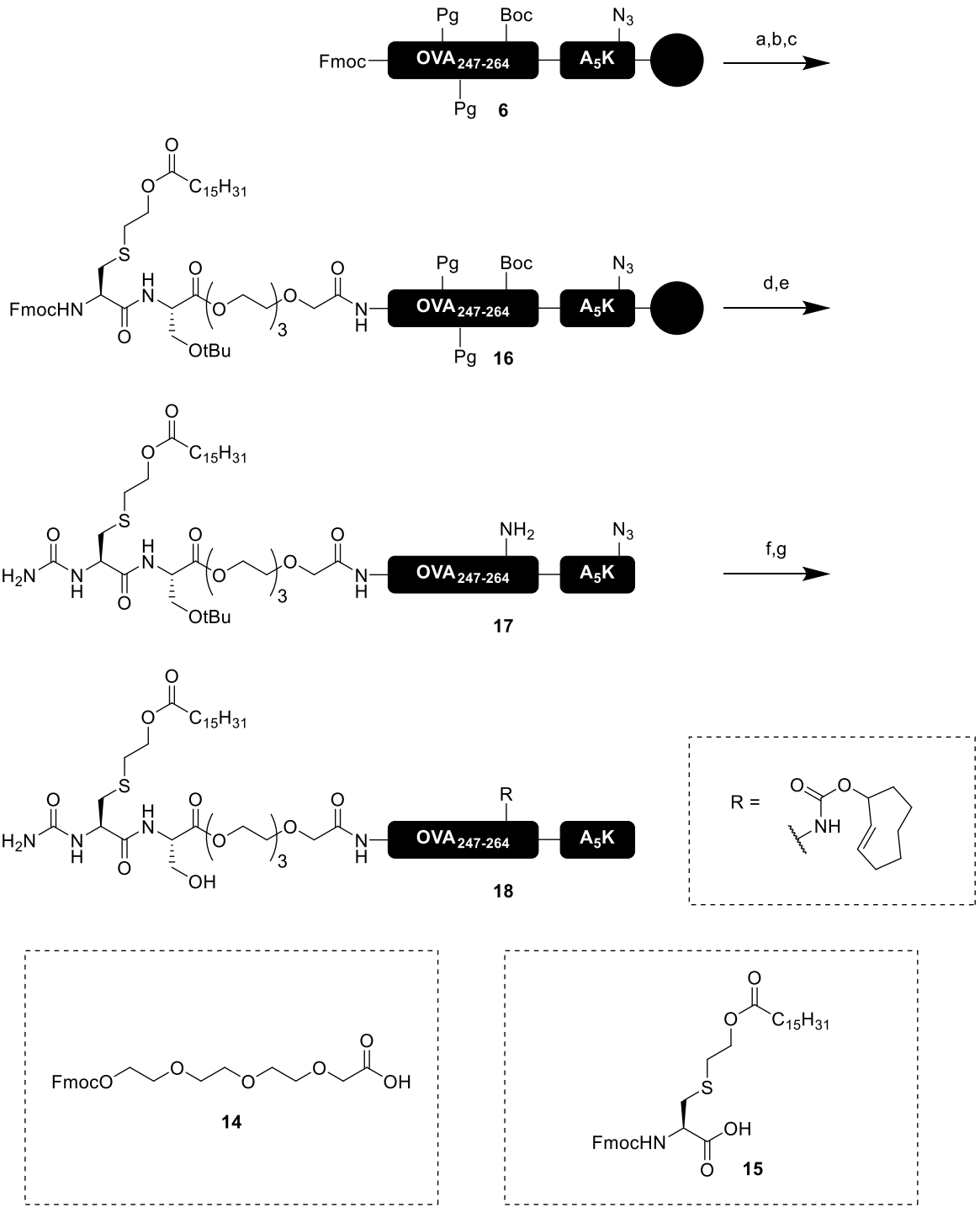

Figure 7. Synthesis of TCO-protected model conjugate vaccine **19**. Reagents and conditions: a) i) 20% (v/v) piperidine, DMF ii) **15**, HCTU, DiPEA, DMF b) i) 20% (v/v) piperidine, DMF ii) Fmoc-Ser(tBu)-OH, DIC, DMAP, DMF c) i) 20% (v/v) piperidine, DMF ii) **16**, HCTU, DiPEA, DMF d) 20% (v/v) piperidine, DMF ii) TMS-NCO, iPrOH, DCM e) TFA, TIS, H_2O f) TCO-Osu, DiPEA, DMF g) i) PMe_3, H_2O, DMF ii) RP-HPLC, 7.9%

The synthesis of the TLR-conjugate peptide (Figure 7) was started from resin-bound peptide **6**. This peptide was manually elongated with PEG spacer **14**, followed by liberation of the Fmoc-protected alcohol. This alcohol was condensed with Fmoc-Ser(tBu)-OH, mediated by DIC and catalytic DMAP. Next, the peptide was further elongated using cysteine building block **15**,

producing resin-bound peptide **16**. This was followed, after Fmoc removal, by formation of an N-terminal urea using a mixture of TMS-isocyanate and isopropanol in DCM, as reported by van de Ende *et al.*[44] This conversion proceeded sluggishly, with a single treatment not yielding full conversion of the amine. A second, longer treatment of the resin with the same TMS-isocyanate solution did fully convert the N-terminal amine to the urea. This peptide was then released from resin using the standard TFA cocktail (95:2.5:2.5, TFA/TIS/H_2O) and precipitated from cold diethyl ether, yielding crude peptide **17**. Again, residual TFA was removed by toluene co-evaporation, and DiPEA and TCO-OSu in DMF were added to the crude peptide. The reaction followed by LC-MS analysis. After complete consumption of **17** was observed, Staudinger reduction was initiated, producing crude **18**. RP-HPLC yielded the desired TCO protected conjugate peptide in 7.9% yield. The biological evaluation of this construct and their associated controls was not performed due to time restrictions.

Conclusion

The synthesis of peptides containing a 2-TCO protected lysine residue together with additional lysine residues is complicated. This is primarily due to the high acid sensitivity of the *trans*-cyclooctene group. Here, a synthetic method for such peptides was developed. By using azide groups as amine protecting groups, the lysine for TCO-modification could be selectively deprotected and modified. Subsequent Staudinger reduction allowed the unmasking of the azide protected amine groups.

This was exemplified with the synthesis of the model antigen peptide $OVA_{247\text{-}264}A_5K$, bearing a TCO group on the Lys_{263} residue, while leaving the C-terminal lysine unprotected. The compatibility of the approach with other functionalities was further exemplified by the synthesis of a TCO-caged mini-uPam-$OVA_{247\text{-}264}A_5K$ conjugate peptide. The base-labile ester groups in this peptide would prevent the synthesis using existing methods.

An initial T-cell activation assay using the TCO-caged $OVA_{247\text{-}264}A_5K$ peptide (**9**) showed very low levels of background activation, indicating the TCO cage is capable of blocking T-cell activation. Treatment with tetrazine **13** resulted in T-cell activation, indicating both successful deprotection of the epitope and that these protected peptides are processed and presented by immune cells. These results will enable the further study of the antigen processing and presentation of longer peptides.

Experimental

General procedure for automated SPPS

Peptides were synthesized using automated Fmoc-SPPS on a Liberty Blue^{tm} automated microwave peptide synthesizer (CEM corporation). Synthesis was performed 100 µmol scale on Tentagel S RAM resin (loading 0.20-0.25 mmol/g, Rapp Polymere GmbH, Germany). Resin was first swollen for 5 minutes in DMF prior to amino acid coupling. Activation was achieved using DIC/Oxyma coupling as is recommended by the manufacturer. The following amino acids were used: Fmoc-Ala-OH, Fmoc-Asn(Trt)-OH, Fmoc-Asp(OtBu)-OH, Fmoc-Gln(Trt)-OH, Fmoc-Glu(OtBu), Fmoc-Gly-OH, Fmoc-Ile-OH, Fmoc-Leu-OH, Fmoc-Lys(Boc)-OH, Fmoc-Lys(N_3)-OH, Fmoc-Phe-OH, Fmoc-Ser(tBu)-OH, Fmoc-Tyr(tBu)-OH, Fmoc-Val-OH. All amino acids were obtained from Novabiochem except Fmoc-Lys(N_3)-OH which was synthesized in house.[45] Standard coupling was achieved using 5 equivalents amino acid as a 0.2 M amino acid/DMF solution, 5 equivalents DIC as a 0.5 M of DIC/DMF solution and 5 equivalents Oxyma as a 1 M Oxyma/DMF solution (also containing 0.2 M DiPEA), at 90°C for 2 minutes. Standard Fmoc deprotection was achieved by 20% (v/v) piperidine in DMF at 90°C for 90 seconds, repeated once. To analyze the quality of the peptide, a small amount of resin (~1mg) was treated with 200 µL of a TFA cocktail (95:2.5:2.5, TFA/H_2O/TIS) for 2 hours, after which the TFA was filtered into 800 µL of ice cold Et_2O. After five minutes the formed precipitate was collected by centrifugation and the supernatant discarded. The pellet was dissolved in 200 µL 1:1:1 H_2O/MeCN/tBuOH and subjected to LC-MS analysis. Peptides were characterized using electrospray ionization mass spectrometry (ESI-MS) on a Thermo Finnigan LCQ Advantage Max LC-MS instrument with a Surveyor PDA plus UV detector on an analytical C18 column (Phenomenex, 3 µm, 110 Å, 50 mm × 4.6 mm) in combination with buffers A (H_2O), B (MeCN), and C (1% aq TFA). Quality of crude was evaluated with a linear gradient of 10-90% B with a constant 10% C over 9 minutes, unless stated otherwise.

General procedures for manual SPPS

Manual elongation of peptides was carried out in a fritted syringe at either 100 or 20 µmol scale. Fmoc deprotection was achieved using 20 % (v/v) piperidine in DMF in two steps, reacting 3 and 7 minutes respectively. All amino acids were coupled using 5 equivalents of amino acid together with 5 equivalents of HCTU (as a 0.5 M solution) and 10 equivalents DiPEA for 45 minutes, except for Fmoc-Lys(N_3)-OH, which was coupled using 2 equivalents together with 2 equivalents HCTU (as a 0.2 M in DMF solution) and 4 equivalents of DiPEA for 90 minutes. Analysis of the quality of the resin-bound peptide was carried out as above.

General procedure for peptide purification

Crude peptides were dissolved in a mixture of DMSO:H_2O:MeCN:tBuOH (typically 3:1:1:1) and subjected to RP-HPLC purification on a Agilent 1260 Infinity II semiprep system. This machine was equipped with a Nucleodur C18 gravity column (5 µm, 250 x 10.0 mm) using a flow of 5 mL/min and buffers A = 1% AcOH in H_2O and B = MeCN. Fraction collection was triggered by detection of the target peptide mass on a coupled mass detector (Agilent InfinityLab LC/MSD XT). Quality of purified peptides was determined using an electrospray ionization mass spectrometry (ESI-MS) on a Thermo Finnigan LCQ Advantage Max LC-MS instrument with a Surveyor PDA plus UV detector on an analytical C18 column (Phenomenex, 3 µm, 110 Å, 50 mm × 4.6 mm) in combination with buffers A (H_2O), B (MeCN),

and C (1% aq TFA). Quality of the peptides was evaluated with a linear gradient of 10-90% B with a constant 10% C over 9 minutes.

Fmoc-Tyr(tBu)-Ser(tBu)-Phe-Lys(Boc)-Ala-Lys(N_3)-RAM-Tentagel S (1)

The peptide was synthesized on a 50 µmol scale using the general manual SPPS procedures. **LC-MS** RT = 6.1 min (C18, 10-90% B over 9 minutes) **LRMS** calcd $[M+H]^+$ = 990.48 observed M/z = 990.47

N_3-Tyr-Ser-Phe-Lys-Ala-Lys(N_3)-NH_2 (3)

25 µmol of resin bound peptide **1** was swelled in DMF for 30 minutes followed by Fmoc removal according to the general procedure. ISA·H_2SO_4 (3 eq, 21 mg, 75 µmol) and DiPEA (5 eq, 21.8 µL, 125 µmol) were dissolved in anhydrous DMF (1 mL) and added to the drained resin. The resin was reacted under gentle agitation for 1 hour, after which the resin was drained and thoroughly washed with DMF (3 x 5 mL) and DCM (3 x 5 mL). Next, a TFA cocktail was added (1 mL, 95:2.5:2.5 TFA/TIS/H_2O) to the drained resin and this suspension was incubated for 1 hour, before draining the TFA into a centrifuge tube containing ice cold Et_2O (10 mL). The obtained suspension was kept on ice for 15 minutes followed by centrifugation. The supernatant was discarded and the pellet washed with Et_2O (2 mL). The crude peptide was transferred to a roundbottom flask with MeOH and concentrated *in vacuo*. This yielded 18.1 mg (22.8 µmol) of crude peptide **3**. **LC-MS** RT = 5.0 min (C18, 10-90% B over 9 minutes) **LRMS** calcd $[M+H]^+$ = 794.40 observed M/z = 794.27

Tyr-Ser-Phe-Lys(TCO)-Ala-Lys-NH_2 (5)

The crude peptide **3** (22.8 µmol) was co-evaporated with toluene (3 x 1 mL) and put under N_2. TCO-OSu (1.1 eq, 6.7 mg, 25 µmol) and DiPEA (5 eq, 20 µL, 115 µmol) were dissolved in anhydrous DMF (2.3 mL) and this solution was added to the flask containing the crude peptide. After 2 hours, LC-MS analysis indicates full conversion to the TCO protected peptide. **LC-MS** RT = 6.3 min (C18, 10-90% B over 9 minutes) **LRMS** calcd $[M+H]^+$ = 946.48 observed M/z = 946.17 This intermediate was then treated with a 1 M solution of PMe_3 in THF (10 eq, 230 µL, 0.23 mmol) followed by the addition of H_2O (100 eq, 41 µL, 2.3 mmol). After 1 hour LC-MS analysis indicated full consumption of the intermediate. RP-HPLC followed by lyophilization yielded peptide **5** in 2.1 % yield (0.42 mg, 0.47 µmol). **LC-MS** RT = 4.9 min (C18, 10-90% B over 9 minutes) **LRMS** calcd $[M+H]^+$ = 894.50, $[M+2H]^{2+}$ = 447.75 observed M/z = 894.40, 447.60 **HRMS** (ESI) m/z: $[M + 2H^+]$ calcd $C_{45}H_{67}N_9O_{10}$ 894.5084, found 894.5086

Fmoc-Asp(OtBu)-Glu(OtBu)-Val-Ser(tBu)-Gly-Leu-Glu(OtBu)-Gln(Trt)-Leu-Glu(OtBu)-Ser(tBu)-Ile-Ile-Asn(Trt)-Phe-Glu(OtBu)-Lys(Boc)-Leu-Ala-Ala-Ala-Ala-Ala-Lys(N_3)-RAM-Tentagel S (6)

Synthesis was carried out on a 100 µmol scale. The initial Fmoc-Lys(N_3)-OH was coupled using manual SPPS procedures. The peptide was then elongated using automatic SPPS. **LC-MS** RT = 6.7 min (C18, 10-90% B over 9 minutes) **LRMS** calcd $[M+2H]^{2+}$ = 1397.70 observed M/z = 1397.53

N_3-Asp-Glu-Val-Ser-Gly-Leu-Glu-Gln-Leu-Glu-Ser-Ile-Ile-Asn-Phe-Glu-Lys-Leu-Ala-Ala-Ala-Ala-Ala-Lys(N_3)-NH_2 (8)

25 µmol of resin bound peptide **6** was swelled in DMF for 30 minutes followed by Fmoc removal according to the general procedure. ISA·H_2SO_4 (3 eq, 21 mg, 75 µmol) and DiPEA (5 eq, 21.8 µL, 125 µmol) were dissolved in anhydrous DMF (1 mL) and added to the drained resin. The resin was reacted under gentle agitation for 1 hour, after which the resin was drained and thoroughly washed with DMF

(5 x 5 mL). The remaining free N-terminal amines were acetylated using a solution of 10% (v/v) Ac_2O and 5% (v/v) DiPEA in DMF (1 mL total) for 15 minutes, followed by thorough washing with DMF (3 x 5 mL) and DCM (3 x 5 mL). Next, a TFA cocktail was added (1 mL, 95:2.5:2.5 TFA/TIS/H_2O) to the drained resin and this suspension was incubated for 1 hour, before draining the TFA into a centrifuge tube containing ice cold Et_2O (10 mL). The obtained suspension was kept on ice for 15 minutes followed by centrifugation. The supernatant was discarded and the pellet washed with Et_2O (2 mL). The crude peptide was transferred to a roundbottom flask with MeOH and concentrated *in vacuo*. This yielded 41.7 mg (15.2 µmol) of crude peptide **8**. **LC-MS** RT = 6.1 min (C18, 10-90% B over 9 minutes) **LRMS** calcd $[M+2H]^{2+}$ = 1299.65 observed M/z = 1299.47

Asp-Glu-Val-Ser-Gly-Leu-Glu-Gln-Leu-Glu-Ser-Ile-Ile-Asn-Phe-Glu-Lys(TCO)-Leu-Ala-Ala-Ala-Ala-Ala-Lys-NH_2 (9)

The crude peptide **8** (15.2 µmol) was co-evaporated with toluene (3 x 1 mL) and put under N_2. TCO-OSu (1.1 eq, 4.5 mg, 16.7 µmol) and DiPEA (20 eq, 53 µL, 300 µmol) were dissolved in anhydrous DMF (1.5 mL) and this solution was added to the flask containing the crude peptide. After 2 hours, LC-MS analysis indicates full conversion to the TCO protected peptide. **LC-MS** RT = 6.8 min (C18, 10-90% B over 9 minutes) **LRMS** calcd $[M+2H]^{2+}$ = 1375.70 observed M/z = 1375.67. This intermediate was then treated with a 1 M solution of PMe_3 in THF (10 eq, 160 µL, 0.16 mmol) followed by the addition of H_2O (100 eq, 29 µL, 1.6 mmol). After 1 hour LC-MS analysis indicated full conversion to the desired peptide. RP-HPLC followed by lyophilization yielded peptide **9** in 5.4 % yield (2.20 mg, 0.82 µmol). **LC-MS** RT = 5.9 min (C18, 10-90% B over 9 minutes) **LRMS** calcd $[M+2H]^{2+}$ = 1349.71 observed M/z = 1349.53 **HRMS** (ESI) m/z: $[M + 2H^+]$ calcd $C_{121}H_{197}N_{29}O_{40}$ 1349.2209, found 1349.2212

Fmoc-Asp(OtBu)-Glu(OtBu)-Val-Ser(tBu)-Gly-Leu-Glu(OtBu)-Gln(Trt)-Leu-Glu(OtBu)-Ser(tBu)-Ile-Ile-Asn(Trt)-Phe-Glu(OtBu)-Lys(Boc)-Leu-AC-Tentagel S (10)

Tentagel S AC resin (100 µmol, 400 mg, 0.25 mmol/g) was swelled in DMF for 30 minutes. Fmoc-Leu-OH (4 eq, 141 mg, 0.4 mmol) was preactivated with DIC (6 eq, 92 µL, 0.6 mmol) in a 10 mM solution of DMAP in DMF for 1 minute. This solution was added to the drained resin and reacted overnight. The resin was washed with DMF (5 x 10 mL) and capped by treatment of a solution of 10% (v/v) Ac_2O and 5% (v/v) DiPEA in DMF (1 mL) containing 10 mM DMAP for 15 minutes. The resin was again washed (5 x 10 mL) and elongated using the general automated Fmoc-SPPS methods. **LC-MS** RT = 6.4 min (C18, 10-90% B over 9 minutes) **LRMS** calcd $[M+2H]^{2+}$ = 1143.56 observed M/z = 1143.40.

N_3-Asp-Glu-Val-Ser-Gly-Leu-Glu-Gln-Leu-Glu-Ser-Ile-Ile-Asn-Phe-Glu-Lys-Leu-OH (11)

Resin bound peptide **10** (25 µmol) was swelled in DMF, followed by removal of the Fmoc using standard conditions. The resin was thoroughly washed with water (3 x 5 mL). A solution containing ISA·H_2SO_4 (3 eq, 21 mg, 75 µmol) and Na_2CO_3 (4.5 eq, 12 mg, 113 µmol) in H_2O (1 mL) was added and the diazotranfer was allowed to proceed under gentle agitation for 16 hours. The resin was washed with H_2O (3 x 5 mL), MeOH (3 x 5 mL) and DCM (3 x 5 mL) before a TFA cocktail (1 mL, 95:2.5:2.5 TFA/TIS/H_2O) was added to the drained resin. This suspension was incubated for 1 hour, before draining the TFA into a centrifuge tube containing ice cold Et_2O (10 mL). The obtained suspension was kept on ice for 15 minutes followed by centrifugation. The supernatant was discarded and the pellet washed with Et_2O (2 mL). The crude peptide was transferred to a roundbottom flask with MeOH and

concentrated *in vacuo*. This yielded 47.6 mg (22.8 µmol) of the crude peptide **11**. **LC-MS** RT = 5.8 min (C18, 10-90% B over 9 minutes) **LRMS** calcd $[M+2H]^{2+}$ = 1045.02 observed M/z = 1045.33.

Asp-Glu-Val-Ser-Gly-Leu-Glu-Gln-Leu-Glu-Ser-Ile-Ile-Asn-Phe-Glu-Lys(TCO)-Leu-OH (12)

The crude peptide **11** (22.8 µmol) was co-evaporated with toluene (3 x 1 mL) and put under N_2. TCO-OSu (1.1 eq, 5.5 mg, 20.7 µmol) and DiPEA (10 eq, 33 µL, 190 µmol) were dissolved in anhydrous DMF (1.9 mL) and this solution was added to the flask containing the crude peptide. After 2 hours, LC-MS analysis indicates full conversion to the TCO protected peptide. **LC-MS** RT = 6.8 min (C18, 50-90% B over 9 minutes) **LRMS** calcd $[M+2H]^{2+}$ = 1121.06 observed M/z = 1120.90. This intermediate was then treated with a 1 M solution of PMe_3 in THF (10 eq, 190 µL, 0.19 mmol) followed by the addition of H_2O (100 eq, 34 µL, 1.9 mmol). After 2 hours LC-MS analysis indicated full conversion to the desired peptide. RP-HPLC followed by lyophilization yielded peptide **12** in 1.4 % yield (0.70 mg, 0.32 µmol). **LC-MS** RT = 6.3 min (C18, 10-90% B over 9 minutes) **LRMS** calcd $[M+2H]^{2+}$ = 1108.07 observed M/z = 1108.27 **HRMS** (ESI) m/z: $[M + 2H^+]$ calcd $C_{100}H_{159}N_{21}O_{35}$ 1108.0726, found

Fmoc-Cys(C_2H_4OPam)-Ser(tBu)-O-TEG-Asp(OtBu)-Glu(OtBu)-Val-Ser(tBu)-Gly-Leu-Glu(OtBu)-Gln(Trt)-Leu-Glu(OtBu)-Ser(tBu)-Ile-Ile-Asn(Trt)-Phe-Glu(OtBu)-Lys(Boc)-Leu-Ala-Ala-Ala-Ala-Ala-Lys(N_3)-RAM-Tentagel S (16)

The building blocks **14** and **15** were synthesized as described in van de Ende et al.[44] and provided by M.M.E. Isendoorn (Leiden university). Resin-bound peptide **6** (25 µmol) was swelled in DMF and the Fmoc group was removed using the general method. The peptide was manually elongated with compound **14** (4 eq, 43 mg, 100 µmol) mediated by HCTU (4 eq, 200 µL of a 0.5 M solution in DMF) and DiPEA (8 eq, 35 µL, 200 µmol), reacted for 45 min. This was followed by Fmoc removal and the obtained resin-bound ester was condensed with Fmoc-Ser(tBu)-OH (4 eq, 38 mg, 100 µmol) mediated by DIC (6 eq, 23 µL, 150 µmol) in DMF (200 µL) containing 0.1 eq DMAP (12.5 µM), reacted for 1.5 h. The Fmoc was again removed and building block **15** (2 eq, 31 mg, 50 µmol) was coupled, mediated by HCTU (2 eq, 200 µL 0.25 M) and DiPEA (4 eq, 17.4 µL, 100 µmol) for 1.5 hour. The resin was washed with DMF (3 x 5 mL) and DCM (3 x 5 mL), drained, and stored at -20°C until further use. **LC-MS** RT = 9.8 min (C18, 10-90% B over 9 minutes) **LRMS** calcd $[M+2H]^{2+}$ = 1728.89 observed M/z = 1729.20.

NH_2CO-Cys(C_2H_4OPam)-Ser-O-TEG-Asp-Glu-Val-Ser-Gly-Leu-Glu-Gln-Leu-Glu-Ser-Ile-Ile-Asn-Phe-Glu-Lys-Leu-Ala-Ala-Ala-Ala-Ala-Lys(N_3)-NH_2 (17)

The resin bound peptide **16** was swelled in DMF for 30 minutes followed by Fmoc removal using the standard method. The N-terminal urea was introduced by treating the resin with a mixture of TMS-NCO (6 eq, 20 µL, 150 µmol) and isopropanol (12 eq, 22.8 µL, 300 µmol) in DCM (2.5 mL) for 2.5 hour. This step was repeated once to ensure full conversion. Next, a TFA cocktail was added (1 mL, 95:2.5:2.5 TFA/TIS/H_2O) to the drained resin and this suspension was incubated for 1 hour, before draining the TFA into a centrifuge tube containing ice cold Et_2O (10 mL). The obtained suspension was kept on ice for 15 minutes followed by centrifugation. The supernatant was discarded and the pellet washed with Et_2O (2 mL). The crude peptide was transferred to a roundbottom flask with MeOH and concentrated *in vacuo*. This yielded 33.6 mg (10.3 µmol) of crude peptide **17**. **LC-MS** RT = 8.4 min (C18, 10-90% B over 9 minutes) **LRMS** calcd $[M+2H]^{2+}$ = 1639.36 observed M/z = 1639.60.

NH_2CO-Cys(C_2H_4OPam)-Ser-O-TEG-Asp-Glu-Val-Ser-Gly-Leu-Glu-Gln-Leu-Glu-Ser-Ile-Ile-Asn-Phe-Glu-Lys(TCO)-Leu-Ala-Ala-Ala-Ala-Ala-Lys-NH_2 (18)

The crude peptide **17** (10.3 µmol) was co-evaporated with toluene (3 x 1 mL) and put under N_2. TCO-OSu (1.2 eq, 3.2 mg, 12.4 µmol) and DiPEA (20 eq, 36 µL, 200 µmol) were dissolved in anhydrous DMF (1.0 mL) and this solution was added to the flask containing the crude peptide. After 2 hours, LC-MS analysis indicates full conversion to the TCO protected peptide. **LC-MS** RT = 7.8 min (C18, 50-90% B over 9 minutes) **LRMS** calcd $[M+2H]^{2+}$ = 1715.41 observed M/z = 1715.67. This intermediate was then treated with a 1 M solution of PMe_3 in THF (10 eq, 100 µL, 0.10 mmol) followed by the addition of H_2O (100 eq, 18 µL, 1.0 mmol). After 1 hour LC-MS analysis indicated full conversion to the desired peptide. RP-HPLC followed by lyophilization yielded peptide **18** in 7.9 % yield (2.75 mg, 0.81 µmol). **LC-MS** RT = 8.6 min (C18, 10-90% B over 9 minutes) **LRMS** calcd $[M+2H]^{2+}$ = 1702.41 observed M/z = 1702.27 **HRMS** (ESI) m/z: $[M + 2H^+]$ calcd $C_{154}H_{256}N_{32}O_{51}S$ 1701.9144, found 1701.9153

T-cell activation assay

This assay was carried out as described in van de Gracht et al.[17]

References

(1) Li, J.; Chen, P. R. Development and Application of Bond Cleavage Reactions in Bioorthogonal Chemistry. *Nat. Chem. Biol.* **2016**, *12* (3), 129–137. https://doi.org/10.1038/nchembio.2024.

(2) Streu, C.; Meggers, E. Ruthenium-Induced Allylcarbamate Cleavage in Living Cells. *Angew. Chem. Int. Ed.* **2006**, *45* (34), 5645–5648. https://doi.org/10.1002/anie.200601752.

(3) Tu, J.; Xu, M.; Franzini, R. M. Dissociative Bioorthogonal Reactions. *ChemBioChem* **2019**, *20* (13), 1615–1627. https://doi.org/10.1002/cbic.201800810.

(4) Van De Graaff, M. J.; Oosenbrug, T.; Marqvorsen, M. H. S.; Nascimento, C. R.; De Geus, M. A. R.; Manoury, B.; Ressing, M. E.; Van Kasteren, S. I. Conditionally Controlling Human TLR2 Activity via Trans-Cyclooctene Caged Ligands. *Bioconjug. Chem.* **2020**, *31* (6), 1685–1692. https://doi.org/10.1021/acs.bioconjchem.0c00237.

(5) Rossin, R.; Versteegen, R. M.; Wu, J.; Khasanov, A.; Wessels, H. J.; Steenbergen, E. J.; Ten Hoeve, W.; Janssen, H. M.; Van Onzen, A. H. A. M.; Hudson, P. J.; Robillard, M. S. Chemically Triggered Drug Release from an Antibody-Drug Conjugate Leads to Potent Antitumour Activity in Mice. *Nat. Commun. 2018 91* **2018**, *9* (1), 1–11. https://doi.org/10.1038/s41467-018-03880-y.

(6) Versteegen, R. M.; Rossin, R.; Ten Hoeve, W.; Janssen, H. M.; Robillard, M. S. Click to Release: Instantaneous Doxorubicin Elimination upon Tetrazine Ligation. *Angew. Chem. Int. Ed.* **2013**, *52* (52), 14112–14116. https://doi.org/10.1002/anie.201305969.

(7) Li, J.; Jia, S.; Chen, P. R. Diels-Alder Reaction-Triggered Bioorthogonal Protein Decaging in Living Cells. *Nat. Chem. Biol.* **2014**, *10* (12), 1003–1005. https://doi.org/10.1038/nchembio.1656.

(8) Sarris, A. J. C.; Hansen, T.; de Geus, M. A. R.; Maurits, E.; Doelman, W.; Overkleeft, H. S.; Codée, J. D. C.; Filippov, D. V.; van Kasteren, S. I. Fast and PH-Independent Elimination of Trans-Cyclooctene by Using Aminoethyl-Functionalized Tetrazines. *Chem. Eur. J.* **2018**, *24* (68), 18075–18081. https://doi.org/10.1002/chem.201803839.

(9) Wilkovitsch, M.; Haider, M.; Sohr, B.; Herrmann, B.; Klubnick, J.; Weissleder, R.; Carlson, J. C. T.; Mikula, H. A Cleavable C2-Symmetric Trans-Cyclooctene Enables Fast and Complete Bioorthogonal Disassembly of Molecular Probes. *J. Am. Chem. Soc.* **2020**, *142* (45), 19132–19141. https://doi.org/10.1021/jacs.0c07922.

(10) Davies, S.; Qiao, L.; Oliveira, B. L.; Navo, C. D.; Jiménez-Osés, G.; Bernardes, G. J. L. Tetrazine-Triggered Release of Carboxylic-Acid-Containing Molecules for Activation of an Anti-Inflammatory Drug. *ChemBioChem* **2019**, *20* (12), 1541–1546. https://doi.org/10.1002/cbic.201900098.

(11) Versteegen, R. M.; ten Hoeve, W.; Rossin, R.; de Geus, M. A. R.; Janssen, H. M.; Robillard, M. S. Click-to-Release from Trans -Cyclooctenes: Mechanistic Insights and Expansion of Scope from Established Carbamate to Remarkable Ether Cleavage. *Angew. Chemie* **2018**, *130* (33), 10654–10659. https://doi.org/10.1002/ange.201800402.

(12) De Geus, M. A. R.; Groenewold, G. J. M.; Maurits, E.; Araman, C.; Van Kasteren, S. I. Synthetic Methodology towards Allylic: Trans-Cyclooctene-Ethers Enables Modification of Carbohydrates: Bioorthogonal Manipulation of the Lac Repressor. *Chem. Sci.* **2020**, *11* (37), 10175–10179. https://doi.org/10.1039/d0sc03216f.

(13) Blackman, M. L.; Royzen, M.; Fox, J. M. Tetrazine Ligation: Fast Bioconjugation Based on Inverse-Electron-Demand Diels-Alder Reactivity. *J. Am. Chem. Soc.* **2008**, *130* (41), 13518–13519. https://doi.org/10.1021/ja8053805.

(14) Zhang, G.; Li, J.; Xie, R.; Fan, X.; Liu, Y.; Zheng, S.; Ge, Y.; Chen, P. R. Bioorthogonal Chemical

Activation of Kinases in Living Systems. *ACS Cent. Sci.* **2016**, *2* (5), 325–331. https://doi.org/10.1021/acscentsci.6b00024.

(15) Rossin, R.; van Duijnhoven, S. M. J.; ten Hoeve, W.; Janssen, H. M.; Kleijn, L. H. J.; Hoeben, F. J. M.; Versteegen, R. M.; Robillard, M. S. Triggered Drug Release from an Antibody–Drug Conjugate Using Fast "Click-to-Release" Chemistry in Mice. *Bioconjug. Chem.* **2016**, *27* (7), 1697–1706. https://doi.org/10.1021/acs.bioconjchem.6b00231.

(16) Wu, K.; Yee, N. A.; Srinivasan, S.; Mahmoodi, A.; Zakharian, M.; Mejia Oneto, J. M.; Royzen, M. Click Activated Protodrugs against Cancer Increase the Therapeutic Potential of Chemotherapy through Local Capture and Activation. *Chem. Sci.* **2021**, *12* (4), 1259–1271. https://doi.org/10.1039/D0SC06099B.

(17) van der Gracht, A. M. F.; de Geus, M. A. R.; Camps, M. G. M.; Ruckwardt, T. J.; Sarris, A. J. C.; Bremmers, J.; Maurits, E.; Pawlak, J. B.; Posthoorn, M. M.; Bonger, K. M.; Filippov, D. V; Overkleeft, H. S.; Robillard, M. S.; Ossendorp, F.; van Kasteren, S. I. Chemical Control over T-Cell Activation in Vivo Using Deprotection of Trans -Cyclooctene-Modified Epitopes. *ACS Chem. Biol.* **2018**, *13* (6), 1569–1576. https://doi.org/10.1021/acschembio.8b00155.

(18) Nordlander, J. E.; Kotian, K. D.; Raff, D. E.; Njoroge, F. G.; Winemiller, J. J.; Njoroge, G. F.; Winemiller, J. J. Regiochemistry, Stereochemistry, and Mechanism of Addition of Trifluoroacetic Acid to (Z)-Cyclooctene. *J. Am. Chem. Soc.* **1984**, *106* (5), 1427–1432. https://doi.org/10.1021/ja00317a039.

(19) La–Venia, A.; Dzijak, R.; Rampmaier, R.; Vrabel, M. An Optimized Protocol for the Synthesis of Peptides Containing Trans-Cyclooctene and Bicyclononyne Dienophiles as Useful Multifunctional Bioorthogonal Probes. *Chem. – A Eur. J.* **2021**, *27* (54), 13632–13641. https://doi.org/https://doi.org/10.1002/chem.202102042.

(20) Dicker, K. T.; Song, J.; Moore, A. C.; Zhang, H.; Li, Y.; Burris, D. L.; Jia, X.; Fox, J. M. Core-Shell Patterning of Synthetic Hydrogels: Via Interfacial Bioorthogonal Chemistry for Spatial Control of Stem Cell Behavior. *Chem. Sci.* **2018**, *9* (24), 5394–5404. https://doi.org/10.1039/c8sc00495a.

(21) Pawlak, J. B.; Gential, G. P. P.; Ruckwardt, T. J.; Bremmers, J. S.; Meeuwenoord, N. J.; Ossendorp, F. A.; Overkleeft, H. S.; Filippov, D. V.; Van Kasteren, S. I. Bioorthogonal Deprotection on the Dendritic Cell Surface for Chemical Control of Antigen Cross-Presentation. *Angew. Chem. Int. Ed.* **2015**, *54* (19), 5628–5631. https://doi.org/10.1002/ANIE.201500301.

(22) Sieber, P. A New Acid-Labile Anchor Group for the Solid-Phase Synthesis of C-Terminal Peptide Amides by the Fmoc Method. *Tetrahedron Lett.* **1987**, *28* (19), 2107–2110. https://doi.org/10.1016/S0040-4039(00)96055-6.

(23) Alsina, J.; Albericio, F. Solid-Phase Synthesis of C-Terminal Modified Peptides. *Pept. Sci.* **2003**, *71* (4), 454–477. https://doi.org/10.1002/BIP.10492.

(24) Rijkers, D. T. S.; Van Vugt, H. H. R.; Jacobs, H. J. F.; Liskamp, R. M. J. A Convenient Synthesis of Azido Peptides by Post-Assembly Diazo Transfer on the Solid Phase Applicable to Large Peptides. *Tetrahedron Lett.* **2002**, *43* (20), 3657–3660. https://doi.org/10.1016/S0040-4039(02)00629-9.

(25) Hansen, M. B.; Van Gurp, T. H. M.; Van Hest, J. C. M.; Löwik, D. W. P. M. Simple and Efficient Solid-Phase Preparation of Azido-Peptides. *Org. Lett.* **2012**, *14* (9), 2330–2333. https://doi.org/10.1021/ol300740g.

(26) Marine, J. E.; Liang, X.; Song, S.; Rudick, J. G. Azide-Rich Peptides via an on-Resin Diazotransfer Reaction. **2015**, *104* (4), 419–426.

(27) Goddard-Borger, E. D.; Stick, R. V. An Efficient, Inexpensive, and Shelf-Stable Diazotransfer Reagent: Imidazole-1-Sulfonyl Azide Hydrochloride. *Org. Lett.* **2007**, *9* (19), 3797–3800. https://doi.org/10.1021/ol701581g.

(28) Potter, G. T.; Jayson, G. C.; Miller, G. J.; Gardiner, J. M. An Updated Synthesis of the Diazo-Transfer Reagent Imidazole-1-Sulfonyl Azide Hydrogen Sulfate. *J. Org. Chem.* **2016**, *81* (8), 3443–3446. https://doi.org/10.1021/acs.joc.6b00177.

(29) Lundquist IV, J. T.; Pelletier, J. C. A New Tri-Orthogonal Strategy for Peptide Cyclization. *Org. Lett.* **2002**, *4* (19), 3219–3221. https://doi.org/10.1021/ol026416u.

(30) Staudinger, H.; Meyer, J. Über Neue Organische Phosphorverbindungen III. Phosphinmethylenderivate Und Phosphinimine. *Helv. Chim. Acta* **1919**, *2* (1), 635–646. https://doi.org/10.1002/HLCA.19190020164.

(31) Meldal, M.; Juliano, M. A.; Jansson, A. M. Azido Acids in a Novel Method of Solid-Phase Peptide Synthesis. *Tetrahedron Lett.* **1997**, *38* (14), 2531–2534. https://doi.org/10.1016/S0040-4039(97)00393-6.

(32) Lundquist IV, J. T.; Pelletier, J. C. Improved Solid-Phase Peptide Synthesis Method Utilizing α-Azide-Protected Amino Acids. *Org. Lett.* **2001**, *3* (5), 781–783. https://doi.org/10.1021/ol0155485.

(33) Castro, V.; Blanco-Canosa, J. B.; Rodriguez, H.; Albericio, F. Imidazole-1-Sulfonyl Azide-Based Diazo-Transfer Reaction for the Preparation of Azido Solid Supports for Solid-Phase Synthesis. *ACS Comb. Sci.* **2013**, *15* (7), 331–334. https://doi.org/10.1021/co4000437.

(34) Khan, S.; Bijker, M. S.; Weterings, J. J.; Tanke, H. J.; Adema, G. J.; van Hall, T.; Drijfhout, J. W.; Melief, C. J. M.; Overkleeft, H. S.; van der Marel, G. A.; Filippov, D. V; van der Burg, S. H.; Ossendorp, F. Distinct Uptake Mechanisms but Similar Intracellular Processing of Two Different Toll-like Receptor Ligand-Peptide Conjugates in Dendritic Cells. *J. Biol. Chem.* **2007**, *282* (29), 21145–21159. https://doi.org/10.1074/jbc.M701705200.

(35) Rosalia, R. A.; Quakkelaar, E. D.; Redeker, A.; Khan, S.; Camps, M.; Drijfhout, J. W.; Silva, A. L.; Jiskoot, W.; Hall, T. van; Veelen, P. A. van; Janssen, G.; Franken, K.; Cruz, L. J.; Tromp, A.; Oostendorp, J.; Burg, S. H. van der; Ossendorp, F.; Melief, C. J. M. Dendritic Cells Process Synthetic Long Peptides Better than Whole Protein, Improving Antigen Presentation and T-Cell Activation. *Eur. J. Immunol.* **2013**, *43* (10), 2554–2565. https://doi.org/10.1002/EJI.201343324.

(36) Rötzschke, O.; Falk, K.; Stevanovic, S.; Jung, G.; Walden, P.; Rammensee, H. -G. Exact Prediction of a Natural T Cell Epitope. *Eur. J. Immunol.* **1991**, *21* (11), 2891–2894. https://doi.org/10.1002/EJI.1830211136.

(37) Saito, N. G.; Paterson, Y. Contribution of Peptide Backbone Atoms to Binding of an Antigenic Peptide to Class I Major Histocompatibility Complex Molecule. *Mol. Immunol.* **1997**, *34* (16–17), 1133–1145. https://doi.org/10.1016/S0161-5890(97)00140-5.

(38) Fan, X.; Ge, Y.; Lin, F.; Yang, Y.; Zhang, G.; Ngai, W. S. C.; Lin, Z.; Zheng, S.; Wang, J.; Zhao, J.; Li, J.; Chen, P. R. Optimized Tetrazine Derivatives for Rapid Bioorthogonal Decaging in Living Cells. *Angew. Chem. Int. Ed.* **2016**, *55* (45), 14046–14050. https://doi.org/10.1002/anie.201608009.

(39) Immunology, N.; Nolan, J. P.; Matilla, G. P.; Crabtree, P.; Herzenberg, G. R. Measurement of Ligand-Induced Activation in Single Viable T Cells Using the LacZ Reporter Gene. *Proc. Natl. Acad. Sci.* **1991**, *88* (9), 3972–3976. https://doi.org/10.1073/PNAS.88.9.3972.

(40) Sanderson, S.; Shastri, N. LacZ Inducible, Antigen/MHC-Specific T Cell Hybrids. *Int. Immunol.* **1994**, *6* (3), 369–376. https://doi.org/10.1093/INTIMM/6.3.369.

(41) Zom, G. G. P.; Khan, S.; Filippov, D. V.; Ossendorp, F. TLR Ligand-Peptide Conjugate Vaccines.

Toward Clinical Application. In *Advances in Immunology*; Academic Press, 2012; Vol. 114, pp 177–201. https://doi.org/10.1016/B978-0-12-396548-6.00007-X.

(42) Hanna, C. C.; Ashhurst, A. S.; Quan, D.; Maxwell, J. W. C.; Britton, W. J.; Payne, R. J. Synthetic Protein Conjugate Vaccines Provide Protection against Mycobacterium Tuberculosis in Mice. *Proc. Natl. Acad. Sci. U. S. A.* **2021**, *118* (4). https://doi.org/10.1073/pnas.2013730118.

(43) Zom, G. G.; Khan, S.; Britten, C. M.; Sommandas, V.; Camps, M. G. M.; Loof, N. M.; Budden, C. F.; Meeuwenoord, N. J.; Filippov, D. V.; van der Marel, G. A.; Overkleeft, H. S.; Melief, C. J. M.; Ossendorp, F. Efficient Induction of Antitumor Immunity by Synthetic Toll-like Receptor Ligand-Peptide Conjugates. *Cancer Immunol. Res.* **2014**, *2* (8), 756–764. https://doi.org/10.1158/2326-6066.CIR-13-0223.

(44) Ende, T. C.; Heuts, J. M. M.; Gential, G. P. P.; Visser, M.; Graaff, M. J.; Ho, N. I.; Jiskoot, W.; Valentijn, A. R. P. M.; Meeuwenoord, N. J.; Overkleeft, H. S.; Codée, J. D. C.; Burg, S. H.; Verdegaal, E. M. E.; Marel, G. A.; Ossendorp, F.; Filippov, D. V. Simplified Monopalmitoyl Toll-like Receptor 2 Ligand Mini-UPam for Self-Adjuvanting Neoantigen-Based Synthetic Cancer Vaccines. *ChemBioChem* **2021**, *22* (7), 1215–1222. https://doi.org/10.1002/cbic.202000687.

(45) Sminia, T. J.; Pedersen, D. S. Azide- and Alkyne-Functionalised α- And β 3-Amino Acids. *Synlett* **2012**, *23* (18), 2643–2646. https://doi.org/10.1055/S-0032-1317445/ID/JR000-12.

7

Summary and future prospects

R.C. Reijnen contributed to the thioflavin T assays described in this chapter.

S. Wijngaarden contributed to the protein synthesis described in this chapter.

This thesis has described novel synthetic methods to produce a variety of (glyco)peptides and their application in the study of various immunological processes. The first part of the thesis describes novel insights into the pathogenesis of multiple sclerosis, in the form of new findings in the areas of lectin-driven immunotolerance and a biochemical comparison between human and animal model antigen.[1,2] The next part describes novel multivalently glycosylated peptides, that can be used to study lectin binding and lectin mediated antigen uptake.[3,4] The final part of the thesis describes a novel method to produce *trans*-cyclooctene protected peptides, an exciting new category of molecular tools within chemical biology that have recently been developed.[5]

Chapter 2 describes the synthesis of a series of N-glycosylated Fmoc-asparagine building blocks for solid phase peptide synthesis (SPPS). Four different glycan structures were synthesized: GlcNAc, LacNAc (Galβ1-4GlcNAc), Fucα1-3GlcNAc and Lewis X (Galβ1-4(Fucα1-3)GlcNAc, Le^X). The building blocks were constructed from the protected glycosyl azides and coupled to the sidechain of asparagine using a one-pot, two step procedure involving Staudinger reduction of the azide followed by regioselective ring-opening of Fmoc-aspartic anhydride. Using standard Fmoc-SPPS conditions, these building blocks were incorporated into the immunodominant peptide of myelin oligodendrocyte glycoprotein (MOG), MOG_{31-55}, at the site of native N-glycosylation (Asn_{31}). Using an ELISA based assay, binding of the Le^X decorated neoglycopeptide to DC-SIGN was proven. Furthermore, a Le^X dependent effect on cytokine secretion, specifically a decrease of IL12p70 secretion, was found when moDCs were treated with peptides in presence of LPS. The effect of glycosylation on the citrullination driven aggregation of MOG_{31-55} was also investigated. Here a glycosylation-dependent decrease in aggregation propensity was found.

Synthesis and immunological evaluation of neoglycopeptides bearing these *N*-glycosylated asparagine residues could lead to a better understanding of glycosylation mediated cytokine secretion. Since these building blocks are far easier to obtain in synthetically useful quantities then native, Le^X decorated N-glycosylated asparagine, while still containing a native glycosidic linkage to the peptide, they could be highly useful in situations were side effects resulting from non-native linkages are to be avoided. Furthermore, the interplay of glycosylation and citrullination on the aggregation of MOG_{31-55} remains an interesting topic.

With the GlcNAc decorated MOG_{31-55} peptides easily available, native N-glycan structures could be introduced by the use of engineered *endo*-β-N-acetylglucosaminidase (ENGase) enzymes.[6] ENGase enzymes are naturally able to cleave the glycosidic bond between the two GlcNAc residues in the chitobiose core of an *N*-glycan, but directed mutagenesis produced enzymes that can instead ligate a GlcNAc decorated asparagine together with a glycan containing a reducing end GlcNAc, provided this GlcNAc is provided as the oxazoline.[7] Using this approach, peptides bearing native *N*-glycans, for instance the high-mannose type[8] or sialylated complex type,[9] can be synthesized.[10] Using these methods, different forms of natively glycosylated MOG_{31-55} could be produced, and the effects of native glycosylation on citrulline driven aggregation evaluated.

Chapter 3 reports the evaluation of a series of citrullinated peptides derived from the myelin protein myelin oligodendrocyte glycoprotein (MOG). Previous work has found that the murine sequence of the immunodominant peptide MOG_{35-55} displayed amyloid-like aggregation behavior after citrullination.[2] The MOG protein, and particularly the immunodominant region, have a high degree of similarity between species, and the only amino acid substitution between the murine and human sequence is a Ser-to-Pro substitution on position 42. Experiments described in chapter 3 indicate that this single substitution fully inhibits the aggregation. Some further chemical mutagenesis experiments were carried out, replacing

Ser_{42} with various serine isosteres, indicating serine to be crucial for the citrullination driven aggregation.

An additional surprising difference between the marmoset Ser_{42} containing citrullinated MOG_{35-55} peptides and the human Pro_{42} containing variants came from an antigen cross-presentation assay. Using B- and T-cells from marmosets previously immunized with $hMOG_{35-55}$,[11] it was found that one of the non-aggregating human MOG_{35-55} variants was better able to activate T-cells than the corresponding aggregating marmoset variant. Specifically, the marmoset peptide $mMOG_{35-55}Cit_{46,52}$, a strongly aggregating peptide, did not produce any T-cell response, while the non-aggregating $hMOG_{35-55}Cit_{46,52}$ did. Given the complexity of the underlying immunology, determining the precise cause of this discrepancy can be multi-factorial. In this chapter, two major hypotheses for the difference in T-cell activation are proposed and evaluated.

The first hypothesis involved the presentation of the antigen to the T-cell. In order for an antigen to elicit a T-cell response, an epitope, a peptide usually 8 or 9 residues in length, has to be loaded into a Major Histocompatibility Complex (MHC), and this epitope-MHC complex has to be recognized by a T-cell receptor (TCR). The precise structure of this epitope-MHC complex, especially the exact binding mode of the epitope, is often critical for TCR recognition. The critical question here is whether the citrullination pattern leading to aggregation affects the position of the amino acid sidechains in the MHC-complex. While the structure of the MHC-peptide complex has not been determined experimentally, computational methods can be used to study these interactions *in silico* by docking the peptide into the MHC crystal structure. This method will be applied to evaluate whether differences in presentation of the epitope are to be expected to play a role in the observed differences in T-cell activation.

The second hypothesis was that the amyloid-like aggregation behavior prevents the proteolytic liberation of the minimal epitope from the aggregated longer MOG-peptide fragments, leading to reduced antigen presentation. The epitope, to be loaded into an MHC, needs to be liberated from the full 21-mer peptide incubated with the cell. To produce this epitope, which is only 9 residues in length, partial degradation of the longer peptide is required. This process is called antigen processing and is quite difficult to study, due to the amount of enzymes and cell-compartments it involves.[12] Still, differences in degradation of the peptide, caused by either the introduction of the citrulline residues in the peptide sequence, or by the difference between the Ser-containing marmoset peptide compared to the Pro-containing human one, could lead to differences in peptide degradation. This hypothesis was approached from two directions. First, it was investigated whether smaller peptides derived from $mMOG_{35-55}$-$Cit_{46,52}$ retained the ability to aggregate, which could prevent loading of this peptide into MHC complexes (thereby preventing T-cell activation). To answer this question, the citrullinated forms of the MHC binding epitope (MOG_{40-48}),[13] as well as C- and N-terminally extended versions of this peptides, were evaluated for their aggregation propensity. Alternatively, the liberation of the specific epitope could be impeded by the inability of a specific enzyme to perform its proteolytic function, or by a specific enzyme

destructively processing the key epitope. Previously, Cathapsin G (CatG) degradation was implicated as major factor in the degradation of MOG_{35-55} antigens[14,15] and has also been shown to be critical in the degradation of a different myelin antigen (myelin basic protein, MBP) by B-cells.[16] Therefore, the degradation of the different MOG_{35-55} peptides by this enzyme was investigated.

Docking of MOG_{40-48} peptides into HLA-E

While the antigenicity of citrullinated $hMOG_{35-55}$ has never been studied in the marmoset system, previous work in mice[17] showed that citrullination of $mMOG_{35-55}$-Cit_{46} strongly diminished the immune response observed from T-cells of $mMOG_{35-55}$ immunized animals, similar to absence of T-cell responses against $mMOG_{35-55}$-$Cit_{46,52}$ seen in Chapter 3. The presentation of $hMOG_{35-55}$ to T-cells via EBV infected marmoset B-cells is considered to take place via presentation on the non-classical MHC class I receptor Caja-E.[13] Since no crystal structures of the peptide-MHC complexes are available, it is unknown whether the presentation of the human and marmoset MOG_{40-48} in the relevant MHC displays the same TCR (T-cell receptor) contact residues.

To evaluate binding difference inside the Caja-E complex, an *in silico* docking approach was used to predict the binding of the different MOG_{40-48} epitopes to this MHC. This approach was previously used to study the effect of citrullination on a key T-cell epitope of a protein involved in rheumatoid arthritis, where a large perturbation of a residue was predicted for the citrullinated peptide, potentially explaining the lack of T-cell response against this peptide.[18] If docking of the different MOG_{40-48} epitopes shows a similar perturbation only for $mMOG_{40-48}$-Cit_{46}, this could help explain the observed effect. While no crystal structures of Caja-E have been reported, the amino acid sequence shows extremely high similarity to human HLA-E, for which multiple structures are available. Careful examination of the polymorphisms present between Caja-E and HLA-E showed that no amino acid polymorphisms were present in the binding cleft (Figure S1). Therefore, the available HLA-E structures were considered decent models for the study.

For the purpose of the docking study, it was assumed that citrullination of Arg_{46} and Arg_{52} would not lead to different processing of the peptide, and therefore would produce a different 9-mer epitope from MOG_{40-48}. The following four different forms of MOG_{40-48} expected to be produced by the B-cell during processing were docked: $hMOG_{40-48}$, $mMOG_{40-48}$, $hMOG_{40-48}$-Cit_{46} and $mMOG_{40-48}$-Cit_{46}. When comparing the poses found when docking either the human or marmoset form of the epitope (Figure 1A), the N-terminal part of the peptides seems to overlay quite well, even on the position of the Pro/Ser polymorphism. The rest of the sequence shows less overlap, with the central phenylalanine showing a large shift in location in the binding cleft. The C-terminal valine again overlaps well between the two peptides, indicating correct docking of the peptide's carboxylic acid.

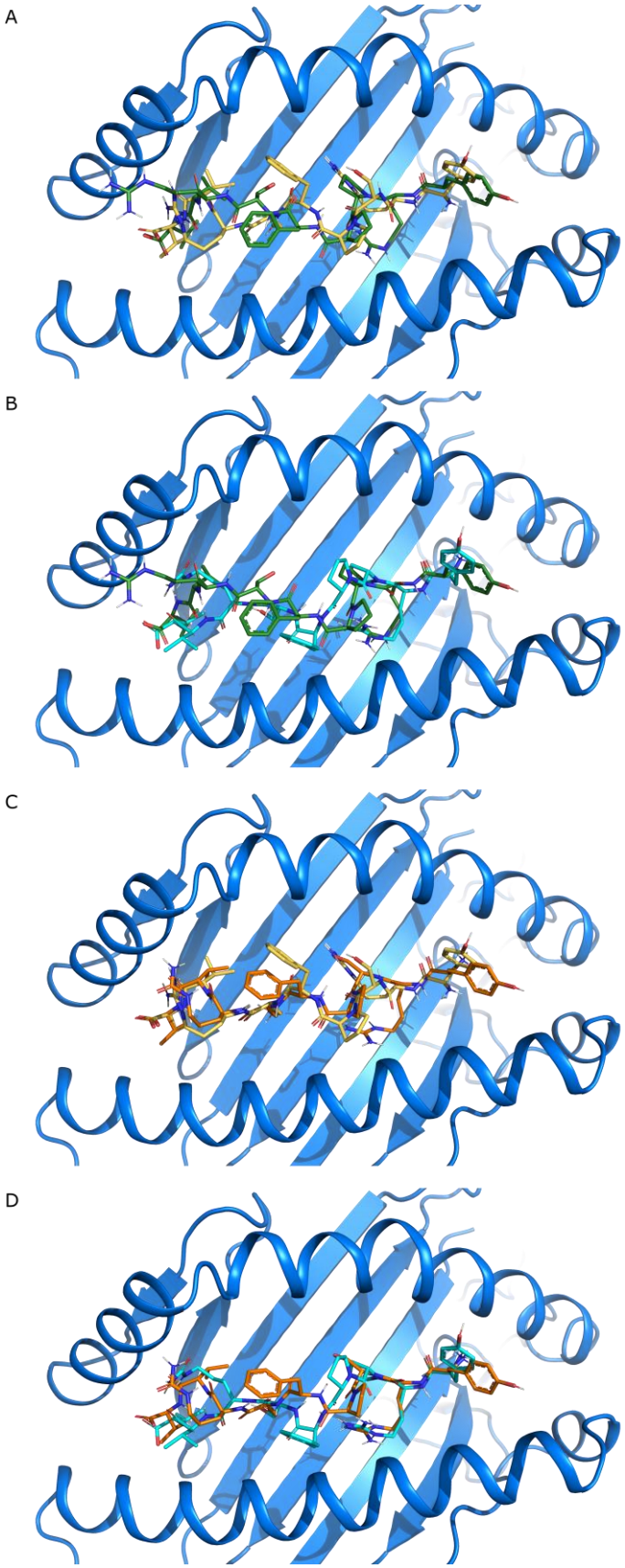

Figure 1. Resulting poses after docking the four different MOG_{40-48} peptides into HLA-E. The following colors were used to denote the different peptides: $hMOG_{40-48}$ (green), $mMOG_{40-48}$ (yellow), $hMOG_{40-48}$-Cit_{46} (cyan), $mMOG_{40-48}$-Cit_{46} (orange) A) $hMOG_{40-48}$ compared with $mMOG_{40-48}$ B) $hMOG_{40-48}$ and $hMOG_{40-48}$-Cit_{46} C) $mMOG_{40-48}$ and

mMOG$_{40-48}$-Cit$_{46}$ D) hMOG$_{40-48}$-Cit$_{46}$ and mMOG$_{40-48}$-Cit$_{46}$. These docking studies were performed by A.P.A. Janssen (Leiden university).

When comparing the human wildtype and citrullinated form (Figure 1B), good overlap was again observed for the three N-terminal residues. On the C-terminal side, the backbone of the citrullinated residue is twisted, resulting in the citrulline pointing more inward into the cleft, making the penultimate valine solvent exposed. The docked poses found for wildtype mMOG$_{40-48}$ and its citrullinated counterpart (Figure 1C) are highly similar, with the backbone closely overlapping over its entire length.

Figure 1D shows the overlay of the docking poses found for the human and marmoset citrullinated peptides. Based on the results of the T-cell presentation assay (Chapter 3) this is where the largest differences are expected. However, as expected from the high degree of overlap between both wildtype peptides and their citrullinated counterparts, the same pattern is found in the direct comparison, with the N-terminus overlapping well and the C-terminus showing a conformational difference. Taken together, these findings do not give a strong basis to explain the differences found in the T-cell activation assays. This suggests that differences in antigen processing is the major factor in the changes in antigen presentation. This could be due to the altered solubility/aggregation of the processed peptides, for instance by aggregation sequestering the epitope inside insoluble aggregates. Altered processing, either due to partially processed peptides forming aggregates, or due to differential proteolysis of peptides due to citrullination could also be relevant. These ideas will be explored in the rest of this chapter.

Aggregation of truncated peptides

Having shown that the human-variant of MOG$_{35-55}$ did not aggregate upon citrullination like the marmoset citrullinated peptide, it was next assessed whether truncated versions of the marmoset peptide retained their ability to aggregate. Since APCs would likely (partially) degrade internalized peptide, the aggregation behavior of peptide fragments could be just as important as that of the parent peptides, in an immunological setting.

First, the minimal MHC class I-restricted epitope peptide, MOG$_{40-48}$, was evaluated. Since this peptide contains two of the key arginine residues within the sequence (Arg$_{41}$ and Arg$_{46}$), a question was whether the citrullinated variants of this short 9-mer peptide could induce amyloid-like aggregation similar to that seen with the parent peptide. The three possible citrullinated variants of the mMOG$_{40-48}$ peptide, mMOG$_{40-48}$-Cit$_{41}$, mMOG$_{40-48}$-Cit$_{46}$ and mMOG$_{40-48}$-Cit$_{41,46}$ were synthesized on chlorotrityl resin, to obtain the free C-terminal carboxylic acid (Table 1). These were then tested in the same ThT assay as described in Chapter 3. None of these peptides showed any increase in ThT fluorescence over the 16 hour time

period, indicating none of the three the citrullinated peptides showed amyloidogenic properties as determined by ThT (Figure 2).

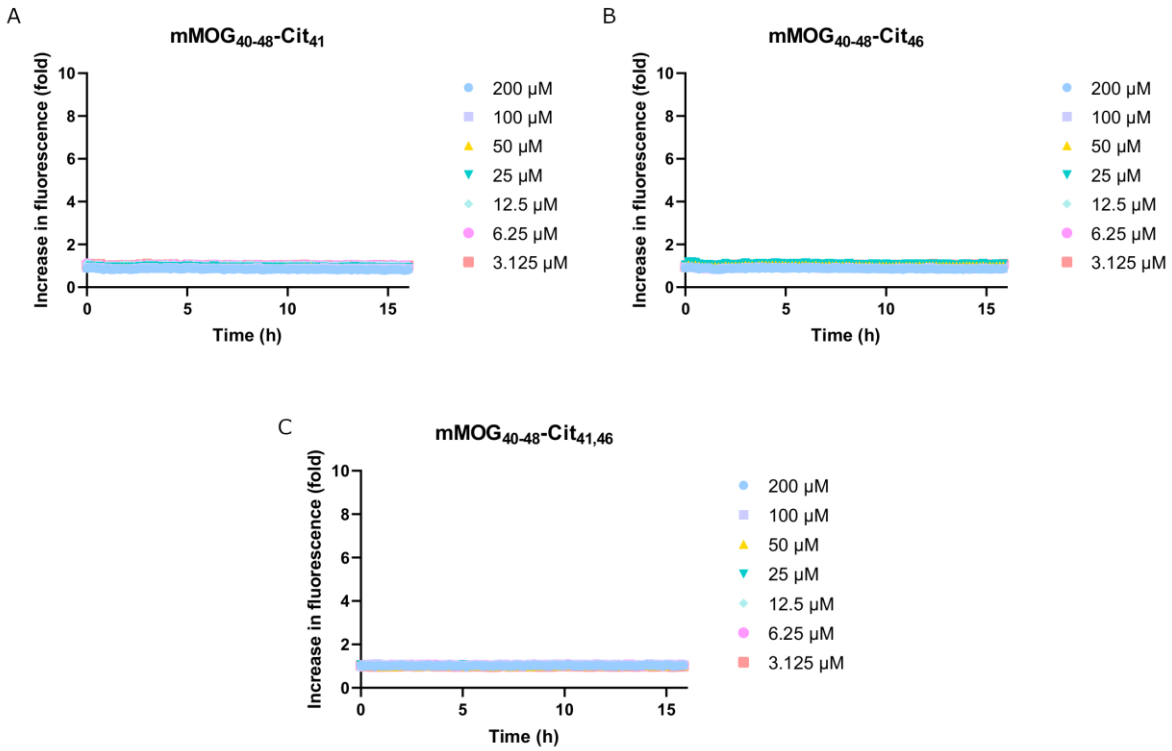

Figure 2. ThT aggregation assays showing the aggregation properties of citrullinated mMOG$_{40-48}$ peptides. A) mMOG$_{40-48}$-Cit$_{41}$. B) mMOG$_{40-48}$-Cit46. C) mMOG$_{40-48}$-Cit$_{41,46}$

Since the 9-mer T-cell epitopes did not show any amyloid-like aggregation, a key question was what the shortest aggregating sequence would be. Additionally, the aggregation kinetics of any shorter aggregating sequences could be important during antigen processing; rapid amyloidogenesis of a partially processed antigen could obstruct further degradation and MHC loading. To investigate this line of reasoning, a series of peptides was synthesized, each stepwise elongated by one residue on both the C- and N-terminus. All of these peptides were synthesized as the free carboxylic acid, to simulate degradation products that could be produced when mMOG$_{35-55}$-Cit$_{46,52}$ is degraded intracellularly. An overview of these synthetic, stepwise elongated peptides is given in Table 1.

Table 1. Overview of all novel peptides synthesized in this Chapter. Arginine residues that were replaced with citrulline are highlighted in boldface. All yields are after RP-HPLC and based on the manufacture specified resin loading.

Name	Sequence	Yield (%)
mMOG$_{40-48}$-Cit$_{41}$	Y**R**SPFSRVV	31
mMOG$_{40-48}$-Cit$_{46}$	YRSPFS**R**VV	29
mMOG$_{40-48}$-Cit$_{41,46}$	Y**R**SPFS**R**VV	33
mMOG$_{39-49}$-Cit$_{46}$	WYRSPFS**R**VVH	17
mMOG$_{38-50}$-Cit$_{46}$	GWYRSPFS**R**VVHL	27
mMOG$_{37-51}$-Cit$_{46}$	VGWYRSPFS**R**VVHLY	27
mMOG$_{36-52}$-Cit$_{46}$	EVGWYRSPFS**R**VVHLYR	13
mMOG$_{36-52}$-Cit$_{46,52}$	EVGWYRSPFS**R**VVHLY**R**	27
mMOG$_{35-53}$-Cit$_{46,52}$	MEVGWYRSPFS**R**VVHLY**R**N	27

The first three extensions, mMOG$_{39-49}$-Cit$_{46}$ (Figure 3A), mMOG$_{38-50}$-Cit$_{46}$ (Figure 3B) and mMOG$_{37-51}$-Cit$_{46}$ (Figure 3C) showed no increase in ThT fluorescence. However, the next extension, mMOG$_{36-52}$-Cit$_{46}$, showed a minor increase in ThT fluorescence over time (Figure 3D). The peptide containing 2 citrulline residues, mMOG$_{35-55}$-Cit$_{46,52}$, yielded a more pronounced aggregation (Figure 3E), that was further compounded when the N- and C-termini were extended by an additional amino acid (mMOG$_{35-53}$-Cit$_{46,52}$; Figure 3F). This compound showed aggregation behavior in line with the parent peptide mMOG$_{35-55}$-Cit$_{46,52}$ (Chapter 3, Figure 2F). The only caveat was that the lower concentrations did not show any increase in ThT fluorescence, in stark contrast to the full-length peptide.

These results imply it is primarily the non-processed peptide that is involved in amyloid-like aggregation and aggregation of a citrullinated, partially processed peptide is unlikely to be a key factor in the observed lack of T-cell activation. The key question that remains is whether the aggregation of the parent peptide by itself inhibits processing at the earliest point in the process.

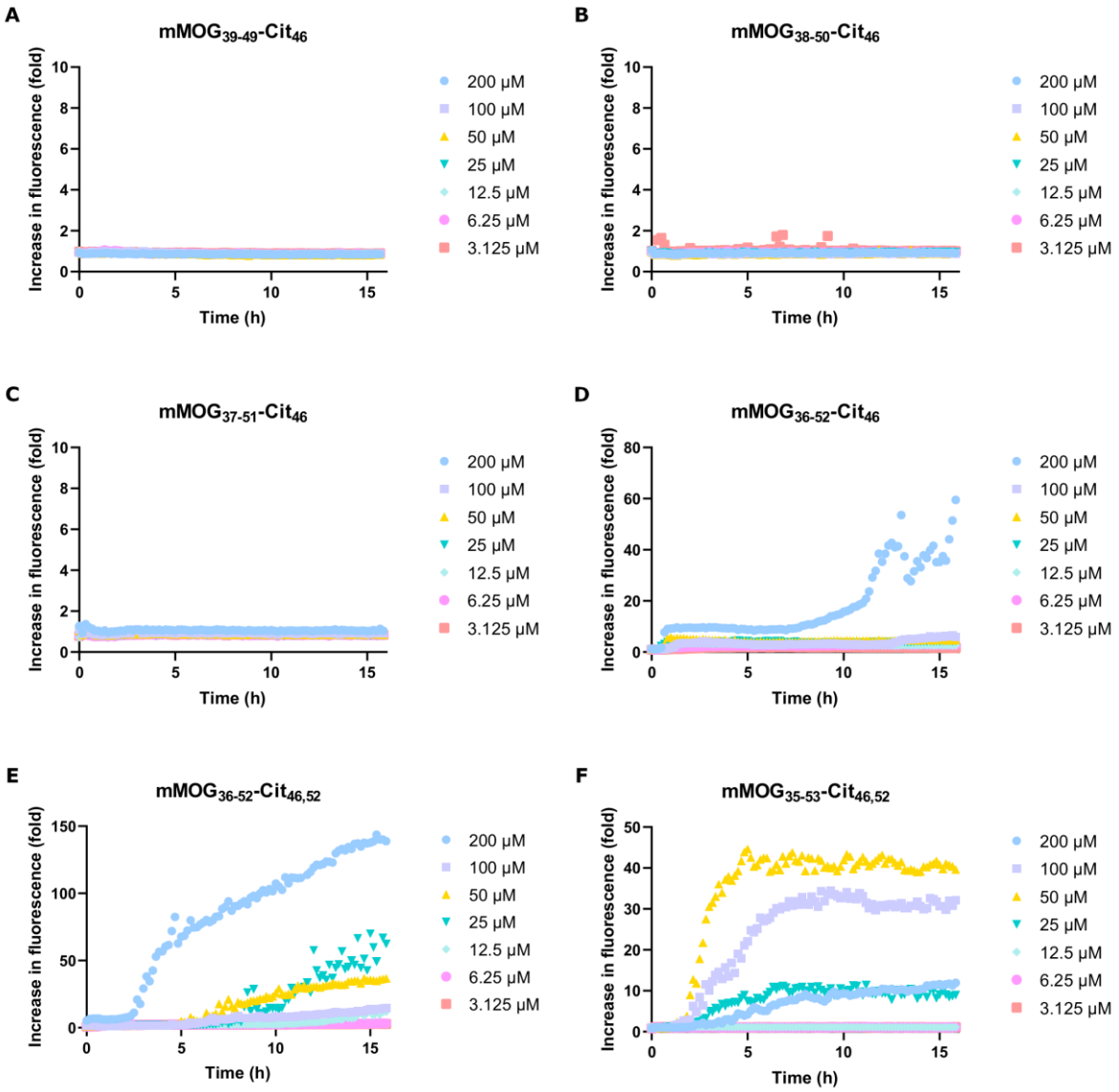

Figure 3. ThT aggregation assays of the stepwise elongated core epitope peptides. All sequences were based on the marmoset peptide sequence and in each step the peptide was elongated with one amino acid on both N- and C-terminus. A) mMOG$_{39-49}$-Cit$_{46}$. B) mMOG$_{38-50}$-Cit$_{46}$. C) mMOG$_{37-51}$-Cit$_{46}$. D) mMOG$_{36-52}$-Cit$_{52}$. E) mMOG$_{36-52}$-Cit$_{46,52}$. F) mMOG35-53-Cit$_{46,52}$

Alternative degradation by an endolysosomal protease

Cathepsin G (CatG) has been implicated as a crucial protease in the processing of MOG$_{35-55}$. Previous work suggested that this serine protease would destructively process the critical MOG$_{40-48}$ epitope, unless Arg$_{46}$ was citrullinated.[14,15] Destructive processing of amyloid autoantigen in B cells has also been implicated as an important mechanism for tolerance to myelin basic protein.[16] To more clearly understand the effect of citrullination on the degradation of the human and marmoset forms of MOG$_{35-55}$, both the non-citrullinated and Cit$_{46,52}$ forms of marmoset and human MOG$_{35-55}$ were incubated with purified hCatG for 24 hours at 37°C and pH 5. At timepoints 0, 1, 2, 4 and 24 hours a sample was taken and measured

by LC-MS. The disappearance of the starting peptides was quantified and the data was plotted in Figure 4A.

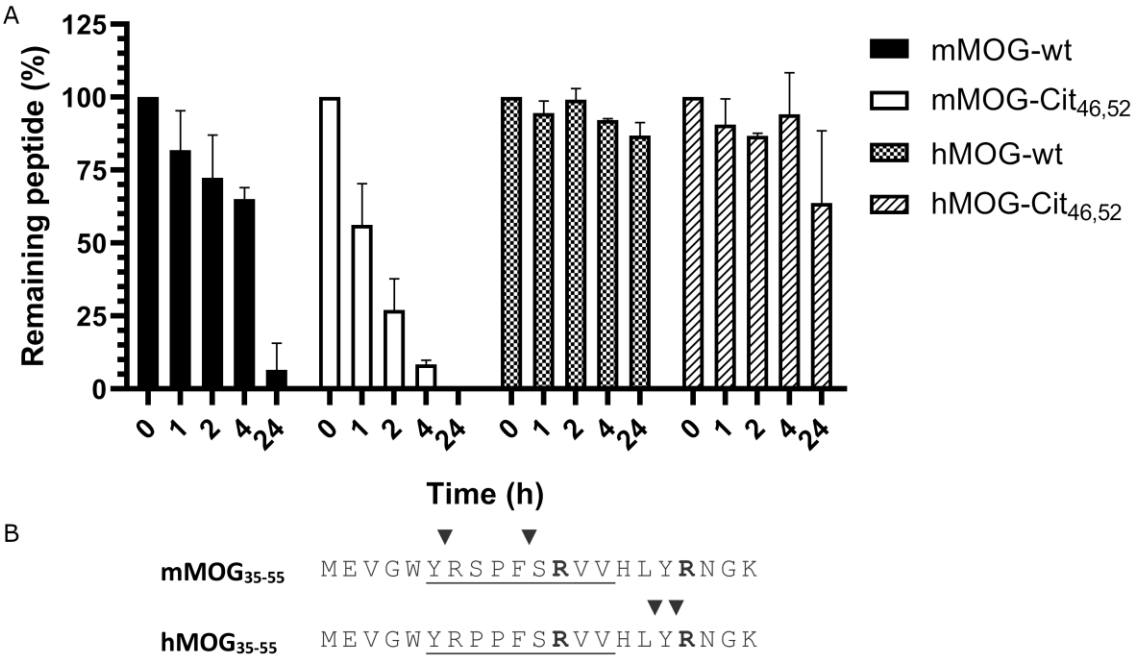

Figure 4. A) Degradation of peptides with human Cathepsin G at 37°C and pH 5. Peptides (10 µM) were incubated with hCatG (250 ng/mL) and samples were taken out at the stated time points and enzymatic activity was stopped by dilution of a 45:45:10 mixture of H_2O/MeCN/TFA. The samples were analyzed using LC-MS and amount of degradation determined by comparison of peak area against an internal standard. The graph shows the average of two independent experiments for each peptide. B) Mass spectrometry analysis was used to determine the cleavage sites of hCatG by analyzing the mass-spectra of the fragments formed after degradation. Arrows indicated detected cleavage sites. The immunodominant epitope MOG_{40-48} is underlined and the citrullinated arginine residues highlighted in bold.

The marmoset peptide $mMOG_{35-55}$ showed clear degradation over time, with the peptide being almost fully degraded after 24 hours. In contrast to what was seen by Jagessar *et al.*[14], the peptide containing citrulline on position 46 (as well as on position 52) was degraded by hCatG at an increased rate, with almost all peptide cleaved after only 4 hours. Earlier work on the sequence preference of hCatG showed that an acidic, negatively charged residue is preferred on the P2' position,[19] which could explain why neutral citrulline in P2' results in a higher rate of hydrolysis compared to positively charged arginine.

For the human peptides, degradation occurred sluggishly for either sequence. This might be explained by examining the peptide fragments formed by hCatG for the different peptides. For each peptide fragment detected in LC-MS, the mass was assigned to a fragment of the respective parent peptide (Figure 4B). This analysis indicated that the marmoset sequence gets rapidly degraded by cleavage in the middle of the T-cell epitope, between the Phe_{44} and Ser_{45} residues. This is followed at a slower rate by a cleavage after Tyr_{40}. The presence of the Pro_{42} residue in the human sequence (instead of Ser_{42} in the marmoset sequence) seems to completely abrogate these cleavage sites, instead preferring two more productive cleavage sites on the C-terminal end of the sequence.

In conclusion, the unexpected T-cell activation by the cross-presentation of $hMOG_{35-55}$-$Cit_{46,52}$, in comparison to the immunologically inactive $mMOG_{35-55}$-$Cit_{46,52}$ remains not fully explained. The observed cross-reactivity for $hMOG_{35-55}$-$Cit_{46,52}$ in $hMOG_{35-55}$ marmosets is however quite interesting, as this is in contrast with the findings in a similar murine model,[17] where $mMOG_{35-55}$ immunized mice did not show cross-reactivity with $mMOG_{35-55}$-Cit_{46}. Further study of the biophysical and biochemical differences between these peptides is therefore necessary for the development of better animal models of multiple sclerosis.

However, these experiments and the experiments described in Chapter 3, as well as most work on the citrullination of MOG, have been carried out on peptide level. It is expected that substantial differences between the wild-type and (site-specifically) citrullinated protein could exist. Non-site-specifically citrullinated proteins can be generated *in vitro* by treatment with recombinant peptidyl arginine deiminase (PAD) enzymes, but these would not enable the study of the exact role of different citrullination sites. Alternatively, chemical or chemoenzymatic semi-synthesis of the entire protein would be able to generate site-specifically modified material. Here, synthetic peptides are ligated together using either native chemical ligation (NCL)[20,21] or enzymatic ligation to produce native amide bonds. These types of approaches enable peptide chemists to get around the typical limitations of synthetic peptide chemistry, which usually is limited to the synthesis of peptides <50 amino acids, to produce longer peptides and (small) proteins. Both of these methods involve the ligation of unprotected synthetic peptides to synthetic or expressed protein fragments in aqueous buffer. However, both methods differ in the functional requirements of the fragments that are to be ligated.

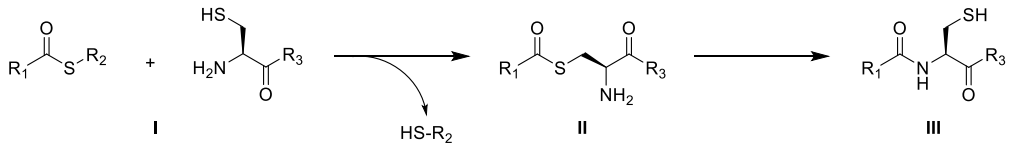

Figure 5. General mechanism of native chemical ligation. R_1 and R_3 denote two peptide chains, while R_2 denotes the thiol catalyst.

In native chemical ligation, a cysteine residue on the N-terminus of one peptide fragment reacts with a thioester on the C-terminus of the other (or the same, when cyclisation is desired). This nucleophilic attack of the cysteine thiol onto the carbonyl results (Figure 5, I) in a thioester exchange, producing intermediate II. The N-terminal amine of the cysteine can then perform a nucleophilic attack on the carbonyl, performing a S-to-N shift via a 5 membered ring transition state and forging a peptide bond, effectively condensing the two peptide fragments. However, cysteine is a quite rare amino acid in native human proteins (1.5-2.2% of all amino acids in the proteome)[22,23] and the requirement for this amino acid at the ligation site somewhat limits the application. To alleviate this, desulphurization chemistry was developed, enabling the conversion of cysteine residues into alanine. In this way, the scope of native chemical ligation reactions was expanded to more common alanine containing junctions.[24,25]

Here, the application of these approaches is evaluated for the synthesis of site-specifically citrullinated extracellular domain of MOG. Since the arginine residues of interest (Arg_{41}, Arg_{46}, Arg_{52}) are all in close proximity of each other and relatively close to the N-terminus of the protein, a semisynthetic approach was considered initially. This would involve the production of the C-terminal part of the protein using recombinant expression, while the N-terminal region would be produced synthetically. Only two cysteine residues are present in the sequence of MOG_{1-125}, one on position 24 and another on position 98. Neither of these are in a beneficial position for ligation with a peptide fragment that contains the desired citrulline replacements, so an alanine-to-cysteine replacement was considered instead. A viable ligation site was found between Gln_{61} and Ala_{62}, producing two fragments, MOG_{1-61} and $MOG_{62-125}A_{61}C$. The unnatural cysteine in position 62 can be removed post-ligation using a desulphurization reaction, reducing the residue to the natural alanine. This will, however, have the drawback of simultaneously reducing the natural Cys_{98} to alanine.

Looking at the SPPS based part of the route, the MOG_{1-61} peptide required for the N-terminal half of the protein is still on the large side for synthetic peptide chemistry. To alleviate this, a second disconnect between Pro_{23} and Cys_{24} was added, in order to reduce the complexity, and therefore potentially increase the yield, of the SPPS part of the route. To provide regioselectivity, the cysteine residue on the N-terminus of the MOG_{24-61} fragment will initially be protected as a thiazolidine, ensuring regioselectivity in the first ligation. This approach is outlined in Figure 6.

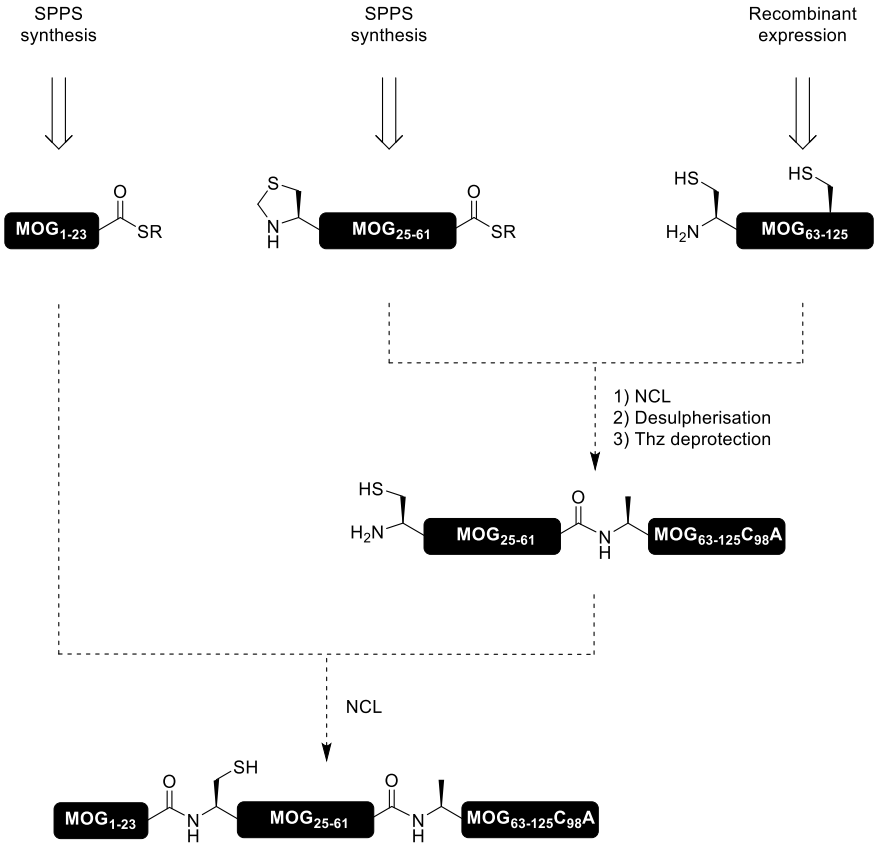

Figure 6. Initial semisynthetic approach towards MOG_{1-125}.

Since ligation on proline-thioesters is known to be difficult,[26] this ligation junction was evaluated first. The MOG_{1-23} peptide was synthesized bearing two different thioester surrogates on the C-terminus. Thioester surrogates are commonly used during the SPPS assembly of peptides for NCL, since thioesters themselves are not stable to all steps in Fmoc-SPPS (i.e. Fmoc deprotection with piperidine/DMF).[27] MOG_{1-23} was synthesized bearing either the bis(2-sulfanylethyl)amido (SEA)[28] (**1**) or *N*-acyl-benzimidazolinone (NBz)[29] (**2**) group on the C-terminus. Both of these were ligated under various different conditions with a test peptide consisting of the first six amino acids after the ligation junction (MOG_{24-29}, **3**). These experiments (Figure 7A) showed that the NBz thioester surrogate **2** shows the most promise for this thioester junction. The optimal conditions were 6 M guanidine in 200 mM NaPi buffer, pH 7.0, with 200 mM mercaptophenylacetic acid (MPAA) as thiol catalyst and 50 mM triscarboxyethylphosphine (TCEP).

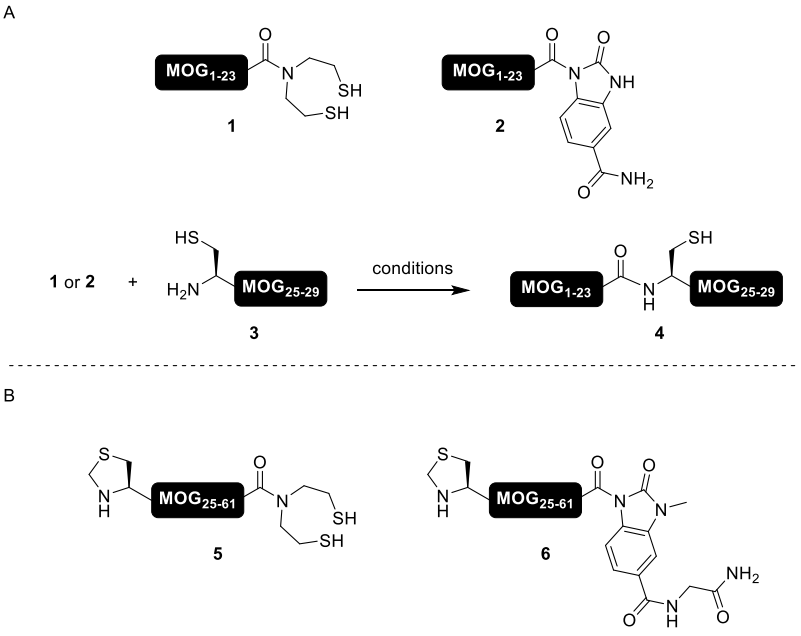

Figure 7. A) MOG_{1-23} peptide as a C-terminal SEA (**1**) and NBz (**2**) derivative and the test ligations performed on these peptides with MOG_{24-29} (**3**). B) Structure of the C-terminal SEA (**5**) and MeNBz (**6**) derivatives of MOG_{24-61}.

The synthesis of the middle fragment (MOG_{24-61}) was initialized on solid support containing the SEA linker using, after the loading of the first amino acid, standard Fmoc-SPPS conditions. LC-MS analysis of the crude peptide indicated a multitude of monodehydrated (Δm = -18 Da) or bisdehydrated (Δm = -36 Da) species, which were assumed to be the result of aspartimide formation.[30] Dimethoxybenzyl protection[31] of the peptide backbone at the $Aps_{58}Gly_{59}$ dipeptide was applied, which limited but not abolished the aspartimide formation. When, as an additional measure, a small percentage (1% (v/v)) of formic acid was introduced into the Fmoc deprotection solution (20% (v/v) piperidine in DMF), as described by Michels *et al.*,[32] this side reaction was fully suppressed, allowing synthesis of SEA peptide **5**. To evaluate a different latent thioesters for this ligation reaction, the MOG_{24-61} peptide was also synthesized as an *N*-acyl-*N'*-methyl-benzimidazolinone (MeNBz)[33] thioester surrogate (**6**). However, the

MeNBz acylurea moiety was found to be unstable on this peptide during RP-HPLC purification, resulting in contamination of the isolated peptide with hydrolyzed peptide, and this option was abandoned.

For the expression and subsequent purification of the $MOG_{62\text{-}125}A_{62}C$ fragment (**7**), a construct was created bearing a His_6-tag followed by a TEV cleavage site at the N-terminal site of the peptide. The His-tag would aid purification of the peptide, while the TEV cleavage site would enable liberation of the N-terminal cysteine required for ligation. While expression and purification of this protein fragment could be conducted without incident, removal of the His-tag via TEV cleavage did not proceed as planned. After addition of the TEV protease, disappearance of the protein construct was observed by both SDS-PAGE and LC-MS, but the cleaved fragment was not observed. The was assumed to be caused by a lack of solubility of the fragment in the protease buffer. This, combined with a concern about the importance of the Cys_{98} residue, shown to form a disulfide bond with Cys_{24},[34] that would be mutated to alanine using this approach, instigated an investigation into alternative synthetic routes.

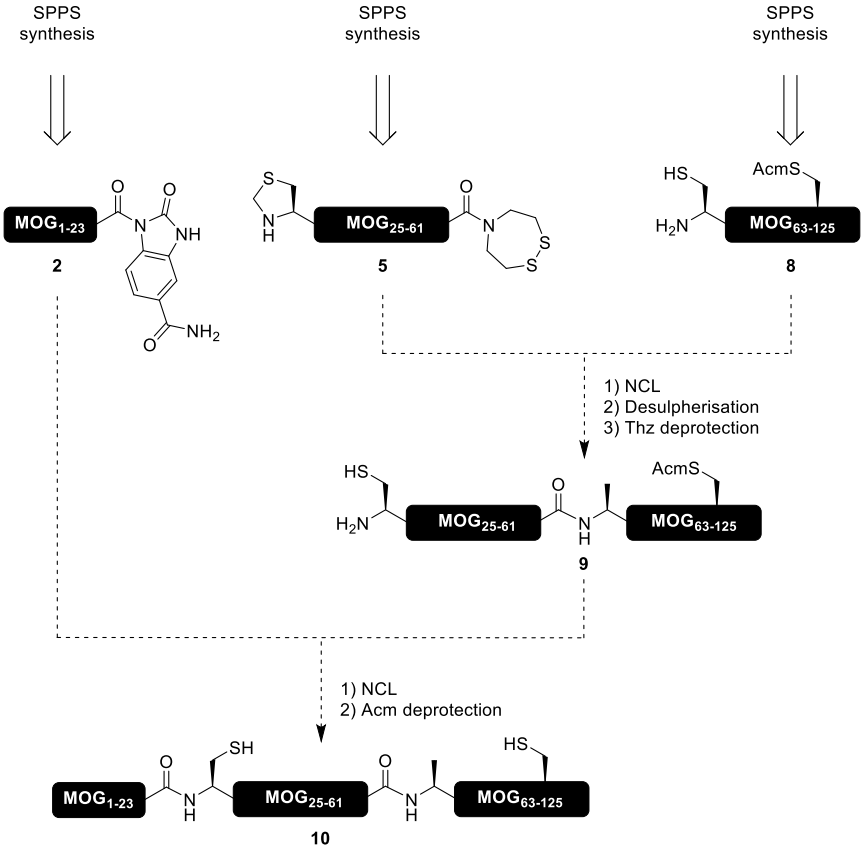

Figure 8. Proposed synthesis of $MOG_{1\text{-}125}$ utilizing three synthetic peptides and two ligation steps.

First, a chemical synthesis based on the already designed semisynthetic approach was considered (Figure 8), producing the $MOG_{62\text{-}125}A_{62}C$ fragment using SPPS instead of recombinant expression. This would allow the incorporation of an acetamidomethyl (Acm) protecting group on Cys_{98}, facilitating selective desulfurization of Cys_{62}. However, at 64 residues, this peptide would be outside the range of easily synthesizable peptides. In an

attempt to synthesize this long peptide, all amino acid couplings were carried out as double couplings, that is repetition of the coupling cycle before Fmoc deprotection. Additionally, pseudoproline protected dipeptides[35] were applied on the $Phe_{96}Thr_{97}$ and $Val_{81}Thr_{82}$ positions, which have been used to great effect during the chemical synthesis of other long peptides.[36] However, even when combining all of these techniques, the quality of the crude peptide was poor and the desired $MOG_{62\text{-}125}A_{62}C$ (**8**) could not be isolated.

In order to simplify the solid support synthesis of the peptides, an additional NCL disconnect between Thr_{97} and Cys_{98} was envisioned (Figure 9). While this simplification of the peptide synthesis should allow for easier purification and higher yields of the peptide fragments, this comes at the cost of additional steps during the assembly of the protein. To facilitate facile desulfurization of Cys_{62}, that is without the need for additional protecting group manipulations, the ligation between fragment **11** and **12** was selected as the first ligation. This required an inert latent thioester on the C-terminus of this fragment, for which a hydrazide function was selected.[37] Since the activation of the hydrazide function requires low pH, the thiazolidine group used previously as N-terminal protection for peptide **5** would no longer be orthogonal. An Acm group was chosen instead as an orthogonal protective group for the N-terminal cysteine in peptide **11**.

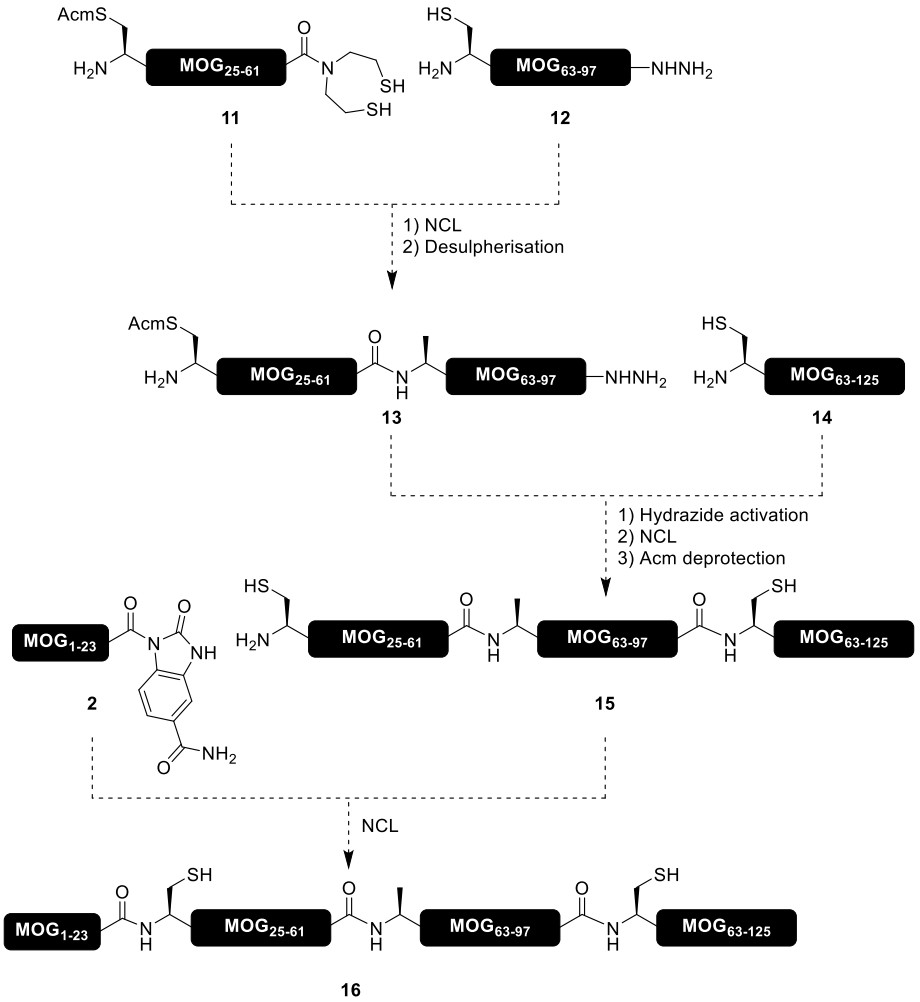

Figure 9. Total chemical synthesis of MOG1-125 using a four peptide three ligation approach. All peptides (**2**, **11**, **12** and **14**) were produced synthetically using SPPS.

Synthesis of all four of these peptides proceeded smoothly, and the ligation of fragments **11** and **12** was evaluated. For NCL reactions, the usual catalyst is the thiophenyl derivative MPAA. However, aromatic thiols have been shown to negatively interfere with the radical desulfurization chemistry.[38] Therefore, alternative catalysts have been proposed to enable one-pot ligation-desulfurization approaches. The most promising of these catalysts is trifluoroethanethiol (TFET),[39] and the ligation reaction was first evaluated using this catalyst, using **5** instead of **11** (Figure 10). Regrettably, only a small amount of ligation was observed, with both starting peptides showing significant degradation. As an alternative, a ligation reaction using a concentration of MPAA lower than normal was considered. This smaller amount of MPAA could then be removed using diethylether washes, potentially enabling one-pot ligation-desulfurization, although in a more laborious manner. These reactions seemed to proceed more effectively, with around 50% conversion observed after 24h. Oxidation, both in the form of disulfide formation with MPAA as well as methionine oxidation, was however a major side reaction.

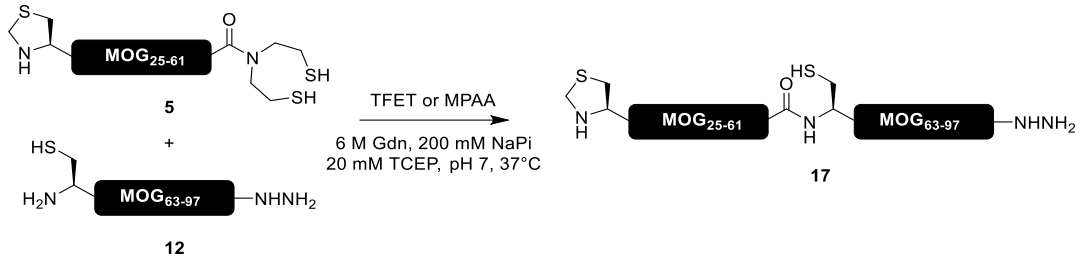

Figure 10. Attempted ligation of fragments **5** and **12**. Both TFET and MPAA were evaluated as thiol catalysts for this ligation.

As a third and final attempt, a chemoenzymatic ligation approach was considered. For this, Omniligase-1,[40] an enzyme capable of catalyzing the ligation between a peptide ester and a free N-terminus, was applied. This enzyme is an example of the class of peptide ligases, which were recently reviewed by Nuijens *et al*.[41] Omniligase itself is an modified form of another ligase enzyme, Subtiligase, engineered to broaden the substrate scope. As the name implies, the resulting enzyme has a broad substrate sequence scope for both the peptide ester and the amine fragment. Furthermore, it also has an improved S/H ratio, that is the ratio between productive ligation and peptide ester hydrolysis. Because of these features, Omniligase-1 is under active investigation as the enzyme of choice for chemo-enzymatic peptide synthesis (CEPS) of pharmaceutical peptides, like the GLP-agonist peptide exenatide.[42]

For the chemoenzymatic synthesis of $MOG_{1\text{-}125}$, a strategy using a single disconnect was considered optimal, as this would circumvent laborious protecting group manipulations. Since no PTMs are desired in the C-terminal fragment of the protein, a semisynthetic approach was taken. As for the ligation junction, the $Val_{47}Val_{48}$ junction was chosen, as the ligase has been shown to prefer aliphatic amino acids on both the C-terminal and N-terminal side of the ligation junction.[43] There are however two downsides to this ligation junction: i) it removes the ability to study citrullination of Arg_{52}, and ii) the critical Arg_{46}Cit modification would be in the P2 pocket of the ligase. Since the tolerance of the enzyme towards of citrulline residues inside the enzyme pocket has not previously been tested, this had to be evaluated before synthesis of the full protein could be attempted.

The tolerance of the enzyme for citrulline in P2 was evaluated by a test ligation between $MOG_{48\text{-}53}$ (VHLYRN) as the nucleophilic fragment and $MOG_{43\text{-}47}$ (PFSXV, with X = Arg or Cit) C-terminally functionalized with a carboxyamidomethyl-leucine (OCamL) ester, the preferred C-terminal ester of Omniligase-1.[44] The N-terminal proline on the $MOG_{43\text{-}47}$ fragments prevents homoligation, ensuring that the ligated $MOG_{43\text{-}53}$ fragment and hydrolysis of the Cam ester are the only observed products. Under these conditions, both ligations show full consumption of the peptide ester fragment in two hours (Figure 11). For arginine containing ester **18**, a S/H (Synthesis/Hydrolysis) ratio of 2.0 was observed. The ratio was slightly worse for citrulline containing peptide **19** at 1.6. While these ratios are not as high as those obtained with other peptide esters tested with Omniligase-1, this result does indicate that citrulline is tolerated in the P2 pocket, potentially enabling the synthesis of the desired citrullinated MOG protein, as well as other citrullinated proteins.

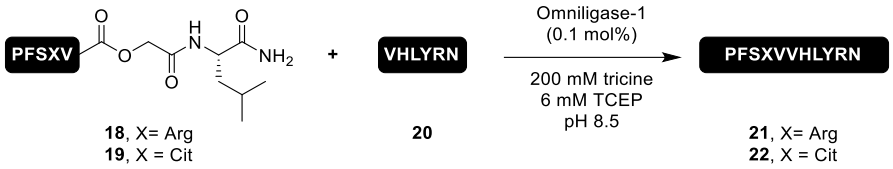

Figure 11. Test ligation reactions to determine the tolerance for citrulline in the P2 pocket of omniligase-1.

Next, the MOG_{48-125} fragment required for the ligation was expressed. This fragment was initially expressed C-terminally fused to a TEV cleavage site, followed by His_6 extension, creating the MOG_{48-125}-TEV-His_6 fusion protein **24**. This polypeptide was expressed and purified in a similar manner as the His_6-TEV-$MOG_{62-125}A_{62}C$ polypeptide (**7**) described above. Removal of the His-Tag via TEV protease was left for a later stage, since a C-terminal modification should not interfere with the ligation experiments. For the peptide ester part of the ligation, a peptide covering the native sequence of MOG_{27-47}, C-terminally extended with OCam followed by LKK was synthesized (**23**). These extra C-terminal lysines are not required for the ligation, but are tolerated by the enzyme and could help solubility of the peptide ester. This fragment again contained an N-terminal proline, preventing homoligation.

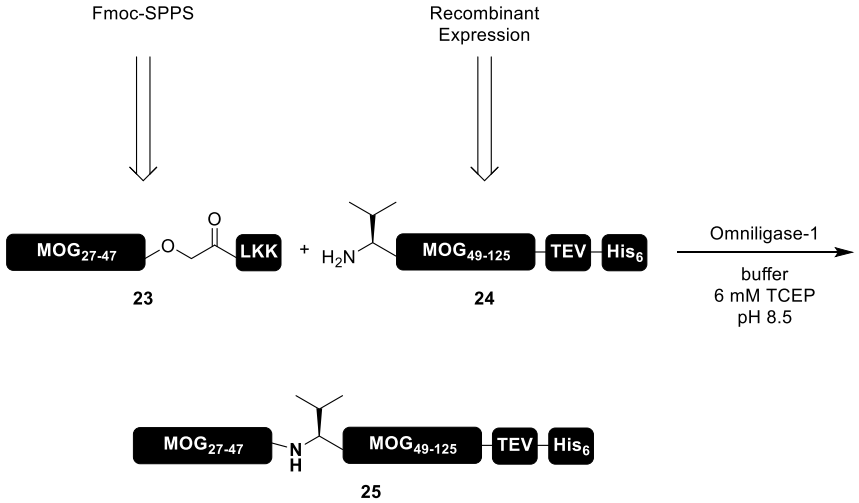

Figure 12. Test ligations with Omniligase-1 using expressed protein fragment **24** together with synthetic peptide **23**. A variety of different buffer compositions were tested, as outlined in table S1.

Since the protein fragment was expressed in inclusion bodies, solubilization with chaotropic agents was required. The protein could be solubilized with either 8 M urea or 6 M guanidine, with guanidine giving better recovery of protein. However, Omniligase-1 is hindered by the presence of chaotropic agents, and does not tolerate urea concentrations > 6 M or guanidine concentrations > 2 M.[43] Therefore, chaotrope concentrations were lowered after purification of the protein fragments by ultrafiltration over a 3 kDa molecular weight cut-off filter. Furthermore, both sodium phosphate and tricine buffers were evaluated, as the employed buffer salt can also influence the enzymatic ligation. For all conditions tested, complete consumption of peptide ester **23** was observed by LC-MS analysis after 4h. It was confirmed that this was primarily due to enzymatic hydrolysis, and not hydroxide mediated hydrolysis due to the high pH of the buffer, as incubation of peptide **23** in ligation buffer for up to 4 hours

yielded negligible hydrolysis. All ligation reactions were followed over time by LC-MS, at 0, 1, 2 and 4 hours. Since the peaks of polypeptide **24** and **25** did not separate on C18-column, conversion was estimated by SDS-PAGE analysis of the reaction mixtures after 4 hours. A complete overview of all ligation conditions is given in supplementary Table S1.

Briefly, while guanidine achieved the highest protein concentration and therefore the best conversion, a 2 M concentration was not enough to keep the protein soluble at room temperature. The same was found for 2 M urea, where also precipitation was observed. 4 M urea in tricine buffer was chosen as the best combination, with a compromise between protein solubility and ligase activity.

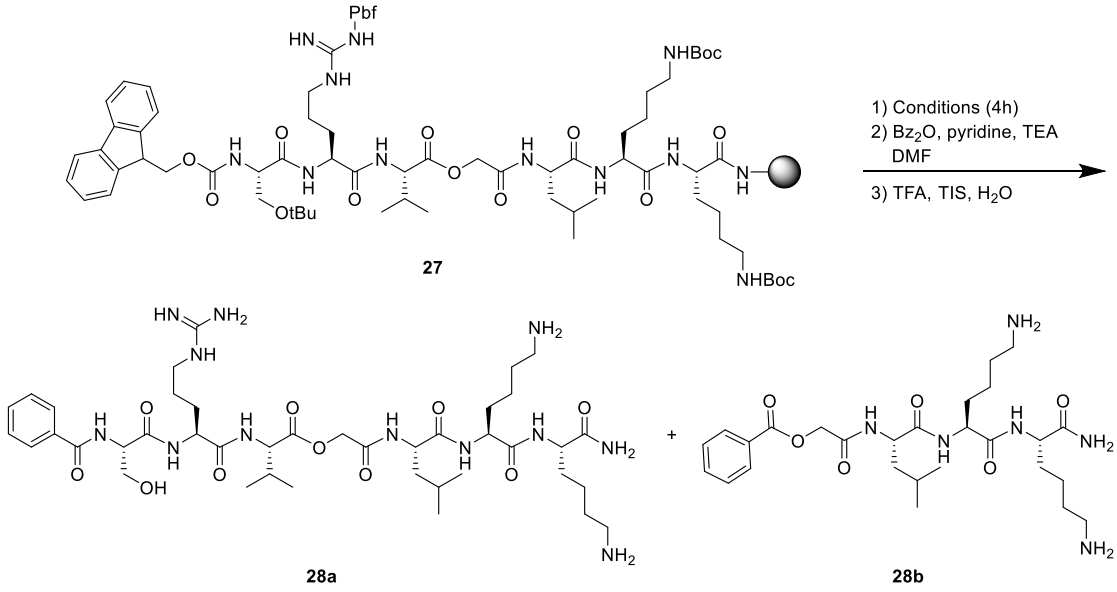

Figure 13. Demonstration of the experiment used to evaluated the stability of resin-bound ester **27** when treated with various Fmoc-deprotection conditions.

To evaluate the efficiency of these conditions for the semisynthesis of MOG_{1-125}, the synthesis of the N-terminal peptide MOG_{1-47}-OCamLKK (**26**) was required. To achieve a high quality crude product after SPPS, and therefore high yields of this substantial peptide, the SPPS needed to be properly optimized beforehand. The ester at the C-terminal side of the peptide could suffer from unintentional aminolysis (or hydrolysis if water is present) during the many Fmoc-deprotection steps required, especially at the elevated temperatures commonly used in microwave assisted peptide synthesis. A selection of commonly employed Fmoc-deprotection mixtures were tested on resin bound peptide **27**, consisting of the three C-terminal amino acids of MOG_{1-47} coupled to the OCamLKK ester. These deprotection solutions were tested at room temperature, 50°C and 90°C, in each case for 4 hours. After the removal of the deprotection solution, the resin was treated with a mixture of benzoic anhydride, pyridine and triethylamine in DMF, to benzoylate both the free amine and alcohol functions. Next, the peptides were liberated from resin with TFA (95:2.5:2.5, TFA/H_2O/TIS) and analyzed by LC-MS. Using this approach, the ratio of intact versus deacylated peptide was determined

by ratio of the peak areas as determined by LC-UV. An overview of the results is shown in Table 2.

Table 2. Overview of the effect of different deprotection conditions on the stability of the ester bond in immobilized peptide **27**. For each condition, the peak area of the peak assigned to **28a** is given as a percentage of the total peak area in the chromatogram. All percentages as given as volume percent (v/v) of the solution in DMF, except for piperazine which is given as a weight percentage instead (w/v). RT = room temperature, ND = not detected.

	Temperature		
Condition	RT	50°C	90°C
20% Piperidine	>95%	88%	25%
20% Piperidine + 1% CHOOH	>95%	95%	84%
5% Piperazine	>95%	>95%	42%
50% Morpholine	>95%	95%	43%
2% DBU	>95%	73%	ND

At 90°C, the standard 20% (v/v) piperidine in DMF solution is quite capable of cleaving the ester bond, even on a sterically hindered residue like valine. By buffering the solution with the addition of formic acid, this reaction can be almost completely suppressed. At 50°C, the ester bond is nearly completely retained, indicating that temperature is the most critical factor for this side reaction. At room temperature, nearly no cleavage of the peptide ester was observed for any of the deprotection solutions. Therefore, the synthesis of peptide **26** carried out using room temperature Fmoc-deprotection protocols in the automated peptide synthesizer. By using these conditions and a combination of manual and automated SPPS protocols, peptide **26** was isolated in 7% yield.

This peptide ester was then used in a test ligation with protein fragment **24**, using the same conditions as described for the test ligations with peptide **23**. However, during these reactions, both ligation and enzyme catalyzed hydrolysis proceeded exceptionally slow. Furthermore, peptide **23** was found to be unstable on storage, with, besides expected methionine oxidation, an unknown degradation product appearing upon prolonged storage. Therefore, further optimization of this ligation reaction is required before semisynthesis of $MOG_{1\text{-}125}$ can be achieved.

Chapter 4 describes the synthesis of a series of antigenic peptides bearing N-terminal glycoclusters and a C-terminal fluorophore. The antigen of choice is the well-studied ovalbumin-derived peptide $OVA_{247\text{-}264}$, containing the $CD8^+$ T-cell restricted epitope $OVA_{257\text{-}264}$. The fluorophore allows for the detection of the glycosylated peptides upon binding to a lectin, like the mannose receptor (MR), using a technique called glyco-PAINT.[3] By direct incorporation of the fluorophore onto the glycoconjugate antigen, the MR binding and uptake of these peptides can be directly measured using the glyco-PAINT technique. By combining

glycocluster, antigen and fluorophore into a single construct, the opportunity arrives to directly correlate MR binding with T-cell activation. This could contribute to the understanding of the effect glycosylation has on antigen cross-presentation, a topic of active research and debate.[4,45] Furthermore, the synthetic techniques used in this chapter could also be used for the generation of synthetic, glycosylated vaccine candidates.

Synthesis of these conjugate peptides did not proceed without problems. The oligosaccharides were introduced with copper catalyzed click chemistry (CuAAC) using propargylated glycans. To facilitate this conjugation, a series of azidolysine residues were included on the N-terminal side of the peptide. However, incorporation of multiple azidolysine residues critically lowered the solubility of the resulting peptides, severely hindering the following CuAAC reactions. To alleviate this, a flexible PEG based spacer was introduced between the N-terminus of the antigenic peptide and the glycocluster, greatly increasing solubility and enabling the synthesis several glycosylated peptides. Furthermore, determining the effect of the PEG spacer on the MR binding kinetics of the glycoconjugates could give valuable information for further design of antigen-glycocluster conjugates.

For further development in this area, peptides containing a $CD4^+$ T-cell restricted epitope could also be similarly decorated with glycocluster and fluorophore. A useful model epitope to consider here is the $OVA_{323-339}$ peptide for which, just like $OVA_{247-264}$, a variety of specific T-cell have been developed. Some initial explorations into these peptides were made, as shown in Figure 14A.

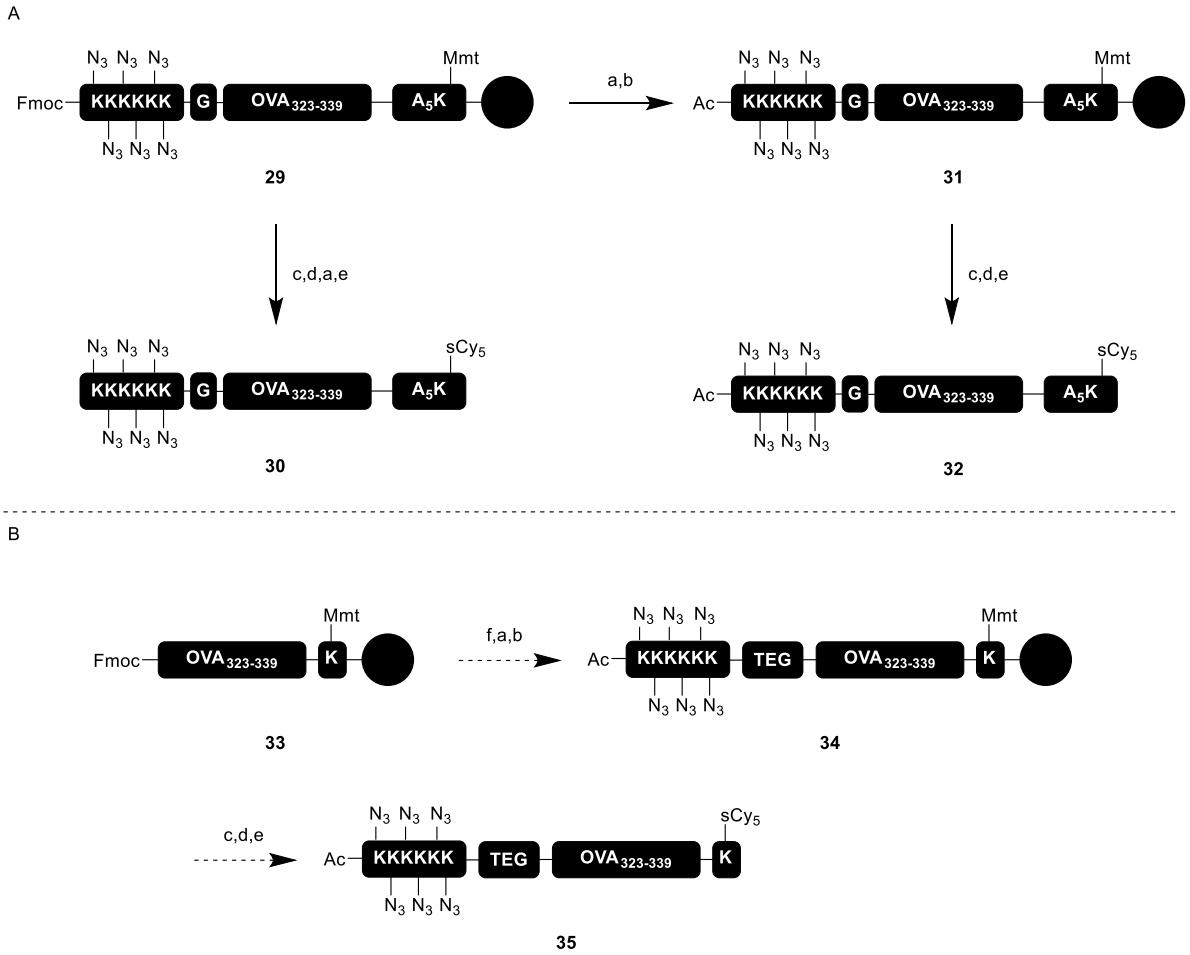

Figure 14. A) Failed synthesis of $OVA_{323-339}$ based model antigenic peptides **30** and **32**. B) Proposed synthesis of new $OVA_{323-339}$ model antigenic peptide **35**. Reagents and conditions: a) 20% (v/v) piperidine, DMF b) Ac_2O, DiPEA, DMF c) AcOH, TFE, DCM d) sCy5-OH, HCTU, DMF e) TFA, TIS, H_2O f) Fmoc-SPPS.

First, a similar approach to the $OVA_{247-264}$ based peptides was taken. The C-terminus of the epitope was extended with the amino acid sequence AAAAAK, the lysine bearing the highly acid labile Mmt protective group. N-terminally, the peptide was extended with a glycine residue, followed by six azidolysine residues. Using standard automated SPPS conditions, immobilized peptide **29** was obtained. The Mmt protective group was then selectively removed with AcOH and TFE in DCM. Next, the fluorophore was incorporated, using HCTU as a mediator. Finally, the N-terminal Fmoc was removed and the peptide liberated from the support. This yielded a very poor quality crude, with high amounts of double fluorophore modified material present, as well as many unidentified side products. Recovery of the desired peptide **30** from this mixture using RP-HPLC was unsuccessful. The issue of undesired over labeling of the N-terminus of the peptide was addressed by acetylation, as was done for the $OVA_{247-264}$ derived model peptide, to produce resin-bound peptide **31**. The C-terminal lysine was, after Mmt cleavage, again modified with fluorophore. After cleaving the peptide from the support, the level of fluorophore incorporation, however, was found to be low. Furthermore, the crude material was highly insoluble, making RP-HPLC challenging.

Instead, a new scaffold based around the $MOG_{323-339}$ peptide could be considered (Figure 14B). The synthesis would start from peptide **33**, removing the C-terminal penta-alanine spacer. N-terminally, the same TEG spacer using in chapter 4 could be incorporated between the N-terminus of the epitope and the azidolysine cluster (**34**). This combination of changes should hopefully increase solubility of the scaffold sufficiently to allow for efficient synthesis and purification of peptide **35**.

Chapter 5 outlines the synthesis of a cyclic, pentavalent scaffold conjugated with glycans via CuAAC chemistry. This scaffold consists of a series of six lysine residues, five used as carbohydrate attachment points. The sixth lysine was used to conjugate a fluorophore to the scaffold, creating a trackable, multivalent glycoconjugate. To realize this goal, a combination of on-resin chemistry, to build the scaffold, and off-resin conjugation reactions were used. To create the cyclic core of the molecule, on-resin cyclization of the peptide backbone was used, using a head-to-tail cyclization approach as has been reported many times in the literature. However, like in many other cases, on-resin dimerization during the cyclization phase was a major obstacle, resulting in very little product formation. The length of the linear peptide, which was significantly greater than the length of the typical linear peptide of most published cyclization reactions, seemed to play a major part here. By changing the design slightly, going from a 6-carbon to a 4-carbon spacer amino acid between the carbohydrate attachment points, the cyclization was carried out successfully. Next, long, polyethylene glycol (PEG) based spacers were introduced onto the five lysine residues. To accomplish this, all five of these residues needed to be deprotected without damaging the labile resin linkage. Using highly acid labile monomethoxytrityl groups in combination with a mildly acidic deprotection solution, very high conversion with good retention of the resin linker was achieved. Finally, CuAAC mediated glycan conjugation, using the methods from Chapter 4, followed by fluorophore labeling, produced the desired labeled glycoconjugates.

With this effective method in hand, glycoconjugates with different valencies can be produced in a straightforward manner, assuming the length of the peptide backbone won't interfere with the cyclization step. Since there are many tetravalent lectins with important functions in immunology, like DC-SIGN[46] and the cation-independent mannose-6-phosphate receptor (CI-MPR),[47] a tetravalent design would be an interesting next step. Using the chemistry developed in Chapter 5, such a ligand could be relatively straightforward to synthesize. A clickable ligand for the CI-MPR, bearing a non-hydrolyzable phosphonate on the 6-carbon of mannose was recently published.[48] This molecules, however, has an alkyne as the conjugation group, necessitating the design and synthesis of a scaffold bearing azide handles for the conjugation. The synthesis of these scaffolds is described in Figure 15.

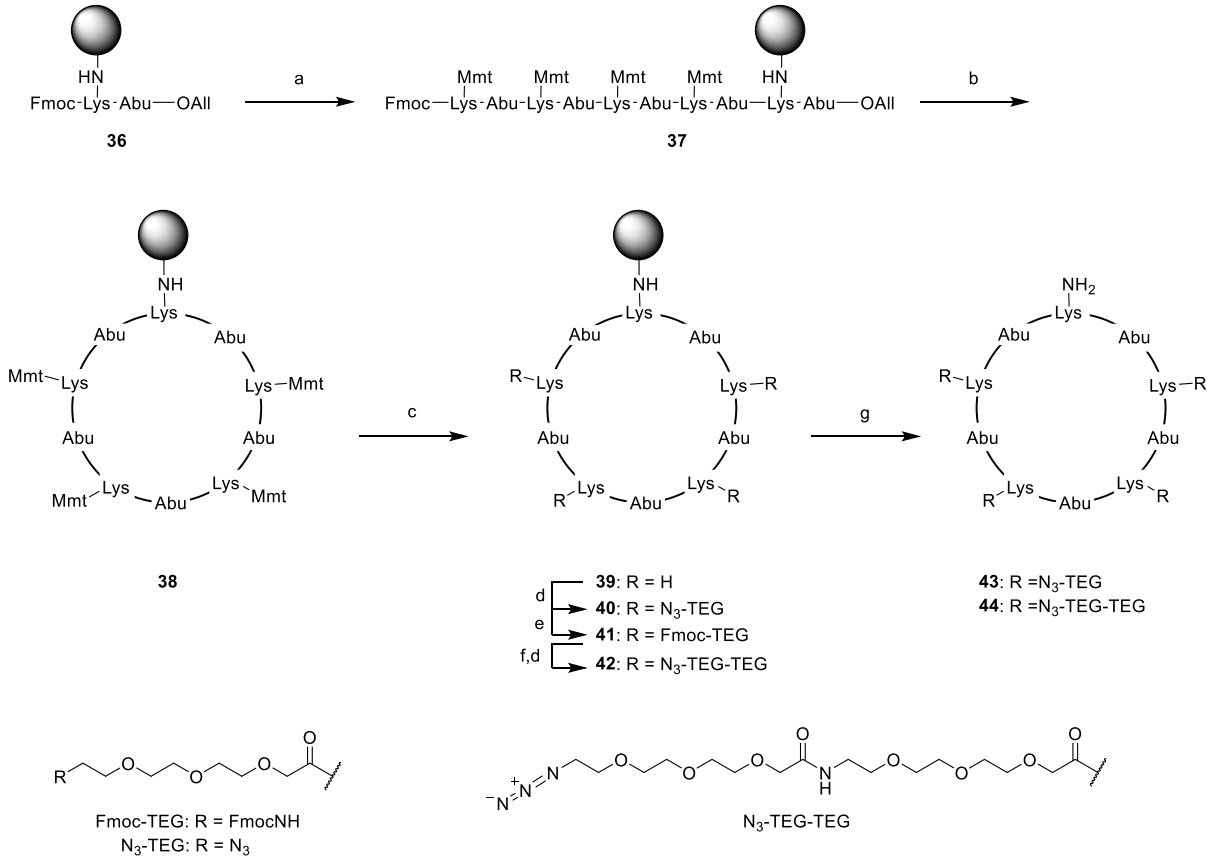

Figure 15. Synthesis of cyclic scaffolds **43** and **44** using the chemistry developed in Chapter 5. Reagents and conditions: a) Fmoc-SPPS b) i) $Pd(PPh_3)_4$, $PhSiH_3$, DCM ii) 2% (v/v) DBU, DMF iii) PyAOP, DiPEA, DMF c) AcOH, TFE, DCM d) N_3-TEG-OH, HCTU, DiPEA, DMF e) Fmoc-TEG-OH, HCTU, DiPEA f) 20% (v/v) piperidine, DMF g) i) TFA, H_2O, TIS ii) RP-HPLC (**43**: 9.8%), (**44**: 4.6%).

The synthesis started of as described in Chapter 5 from a dipeptide immobilized onto the solid support via a sidechain carbamate linkage (**36**). Standard Fmoc-SPPS conditions were used to elongate the peptide N-terminally (**37**). Using $Pd(PPh_3)_4$ and $PhSiH_3$ in DCM, the allyl ester was removed. After Fmoc deprotection using 2% (v/v) DBU in DMF, on-resin cyclization was carried out using PyAOP as the activator. Successful cyclization was confirmed by LC-MS analysis of a small portion of deprotected peptide, using the approach outlined in Chapter 5. The Mmt groups on immobilized peptide **38** were then removed using the AcOH/TFE cocktail (1:2:7 AcOH/TFE/DCM), producing immobilized cyclic peptide **39**. Since the requirements for good multivalent binding to CI-MPR are not known, two scaffolds with different lengths of spacer between the peptide backbone and the glycans were build. Half of **39** was acylated with N_3-PEG-OH, creating **40**. Acidic cleavage and RP-HPLC yielded **43** in 9.8% yield. The other half of **39** was first coupled with Fmoc-TEG-OH, producing **41**. The Fmoc-group was removed under standard conditions and N_3-TEG-OH was coupled, producing **42**. This compound was also released from the resin and purified, yielding **44** in 4.6% yield. The conjugation of these scaffolds with the mannose-6-phosphate ligand and a fluorophore remains to be explored.

Chapter 6 described development of a novel method for the synthesis of peptides containing a lysine residue protected with an allylic TCO group. Since TCO groups are rather sensitive to acidic conditions, direct Fmoc-SPPS synthesis of these peptides using, a TFA based global deprotection step, is not feasible. The novel approach involves the use of azide groups to mask all additional amines in the peptide (*i.e.* the N-terminus as well as additional lysine residues in the sequence). After global deprotection, the allylic TCO is introduced using an activated TCO carbonate. Following successful introduction of the modification, all azides are reduced to the corresponding amines using a Staudinger reduction with trimethylphosphine. This enables the synthesis of longer, TCO-caged peptides, containing multiple lysine residues. Furthermore, by not relying on a nucleophilic base-labile protecting group, like earlier works have done,[5,49] functions labile to nucleophilic base could also be introduced to the molecule, as was exemplified by the synthesis of a TCO-caged peptide containing a fatty acid ester.

Experimental

General methods for automated SPPS

Peptides were synthesized using automated Fmoc-SPPS on a Liberty Blue^{tm} automated microwave peptide synthesizer (CEM corporation). Synthesis was performed on a 100 µmol scale on Tentagel S RAM resin (loading 0.20-0.25 mmol/g, Rapp Polymere GmbH, Germany), unless stated otherwise. Resin was first swollen for 5 minutes in DMF prior to amino acid coupling. Activation was achieved using DIC/Oxyma coupling as is recommended by the manufacturer. The following amino acids were used: Fmoc-Ala-OH, Fmoc-Arg(Pbf)-OH, Fmoc-Asn(Trt)-OH, Fmoc-Asp(OtBu)-OH, Fmoc-Cit-OH, Fmoc-Cys(Acm)-OH, Fmoc-Cys(Trt)-OH, Fmoc-Gln(tBu)-OH, Fmoc-Glu(OtBu), Fmoc-Gly-OH, Fmoc-His(Boc)-OH, Fmoc-Ile-OH, Fmoc-Leu-OH, Fmoc-Lys(Boc)-OH, Fmoc-Met-OH, Fmoc-Phe-OH, Fmoc-Pro-OH, Fmoc-Ser(tBu)-OH, Fmoc-Thr(tBu)-OH, Fmoc-Trp(Boc)-OH, Fmoc-Tyr(tBu)-OH, Fmoc-Val-OH and Boc-Thz-OH. All amino acids were obtained from Novabiochem or Sigma Aldrich. Standard coupling was achieved using 5 equivalents amino acid as a 0.2 M amino acid/DMF solution, 5 equivalents DIC as a 0.5 M of DIC/DMF solution and 5 equivalents Oxyma as a 1 M Oxyma/DMF solution (also containing 0.2 M DiPEA), at 90°C for 2 minutes. Standard Fmoc deprotection was achieved by 20% (v/v) piperidine in DMF at 90°C for 90 seconds, repeated once. For peptide **5**, **6** and **11**, 1% (v/v) of formic acid was added to the deprotection solution and the Fmoc deprotection was carried out at room temp for 2 x 5 min instead. To analyze the quality of a resin bound peptide, a small amount of resin (~1mg) was treated with 200 µL of a TFA cocktail (95:2.5:2.5, TFA/H_2O/TIS) for 2 hours, after which the TFA was filtered into 800 µL of ice cold Et_2O. After five minutes the formed precipitate was collected by centrifugation and the supernatant discarded. The pellet was dissolved in 200 µL 1:1:1 H_2O/MeCN/tBuOH and subjected to LC-MS analysis. Peptides were characterized using electrospray ionization mass spectrometry (ESI-MS) on a Thermo Finnigan LCQ Advantage Max LC-MS instrument with a Surveyor PDA plus UV detector on an analytical C18 column (Phenomenex, 3 µm, 110 Å, 50 mm × 4.6 mm) in combination with buffers A (H_2O), B (MeCN), and C (1% aq TFA). Quality of crude was evaluated with a linear gradient of 10-90% B with a constant 10% C over 10 minutes. For mass analysis of peptides by low-resolution mass spectrometry (LRMS), calculated masses (calcd) were based on the most abundant isotopic pattern.

General methods for manual SPPS

Manual elongation of peptides was carried out in a fritted syringe at either 25 or 5 µmol scale. Fmoc deprotection was achieved using 20 % (v/v) piperidine in DMF in two steps, reacting 3 and 7 minutes respectively. Fmoc-Gly-OH was coupled using 5 equivalents of amino acid together with 5 equivalents of HCTU (as a 0.5 M solution) and 10 equivalents DiPEA for 45 minutes. Analysis of the quality of the resin-bound peptide was carried out as above.

General methods for resin cleavage and RP-HPLC purification

Global deprotection and resin cleavage of peptides was accomplished using a 95:2.5:2.5 mixture of TFA/TIS/H_2O for 3 hours, or a 90:2.5:2.5:2.5:2.5 mixture of TFA/Me_2S/thioanisole/H_2O/TIS for peptides containing a free cysteine, followed by precipitation from cold diethyl ether (1:9 ratio TFA to ether) and recovery of the precipitate by centrifugation. Crude, tryptophan containing peptides were

dissolved in MilliQ water and lyophilized overnight in order to remove the residual carboxylate. Preparative reverse phase HPLC on a Waters AutoPurification system (eluent A: H_2O + 0.2% TFA; eluent B: ACN) with a preparative Gemini C18 column (5 µm, 150 x 21.2 mm) yielded the final products after lyophilization. Quality of purified peptides was determined using a Thermo Scientific Vanquish UHPLC coupled to a Thermo Scientific LCQ Fleet ion trap electron spray ionization mass spectrometer (ESI-MS) using an analytical C18 column (Phenomenex, 3 µm, 110 Å, 50 mm × 4.6 mm) in combination with buffers A (H_2O), B (MeCN), and C (1% aq TFA). Quality of the peptides was evaluated with a linear gradient of 10-50% B with a constant 10% C over 9 minutes or a linear gradient of 5-65% B with a constant 10% C over 30 minutes.

Yields and analysis of peptides described in Table 1

Table 3. Overview of all synthesized peptides. [a] synthesis was previously described in Araman *et al.*[2]

Name	Sequence	Expected mass [M+2H]	Found mass [M+2H]	Yield (%)
mMOG$_{40-48}$-Cit$_{41}$	Y*Cit*SPFSRVV-OH	556.3	556.5	31.0
mMOG$_{40-48}$-Cit$_{46}$	YRSPFS*Cit*VV-OH	556.3	556.4	29.0
mMOG$_{40-48}$-Cit$_{41,46}$	Y*Cit*SPFS*Cit*VV-OH	556.8	556.9	32.7
mMOG$_{39-49}$-Cit$_{46}$	WYRSPFS*Cit*VVH-OH	718.3	718.1	17.2
mMOG$_{38-50}$-Cit$_{46}$	GWYRSPFS*Cit*VVHL-OH	803.4	803.2	26.8
mMOG$_{37-51}$-Cit$_{46}$	VGWYRSPFS*Cit*VVHLY-OH	934.6	934.5	27.4
mMOG$_{36-52}$-Cit$_{46}$	EVGWYRSPFS*Cit*VVHLYR-OH	1077.3	1077.1	13.3
mMOG$_{36-52}$-Cit$_{46,52}$	EVGWYRSPFS*Cit*VVHLY*Cit*-OH	1077.7	1077.6	27.2
mMOG$_{35-53}$-Cit$_{46,52}$	MEVGWYRSPFS*Cit*VVHLY*Cit*-OH	1200.4	1200.1	27.4

Experimental for MOG (semi)synthesis

Gly-Gln-Phe-Arg-Val-Ile-Gly-Pro-Arg-His-Pro-Ile-Arg-Ala-Leu-Val-Gly-Asp-Glu-Val-Glu-Leu-Pro-SEA (1)

500 µmol Tentagel PS chlorotrityl resin (1,44 µmol/g) was loaded with SEA linker in a 1:10 ratio followed by capping, as described by Ollivier et al.[28] This was followed by coupling of Fmoc-Pro-OH using 10 eq. amino acid and 9.5 eq HATU (as 0.5 M solution in DMF) together with 20 eq. DiPEA for one hour. Capping of unreacted secondary amines was carried out using a solution containing 10% (v/v) Ac_2O and 5% (v/v) DiPEA in DMF for 10 minutes, repeated once. An Fmoc loading test was carried out,[50] and loading was determined to be 0.12 mmol/g. The peptide was then further synthesized using the general manual SPPS conditions. Global deprotection followed by RP-HPLC purification yielded compound **1** as a white solid (11.5 mg, 4.3 µmol, 10%) **LC-MS** RT = 4.1 min (C18, 10-90% B over 9 minutes) **LRMS** calcd $[M+2H]^{2+}$ = 1337.7, $[M+3H]^{3+}$ = 892.5 observed M/z = 1338.1, 892.5

Gly-Gln-Phe-Arg-Val-Ile-Gly-Pro-Arg-His-Pro-Ile-Arg-Ala-Leu-Val-Gly-Asp-Glu-Val-Glu-Leu-Pro-NBz (2)

Dawson DBz AM resin (100 µmol, 0.47 mmol/g), preloaded with the diaminobenzamide (DBz) linker,[29] was acylated with Fmoc-Pro-OH using 5 equivalents of amino acid, 4.9 equivalents HATU (as a 0.5 M HATU solution in DMF) and 11 equivalents DIPEA for 90 minutes. The peptide was then further synthesized using the general manual SPPS conditions. To form the urea function of the NBz moiety, the Fmoc-protected resin was first treated with 5 equivalents of p-nitro-choloroformate in degassed DCM (0.25 M) for one hour. This was followed, after thorough washing, by treatment of the resin with a solution of N-methylmorphline (NMM) in DMF (0.5M) for 2 hours at 60°C. Global deprotection followed by RP-HPLC purification yielded compound **2** as a white solid (10.7 mg, 3.9 µmol, 3.9%) **LC-MS** RT = 14.2 min (C18, 5-65% B over 30 minutes) **LRMS** calcd $[M+2H]^{2+}$ = 1357.8, $[M+3H]^{3+}$ = 905.5 observed M/z = 1358.3, 906.0

Cys-Arg-Ile-Ser-Pro-Gly-NH_2 (3)

Peptide was synthesized on a 100 µmol scale on Tentagel S RAM resin using the standard condition for manual SPPS. Global deprotection followed by RP-HPLC purification yielded compound **3** as a white solid (46.3 mg, 73.4 µmol, 73%) **LC-MS** RT = 3.4 min (C18, 10-90% B over 9 minutes) **LRMS** calcd $[M+H]^{+}$ = 631.3 observed M/z = 631.4

Thz-Arg-Ile-Ser-Pro-Gly-Lys-Asn-Ala-Thr-Gly-Met-Glu-Val-Gly-Trp-Tyr-Arg-Pro-Pro-Phe-Ser-Arg-Val-Val-His-Leu-Tyr-Arg-Asn-Gly-Lys-Asp-Gln-Asp-Gly-Asp-Gln-SEA (5)

500 µmol Tentagel PS chlorotrityl resin (1,44 µmol/g) was loaded with SEA linker in a 1:10 ratio followed by capping, as described by Ollivier et al.[28] This was followed by coupling of Fmoc-Gln(Trt)-OH using 10 eq. amino acid and 9.5 eq HATU (as 0.5 M solution in DMF) together with 20 eq. DiPEA for one hour. Capping of unreacted secondary amines was carried out using a solution containing 10% (v/v) Ac_2O and 5% (v/v) DiPEA in DMF for 10 minutes, repeated once. The peptide was then further synthesized using the general automated SPPS conditions, using the formic acid containing Fmoc deprotection solution (1:20:79 CHOOH/piperidine/DMF). The $Asp_{58}Gly_{59}$ dipeptide was incorporated as the Fmoc-Asp(OtBu)-(Dmb)Gly-OH dipeptide building block. Global deprotection followed by RP-HPLC purification yielded compound **5** as a white solid (31.6 mg, 7.1 µmol, 14%). **LC-MS** RT = 13.8 min (C18, 5-65% B over 30 minutes) **LRMS** calcd $[M+3H]^{3+}$ = 1489.7, $[M+4H]^{4+}$ = 1117.5 observed M/z = 1489.4, 1117.4

Thz-Arg-Ile-Ser-Pro-Gly-Lys-Asn-Ala-Thr-Gly-Met-Glu-Val-Gly-Trp-Tyr-Arg-Pro-Pro-Phe-Ser-Arg-Val-Val-His-Leu-Tyr-Arg-Asn-Gly-Lys-Asp-Gln-Asp-Gly-Asp-Gln-MeNBz-Gly-NH_2 (6)

Peptide **6** was synthesized on a 100 µmol scale on Tentagel S RAM resin. The initial Gly residue was coupled manually, followed by manual coupling of the MeDBz linker, using 5 equivalents of Fmoc-MeDbz-OH, 5 equivalents HCTU as a 0.5 M HCTU/DMF solution and 5.5 equivalents DIPEA for 1 hour. Following Fmoc deprotection, Fmoc-Gln(Trt)-OH was coupled using 5 equivalents of amino acid, 4.9 equivalents HATU (as a 0.5 M HATU solution in DMF) and 11 equivalents DIPEA for 90 minutes. The peptide was then further synthesized using the general automated SPPS conditions, using the formic acid containing Fmoc deprotection solution (1:20:79 CHOOH/piperidine/DMF). The $Asp_{58}Gly_{59}$ dipeptide was incorporated as the Fmoc-Asp(OtBu)-(Dmb)Gly-OH dipeptide building block. Transformation of the MeDBz group into the MeNBz group was carried out as described by Blanco-

Canosa *et al.*[33] Global deprotection followed by RP-HPLC purification yielded 25.6 mg of peptide **6** as an inseparable mixture with the hydrolyzed peptide. **LC-MS** RT = 6.2 min (C18, 10-90% B over 9 minutes) **LRMS** calcd $[M+3H]^{3+}$ = 1527.1, $[M+4H]^{4+}$ = 1145.6 observed M/z = 1527.0, 1145.5. The co-eluting hydrolyzed peptide was also detected: calcd $[M+3H]^{3+}$ = 1450.0, $[M+4H]^{4+}$ = 1087.8 observed M/z = 1450.3, 1088.0.

Cys-Pro-Glu-Tyr-Arg-Gly-Arg-Thr-Glu-Leu-Leu-Lys-Asp-Ala-Ile-Gly-Glu-Gly-Lys-Val-Thr-Leu-Arg-Ile-Arg-Asn-Val-Arg-Phe-Ser-Asp-Glu-Gly-Gly-Phe-Thr-$NHNH_2$ (12)

2-Chlorotrityl chloride resin (200 µmol, 1.36 mmol/g) was modified with hydrazine monohydrate as described by Zheng *et al*.[51] Fmoc-Thr(tBu)-OH was manually coupled onto the hydrazine and a loading test was carried out, finding a loading of 0.3 mmol/g. The peptide was then further synthesized using the general automated SPPS conditions, using the formic acid containing Fmoc deprotection solution (1:20:79 CHOOH/piperidine/DMF). The $Val_{80}Thr_{81}$ dipeptide was incorporated as the Fmoc-Val-Thr(ψ(Me,Me)pro)-OH pseudoproline dipeptide building block. Global deprotection followed by RP-HPLC purification yielded compound **12** as a white solid (14.2 mg, 3.5 µmol, 7.7%). **LC-MS** RT = 3.7 min (C18, 10-50% B over 9 minutes) **LRMS** calcd $[M+3H]^{3+}$ = 1366.7, $[M+4H]^{4+}$ = 1025.3 observed M/z = 1367.2, 1025.8

Cys-Phe-Phe-Arg-Asp-His-Ser-Tyr-Gln-Glu-Glu-Ala-Ala-Met-Glu-Leu-Lys-Val-Glu-Asp-Pro-Phe-Tyr-Trp-Val-Ser-Pro-Gly-OH (14)

The peptide was synthesized using the standard methods for automated peptide synthesis starting from glycine preloaded Tentagel S Ac. Global deprotection followed by RP-HPLC purification yielded compound **14** as a white solid (4.9 mg, 1.5 µmol, 1.4%) **LC-MS** RT = 16.8 min (C18, 5-65% B over 30 minutes) **LRMS** calcd $[M+3H]^{3+}$ = 1127.8 observed M/z = 1128.1

Val-His-Leu-Tyr-Arg-Asn-NH_2 (20)

Synthesized on Tentagel S RAM resin (50 µmol) using the standard conditions for manual SPPS. Global deprotection followed by RP-HPLC purification yielded compound **20** as a white solid (26.5 mg, 33.2 µmol, 66%). **LC-MS** RT = 3.7 min (C18, 10-90% B over 9 minutes) **LRMS** calcd $[M+H]^{+}$ = 800.45 observed M/z = 800.53

General procedure for the on-resin synthesis of OCam peptide esters

The OCam function is introduced onto the resin by coupling 2 equivalents of Fmoc-OCH_2COOH, activated with 2 equivalents of HCTU (as 0.2 M in DMF) and 4 equivalents of DiPEA for 90 minutes. After Fmoc removal following the standard protocols, the C-terminal amino acid is acylated onto the alcohol using 4 equivalents of Fmoc-amino acid, together with 6 equivalents of DIC and 0.4 equivalents of DMAP. This reaction was allowed to proceed for 45 minutes. For sterically hindered amino acids, the procedure is repeated once. The Fmoc group is then removed by treatment with 20 % (v/v) piperidine for 2 minutes, repeated once, in order to limit aminolysis. The following amino acid is then coupled as normal. In order to limit diketopiperazine formation, the next Fmoc group was removed using 2% (v/v) DBU in DMF for 10 minutes. This free amine was, after thorough washing (5 x DMF) immediately coupled with the next amino acid using standard protocols. From this point on, the synthesis of the peptide was carried out as normal using either manual or automated Fmoc-SPPS protocols.

Pro-Phe-Ser-Arg-Val-OCam-Leu-NH_2 (18)

Peptide was synthesized on Tentagel S RAM resin (50 µmol) using the procedures for introduction of OCam esters followed by manual synthesis. Global deprotection followed by RP-HPLC purification yielded compound **18** as a white solid (24,8 mg, 32.0 µmol, 64%) **LC-MS** RT = 5.3 min (C18, 10-50% B over 9 minutes) **LRMS** calcd $[M+H]^+$ = 775.44 observed M/z = 775.60

Pro-Phe-Ser-Cit-Val-OCam-Leu-NH_2 (19)

Peptide was synthesized on Tentagel S RAM resin (50 µmol) using the procedures for introduction of OCam esters followed by manual synthesis. Global deprotection followed by RP-HPLC purification yielded compound **19** as a white solid (22,7 mg, 29.3 µmol, 59%). **LC-MS** RT = 5.5 min (C18, 10-50% B over 9 minutes) **LRMS** calcd $[M+2H]^{2+}$ = 776.42 observed M/z = 776.60

Pro-Gly-Lys-Asn-Ala-Thr-Gly-Met-Glu-Val-Gly-Trp-Tyr-Arg-Pro-Pro-Phe-Ser-Arg-Val-OCam-Leu-Lys-Lys-NH_2 (23)

Peptide was synthesized on Tentagel S RAM resin (100 µmol) using the procedures for introduction of OCam esters followed by manual synthesis. Global deprotection followed by RP-HPLC purification yielded compound **23** as a white solid (80.7 mg, 30.2 µmol, 30%) **LC-MS** RT = 5.2 min (C18, 10-90% B over 9 minutes) **LRMS** calcd $[M+3H]^{3+}$ = 892.81 observed M/z = 893.17

Ac-Gly-Gln-Phe-Arg-Val-Ile-Gly-Pro-Arg-His-Pro-Ile-Arg-Ala-Leu-Val-Gly-Asp-Glu-Val-Glu-Leu-Pro-Cys-Arg-Ile-Ser-Pro-Gly-Lys-Asn-Ala-Thr-Gly-Met-Glu-Val-Gly-Trp-Tyr-Arg-Pro-Pro-Phe-Ser-Arg-Val-OCam-Leu-Lys-Lys-NH_2 (26)

Peptide was synthesized on Tentagel S RAM resin (100 µmol) using the procedures for introduction of OCam esters followed by automated synthesis. After Fmoc deprotection, the N-terminus was acetylated using 10% (v/v) Ac_2O and 5% (v/v) DiPEA in DMF for 15 minutes. Global deprotection followed by RP-HPLC purification yielded compound **26** as a white solid (42.2 mg, 7.4 µmol, 7%) **LC-MS** RT = 14.9 min (C18, 5-65% B over 30 minutes) **LRMS** calcd $[M+4H]^{4+}$ = 1429.52 observed M/z = 1429.83

Recombinant expression of His-tagged MOG-fragments

Expression and purification of His-tagged MOG fragments was carried out as described by Araman *et al.*[2] with a few minor changes: For the MOG_{49-125}-TEV-His_6 fragment, four different solubilization buffers were tested: 6 M Gdn·HCl, 200 mM NaPi, 300 mM NaCl, pH 8; 6 M Urea, 200 mM NaPi, 300 mM NaCl, pH 8; 6 M Urea, 200 mM Tricine, 300 mM NaCl, pH 8; 8 M Urea, 200 mM Tricine, 300 mM NaCl, pH 8.5; Desalting buffers with the same compositions (minus the NaCl) were used in tandem.

General protocol for NCL

Ligation buffer (6 M Gdn·HCl, 200 mM NaPi, pH 7.2) was degassed with N2 for 30 minutes prior to use. TCEP·HCl and the desired thiol catalyst (MPAA or TFET) were dissolved in this buffer, pH adjusted to the desired value, and the resulting solution was again degassed with N2. Then, the thioester fragment (1.0 eq, 2 mM) and cysteine fragment (1.5 eq., 3 mM) are dissolved in 100 µL of this mixture. The ligation mixture was shaken at 600 rpm at the specified temperature. Fresh TCEP (as 100 mM solution in ligation buffer) was added after 4 and 24. Time points (0, 1,2,4,24 and (for proline ligation) 48 hours) were taken as aliquots of 10 µl, acidified with 10µl 20% (v/v) aqueous TFA and stored at -80°C. The aliquot was diluted with 30 µl buffer prior to LC-MS analysis.

Omniligase-1 ligation of Arg and Cit containing model peptides

The peptide ester and the amine fragments were prepared as 10 mM stock solutions in ligation buffer (200 mM tricine, pH 8.5). From these, a reaction mixture was made containing 1 mM of both peptides and 6 mM TCEP, in a total volume of 200 µL ligation buffer. The pH was calibrated to be 8.5 and Omniligase-1 was added (1 µL of a 5 mg/mL stock). Samples were taken at 0, 1 2 and 4 hours by diluting 10 µL of ligation mixture in 90 µL of quenching solution (2:9:9 TFA:MeCN:H_2O). These samples were analyzed by LC-MS.

Omniligase-1 ligation onto $MOG_{49\text{-}125}$-TEV-His_6

Reduction of chaotrope concentration in protein solution was carried out as follows: 500 µL of protein solution was applied to an Amicon Ultra-0.5 Centrifugal Filter (3 kDa NMWCO), which was spun at the manufacturers recommended speed (14000 rcf) and 8°C until half of the solution had run through the filter. Then, the sample was diluted with chaotrope-free buffer to achieve the desired chaotrope concentration. When necessary, this procedure was repeated.

Peptide ester (5 or 10 equivalents, based on protein concentration) was dissolved in 100 µL of protein solution in denaturing buffer. TCEP was added from a 100 mg/mL solution to make the final TCEP concentration 6 mM (1.5 µL). The pH was set to 8.5 and Omniligase-1 was added from a 5 mg/mL stock solution. LC-MS samples were taken at 0, 1 2 and 4 hours by diluting 10 µL of ligation mixture in 90 µL of quenching solution (2:9:9 TFA:MeCN:H_2O). Additional samples for SDS-PAGE analysis were taken by diluting 2.5 µL of reaction mixture with 12.5 µL denaturing buffer (8 M Urea, 200 mM tricine, pH 8.5), followed by an equal volume (15 µL) loading buffer (Laemmli).

Carboxyamidometyl-ester stability tests

1 µmol of resin-bound peptide **27** (Fmoc-Ser(tBu)-Arg(Pbf)-Val-OCam-Leu-Lys(Boc)-Lys(Boc)-RAM) was added into a vial and 500 µL of the deprotection solution under investigation was added. The vial was screwed close and put in a heating block, were it was stirred for 4 hours at the indicated temperatures (RT, 50°C or 90°C). After the four hours had elapsed, the vials were cooled back to room temperature and the resin was transferred to a fritted syringe and thoroughly washed with DMF. Next, the resin was treated with 0.5 mL capping solution containing 0.5 M Bz_2O, 0.5 M DiPEA and 0.1 M pyridine in DMF for 30 minutes. After capping, the peptides were cleaved from resin (95:2.5:2.5 TFA/H_2O/TIS, 200 µL, 1 hour), precipitated from cold Et_2O and recovered by centrifugation. The pellets were dissolved in 1 mL of 1:1:1 MeCN/tBuOH/H_2O and subjected to LC-MS analysis.

Experimental for $OVA_{323\text{-}339}$ glycocluster-scaffold-peptides

General procedure for peptides synthesis

All solid support peptide synthesis, including selective Mmt deprotection and fluorophore incorporation, was carried out as described in Chapter 4.

Fmoc-Lys(N_3)-Lys(N_3)-Lys(N_3)-Lys(N_3)-Lys(N_3)-Lys(N_3)-Gly-Ile-Ser(tBu)-Gln(Trt)-Ala-Val-His(Boc)-Ala-Ala-His(Boc)-Ala-Glu(OtBu)-Ile-Asn(Trt)-Glu(OtBu)-Ala-Gly-Arg(Pbf)-Ala-Ala-Ala-Ala-Ala-Lys(Mmt)-RAM-Tentagel S (29)

The synthesis was carried out on Tentagel S RAM resin (25 µmol) using a combination of manual and automatic SPPS conditions. **LC-MS** RT = 7.7 min (C18, 10-90% B over 9 minutes) **LRMS** calcd $[M+2H]^{2+}$ = 1730.90, $[M+3H]^{3+}$ = 1154.26 observed M/z = 1730.80, 1154.60

Lys(N_3)-Lys(N_3)-Lys(N_3)-Lys(N_3)-Lys(N_3)-Lys(N_3)-Gly-Ile-Ser-Gln-Ala-Val-His-Ala-Ala-His-Ala-Glu-Ile-Asn-Glu-Ala-Gly-Arg-Ala-Ala-Ala-Ala-Ala-Lys(sCy5)-RAM-Tentagel S (30)

Immobilized peptide **29** (5 µmol) was selectively deprotected followed by incorporation of the sCy5 fluorophore, according to the general methods. The Fmoc-group was then removed using standard conditions and the peptide liberated from resin. **LC-MS** RT = 5.0 min (C18, 10-90% B over 9 minutes) **LRMS** calcd $[M+2H]^{2+}$ = 1931.96, $[M+3H]^{3+}$ = 1288.31 observed M/z = 1921.25, 1288.50

Lys(N_3)-Lys(N_3)-Lys(N_3)-Lys(N_3)-Lys(N_3)-Lys(N_3)-Gly-Ile-Ser-Gln-Ala-Val-His-Ala-Ala-His-Ala-Glu-Ile-Asn-Glu-Ala-Gly-Arg-Ala-Ala-Ala-Ala-Ala-Lys(sCy5)-RAM-Tentagel S (31)

Immobilized peptide **29** (5 µmol) was N-terminally acetylated following the general protocol. The Mmt group was then selectively deprotected, followed by incorporation of the sCy5 fluorophore, according to the general methods. Finally, the peptide was liberated from resin. **LC-MS** RT = 6.0 min (C18, 10-90% B over 9 minutes) **LRMS** calcd $[M+2H]^{2+}$ = 1953.97, $[M+3H]^{3+}$ = 1302.31 observed M/z = 1953.50, 1302.50

Experimental for cyclic scaffolds

General procedure for peptides synthesis

All solid support peptide synthesis, including head-to-tail cyclization and selective Mmt deprotection, was carried out as described in Chapter 5.

***Cyclo*(-Lys-Abu-Lys(TEG-N_3)-Abu-Lys(TEG-N_3)-Abu-Lys(TEG-N_3)-Abu-Lys(TEG-N_3)-Abu-) (43)**

Peptide synthesis was initiated on a 25 µmol scale. Following the general procedures for cyclization and sidechain modification, compound **43** was isolated using RP-HPLC in 9.8% (4.6 mg, 2.4 µmol) yield. **LC-MS** RT = 5.2 min (C18, 10-90% B over 9 minutes) **LRMS** calcd $[M+H]^{+}$ = 1927.1, $[M+2H]^{2+}$ = 964.10; observed M/z = 1926.87,964.07

***Cyclo*(-Lys-Abu-Lys(TEG-TEG-N_3)-Abu-Lys(TEG-TEG-N_3)-Abu-Lys(TEG-TEG-N_3)-Abu-Lys(TEG-TEG-N_3)-Abu-) (44)**

Peptide synthesis was initiated on a 25 µmol scale. Following the general procedures for cyclization and sidechain modification, compound **44** was isolated using RP-HPLC in 4.5% (3.0 mg, 1.1 µmol) yield. **LC-MS** RT = 4.4 min (C18, 10-90% B over 9 minutes) **LRMS** calcd $[M+2H]^{2+}$ = 1342.75, $[M+3H]^{3+}$ = 895.5; observed M/z = 1342.83, 895.58

Biophysical, biochemical and computational assays

ThT Fluorescence Aggregation Assays

Aggregation assays were carried out in 96-well plate format using a Infinite M1000 Pro Tecan plate reader. The excitation and emission wavelengths were set to 444 nm and 485 nm respectively, with a

bandwidth of 10 nm. For each peptide under investigation, a 200 µM stock in sodium ascorbate buffer (20 mM, pH=5) was prepared and from this stock a serial diluted was made using the same buffer. Of these solutions, 199 µL of peptide stock was added into a well and mixed with 1 µL of 1 mM Thioflavin T stock solution, prepared in the same NaOAc buffer, for a final dye concentration of 5 µM. Every concentration of peptide was measured in triplicate. The plate was kept at 37°C and the fluorescence was measured every ten minutes for 16 hours. The fluorescence was normalized against a well containing 5 µM Thioflavin T in buffer that was measured alongside the assay.

Molecular Docking

The structures of HLA-E were retrieved from the Protein Data Bank using ICM Molsoft's inbuilt feature. The two entries with a resolution < 2.5 Å were visually inspected and 6GH1 was selected for its slightly better resolution. Of this structure chain A and peptide P were converted to an ICM object, with 'optimize hydrogens' set to true. 'Tight' water molecules were retained, leading to a conserved water molecule being present in the binding cleft near the peptides N-terminus. This water molecule is present in around half of the structures in the PDB. The bound 9-mer epitope was isolated to a separate object and used as template to select the binding cleft by selecting all atoms of the protein in a 5.0 Å radius. A pocket box was defined around this selection using default settings. The MOG_{40-48} epitopes of human (YRPPFSRVV) and mouse (YRSPFSRVV) and their 46-Citr variants were loaded from an SD-file and docked with the 'thoroughness' parameter set to 10, the 10 best poses were retained. The resulting poses were manually inspected and visualised using the Open Source PyMOL application.

Cathepsin G degradation assay

Peptides (10 µM) were dissolved in 200 µL sodium acetate buffer (150 mM, pH 5) and 50 ng of human cathepsin G (Abcam, ab91122) was added as 0.5 µL of a 0.1 mg/mL stock solution in NaOAc buffer (150 mM NaOAc, 150 mM NaCl, pH 5.5). The enzymatic reactions were incubated at 37°C and gently mixed at 600 RPM using an Eppendorf® ThermoMixer® C equipped with an Eppendorf® SmartBlock® for 1.5 mL epps. At specific timepoints (0, 1, 2, 4 and 24 hours) a 20 µL sample was taken. This sample was diluted with a quenching buffer (20 µL, 45:45:10 H_2O/MeCN/TFA) containing 100 µM Cbz-Phe-OH as an internal standard. These samples were analysed on a Thermo Scientific Vanquish UHPLC coupled to a Thermo Scientific LCQ Fleet ion mass spectrometer using a gradient of 5-65% B with constant 10% C over 30 minutes (buffer A: H_2O; buffer B: MeCN; buffer C: 1% TFA in H_2O). The peak at RT = 20.4 minutes was determined to belong to the internal standard and the ratio of the area under this peak to the area under the starting peptide peak was determined for all time points, using 220 nm as the absorption wavelength. The peak area ratio at t = 0 was set to 100%. Newly produced fragments were assigned to peptide sequences by analysis of the ESI+ mass spectrum.

Supporting Figures

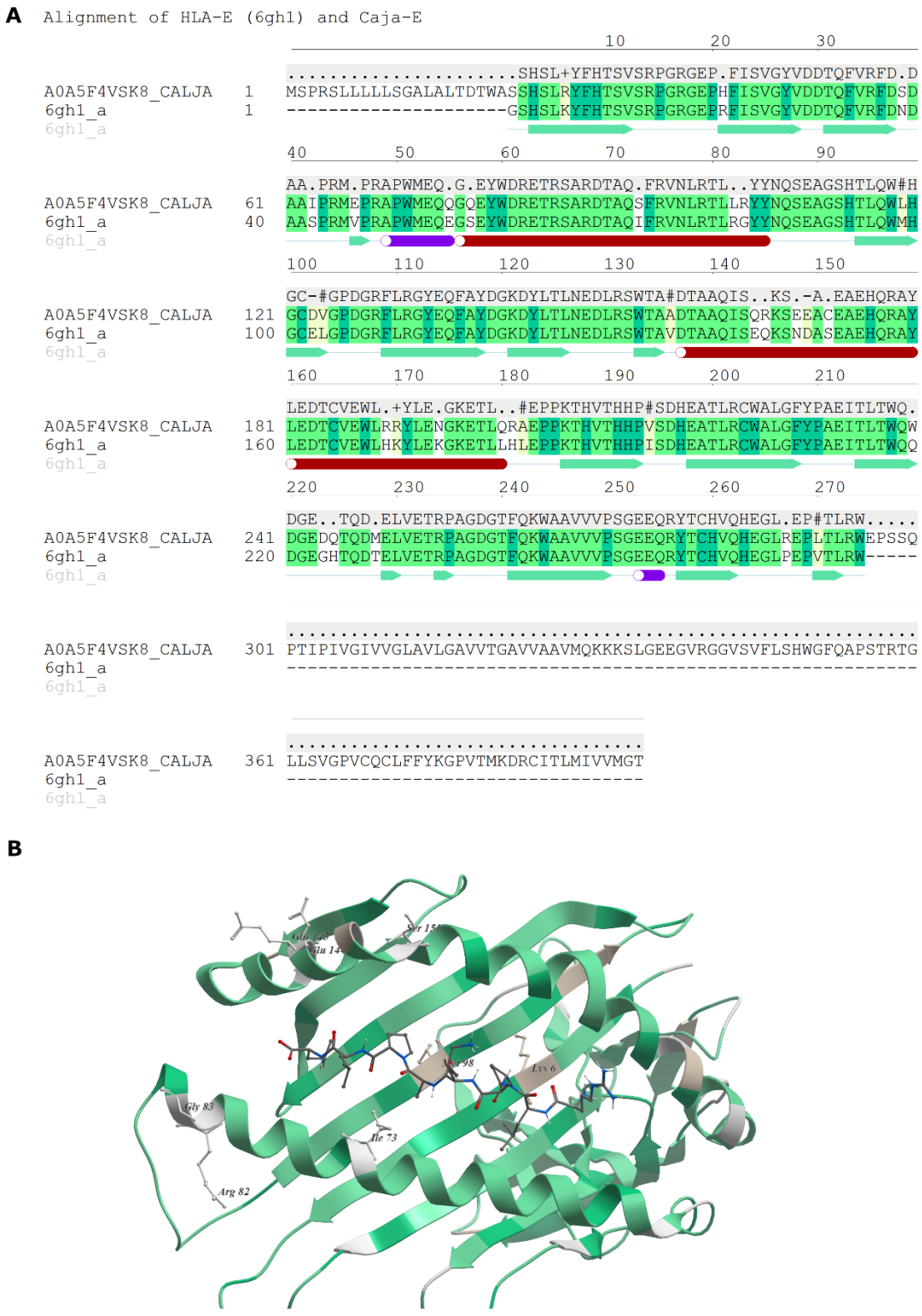

Figure S1. A) Alignment of amino acid sequence between HLA-E (PDB 6gh1, 6gh1_a) and Caja-E (A0A5F4VSK8_CALJA) B) HLA-E crystal structure (PDB 6gh1) showing the peptide binding groove. All residues not identical to those in Caja-E are highlighted in gray. Image generated by A.P.A. Janssen (Leiden university).

Table S1. Overview of ligation conditions tested on MOG27-47-OCamLKK (**23**) with MOG48-125-TEV-His_6 (**24**).

#	Buffer composition	Enzyme (μg/mL)	[Protein fragment] (μM)	Peptide (eq.)	Remarks
1	2 M guanidine 200 mM phosphate	500	360	5	low conversion (~20%), precipitated
2	2 M guanidine 200 mM phosphate	500	360	10	moderate conversion (~50%), precipitated
3	1.5 M guanidine 200 mM phosphate	500	250	5	low conversion (~20%), precipitated
4	1.5 M guanidine 200 mM phosphate	500	250	10	moderate conversion (~50%), precipitated
5	1 M guanidine 200 mM phosphate	500	180	5	very low conversion (<10%), precipitated
6	1 M guanidine 200 mM phosphate	500	180	10	low conversion (~20%), precipitated
7	6 M urea 200 mM tricine	250	190	10	moderate conversion (~40%)
8	6 M urea 200 mM phosphate	250	230	10	moderate conversion (~40%)
9	4 M urea 200 mM tricine	250	235	10	moderate conversion (~40%)
10	4 M urea 200 mM phosphate	250	185	10	moderate conversion (~40%)
11	4 M urea 200 mM tricine	50	235	10	moderate conversion (~40%)
12	4 M urea 200 mM phosphate	50	185	10	moderate conversion (~40%)
13	2 M urea 200 mM tricine	50	170	10	moderate conversion (~40%), precipitated
14	2 M urea 200 mM phosphate	50	200	10	moderate conversion (~40%), precipitated

References

(1) Doelman, W.; Marqvorsen, M. H. S.; Chiodo, F.; Bruijns, S. C. M.; van der Marel, G. A.; van Kooyk, Y.; van Kasteren, S. I.; Araman, C. Synthesis of Asparagine Derivatives Harboring a Lewis X Type DC-SIGN Ligand and Evaluation of Their Impact on Immunomodulation in Multiple Sclerosis. *Chem. Eur. J.* **2021**, *27* (8), 2742–2752. https://doi.org/10.1002/chem.202004076.

(2) Araman, C.; van Gent, M. E.; Meeuwenoord, N. J.; Heijmans, N.; Marqvorsen, M. H. S.; Doelman, W.; Faber, B. W.; 't Hart, B. A.; Van Kasteren, S. I. Amyloid-like Behavior of Site-Specifically Citrullinated Myelin Oligodendrocyte Protein (MOG) Peptide Fragments inside EBV-Infected B-Cells Influences Their Cytotoxicity and Autoimmunogenicity. *Biochemistry* **2019**, *58* (6), 763–775. https://doi.org/10.1021/acs.biochem.8b00852.

(3) Riera, R.; Hogervorst, T. P.; Doelman, W.; Ni, Y.; Pujals, S.; Bolli, E.; Codée, J. D. C.; van Kasteren, S. I.; Albertazzi, L. Single-Molecule Imaging of Glycan–Lectin Interactions on Cells with Glyco-PAINT. *Nat. Chem. Biol.* **2021**, *17* (12), 1281–1288. https://doi.org/10.1038/s41589-021-00896-2.

(4) Li, R. J. E.; Hogervorst, T. P.; Achilli, S.; Bruijns, S. C.; Arnoldus, T.; Vivès, C.; Wong, C. C.; Thépaut, M.; Meeuwenoord, N. J.; van den Elst, H.; Overkleeft, H. S.; van der Marel, G. A.; Filippov, D. V.; van Vliet, S. J.; Fieschi, F.; Codée, J. D. C.; van Kooyk, Y. Systematic Dual Targeting of Dendritic Cell C-Type Lectin Receptor DC-SIGN and TLR7 Using a Trifunctional Mannosylated Antigen. *Front. Chem.* **2019**, *7*, 650. https://doi.org/10.3389/fchem.2019.00650.

(5) van der Gracht, A. M. F.; de Geus, M. A. R.; Camps, M. G. M.; Ruckwardt, T. J.; Sarris, A. J. C.; Bremmers, J.; Maurits, E.; Pawlak, J. B.; Posthoorn, M. M.; Bonger, K. M.; Filippov, D. V; Overkleeft, H. S.; Robillard, M. S.; Ossendorp, F.; van Kasteren, S. I. Chemical Control over T-Cell Activation in Vivo Using Deprotection of Trans -Cyclooctene-Modified Epitopes. *ACS Chem. Biol.* **2018**, *13* (6), 1569–1576. https://doi.org/10.1021/acschembio.8b00155.

(6) Fairbanks, A. J. The ENGases: Versatile Biocatalysts for the Production of Homogeneous N-Linked Glycopeptides and Glycoproteins. *Chem. Soc. Rev.* **2017**, *46* (16), 5128–5146. https://doi.org/10.1039/C6CS00897F.

(7) Fujita, M.; Shoda, S. ichiro; Haneda, K.; Inazu, T.; Takegawa, K.; Yamamoto, K. A Novel Disaccharide Substrate Having 1,2-Oxazoline Moiety for Detection of Transglycosylating Activity of Endoglycosidases. *Biochim. Biophys. Acta - Gen. Subj.* **2001**, *1528* (1), 9–14. https://doi.org/10.1016/S0304-4165(01)00164-7.

(8) McIntosh, J. D.; Brimble, M. A.; Brooks, A. E. S.; Dunbar, P. R.; Kowalczyk, R.; Tomabechi, Y.; Fairbanks, A. J. Convergent Chemo-Enzymatic Synthesis of Mannosylated Glycopeptides; Targeting of Putative Vaccine Candidates to Antigen Presenting Cells. *Chem. Sci.* **2015**, *6* (8), 4636–4642. https://doi.org/10.1039/c5sc00952a.

(9) Bosques, C. J.; Imperiali, B. The Interplay of Glycosylation and Disulfide Formation Influences Fibrillization in a Prion Protein Fragment. *Proc. Natl. Acad. Sci.* **2003**, *100* (13), 7593–7598. https://doi.org/10.1073/pnas.1232504100.

(10) Liu, C. P.; Tsai, T. I.; Cheng, T.; Shivatare, V. S.; Wu, C. Y.; Wu, C. Y.; Wong, C. H. Glycoengineering of Antibody (Herceptin) through Yeast Expression and in Vitro Enzymatic Glycosylation. *Proc. Natl. Acad. Sci. U. S. A.* **2018**, *115* (4), 720–725. https://doi.org/10.1073/pnas.1718172115.

(11) Jagessar, S. A.; Kap, Y. S.; Heijmans, N.; Van Driel, N.; Van Straalen, L.; Bajramovic, J. J.; Brok, H. P. M.; Blezer, E. L. A.; Bauer, J.; Laman, J. D.; 'T Hart, B. A. Induction of Progressive Demyelinating Autoimmune Encephalomyelitis in Common Marmoset Monkeys Using MOG34-56 Peptide in Incomplete Freund Adjuvant. *J. Neuropathol. Exp. Neurol.* **2010**, *69* (4), 372–385. https://doi.org/10.1097/NEN.0b013e3181d5d053.

(12) Embgenbroich, M.; Burgdorf, S. Current Concepts of Antigen Cross-Presentation. *Front. Immunol.* **2018**, *0* (JUL), 1643. https://doi.org/10.3389/FIMMU.2018.01643.

(13) Jagessar, S. A.; Heijmans, N.; Blezer, E. L. A.; Bauer, J.; Blokhuis, J. H.; Wubben, J. A. M.; Drijfhout, J. W.; van den Elsen, P. J.; Laman, J. D.; Hart, B. A. '. Unravelling the T-Cell-Mediated Autoimmune Attack on CNS Myelin in a New Primate EAE Model Induced with MOG 34-56 Peptide in Incomplete Adjuvant. *Eur. J. Immunol.* **2012**, *42* (1), 217–227. https://doi.org/10.1002/eji.201141863.

(14) Jagessar, S. A.; Holtman, I. R.; Hofman, S.; Morandi, E.; Heijmans, N.; Laman, J. D.; Gran, B.; Faber, B. W.; van Kasteren, S. I.; Eggen, B. J. L.; 't Hart, B. A. Lymphocryptovirus Infection of Nonhuman Primate B Cells Converts Destructive into Productive Processing of the Pathogenic CD8 T Cell Epitope in Myelin Oligodendrocyte Glycoprotein. *J. Immunol.* **2016**, *197* (4), 1074–1088. https://doi.org/10.4049/jimmunol.1600124.

(15) Morandi, E.; Jagessar, S. A.; 't Hart, B. A.; Gran, B. EBV Infection Empowers Human B Cells for Autoimmunity: Role of Autophagy and Relevance to Multiple Sclerosis. *J. Immunol.* **2017**, *199* (2), 435–448.

(16) Burster, T.; Beck, A.; Tolosa, E.; Marin-Esteban, V.; Rötzschke, O.; Falk, K.; Lautwein, A.; Reich, M.; Brandenburg, J.; Schwarz, G.; Wiendl, H.; Melms, A.; Lehmann, R.; Stevanovic, S.; Kalbacher, H.; Driessen, C. Cathepsin G, and Not the Asparagine-Specific Endoprotease, Controls the Processing of Myelin Basic Protein in Lysosomes from Human B Lymphocytes. *J. Immunol.* **2004**, *172* (9), 5495–5503. https://doi.org/10.4049/JIMMUNOL.172.9.5495.

(17) Carrillo-Vico, A.; Leech, M. D.; Anderton, S. M. Contribution of Myelin Autoantigen Citrullination to T Cell Autoaggression in the Central Nervous System. *J. Immunol.* **2010**, *184* (6), 2839–2846. https://doi.org/10.4049/jimmunol.0903639.

(18) Van Leeuwen, T.; Araman, C.; Pieper Pournara, L.; Kampstra, A. S. B.; Bakkum, T.; Marqvorsen, M. H. S.; Nascimento, C. R.; Groenewold, G. J. M.; Van Der Wulp, W.; Camps, M. G. M.; Janssen, G. M. C.; Van Veelen, P. A.; Van Westen, G. J. P.; Janssen, A. P. A.; Florea, B. I.; Overkleeft, H. S.; Ossendorp, F. A.; Toes, R. E. M.; Van Kasteren, S. I. Bioorthogonal Protein Labelling Enables the Study of Antigen Processing of Citrullinated and Carbamylated Auto-Antigens. *RSC Chem. Biol.* **2021**, *2* (3), 855–862. https://doi.org/10.1039/D1CB00009H.

(19) Thorpe, M.; Fu, Z.; Chahal, G.; Akula, S.; Kervinen, J.; De Garavilla, L.; Hellman, L. Extended Cleavage Specificity of Human Neutrophil Cathepsin G: A Low Activity Protease with Dual Chymase and Tryptase-Type Specificities. *PLoS One* **2018**, *13* (4), e0195077. https://doi.org/10.1371/JOURNAL.PONE.0195077.

(20) Dawson, P. E.; Muir, T. W.; Clark-Lewis, I.; Kent, S. B. H. Synthesis of Proteins by Native Chemical Ligation. *Science* **1994**, *266* (5186), 776–779. https://doi.org/10.1126/science.7973629.

(21) Agouridas, V.; El Mahdi, O.; Diemer, V.; Cargoët, M.; Monbaliu, J. C. M.; Melnyk, O. Native Chemical Ligation and Extended Methods: Mechanisms, Catalysis, Scope, and Limitations. *Chemical Reviews*. American Chemical Society June 26, 2019. https://doi.org/10.1021/acs.chemrev.8b00712.

(22) Miseta, A.; Csutora, P. Relationship Between the Occurrence of Cysteine in Proteins and the Complexity of Organisms. *Mol. Biol. Evol.* **2000**, *17* (8), 1232–1239. https://doi.org/10.1093/OXFORDJOURNALS.MOLBEV.A026406.

(23) Carugo, O. Amino Acid Composition and Protein Dimension. *Protein Sci.* **2008**, *17* (12), 2187–2191. https://doi.org/10.1110/PS.037762.108.

(24) Yan, L. Z.; Dawson, P. E. Synthesis of Peptides and Proteins without Cysteine Residues by Native Chemical Ligation Combined with Desulfurization. *J. Am. Chem. Soc.* **2001**, *123* (4), 526–533.

https://doi.org/10.1021/ja003265m.

(25) Wan, Q.; Danishefsky, S. J. Free-Radical-Based, Specific Desulfurization of Cysteine: A Powerful Advance in the Synthesis of Polypeptides and Glycopolypeptides. *Angew. Chem. Int. Ed.* **2007**, *46* (48), 9248–9252. https://doi.org/10.1002/ANIE.200704195.

(26) Hackeng, T. M.; Griffin, J. H.; Dawson, P. E. Protein Synthesis by Native Chemical Ligation: Expanded Scope by Using Straightforward Methodology. *Proc. Natl. Acad. Sci.* **1999**, *96* (18), 10068–10073. https://doi.org/10.1073/PNAS.96.18.10068.

(27) Camarero, J.; Mitchell, A. Synthesis of Proteins by Native Chemical Ligation Using Fmoc-Based Chemistry. *Protein Pept. Lett.* **2005**, *12* (8), 723–728. https://doi.org/10.2174/0929866054864166.

(28) Ollivier, N.; Dheur, J.; Mhidia, R.; Blanpain, A.; Melnyk, O. Bis(2-Sulfanylethyl)Amino Native Peptide Ligation. *Org. Lett.* **2010**, *12* (22), 5238–5241. https://doi.org/10.1021/ol102273u.

(29) Blanco-Canosa, J. B.; Dawson, P. E. An Efficient Fmoc-SPPS Approach for the Generation of Thioester Peptide Precursors for Use in Native Chemical Ligation. *Angew. Chem. Int. Ed.* **2008**, *47* (36), 6851–6855. https://doi.org/10.1002/ANIE.200705471.

(30) Yang, Y.; Sweeney, W. V.; Schneider, K.; Thörnqvist, S.; Chait, B. T.; Tam, J. P. Aspartimide Formation in Base-Driven 9-Fluorenylmethoxycarbonyl Chemistry. *Tetrahedron Lett.* **1994**, *35* (52), 9689–9692. https://doi.org/10.1016/0040-4039(94)88360-2.

(31) Cardona, V.; Eberle, I.; Barthélémy, S.; Beythien, J.; Doerner, B.; Schneeberger, P.; Keyte, J.; White, P. D. Application of Dmb-Dipeptides in the Fmoc SPPS of Difficult and Aspartimide-Prone Sequences. In *International Journal of Peptide Research and Therapeutics*; Springer, 2008; Vol. 14, pp 285–292. https://doi.org/10.1007/s10989-008-9154-z.

(32) Michels, T.; Dölling, R.; Haberkorn, U.; Mier, W. Acid-Mediated Prevention of Aspartimide Formation in Solid Phase Peptide Synthesis. *Org. Lett.* **2012**, *14* (20), 5218–5221. https://doi.org/10.1021/ol3007925.

(33) Blanco-Canosa, J. B.; Nardone, B.; Albericio, F.; Dawson, P. E. Chemical Protein Synthesis Using a Second-Generation N-Acylurea Linker for the Preparation of Peptide-Thioester Precursors. *J. Am. Chem. Soc.* **2015**, *137* (22), 7197–7209. https://doi.org/10.1021/jacs.5b03504.

(34) Clements, C. S.; Reid, H. H.; Beddoe, T.; Tynan, F. E.; Perugini, M. A.; Johns, T. G.; Bernard, C. C. A.; Rossjohn, J. The Crystal Structure of Myelin Oligodendrocyte Glycoprotein, a Key Autoantigen in Multiple Sclerosis. *Proc. Natl. Acad. Sci.* **2003**, *100* (19), 11059–11064. https://doi.org/10.1073/PNAS.1833158100.

(35) White, P.; Keyte, J. W.; Bailey, K.; Bloomberg, G. Expediting the Fmoc Solid Phase Synthesis of Long Peptides through the Application of Dimethyloxazolidine Dipeptides. *J. Pept. Sci.* **2004**, *10* (1), 18–26. https://doi.org/10.1002/PSC.484.

(36) El Oualid, F.; Merkx, R.; Ekkebus, R.; Hameed, D. S.; Smit, J. J.; de Jong, A.; Hilkmann, H.; Sixma, T. K.; Ovaa, H.; El Oualid, F.; Merkx, R.; Ekkebus, R.; Hameed, D. S.; de Jong, A.; Hilkmann, H.; Ovaa, H.; Smit, J. J.; Sixma, T. K. Chemical Synthesis of Ubiquitin, Ubiquitin-Based Probes, and Diubiquitin. *Angew. Chem. Int. Ed.* **2010**, *49* (52), 10149–10153. https://doi.org/10.1002/ANIE.201005995.

(37) Fang, G. M.; Li, Y. M.; Shen, F.; Huang, Y. C.; Li, J. Bin; Lin, Y.; Cui, H. K.; Liu, L. Protein Chemical Synthesis by Ligation of Peptide Hydrazides. *Angew. Chem. Int. Ed.* **2011**, *50* (33), 7645–7649. https://doi.org/10.1002/ANIE.201100996.

(38) Jin, K.; Li, X. Advances in Native Chemical Ligation–Desulfurization: A Powerful Strategy for Peptide and Protein Synthesis. *Chem. – A Eur. J.* **2018**, *24* (66), 17397–17404.

https://doi.org/10.1002/CHEM.201802067.

(39) Thompson, R. E.; Liu, X.; Alonso-García, N.; Pereira, P. J. B.; Jolliffe, K. A.; Payne, R. J. Trifluoroethanethiol: An Additive for Efficient One-Pot Peptide Ligation - Desulfurization Chemistry. *J. Am. Chem. Soc.* **2014**, *136* (23), 8161–8164. https://doi.org/10.1021/ja502806r.

(40) Schmidt, M.; Toplak, A.; Quaedflieg, P. J. L. M.; Ippel, H.; Richelle, G. J. J.; Hackeng, T. M.; van Maarseveen, J. H.; Nuijens, T. Omniligase-1: A Powerful Tool for Peptide Head-to-Tail Cyclization. *Adv. Synth. Catal.* **2017**, *359* (12), 2050–2055. https://doi.org/10.1002/ADSC.201700314.

(41) Nuijens, T.; Toplak, A.; Schmidt, M.; Ricci, A.; Cabri, W. Natural Occurring and Engineered Enzymes for Peptide Ligation and Cyclization. *Front. Chem.* **2019**, *7*, 829. https://doi.org/10.3389/fchem.2019.00829.

(42) Pawlas, J.; Nuijens, T.; Persson, J.; Svensson, T.; Schmidt, M.; Toplak, A.; Nilsson, M.; Rasmussen, J. H. Sustainable, Cost-Efficient Manufacturing of Therapeutic Peptides Using Chemo-Enzymatic Peptide Synthesis (CEPS). *Green Chem.* **2019**, *21* (23), 6451–6467. https://doi.org/10.1039/C9GC03600H.

(43) Schmidt, M.; Nuijens, T. Chemoenzymatic Synthesis of Linear- and Head-to-Tail Cyclic Peptides Using Omniligase-1. In *Enzyme-Mediated Ligation Methods*; Nuijens, T., Schmidt, M., Eds.; Springer New York: New York, NY, 2019; pp 43–61. https://doi.org/10.1007/978-1-4939-9546-2_4.

(44) Nuijens, T.; Toplak, A.; van de Meulenreek, M. B. A. C.; Schmidt, M.; Goldbach, M.; Quaedflieg, P. J. L. M. Improved Solid Phase Synthesis of Peptide Carboxyamidomethyl (Cam) Esters for Enzymatic Segment Condensation. *Tetrahedron Lett.* **2016**, *57* (32), 3635–3638. https://doi.org/10.1016/J.TETLET.2016.06.132.

(45) Burgdorf, S.; Kautz, A.; Böhnert, V.; Knolle, P. A.; Kurts, C. Distinct Pathways of Antigen Uptake and Intracellular Routing in CD4 and CD8 T Cell Activation. *Science* **2007**, *316* (5824), 612–616. https://doi.org/10.1126/science.1137971.

(46) Mitchell, D. A.; Fadden, A. J.; Drickamer, K. A Novel Mechanism of Carbohydrate Recognition by the C-Type Lectins DC-SIGN and DC-SIGNR. Subunit Organization and Binding to Multivalent Ligands. *J. Biol. Chem.* **2001**, *276* (31), 28939–28945. https://doi.org/10.1074/jbc.M104565200.

(47) Ghosh, P.; Dahms, N. M.; Kornfeld, S. Mannose 6-Phosphate Receptors: New Twists in the Tale. *Nat. Rev. Mol. Cell Biol. 2003 43* **2003**, *4* (3), 202–213. https://doi.org/10.1038/nrm1050.

(48) Reintjens, N. R. M. M.; Tondini, E.; Vis, C.; McGlinn, T.; Meeuwenoord, N. J.; Hogervorst, T. P.; Overkleeft, H. S.; Filippov, D. V.; Marel, G. A. van der; Ossendorp, F.; Codée, J. D. C. C.; van der Marel, G. A.; Ossendorp, F.; Codée, J. D. C. C. Multivalent, Stabilized Mannose-6-Phosphates for the Targeted Delivery of Toll-Like Receptor Ligands and Peptide Antigens. *ChemBioChem* **2021**, *22* (2), 434–440. https://doi.org/10.1002/CBIC.202000538.

(49) La–Venia, A.; Dzijak, R.; Rampmaier, R.; Vrabel, M. An Optimized Protocol for the Synthesis of Peptides Containing Trans-Cyclooctene and Bicyclononyne Dienophiles as Useful Multifunctional Bioorthogonal Probes. *Chem. – A Eur. J.* **2021**, *27* (54), 13632–13641. https://doi.org/https://doi.org/10.1002/chem.202102042.

(50) Boll, E.; Drobecq, H.; Ollivier, N.; Blanpain, A.; Raibaut, L.; Desmet, R.; Vicogne, J.; Melnyk, O. One-Pot Chemical Synthesis of Small Ubiquitin-like Modifier Protein–Peptide Conjugates Using Bis(2-Sulfanylethyl)Amido Peptide Latent Thioester Surrogates. *Nat. Protoc. 2014 102* **2015**, *10* (2), 269–292. https://doi.org/10.1038/nprot.2015.013.

(51) Zheng, J. S.; Tang, S.; Qi, Y. K.; Wang, Z. P.; Liu, L. Chemical Synthesis of Proteins Using Peptide Hydrazides as Thioester Surrogates. *Nat. Protoc. 2013 812* **2013**, *8* (12), 2483–2495.

https://doi.org/10.1038/nprot.2013.152.

Nederlandse samenvatting

Dit proefschrift beschrijft nieuwe synthetische methodologie voor het produceren van verscheidende (glyco)peptiden en de toepassing van deze peptiden in het bestuderen van verscheidende immunologische processen. Het eerste deel van het proefschrift gaat over nieuwe inzichten in het ontstaan van de ziekte multiple sclerose, door onderzoek te doen naar lectine gestuurde immunotolerantie en een biochemische studie naar verschillen tussen een belangrijk menselijk antigeen en de dierlijke vorm van dit molecule. Het tweede deel omschrijft nieuwe multivalent geglycosyleerde peptides, welke gebruikt kunnen worden om lectine interacties en lectine-gestuurde antigeen opname te bestuderen. Het laatste stuk van deze thesis omschrijft een nieuwe manier om peptides met een *trans*-cyclooctene beschermde lysine te produceren, welke een interessante nieuwe categorie van moleculair gereedschap binnen de chemische biology.

Hoofdstuk 2 beschrijft de synthese van een serie *N*-geglycosyleerde Fmoc-asparagine bouwstenen voor de vastedrager synthese. Vier verschillende sacharide structuren werden gesynthetiseerd: GlcNAc, LacNAc (Galβ1-4GlcNAc), Fucα1-3GlcNAc en Lewis X (Galβ1-4(Fucα1-3)GlcNAc, Le^X). De bouwstenen werden gemaakt vanuit de beschermde glycosyl azides welke gekoppeld werden met asparagine door gebruikt te maken van een éénpots, tweestappen transformatie, gebruikmakend van een Staudinger reductie van de azide, gevolgd door regioselectieve opening van het cyclisch anhydride van Fmoc-asparaginezuur. Door gebruik te maken van standaard vastedrager peptide synthese zijn deze bouwstenen verwerkt in de immunologisch dominante peptide van het eiwit myeline oligodendrocyt glycoproteïne (MOG), MOG_{31-55}. Deze peptide bevat het residue dat onder natuurlijke omstandigheden *N*-geglycosyleerd wordt, Asn_{31}, welke hier vervangen werd met de *N*-geglycosyleerde asparagines. Door gebruikt te maken van een immunoadsorbtie methode (ELISA) kon bewezen worden dat de Le^X bevattende peptide kan binden aan de DC-SIGN receptor. Verder werd aangetoond dat er een Le^X gedreven effect van de peptiden is op de cytokine uitscheiding; moDCs behandeld met de peptide met of zonder Le^X glycaan lieten een vermindering van IL12p70 zien voor de Le^X bevattende peptide, als de peptides samen met LPS gegeven werden. Het effect van glycosylatie op de eerder beschreven citrulline gestuurde aggregatie van MOG_{31-55} was ook onderzocht. Er bleek een suikerafhankelijk verlaging in de mate van aggregatie te zijn.

In **hoofdstuk 3** wordt een serie gecitrullineerde peptides afgeleid van myeline oligodendrocyt glycoproteïne (MOG) onderzocht op hun biofysische en immunologische eigenschappen. Eerder werk vond dat de immunologisch dominante peptide MOG_{35-55}, afgeleid van de muis variant van MOG, amyloïde aggregatie vertoond, als één of meer van de arginine residuen gecitrullineerd zijn. Het eiwit MOG, en in het bijzonder de immunologisch dominante regio, hebben een zeer hoge mate van gelijkheid tussen verschillende diersoorten. Tussen de menselijke en muizenpeptide is slechts een enkel aminozuur verschil, in de vorm van een serine-naar-proline variatie op positie 42. In het hoofdstuk worden experimenten beschreven

die laten zien dat deze enkele substitutie de aggregatie volledig laat verdwijnen. Verdere analyse, waarbij peptides met verscheidende, op serine lijkende, aminozuren op positie 42 gemaakt werden, lieten zien dat de aggregatie sterk van dit serineresidue afhankelijk lijkt te zijn. Een verdere verassende vondst op immunologisch gebied was dat de onderzochte gecitrullineerde peptides zich anders gedroegen in een antigeen kruispresentatie experiment. Hiervoor werden B- en T-cellen van penseelaapjes, eerder geïmmuniseerd met humaan MOG_{35-55}, gebruikt. De niet-aggregerende humane peptide $hMOG_{35-55}$-$Cit_{46,52}$, liet een sterke respons, in de vorm van hoge mate van T-cel proliferatie, zien bij dit experiment. De gelijk gecitrullineerde muizenpeptide, $mMOG_{35-55}Cit_{46,52}$, een zeer effectief aggregerende peptide, liet geen enkele vorm van T-cell activatie zien.

In **hoofdstuk 4** wordt de synthese van een stel antigene peptiden met N-terminale glycoclusters en een C-terminale fluorofoor beschreven. Het gekozen antigeen is het welbekende peptide $OVA_{247-264}$, afgeleid van kippenovalbumine (OVA). Deze peptide bevat het $CD8^+$ T-cel specifieke epitoop $OVA_{257-264}$. De fluorofoor maakt het mogelijk om de binding van de glycopeptide aan een lectine, bijvoorbeeld de mannosereceptor (MR), te visualiseren. Hiervoor werd gebruikt gemaakt van de recent ontwikkelde glycoPAINT techniek. Door de fluorofoor covalent te koppelen aan het antigene glycoconjugaat, kan zowel de lectinebinding als de opname van het molecule gemeten worden. Door de combinatie van glycocluster, antigeen en fluorofoor in een enkel construct word het mogelijk om met directe metingen de relatie tussen MR binding en T-cel activatie te bepalen. Dit zou kunnen bijdragen aan een beter begrip van het effect dat glycosylering van antigenen heeft op antigeen kruispresentatie, een onderwerp waar nog veel onderzoek naar nodig is.

De synthese van de conjugaten verliep niet vlekkeloos. De introductie van de oligosacharides verliep door middel van koper gekatalyseerde ‘click’ chemie (CuAAC), gebruikmakend van propargylgroep bevattende oligosacharides. Deze suikers werden doormiddel van deze click reactie gekoppeld aan een serie azidolysineresiduen aan de N-terminale kant van peptiden. Deze reactie verliep niet zonder problemen; peptiden met meerdere azidolysineresiduen bleken zeer slecht oplosbaar, wat de koper gekatalyseerde conjugatiereactie verhinderede. Om dit te verhelpen werd een flexibele triethyleneglycol spacer tussen de antigene peptide en het glycocluster geïntroduceerd. Deze verandering verhoogde de oplosbaarheid van de peptides voldoende om succesvol verschillende glycoconjugaten te produceren. Verder geeft dit een mogelijkheid om het effect van deze PEG spacer op de MR bindingskinetiek te bepalen, wat waardevolle inzichten zal kunnen opleveren voor de verdere ontwikkelingen van antigeen-glycocluster conjugaten.

Hoofdstuk 5 beschrijft de synthese van een cyclisch, pentavalente peptide die als platform dient voor de conjugatie van suikers via CuAAC chemie. De cyclische peptide bestaat uit 6 lysineresiduen, waarvan vijf dienen als conjugatieposities voor de suikergroepen. De zesde lysine werd gebruikt om een fluorofoor te koppelen, wat resulteerde in een traceerbaar multivalent glycoconjugaat. Om dit doel te bereiken werd een combinatie van vastedrager chemie, waarop de cyclische peptide gebouwd werd, en oplossingschemie, om de suiker- en

fluorofoorconjugaties mogelijk te maken, gebruikt. Om de cyclische kern van het molecule te maken werd gebruik gemaakt van een welbekende kop-staart cyclisatiemethode op de vaste drager. Hierbij werd een probleem ondervonden, in de vorm van onbedoelde dimerisatie op de drager, een vaker voorkomend probleem volgens de chemische literatuur. De lengte van de lineaire startpeptide, welke significant groter was dan die gezien word bij de meeste gerapporteerde cyclisatiereacties, bleek het obstakel. Door het ontwerp minimaal aan te passen door de afstand tussen de lysineresiduen te verkleinen van zes koolstofatomen naar vier, kon de cyclisatie toch succesvol uitgevoerd worden. Op deze cyclische peptide werden, op de vijf lysines bedoelt voor suikerconjugatie, lange polyethylenederivaten gekoppeld, om voldoende afstand tussen de suikers en de cyclische kern te waarborgen. Om dit voor elkaar te krijgen moesten deze vijf lysineresiduen volledig ontschermd worden, zonder hierbij ook de peptide per abuis van de drager af te splitsen. Door gebruik te maken van de zeer zuurlabile monomethoxytrityl beschermgroep op deze vijf lysineresiduen, in combinatie met een zeer mild zure ontschermcocktail, kon een zeer hoge mate van volledige ontmaskering bereikt worden, zonder de gevoelige verbinding met de drager te beschadigen. Dit molecule was daarna, gebruikmakend van de chemie ontwikkeld in hoofdstuk 4, gekoppeld met oligosaccharides. Deze conjugatie werd gevolgd door labeling met een fluorofoor, wat de gewenste eindproducten opleverde.

In **hoofdstuk 6** wordt de ontwikkeling van een nieuwe methode voor de synthese van peptides die een allylische *trans*-cyclooctene (TCO) beschermd lysineresidue bevatten beschreven. Omdat de TCO functionaliteit zeer zuurgevoelig is, is de direct synthese van dit soort peptides door middel van Fmoc-SPPS erg moeilijk, omdat deze vorm van vastedrager synthese altijd gebruik maakt van een globale ontschemstap met trifluorazijnzuur (TFA). De nieuwe aanpak beschreven in dit hoofdstuk omvat het gebruik van azides als aminebeschermgroep voor de overige amines in de peptide, dat wil zeggen de N-terminus en alle andere lysineresiduen. Na de globale ontscherming met TFA word de TCO in oplossing geintroduceerd als een geactiveerd carbonaat. Na de succesvolle introductie van de TCO functionaliteit, kunnen de overige amines onthult worden door gebruik te maken van een Staudinger reductie met trimethylfosfine. Deze aanpak maakt het mogelijk om langere TCO bevattende peptiden te produceren dan tot nu toe haalbaar was. Omdat deze methode, anders dan eerder beschreven synthetische strategieën, ook geen gebruik maakt van nucleofiele bases tijdens de ontschermstap, kunnen functionaliteiten gevoelig voor dit soort condities ook geïntroduceerd worden. Om dit te demonstreren werd een TCO-beschermede peptide gemaakt die ook een vetzuurester bevat.

List of publications

Synthesis of peptides containing a combination of free and 2-*trans*-cyclooctene carbamate protected lysine residues
W. Doelman, M.A.T. van de Plassche, N.A.M. Ligthart, M. Isendoorn, L. Reinalda, D. Filippov, G.J. van der Heden-van Noort, S.I. van Kasteren
manuscript in preparation

Citrullinated human and murine MOG_{35-55} display distinct biophysical and biochemical behavior
W. Doelman, R.C. Reijnen, N. van Driel, N. Dijksman, B.A. 't Hart, I. Philippens, M.C. Araman, W. Baron, S.I. van Kasteren
manuscript in preparation

Bio-orthogonal peptide enrichment from complex samples using a Rink-amide-based catch-and-release
W. Doelman*, T. van Leeuwen*, R.W.R. van den Kieboom, B.I. Florea, S.I. van Kasteren
**These authors contributed equally to this work*
manuscript in preparation

Synthesis of glycopeptides and glycopeptide conjugates
W. Doelman, S.I. van Kasteren
Org. Biomol. Chem. **2022**, *20*, 6487-6507
DOI: 10.1039/d2ob00829g

Single-molecule imaging of glycan–lectin interactions on cells with Glyco-PAINT
R. Riera*, T.P. Hogervorst*, W. Doelman, Y. Ni, S. Pujals, E. Bolli, J.D.C. Codée, S.I. van Kasteren, L. Albertazzi
**These authors contributed equally to this work*
Nat. Chem. Biol. **2021**, *17*, 1281–1288
DOI: 10.1038/s41589-021-00896-2

Synthesis of Asparagine Derivatives Harboring a Lewis X Type DC-SIGN Ligand and Evaluation of their Impact on Immunomodulation in Multiple Sclerosis
W. Doelman, M.H.S. Marqvorsen, F. Chiodo, S.C.M. Bruijns, G.A. van der Marel, Y. van Kooyk, S.I. van Kasteren, C. Araman
Chem. Eur. J. **2021**, *27*, 2742-2752
DOI: 10.1002/chem.202004076

Efficient synthesis and enzymatic extension of an *N*-GlcNAz asparagine building block
M.H.S. Marqvorsen, S. Paramasivam, W. Doelman, A.J. Fairbanks, S.I. van Kasteren
Chem. Commun. **2019**, *55*, 5287-5290
DOI: 10.1039/c9cc02051a

Amyloid-like Behavior of Site-Specifically Citrullinated Myelin Oligodendrocyte Protein (MOG) Peptide Fragments inside EBV-Infected B-Cells Influences Their Cytotoxicity and Autoimmunogenicity
M.C. Araman, M.E. van Gent, N.J. Meeuwenoord, N. Heijmans, M.H.S. Marqvorsen, W. Doelman, B.W. Faber, B.A. 't Hart, S.I. van Kasteren
Biochemistry **2019**, *58*, 763–775
DOI: 10.1021/acs.biochem.8b00852

Fast and pH-Independent Elimination of *trans*-Cyclooctene by Using Aminoethyl-Functionalized Tetrazines
A.J.C. Sarris, T. Hansen, M.A.R. de Geus, E. Maurits, W. Doelman, H.S. Overkleeft, J.D.C. Codée, D.V. Filippov, S.I. van Kasteren
Chem. Eur. J. **2018**, *24*, 18075-18081
DOI: 10.1002/chem.201803839

Structure-kinetic relationship studies of cannabinoid CB2 receptor agonists reveal substituent-specific lipophilic effects on residence time
M. Soethoudt, M.W.H. Hoorens, W. Doelman, A. Martella, M. van der Stelt, L.H. Heitman
Biochem. Pharmacol. **2018**, *152*, 129-142
DOI: 10.1016/j.bcp.2018.03.018

ORCID: 0000-0002-5138-9402

Curriculum Vitae

Ward Doelman was born in Utrecht, on the 25th of January, 1994. In 2015, he obtained his BSc degree in Life Science & Technology from the Leiden University and Delft University of Technology, with the distinction *cum laude*. During his bachelor studies he performed a research internship under the guidance of Dr. G.P.P. Gential and Dr. D.V. Filippov. The thesis written as part of this research was titled "Towards double labeled peptides for antigen processing research" and dealt with the synthesis of an antigenic peptide containing several orthogonally conjugatable functions.

When starting his master's degree, he switched majors and started the MSc program Chemistry (specialization research in chemical biology) at Leiden University. During his master education he performed two research internships within Leiden University. The first was under the supervision of Dr. M. Soethoudt, Prof. Dr. L.H. Heitman and Prof. Dr. M. van der Stelt. The title of the research project was "Structure-kinetics relationships for a library of LEI101 derived CB_2 agonists". This project involved both the profiling of the binding kinetics of unlabeled agonist for the CB_2-GPCR using radioligand competition assays, as well as functional assays related to GPCR activation. Next, chemical immunology came into focus, with a research project in the van Kasteren group, supervised by Dr. M.J. van de Graaff and Prof. Dr. S.I. van Kasteren. The master thesis written about this research was titled "Towards the synthesis of sulfated Lewis X trisaccharides for cross-presentation research" and dealt with the synthesis of several immune relevant sulfated oligosaccharides. He obtained his MSc degree in 2017 with the distinction *summa cum laude* and also received the Unilever research award 2017 for his master thesis.

After obtaining his master's degree, he stayed in the group of Prof. Dr. van Kasteren as a PhD student, where the research outlined in this thesis was performed. During his PhD, he has collaborated with several Dutch experts on multiple sclerosis research: Prof. Dr. B.A. 't Hart (BPCR), Prof. Dr. Y. van Kooyk (vUMC) and Dr. W. Baron (UMCG). The glycoPAINT technique was developed as a collaboration with the group of Prof. Dr. L. Albertazzi (TUe). He also briefly collaborated with an industrial partner, EnzyTag B.V. (Nuth, the Netherlands), on a protein semisynthesis project. During his PhD he also supervised the research internships of two bachelor students and five master students, as well as teaching several seminars and supervising several practical courses, all aimed at first year bachelor students.

He also presented his research at various conferences. He gave oral presentations at the Wageningen synthetic organic chemistry meeting (2019), the Bioorthogonal & Bioresponsive conference (2021) and CHAINS (2021). He also presented parts of his research in the form of posters at Eurocarb (2019) and CHAINS (2017, 2018, 2019).

Currently, he continues his research as a postdoctoral scientist at Leiden University.

Dankwoord

En dan uiteindelijk de laatste pagina's van het proefschrift. Het dankwoord is, grappig genoeg, vaak tegelijk het meest persoonlijke en het meest formalistische deel van een thesis. Je kan een chemisch lab niet persoonlijk draaiend houden, en dat moet je ook niet willen. Mijn dank gaat uit naar alle personen die mij de afgelopen jaren op professioneel en persoonlijk vlak hebben bijgestaan.

Allereest wil ik natuurlijk Sander bedanken. Vanaf de eerste dag van mijn promotie heb je mij je volle vertrouwen gegeven. Je gaf me vreemde en moeilijke vraagstukken om op te lossen, en gaf mij tegelijk ook de ruimte om mijn eigen ideeën te ontplooien. Ik heb van jou geleerd dat een goede wetenschapper meer moet kunnen dan het uitvoeren van sterke proeven, en ik neem alles wat je me verteld hebt mee in mijn volgende stappen als jonge wetenschapper. Ook wil ik je bedanken voor alle samenwerkingen die jij mogelijk gemaakt hebt; jouw flexibiliteit en openheid voor andere invalshoeken hebben heel veel toegevoegd aan mijn thesis en mijn wetenschappelijk kennis. Ook mijn tweede promotor, Hermen, moet ik natuurlijk bedanken; jouw advies met je rechtdoorzee maar zeer nauwkeurige schrijfstijl heeft mijn thesis strakker op papier gezet dan ik het alleen zou kunnen.

Maar niet alleen Sander heeft geholpen bij mijn wetenschappelijke ontwikkeling; ik heb veel geleerd van de samenwerking met verschillende postdocs in onze groep. Mikkel, your passion for and knowledge of carbohydrate chemistry has only helped to further increase my own. Our collaboration on the synthesis of glycosylated asparagine derivatives has yielded two papers and a strong friendship. Can, where Mikkel inspired my love of carbohydrates, you taught me about the wonderful world of peptides, which has become the central theme of my Thesis. For nearly three years, we fought with our beloved MOG antigens. Together, we studied their amyloidogenic potential, until we were defeated by a single amino acid. Building the entire, post-translationally modified protein turned out to be a bridge too far, but regardless I treasured all the time we spent together in and out of the lab. Merel, jij begon bij ons in de groep toen ik al vrij ver in mijn PhD traject zat, dus misschien kon je me wat minder leren dan de anderen. Je gezelligheid en optimisme daarentegen, kwamen op een goed moment, en we hebben samen ook nog eens een erg cool project gestart.

Verder zijn er nog vele andere mensen in en rond de labs die ik wil bedanken. Dima, jij bent de man waar ik altijd op kon vertrouwen als er iets echt geks gebeurde in de peptidechemie. Hans en Nico, jullie hebben mij enorm geholpen met het analyseren en zuiveren van alle gekkigheid die ik de afgelopen jaren gesynthetiseerd heb, waarvoor ik jullie eeuwig dankbaar ben. Ook belangrijk zijn alle collega's waarmee ik de afgelopen jaren een lab gedeeld heb; Lab DM3.17 is al meer dan vijf jaar mijn werkplek, en ik sta daar nog steeds met veel plezier. Ook ieder ander waar ik de afgelopen jaren ideeën mee heb uitgewisseld, technieken van heb geleerd of gewoon een kopje koffie (of iets anders) mee gedronken heb worden allemaal gewaardeerd. Dit geld natuurlijk ook voor mijn collega's in het biolab, vooral voor de mensen die mij geholpen hebben met experimenten die een stukje verder uit mijn comfortzone waren.

Ook mijn samenwerkingspartners moet ik bedanken. Bert en Wia, met jullie kennis van neuroimmunology hebben we erg veel interessant onderzoek naar het ontstaan van multiple sclerosis kunnen uitvoeren. Fabrizio Chiodo en Yvette van Kooyk, jullie hebben het Lewis X verhaal naar een hoger plan getild met jullie expertise. Ingrid Philippens, dank je wel voor je bereidheid om tijd vrij te maken om onze gekke peptides te testen in een immunologisch experiment. Roger and Lorenzo, working together on the development of glycoPAINT was a fantastic experience, that resulted in a beautiful paper. Anna en Leendert, hoewel de MOG-semisynthese pittiger bleek dan we ons initieel voorstelden, heb ik erg genoten van onze samenwerking. Dankjewel dat ik jullie lab in Nuth mocht bezoeken, ik heb er zeer veel geleerd. Diana, Tyrza, Nina en Luuk, jullie hulp bij mijn projecten word ook zeer gewaardeerd. Laten we samen een paar mooie papers maken van al het werk dat we gedaan hebben!

De studenten die ik de afgelopen jaren begeleid heb moet ik natuurlijk ook bedanken: Rudy, Femke, Duncan, Lars, Sven, Roos en Robin. Jullie hebben allemaal hard gewerkt en op jullie eigen wijze een bijdrage geleverd aan mijn proefschrift. Ik heb ervan genoten om jullie te leren kennen en door jullie vragen en interesse nieuwe dingen te leren. Mijn PhD was niet zo leuk en afwisselend geweest zonder jullie.

Als laatste wil ik natuurlijk ook mijn familie en vriendin bedanken. Pap en mam, meestal begrepen jullie weinig van wat ik aan het doen was, maar jullie waren altijd blij dat ik het aan het doen was. Lieve Merel, je bent er altijd voor me geweest, ook als ik chagrijnig was door een mislukt experiment of druk was met een deadline. Het zit er eindelijk op, nu is het tijd om samen op avontuur te gaan.